The Effect of Sub-Optimal Temperature on the Cellular Metabolism of Wheat and *Arabidopsis thaliana*

Bo Eng Cheong

ORCID Identifier (0000-0002-6423-2148)

Thesis submitted in total fulfilment for the degree of

Doctor of Philosophy

November 2020

The School of BioSciences

The University of Melbourne

Abstract

Low or suboptimal temperature stress is one of the primary abiotic conditions limiting the growth and productivity of economic crops in many regions of the world. Wheat is one of the major crops in Australia, it is grown during winter to avoid hot summers and they flower in early spring. The sensitive flowering stage of wheat is therefore frequently exposed to spring frost. In Australia, the frequency of spring frosts during the flowering stage has increased significantly since 1960, and the reoccurrence of frost events led to an estimated $360 million of losses in the Australian wheat industry per annum. It is therefore important for breeders to minimize the loss via the development of more chilling/frost-tolerant wheat varieties, especially during their reproductive stages. Two approaches could be employed to achieve this goal. The first one is by employing metabolomics approaches to understand the underlying molecular mechanisms involved in cold responses of wheat upon cold stress. The second approach is via bioengineering of cold responsive genes into wheat to create chilling/frost-tolerant varieties. With this in mind, my PhD study was carried out with three main objectives. The first objective was to investigate and understand metabolic traits involved in the cold acclimation of two Australian wheat varieties with contrasting cold tolerance using targeted metabolomics and lipidomics approaches. The cold-sensitive variety used in this study was Wyalkatchem and the cold tolerant variety used was Young. The second objective of this study was to identify potential metabolite and lipid responsible for chilling tolerance in the two studied wheat varieties. The third objective was to evaluate the potential of REIL (Required for isotropic bud growth1 – like) protein as cold acclimation factor in *Arabidopsis thaliana* for potentially enhancing wheat cold tolerance.

Chapter 1 consists of a review of the recent literature covering cold stress responses (physiologically and metabolically) of plants and how plants adopt to cold stress. It describes how metabolomics and lipidomics can be used as promising tools to decipher cold stress responses in wheat and discuss the role of cold-induced genes to increase cold tolerance in plants. The targeted protein in this study, REIL, as a new potential cold acclimation factor in *Arabidopsis thaliana* and wheat is also reviewed.

To achieve the first and second objectives of this study, work described in **Chapter 2** was conducted to investigate the cold acclimation of two Australian wheat varieties with contrasting cold tolerance using targeted metabolomics and lipidomics approaches. The selected cold-sensitive spring wheat variety used in this study was Wyalkatchem and the selected cold-tolerant spring wheat variety was Young. Samples of flag leaves and spikes at the

young microspore stage were collected and analysed in this study. The results obtained provide us with a better understanding of the cold responses of wheat, and pointed out the potential of several sugars, amino acids, amines and glycerolipids to confer cold-tolerance to the Young variety. The outcomes gained from this study have been published in Cheong et al., (2019) for the study on flag leaves, and in Cheong et al., (2020) for the study on spikes. The outcomes also pointed out the profound potential of lipid species as biomarkers that can be explored to distinguish the two varieties. This further motivated us to expand the lipidomics study on the underground part of wheat, the roots (**Chapter 3**). There are limited cold stress studies on the lipidome of whole roots and to the best of our knowledge, no data are available on responses of specific root developmental zones. In **Chapter 3**, the lipid profiles of the spatial root zones derived from young seedlings of Wyalkatchem and Young grown at optimal, chilling and freezing temperatures were investigated. The outcomes indicate the involvement of not only glycerolipids in discriminating Young from Wyalkatchem, but sphingolipids are also involved in conferring cold-tolerance of Young.

Next, to fulfil the third objective of this study, REIL, a protein that has been postulated to act as a potential cold acclimation factor in the mature leaves of *Arabidopsis thaliana,* was evaluated in roots in **Chapter 4**, followed by the evaluation of its potential in wheat in **Chapter 5**. REIL proteins have been postulated to be involved in late ribosomal biogenesis and affect the accumulation of 60S large subunits in the mature leaves of *A. thaliana* upon cold stress. To validate these roles in *A. thaliana*, a systematic analysis of roots grown at optimized and cold temperatures was conducted in **Chapter 4**. The outcomes substantiate the role of REIL proteins as a cold acclimation factor in Arabidopsis by being involved in ribosomal biogenesis during cold acclimation. In **Chapter 5**, three REIL homologs are found to be expressed in wheat. Evaluation of the *REIL* expressions in wheat subjected to cold stress through the re-analyses of published transcriptomics datasets show the potential cold and heat responsiveness of *REILs*. A real-time PCR analysis was then performed to evaluate the *REIL* expressions in Wyalkatchem and Young under cold stress, but no significant changes of expressions were observed in both varieties upon cold stress. It is then yet-to-be-known whether the cold acclimation function of REIL is conserved among dicots (*A. thaliana*) and monocots (wheat). Therefore, more in-depth investigation such as overexpression or silencing of the *REIL* expression in Australian spring wheat varieties is needed.

The last chapter of this thesis (**Chapter 6**) summarizes the key results from each research chapter (**Chapter 2 to 5**) and also discusses the future directions and perspectives.

Declaration

This is to certify that

i. the thesis comprises only my original work, except where indicated in the Preface;

ii. due acknowledgement has been made in the text to all other material used; and

iii. the thesis is fewer than 100 000 words in length, exclusive of tables, maps, bibliographies and appendices.

Signature:

Bo Eng Cheong

School of BioSciences

The University of Melbourne

Parkville, Victoria 3010

Preface

The work presented in this thesis has been conducted primarily by myself with more than 50% of contribution, including experimental work, data processing, data analysis, data interpretation, manuscript writing and drafting of the thesis. My supervisors Prof. Ute Roessner, Dr. William Ho and Dr. Joachim Kopka have been involved in the project planning, the design of experiments and supervision. Some work presented has been generated in collaboration with other researchers as indicated below.

Chapter 2 – The work in this chapter has been performed in collaboration with Dr. Rudy Dolferus from CSIRO Agriculture and Food, Canberra, Australia. The wheat cold stress experiment has been performed by Dr. Dolferus's team using the frost chamber available at CSIRO. The cold-stressed plant materials have then been harvested and sent to us (School of BioSciences, University of Melbourne) for subsequent extractions and targeted metabolomics and lipidomics analyses which have been performed by me. I also have carried out the data processing, data analysis and interpretation with the assistance and guidance provided by Metabolomics Australia (for metabolomics) and Dr. Thusitha Rupasinghe (for lipidomics, School of BioSciences).

Chapter 3 – The seeds of the wheat varieties used in this study have been provided by Dr. Rudy Dolferus. The growing of the wheat seedlings, the cold stress experiment, harvesting of samples and lipid extraction have been performed by me. The lipidomics experiment, data processing, data analysis and interpretation have been performed with the assistance and guidance from Dr. Dingyi Yu (School of BioSciences).

Chapter 4 – All the experimental work and data analyses in this study have been performed by me, with guidance from Dr. Joachim Kopka and Dr. Olga Beine-Golovchuk from the Max-Planck-Institute for Molecular Plant Physiology (Golm, Germany), with two exceptions. The microarray experiment has been performed using the service provided by ATLAS Biolabs GmbH (Berlin, Germany). The proteomics experiment has been performed by Dr. Aleksandra Skirycz and Dr Michal Gorka from MPIMP, Germany.

Chapter 5 – The cold-stressed wheat material used in the qRT-PCR of this study has been provided by Dr. Rudy Dolferus. All other experiments and data analysis have been performed by me.

Acknowledgements

First of all, I would like to thank God the Almighty for showering me with abundance of strengths, courage, wisdoms and good health to walk through the four years of my PhD study. Without these blessings, I know I may not have been able to complete my study successfully.

My deepest and sincerest gratitude goes to Prof. Ute Roessner, my main supervisor who has been so lovely, kind and patience to guide and support me right from the moment I first contacted her to apply for a PhD opportunity until the moment I completed and submitted my thesis. A million "thank you" to you Ute! You will be my role model on how to be a good supervisor for my future students!

I am also extremely grateful to both of my co-supervisors, Dr. William Ho and Dr. Joachim Kopka, who have been so patient and provided me with invaluable guidance and advice throughout this research. I am truly in-debt to you William for always being willing to spend your midnight time to go through my requests and provide your feedback immediately so that my progress did not get delayed. To Joachim, although the time we worked together was only one year at MPIMP, Germany, it was my great honour to work and learn from you.

I would also like to express my great gratitude to Dr. Rudy Dolferus from CSIRO, Canberra. Thank you so much Rudy for leading our collaboration with us to study wheat cold stress and providing me with the varieties and information used in this study. Your kind guidance and support are highly appreciated. How lucky am I to have an additional mentor for my studies in addition to my lovely supervisors!

I would also like to offer my sincere gratitude and appreciation to my beloved colleagues from the Roessner lab – Allene, Berin, Carl, Cheka, Daniel, Dingyi, Federico, Martino, Pipob, Robert, Sneha, Tannaz and Thusi; and from the Kopka lab – Alex, Christopher, Ines, Olga, Didi (from MPIMP) for their kind friendship, cheers, assistance, patience and advice throughout my study. I also thank the team from Metabolomics Australia – Adrian, Himasha, Kim, Niru, Roshan, Siria and Veronica for having provided me with invaluable technical assistance in the execution of my metabolomics experiments.

Finally, I would like to specially thank my mother and sister for the love and moral support during these four years of study. Thank you for calling me every week to remind me to eat well, sleep well, because, without a healthy body, there will be no successful PhD. Also, a big thank you to my beloved husband, Arthur, who has been enormously supportive and unselfishness to support me to pursue my PhD dream. I know my dream would have not come true without your love and support. Thank you!

Publications

Cheong, B.E., Ho, W.W.H., Biddulph, B., Wallace, X., Rathjen, T., Rupasinghe, T.W.T., Roessner, U., & Dolferus, R. (2019). Phenotyping reproductive stage chilling and frost tolerance in wheat using targeted metabolome and lipidome profiling. *Metabolomics* **15:** Article 144. DOI: 10.1007/s11306-019-1606-2.

Cheong, B.E., Onyemaobi, O., Ho, W.W.H., Biddulph, B., Rupasinghe, T.W.T., Roessner, U., & Dolferus, R. (2020). Phenotyping the chilling and freezing responses of young microspore stage wheat spikes using targeted metabolome and lipidome profiling. *Cells* **9:** Article 1309. DOI: 10.3390/cells9051309.

Both of the papers are presented in Chapter 2

Publication-in-progress

Cheong, B.E., Beine-Golovchuk, O., Gorka, M., Ho, W.W.H., Martinez-Seidel, F., Firmino, A.A.P., Skirycz, A., Roessner, U., & Kopka, J. (2020). Arabidopsis REI-LIKE proteins activate ribosome biogenesis during cold acclimation. The preprint has been posted to bioRxiv (https://www.biorxiv.org/) with accession number 954396 and can also be accessed using doi: https://doi.org/10.1101/2020.02.18.954396. The manuscript has been submitted to the journal *Scientific Reports* for consideration of publication.

The manuscript is presented in Chapter 4

Conference Abstracts

[ORAL] Abstract Title: Phenotyping chilling and frost tolerance in reproductive stage wheat tissues using targeted metabolome and lipidome profiling. **Cheong, B. E.,** Ho, W. W. H., Biddulph, B., Wallace, X., Rathjen, T., Rupasinghe, T.W.T., Roessner, U., & Dolferus, Rudy. (2019). The 8th Asian-Oceanian Symposium on Plant Lipids, Canberra, Australia.

[POSTER] Abstract Title: Phenotyping reproductive stage chilling and frost tolerance in wheat using targeted metabolome and lipidome profiling. **Cheong, B. E.,** Ho, W. W. H., Biddulph, B., Wallace, X., Rathjen, T., Rupasinghe, T.W.T., Roessner, U., & Dolferus, Rudy. (2019). Australian Society of Plant Scientists Conference – Bringing Plant Science Together, Melbourne, Australia.

Abbreviations

Abbreviation	Full name
°C	Celsius degree
ABA	Abscisic acid
ASG	Acylated steryl glycoside
BA	Benzoic acid
CA	trans-Cinnamic acid
Cer	Ceramide
CO_2	Carbon dioxide
CL	Cardiolipin
DAG	Diacylglycerol
DGDG	Digalactosyl diacylglycerol
DGMG	Digalactosyl monoacylglycerol
DNA	Deoxyribonucleic acid
FA	Fatty acids
GABA	Gamma-aminobutyric acid
GC	Gas chromatography
GC-MS	Gas chromatography - mass spectrometry
GC-TOF-MS	Gas chromatography -time-of-flight - mass spectrometry
GC-QqQ-MS	Gas chromatography – triple quadruple – mass spectrometry
HexCer	Monohexosyl ceramide
H_2O_2	Hydrogen peroxide
IAA	Indole-3-acetic acid
IBA	Indole-3-butyric acid
ICA	Indole-3-carboxylic acid
JA	Jasmonic acid
JA-ile	Jasmonoyl-isoleucine
LC	Liquid chromatography
LC-HRMS	Liquid chromatography - high resolution - mass spectrometry
LC-MS	Liquid chromatography - mass spectrometry
LC-MS/MS	Liquid chromatography tandem - mass spectrometry

LC-ESI-QqTOF	Liquid chromatography – electrospray ionization- quadrupole time-of-flight – mass spectrometry
LC-QqQ-MS	Liquid chromatography – triple quadruple - mass spectrometry
MGDG	Monogalactosyl diacylglycerol
MGMG	Monogalactosyl monoacylglycerol
OPDA	12-Oxo phytodienoic acid
μm	Micrometre
Mg^{2+}	Magnesium ion (II)
mRNA	Messenger ribonucleic acid
MS	Mass spectrometry
MS/MS	Tandem mass spectrometry
N_2	Nitrogen
Na_2CO_3	Sodium carbonate
NaCl	Sodium chloride
NADPH	Nicotinamide adenine dinucleotide phosphate
NH^{4+}	Ammonium ion
O_2	Oxygen
O^{2-}	Superoxide radical
OH^-	Hydroxyl radical
PA	Phosphatidic acid
PC	Phosphatidylcholine
PCR	Polymerase chain reaction
PE	Phosphatidylethanolamine
PG	Phosphatidylglycerol
PI	Phosphatidylinositol
PIP	Phosphatidylinositol phosphate
PLC	Phospholipase C
PLD	Phospholipase D
PS	Phosphatidylserine
qRT-PCR	Quantitative reverse transcription polymerase chain reaction
REIL	Required for isotropic bud growth1 – like protein
RNA	Ribonucleic acid
ROS	Reactive oxygen species

SA	Salicylic acid
SQDG	Sulfoquinovosyl diacylglycerol
SE	Steryl ester
SG	Steryl glycoside
SQMG	Sulfoquinovosyl monoacylglycerol
ST	Steryl derivative
TAG	Triacylglycerol
TCA	Tricarboxylic acid
w/v	weight/volume percentage
v/v	volume/volume percentage
YM	Young microspore

Table of Contents

Abstract ..... **.i**
Declaration ..... **.iii**
Preface ..... **.iv**
Acknowledgements ..... **.v**
Publications ..... **.vi**
Conference Abstracts ..... **.vii**
Abbreviations ..... **.viii**
Table of Contents ..... **..xi**
List of Figures ..... **..xviii**
List of Tables ..... **xxii**
List of Supplemental Figures ..... **xxiii**
List of Supplemental Table ..... **...xxv**
List of Supplemental Data ..... **...xxviii**

Chapter 1 ..... **1**
Literature Review **1**
1.1 Cold Stress in Plants: The Physiological and Metabolic Responses **2**
1.1.1 Cold Stress in *Arabidopsis thaliana*: The Physiological and Metabolic Responses **3**
1.1.2 Cold Stress in Wheat (*Triticum aestivum*): The Physiological and Metabolic Response **5**
1.1.3 Wheat and Frost Events in Australia: The Dilemma of Australian Farmers **9**

1.2 Plant Strategies to Sustain in Suboptimal or Cold Temperature **13**
1.2.1 Strategy 1: Activation of Transcription Factors and Stress-responsive Genes **14**
1.2.2 Strategy 2: Remodeling of Plasma and Subcellular Membranes **16**
1.2.3 Strategy 3: Acceleration of Osmolytes Biosynthesis during Cold Stress **21**
1.2.4 Strategy 4: Synthesis of Stress-Induced Phytohormones **22**

1.3 Metabolomics and Lipidomics for the Understanding of Cold Stress in Plants **22**
1.3.1 Metabolomics and Lipidomics as Promising Tools to Understand Cold Stress Response in Australian Wheat and Breeding of Cold-tolerant Cultivars **26**

1.4 Engineering of Cold-induced Transcription Factors to Increase the Cold Tolerance in Plants **27**

1.5 REIL Protein as a New Potential Cold Acclimation Factor in *Arabidopsis thaliana* and Wheat **29**

1.6 Aims of this Thesis **39**

Chapter 2 ..... **42**
Metabolomics and Lipidomics Studies of Cold-Tolerant and Cold-Sensitive Wheat Varieties from Australia **42**

Preface to Chapter 2 ..... **43**

Part I..... **43**

2.1 Abstract..... **46**

2.2 Introduction..... **47**

2.3 Materials and Methods..... **49**
2.3.1 Controlled Environment for Wheat Growing, Cold Treatment and Sample Collection..... **49**
2.3.2 Analysis of Sugars, Organic Acids, Amino Acids, Amines and Phytohormones..... **50**
2.3.3 Analysis of Lipid Content..... **53**
2.3.4 Data Processing and Statistical Analysis of Metabolite Data..... **54**

2.4 Results..... **55**
2.4.1 Establishment of A Controlled Environment Assay for Chilling Tolerance..... **55**
2.4.2 Four-day Chilling Treatment Induces Significant Changes in Metabolites and Lipids in Young and Wyalkatchem..... **56**
2.4.3 A Four-Day Chilling Time Course Reveals Significant Differences in Cold Acclimation in Wyalkatchem and Young Flag Leaves..... **57**
2.4.4 Young and Wyalkatchem Show Significant Varietal Differences in Cold Acclimation across Time Points..... **59**
2.4.5 Quantitative Changes in Two Groups of Lipids May Account for Differences in Membrane Fluidity and Cold Tolerance between Young and Wyalkatchem..... **63**

2.5 Discussion..... **67**
2.5.1 Wheat Chilling and Frost Tolerance: Field vs. Controlled Environment Phenotyping..... **67**
2.5.2 Metabolomics as Alternative Phenotyping Tool for Chilling and Frost Tolerance in Wheat..... **68**
2.5.3 Effect of Prolonged/Consecutive Chilling Treatments on Wheat Flag Leaf Metabolites and Lipids..... **69**

2.6 Conclusion..... **72**

2.7 Acknowledgements..... **73**

2.8 Author Contributions..... **73**

2.9 Funding..... **73**

2.10 **Part II**..... **74**

2.10.1 Abstract..... **76**

2.10.2 Introduction..... **77**

2.10.3 Materials and Methods…….... **79**
2.10.3.1 Controlled for Environment Wheat Growth, Cold Treatment and Tissue Sampling……..…. **79**
2.10.3.2 Analysis of Sugars, Organic Acids, Amino Acids and Amines…...… **80**
2.10.3.3 Analysis of Lipids……..... **82**
2.10.3.4 Processing of Raw Data……...… **83**
2.10.3.5 Statistical Analysis of Metabolite and Lipid Data……...… **83**

2.10.4 Results…… **84**
2.10.4.1 Metabolite and Lipid Profiling Using YM Stage Wheat Spikes…….. **84**
2.10.4.2 Cold Treatment Affects Spike Metabolites in Wyalkatchem More Than Young Spikes…….. **86**
2.10.4.3 Varietal Differences in Metabolite and Lipid Levels Before and After Cold Treatment……..…. **88**
2.10.4.4 Differences in Primary Metabolite Levels between Spikes and Flag Leaves of Wyalkatchem and Young……...……. **93**
2.10.4.5 Differences in Metabolite and Lipid Levels between Spikes and Flag Leaves of Wyalkatchem and Young……...……. **96**

2.10.5 Discussion…… **96**
2.10.5.1 Are Wheat Spikes or Flag Leaves Better for Cold Tolerance Phenotyping?..... **96**
2.10.5.2 Spikes of Cold-Tolerant Young Are Potentially Better Prepared for Low Temperature Stress…… **99**
2.10.5.3 Lipid Remodeling is Critical for Cold Acclimation in Wheat Spikes……... **100**

2.10.6 Conclusion……..…... **103**

2.10.7 Author Contributions……. **104**

2.10.8 Funding……..... **104**

2.10.9 Acknowledgements……...…… **104**

2.10.10 Conflicts of Interest……..…… **105**

2.10.11 Supplemental Figures……..... **105**

Chapter 3..... **112**
The Effect of Cold Stress onto the Tissue-Specific Root Lipidome of Two Wheat Varieties with Contrasting Cold Tolerance…….……... **112**

Preface to Chapter 3…… **113**

3.1 Introduction……... **114**

3.2 Materials and Methods **115**
3.2.1 Chemicals and Reagents **115**
3.2.2 Lipid Nomenclature, Notation and Abbreviations **117**
3.2.3 Plant Material and Growth Conditions **118**
3.2.4 Stress Treatment and Harvest of Root Samples **118**
3.2.5 Lipid Extraction **119**
3.2.6 LC-ESI-MS/MS Analysis **120**
3.2.7 Data Processing **120**
3.2.8 Statistical Analysis **120**

3.3 Results **121**
3.3.1 Targeted Profiling Using Scheduled Parallel Reaction Monitoring Assays Enables the Profiling of the Complex Lipidome in Different Wheat Root Developmental Zones **121**
3.3.2 Comparisons of Lipid Profiles of the Developmental Root Zones in Each Wheat Variety at the Unstressed Stage **122**

3.3.3 Comparisons of Lipid Profiles of the Developmental Root Zones in Each of the Wheat Variety Subjected to Chilling and Freezing Stresses **125**
3.3.4 Varietal Difference: Lipid Profiles of the Developmental Root Zones of Young and Wyalkatchem under Control, Chilling and Freezing Conditions **139**

3.4 Discussion **143**
3.4.1 Lipid Composition at The Unstressed Stage Reveal Differences among The Three Developmental Root Zones in Each Wheat Variety **143**
3.4.2 Cold Stress Mainly Alters the Glycerolipid and Sphingolipid Composition of the Root Zones, which Also Reveals the Main Differences between the Cold-Sensitive and Cold-Tolerant Varieties **146**

3.5 Conclusion **150**

3.6 Supplemental Figures **150**

Chapter 4 ..... **154**
Systemic Analysis of REIL Protein Function in Cold Acclimated *Arabidopsis thaliana* Roots **154**

Preface to Chapter 4 ..... **155**

4.1 Abstract **157**

4.2 Introduction **158**

4.3 Materials and Methods **160**
4.3.1 Plant Materials **160**
4.3.2 Photographic Documentation **161**
4.3.3 Hydroponic System for Growth, Controlled Temperature Shift and Sampling of Arabidopsis Root Materials **161**

4.3.4 Temperature Shift Experiments and Root Harvests **162**
4.3.5 Sucrose Density Gradient Analysis of Ribosome Preparations from Arabidopsis Root Tissue **162**
4.3.6 KCl-Sensitivity Test of Ribosome Complexes **164**
4.3.7 Transcriptome Analysis **164**
4.3.8 Functional Enrichment Analyses of Gene Expression Data **165**
4.3.9 Proteome Analysis of Ribosome Preparations from Arabidopsis Root Tissue **165**
4.3.10 Association Analysis of Changes in Transcript and Relative Protein Abundance..... **167**
4.3.11 Statistical Analyses and Data Visualizations..... **168**

4.4 Results..... **168**
4.4.1 Hydroponic Growth of *reil* Mutant Plants Compared to the Arabidopsis Col-0 Wild Type **168**
4.4.2 Analyses of Ribosome Complex Abundances from Roots Confirms Association of REIL Deficiency with Delayed 60S LSU Accumulation After Cold Shift..... **169**
4.4.3 Changes of Ribosome Complex Abundances Reveal Inter-Complex Correlations and Compensation Responses to REIL Deficiency..... **172**
4.4.4 REIL Deficiency Deregulates Transcriptional Temperature Acclimation Responses in Roots..... **176**
4.4.5 REIL Deficiency Affects Transcription of Root Morphogenesis Genes and Activates Expression of Cytosolic Ribosome and Translation Related Genes..... **177**
4.4.6 Constitutive Transcriptional Compensation Responses to REIL Deficiency Indicate Interaction of Cytosolic Ribosome Maturation with Nucleolar rRNA Biogenesis and Translation Initiation..... **181**
4.4.7 Proteome Analysis of Ribosome Preparations from Arabidopsis Root Tissue..... **185**
4.4.8 60S RPs and RP Paralogs Differentially Accumulate in Non-Translating 60S Fractions of *reil* Double Mutants..... **187**
4.4.9 Homologs of Yeast 66S Pre-Ribosome Constituents and 60S Biogenesis Factors Accumulate in Non-Translating 60S Fractions of *reil* Double Mutants..... **189**
4.4.10 40S RPs and Eukaryotic Translation Initiation Factors Differentially Accumulate In Non-Translating 40S Fractions of *reil* Double Mutants..... **191**
4.4.11 Association of Differential Accumulation of RPs and RAPs in Non-Translating 40S and 60S Fractions of *reil* Double Mutants with Differential Gene Expression..... **192**

4.5 Discussion..... **193**
4.5.1 The Mixotrophic *in vitro* Cultivation System: Requirements and Biases..... **193**
4.5.2 REIL Deficiency Reveals Requirement for *de novo* Synthesis of Eukaryote Ribosomes After Cold Shift..... **195**
4.5.3 Effects of REIL Deficiency on Translation Initiation..... **197**
4.5.4 Effects of REIL Deficiency On Ribosome Biogenesis..... **198**
4.5.5 REIL Deficiency Affects the RP Paralog Composition of Non-Translating 40S SSU and 60S LSU Fractions..... **200**

4.6 Conclusion **162**

4.7 Supplemental Figures..... **202**

Chapter 5 ..... **211**
Evaluation of REIL as Potential Cold Acclimation Factor in Wheat **211**

Preface to Chapter 5..... **212**

5.1 Introduction **213**

5.2 Materials and Methods **214**
5.2.1 Analysis of the Topology of Wheat (cv. Chinese Spring) *REIL* Gene Sequences Retrieved from Ensembl Plants..... **214**
5.2.2 Evaluation of *REIL* Expression in Wheat Subjected to Cold, Drought Heat Stress using Published Transcriptomics Data from Li et al. (2015) Liu et al. (2015)..... **214**
5.2.2.1 Reprocessing of Reads and Re-mapping to the Latest Wheat Genome Released by International Wheat Genome Sequencing Consortium (IWGSC)..... **214**
5.2.2.2 Differential Gene Expression (DGE) Analysis of *REIL*s in Wheat Subjected to Cold, Drought and Heat Stress..... **215**
5.2.3 Evaluation of *REIL* Expression in Wheat Subjected to Cold Stress Using Quantitative Real Time Polymerase Chain Reaction (PCR)..... **215**
5.2.3.1 Controlled Environment for Wheat Growing, Cold Treatment and Sample Collection..... **215**
5.2.3.2 Extraction of Total RNA..... **216**
5.2.3.3 Reverse Transcription of Total RNA to Synthesize First Strand cDNA..... **217**
5.2.3.4 Quantitative Real Time PCR Analysis..... **218**
5.2.4 Phylogenetic Analysis of REIL Proteins in Wheat and *Arabidopsis thaliana*..... **218**

5.3 Results **219**
5.3.1 Analysis of the Topology of Wheat (cv. Chinese Spring) *REIL* Gene Sequences Retrieved from Ensembl Plants..... **219**
5.3.2 Evaluation of *REIL* Expression in Wheat Subjected to Cold, Drought Heat Stress Using Published Transcriptomics Data from et al. (2015) and Liu et al. (2015)..... **220**
5.3.3 Evaluation of *REIL* Expression in Wheat Subjected to Cold Stress Using Quantitative Real Time Polymerase Chain Reaction (qRT-PCR)..... **220**
5.3.4 Phylogenetic Analysis of REIL Proteins in Wheat and *Arabidopsis thaliana*..... **221**

5.4 Discussion **224**

5.5 Conclusion **226**

5.6 Supplemental Information **226**

Chapter 6 Conclusions and Future Directions **227**

6.1 Summary of Key Results from this Research and Future Directions…….. **229**

6.2 Concluding Remarks…… **236**

References **238**

Appendices…… **277**
A) Supplemental Data and Tables for Chapter 2, Part I…….. **278**
A) Supplemental Data and Tables for Chapter 2, Part II…….. **294**
B) Supplemental Data and Tables for Chapter 3…….. **302**
C) Supplemental Data and Tables for Chapter 4…….. **312**
D) Supplemental Data and Tables for Chapter 5…….. **314**
Publication (Cheong et al., 2019)…… **330**
Publication (Cheong et al., 2020)…… **349**

List of Figures

Figure 1-1: Life cycle of *Arabidopsis thaliana*. (A) *A. thaliana* of the accession Columbia (Col) at different stages of its life cycle, from seed (bottom left) to seedling (11 days), to vegetative growth (39 days), and to reproductive growth (45 days)……..……..**4**

Figure 1-2: A wheat plant and genome……...…….**7**

Figure 1-3: Wheat sowing and harvesting time, and the major production regions in Australia……..**10**

Figure 1-4: Susceptibility of wheat to frost during the development cycle……...…**11**

Figure 1-5: How frost is formed, heat is captured in the soil during the day and radiates out during the night into the canopy…….**12**

Figure 1-6: Western Australia (WA) experienced the worst frost damage in year 2016 and 2018…….**13**

Figure 1-7: Overview of common tolerance mechanisms triggered by plants in responses to cold stress……...….**14**

Figure 1-8: Schematic representation of the cold response in plant cells……..…**17**

Figure 1-9: Model of the Arabidopsis CBF cold acclimation pathway……...……..**18**

Figure 1-10: A plant cell with its plasma and subcellular membrane……....**19**

Figure 1-11: Examples of some common glycerophospholipids and glycolipids found in plants……...……**21**

Figure 1-12: Eukaryotic ribosome biogenesis and translation initiation……...…**32**

Figure 1-13. Topology and phylogenetic analysis of *Arabidopsis thaliana REIL* genes and plant REIL proteins…….**33**

Figure 1-14. The aberrant leaf phenotypes of the *reil1-1 reil2-1* double mutant and of the *reil2-1* single mutant……**36**

Figure 1-15. Developmental phenotypes of the Arabidopsis wild type (Col-0) and *reil1-1 reil2-1* mutant under standard and different suboptimal temperature regimes...……**37**

Figure 1-16: Relative abundance of rRNAs within total RNA preparations and of 60S and 50S large ribosomal subunits from total ribosome preparations before and after the shift to 10°C……**38**

Figure I-2-1: Log_2-fold changes of primary metabolites in the flag leaves of the cold-sensitive Wyalkatchem (W) and cold-tolerant Young (Y) after one night (TP_1 vs. TP_0) and prolonged (TP_3 vs. TP_1) of cold treatment……...**60**

Figure I-2-2: Log_2-fold changes of phospholipids in the flag leaves of the cold-sensitive Wyalkatchem (W) and cold-tolerant Young (Y) after one night (TP_1 vs. TP_0) and prolonged (TP_3 vs. TP_1) of cold treatment……...**61**

Figure I-2-3: Log_2-fold changes of primary metabolites in the flag leaves of cold-tolerant Young (Y) compared to the cold-sensitive Wyalkatchem (W) at each time point……**64**

Figure I-2-4: Log_2-fold changes of phospholipids in the flag leaves of the cold-tolerant Young (Y) compared to the sensitive Wyalkatchem (W) at each time point……**65**

Figure I-2-5: Unsaturation to saturation ratio in Wyalkatchem and Young across the four-day of cold treatment……...…..**66**

Figure II-2-1: Schematic diagram showing the controlled environment design of the cold treatments and lighting conditions (see Materials & Methods section). Yellow bars show day-light conditions, dark bars dark conditions. Arrows labelled TPx indicate where samples were harvested from wheat plants……...**85**

Figure II-2-2: Pairwise comparisons of normalized and log_2-transformed primary metabolites and lipids in the spikes of cold-sensitive Wyalkatchem and cold-tolerant Young after one night (TP_1 vs. TP_0) and prolonged (TP_3 vs. TP_1) of cold treatment……**87**

Figure II-2-3: Log_2-fold changes of primary metabolites in spikes of cold-tolerant Young (Y) compared to cold-sensitive Wyalkatchem (W) at each time point……**90**

Figure II-2-4: Log_2-fold changes of lipids in the spikes of cold-tolerant Young (Y) compared to cold-sensitive Wyalkatchem (W) at each time point……..**91**

Figure II-2-5: Comparison of unsaturated to saturated lipid ratio between Wyalkatchem and Young, and in each variety across the time points……..**92**

Figure II-2-6: Comparison of primary metabolites involved in glycolysis and the tricarboxylic acid (TCA) cycle, the two main energy-providing pathways of the cell……**94**

Figure II-2-7: Comparison of amino acid and amine levels (in concentration unit picomole/mg of fresh weight and log_2-transformed), as well as their relationship to the main energy providing pathways (glycolysis and TCA cycle)……....**95**

Figure II-2-8: Differences in differentially expressed lipid species between flag leaves and spikes of cold-tolerant Young and cold-sensitive Wyalkatchem……....**97**

Figure 3-1: The three root zones analysed in this study. DZ = root cap and division zone, EZ = elongation zone, MZ = maturation zone……...**119**

Figure 3-2: The distribution of individual lipids within the 21 lipid classes (in % based on total lipid abundance set to 100%) in each specific root zone of cold-sensitive Wyalkatchem and cold-tolerant Young at the unstressed stage……..**125**

Figure 3-3: The distribution of the 21 lipid classes (in %) in each specific root zone of cold-sensitive Wyalkatchem and cold-tolerant Young at the unstressed stage and after subjected to chilling (4°C) and freezing (-3°C) stress……..**128**

Figure 3-4: Log_2-fold changes of DAG, Cer and HexCer species in the division zone (DZ) of the cold-sensitive Wyalkatchem and cold-tolerant Young after exposed to (A) chilling and (B) freezing stresses……....**130**

Figure 3-5: Log_2-fold changes of PC, PE and PG species in the division zone (DZ) of the cold-sensitive Wyalkatchem and cold-tolerant Young after exposed to (A) chilling and (B) freezing stresses……..**131**

Figure 3-6: Log_2-fold changes of DAG, Cer and HexCer species in the elongation zone (EZ) of the cold-sensitive Wyalkatchem and cold-tolerant Young after exposed to (A) chilling and (B) freezing stresses……..**134**

Figure 3-7: Log_2-fold changes of PC, PE and PG species in the elongation zone (EZ) of the cold-sensitive Wyalkatchem and cold-tolerant Young after exposed to (A) chilling and (B) freezing stresses……....**135**

Figure 3-8: Log_2-fold changes of DAG, Cer and HexCer species in the maturation zone (MZ) of the cold-sensitive Wyalkatchem and cold-tolerant Young after exposed to (A) chilling and (B) freezing stresses……..**137**

Figure 3-9: Log_2-fold changes of PC, PE and PG species in the maturation zone (MZ) of the cold-sensitive Wyalkatchem and cold-tolerant Young after exposed to (A) chilling and (B) freezing stresses……**138**

Figure 3-10: Examples of (A) glycerophospholipid and (B) sphingolipids analysed in this study……..**145**

Figure 4-1: Sucrose density gradient analyses of ribosome complexes from equal fresh weight amounts of hydroponically grown total root material before (0 day) and at 1, 3, 7, or 21 days after shift from 20°C (day)/ 18°C (night) to 10°C (day) and 8°C (night)…….**172**

Figure 4-2: Relative quantification of abundances of ribosome complexes from non-acclimated (0 day) and 10°C cold acclimating *reil* mutants at 1, 3, 7, or 21 days after shift (cf. Fig. 4-1)…….**173**

Figure 4-3: Correlation analyses of log_2-transformed ratios of ribosome complex abundances comparing the cold induced changes of abundances relative to wild type of the 40S SSU (A) and of the 80S monosome fractions (B) to the changes of the 60S LSU fraction across all *reil* mutants (cf. Fig. 4-2)…….....**174**

Figure 4-4: *In vitro* KCl-sensitivity test of monosomes and polysomes that were prepared from roots sampled at 21 days after start of 10°C cold-acclimation…….**175**

Figure 4-5: Functional enrichment and transcript correlation analyses of differential gene expression in the roots of Col-0, and *the reil1-1 reil2-1* and *reil1-1 reil2-2* double mutants at the non-acclimated state (0 day, 20°C) and shifted to 10°C cold for 1 day or 1 week. Differential gene expression was determined relative to non-acclimated Col-0 at optimized temperature 20°C……..**179**

Figure 4-6: Functional enrichment analyses of differential gene expression in roots of Col-0, and the *reil1-1 reil2-1* and *reil1-1 reil2-2* double mutants at the non-acclimated state (0 day, 20°C) and shifted to 10°C cold for 1 day or 1 week. Differential gene expression was determined relative to non-acclimated Col-0 at optimized temperature 20°C……..**180**

Figure 4-7: Differential expression of cytosolic and plastid ribosome genes in *reil1-1 reil2-1* and *reil1-1 reil2-2* double mutant roots at the non-acclimated state (0 day, 20°C) and shifted to 10°C cold for 1 day or 7 days……...**182**

Figure 4-8: Differential expression of six genes that accumulate constitutively in *reil1-1 reil2-1* and *reil1-1 reil2-2* double mutant roots (means +/- standard error, n = 3)……...**184**

Figure 4-9: Changes of RP composition in the non-translating 60S LSU and 40S SSU fractions of the *reil1 reil2* double mutants 7 days after shift to 10°C and prior to cold shift at 20°C….**188**

Figure 4-10: Changes of the composition of ribosome associated proteins in the non-translating 60S fractions of the *reil1 reil2* double mutants 7 days after shift to 10°C and prior to cold shift at 20°C……..**190**

Figure 4-11: Changes of the composition of translation initiation factor 3 proteins in the non-translating 40S fraction of the *reil1 reil2* double mutants 7 days after shift to 10°C and prior to cold shift at 20°C……..….**192**

Figure 5-1: Graphic representation for the experimental design and cold treatment of Wyalkatchem and Young in controlled environment. The cold treatment was set for consecutive of two days, instead of four days like have been described in Chapter 2…….**217**

Figure 5-2: The Genomic Sequence Topology of the REIL Proteins from *Triticum aestivum* (wheat, Chinese Spring variety)……...….**221**

Figure 5-3: The relative expression of *REIL7A, REIL7B* and *REIL7D* to Ubiquitin genes in the flag leaves of Wyalkatchem and Young before and after cold treatment……..……...**223**

Figure 5-4: Molecular phylogenetic analysis of *Arabidopsis thaliana* and wheat REIL proteins by Maximum Likelihood method…….**224**

List of Tables

Table I-2-1: Metabolites and lipids that changed significantly over the four-day of cold stress in the flag leaves of cold-sensitive Wyalkatchem (W) and cold-tolerant Young (Y), analyzed by One-way ANOVA with FDR-adjusted $p < 0.05$ as significance, followed by Tukey Test……..**58**

Table 3-1: Summary of the detected and measured 21 classes of lipids and the number of lipid species per class in the root developmental zones……....**123**

Table 3-2: Varietal Differences of the Lipid Profiles of Three Developmental Root Zones Under Control, Chilling and Freezing Conditions……**142**

Table 5-1: Reaction mixture recipe for each sample……...……**217**

Table 5-2: Reaction mixture and primer mixture recipes for each sample……...…...**218**

Table 5-3: Differential gene expression (DGE) analysis of *REIL* genes in wheat variety TAM107 subjected to subjected to heat, drought or combination of the two stress; and in wheat variety Manitou subjected to cold stress……...**222**

Table 5-4: Expression changes (in fold-change) of *REIL* genes in the flag leaves of Wyalkatchem and Young in response to cold stress. Statistical significant differences ($p < 0.05$) between the control and cold-treated samples were analyzed by using Student's *t*-test…….**223**

List of Supplemental Figures

Fig. I-S2-1: Schematic of the controlled environment chilling tolerance assay……..**106**

Fig. I-S2-2: Log_2-fold changes of primary metabolite recoveries in the flag leaves of the cold-sensitive Wyalkatchem (W) and cold-tolerant Young (Y) after one night (TP_2 vs TP_1) and prolonged (TP_4 vs TP_3) of cold treatment…….....**107**

Fig. I-S2-3: Log_2-fold changes of phospholipid recoveries in the flag leaves of the cold-sensitive Wyalkatchem (W) and cold-tolerant Young (Y) after one night (TP_2 vs TP_1) and prolonged (TP_4 vs TP_3) of cold treatment…….……**108**

Fig. II-S2-1: Log_2-fold changes of primary metabolite concentrations in the spikes of cold-sensitive Wyalkatchem (W) and cold-tolerant Young (Y)……...……**109**

Fig. II-S2-2: Log_2-fold changes of lipid concentrations in the spikes of the cold-sensitive Wyalkatchem (W) and cold-tolerant Young (Y)……..……**110**

Fig. II-S2-3: Differences in differentially expressed primary metabolites between flag leaves and spikes of cold-tolerant Young and cold-sensitive Wyalkatchem……...**111**

Fig. S3-1: Plant materials and growth conditions for the two wheat varieties used in this study……..…**151**

Fig. S3-2: Varietal differences of glycerophospholipids and galactosyl glycerolipids of the three developmental root zones at the control and after cold stress conditions……**152**

Fig. S3-3: Varietal differences of sterols, diacylglycerols (DAG) and sphingolipids (Cer and HexCer) of the three developmental root zones at the control and after cold stress conditions……..…**153**

Fig. S4-1: Hydroponic growth system of *Arabidopsis thaliana* Col-0 wild type and mutants. The system was feasible for temperature shift experiments in the vegetative phase and for rapid sampling of pooled material of whole root or shoot systems.……...……...…**202**

Fig. S4-2: Exemplary documentation of shoot systems of hydroponically cultivated *Arabidopsis thaliana* wild type (Col-0), of the single mutants, *reil1-1*, *reil2-1*, *reil2-2*, and of the double mutants, *reil1-1 reil2-1* (DKO1) and *reil1-1 reil2-2* (DKO2), before (0 day) and 7 or 21 days after shift from 20°C (day)/ 18°C (night) to 10°C (day) and 8°C (night)……...….**203**

Fig. S4-3: Exemplary documentation of hydroponic root systems of *Arabidopsis thaliana* wild type (Col-0), of the single mutants, *reil1-1*, *reil2-1*, *reil2-2*, and of the double mutants, *reil1-1 reil2-1* (DKO1) and *reil1-1 reil2-2* (DKO2), before (0 day) and 7 or 21 days after shift from 20°C (day)/ 18°C (night) to 10°C (day) and 8°C (night)……..**204**

Fig. S4-4: Differential expression of selected cold responsive genes in the roots of Col-0, and the *reil1-1 reil2-1* and *reil1-1 reil2-2* double mutants at the non-acclimated state (0 day, 20°C)

and shifted to 10°C cold for 1 day or 7 days……**205**

Fig. S4-5: Reduced transcript levels of the *reil 1* and *reil2* genes in the *reil1-1 reil2-1* and *reil1-1 reil2-2* double mutants……..……**206**

Fig. S4-6: Functional enrichment analyses of differential gene expression in the roots of Col-0, and the *reil1-1 reil2-1* and *reil1-1 reil2-2* double mutants at the non-acclimated state (0 day, 20°C) and shifted to 10°C cold for 1 day or 7 days……..…**207**
…
Fig. S4-7: Proteomic characterization of ribosome preparations obtained from root material by sucrose density gradient fractionation experiments DS1 and DS2, i.e. the root subset of Pride repository data set PXD016292……**208**

Fig. S4-8: Distribution analysis of RPP2D (A), RPP0B (B), RPL3A (C), and RPL3B (D) across the sampled ribosome fractions and analyzed conditions, DS1 orange, DS2 blue……**209**

Fig. S4-9: Association analysis of changes in root transcript abundance and relative protein abundance in non-translating 40S and 60S (60S/80S) fractions of *reil1 reil2* mutants compared to *Arabidopsis thaliana* Col-0 wild type…….……..**210**

List of Supplemental Tables

Table I-S2-1: The Multiple Reaction Monitorings (MRMs) established for the authentic sugars, organic acids, amino acids/amines and phytohormones used for identification and quantification in this study.....…….……**285**

Table I-S2-2: The Multiple Reaction Monitorings (MRMs) established for the five external authentic lipids, and 70 phospholipids used for identification in this study…….**289**

Table I-S2-3: Concentrations for the measured metabolites (sugars, organic acids, aminoacids/amines and phytohormones) in the Wyalkatchem's and Young's flag leaves across all the time points……..…**293**

Table I-S2-4: Lipid responses for the measured phospholipids in the Wyalkatchem's and Young's flag leaves across all the time points……..**293**

Table I-S2-5: Fold changes ± sem for the pair-wise comparisons of metabolites in Young and Wyalkatchem……**293**

Table I-S2-6: Fold changes ± sem for the pair-wise comparisons of phospholipids in Young and Wyalkatchem……..**293**

Table I-S2-7: Multiple comparisons of metabolites in Wyalkatchem, Young, Wyalkatchem vs. Young across all the time points by using One-Way ANOVA, with FDR-adjusted $p < 0.05$ as significance……...**293**

Table I-S2-8: Multiple comparisons of phospholipids in Wyalkatchem, Young, Wyalkatchem vs. Young across all the time points by using One-Way ANOVA, with FDR-adjusted $p < 0.05$ as significance……...**293**

Table I-S2-9: Tukey test for metabolites that significantly changed in Wyalkatchem, Young, Wyalkatchem *vs.* Young……...**293**

Table I-S2-10: Tukey test for phospholipids that significantly changed in Wyalkatchem, Young, Wyalkatchem *vs.* Young……..**293**

Table I-S2-11: The unsaturation to saturation ratio in Wyalkatchem and Young……...**293**

Table I-S2-12: Group of 11 lipids that consistently higher in Wyalkatchem compared to Young……**293**

Table I-S2-13: Group of 18 lipids that consistently higher in Young compared to Wyalkatchem……**293**

Table II-S2-1: Multiple Reaction Monitoring (MRMs) established for authentic sugars, organic acids, amino acids and amines used for identification and quantification of these compounds in this study…….....……...**294**

Table II-S2-2: Multiple Reaction Monitoring (MRMs) established for the seven external authentic lipids, and 95 phospholipids used for identification of these compounds in this study……..**297**

Table II-S2-3: Concentrations of primary metabolites (sugars, organic acids, amino acids and amines) measured in Wyalkatchem and Young spikes across all time points……..…**300**

Table II-S2-4: Normalized lipid responses for the measured lipids in the Wyalkatchem and Young spikes across all the time points……**300**

Table II-S2-5: Fold changes ± sem for the pair-wise comparisons of metabolites in Young and Wyalkatchem spikes…….**300**

Table II-S2-6: Fold changes ± sem for the pair-wise comparisons of lipids in Young and Wyalkatchem spikes. ……..……..**300**

Table II-S2-7: Multiple comparisons of primary metabolites in Wyalkatchem, Young, Wyalkatchem vs. Young across all time points using One-Way ANOVA (with FDR-adjusted $p<0.05$), followed by Tukey test to determine which specific two groups are significantly different…….**301**

Table II-S2-8: Multiple comparisons of phospholipids in Wyalkatchem, Young, Wyalkatchem vs. Young across all time points using One-Way ANOVA (with FDR-adjusted $p<0.05$), followed by Tukey test to determine which specific two groups are significantly different…**301**

Table II-S2-9: Changes in the unsaturated to saturated lipid ratio in Wyalkatchem and Young during the time-course experiment…….……..**301**

Table II-S2-10: One-Way ANOVA analysis and Tukey test for comparison of primary metabolite levels between flag leaves and spikes in Wyalkatchem and Young……...**301**

Table S3-1: Fold-changes of total 273 lipid species in the three developmental root zones of cold-sensitive Wyalkatchem and cold-tolerant Young at the unstressed stage (control 21°C), after subjected to chilling (4°C) and freezing (-3°C) stress……..**302**

Table S4-1: Abundance analysis of ribosome complexes (40S SSU, 60S LSU, 80S monosomes and polysomes) from roots of single-paralog *reil* mutants (*reil1-1*, *reil2-1*, *reil2-2*) and double mutants (*reil1-1 reil2-1* and *reil1-1 reil2-2*) compared to wild type Col-0 at non-acclimated (20°C, 0 day) and cold-acclimating states (10°C, 1 day, 3 days, 7 days, and 21 days)……**312**

Table S4-2: Gene expression profiles and statistical data analyses of roots from the non-acclimated and 10°C cold acclimating *reil1-1 reil2-1* and *reil1-1 reil2-2* mutants compared to Col-0 wild type……..**312**

Table S4-3: Functional enrichment analysis of differential gene expression in non-acclimated (0 day) and cold-acclimating roots of *Arabidopsis thaliana* Col-0 and the *reil1-1 reil2-1* and *reil1-1 reil2-2* mutants at 1 day or 7 days after shift to 10°C cold……...**312**

Table S4-4: Proteomic characterization of ribosome preparations obtained from root material by sucrose density gradient fractionation experiments DS1 and DS2 (Selection of analyzed samples from Pride repository data set PXD016292)……...**313**

Table S4-5: Fold changes (FC) of total RP abundances in the proteomic analyses of roots from the *reil1 reil2* double mutants compared to Col-0 wild type at 20°C and 7 days after shift to 10° C cold……**313**

Table S4-6: List and specificity analysis of detected cytosolic RPs and ribosome associated proteins…….…….**313**

Table S4-7: Differential accumulation of cytosolic RPs and RP associated proteins (RAPs) in non-translating ribosome fractions of the *reil1-1 reil2-1* (DS2) and *reil1-1 reil2-2* (DS1) mutants relative to *Arabidopsis thaliana* Col-0 wild type……**313**

Table S5-1: Primers used in this study…….**328**
.
Table S5-2: Relative expression of *REIL* compared to Ubiquitin in each of the wheat variety……....**328**

List of Supplemental Data

Data I-S2-1: Methodology for Phytohormone Analysis…….....……**278**

Data S5-1: The coding sequences of *Arabidopsis thaliana REIL1* and *REIL2*……**314**

Data S5-2: REIL amino acid sequences used for phylogenetic tree construction……...……**315**

Data S5-3: Multiple sequence alignments and phylogenetic analysis of REIL proteins in *Arabidopsis thaliana* and different wheat varieties…….……**320**

CHAPTER 1

Literature Review

1.1 Cold Stress in Plants: The Physiological and Metabolic Responses

Every plant species has a specific range of optimal temperatures, at which they exhibit maximal growth rate and development. Changes such as physiological, biochemical, metabolic and molecular fluctuation occur when ambient temperature deviates from the optimal (Guy et al., 2008). Low temperatures (cold and frost) represent a severe threat to plant survival and economic crop productivity in many regions (Kosova et al., 2012). Different plant species vary in their degree of adaptation to low temperatures. Tropical and subtropical plants are sensitive to chilling conditions (20°C) and cannot survive frost events (< 0°C). For example, rice grown in temperate climate zones will experience substantial yield losses due to cold spells during flowering (< 17°C) which causes pollen sterility (Hayase et al., 1969; Satake et al., 1969; Nishiyama, 1984; Oliver et al., 2005). Tomato, like many horticultural crops, originated from sub-tropical areas. Below 12°C almost no growth is expected for tomato. Chilling injury occurs when tomato plants are exposed to these temperatures for a long period of time (Criddle et al., 1997). Temperate climate zone plants are generally more tolerant to chilling conditions but show various degrees of frost tolerance. For example, wheat can tolerate severe frosts during vegetative growth, but is frost-sensitive during flowering in early spring. Chilling conditions during the flowering stage also cause pollen sterility in wheat (Demotes-Mainard et al., 1996; Rerkasem, 1996; Subedi et al., 1998a&b; Subedi et al., 2000; Chakrabarti et al., 2011).

Plants usually start to experience cold stress at the temperature between 0 and 15°C. Above zero-degree temperatures (chilling; 10 to 0°C) cause an acclimation response in plant tissues. Below zero-degree temperatures (frost) cause an additional challenge to plant tissues due to the formation of ice crystals. Exposure of plants to cold stress leads to several consequences such as oxidative stress, disintegration or damage of the plasma membrane, cell dehydration (water loss due to ruptured membrane), solute and ion leakage, dysfunction of metabolisms, inhibition of phloem transport, inhibition in respiration, photoinhibition, delays in leaf development, chlorosis, and wilting (reviewed in Yadav, 2010).

All of these may eventually damage the plants. To overcome such circumstances, plants will try to develop freezing tolerance through a process called cold acclimation, where extensive re-programming of gene expression and metabolism is involved (Palta and Weiss, 1993; Guy, 1999; Wanner and Junttila, 1999; Thomashow, 1999, 2001, 2010; Cook et al., 2004; Kaplan et al., 2004; Usadel et al., 2008). The ability of plants to develop freezing tolerance during cold acclimation is a determining factor for their survival (Gulick et al., 2005). The process of how the

plants acquire freezing tolerance via several strategies will be discussed in detail in Part 1.2 in this chapter.

1.1.1 Cold Stress in *Arabidopsis thaliana*: The Physiological and Metabolic Responses

Arabidopsis thaliana is a flowering plant that has been used in classical genetic work for over 40 years and an extensive genetic and ecological literature exist (Meyerowitz et. al., 1991). Arabidopsis is a small, annual or winter annual, rosette plant (**Fig. 1-1**). It belongs to the taxonomic family of the Brassicaceae in the eudicotyledonous group of angiosperm vascular plants, and is a member of the mustard family, along with some more familiar plants, such as cabbages and radishes (Kramer U, 2015; Meyerowitz et al., 1991). It is a harmless weed of no food or other economic value. Nonetheless, Arabidopsis is of considerable value as a model plant in molecular genetic research. It has a generation time of only 5 weeks, it can produce more than 10,000 seeds per plant, it is of such small size that can be grown in a small space. The small flowers contain both anthers and pistils, and the plant typically self-fertilizes. Self-fertilization allows new mutations to be made homozygous rapidly with minimal effort (Meyerowitz et al., 1991).

The popularity of Arabidopsis as a central genetic model and universal reference organism in plant and crop science rapidly gained momentum when researchers successfully began to combine genetics with powerful molecular biology methods. The Arabidopsis reference genome sequence was published as the first nuclear genome of a flowering plant in 2000 (http://www.arabidopsis.org/) (Arabidopsis Genome Initiative, 2000; Somerville and Koornneef, 2002; Koornneef and Meinke, 2010). It has a very small nuclear genome, with a genome size of ~135 Mb, and a haploid chromosome number of five (http://plants.ensembl.org/Arabidopsis_thaliana/Info/Index). The ease and speed with which experiments can be conducted on Arabidopsis has allowed enormous fundamental progress in our knowledge of the molecular principles of plant development, cell biology, metabolism, physiology, genetics, epigenetics and system biology (https://www.arabidopsisbook.org/).

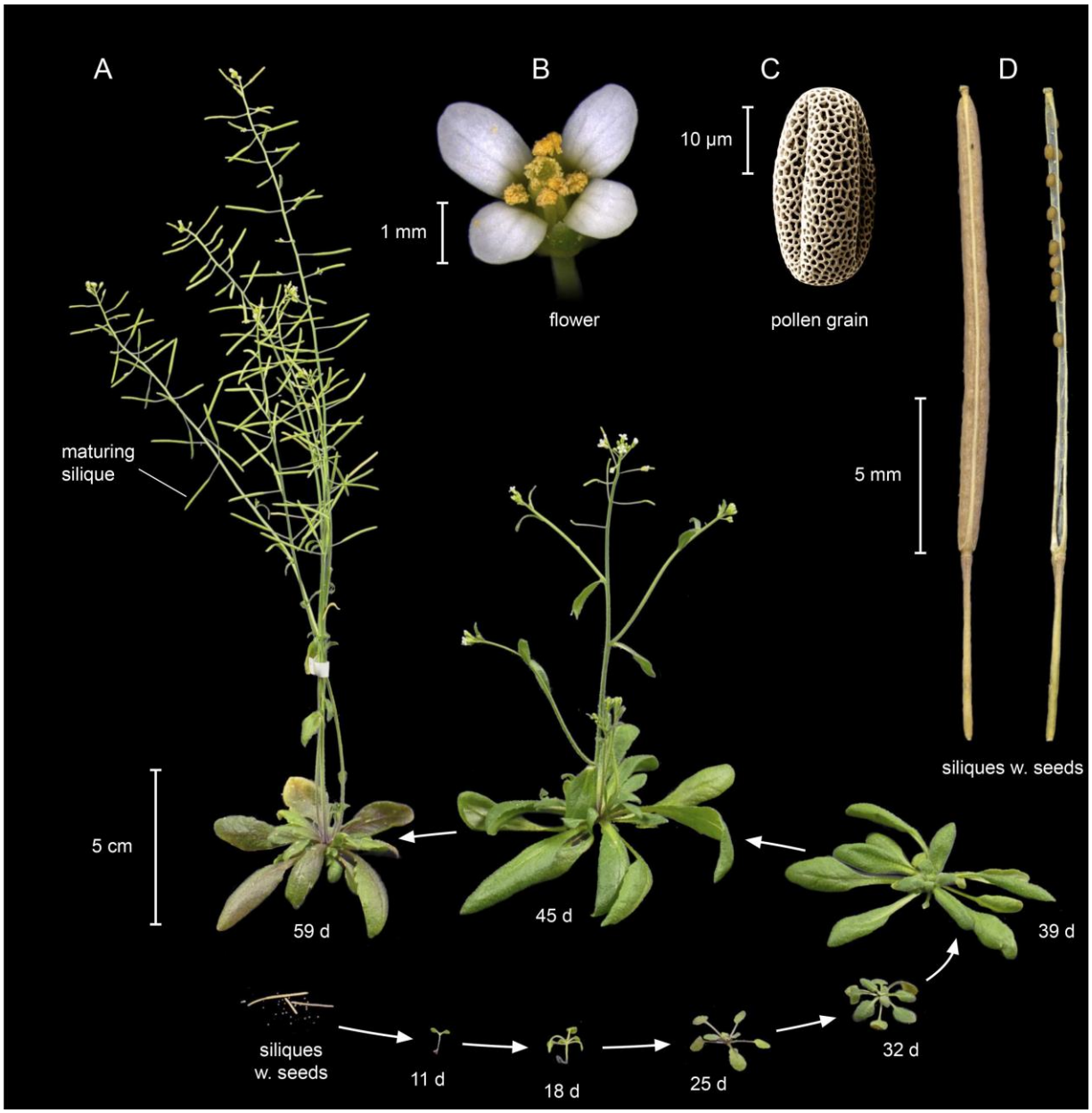


Figure 1-1. Life cycle of *Arabidopsis thaliana*. **(A)** *A. thaliana* of the accession Columbia (Col) at different stages of its life cycle, from seed (bottom left) to seedling (11 days), to vegetative growth (39 days), and to reproductive growth (45 days). Photographs of **(B)** a flower, **(C)** a pollen grain (scanning electron micrograph), and **(D)** mature siliques (seed pods; left: closed; right: open with a few remaining un-shattered seeds) at higher magnification. Image credits: B and C, Maria Bernal and Peter Huijser; other photographs, Ines Kubigsteltig and Klaus Hagemann (Source of figure: Kramer U, 2015).

The optimal growth temperature for Arabidopsis ranges from 23°C to 25°C. At lower temperatures, growth is slow, and flowering is delayed (The Arabidopsis Biological Resource Center, https://abrc.osu.edu/). Chilling was shown to interrupt the circadian-regulated transcription of several nuclear-encoded photosynthetic genes in chilling-tolerant Arabidopsis (Kreps and

Simon, 1997). Hasdai and colleagues (2006) reported the physiological and morphological responses of various Arabidopsis ecotypes grown under chilling (14°C) and cold (6°C) temperatures, on the ecotypes' basal freezing tolerance levels. Seedlings of Arabidopsis plants were extremely sensitive to low growth temperatures, in which the hypocotyls and petioles were much longer and the angles of the second pair of true leaves were much greater in plants grown at 14°C than in those grown at 22°C. Flowering time was also markedly delayed at low growth temperatures. Other marked responses to low temperatures were changes in pigmentation, which appeared to be both ecotype specific and temperature dependent and resulted in various visual phenotypes such as chlorosis, necrosis or enhanced accumulation of anthocyanins. The observed decreases in chlorophyll contents and accumulation of anthocyanins were much more prominent in plants grown at 6°C than in those grown at 14°C. It was concluded that Arabidopsis ecotypes responded differentially to cold (6°C), chilling (14°C) and freezing temperatures. On the other hand, Strand et al. (1997) have shown that rapid chilling inhibited phloem export, leading to a rapid accumulation of soluble sugars (hexose phosphates, sucrose, glucose, fructose) and severely suppressed photosynthesis (via suppression of photosynthetic gene expression) in Arabidopsis during a short term shift from 23°C to low temperatures (5°C). Strand et al. (1999) then also conducted another experiment where they compared Arabidopsis leaves shifted to 5°C for 10 days and then also the new leaves which developed after shifting to 5°C with control leaves on plants that had been left at 23°C. Leaf development at 5°C resulted in the recovery of photosynthesis to rates comparable with those achieved by control leaves at 23°C. This phenomenon shown in Arabidopsis is known as cold acclimation, and has also been reported by Thomashow (1999, 2001 and 2010). Cold acclimation involves the extensive activation of transcription factors, cold-responsive genes and networks. The process is complex, yet it is the first and most important strategy for plants to be able to acclimate in chilling temperature and survive in freezing temperature (will be further discussed in Part 1.2.1).

1.1.2 Cold Stress in Wheat (*Triticum aestivum*): The Physiological and Metabolic Response

Wheat (*Triticum aestivum L.*) is the most widely cultivated crop on Earth, which was grown on 220 million hectares of farmland worldwide in the year 2016. Wheat production was 749 million tons in 2016 and the production needs to increase by 60% to feed the projected 9.6 billion world population by year 2050 (International Wheat Genome Sequencing Consortium,

www.wheatgenome.org). Wheat yields and production therefore have great impact on the global economy, food security and human sustainability.

As illustrated in **Fig. 1-2B**, bread wheat is hexaploid (AABBDD), with a genome size estimated at ~17 Gb, composed of three closely-related and independently maintained genomes (wheat A, B and D, each comprising 7 chromosomes) that are the result of a series of naturally occurring hybridisation events. The ancestral progenitor genomes are considered to be *Triticum urartu* (the A-genome donor) and an unknown grass thought to be related to *Aegilops speltoides* (the B-genome donor). This first hybridisation event produced tetraploid emmer wheat (AABB, *T. dicoccoides*) which hybridized again with *Aegilops tauschii* (the D-genome donor) to produce modern bread wheat (http://plants.ensembl.org/Triticum_aestivum/Info/Index). In August 2018, the International Wheat Genome Sequencing Consortium (IWGSC) published in the international journal *Science* (Appels et al., 2018) a detailed description of the genome of bread wheat, in which the sequence of the model wheat variety Chinese Spring was fully reported (**Fig. 1-2C**). This work sheds light and paves the way for the production of wheat varieties better adapted to climate challenges, with higher yields, enhanced nutritional quality and improved sustainability.

A key challenge for wheat breeding is the improvement of varieties with tolerance to multiple biotic and abiotic stresses while maintaining stable yields (Appels et al., 2018; Ortiz et al., 2008). Among the stresses, low temperature is one of the primary stresses limiting the growth and productivity of wheat (Fowler et al., 1996b). Wheat, which is a temperate climate zone plant, has an optimum growth temperature range of 17–23°C (Porter and Gawith, 1999). Winter cereals sense chilling when exposed to temperatures colder than 10°C (Fowler et al., 1996b). The capacity to withstand cold temperatures in wheat may vary depending on the genetic background and variability. Some wheat varieties are cold tolerant, while some are cold sensitive. Nonetheless, all of these varieties need to go through a similar process during the exposure to low, non-freezing temperatures to acquire freezing tolerance. This process of cold acclimation (Fowler and Gusta, 1979) is not restricted to cereal crops, but as previously mentioned, also happens to other plants including the model plant Arabidopsis.

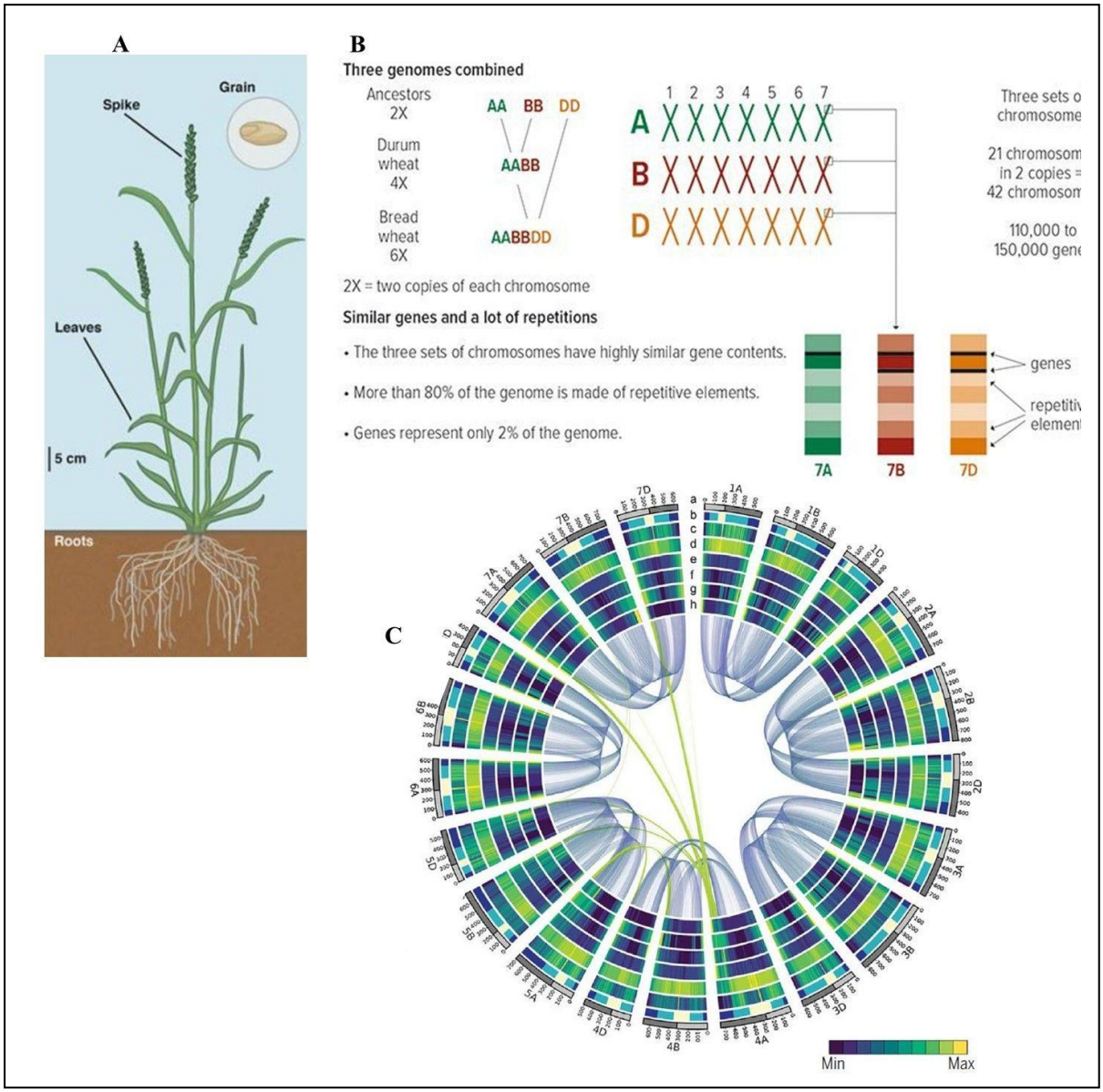


Figure 1-2. A wheat plant and genome. **(A)** Schematic illustration of a mature wheat plant and high-level tissue definitions for roots, leaves, spike and grain. **(B)** Bread wheat genome is complex due to the co-existence in wheat of the genomes from three progenitor species, called genomes A, B and D. **(C)** With complete access to the ordered sequence of all 21 wheat chromosomes, the context of regulatory sequences, and the interaction network of expressed genes, breeders and researchers now have the ability to rewrite the story of wheat crop improvement. (Source of pictures: Modified from Appels et al. 2018 and International Wheat Genome Sequencing Consortium).

Together with cold acclimation, the vernalization response is the second important mechanism that cereals and other plants evolved to cope with low-temperature stress. Wheat varieties are traditionally classified as two general types: winter wheat with variable low temperature requirement for a proper flowering time (vernalization) and spring wheat without

the vernalization requirement (Yan et al., 2015). Vernalization, which is the requirement of a prolonged exposure to low temperatures (4 and 6°C for 4–6 weeks) to accelerate flowering, is particularly important for winter wheat to prevent premature flower development during winter and protect the environmentally sensitive floral organs (Loukoianov et al., 2005; Porter and Gawith, 1999). In both the winter and spring wheat, genes for vernalization (*Vrn*) and photoperiod (*Ppd*) responses determine the flowering habit. Winter-habit wheat genotypes require vernalization to flower, whereas spring wheat genotypes can flower without vernalization. Spring wheat genotypes flower either if the *Ppd-1* gene is present (*Ppd* is a gene that conveys photoperiod insensitivity) or once the long day photoperiod requirement is met (Santra et al., 2009). Vernalization requirement is primarily controlled by alleles at three orthologous loci, *Vrn-A1*, *Vrn-B1* and *Vrn-D1*, which are located on the long arms of chromosomes 5A, 5B and 5D, respectively. Collectively, these three genes are referred to as *Vrn-1* loci. Dominant alleles of each locus are designated as *Vrn-A1*, *Vrn-B1*, and *Vrn-D1*, whereas the recessive alleles are designated as *vrn-A1*, *vrn-B1*, and *vrn-D1*. The presence of a dominant *Vrn-1* allele in any genome confers spring growth habit, whereas the presence of recessive alleles in the homozygous state across *Vrn-1* loci confers winter growth habit (Santra et al., 2009; Dubcovsky et al., 2006; Loukoianov et al., 2005).

To date, several studies have been reported for the investigation of physiological and metabolic responses of both winter and spring wheat subjected to cold stress. Hurry et al. (1995) investigated the effect of long-term (months) exposure to low temperature (5°C) on growth, photosynthesis, and carbon metabolism in spring (cv. Dragon) and winter (cv. Portal) cultivars of wheat. They discovered that winter wheat was able to maintain higher net assimilation rates and higher *in situ* CO_2 exchange rates than the respective cold-grown spring cultivars. Associated with the high photosynthetic rates of cold-grown winter cultivars, was a 2-fold increase per unit of protein in both stromal and cytosolic fructose-1 ,6-bisphosphatase activity and a 1.5- to 2-fold increase in sucrose-phosphate synthase activity. The spring wheat cultivar did not increase in photosynthetic enzyme activity on a per unit of protein basis. The winter wheat cultivar also increased the soluble/insoluble carbohydrate ratio and the levels of photosynthetic and sucrose biosynthetic enzymes. In contrast, the spring cultivar showed a reduced soluble/insoluble carbohydrate ratio and only small changes in enzymatic activity.

On the other hand, Equiza et al. (1997, 2001) reported the changes of shoot and root growth rates as well as carbohydrate accumulation in several winter cultivars (cv. ProINTA Pincen, cv. ProINTA Puntal) and spring cultivars (cv. Buck Pataco, San Agustin INTA) cultivated at either 25

or 5 °C. At 5 °C, relative growth rate (RGR) of shoots was similarly reduced in all cultivars, but RGR of roots was more affected in winter wheats. This difference resulted in smaller root to shoot ratios in winter wheats compared to spring wheats. Although winter cultivars developed relatively smaller root systems at 5°C, this characteristic was compensated by a low stomatal frequency and increased thickness of epidermal cell walls in leaves. A decrease in the osmotic potential of shoots and roots was observed in parallel with sugar accumulation, this decrease was more marked in winter cultivars. The winter cultivars accumulated more soluble sugars in shoots and roots than spring cultivars. Higher soluble sugar content leads to a decreased osmotic potential, which favored water uptake and retention by roots. These results indicate a different morpho-anatomical and physiological plasticity of winter and spring cultivars during development at low temperature (Equiza et al, 1997; Equiza et al., 2001).

1.1.3 Wheat and Frost Events in Australia: The Dilemma of Australian Farmers

Wheat is one of the major winter crops grown in Australia. Australia is the eighth largest wheat producing country in the world with the production of about 22 million tons per annum (Food and Agriculture Organization of the United Nations, http://www.fao.org/faostat/en/#data/QC/visualize). There are various types of wheat produced in Australia, including Australian Prime Hard, Australian Hard, Australian Premium White, Australian Noodle Wheat, Australian Standard White, Australian Premium Durum, and Australian Soft (Source: Australian grain production – a snapshot, https://www.aegic.org.au/australian-grain-production-a-snapshot/). The main producing state, Western Australia, generates about 50% of Australia's total wheat production, followed by New South Wales, South Australia, Victoria and Queensland (**Fig. 1-3**). In Australia, spring wheat is sown in autumn and harvested in late spring or early summer (Zheng et al., 2015; **Fig. 1-3**). Most of the Australian wheat is exported and sold overseas to Asian and Middle East regions including Indonesia, Japan, South Korea, Malaysia, Vietnam and Sudan (www. https://www.agriculture.gov.au/ag-farm-food/crops/wheat).

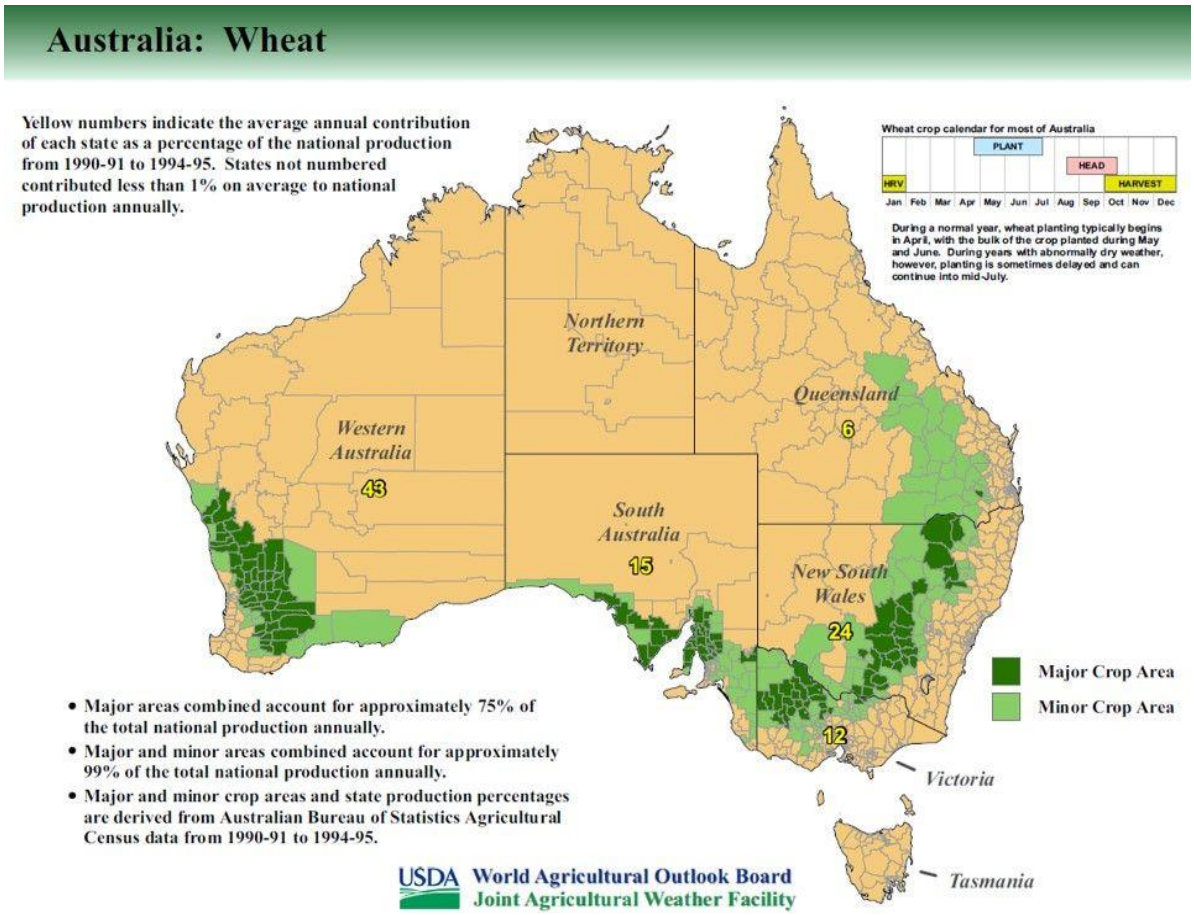


Figure 1-3. Wheat sowing and harvesting time, and the major production regions in Australia. (Source: https://www.usda.gov/oce/weather/pubs/Other/MWCACP/Graphs/aus/AusWheat.pdf).

Climate change and the associated changes in atmospheric conditions have increased the probability of weather extremes, resulting in more frequent crop losses including wheat production (Lobell and Gourdji, 2012). Low temperatures, such as chilling (0–12°C) and freezing (<0°C), are one of the major yield-limitations to wheat productivity. Wheat can tolerate relatively severe frosts during vegetative growth, but is frost-sensitive during the reproductive or flowering stage (**Fig. 1-4**). Under very severe frost (for example -8°C) or multiple minor frost events (several nights of -2° to -4°C), all wheat varieties at the flowering stage are susceptible, resulting in up to 100% sterility. Warmer winters and more frequent spring frosts have increasingly affected wheat yields in China from 1961 to 2000 (Li et al., 2014; Li et al., 2015).

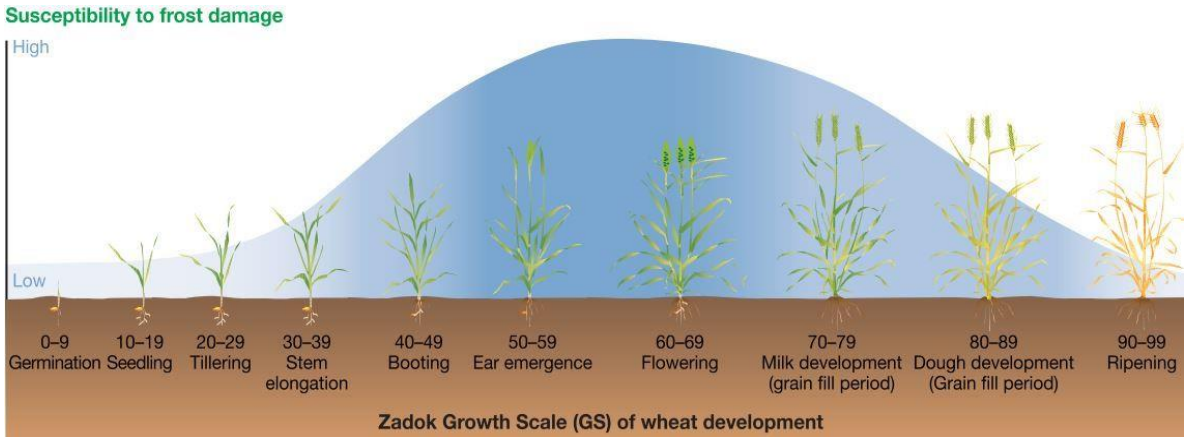


Figure 1-4. Susceptibility of wheat to frost during the development cycle.
(Source: https://www.agric.wa.gov.au/sites/gateway/files/GRDC-Managing-Frost-Risk-Tips-and-Tactics).

In Southern Australia, the frequency of spring frosts has increased significantly since 1960 and the overall length of the frost season has increased by one month, resulting in more frequent occurrences of frost damage to wheat crops during flowering (Crimp et al., 2015; Zheng et al., 2015). In contrast to drought stress, which establishes progressively over weeks, yield losses of wheat are mainly due to chilling and frost conditions that are often caused by short events occurring at night or early morning hours (also known as 'cold spells'). Radiant frosts in spring are caused by heat loss from the soil surface to the night sky on cold and dry days with clear skies. This leads to rapid cooling of the crop canopy (Marcellos and Single, 1975). Together with the calm conditions when atmospheric humidity is relatively low (with a dew point less than 2.2°C), a radiant frost is likely to occur (**Fig. 1-5**). Part of the problems with frost is that effects of frost periods are often unobservable until grain-fill and when the crop is harvested. More seriously, a white coat layer of ice crystals not necessarily seen on crops can already lead to frost damages (Source: https://www.agric.wa.gov.au/frost/managing-frost-risk).

Reoccurring of frost events have cost the Australian wheat industry an estimated $360 million of direct and indirect yield losses annually (March et al., 2015; Zheng et al., 2015). In September 2016, the Western Australia (WA) farmers have experienced severe frost damage on their wheat crops, which has been considered to be the worst in the last decade. Within one month, frost, water logging and isolated dry conditions have wiped $140 million dollars off the total value of harvest in Western Australia in 2016 (**Figure 1-6A**; Source: http://www.abc.net.au/news/2016-10-05/frost-hits-wa-crop-value/7903250). In September 2018, a record-breaking cold spell in the

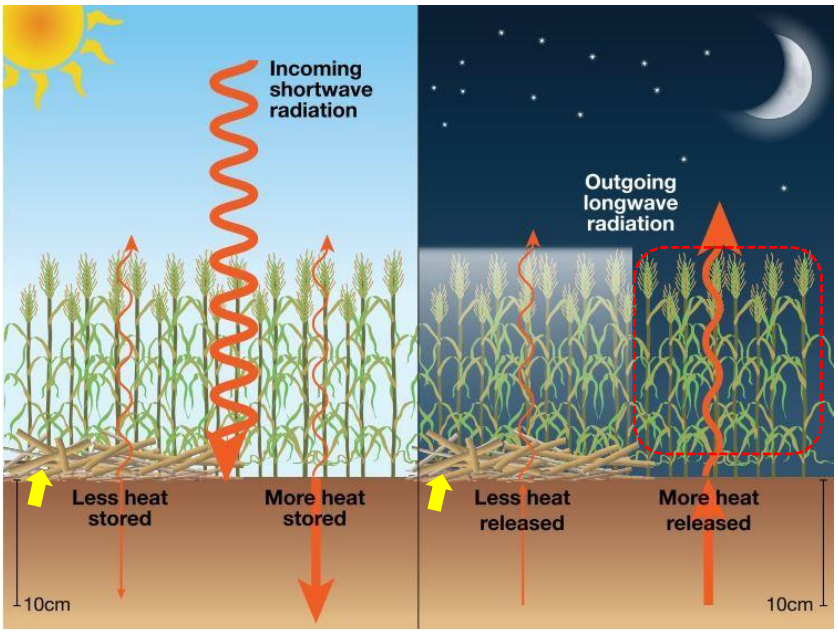


Figure 1-5. How frost is formed, heat is captured in the soil during the day and radiates out during the night into the canopy. Region circled with red line indicates the area where frost may happen easily. Farming practices that manipulate the storage and release of heat using soil heat bank (indicated by yellow arrows) into the crop canopy at night are important to reduce the impact of a frost event. (Source: Modified from https://www.agric.wa.gov.au/sites/gateway/files/GRDC-Managing-Frost-Risk-Tips-and-Tactics).

Western Australia's agricultural heartland has shattered farmers' hopes of enjoying a bumper crop harvest (**Figure 1-6B**; Source: https://www.abc.net.au/news/2018-09-16/wa-farmers-facing-frost-damage-as-chilly-spell-sweeps-south/10253186). In September 2019, two weeks of extreme weather causing frost and heat damage wiped $750 million off Western Australia's upcoming grain harvest (Source: https://www.abc.net.au/news/rural/2019-09-16/giwa-slashes-crop-forecast/11517752).

Minimising the loss caused by chilling and frost events is therefore critical for breeders in Australia. One of the solutions is via the development of more frost-tolerant wheat cultivars. To achieve this goal, we first need to understand the underlying molecular mechanisms of cold responses of Australian wheat subjected to cold stress. Apart from transcriptomic studies, metabolome and lipidome profiling are also believed to contribute to the unravelling of cold and frost mechanism in wheat. This may enable breeders to develop more frost-tolerant cultivars in the future.

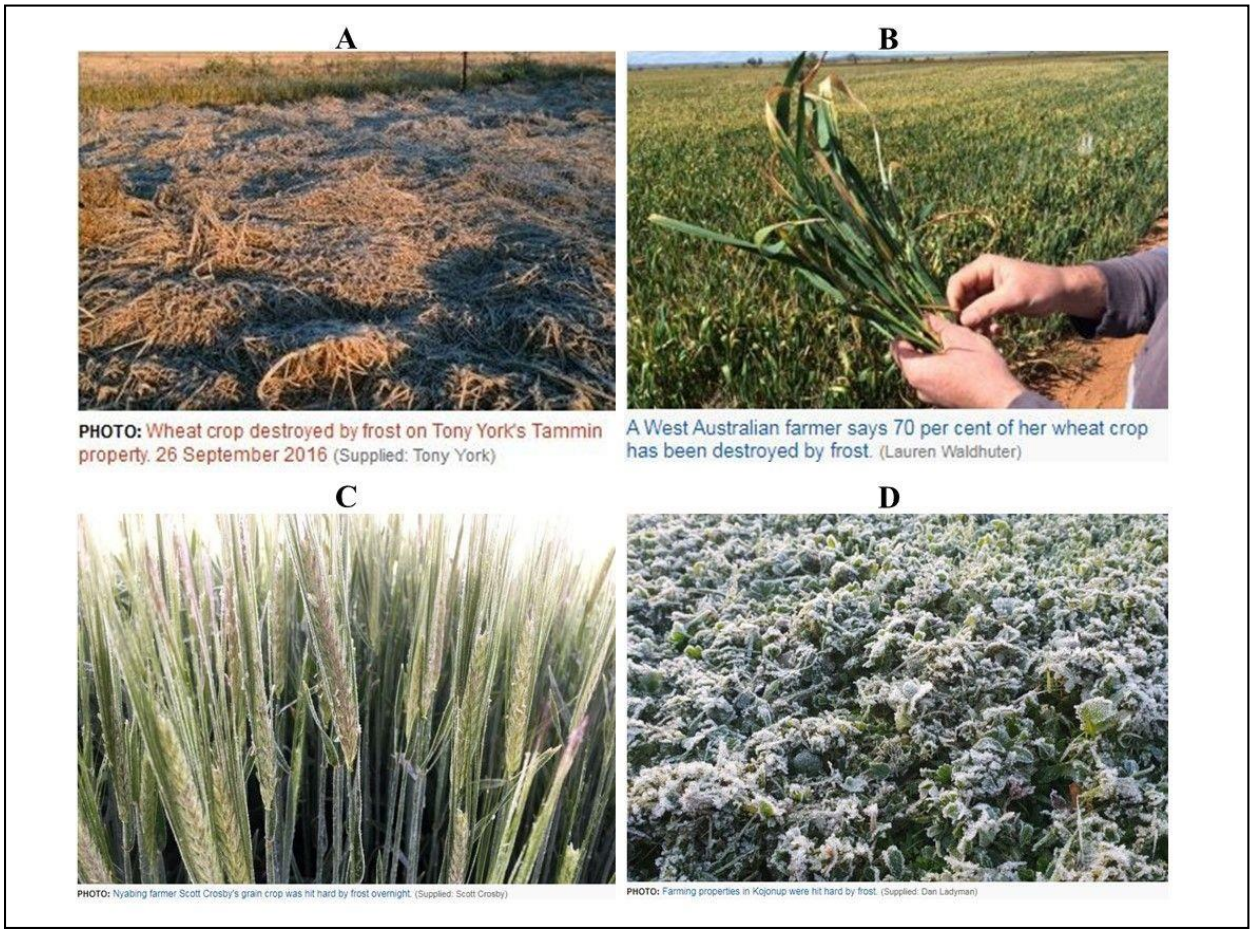


Figure 1-6. (A) Western Australia (WA) experienced the worst frost damage on cereal crops in the last decade, wiped $140 million dollars off the total value of harvest in WA (Sources: http://www.abc.net.au/news/2016-10-05/frost-hits-wa-crop-value/7903250). **(B)** Frost wipes out 70 per cent of a WA farmer's wheat crop (Source: https://www.abc.net.au/news/rural/2016-10-05/frost-devastation-in-konindin/7906428). **(C** and **D)** A record-breaking cold spell in Western Australia's. Farmers woke up to discover heavy frost gripping their wheat and barley crops, which were expected to deliver a combined 14 million ton harvest in 2018 (Source: https://www.abc.net.au/news/2018-09-16/wa-farmers-facing-frost-damage-as-chilly-spell-sweeps-south/10253186).

1.2 Plant Strategies to Sustain in Suboptimal or Cold Temperature

Plants acquired several strategies to develop cold or freezing tolerance. These include (a) the activation of transcription factors and stress-responsive genes, (b) detoxification of reactive oxygen species (ROS) produced from damaged plasma membranes, (c) remodeling of the plasma membrane through regulation of lipid metabolism, (d) synthesis of anti-freeze proteins to inhibit ice formation in the apoplast, (e) synthesis of osmolytes acting as osmoprotectants in cells to prevent dehydration, and (f) synthesis of stress-induced phytohormones such as abscisic acid (ABA), salicylic acid (SA), jasmonic acid (JA) and ethylene (**Fig. 1-7**). Among them, strategies

(a), (c), (e) and (f) are of interest in this study as they involve the regulation of primary metabolism at the cellular and membrane level (reviewed and modified from Yadav, 2010).

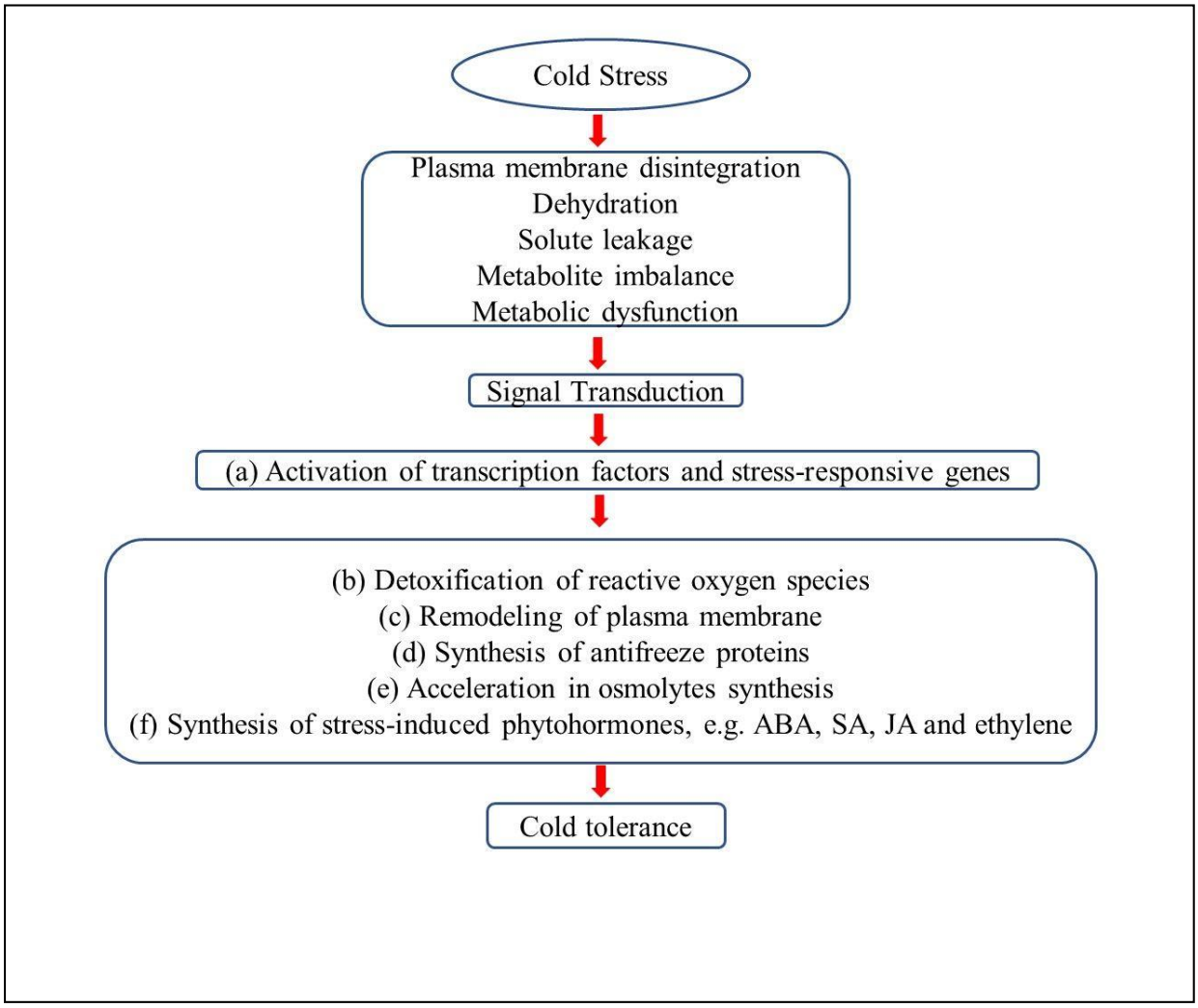


Figure 1-7. Overview of common tolerance mechanisms triggered by plants in responses to cold stress (modified from Yadav, 2010).

1.2.1 Strategy 1: Activation of Transcription Factors and Stress-responsive Genes

To date, the precise mechanism for low temperature sensing and acclimation is not well understood. However, the characterization of cold related transcription factors and cold regulated genes have given important insight into the signaling pathways and the regulation of genes associated with cold acclimation (Thomashow 1999, 2001; Monroy et al., 2007; Winfield et al.,

2010). As illustrated in **Fig. 1-8**, an alteration of membrane fluidity appears to be the primary sensing event followed by an influx of calcium into the cytosol (Winfield et al., 2010), and the activation of a signaling cascade of transducers, some of which are protein kinases (RLKs). Two well-characterized protein kinases that participate in these cascades are CDPKs (Martin and Busconi 2001) and MAPK (Teige et al., 2004). Although the ultimate primary targets of the cold signaling cascade have not been identified, they are likely to be downstream transcription factors such as WRKY transcription factors and the ICE1 (*INDUCER OF CBF EXPRESSION 1*), a constitutively expressed MYC-like bHLH transcription factor (Chinnusamy et al. 2006). ICE1 in turn regulates the cold-induced expression of *CBF* (*C-REPEAT BINDING FACTOR*) belonging to the *AP2* (*APETALA 2)* family.

An important step in understanding cold-regulated gene expression came with the discovery of the transcription factors called CBF or also known as DREB1 (*DEHYDRATION-RESPONSIVE ELEMENT-BINDING FACTOR 1*). *CBF1*, *2* and *3* genes (corresponding to *DREB1b*, *DREB1c* and *DREB1a*, respectively) are present in tandem array on chromosome 4 in Arabidopsis and are rapidly induced (within 15 min) in response to low temperature, reaching peak expression about two hours after exposure to cold (Gilmour et al. 1998, Liu et al., 1998, Stockinger et al. 1997). The CBF transcription factors were the first transcriptional activators demonstrated to have a role in controlling the expression of cold-responsive genes with a role in cold acclimation (Van Buskirk et al., 2006). The CBF transcription factors altered the expression of more than 100 CBF-targeted genes, known as the CBF regulon, which contribute to an increase in freezing tolerance (Park et al., 2015). The cold responsive genes that were found to be upregulated by CBF in response to low temperature were given a variety of names including *COR* (*COLD REGULATED*), *LTI* (*LOW-TEMPERATURE INDUCED*), *KIN* (*COLD-INDUCED*), *RD* (*RESPONSIVE TO HYDRATION*), *ERD* (*EARLY RESPONSIVE TO DEHYDRATION*) genes, to name a few (**Fig. 1-9**). The transcript levels for these genes were found to increase greatly within a few hours of plants being exposed to low temperature. Then, they remained elevated for the duration of the cold exposure, but quickly return to pretreatment levels upon returning the plants to warm temperatures (reviewed in Thomashow 1999).

The mechanisms by how the CBF regulon increases freezing tolerance are not completely understood, but involve the action of genes that encode cryoprotective proteins, such as *COR15a* (Steponkus et al., 1998) and enzymes involved in the biosynthesis of low-molecular-weight cryoprotectants, including proline and raffinose (Cook et al., 2004; Gilmour et al., 2000 & 2004;

Kaplan et al., 2007; Taji et al., 2002). Besides, up-regulation is also observed for genes encoding cold-inducible proteins that function in survival at low temperatures, including the late embryogenesis abundant (LEA) proteins, which are hydrophilic proteins abundantly expressed during seed maturation and in response to cold or dehydration, and enzymes for sugar metabolism and fatty acid desaturation (Fowler and Thomashow 2002; Maruyama et al., 2004; Seki et al., 2001). It has been noted that major frost tolerance QTLs in diploid wheat (*Triticum monococcum*) and barley are mapped to *DREB1/CBF* genes (Vagujfalvi et al., 2003; Francia et al., 2007; Knox et al., 2008), and frost tolerance is correlated with the expression levels of linked *DREB1/CBF* genes (Knox et al., 2008).

1.2.2 Strategy 2: Remodeling of Plasma and Subcellular Membranes

Maintaining of the integrity and fluidity of membranes is of fundamental importance for plants to survive high or low temperature stress (Zheng et al., 2011). Plasma and subcellular membranes are lipid bilayers. The plasma membrane surrounds the cytoplasm of cells and generally functions as a barrier to separate the intracellular compartment from the extracellular environment, whilst subcellular membranes surround the organelles to form compartments inside the cell. Plasma and subcellular membranes are mainly built from lipids and proteins, in which the membrane proteins are either integrated or peripherally attached to the plasma membrane. Primary functions of plasma membrane proteins include receptors, kinases or G proteins mediating signal transduction, transporters and channels for trafficking, for instance. In contrast, plasma membrane lipids forming the lipid bilayer structure are composed of three main categories of lipids: (1) phosphoglycerolipids and glycosylglycerolipids, (2) sphingolipids and (3) sterols. These lipids confer structurally protection to the cell membranes, are involved in remodeling to maintain the fluidity during temperature stress, and act as signaling molecules upon temperature stress. (Testerink and Munnik, 2005; Sperling et al., 2005; Cacas et al., 2012; Dutilleul et al., 2012; Dormann 2013; Hou et al., 2016; Minami et al., 2017) (**Fig. 1-10**).

Glycerolipids, such as phosphoglycerolipids and glycolipids, are the major constituents of membranes (**Fig. 1-11**). In response to changes in temperature, plants can adjust the glycerolipid composition of their membranes to maintain the integrity and optimal fluidity of these membranes. For example, at temperatures <0 °C, the amounts of lyso-phospholipids increase rapidly by five- to 10-fold (Welti et al. 2002). Glycerolipids in the plasma membrane and the multiple subcellular

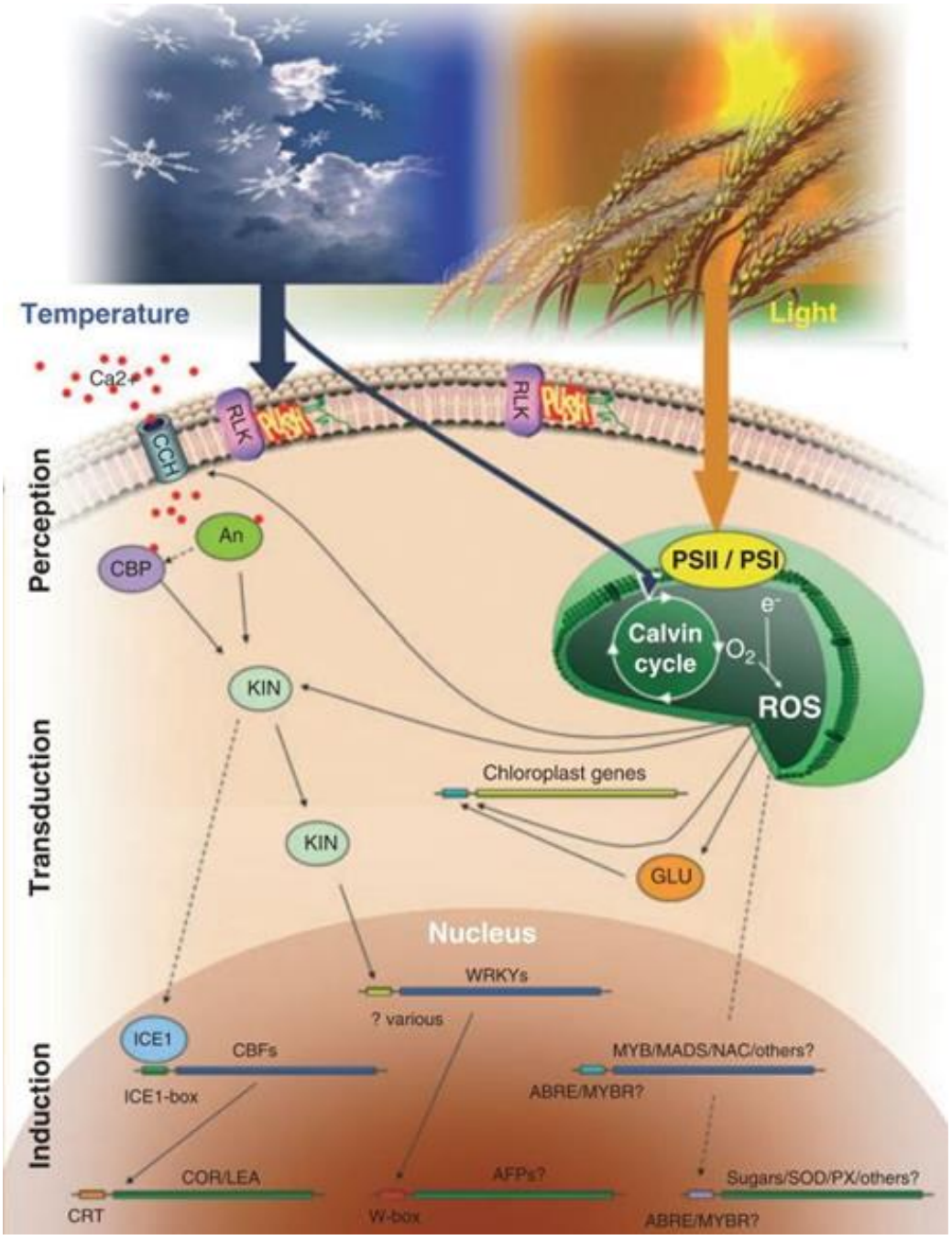


Figure 1-8. Schematic representation of the cold response in plant cells. The coloured rods in the nucleus represent genes; those with the coding region coloured blue are transcription factors (eg. CBFs, WRKYs), those coloured green represent genes for effector molecules (eg. *COR*/*LEA*). Each gene is represented with only one cis-acting promoter region, but several may be present. Ice1 is a constitutive protein that is localized to the nucleus. Membrane-bound kinases (RLK) might be involved in signal transduction as a result of the mechanical stress resulting from membrane rigidification. The annexins (An) and calcium-binding proteins (CBP) are activated by binding calcium. ABRE, ABA response element; CBF, C-repeat Binding Factors; CBP, calcium binding proteins, CCH, calcium channel; GLU, glutathione; KIN, kinases and phosphatases; RLK, receptor-like kinase, ROS, reactive oxygen species (Source: Winfield et al., 2010).

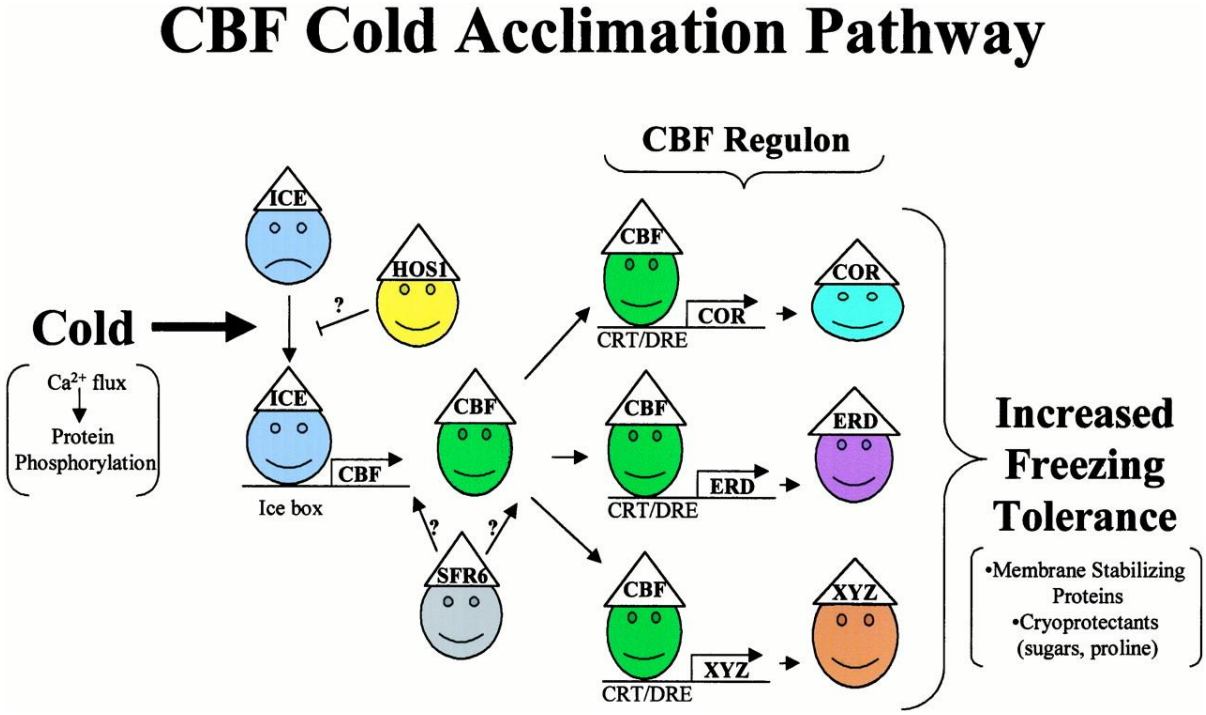


Figure 1-9. Model of the Arabidopsis CBF cold acclimation pathway. Low temperature leads to rapid induction of the *CBF/DREB1* genes that in turn results in expression of the *CBF* regulon of *CRT/DRE*-regulated genes. Action of the *CBF* regulon, which includes *COR*, *ERD*, and presumably yet to be discovered ("*XYZ*") cold-regulated genes, results in an increase in plant freezing tolerance. Cold-induced expression of the *CBF/DREB1*genes has been proposed to involve the action of a regulatory protein present at warm temperature designated ICE (inducer of *CBF* expression). Low temperature is envisioned to either activate the ICE protein or other protein(s) with which it interacts. Such activation may involve alterations in protein phosphorylation caused by a cold-induced influx of calcium. The SFR6 protein appears to act between *CBF/DREB1* transcription and induction of the *CRT/DRE*-regulated genes whereas *HOS1* appears to act upstream of CBF transcription (Source: Thomashow 2001).

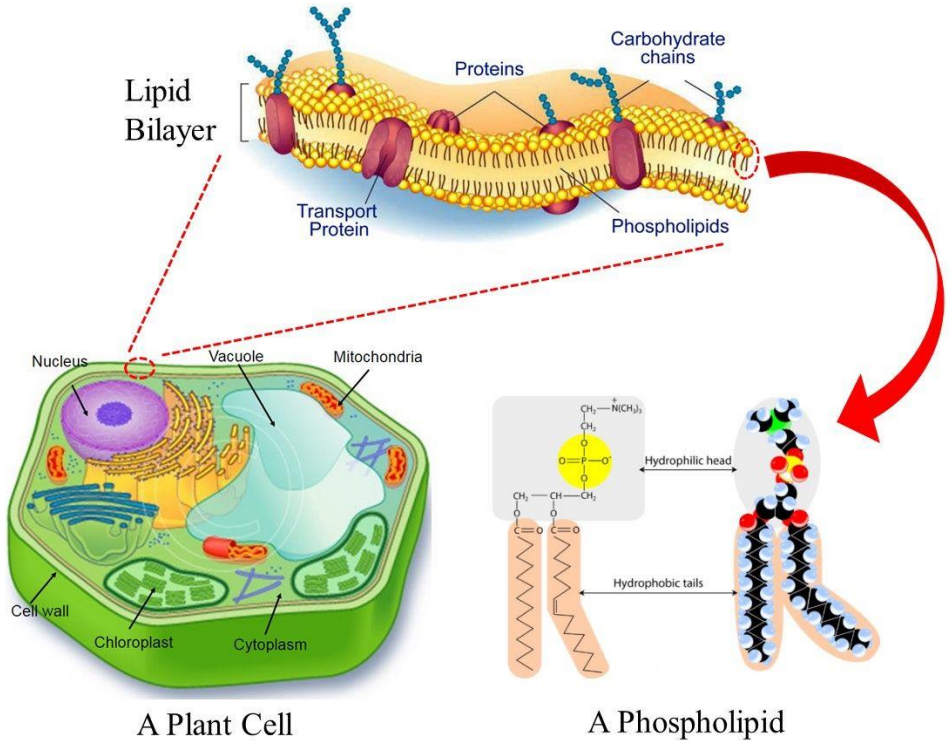


Figure 1-10. A plant cell with its plasma and subcellular membrane. The membranes are lipid bilayers and majority of the lipids are phospholipids with hydrophilic head and hydrophobic tail (Image sources: http://slideplayer.com/slide/5869473; https://chem.libretexts.org/ and http://biology.tutorpace.com/plasma-membrane-online-tutoring).

membranes consist of two kinds of fatty acids: unsaturated and saturated fatty acids. Changes in the degree of unsaturation of membrane glycerolipids, which affect membrane fluidity, are well known and occur when plants encounter low or high temperatures (Zheng et al., 2011). In general, lipids built up from more unsaturated fatty acids were shown to stay fluid at lower temperatures. Consistent with this physical property, cold-tolerant plants usually have a higher proportion of unsaturated fatty acids in their plasma membrane compared to the cold-sensitive ones (Steponkus et al., 1993). At low temperatures, the degree of unsaturation of fatty acids is increased through the regulation of several fatty acid biosynthesis pathways (Harwood 1998). Cold acclimation increases the ratio of unsaturated to saturated fatty acids (Sakai & Larcher 1987). For example, in chickpea (*Cicer arietinum*), low temperature resulted in a 31% increase in the degree of unsaturation of fatty acids, from a DBI (Double Bond Index) of 1.18 per fatty acid to one of 1.54 (Bakht et al., 2006).

The degree of unsaturation of fatty acid chains is mainly controlled by a group of enzymes known as fatty acid desaturases (FAD). When plants are subjected to heat or cold stress, FADs

regulate the remodeling of the membrane composition and modify fatty acid types or chains. In agreement with this claim, a transcriptomic study by Qin et al. (2008) revealed the down-regulation of *FAD3* transcripts in endoplasmic reticulum when both the heat-tolerant wheat 'TAM107' and heat susceptible wheat 'Chinese Spring' were subjected to heat stress. In 2000, Murakami et al. also reported that a double mutant in *Arabidopsis*, *fad7fad8,* (localised in the chloroplast membrane) could better acclimate to higher temperatures. Martiniere et al. (2011) reported that in cold conditions, plasma membranes of a linolenic acid-deficient *fad2* desaturase ethyl methanesulfonate (EMS) Arabidopsis mutant accumulated more saturated fatty acids with an increase of membrane viscosity compared to the wild type line Columbia-0. These findings indicated the importance of *FAD* in the regulation of membrane lipid metabolism in response to temperature changes.

Besides *FAD*, lipid transfer proteins (LTP) also play significant roles in the remodeling of membrane lipid compositions of plants under heat or cold stress. Changes of LTP activity can lead to alterations in membrane composition and affect cold tolerance. Plant LTPs form a group of highly-conserved proteins responsible for transporting of phosphoglycerolipids such as phosphatidylcholine (PC), phosphatidylethanolamine (PE), phosphatidylglycerol (PG), phosphatidylserine (PS), phosphatidylinositol (PI) and other fatty acid groups between cell membranes. A transcriptomics study performed by Gulick and colleagues (2005) found that the *LTP* genes were significantly up-regulated in both winter-wheat 'Norstar' and spring-wheat 'Glenlea' when exposed to 6°C during the day, 2°C during the night, and cold-acclimated for six days.

Due to the numerous alterations of lipid species involved in the remodeling of plasma and subcellular membranes during heat or cold stress, identification and understanding of lipid species are thus important. Findings of this PhD study can potentially assist the development of cold- and frost-tolerant crop varieties in future.

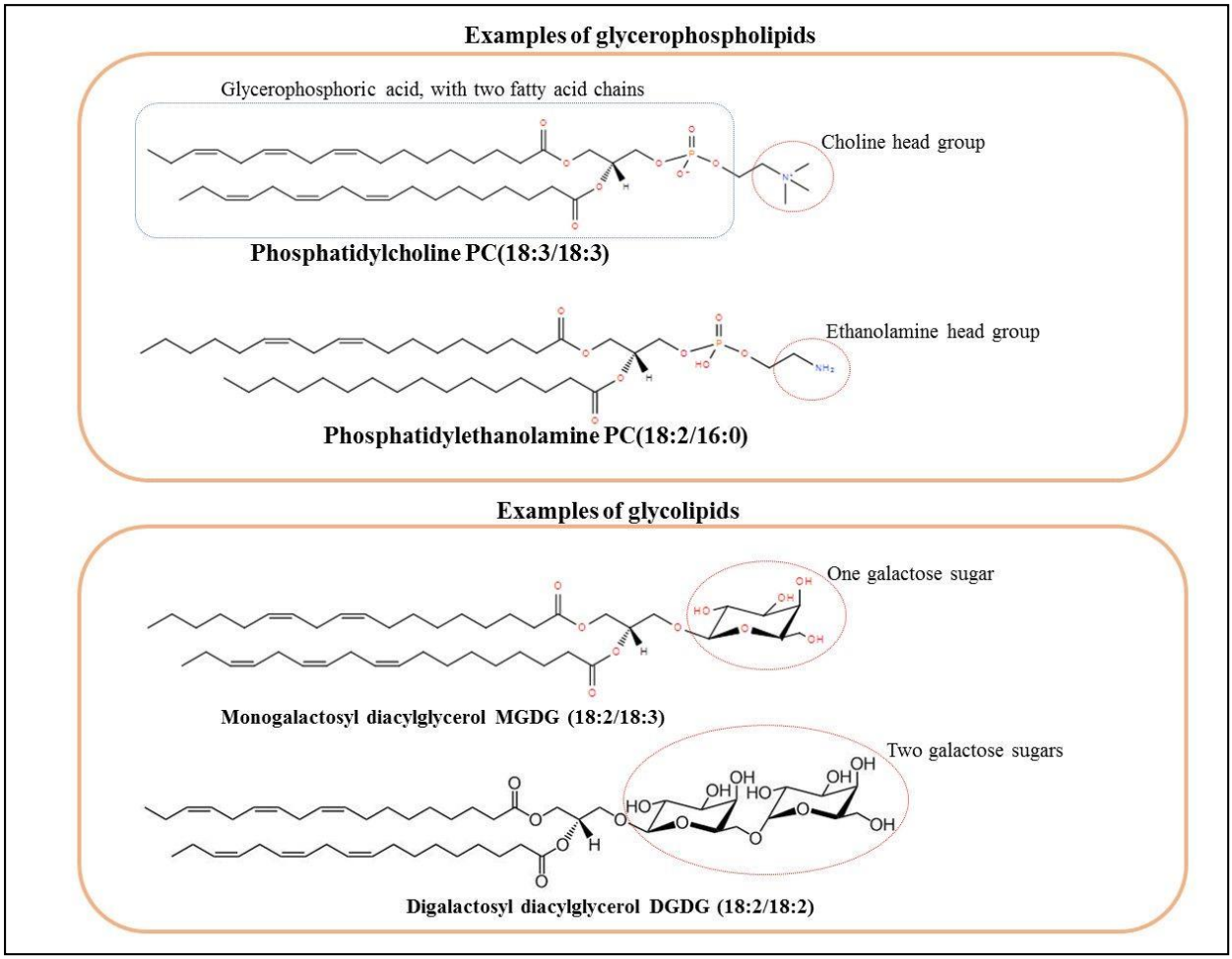


Figure 1-11. Examples of some common phosphoglycerolipids and glycolipids found in plants. The structures of the lipids are extracted from LIPID MAPS (www.lipidmaps.org).

1.2.3 Strategy 3: Acceleration of Osmolytes Biosynthesis during Cold Stress

When plants are exposed to cold stress, several cellular metabolites, which function as osmolytes, are produced. Osmolytes are chemical inert compounds involved in osmotic adjustment. They operate by lowering cellular osmotic potential to facilitate water retention. Also, their compatible solute behavior allows them to function as stabilisers of enzymes, membranes and other cellular components (Yadav, 2010). Osmolytes are also involved in re-tailoring of membrane lipid compositions so as to achieve an optimised liquid/crystalline physical structure necessary for proper membrane function (Yadav, 2010). To date, the well-studied osmolytes include soluble sugars (e.g. sucrose, raffinose, trehalose), sugar alcohols (e.g. sorbitol and mannitol), amino acids (proline) and polyamines. Of these, proline has drawn much attention due to its additional role

contributing to the stabilization of sub-cellular structures (e.g. membranes and proteins), scavenging free radicals, and buffering cellular redox potential under stressed conditions (Yadav, 2010). Another two amino acids or amines, citrulline and gamma-aminobutyric acid (GABA), are also reported to play important cryo-protective roles for plants under cold stress. Citrulline has hydroxyl radical scavenging and antioxidant properties and can protect DNA and enzymes from oxidative injuries during drought and water deficit conditions (Kawasaki et al., 2000; Akashi et al., 2001; Rimando et al., 2005; Kusvuran et al., 2013). Meanwhile, GABA can stabilize and protect proteins and membranes from freezing damage (Bouche and Fromm, 2004; Mazzucotelli et al., 2006).

1.2.4 Strategy 4: Synthesis of Stress-Induced Phytohormones

Phytohormones also play a major role in plants when they are exposed to extreme temperature. Abscisic acid (ABA) is the most extensively studied phytohormone that is highly induced during cold stress. Zhang et al. (2005) showed the importance of ABA to act as a secondary signal to induce the expression of phospholipase D (AtPLD) in *Arabidopsis thaliana*. PLDs were found to hydrolyze structural phospholipids such as PC, PG, and PE to produce phosphatidic acid (PA), an important secondary messenger that further activated the intracellular signalling cascade to induce gene expression during osmotic stress and dehydration (Meijer and Munnick, 2003). Besides ABA, salicylic acid (SA) and ethylene were also reported to play a role in the signal transduction pathway of cold responses (Horvath et al., 2007; Machakova et al., 1989). Recently, the role of jasmonates (JA) and derivatives in the breakage of seed dormancy by cold stratification (imbibed at 4°C for 84 hrs before transferred to room temperature) in wheat was also reported (Xu et al., 2016).

1.3 Metabolomics and Lipidomics for the Understanding of Cold Stress in Plants

Over the past decades, the metabolomics and lipidomics fields have benefited from advances in analytical instrumentation, especially mass spectrometry (MS)-based equipment (Hall, 2005; Horn and Chapman, 2014). To date, gas chromatography (GC) and liquid chromatography (LC) coupled with MS are the most two common techniques used for high-throughput metabolite and lipid profiling in plants under cold stress due to their high sensitivity and resolution (reviewed in Guy et al., 2008; Shulaev et al., 2008 and Welti et al., 2007). One successful example of metabolomics study of plants exposed to low temperature stress was shown by Cook et al., 2004. They reported the increment of 325 metabolites (out of 434) in *Arabidopsis* Wassilewskija-2 (Ws-2)

overexpressing the C-repeat responsive element-binding factor 3 (CBF3) in response to low temperature (4°C) using GC-time-of-flight (TOF)-MS. This included several metabolites which had previously been shown to accumulate in *Arabidopsis* plants upon exposure to low temperature, such as the amino acid proline and the sugars glucose, fructose, sucrose and raffinose. Increases were also found in aspartate, ornithine and citrulline, where Cook and colleagues suggested these patterns of these metabolites to demonstrate an upregulation of the urea cycle. Besides, they also pointed to increases of a-ketoglutarate, fumarate, malate and citrate in their study demonstrating an upregulation of the citric acid cycle upon low temperature.

With the successful metabolomics studies of cold stress in Arabidopsis (Cook et al., 2004; Kaplan et al., 2004, 2007; Guy et al., 2008), this field was further expanded to important crop plants such as rice and wheat. Maruyama and colleagues (2014) used GC-TOF-MS and CE-MS to study the effects of cold and dehydration on rice ('Nipponbare') and managed to identify and analyse 152 metabolites according to their retention time indices and specific mass fragments. This included sugars such as glucose, fructose, sucrose, amino acids and amines such as glycine, leucine, proline, GABA and many more. On the other hand, they also used LC-MS to measure and analyse phytohormone profiles of rice plants exposed to cold and dehydration. The metabolomics results obtained enabled them to perform integrated analysis with gene expression results which led to the finding that genes encoding enzymes involved in starch degradation, sucrose metabolism, and the glyoxylate cycle were upregulated in rice plants exposed to cold or dehydration and that these changes are correlated with the accumulation of glucose (Glc), fructose, and sucrose. The high expression levels of genes encoding isocitrate lyase and malate synthase in the glyoxylate cycle correlated with increased Glc levels in rice, but not in Arabidopsis under dehydration conditions. This indicates that the regulation of the glyoxylate cycle may be involved in Glc accumulation under dehydration conditions in rice but not in Arabidopsis. In addition, the integrated analysis of phytohormones and gene transcripts revealed an inverse relationship between the effects of abscisic acid (ABA) signaling and cytokinin (CK) signaling under cold and dehydration stresses. Cold and dehydration increased the effect of ABA signaling and decrease the effect of CK signaling.

On the other hand, Juhasz et al. (2015) applied metabolomics to identify the differences that are characteristic for cold acclimation and transition in wheat, from the vegetative to the reproductive phases, both in a *T. monococcum* accession KU 104-1 and *T. aestivum* cv. (cultivar) Chinese Spring and investigated the involvement of chromosome 5A and its VRN1 (vernalization

gene) region in these two processes. Samples were taken from the shoots and crowns during four developmental stages: plants grown at 20/17°C, after cold treatment but still during the vegetative phase, at the double ridge and during spikelet formation. Targeted metabolite analysis using gas chromatography-mass spectrometry was employed. They managed to measure 47 compounds and annotated 38 of them. This included amino acids, organic acids, sugars and sugar alcohols. In general, cold increased the levels of primary metabolites both in the shoots and crowns. Significant increases in the proline levels were observed in most of the treated samples. Increases were also detected in the fructose, trehalose, raffinose, maltose, turanose, sucrose, glucose, galactinol, GABA, glutamine and asparagine levels. In conclusion, the results of their study demonstrated that the levels of compatible solutes increased in response to cold treatment but not at the same scale for all lines and also not equally in the shoots and crowns. The distinct and overlapping accumulation patterns of metabolites suggest the complex genetic regulation of metabolism in the shoots and crowns.

For plant lipidomics studies upon cold stress, Welti et al. (2002) were the first to report a comprehensive lipid profiling on *Arabidopsis* exposed to cold (4°C) and freezing (-2°C and -8°C) stress using LC-electrospray ionisation (ESI)-triple quadrupole (QqQ)-tandem MS. They discovered that freezing at a sub-lethal temperature induced declines in many molecular species of phosphatidylcholine (PC), phosphatidylethanolamine (PE), and phosphatidylglycerol (PG) but induced an increase in phosphatidic acid (PA) and lysophospholipids. To probe the metabolic steps generating these changes, they further analyzed the lipids of *Arabidopsis* deficient in the most abundant phospholipase D, phospholipase D (PLDα). Again, they found that the PC content dropped only half as much, and PA levels rose only half as high in the PLDα-deficient plants as in wild-type plants. In contrast, neither PE nor PG levels decreased significantly in wild-type plants compared to PLDα-deficient plants. Their study suggests that PC species were the major *in vivo* substrates of PLDα. The action of PLDα during freezing is of special interest because *Arabidopsis* plants that are deficient in PLDα have improved tolerance to freezing. The greater loss of PCs and increase in PAs in wild-type plants as compared with PLDα-deficient plants may be responsible for destabilizing membrane bilayer structures, resulting in a greater propensity toward membrane fusion and cell death in wild-type plants. The finding from this study became an important reference for other plant researchers to expand their lipidomics studies to cold stressed important crops such as rice (Zheng et al., 2016), wheat (Li et al., 2015) and barley (Margutti et al., 2019), which will be described below.

Zheng et al. (2016) reported the investigation of the responses of the glycerolipidomes of rice and Arabidopsis using LC-ESI-QqQ MS after exposure of the plants to chilling (4 and 10 °C) and freezing (−6 and −12 °C) temperatures, respectively. Rice is a chilling-sensitive plant that dies after the temperature falls to 4 °C (Shinkawa et al., 2013). In contrast, after acclimation to cold at 4 °C, Arabidopsis can tolerate freezing temperatures as low as −6 °C (Li et al., 2004). They discovered that Arabidopsis contains higher levels of galactolipids than rice and has a higher double bond index (DBI). Arabidopsis contained lower levels of high melting point phosphatidylglycerol (PG) molecules and has a lower average acyl chain length (ACL), thus could make the membranes of Arabidopsis more fluid at low temperatures. Meanwhile, they also observed noticeable phospholipid degradation occurring during the recovery culture period of non-lethal chilling treated rice, which did not occur in non-lethal freezing treated Arabidopsis. Glycerolipids with larger head groups were also observed to be synthesised more in Arabidopsis than in rice at sub-lethal low temperature. The ability to synthesize glycerolipids containing a larger head group may correlate with low temperature tolerance. Both the levels of phosphatidic acid (PA) and phosphatidylinositol (PI), which have been reported to act as signaling molecules, rose in both plant species after low-temperature treatment.

On the other hand, Li et al. (2015a) conducted the glycerolipidome studies on three different plant species (Arabidopsis, wheat and *Atriplex lentiformis*) under different temperature stresses (cold and heat stress for Arabidopsis, heat stress for *A. lentiformis* and cold stress for wheat). They reported the significance of the glycerolipid pathway balance in temperature-induced lipid compositional changes in three plant species that have distinctive modes of lipid pathway interactions. Photosynthetic tissues of higher plants contain 60–70% trienoic fatty acids. The so-called “C18:3” plants are generally the most advanced families of angiosperms (pea, spinach, wheat and etc.) whose position sn-2 of the galactolipids is esterified exclusively by polyunsaturated fatty acids with 18 carbon atoms. The “C16:3” plants are from the families of angiosperms (eg. Brassicaceae) whose position sn-2 of the galactolipids is esterified by polyunsaturated fatty acids with 16 or 18 carbon atoms (Dubacq et al., 1983). *Arabidopsis thaliana*, a model “C16:3” plant, was raised at low (10°C), high (30°C), or standard (22°C) growth temperature, under similar light intensity and with an identical light cycle (16 h/8 h). Wheat, a “C18:3” plant and also a valuable system in which to assess metabolic response to low temperature in cold adaptation and cold acclimation for freezing tolerance were grown at 23°C for 2 weeks (control) and then shifted to 4°C for another 2 weeks. *Atriplex lentiformis* of the Chenopodiaceae

family is a unique species in regard to fatty acid phenotype: it switches from that of a "C16:3" plant to "C18:3" under extreme heat. To assess the effect of high temperatures, *A. lentiformis* plants were grown at 23°C or 43°C for 8 weeks. Lipid compositions of Arabidopsis, *A. lentiformis*, and wheat which were grown at various temperatures were first quantitatively assessed by two-dimensional TLC (2D-TLC), followed by gas chromatography quantification of fatty acid methyl esters. Relative contributions of the prokaryotic and eukaryotic pathways were then delineated through stereo-specific analysis of fatty acid distribution in various lipid classes. Lipid profiles for *A. lentiformis* and wheat were further interrogated at the level of head group, carbon chain length, and double bonds of the acyl groups through electrospray ionization tandem mass spectrometry (ESI-MS/MS). They found that in Arabidopsis, a typical "C16:3" plant, low temperature induced an augmented prokaryotic pathway, whereas high temperature enhanced the eukaryotic pathway. *Atriplex lentiformis* switched its lipid profile from "C16:3" to "C18:3" when it encountered heat and reduced its overall lipid desaturation through drastically increasing the contribution of the eukaryotic pathway. In wheat, which is a "C18:3" plant, low temperature caused a reduced contribution from the ER pathway to chloroplast lipid biosynthesis. Together with transcriptomics data, these studies demonstrated that metabolic adjustments from different intracellular glycerolipid pathways represented a major regulatory mechanism through which the provision of lipid substrates for membrane desaturation is regulated under temperature stress.

Margutti et al. (2019) conducted a cold stress study on barley seedlings (4°C for 6 hrs and 36 hrs, respectively) and analysed the glycerolipidomes of the leaves and roots using the ESI-MS/MS platform. They observed that that the level of phospholipids and galactolipids was higher in roots than in leaves, although the phospholipid to galactolipids ratio was similar for both tissues. Compared with plants grown at control temperature at 25 °C, the chilling treatment produced contrasting responses in phospholipids and galactolipids. A slight increasing trend in unsaturated fatty acid-enriched phospholipids was observed in leaves during 6 hrs of chilling. By contrast, there was a decrease in plastidic and extraplastidic phospholipids in roots during 36 hrs of chilling. The contrasting and spatial-temporal behaviour of the plant tissues may indicate a particular chilling sensing mechanism of the plant in response to external environmental fluctuations.

1.3.1 Metabolomics and Lipidomics as Promising Tools to Understand Cold Stress Response in Australian Wheat and Breeding of Cold-tolerant Cultivars

As mentioned earlier, minimising the loss caused by chilling and frost events is critical for breeders in Australia. One of the solutions is by the development of more cold/frost-tolerant wheat cultivars. We first need to understand the underlying molecular mechanisms of Australian wheat cultivars subjected to cold stress using functional genomics, transcriptomics, metabolomics and lipidomics approaches. While some of the genetic diversity of Australian wheat have been profiled and sequenced (Edward et al., 2012) and also QTL mapping for abiotic stress tolerance in cereals have been done (Dolferus et al., 2013; Hill et al., 2013), there is a lack of reports on the comprehensive metabolite profiling of Australian wheat subjected to cold stress to date. Referring to the successful examples mentioned in part 1.3 above, metabolomics and lipidomics via high-end mass spectrometry could serve as promising tools to understand cold stress response in Australian wheat cultivars.

1.4 Engineering of Cold-induced Transcription Factors to Increase the Cold Tolerance in Plants

Development of transgenic plants for cold tolerance is a fast and effective biotechnological tool to improve agricultural crops. Engineering genes encoding transcription factors are found useful for the improvement of stress tolerance in plants (reviewed in Yadav, 2010). The CBF/DREB transcription factors were the first transcriptional activators demonstrated to have a role in controlling the expression of cold-responsive genes to contribute to cold acclimation (Van Buskirk et al., 2006). The *CBF* genes encoding transcription factors that belong to the *AP2/ERF* (*APETALA 2/ETHYLENE-RESPONSIVE ELEMENT BINDING FACTOR*) domain family of DNA-binding proteins (Cook et al., 2004). The proteins encoded by these *CBF1*, *2* and *3* genes are transcriptional activators which contain *AP2/ERF* DNA binding domains that recognize the *CRT/DRE* element present in the promoters of *COR* (*COLD RESPONSIVE*) and other cold-regulated genes. Constitutive overexpression of *CBF1, 2* or *3* in transgenic Arabidopsis plants results in constitutive expression of the *COR* and other *CRT/DRE*-containing target genes and an increase in whole plant freezing tolerance in the absence of a cold stimulus (Gilmour et al. 2000, Gilmour et al. 2004, Jaglo-Ottosen et al. 1998, Kasuga et al. 1999, Liu et al. 1998). Metabolomics analyses demonstrate that cold stress induces the accumulation of many metabolites, such as sugars, and a large portion of these metabolites also accumulate in transgenic Arabidopsis constitutively overexpressing *DREB1s/CBFs* (Cook et al., 2004; Maruyama et al., 2009). Furthermore, overexpression of Arabidopsis *DREB1/CBF* genes improves freezing tolerance in oilseed rape (Jaglo et al., 2001) and confers chilling tolerance in tomato, tobacco and rice (Hsieh

et al., 2002; Kasuga et al., 2004; Ito et al., 2006). In addition, Morran and colleagues (2011) have investigated the possibility of modulating the transcriptional regulation of drought and cold responses in wheat and barley, with the aim to increase drought and frost tolerance. They overexpressed the TaDREB2 and TaDREB3 transcription factors isolated from wheat grain, together with constitutive expression of promoter (double 35S) and drought-inducible promoter (maize Rab17) in wheat and barley plants. Both the TaDREB2 and TaDREB3 transgenic plants showed improved survival under severe drought conditions relative to non-transgenic controls. In addition to drought tolerance, both TaDREB2 and TaDREB3 transgenic plants with constitutive overexpression of the transgene showed a significant improvement in frost tolerance. The increased expression of TaDREB2 and TaDREB3 led to elevated expression in the transcripts of ten other *CBF/DREB* genes and a large number of stress responsive *LEA/COR/DHN* genes known to be responsible for the protection of cell from damage and desiccation under stress.

Despite of conferring enhanced cold tolerance to the plants, constitutive overexpression of the *CBF/DREB* genes in Arabidopsis using 35S cauliflower mosaic virus (CaMV) promoter have been reported to cause stunted growth under normal growth conditions, a decrease in seed yield and a delay in flowering (Liu et al., 1998; Kasuga et al., 1999; Gilmour et al., 2000, Gilmour et al., 2004; Dubouzet et al., 2003). However, not all the overexpression of *CBFs* will cause those impacts of cold tolerance in the plants. Constitutive expression of traits that are normally induced in response to environmental stress will not always lead to impact in the absence of that stress (Jackson et al., 2004). Jackson et al. (2004) reported that the overexpression of *CBF1* in Arabidopsis did not show impact of cold tolerance (evaluated by the reduction of fruit/seed number) in the control environment, instead showing a marginal fitness benefit (increased in fruit number) in the cold environment. Meanwhile, the overexpression of *CBF2* and *3* showed impact of cold tolerance (reduction of fruit number) in both control and cold environments. Zhen et al. (2011) also reported the similar findings in which all the constitutive *CBFs* overexpression lines exhibited high survival under cold exposure. The *CBF1* overexpression lines displayed no cost of cold tolerance by maintaining the fitness (fruit number production) comparable to the wild type and null vector control lines. In contrast, overexpression lines *CBF2* and *CBF3* exhibited significantly lower fitness compared to the null vector line, indicating a clear impact of cold tolerance.

There were several attempts to overcome the problems of these impact of cold tolerance by cutting down the duration of *CBF/DREB* overexpression using stress-inducible promoters,

instead of the constitutive promoter. The first such attempt was undertaken in 1999 (Kasuga et al., 1999). They used the rd29A promoter for the expression of *DREB1A* which gave rise to minimal effects on plant growth while providing an even greater tolerance to stress conditions than the CaMV promoter. The rd29A promoter was later used by several other groups for the expression of DREB factors in other plants such as tobacco (Kasuga et al., 2004) and wheat (Hao et al., 2005). Usage of other stress-inducible promoters for the overexpression of *CBF* were also reported. Morran et al., (2011) reported that transgenic wheat and barley with constitutive overexpression of *CBFs* showed slower growth, delayed flowering and had lower grain yields relative to the non-transgenic controls, though improved survival under severe drought and frost conditions relative to non-transgenic controls were observed. However, the undesired changes were alleviated by using a drought-inducible promoter, maize Rab17. Hsieh et al., 2002 also reported that tomato plants over-expressing the Arabidopsis *CBF1* gene under the control of barley abrc1 or cor15A stress-inducible promoters showed normal development and drought tolerance.

1.5 REIL Protein as a New Potential Cold Acclimation Factor in *Arabidopsis thaliana* and Wheat

The successful study of DREB1/CBF transcription factors as cold acclimation factor in Arabidopsis, and their application in other plants led to the hypothesis that there might be other new transcription factors that could act as potential cold acclimation factor in plants. In this study, we chose to study the Arabidopsis REIL protein as our starting point and the importance of this protein is discussed in this section and the last section of this chapter.

The Arabidopsis REIL protein obtains its name from the yeast homolog Rei1 proteins (Required for isotropic bud growth1 protein) [Iwase and Toh-e, 2004; Schmidt et al., 2013]. In Arabidopsis, there are two REI1-LIKE (REIL) proteins called REIL1 and REIL2. REIL1 is encoded by At4g31420 and the REIL2 paralog is encoded by At2g24500. The REIL1 and REIL2 are homologs of the yeast Rei1 and paralog Reh1 proteins. Both the Arabidopsis REIL proteins are plant zinc finger proteins with four C2H2-type zinc finger domains. In Arabidopsis, there are only 32 proteins that contain four zinc finger domains and the REIL protein is one among them (Englbrecht et al., 2004; Ciftci-Yilmaz and Mittler, 2008; Schmidt et al., 2013). The Arabidopsis REIL genes were also previously annotated as putative sequence-specific DNA-binding transcription factors (http://www.arabidopsis.org; Schmidt et al., 2013).

The biogenesis of eukaryotic ribosomes is a fundamental process involving hundreds of ribosome biogenesis factors (RBFs) in three compartments of the cell, namely the nucleolus, nucleus, and cytoplasm (Weis et al., 2015). In yeast, both the Rei1 and Reh1 are known to function as one of the RBFs that participate in the late cytoplasmic 60S ribosomal subunit maturation step. In the cytoplasmic 60S maturation (**Fig. 1-12A**), Rei1 is thought to be recruited to the cytosolic pre-60S subunit by Rlp24p (Ribosomal-like protein24). Rlp24p needs to be removed before Rei1p can load onto the cytosolic 60S pre-ribosome. Both the yeast Rei1 and Reh1 were found to insert their C-terminus into the polypeptide exit tunnel of the non-translating immature 60S subunit. Jjj1p (Type III j-protein 1) is a Hsp40 (Heat shock protein 40) heat shock chaperone which cooperates with Rei1p to remove Alb1p (ARX1 little brother1) from the pre-60S subunit. This step initiates Arx1p (ribosomal export complex1) and Alb1p recycling to the nucleus. Arx1p release, in turn, is thought to be prerequisite of the final releases of Tif6p (translation initiation factor6) and Nmd3p (Non-sense-mediated mRNA decay3 protein) from the pre-60S subunit. These processes form the final control point that renders the cytosolic pre-60S ribosomal subunits of yeast mature and translationally active ribosomes (Schmidt et al., 2014; Greber et al., 2016). Apart from that, these Rei1 and Reh1 proteins are also required by yeast to maintain growth in suboptimal or cold condition. The yeast *reh1* mutant has no effect on growth in the cold, the *rei1* mutant is cold sensitive even at moderately suboptimal temperatures (23-25°C), whereas the *rei1reh1* double mutant is more cold sensitive (Iwase and Toh-e, 2004; Lebreton et al., 2006; Parnell and Basu, 2009).

For the model plant *Arabidopsis thaliana*, the ribosome biogenesis, especially the maturation of 60S, has been extensively reviewed in Weis et al. (2015), Saez-Vasquez and Delseny (2019). The Arabidopsis genome contains homologs for most 60S RBFs, indicating that the mechanisms of 60S assembly are conserved in animals, yeast and plants. With a few exceptions, most of these protein homologs of yeast and human 60S RBFs are encoded by single-copy genes in Arabidopsis (Saez-Vasquez and Delseny, 2019). The disruption or inhibition of these orthologous genes causes pre-60S processing deficiencies along with lethality during gametogenesis or embrogenesis, or non-lethal defects in plant growth and developmental such as pointed leaves, aberrant flower morphogenesis, slower seedling growth, impaired root growth and more (Weis et al., 2015).

To investigate whether REIL functions in 60S ribosomal biogenesis and the requirement for growth at cold conditions are conserved in Arabidopsis (as observed in the yeast), Schmidt et

al. (2013; 2014) first studied the topology of the *A. thaliana* REIL genes, then isolated transfer DNA (T-DNA) mutants of the REIL genes and tested their growth response to suboptimal temperature. In the study presented by Schmidt et al. (2013), they discovered that REI1-LIKE protein REIL1 was encoded by At4g31420 and the REIL2 paralog was encoded by At2g24500. REIL genes represent a small gene family and belong to the few (18.8%) evolutionarily conserved zinc finger proteins (Englbrecht et al., 2004; Ciftci-Yilmaz and Mittler, 2008). The *A. thaliana* REIL genes have five exons, which encode a 404-amino acid for REIL1 protein with gene model At4g31420.1, and a 395-amino acid for REIL2 protein with gene model At2g24500.1. REIL1 has a putative splice site variant, At4g31420.2, which adds an additional Ser at position 281 of REIL1 but leaves the protein otherwise unchanged. The four zinc finger domains of REIL proteins are positioned in two pairs, ZF1/ZF2 and ZF3/ZF4, at the N terminus and in the center of the sequence. Two additional highly conserved domains, here provisionally termed CD1 and CD2, are located close to the C terminus (**Fig. 1-13A**). The two genes REIL1 and REIL2 are conserved among *A. thaliana*, *Arabidopsis lyrata* ssp. lyrata, and *Thellungiella halophile* (**Fig. 1-13B**). The Schmidt et al. studies (2013; 2014) also described the evolution of *Arabidopsis* REIL proteins that diverged from yeast prior to the duplication events (Fig.13B). In contrast to the four zinc finger domains present in Arabidopsis REIL1 and REIL2 that are arranged in two C2H2 zinc finger pairs, namely ZF1/ZF2 at the N terminus and ZF3/ZF4 in the middle of the protein (Schmidt et al., 2013), the yeast paralogs contain only three zinc fingers (Iwase and Toh-e, 2004; Greber et al., 2012).

Schmidt and colleagues (2013, 2014) discovered partial conservation of *Arabidopsis* REIL functions with the yeast homolog Rei1 and paralog Reh1, which are to function as ribosome biogenesis factor for 60S subunit and are also required for plant growth in the cold. Interestingly, the *A. thaliana* REIL paralogs are required specifically for plant growth at suboptimal/cold temperature (10°C) but not for growth at the optimal temperature (20°C). A *reil1-1 reil2-1* double mutant's growth is arrested at 10°C prior to the emergence of the first rosette leaf. Two allelic *reil2* single mutants, *reil2-1* and *reil2-2*, form small spoon-shaped leaves at 10°C. This phenomenon was reverted after shifting plants back to the optimal temperature, 20°C. Except for a slightly delayed germination, a *reil1-1* single mutant showed no further growth phenotype under the currently investigated conditions (**Fig. 1-14**; Schmidt et al., 2013). Interestingly, heterologous expression of *Arabidopsis* REIL1 but not of REIL2 complemented the temperature-dependent growth defect of the yeast *rei1* mutant. Considering that gene duplication events apparently created

the two paralogs in yeast and Arabidopsis independently, convergent evolution of the role of REIL proteins for growth at suboptimal temperature can be proposed.

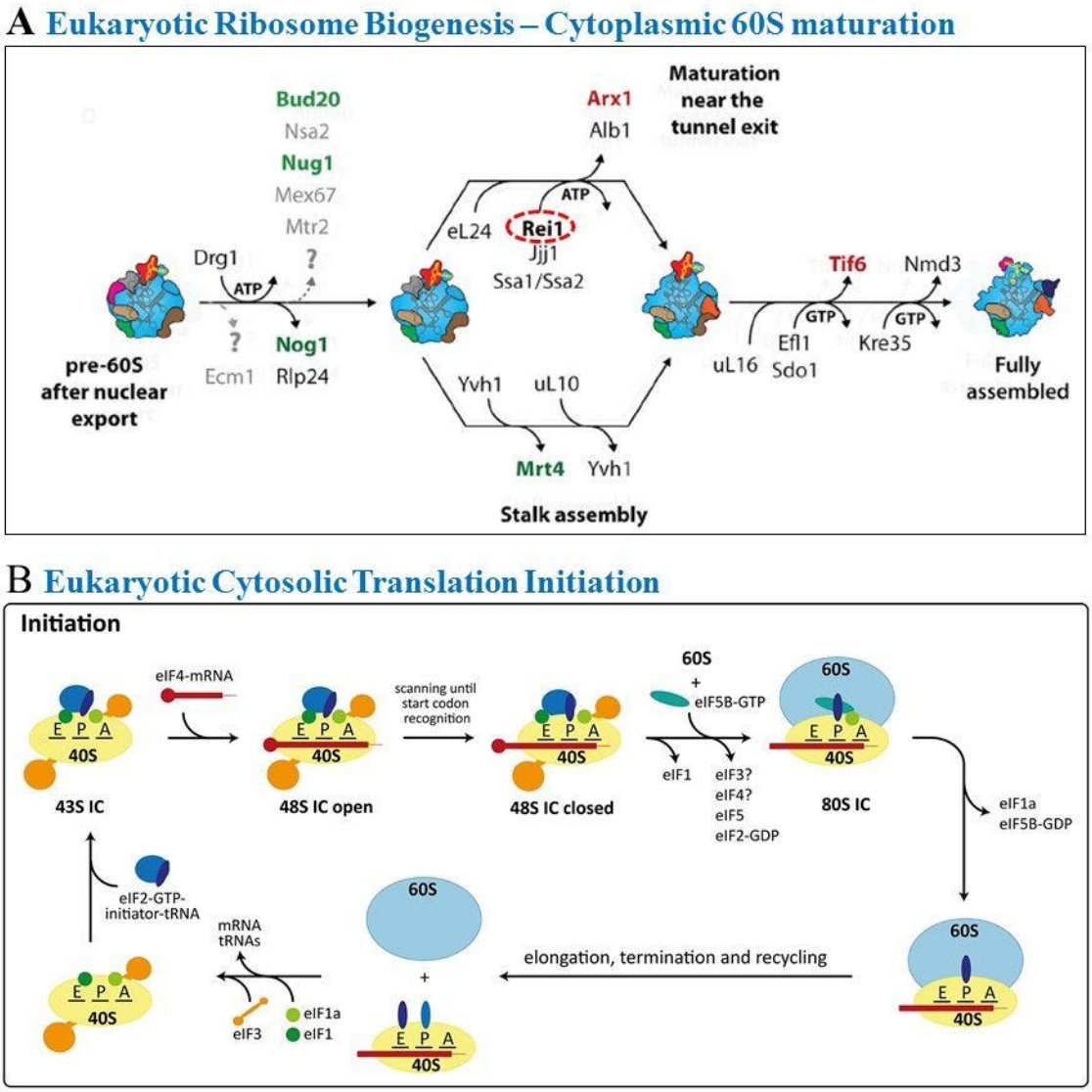


Figure 1-12. Eukaryotic ribosome biogenesis and translation initiation. **(A)** The flow scheme represents the current model of the yeast cytosolic 60S maturation machinery starting with the pre-60S subunit after export from the nucleus and ending with the translational active 60S ribosomal subunit. The direct mechanistic interaction partners of the yeast Rei1 protein within the model are indicated by red circle. **(B)** The diagram illustrating the involvement of the 40S, 60S and 80S in the eukaryotic cytosolic translation initiation (Sources: Diagram A is taken from Greber et al., 2016 and B are taken from The Ban Lab, ETH Zurich (http://www.bangroup.ethz.ch/research/eukaryotic_ribosome.html).

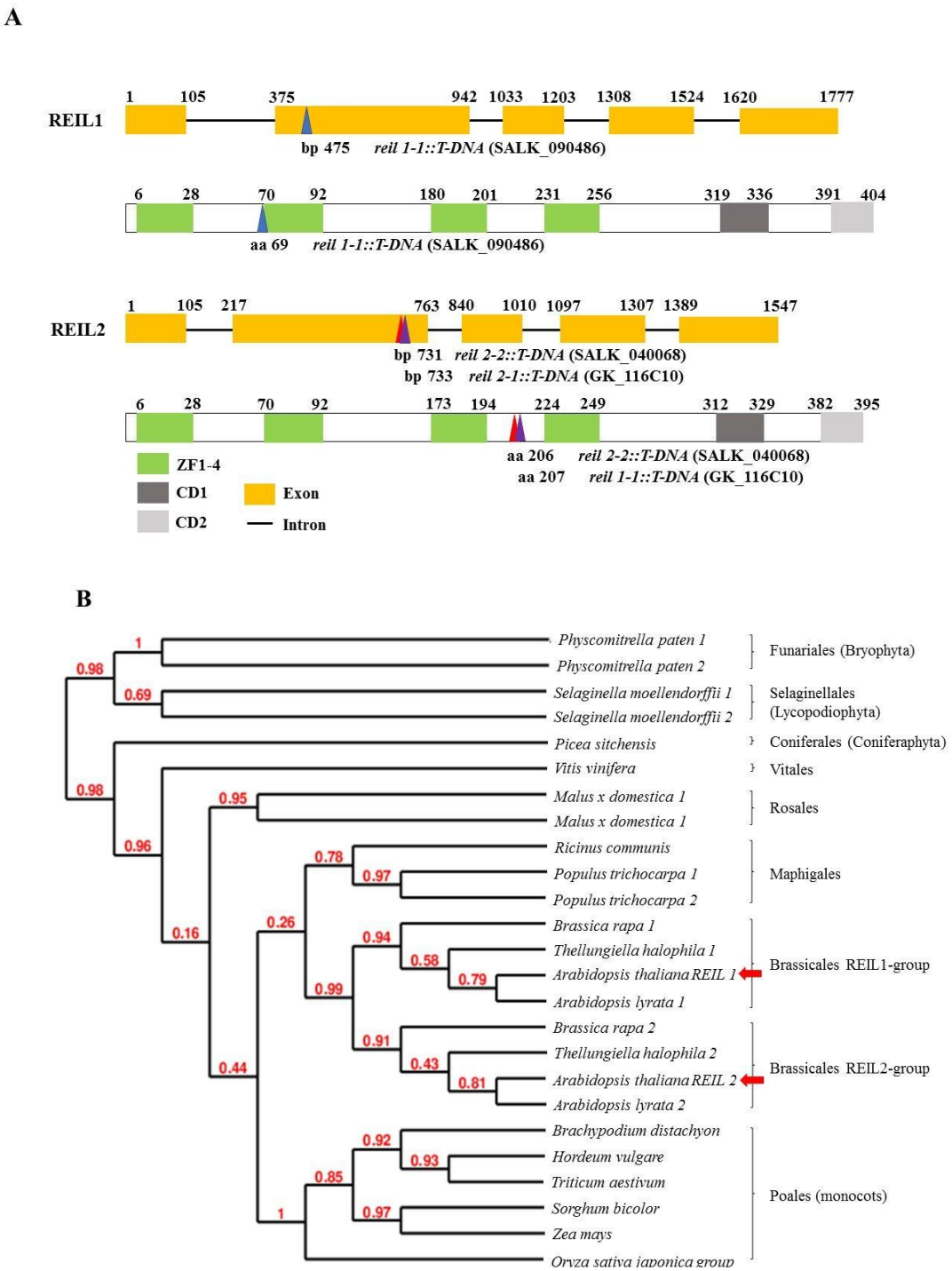


Figure 1-13. (A) Topology of *A. thaliana* REIL genes and proteins. The REIL1 and REIL2 genes have five conserved exons. The respective REIL proteins, namely the 404-amino acid REIL1 and the 395-amino acid REIL2 protein, contain four zinc finger domains and two additional conserved domains, CD1 and CD2. The mutants, *reil1-1* (SALK_090486), *reil2-1* (GK_166C10), and *reil2-2* (SALK_040068), carry T-DNA insertions in exon 2 (compare with arrowheads). **(B)** Phylogenetic analysis of the plant REIL proteins. The plant REIL proteins were subject to gene duplications, which occurred independently in several plant phylae. The REIL1 and the REIL2 paralogs of *A. thaliana* (indicated by red arrows) originated from gene duplication during the speciation of the Brassicales (modified from Schmidt et al., 2013).

To take the next step toward the functional analysis of *Arabidopsis* REIL proteins studied by Schmidt et al., (2013, 2014), Beine-Golovchuk et al., (2018) have conducted a study to investigate both the evidence of functional conservation and indications of plant-specific functions of the *Arabidopsis* REIL proteins, which may have been added on the evolutionary path toward the multicellular embryophyte *Arabidopsis*. For this purpose, they first established the previously created double mutant *reil1-1 reil2-1* as a valid plant system for the investigation of REIL function in *Arabidopsis's* mature leaves. They characterized the *reil1-1 reil2-1* acclimation process to low temperature (10°C) in comparison with the *Arabidopsis* Columbia-0 (Col-0) wild type. They confirmed the previous observation (Schmidt et al., 2013) that young developing rosette leaves grown at standard temperature (20 °C) had a mild pointed-leaves phenotype (**Fig. 1-15A**). This leaf phenotype is a characteristic of many cytosolic ribosomal mutants (Van Lijsebettens et al., 1994; Horiguchi et al., 2012). When the wild type and mutant plants were grown at constant low-temperature conditions at 10°C/8°C (day/night), the mutant plants survived at least 13 weeks after germination and transfer to soil but remained extremely dwarfed (**Fig. 1-15B**). In the temperature shift regime transferring plants from 20°C to 10°C, growth and development of the mutant were again arrested after the shift (**Fig. 1-15C**). In the temperature shift from 20°C to a lower temperature 4°C/4°C (day/night) regime, both mutant plants and the wild type were growth arrested (**Fig. 1-15D**). In conclusion, the *reil1-1 reil2-1* mutant stops growth and development when exposed to low temperature.

Beine-Golovchuk et al. (2018) also reported that in contrast to yeast, REIL1 may be present in the translating ribosome. Their study revealed that wild-type *Arabidopsis* remodels the cytosolic translation machinery when grown at 10°C by accumulating cytosolic ribosome subunits, particularly 60S subunits, and by inducing the expression of cytosolic ribosomal RNA, ribosomal genes, ribosome biogenesis factors, and translation initiation or elongation factors (**Fig. 1-16**). Therefore, they suggested that *Arabidopsis* REIL proteins may influence cold-induced plant ribosome remodeling and enhance the accumulation of cytosolic ribosome subunits after cold shifts either by *de novo* synthesis or by recycling them from the translating ribosome fraction. In the *reil1-1 reil2-1* mutant, all physiological processes associated with growth were delayed, although the plants still maintained cellular integrity or acquired freezing tolerance. REIL proteins were also found to involve in plant-specific processes that do not exist in yeast. For example, the double mutant *reil1-1 reil2-1* already exhibited cold-acclimation responses at the non-acclimated

state (optimal temperature, 20°C), including the activation of the DREB/CBF regulon. REIL function therefore may contribute to "temperature perception or signal transduction" by suppressing "premature cold responses" during growth at non-stressful temperatures.

Another recent cold stress study on REIL using Arabidopsis seedlings published by Yu et al. (2020) also reported the importance of REIL2 protein in conferring cold stress tolerance to plants by promoting rRNA processing and CBF protein translation. Via screening of the Arabidopsis transfer DNA (T-DNA) insertion library, Yu and colleagues identified a cold-hypersensitive mutant, which they named it stch4 (sensitive to chilling 4). This *STCH4* was annotated to be in the gene *REIL2* (At2g24500) (Schmidt et al., 2013). Overexpression of STCH4 conferred chilling and freezing tolerance in Arabidopsis overexpression lines compared to the Col-0 wild type and *stch* mutant lines, when grown at 4°C. Besides, they also showed that the *stch4* mutation reduces CBF protein levels and thus delayed the induction of C-repeat binding factor regulon or the cold late-responsive genes such as *COR15a* and *RD29a*. In addition, ribosomal RNA processing was reduced in *stch4* mutants, especially under cold stress. STCH4 was then thought to be associated with multiple ribosomal proteins, and these interactions were modulated by cold stress. In conclusion, their results suggested that the ribosome is a regulatory node for cold stress responses and that STCH4 promoted an altered ribosomal composition and functions in low temperatures to facilitate the translation of proteins important for plant growth and survival under cold stress.

Based on the findings reported by Schmidt et al. (2013; 2014), Beine-Golovchuk et al. (2018) and Yu et al. (2020) above, we strongly hypothesize the role of REIL proteins as potential cold acclimation factors in Arabidopsis. Further studies in the other organs such as roots were thought necessary to confirm this. Besides functional analyses, we were also interested to understand if this protein could serve as potential cold acclimation factor in wheat. More details of the objectives that motivate this PhD study are elaborated in the next section and in Chapter 4 and 5.

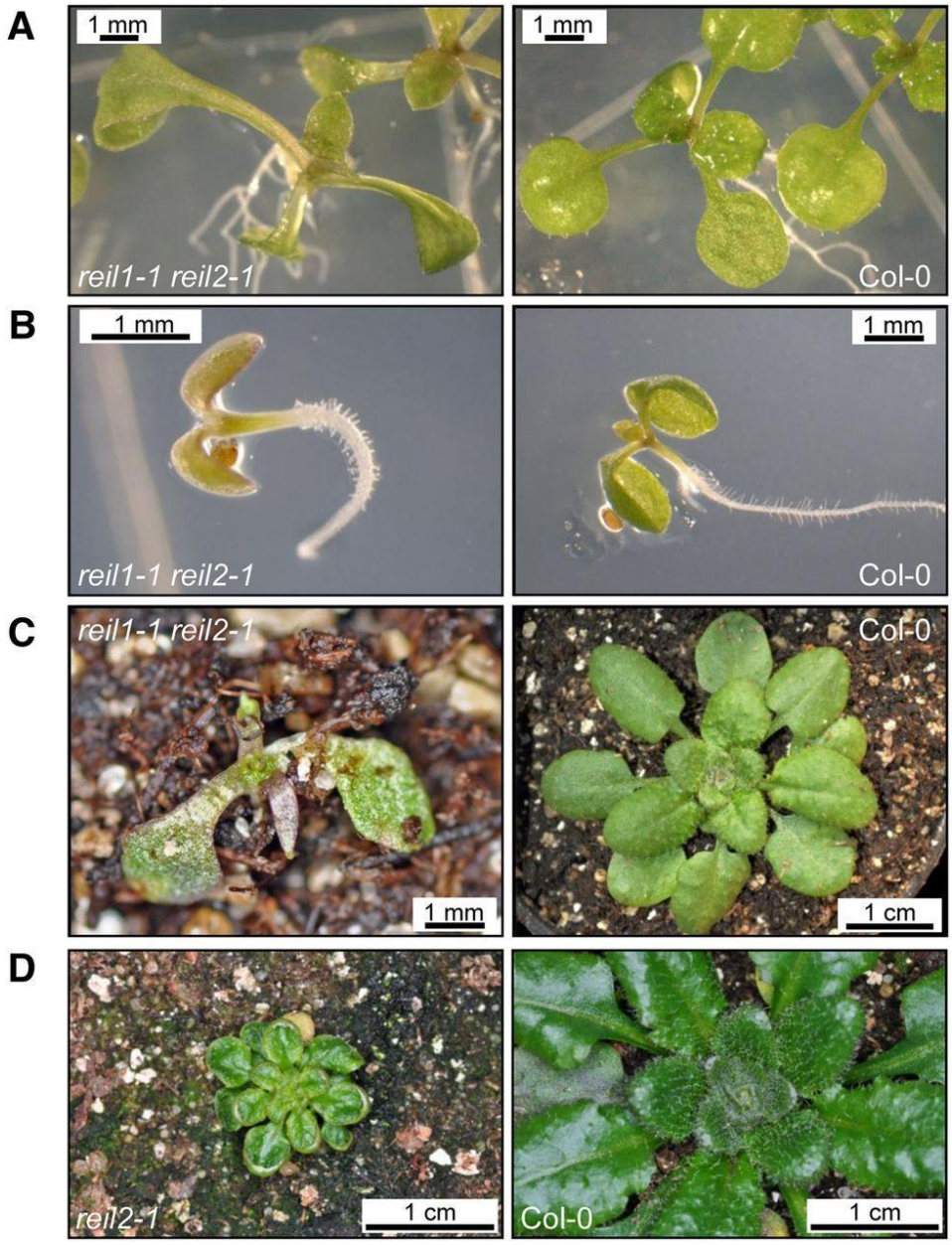


Figure 1-14. The aberrant leaf phenotypes of the *reil1-1 reil2-1* double mutant and of the *reil2-1* single mutant. **(A)** Pointed-leaves morphology of the *reil1-1 reil2-l* double mutant compared with Col-0 after 16 days at 20°C. **(B)** Growth arrest of the *reill-1 reil2-l* double mutant at stage 1.0 (Boyes et al., 2001) after 27 days at 10°C compared with Col-0. **(C)** The phenotype of the *reill-1 reil2-l* double mutant germinated at 10°C, transferred to soil, and kept for 10 weeks strictly at 10°C compared with the wild type. **(D)** The representative phenotype of the *reil2-l* mutant germinated at 10°C, transferred to soil, and kept for 5 to 6 weeks strictly at 10°C compared with the Col-0 wild type (Schmidt et al., 2013).

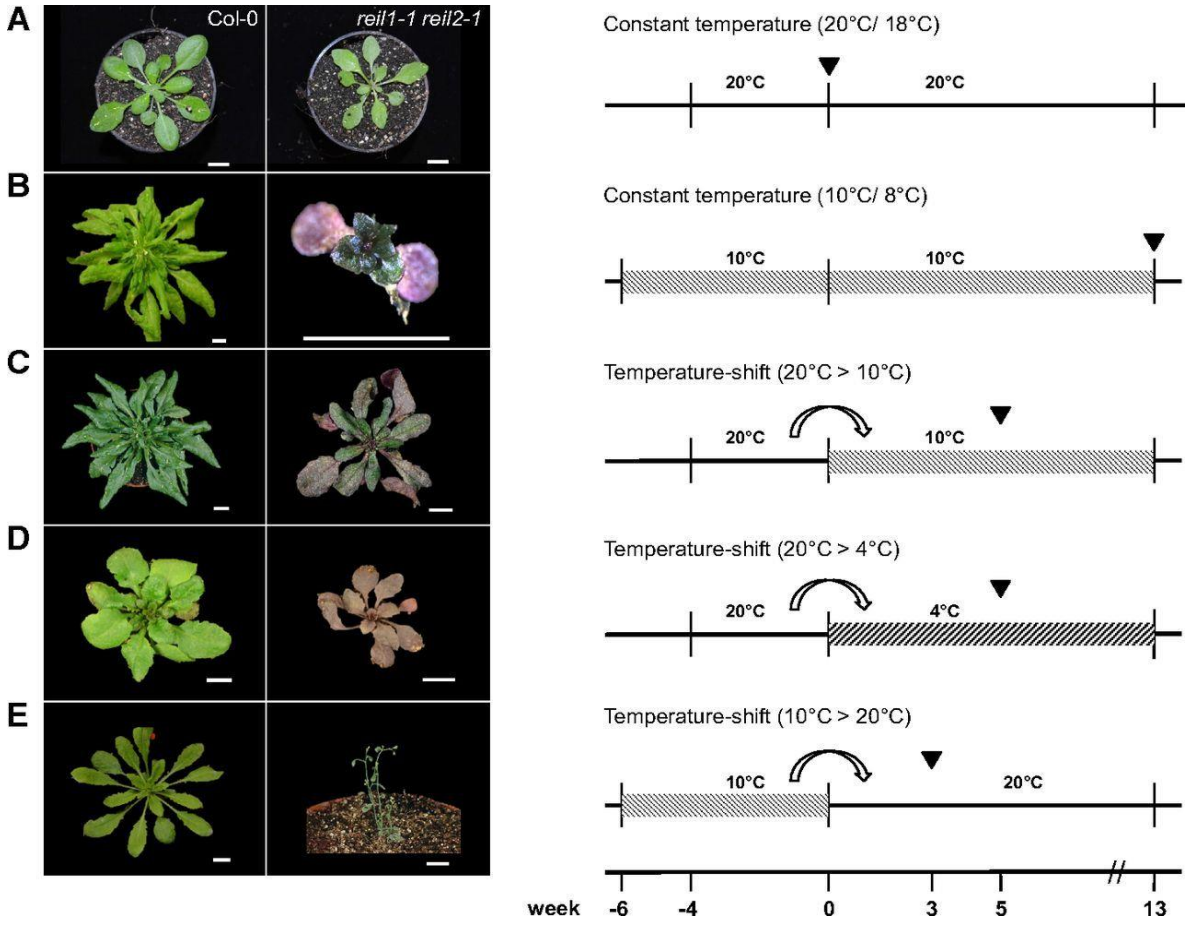


Figure 1-15. Developmental phenotypes of the Arabidopsis wild type (Col-0) and *reil1-1 reil2-1* mutant under standard and different suboptimal temperature regimes. **(A)** Constant standard temperature conditions at 20°C/18°C (day/night). Mutant and wild type plants reached vegetative developmental stage ~1.10 (Boyes et al., 2001) approximately 4 weeks after transfer to soil. Note that the mutant had a mild pointed-leaves phenotype. **(B)** Constant low-temperature conditions at 10°C/8°C (day/night). Mutant plants survived at least 13 weeks after germination and transfer to soil but remained extremely dwarfed, with final rosette diameters less than 1 cm and only five to seven visible leaves. **(C)** Temperature shift from the 20°C to the 10°C regime. In contrast to the acclimating wild type, growth and development of the mutant were arrested. Mutant plants survived at least 13 weeks at low temperatures. **(D)** Temperature shift from the 20°C to a 4°C/4°C (day/night) regime. Mutant plants and the wild type were growth arrested. Mutant survival was not tested. **(E)** Inverse temperature shift from the 10°C to the 20°C regime. In contrast to the de-acclimated wild type, mutant plants entered a rapid flowering program reminiscent of stress-induced early flowering. Temperature shifts in C and D were performed at developmental stage ~1.10 of wild-type and mutant plants at the stages shown in A at week 0. Note that plant age is given by week prior to or post developmental stage ~1.10. Plants were germinated under sterile conditions (Schmidt et al., 2013) and transferred to soil at stage 1.02-1.03 (i.e. at −6 weeks [10°C] or −4 weeks [20°C]). The inverse temperature shift from 10°C to 20°C (E) was performed when the wild type reached stage ~1.10 at 10°C. Co-cultivated mutant plants had stage 1.02-1.03. Arrowheads within the experimental schemes indicate the time at which representative photographs of n ⩾ 10 plants per experiment were taken. Bars = 1 cm (Beine-Golovchuk et al., 2018).

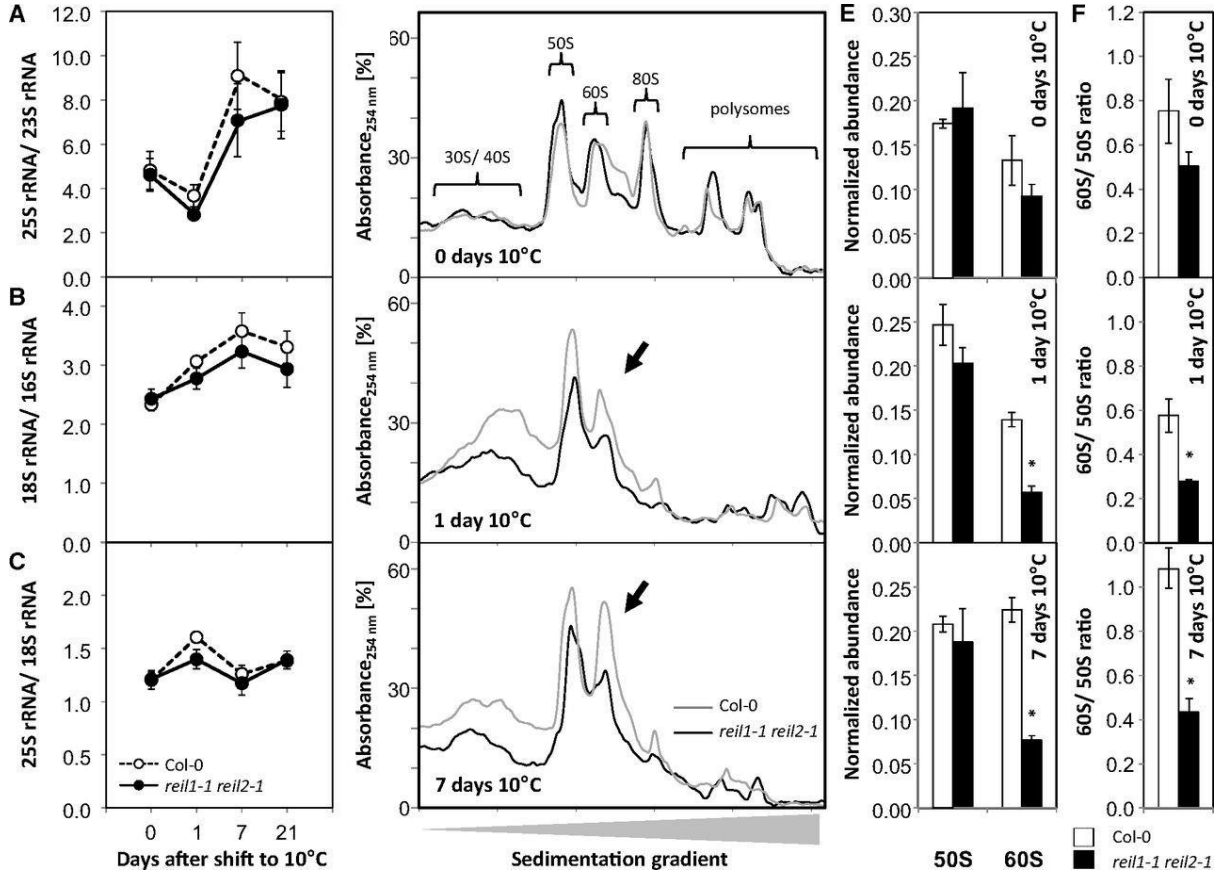


Figure 1-16. Relative abundance of rRNAs within total RNA preparations and of 60S and 50S large ribosomal subunits from total ribosome preparations before and after the shift to 10°C. Complete *reil1-1 reil2-1* rosettes were compared with wild-type (Col-0) rosettes in the non-acclimated state (i.e. at 0 d) and at 1, 7, and 21 d after transfer to the cold according to cultivation scheme C in Figure 15. **(A)** Ratio of the cytosolic 25S large subunit rRNA relative to chloroplast 23S rRNA (P = 0.001). **(B)** Ratio of the cytosolic small subunit 18S rRNA relative to chloroplast 16S rRNA (P = 0.003). **(C)** Ratio of the cytosolic 25S large subunit rRNA and cytosolic 18S small subunit rRNA. For A to C, data are means ± se (n = 3–4 preparations from independent pools of mature rosette leaves). **(D)** Representative sedimentation profiles of total ribosome preparations from ~100 mg fresh weight of rosettes sampled at days 0, 1, and 7 of acclimation to 10°C. The sedimentation analysis was optimized for the separation of the 50S to 60S fractions. Indicated fractions were monitored by blank gradient subtracted absorbance (A_{254}). Fraction identity was verified by rRNA analysis. (E) Analysis of ribosome sedimentation profiles shown in D by calculating the normalized A_{254} abundance of the 60S and 50S fractions relative to the sum of all observed fractions (means ± se of n = 3 preparations from independent pools of mature rosette leaves). (F) Ratio of the 60S fraction relative to the 50S fraction calculated from the data sets of E and F (means ± se of n = 3 preparations from independent pools of mature rosette leaves). The experimental design was according to scheme C in Figure 15. Mutant and wild-type plants were shifted at developmental stage ~1.10. Non-acclimated rosettes were cultivated at 20°C and assayed immediately before the temperature shift. Peak areas of rRNA were determined from total RNA extracts by microfluidic electrophoresis. 23S rRNA was determined by the sum of two naturally occurring post-maturation cleavage products. For A to C, significance (P) of the time effect was tested by two-way ANOVA. For E and F, asterisks indicate significant changes of the mutant compared with the wild type (P < 0.05, heteroscedastic Student's t test) (Beine-Golovchuk et al., 2018).

1.6 Aims of this Thesis

The first objective of this PhD study is to investigate and understand metabolic traits involved in the cold acclimation potential of two Australian wheat varieties with contrasting cold tolerance using targeted metabolomics and lipidomics approaches. The second objective of this study is to identify potential metabolite and lipid markers responsible for chilling tolerance in the two studied wheat varieties. The third objective is to evaluate the potential of REIL proteins as cold acclimation factor in *Arabidopsis thaliana* for potentially enhancing wheat cold tolerance. The knowledge gained from this PhD study may contribute to Australian wheat molecular breeding programs targeted to develop more cold-tolerant wheat varieties in the future. The description of how each of the mentioned objective is achieved related to its respective chapter is elaborated below.

Chapter 2 is conducted to achieve the first and second objectives of this study. This chapter describes the investigation of cold acclimation potential of two Australian wheat varieties with contrasting cold tolerance using targeted metabolomics and lipidomics approaches. The selected cold-sensitive variety for this study is Wyalkatchem and the selected cold-tolerant variety is Young. Wheat is known to be susceptible to cold stress at their reproductive stage. Therefore, flag leaves and spikes at the young microspore (male reproductive development) stage are chosen as the tissue types for the study. The cold stress experiment is conducted in a controlled environment where samples after initial cold exposure (1 day) and prolonged cold exposure to cold (4 days) are harvested and extracted. A comprehensive analysis of metabolites (sugars and derivatives, organic acids, amino acids, amines and/or phytohormones) and glycerolipids of the harvested flag leaf and spike tissues subjected to cold stress is performed using GC and LC coupled to triple quadruple (QqQ) mass spectrometry. Via the outcomes gained from this study, the cold responses of the two wheat varieties with contrasting cold tolerance upon cold stress can be firstly understood, followed by the identification of potential metabolite/lipid markers that can discriminate wheat varieties with differences in cold acclimation.

Chapter 3 is also conducted to achieve the first and second objectives of this study. This chapter describes the spatial root lipidome analysis of cold-stressed wheat varieties from Australia. Cold stress studies on plants are mostly performed using the aerial plant parts, i.e. leaves and spikes. There are limited cold stress studies on whole roots or even rarely on the tissue-specific effects of cold stress on tissues such as the meristem or division zone, elongation zone, and maturation zone.

The outcome gained from **Chapter 2** has pointed out the involvement of certain lipids in the cold response (e.g. membrane remodeling) and as useful biomarkers that can discriminate the two wheat varieties with contrasting cold tolerance. This motivated me to also investigate the tissue-specific lipidomes of roots of the two studied wheat varieties (Wyalkatchem and Young) subjected to cold stress in order to obtain a more comprehensive story of the wheat cold responses and also to identify more potential lipid markers that can distinguish the two wheat varieties. In this study, the lipid profiles of the spatial root zones derived from young seedlings of Wyalkatchem and Young grown at optimal temperature (21°C) and subjected to chilling (4°C) and freezing (-3°C) stresses are investigated. The harvested samples are analysed with a high resolution high performance liquid chromatography (HR-HPLC) coupled with quadruple-time-of-flight (QqTOF) platform via modified parallel reaction monitoring (PRM) methods. Together with the outcomes gained from the studies of flag leaves and spikes in **Chapter 2**, the outcomes obtained from this study (roots) may help us to gain a more comprehensive understanding of lipid metabolisms of wheat in response to cold.

Chapter 4 is conducted to achieve the third objective of this study. This chapter describes the system analysis of REIL protein functions in cold acclimated *Arabidopsis thaliana* roots. REIL proteins have been postulated to act as cold acclimation factor by involving in late ribosomal biogenesis and to affect accumulation of 60S large subunits in *Arabidopsis thaliana* mature leaves and seedlings upon acclimation to low temperature. In order to validate the roles of REIL proteins, a comprehensive system analysis is conducted targeted at understanding the mechanisms of late ribosome biogenesis in which REIL proteins are involved with focus on the roots subjected to cold stress. The comprehensive system analysis includes ribosomal profiling, transcriptomics and proteomics studies of the roots grown and harvested at optimized temperature and at different times after shift to suboptimal/low temperatures. In this study, the role of REIL as potential cold acclimation in *A. thaliana* is confirmed in which REIL proteins are required for the ribosomal biogenesis at low temperature and the first mechanistic insights into the potential roles of REIL proteins are revealed.

Chapter 5 is also conducted to achieve the third objectives of this study, with focus given to wheat. This chapter therefore describes the evaluation of REIL as a potential cold acclimation factor in wheat as the outcomes gained from **Chapter 4** has substantiated the role of REIL proteins as

potential cold acclimation factors in Arabidopsis. Therefore, it is also important to investigate if this protein may also be required for wheat to adapt to cold conditions. In this study, the topology and phylogenetic analyses using the two Arabidopsis REIL proteins and various wheat REIL sequences retrieved from available databases are studied. In addition, data mining using two published transcriptomic datasets from cold- and heat/drought-stressed wheat studies is carried out to evaluate the *REIL* gene expressions upon stresses. Meanwhile, real-time PCR is also conducted to investigate *REIL* expression in the Wyalkatchem and Young varieties when subjected to cold stress. The outcomes gained from this study may provide us some clues of the potential of REIL as cold acclimation factor in wheat upon low temperature stress.

Chapter 6 concludes all the main findings from each of the chapter and suggest future directions for further studies.

CHAPTER 2

Metabolomics and Lipidomics Studies of Cold-Tolerant and Cold-Sensitive Wheat Varieties from Australia

Preface to Chapter 2

This chapter describes the investigation of the cold acclimation potential of two Australian wheat varieties with contrasting cold tolerance using targeted metabolomics and lipidomics approaches. The selected cold-sensitive and -tolerant varieties used for this study are Wyalkatchem and Young, respectively. Wheat is known to be susceptible to cold stress at the reproductive stage. Flag leaves (a source tissue) and spikes (a sink tissue) at the young microspore stage (male reproductive development) are therefore chosen as targets of this study. The work on the flag leaves has been published in the *Metabolomics* journal with the title of "Phenotyping Reproductive Stage Chilling and Frost Tolerance in Wheat Using Targeted Metabolome and Lipidome Profiling" (Cheong et al. 2019), which is presented as the first part (Part I) of this chapter with publication format (page 44 – 73). I claim that I contributed to more than 65% of the work (experimental, data processing, data analysis, interpretation and manuscript writing) to this part, which was proof-read and corrected by all other co-authors. Meanwhile, the analyses performed on the spikes has also been published in the *Cells* Journal, under *Topical Collection: Membrane Lipids in the Interaction of Plants with Their Abiotic and Biotic Environment* (Cheong et al., 2020). The paper is entitled "Phenotyping the Chilling and Freezing Responses of Young Microspore Stage Wheat Spikes Using Targeted Metabolome and Lipidome Profiling". The paper is presented in the second part (Part II) of this chapter as chapter with publication format (page 74 – 105, starts from section 2.10). I claimed that I contributed to more than 60% of this work (experimental, data processing, data analysis, interpretation and manuscript writing) to this part, which has been proof-read and corrected by all other co-authors.

CHAPTER 2

(Part I)

The following work was published in *Metabolomics* (2019) Volume 15: Article 144 (DOI: 10.1007/s11306-019-1606-2). All the numberings of the figures and tables are modified from the original published paper in this chapter to begin with **I-2-x** (I represents Part I; 2 represents Chapter 2; x represents number in sequence) and for supplemental data are begin with **I-S2-x** (S represents supplemental).

Title

Phenotyping Reproductive Stage Chilling and Frost Tolerance in Wheat Using Targeted Metabolome and Lipidome Profiling

Author Names and Affiliations

Bo Eng Cheong[a], William Wing Ho Ho[ae], Ben Biddulph[c], Xiaomei Wallace[b], Tina Rathjen[b], Thusitha W.T. Rupasinghe[d], Ute Roessner[ad], Rudy Dolferus[b*]

[a]: School of BioSciences, The University of Melbourne, Victoria 3010, Australia

[b]: CSIRO Agriculture & Food, GPO Box 1700, Canberra ACT 2601, Australia

[c]: Department of Primary Industries and Regional Development, 3 Baron Hay Court, South Perth, WA 6151, Australia

[d]: Metabolomics Australia, School of BioSciences, The University of Melbourne, 3010 Victoria, Australia

[e]: Melbourne Integrative Genomics, Schools of Mathematics and Statistics and of BioSciences, The University of Melbourne, Victoria 3010, Australia

***Correspondence**

Rudy Dolferus

E-mail: rudy.dolferus@csiro.au

Tel: +61-2-6246 5010

Fax: +61-2-6246 5000

2.1 Abstract

Introduction Frost events lead to A$360 million of yield losses annually to the Australian wheat industry, making improvement of chilling and frost tolerance an important trait for breeding.

Objectives This study aimed to use metabolomics and lipidomics to explore genetic variation in acclimation potential to chilling and to identify metabolite markers for chilling tolerance in wheat.

Methods We established a controlled environment screening assay that is able to reproduce field rankings of wheat germplasm for chilling and frost tolerance. This assay, together with targeted metabolomics and lipidomics approaches, were used to compare metabolite and lipid levels in flag leaves of two wheat varieties with contrasting chilling tolerance.

Results The sensitive variety Wyalkatchem showed a strong reduction in amino acids after the first cold night, followed by accumulation of osmolytes such as fructose, glucose, putrescine and shikimate over a four-day period. Accumulation of osmolytes is indicative of acclimation to water stress in Wyalkatchem. This response was not observed for tolerant variety Young. The two varieties also displayed significant differences in lipid accumulation. Variation in two lipid clusters, resulted in a higher unsaturated to saturated lipid ratio in Young after four days cold treatment and the lipids PC(34:0), PC(34:1), PC(35:1), PC(38:3), and PI(36:4) were the main contributors to the unsaturated to saturated ratio change. This indicates that Young may have superior ability to maintain membrane fluidity following cold exposure, thereby avoiding membrane damage and water stress observed for Wyalkatchem.

Conclusion Our study suggests that metabolomics and lipidomics markers could be used as an alternative phenotyping method to discriminate wheat varieties with differences in cold acclimation.

Keywords

Cold tolerance/Flowering/Lipid/Metabolite/Phenotyping/Wheat

2.2 Introduction

For important food crops, such as cereals, chilling and frost are major constraints to yield and productivity (Gray et al., 1997; Leff et al., 2004; Lobell and Gourdji, 2012). Climate change affects atmospheric conditions, increasing the probability of weather extremes. This is likely to result in more frequent crop losses in the future (Lobell and Gourdji, 2012). Warmer winters and more frequent spring frosts have increasingly affected wheat yields in China between 1961 and 2000 (Li et al., 2014; Li et al., 2015). In Southern Australia, spring frosts have become significantly more frequent since 1960 and the overall length of the frost season has increased by one month, resulting in more frequent occurrences of frost damage to wheat crops (Crimp et al., 2015; Zheng et al., 2015). In Australia, spring wheat varieties are sown in autumn, flower in early spring and are harvested in late spring (Zheng et al., 2015). Radiant frosts in spring are caused by heat loss from the soil surface to the night sky on cold and dry days with clear skies. This leads to a rapid cooling of the crop canopy and associated frost damage if crops are at susceptible stages (Marcellos and Single, 1975). The associated increase in risk of frost damage requires wheat cultivars with improved frost tolerance. Reoccurring frost events cost the Australian wheat industry an estimated A$360 million of direct and indirect yield losses annually (March et al., 2015; Zheng et al., 2015).

Above zero degree temperatures (chilling; typically 10°C to 0°C) cause an acclimation or adaptation response in plant tissues. Below zero degree temperatures (frosts) cause an additional challenge to plant tissues due to the formation of ice crystals. Quantitative and/or qualitative differences in the acclimation response during the chilling period may provide various degrees of frost tolerance. Wheat tolerates frosts during vegetative growth, but becomes more frost-sensitive during flowering in early spring. Chilling conditions during flowering can cause pollen sterility and grain loss in wheat (Demotes-Mainard et al., 1996; Rerkasem, 1996; Subedi et al., 1998a and b; Subedi et al., 2000; Chakrabarti et al., 2011). Exposure of plants to chilling conditions ("hardening") enhances freezing tolerance in a process called cold acclimation (Palta and Weiss, 1993; Guy, 1999; Tomashow, 1999; Wanner and Junttila, 1999). In wheat, cold acclimation during reproductive stages remains poorly characterised. Although most genes involved in cold acclimation are expressed after 24 hours of exposure (Monroy et al., 2007; Kurepin et al., 2013), the full establishment of the response may require prolonged or repeated exposures to cold (Levitt, 1980; Guy, 1990; Ruelland et al., 2009). Cold acclimation can be lost during warmer fluctuating winter conditions, but it remains unclear whether re-acclimation can occur following de-acclimation (Rapacz, 2002; Kalberer et al., 2006; Vitamvas and Prasil, 2008), particularly after

crops transition into reproductive stages. Loss of cold acclimation during spring makes wheat crops particularly vulnerable to unexpected frosts (Frederiks et al., 2011; Frederiks et al., 2012). Cold temperatures, in combination with increasing day-length, accelerate the transition from vegetative to reproductive growth as the vernalization and photoperiod requirements are met (Fowler et al., 2001; Limin and Fowler, 2006). Proper management of sowing time and phenology of wheat (flowering time, response to day-length) minimise frost damage, but the unpredictability of frost events requires genetic improvement in frost tolerance to manage yield stability (Limin and Fowler, 2006; Zheng et al., 2015), particulairy in Southern Australia where the length of the frost season is increasing (Crimp et al., 2015) and crop development cannot be delayed further.

Induction of cold acclimation and freezing tolerance involves physiological and biochemical changes in plants (Wanner and Junttila, 1999). Cold-tolerant plants have a higher proportion of unsaturated fatty acids in the plasma membrane and are better at maintaining membrane fluidity at lower temperatures (Vigh and Horvath, 1979; Steponkus et al., 1993; Bohn et al., 2007). Plants tend to increase the degree of fatty acid unsaturation and the content of phospholipids when they are exposed to low, non-freezing temperatures (Welti et al., 2007). In Arabidopsis, phophatidylcholines (PC), phosphatidylethanolamines (PE), phosphatidylglycerols (PG) and monogalactosyldiacylglycerols (MGDG) containing two polyunsaturated acyl species, including 36:5 (18:2/18:3) and 36:6 (di-18:3), increased during cold acclimation (Welti et al., 2002). Chilling conditions also lead to the accumulation of osmolytes, compatible solutes or cryoprotectants such as sugars (fructose, glucose, trehalose, raffinose) and amino acids or amines such as proline and gamma-aminobutyric acid (GABA). This response is not specific to chilling and is also induced by other stressors that cause osmotic stress (e.g., drought, salinity, heat; Beck et al., 2007). Apart from playing a role in compensating for water loss during osmotic adjustment, osmolytes are also important for protecting membrane integrity and scavenging of reactive oxygen species (Guy, 1999; Wanner and Juntilla, 1999; Smallwood and Bowles, 2002; Valluru et al., 2008; Javadian et al., 2010; Verslues et al., 2006; Janmohammadi, 2012). Cold acclimation in spring and winter Triticum monococcum lines affects the steady-state levels of phytohormones, including abscisic acid (ABA), salicylic acid, ethylene, jasmonic acid, gibberellins, cytokinins and auxin (Horvath et al., 2007; Machakova et al., 1989; Vankova et al., 2014). Increased ABA levels are correlated with cold-induced water deficit in plants. ABA is implicated in plasma membrane lipid alterations during cold stress (Bohn et al., 2007). ABA induces the expression of phospholipase D

(AtPLD) in Arabidopsis, causing hydrolysis of structural phospholipids (Zhang et al., 2005; Meijer and Munnick, 2003).

Studying quantitative and qualitative differences in metabolite and lipid accumulation during cold acclimation is an important tool to understand chilling and frost tolerance in wheat. Targeted metabolomics and lipidomics using gas/liquid chromatography, coupled to a triple-quadruple MS (GC/LC-QqQ-MS) approach offers higher sensitivity, selectivity, reproducibility and robust quantification over a broad dynamic range (Douglas, 2009; Sumner et al., 2015; Jorge et al., 2016). Dias et al. (2015) were able to quantify 76 primary metabolites (sugars, organic acids and amino acids/amines) in two chickpea cultivars with contrasting responses to salinity using GC- and LC-QqQ-MS. Natera et al. (2016) reported the quantification of 63 phospholipids in the roots of two barley genotypes with contrasting responses to salinity using LC-QqQ-MS. We therefore applied these approaches to study the cold acclimation response in wheat.

Reliable phenotyping for chilling and frost tolerance in the field is challenging due to unpredictability, variability in severity, duration, and timing of these events. In this study we established a reliable controlled environment (CE) phenotyping method to discriminate genetic variation in cold and frost tolerance in wheat. This CE phenotyping method, together with targeted metabolomics and lipidomics approaches, were then used to identify quantitative and qualitative differences in metabolite and lipid accumulation in two wheat varieties with differential chilling-tolerance. As starting tissue, we used flag leaves from wheat plants harvested at the young microspore (YM) stage of pollen development, the reproductive stage with highest sensitivity to various abiotic stresses - including cold (Dolferus et al., 2013). The results indicate that two Australian spring wheat varieties with contrasting chilling tolerance (cold-tolerant Young and cold-sensitive Wyalkatchem) differed significantly in the accumulation of metabolites (amino acids, osmolytes) and levels of unsaturated versus saturated membrane lipids, indicating that metabolite profiling could be used to select wheat varieties with differences in cold acclimation.

2.3 Materials and Methods

2.3.1 Controlled Environment for Wheat Growing, Cold Treatment and Sample Collection

Wheat varieties Wyalkatchem (cold-sensitive) and Young (cold-tolerant) used in this study were obtained via the National Frost Initiative, Australia (http://www.nvtonline.com.au/frost/). Seeds were sown in trays (36x25x13cm, LxWxH; 15 plants/tray) filled with soil (100% composted soil,

containing 1g/L fertilizer: 14.4% N/6.6% P/5% K). Plants were grown in the glasshouse under natural lighting conditions and controlled temperature regime (24/16°C, L/D); watering occurred once daily. The young microspore (YM) stage of pollen development was determined using auricle distance measurements (Ji et al., 2010; Dolferus et al., 2013). The Zadoks scale was used to determine growth stages other than YM (Zadoks et al., 1974). Cold treatments were carried out at the YM stage in a Conviron PGC 20 growth chamber. The treatment cycle consisted of 12 hours incubation at 21°C in the light, followed by a linear cooling gradient descending from 21°C to -3°C over a period of 4 hours, then followed by a continuous cold period at -3°C over 8 hours in the dark (12/12 light/dark cycle, using 400µmol/m^2s^1 light intensity; see **Fig. I-S2-1a**). The whole experiment was run over four consecutive days and samples were harvested in the morning immediately after a cold treatment at day one (TP_1 - short cold stress), day four (TP_3 - prolonged cold stress), and corresponding day-time samples were harvested 6 hours into the normal temperature (21°C) light cycle after day one and day four respectively (TP_2 and TP_4; see **Fig. I-S2-1f**). One tray of plants was used as untreated control to harvest T_0 samples. In the trays for stress treatments, tillers that reached the YM stage were tagged before cold treatment. Three flag leaves were harvested from three different tagged plants at each of the time points (TP_0 to TP_4) and pooled as one replicate for metabolite measurements. For each time point, we harvested four biological replicates per variety (n=4) for all the metabolite and lipid analyses, except for phytohormone analyses where three replicates were used (n=3). For sterility measurements, plants were returned to the glasshouse after cold treatment, and spike grain number of tagged tillers was determined at maturity.

2.3.2 Analysis of Sugars, Organic Acids, Amino Acids, Amines and Phytohormones

All chemicals and solvents for metabolite measurements were purchased from Sigma-Aldrich (Australia) and were of analytical or mass spectrometry grades. For sugars, organic acids and amines, tissue extraction was performed according to Dias et al. (2015), with some modifications. Aliquots of frozen leaf material (50 mg per replicate x four replicates) were weighed into Cryomill tubes (Precellys 24, Bertin Technologies). Subsequently, 500 µL of methanol containing 4% of internal standard (from a stock solution containing 0.5 mg/mL of $^{12}C_6$-sorbitol and 0.5 mg/mL $^{13}C_5$-^{15}N-L-valine) was added to the samples, followed by vortexing for 30 sec and homogenization at -10°C using a Cryomill (3 x 45 sec at 6,100 rpm). The samples were then extracted for 15 mins at 30°C in a thermomixer at 850 rpm, and subsequently centrifuged for 5

mins at 4°C at 13,000 rpm. The supernatants were transferred into new tubes, and 500 µL of water containing 0.2% formic acid was added into the Cryomill tubes containing the previously ground tissue pellet. The samples were vortex-mixed for 30 sec, and centrifuged at 13,000 rpm for 5 mins at 4°C. The supernatants were then transferred and combined with the methanolic extracts from the previous centrifugation. A 200 µL of dichloromethane was added to the combined supernatants to separate chlorophylls. The combined supernatants were vortexed, centrifuged at 13,000 rpm for 2 mins at 4°C. The supernatants were taken and stored at -80°C for subsequent sugars, organic acids and amine analyses.

For the analysis of sugars and organic acids, 5 µL and 125 µL aliquots of the supernatants was transferred into new glass vial inserts, and dried in vacuo for sugars and organic acids analyses using GC-QqQ-MS. Prior to the GC-QqQ-MS analysis, the dried extracts were derivatized with methoxyamine hydrochloride in pyridine and bis-(trimethylsilyl)-trifluoroacetamide (BSTFA) as described by Dias et al. (2015). Briefly, all samples were re-dissolved in 20 µL of 30 mg/mL methoxyamine hydrochloride in pyridine and derivatized at 37°C for 120 mins with mixing at 500 rpm. The samples were incubated for 30 min with mixing at 500rpm after addition of 20 µL N,O-bis-(trimethylsilyl)-trifluoroacetamide (BSTFA). Each derivatized sample was allowed to rest for 60 min prior to injection. Later, the derivatized samples (injection volume of 1 µL for each sample) were injected into a GC-QqQ-MS system comprising of a Gerstel 2.5.2 Autosampler, a 7890A Agilent gas chromatograph and a 7000 Agilent triple-quadruple MS (Agilent Santa Clara, USA) with an electron impact (EI) ion source. The instrument settings were the same as described by Dias et al. (2015). For calibration and quantification of sugars and organic acids in the flag leaf samples, we used serial concentrations of calibration authentic standards (**Table I-S2-1**), including 24 sugars (sugars, sugar phosphates, sugar acids and sugar alcohols) and 19 organic acids, derivatized and subjected to GC-QqQ-MS analysis - as described by Dias et al. (2015).

For the amino acid and amine analyses with LC-QqQ-MS, 10 µL of supernatants were transferred into new glass vial inserts. The amino acids and amines in the supernatants were then derivatized with 6-aminoquinolyl-N-hydrosysuccinimidyl carbamate (AQC) reagent as described in Boughton et al. (2011) and Dias et al. (2015). Briefly, 10 µL samples were added to 70 µL of borate buffer (200 mM, pH 8.8 at 25°C) containing 10 mM TCEP, 1 mM ascorbic acid and 50 µM 2-aminobutyrate. The resulting solution was vortexed before adding 20 µL of 6-aminoquinolyl-N-hydrosysuccinimidyl carbamate (AQC) reagent [200 mM dissolved in 100% acetonitrile (ACN)] and then immediately vortexed. The samples were heated with shaking at 55◦C for 10 mins, then

centrifuged at 13,000rpm at room temperature and transferred to HPLC vials containing inserts (Agilent, springless glass inserts, 250 µL) prior to injection. The derivatized samples (injection volume of 1 µL for each sample) were immediately injected into a LC-QqQ-MS system comprising of an Agilent 1200 LC-system coupled to an Agilent 6410 Electrospray Ionization-Triple Quadruple-MS. The settings of the LC-MS instrument were as described by Dias et al. (2015). For calibration and quantification of amino acids and amines in the flag leaf samples, a series of concentrations of calibration authentic standards (**Table I-S2-1**), comprising of 29 amino acids and amines mixed with sulfur-containing compound solution were prepared, derivatized and subjected to LC-QqQ-MS analysis same as described by Dias et al. (2015).

Seven phytohormones and phytohormone-related compounds [salicylic acid (SA), jasmonic acid (JA), jasmonoyl-isoleucine (JA-ile), indole-3-acetic acid (IAA), indole-3-carboxylic acid (ICA), indole-3-butyric acid (IBA) and 2-cis-4-trans-abscisic acid (ABA)], as well as three organic acids which are precursors for phytohormones [(benzoic acid (BA), trans-cinnamic acid (CA) and 12-oxo-phytodienoic acid (OPDA) were analysed in this study. Extraction for phytohormone analysis was carried out using a slightly modified procedure of Cao et al. (2017). Briefly, the flag leaf samples were ground with pestle and mortar in liquid nitrogen and frozen immediately. A 100 mg of sample was weighed for each of the samples and transferred to a dried 2 mL centrifuge tube that was pre-washed with MS grade methanol. 1 mL of extraction solvent, containing 956 µL of 70% methanol and 44 µL of 8.3 µg/mL internal standard mixtures (d_2IAA, d_5BA, d_6ABA, d_6SA, d_7CA, H_2JA), was added to the sample, then vortexed and agitated at 4°C, and spun at 1,400 rpm for 30 mins. The samples were then centrifuged at 16,100 x g for 10 mins. The supernatants were transferred to fresh centrifuge tubes. The residues were re-extracted and centrifuged with 500 µL of extraction solvents (without internal standards). Finally, the first and second supernatant was combined and kept at -80°C until further derivatization steps using methyl-chloroformate (MCF). The subsequent derivatization steps were carried out according to Rawlinson et al. (2015), with some modifications. While Rawlinson et al. used GC coupled with single MS, our analysis used triple quadruple GC-MS (GC-QqQ-MS) with newly developed multiple reaction monitorings (MRMs) which were developed for each of the measured phytohormone and organic acids. Briefly, 600 µL of the supernatant for each sample was taken, dried down and re-dissolved with 160 µL methanol. Then, 8.3 µg/ml of $^{13}C_5$-^{15}N-L-Valine (another internal standard) was added. A 34 µL of pyridine was then added to the mixture, followed by vortexing vigorously for 25-30 sec. A 200 µL of 1% NaOH solution was then added to the mixture.

This ~400 µL mixture was then derivatized with 20 µL of methyl chloroformate (MCF) and vortexed vigorously for 25-30 sec. Another 20 µL of methyl chloroformate (MCF) was added, followed by vortexing. A 400 µL of chloroform was then added to the mixture, vortexed again for 10 sec, followed by an addition of 400 µL of 50 mM sodium bicarbonate. The mixture was vortexed for 10-15 sec and centrifuged for 30 sec at 16,100 x g. The upper aqueous layer was discarded and the bottom organic layer was taken (1 µL for each sample) and injected into a GC-QqQ-MS system comprising a Gerstel 2.5.2 Autosampler, a 7890A Agilent gas chromatograph and a 7010 Agilent triple-quadrupole MS (Agilent, Santa Clara, USA) with an electron impact (EI) ion source. More details for the preparation of calibration and internal standards, extraction, derivatization steps and GC-QqQ-MS instrument settings can be found in **Supplemental Data I-S2-1** (Methodology for phytohormone analysis).

2.3.3 Analysis of Lipid Content

The extraction of lipids was carried according to Folch et al. (1957), with modifications. Briefly, 30 mg freshly frozen flag leaf samples were homogenized in 500 µL of a 2:1 methanol:chloroform mixture using a Cryomill (Precellys 24, Bertin technologies) for 3 x 45 sec at 6,100 rpm (-10°C). The extracts were shaken at 750 rpm for 15 mins at 30°C, and centrifuged at 13,000 rpm for 15 mins. The supernatants were transferred to new tubes, while 500 µL of 2:1 methanol:chloroform mixture was added again to each of the remaining residue, vortexed and centrifuged at 13,000 rpm for 15 mins. The supernatants were combined with the previous supernatants. The combined supernatants were dried down *in vacuo* and re-constituted in 100 µL of 1:1 butanol:methanol for the subsequent LC-QqQ-MS analysis using an Agilent 1200 LC-system coupled to an Agilent 6410 Electrospray Ionization-Triple Quadruple-MS system. An injection of 5 µL of each total lipid extract was chromatographically separated on an Ascentis Express RP-Amide 50 X 2.1 mm, 2.7 µm HPLC column (Sigma-Aldrich, Castle Hill, NSW) using an 8 mins gradient from 0% A to 100 % B, which was then held for 2 mins and followed by a 4 min column re-equilibration with a flow rate of 0.18 mL/min. The mobile phases were: A, 10 mM ammonium formate in water: methanol : tetrahydrofuran (50: 20: 30, v/v/v); B, 10 mM ammonium formate in water : methanol: tetrahydrofuran (5: 20: 75, v/v/v). Lipid species were identified and quantified based on multiple reaction monitorings (MRMs) established using external lipid standards and references from the LIPIDMATCH database (https://github.com/GarrettLab-UF/LipidMatch/releases/tag/v2.0.2) as listed in **Table I-S2-2**, with a 5-20 msec dwell time for the simultaneous measurements of up to

100 compounds. We used optimised parameters for capillary (4000 V), fragmentor (60–160 V) and collision voltages (20-40 V). In all cases, the collision gas was nitrogen with a flow rate of 7 L/min. The external lipid standards used (**Table I-S2-2**) were lysophosphatidylcholine LPC(17:0), phospatidylcholine PC(34:1), phosphatidylethanolamine PE(34:0), phosphatidylglycerol PG(34:1), phosphatidylinositol PI(36:2), phosphatidic acid (PA) and phosphatidylserine PS(34:0). Detected lipid species are annotated as follows: lipid class designation (total number of carbon atoms in the fatty acid chains: total number of double bonds in the fatty acid chains).

2.3.4 Data Processing and Statistical Analysis of Metabolite Data

Raw metabolite and lipid data were processed and analyzed using Quantitative Analysis MassHunter Workstation software for QQQ (Agilent Technologies, Santa Clara, CA, USA). The level of identification was carried out based on the Metabolomics Standards Initiative (MSI) requirements (Sumner et al., 2007). For all measured metabolites (sugars, organic acids, amines and phytohormones), absolute quantities were determined while the concentration unit was expressed as picomole/mg of fresh weight (**Table I-S2-3**), using MSI Level 1 as the identification was based on Multiple Reaction Monitorings (MRMs) established using authentic standards (**Table I-S2-1**). Meanwhile, for lipids, responses were normalized to mg fresh weight (**Table I-S2-4**). Although single authentic lipid species were used for each of the phospholipid class, the identification of individual lipid species was based on the MRM experiment and retention time (MSI Level 2, **Table I-S2-2**). The processed metabolite and lipid data were first subjected to multiple comparison statistical analyses using Analysis of Variance (ANOVA), with a false discovery rate (FDR)-adjusted *p*-value of 0.05 and using the Benjamini-Hochberg method (1995) to determine the metabolites and lipids that changed significantly across all time points or over the four-day cold stress period, followed by the Tukey's honestly significant difference (HSD) post-hoc test in order to determine which pair-wise combinations showed significant differences for both primary metabolites and lipids using Graphpad Prism 7.0 (GraphPad Software, La Jolla California USA). Next, we determined which metabolites/lipids responded specifically to short cold stress (TP_1), prolonged cold stress (TP_3), diurnal fluctuations when the plants were exposed to normal day-time temperature of 21°C for 6h (TP_2 and TP_4). We therefore performed pairwise comparisons of the selected two groups TP_1 vs. TP_0 (for short cold stress), TP_3 vs. TP_1 (for prolonged cold stress), TP_2 vs. TP_1 and TP_4 vs. TP_3 (for recovery and the effect of diurnal fluctuations on metabolite levels) within each variety, and comparisons in every time point

between the two varieties (varietal differences). The comparisons for metabolites were presented as log_2-transformed of fold change values (**Figs. I-2-1 and I-2-3; Table I-S2-5**). A similar approach was also performed for the lipid data (**Figs. I-2-2 and I-2-4; Table I-S2-6**). Statistical significance of differences observed between samples was evaluated with the Student's *t*-test in Excel, with a false discovery rate (FDR)-adjusted *p*-value of 0.05 as the cut-off (Benjamini and Hochberg, 1995). The statistical analysis for the comparison of the unsaturation to saturation ratio between Wyalkatchem and Young at different time points was also performed with Student's *t*-test using GraphPad Prism 7.0 software (GraphPad Software, La Jolla, CA, USA). All bar plots were created using the same software.

2.4 Results

2.4.1 Establishment of A Controlled Environment Assay for Chilling Tolerance

To establish a controlled environment phenotyping method for chilling and frost tolerance in wheat, we used two wheat varieties that consistently performed better (Young) and worse (Wyalkatchem) in terms of grain yield in the Australian National Frost Initiative (NFI) field trials. We used a linear cooling gradient descending from 21°C to -3°C over a period of 4 hours, followed by a continuous cold period at -3°C over 8 hours (**Fig. I-S2-1a**). A four-day chilling treatment at the YM stage showed that the average spike grain number relative to unstressed control plants was consistently higher for Young compared to Wyalkatchem, with Wyalkatchem grain number reduced to an average of 76.3% of control (**Fig. I-S2-1b**). Reduced spike grain number in Wyalkatchem was often associated with the development of larger grains (**Fig. I-S2-1c**). A four-day cold treatment during different stages of reproductive development showed that sensitivity to chilling in Wyalkatchem was highest at Zadok stages 41 to 47 and from 57 to 65, which corresponded to the YM stage and anthesis respectively. Spike grain numbers in Young were not significantly affected at both stages (**Fig. I-S2-1d**). A time course experiment shows that spike grain numbers in Wyalkatchem were reduced considerably after three days of treatment, while in Young spike grain numbers were reduced significantly from five days treatment onwards (**Fig. I-S2-1e**). We therefore standardised on a four-day YM stage treatment to discriminate the two varieties.

2.4.2 Four-day Chilling Treatment Induces Significant Changes in Metabolites and Lipids in Young and Wyalkatchem

To develop a workable field phenotyping method, we focused on cold-induced metabolite changes in the flag leaf, a tissue that is easier to collect in a non-destructive way compared to YM stage spikes. In the field, wheat plants often experience consecutive nights of chilling and frost events throughout flowering, as frost events are linked to large scale climatic patterns and regularly occur over successive nights, while day-time temperatures can be normal (~20°C). Previous chilling events can influence metabolite levels at any harvest time. A time course experiment was therefore designed to identify metabolite changes that were stable over consecutive cold events and were not subject to day-time recovery or to circadian fluctuations. In addition, metabolite markers for chilling tolerance have to accumulate to significantly different levels in the cold-tolerant and sensitive wheat lines.

Using ANOVA multiple comparison analysis and a false discovery rate (FDR)-adjusted *p*-value of 0.05, significant changes of metabolites and lipids were observed in each variety and between the two varieties across all the time points (**Table I-2-1; Tables I-S2-7 and I-S2-8**). Cold treatment of cold-sensitive Wyalkatchem revealed significantly more changes in both primary metabolites (25) and lipids (19) compared to cold-tolerant Young which showed only one metabolite and ten lipid changes across all the time points (**Table I-2-1**). When comparing quantitative and qualitative differences in cold acclimation between the two varieties, a total of 43 metabolites and 47 lipids were found to differ across all time points (**Table I-2-1**). All metabolites and lipids listed in **Table I-2-1** were further analysed with Tukey's honestly significant difference (HSD) *post-hoc* test in order to determine which pair-wise combinations showed significant differences for both primary metabolites and lipids (**Table I-S2-9, Table I-S2-10**). Many pair-wise combinations were shown to differ significantly for both metabolites (387; highlighted in **Table I-S2-9**) and lipids (470; highlighted in **Table I-S2-10**) for the two wheat varieties and across all time points. But only some of these comparisons are relevant for identification of potential metabolite markers for chilling and frost tolerance phenotyping. Comparisons between TP_1 *vs.* TP_0 (short cold treatment) and TP_3 *vs.* TP_1 (stability over prolonged cold treatment during cold acclimation), as well as comparisons between the day and night-time samples (TP_2 *vs*. TP_1 and TP_4 *vs*. TP_3; effect of diurnal fluctuations on metabolite levels), and comparison between these time points for the two wheat varieties are essential to identify those metabolites that could be used as stable markers for cold-tolerance phenotyping. To achieve this particular aim, we performed

additional Student's *t*-test to carry out pair-wise comparisons to identify candidate metabolite markers that are able to differentiate the response in cold acclimation and cold tolerance between the two wheat varieties.

2.4.3 A Four-Day Chilling Time Course Reveals Significant Differences in Cold Acclimation in Wyalkatchem and Young Flag Leaves

Sample comparisons: TP_1 vs. TP_0, TP_2 vs. TP_1, TP_3 vs. TP_1 and TP_4 vs. TP_3 for both varieties

After the first night of cold exposure, the sensitive variety Wyalkatchem showed the most dramatic changes in primary metabolite levels (WTP_1 vs. WTP_0). As shown in **Figure I-2-1**, seven amino acids and amines were significantly decreased, including alanine (–1.9-fold), beta-alanine (–1.7-fold), glycine (–2.9-fold), methionine (–1.7-fold), phenylalanine (–2.9-fold), proline (–2.7-fold) and valine (–2.3-fold). One sugar increased significantly at TP_1: glucose-6-phosphate (+1.8-fold). There was no significant change in phytohormones. Three lipids increased significantly after overnight cold exposure of Wyalkatchem (Fig. 2): PC(34:0) (+1.6-fold), PC(34:1) (+1.6-fold) and PG(36:5) (+1.4-fold). In contrast to Wyalkatchem, the cold tolerant variety Young did not show any significant changes in primary metabolites or lipids at TP_1 compared to TP_0 (**Fig. I-2-1 and I-2-2**).

To test for recovery and the effect of diurnal fluctuations on metabolite levels we harvested the TP_2 samples 6h after the TP_1 samples, when plants were allowed to experience day-light and normal temperatures (21°C) for 6h. Comparison of TP_2 and TP_1 metabolite levels revealed that some of the significant changes we observed at TP_1 in Wyalkatchem flag leaves were partially reversed, but some were maintained and new changes also appeared (**Table I-S2-5, Fig. I-S2-2**). Some amino acids and amine levels changed from being decreased at TP_1 to being significantly increased at TP_2 and regaining T_0 levels: citrulline (+14.9-fold), glycine (+2.3-fold), homoserine (+2.2-fold), methionine (+1.6-fold) and putrescine (+3.0-fold). Tryptophan decreased further at TP_2 compared to TP_1: (–1.9-fold). There were no differences in phytohormone levels, nor were there any significant changes in lipid levels between TP_2 and TP_1 Wyalkatchem flag leaves (**Table I-S2-6, Fig. I-S2-3**). Comparing TP_2 to TP_1 in Young showed a significant increase for citrulline (+2.8-fold) (**Table I-S2-5, Fig. I-S2-2**). There were no significant lipid changes (**Table I-S2-6, Fig. I-S2-3**).

Table I-2-1. Metabolites and lipids that changed significantly over the four-day of cold stress in the flag leaves of cold-sensitive Wyalkatchem (W) and cold-tolerant Young (Y), analyzed by One-way ANOVA with FDR-adjusted $p < 0.05$ as significance, followed by Tukey Test.

Flag leaves_within variety				Flag leaves_between the two varieties	
Wyalkatchem		**Young**		**Wyalkatchem versus Young**	
Metabolites	Lipids	Metabolites	Lipids	Metabolites	Lipids
				2-cis-4-trans-Abscisic acid	LPC(30:6)
2-Oxoglutarate	PC(32:0)		PC(32:0)	2-Oxoglutarate	PC(32:0)
			PC(32:1)	Aconitate	PC(32:1)
Alanine				Alanine	PC(32:2)
				Arabinose	PC(33:1)
	PC(33:2)			Arabitol	PC(33:2)
Arginine				Arginine	PC(33:3)
Asparagine				Asparagine	PC(33:4)
beta-Alanine	PC(34:0)		PC(34:0)	beta-Alanine	PC(34:0)
Citrate	PC(34:1)		PC(34:1)	Citrate	PC(34:1)
Citrulline				Citrulline	PC(34:2)
Fructose	PC(34:3)		PC(34:3)	Fructose	PC(34:3)
				Fructose-6-P	PC(34:4)
GABA	PC(35:0)			GABA	PC(35:0)
	PC(35:1)			Galactitol	PC(35:1)
Glucose				Glucose	PC(35:2)
Glucose-6-P			PC(35:3)	Glucose-6-P	PC(35:3)
Glycine				Glycine	PC(35:4)
Histidine				Histidine	PC(35:5)
				Homoserine	PC(36:1)
	PC(36:2)			Inositol	
	PC(36:3)			Isocitrate	PC(36:3)
Isoleucine	PC(36:4)			Isoleucine	PC(36:4)
Leucine	PC(36:6)			Leucine	PC(36:6)
Lysine				Lysine	PC(37:4)
	PC(38:3)			Maltose	PC(38:3)
Mannose	PC(38:4)			Mannose	PC(38:4)
				Methionine	PC(38:6)
Phenylalanine				Phenylalanine	PC(39:3)
Proline				Proline	PC(41:6)
Putrescine				Putrescine	PE(34:3)
				Quinate	PE(36:4)
				Raffinose	PE(36:6)
				Ribose	PE(38:3)
				Salicylic acid	PE(38:6)
				Serine	PE(40:10)
Shikimate		Shikimate	PG(32:0)	Shikimate	PG(32:0)
Sucrose				Sucrose	PG(32:1)
	PG(34:1)			trans-Cinnamic acid	PG(34:1)
	PG(34:2)			Trehalose	PG(34:2)
Tryptophan	PG(34:3)				PG(34:3)
Tyrosine				Tyrosine	PG(36:4)
Valine	PG(36:5)		PG(36:5)	Valine	PG(36:5)
				Xylose	PG(36:6)
					PI(34:3)
	PI(36:4)				PI(36:4)
			PI(36:5)		PI(36:5)
	PI(36:6)		PI(36:6)		PI(36:6)

After prolonged four-night cold treatment (TP_3), more significant accumulation of sugars and organic acids were observed in Wyalkatchem flag leaves compared to the first overnight exposure to cold (WTP_1; **Fig. I-2-1**). Fructose (+4.1-fold) and glucose (+6.0-fold) increased significantly in Wyalkatchem flag leaves. Also, arabinose (+1.3-fold) and mannose (+1.4-fold) were higher compared to TP_1. Two organic acids, quinate (+1.5-fold) and shikimate (+2.3-fold), and one amine, putrescine (+1.8-fold), were significantly higher. One amino acid, asparagine (+3.9-fold) was markedly lower at WTP_3 compared to WTP_1. Prolonged cold treatment of Wyalkatchem also resulted in more lipid changes at WTP_3 compared to WTP_1. Four lipids were significantly reduced, one being a saturated species PC(32:0) and the remaining three being unsaturated species PC(32:1), PC(36:6), PI(36:6). Another 13 lipids increased significantly; one of them was a saturated lipid, while 12 others were unsaturated species (**Fig. I-2-2, Table I-S2-6**). In Young, none of the primary metabolites were significantly changed at YTP_3 compared to YTP_1 (**Fig. I-2-1**). The most notable changes after prolonged cold stress (YTP_3) in Young flag leaves compared to the shorter cold stress (YTP_1) were in the lipid levels. Fifteen lipids were significantly reduced compared to TP_1, while one polyunsaturated lipid species, PC(38:2), was significantly higher (1.4-fold). Of the 15 lipids with reduced levels, two were saturated species while a majority (13) were unsaturated species (**Fig. I-2-2, Table I-S2-6**). Comparing TP_4 day-time samples to TP_3 in Wyalkatchem and Young revealed that there were no significant differences in primary metabolites (**Table I-S2-5, Fig. I-S2-2**), while only one polyunsaturated lipid species, PC(41:6) was increased (+1.5-fold) in Young flag leaves (**Table I-S2-6, Fig. I-S2-3**).

2.4.4 Young and Wyalkatchem Show Significant Varietal Differences in Cold Acclimation across Time Points

Sample comparisons: WTP vs. YTP at each time point

In the unstressed plants (TP_0), there were no significant differences in the levels of primary metabolites or lipids between Wyalkatchem and Young flag leaves (**Fig. I-2-3 and I-2-4**). However, several metabolites with potential roles in stress responses were slightly higher in Young compared to Wyalkatchem: sucrose (+1.4-fold), mannitol (+1.8-fold), GABA (+3.1-fold), ABA (+1.7-fold). At TP_0, there were no significant differences between Wyalkatchem and Young in terms of lipid content. However, some lipid levels appeared to be different in Wyalkatchem and Young flag leaves. Some lipids were lower in Young compared to Wyalkatchem when a cut-off of 0.1 was used: PC(33:4) (–1.5-fold), PG(36:6) (–1.6-fold) and PI(36:6) (–1.6-fold). Others were

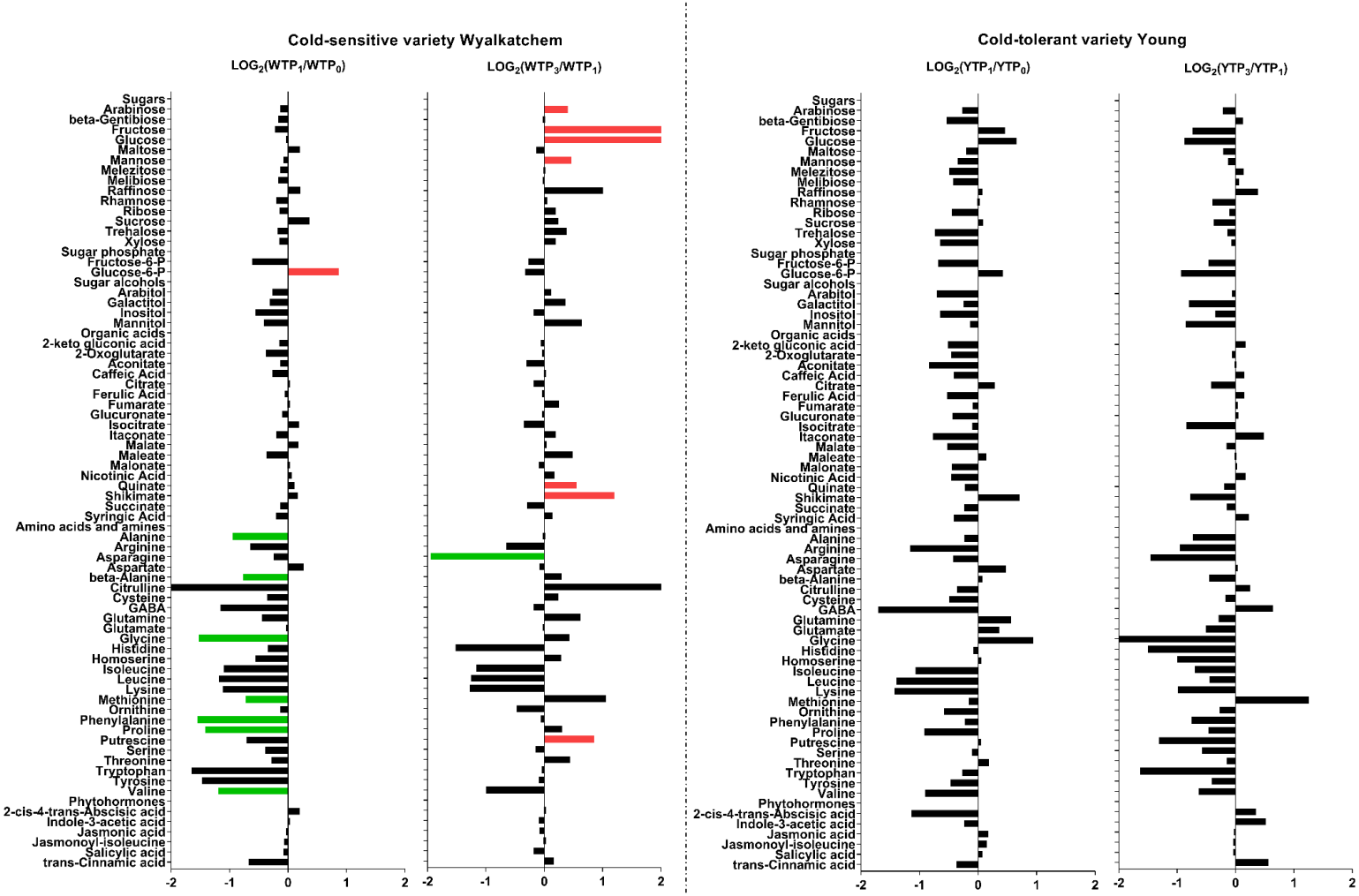


Figure I-2-1. Log_2-fold changes of primary metabolites in the flag leaves of the cold-sensitive Wyalkatchem (W) and cold-tolerant Young (Y) after one night (TP_1 vs. TP_0) and prolonged (TP_3 vs. TP_1) of cold treatment. Fold changes were calculated by dividing the concentration of the variety at a time point (e.g., TP_1) to the concentration of that variety at the previous time point (e.g., TP_0), then Log_2-transformed. Significance of difference was determined by Benjamini and Hochberg method (Benjamini and Hochberg 1995) with false discovery rate (FDR)-adjusted *p*-value of 0.05 as the cut-off. *Green* significant decrease, *Red* significant increase. There were four biological replicates (n = 4) for all the measured metabolites, except phytohormones (n = 3).

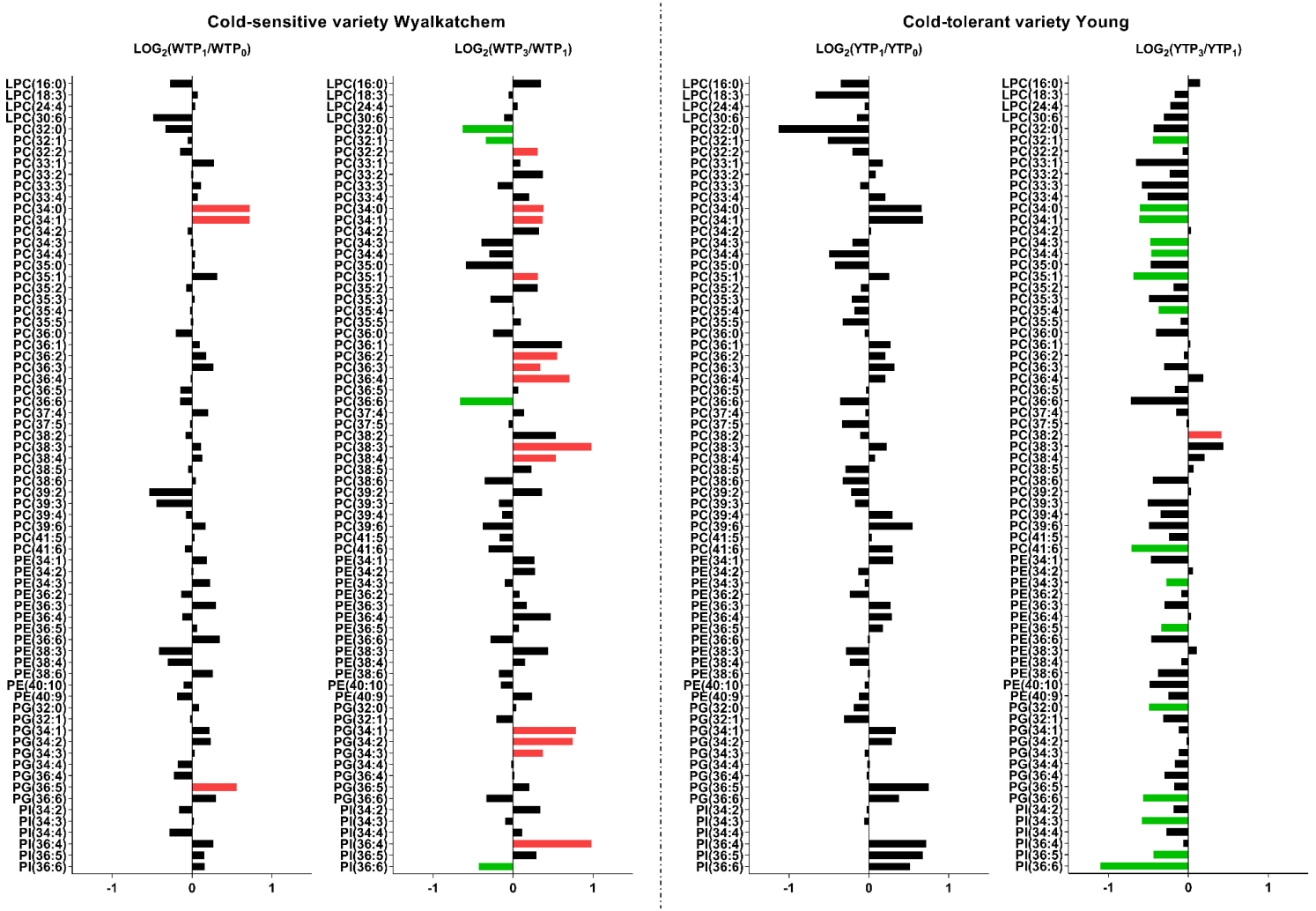


Figure I-2-2. Log_2-fold changes of phospholipids in the flag leaves of the cold-sensitive Wyalkatchem (W) and cold-tolerant Young (Y) after one night (TP_1 vs. TP_0) and prolonged (TP_3 vs. TP_1) of cold treatment. Fold changes were calculated by dividing the normalized response of the variety at a time point (e.g., TP_1) to the normalized response of that variety at the previous time point (e.g., TP_0), then Log_2-transformed. Statistical method and cut-offs are as stated in Fig. 1. *Green* significant decrease, *Red* significant increase. There were four biological replicates (n = 4) for all the measured lipids

higher in Young compared to Wyalkatchem ($p < 0.1$): PC(35:1) (+1.5-fold), PG(34:1) (+1.4-fold) and PG(34:2) (+1.4-fold) (Fig.4). Although these lipids (indicated by asterisks) did not satisfy the significance threshold ($p<0.05$) at TP_0, they did become significantly different ($p<0.05$) after the first night of cold treatment (TP_1; **Fig. I-2-4**). This may indicate that the lipid composition in Wyalkatchem and Young may be different before cold treatment. This is also reflected by the fact that at TP_0, the unsaturated to saturated lipid ratio of Young (218.6 ± 10.6) was significantly lower than in Wyalkatchem flag leave samples (265.2 ± 16.0; **Fig. I-2-5a, Table I-S2-11**).

After overnight exposure to cold (TP_1), two amino acids and amines were significantly higher in Young compared to Wyalkatchem (**Fig. I-2-3**): homoserine (+2.2-fold) and methionine (+2.4-fold). Trehalose (+2.2-fold) was the only sugar that was significantly higher in Wyalkatchem flag leaves. The phytohormone salicylic acid decreased in Young compared to Wyalkatchem (–2.4-fold). Lipids showed the most dramatic difference between the two varieties at TP_1. Fourteen lipid species were significantly higher in Young TP_1 samples and all were polyunsaturated lipids. Thirteen lipid species were significantly higher in Wyalkatchem compared to Young, and all were also unsaturated lipids (**Fig. I-2-4, Table I-S2-6**). The lipid unsaturation to saturation ratio was not significantly different between Wyalkatchem and Young flag leaves at this time point (Fig. 5a). When comparing the TP_2 samples between the two wheat varieties (YTP_2 vs. WTP_2), two metabolites in Young were significantly lower compared to Wyalkatchem (**Fig. I-2-3**): trehalose (–3.0-fold), and asparagine (–2.4-fold). None of the lipid species were significantly different in Young compared to Wyalkatchem at this time point (**Fig. I-2-4, Table I-S2-6**). There was no significant difference in the lipid unsaturation to saturation ratio between the two varieties at TP_2 (**Fig. I-2-5a, Table I-S2-11**).

After prolonged cold stress exposure (TP_3; **Fig. I-2-3**), some metabolites were significantly lower in Young compared to Wyalkatchem, including arabinose (–1.4-fold), fructose (–4.2-fold), glucose (–5.7-fold), mannose (–1.5-fold), quinate (–1.6-fold), shikimate (–2.4-fold), putrescine (–2.4-fold) and salicylic acid (–2.1-fold). Comparison of the lipids at TP_3 again showed the biggest difference between the two varieties. Twenty-five lipid species were significantly lower at TP_3 in Young compared to Wyalkatchem (**Fig. I-2-4, Table I-S2-6**). The total lipid unsaturation to saturation ratio was significantly higher in Young compared to Wyalkatchem at this stage (**Fig. I-2-5a, Table I-S2-11**). Comparison of TP_4 samples between Young and Wyalkatchem (YTP_4 *vs.* WTP_4) showed that only three metabolites were significantly lower in Young compared to

Wyalkatchem (**Fig. I-2-3**): fructose (–2.6-fold), quinate (–1.8-fold) and shikimate (–3.0-fold). In addition, six lipids were significantly lower in Young when compared to Wyalkatchem (**Fig. I-2-4, Table I-S2-6**). They were PC(32:1), PC(34:4), PC(35:4), PC(38:6), PG(32:0) and PG(36:6). All of these six lipids were the same as those found to be lower in Young at previous time points (TP_1 to TP_3). The unsaturation to saturation ratio of Young was again significantly higher than Wyalkatchem at this stage (**Fig. I-2-5a, Table I-S2-11**).

2.4.5 Quantitative Changes in Two Groups of Lipids May Account for Differences in Membrane Fluidity and Cold Tolerance between Young and Wyalkatchem

The time course experiment revealed that the unsaturated to saturated lipid ratio changed progressively from being higher in Wyalkatchem compared to Young at TP_0, to higher in Young at TP_3 and TP_4 (**Fig. I-2-5a**). This shift in unsaturated to saturated lipid ratio is correlated with differences in the expression profile of two main groups of lipids from TP_0 onwards (**Fig. I-2-5b and I-2-5c**). The first group of 11 lipids was higher in Wyalkatchem after the first cold exposure (TP_1) and remained higher than in Young throughout the four-day time course (**Fig. I-2-5b, Table I-S2-12**). In contrast, another group of 18 lipids (**Fig. I-2-5c, Table I-S2-13**) were on average higher in Young compared to Wyalkatchem from the first exposure to cold onwards (TP_1), but 5 members of this group behaved quite differently in the two wheat varieties (**Fig. I-2-5c**). The saturated species PC(34:0), monounsaturated species PC(34:1) and PC (35:1) were significantly increased in both Wyalkatchem and Young after one overnight cold stress event (TP_1), but were then reduced drastically in Young compared to Wyalkatchem after the fourth night of cold stress (TP_3). A fourth lipid, PI(36:4), was increased in Young from time points TP_1 to TP_3, but was induced more strongly in Wyalkatchem after prolonged cold exposure (TP_3). The unsaturated lipid species PC(38:3) was always significantly higher in Young compared to Wyalkatchem from TP_0 onwards and is gradually increased during prolonged cold exposure and was not subjected to diurnal fluctuations (TP_2 and TP_4). PC(38:3) was only increased in Wyalkatchem from TP_3 onwards. The combined changes in these two lipid groups and the differential expression behaviour of some members in these lipid groups may contribute towards the observed increase in the ratio of unsaturated to saturated lipids in Young compared to Wyalkatchem (**Fig. I-2-5a, Table I-S2-11**).

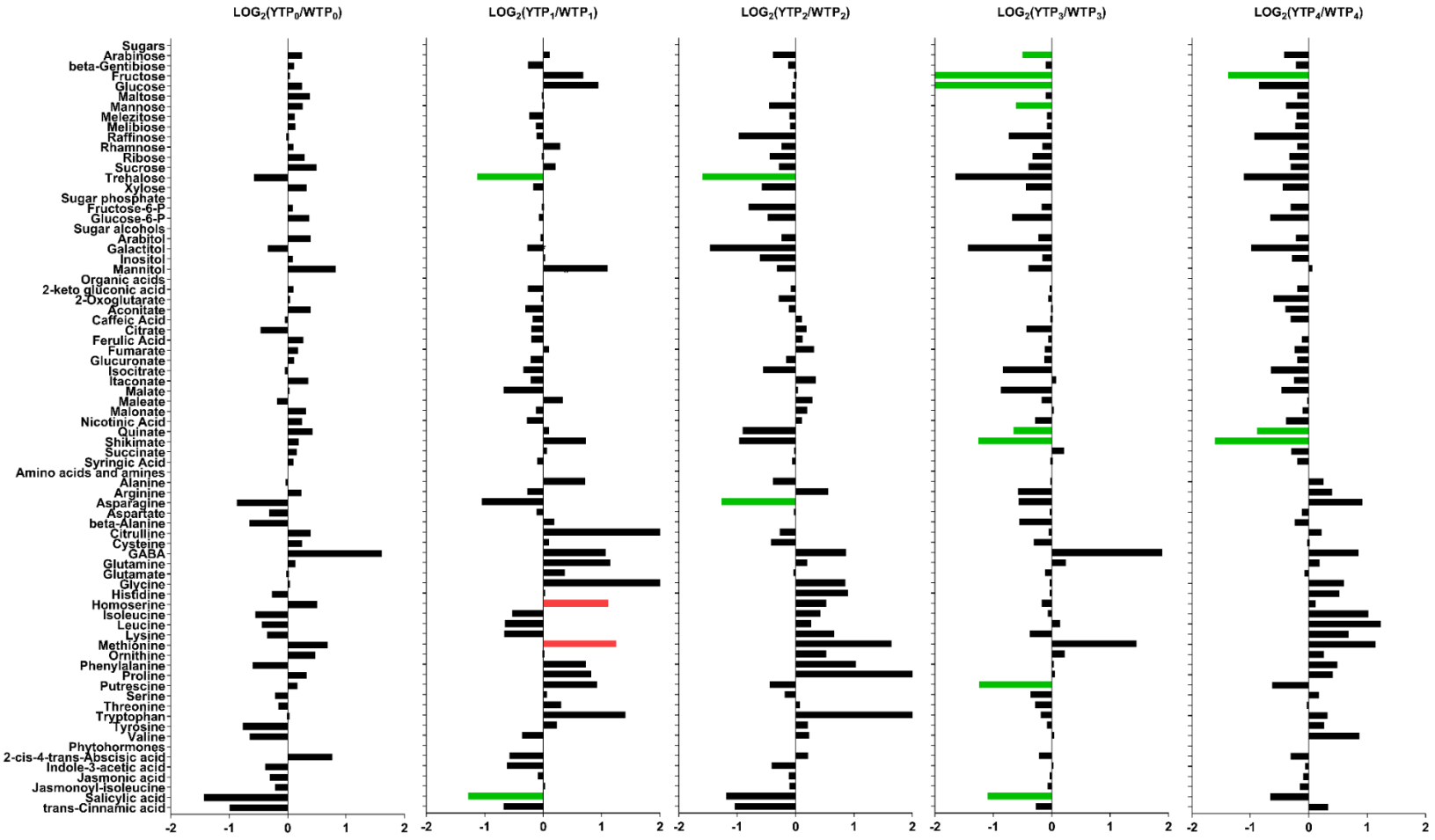


Figure I-2-3. Log_2-fold changes of primary metabolites in the flag leaves of cold-tolerant Young (Y) compared to the cold-sensitive Wyalkatchem (W) at each time point. Fold changes were calculated by dividing the concentration of Y to the concentration of W at that particular time point, then Log_2- transformed. Statistical method and cut-offs are as stated in Fig. 1. *Green* significantly lower in Young/higher in Wyalkatchem; *Red* significantly higher in Young/lower in Wyalkatchem. There were four biological replicates (n = 4) for all the measured primary metabolites, except phytohormones (n = 3).

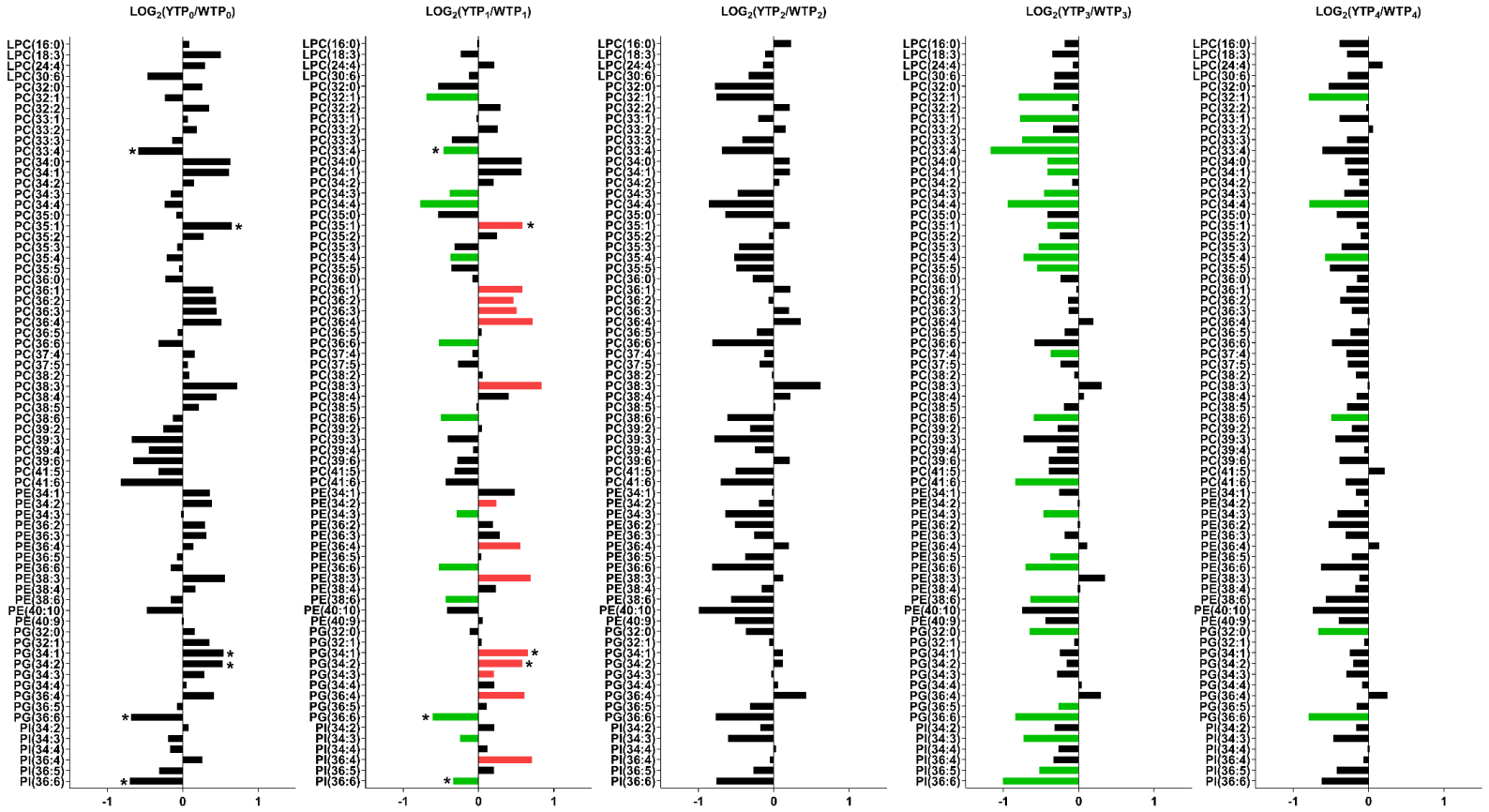


Figure I-2-4. Log_2-fold changes of phospholipids in the flag leaves of the cold-tolerant Young (Y) compared to the sensitive Wyalkatchem (W) at each time point. Fold changes were calculated by dividing the concentration of Y to the concentration of W at that particular time point, then Log_2-transformed. Statistical method and cut-offs are as stated in Fig. 1. *Green* significantly lower in Young/higher in Wyalkatchem; *Red* significantly higher in Young/lower in Wyalkatchem. There were four biological replicates (n = 4) for all the measured lipids. Three lipids: PC(33:4), PG(36:6) and PI(36:6) were lower in Young compared to Wyalkatchem, while another three lipids: PC(35:1), PG(34:1) and PG(34:2) were higher in Young compared to Wyalkatchem when a cut-off of 0.1 was used. Although these six lipids (indicated with asterisks at TP_0 and TP_1) did not satisfy the significance threshold ($p < 0.05$) at TP_0, they did become significantly different after the first night of cold treatment (TP_1).

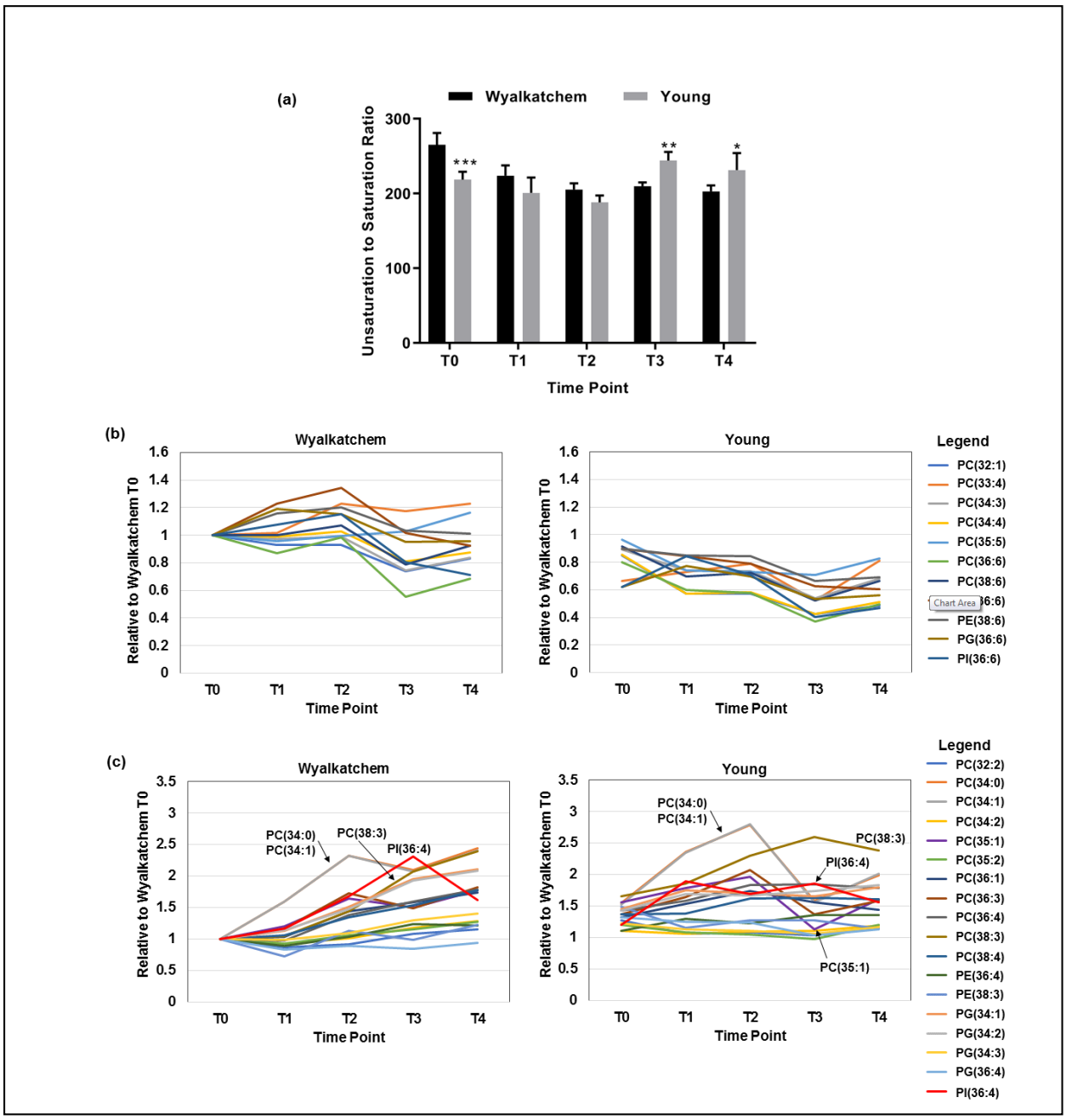


Figure I-2-5. (a) Unsaturation to saturation ratio in Wyalkatchem and Young across the time points. Student's *t*-test was used to compare the ratio values between Wyalkatchem and Young at each time point. Error bars indicate the standard deviation (SD) of four biological replicates (n = 4) and asterisks indicate significance levels: *$p < 0.05$, **$p < 0.01$ and ***$p < 0.001$. **(b)** Expression levels of a group of 11 lipids with higher expression from TP_1 onwards in the cold-sensitive Wyalkatchem compared to Young [(PC(32:1), PC(33:4), PC(34:3), PC(34:4), PC(35:5), PC(36:6), PC(38:6), PE (36:6), PE(38:6), PG(36:6), PI(36:6)]. These lipids had higher levels in Wyalkatchem after the first cold treatment and most of them remained higher than in Young throughout the treatment. **(c)** Expression levels of a group of 18 lipids with higher expression from TP_1 onwards in the cold-tolerant Young compared to Wyalkatchem [(PC(32:2), PC(34:0), PC(34:1), PC(34:2), PC (35:1), PC(35:2), PC(36:1), PC(36:3), PC(36:4), PC(38:3), PC(38:4), PE(36:4), PE(38:3), PG(34:1), PG(34:2), PG(34:3), PG(36:4), PI(36:4)]. Arrows indicate three lipids, PC(34:0), PC(34:1) and PC(35:1), that changed drastically from TP_2 onwards in Young. b and c illustrate how these lipids behaved after long term exposure to cold and how they respond to diurnal rhythms.

2.5 Discussion

2.5.1 Wheat Chilling and Frost Tolerance: Field *vs.* Controlled Environment Phenotyping

In the field, phenotyping for wheat frost tolerance is complicated by the unpredictability and spatial/temporal variation in the severity of frost events (Frederiks et al. 2012). Field phenotyping has focused on the presence/absence of tissue damage and yield effects caused by frosts. Frost events at the critical stage of flowering are often catastrophic, leading to the assumption that there is little genetic variation for frost tolerance in wheat (Frederiks et al., 2012; Zheng et al., 2015; Barlow et al., 2015). Non-freezing, chilling conditions occur far more frequently in the field, but the associated sterility and loss in spike grain number has received less attention (Subedi et al. 1998; Chakrabarti et al., 2011; Smith and Zhao, 2016). In rice, cold-induced pollen sterility causing loss in grain yield is commonly used as a phenotyping trait (Hayase et al., 1969; Satake et al., 1969; Nishiyama, 1984; Oliver et al., 2005). Similar to drought and heat stress, phenotyping for chilling and frost tolerance in the field is compromised by avoidance or escape mechanisms such as phenology of flowering (Fleury et al., 2010; Richards et al., 2010; Shavrukov et al., 2017). Controlled environment phenotyping can overcome some of the pitfalls associated with field work. Occurrence and severity of cold events can be monitored and repeated consistently, as well as their timing during reproductive growth controlled, making it possible to study the physiological and molecular basis of cold tolerance without the interference of avoidance or escape mechanisms or the complexity of changes in frost severity and duration between events. We established a controlled environment screening method based on maintenance of grain number under chilling conditions using two wheat cultivars that were reproducibly shown to be more tolerant (Young) and sensitive (Wyalkatchem) to field chilling and frost conditions. This screening method allowed us to reproduce the field rankings for the two cultivars, as well as the cold tolerance rankings for several other tolerant and sensitive wheat cultivars from the National Frost Initiative (Dolferus et al., unpublished results). Chilling conditions led to a reduction in spike grain number in wheat and we show that the YM and anthesis stages are the two most sensitive stages to chilling stress.

2.5.2 Metabolomics as Alternative Phenotyping Tool for Chilling and Frost Tolerance in Wheat

Tolerance to frost requires the establishment of an acclimation response in plant tissues. Cold acclimation starts below a certain non-freezing threshold temperature before below-zero temperatures cause ice formation and dessication and freezing damage to plant tissues (Livingston et al., 2016). It remains unclear how much time it takes for effective cold acclimation to reach maximal potential, nor do we know whether there is genetic variation in quantitative or qualitative aspects of cold acclimation (Pagter and Arora, 2013; Vankova et al., 2014; Chen et al., 2014; Fiebelkorn and Rahman, 2016). Understanding what acclimation to non-freezing or chilling conditions involves is essential to understand how frost tolerance (cold, chilling/dessication and freezing) can be improved.

Acclimation to abiotic stresses such as cold leads to accumulation of metabolites in plant tissues to protect cellular functions (Morgan, 1992; Ruelland et al., 2009; Ouellet and Charron, 2013; Miura and Furumoto, 2013). Some of these compounds act as osmoprotectants to protect against abiotic stresses that affect the water balance of plants (Vágújfalvi et al., 1999; Uemara et al., 2003; Chen et al., 2014). Osmolytes are small, electrically neutral, water-soluble organic compounds that efficiently maintain osmotic balance and stabilize membranes and macromolecules under water stress conditions. They include betaines, amino acids, polyols and non-reducing sugars (Burg and Ferraris, 2008; Slama et al., 2015; Nahar et al., 2016; Argiolas et al., 2016). Osmolytes also protect membranes and act as scavengers for toxic reactive oxygen species. They are induced by a variety of other abiotic stresses that affect the water balance (drought, heat, salinity), making them therefore less specific markers for cold tolerance per se (Beck et al., 2007). There is no clear evidence available as to how quantitative or qualitative differences in accumulation of these compounds directly contribute to cold tolerance. We compared changes in the concentrations of metabolites and lipids during cold acclimation for two wheat varieties that differ in cold tolerance. Many metabolites are subject to day-night circadian fluctuations and cold or frost events usually occur during the night. It has been demonstrated that there is a substantial overlap between cold and circadian-regulated genes, suggesting that cold acclimation is tightly linked to circadian rhythms (Espinoza et al., 2010; Sanchez et al., 2011). However, it is expected that some compounds that accumulate after an initial chilling or frost event during the night remain present in plant tissues as a protection against subsequent chilling events.

To investigate this, we designed an experiment where we compared metabolite levels in leaves harvested in the morning immediately after a chilling event and six hours later, when plants were allowed to recover in the light at normal temperatures. We also compared these samples for a single and four consecutive chilling cycles. Because our focus is on using metabolites as diagnostic markers for cold acclimation, we first used the easy-to-collect flag leaves.

2.5.3 Effect of Prolonged/Consecutive Chilling Treatments on Wheat Flag Leaf Metabolites and Lipids

Cumulative changes with respect to TP_0, TP_1 and TP_3 for both Wyalkatchem and Young flag leaves show significant changes occurring after the first cold night (TP_1), with additional changes appearing after prolonged cold treatment (TP_3). However, fewer changes were observed in the day-time samples (TP_2 and TP_4), suggesting that partial recovery takes place during normal day temperatures for some metabolites. Day-night fluctuation in levels of some metabolite is likely due to circadian rhythms and fluctuation of photosynthetic activity and associated metabolism and needs to be taken into account for field sampling and cold tolerance phenotyping. After the first night of cold treatment, a significant reduction in the levels of most amino acids and amines was evident in Wyalkatchem, but not in Young. Most amino acids and amines were higher in Young compared to Wyalkatchem from the first overnight cold treatment (TP_1). Interestingly, the amino acids proline and citrulline, which are known to accumulate in plant tissues under a variety of stresses that affect water relations (drought, salinity, cold, heat; Mayer et al., 1990; Ashraf and Foolad, 2007; Lehmann et al., 2010; Hayat et al., 2012; Liang et al., 2013), behaved quite differently in Wyalkatchem compared to Young. Proline was found to decrease significantly after one night of cold treatment in Wyalkatchem but increased in Young flag leaves. Citrulline behaved in a similar fashion, but was only found to change significantly at a more relaxed cut-off of ($p < 0.1$) in both wheat lines. Citrulline has hydroxyl radical scavenging and antioxidant properties and can protect DNA and enzymes from oxidative injuries (Kawasaki et al., 2000; Akashi et al., 2001; Rimando et al., 2005; Kusvuran et al., 2013).

In Young, a significant increase in citrulline was observed in the TP_2 samples. GABA, an amine with cryo-protective properties (Bouche and Fromm, 2004; Mazzucotelli et al., 2006) was also marginally increased - albeit below significance levels. After the prolonged cold treatment (TP_3), amino acid levels in Wyalkatchem did not fully recover and citrulline increased further.

Accumulation of citrulline occurred predominantly in Wyalkatchem and only temporarily in Young (TP_1). Wyalkatchem also showed a three-fold increase for the polyamine putrescine, an amino acid breakdown product with growth-regulatory properties known to play a role in abiotic stresses (Gil and Tuteja, 2010; Shi and Chan, 2014). Shikimate, a substrate for the synthesis of lignin and various aromatic compounds such as quinate (Hermann and Weaver 1999; Guo et al., 2014) was increased in Wyalkatchem but decreased in Young. The enzymes of this pathway have been shown to be involved in defence responses (Kasai et al. 2005). Furthermore, compatible osmolytes such as sugars (arabinose, glucose, glucose-6-P, fructose and raffinose) and the sugar alcohol mannitol also accumulated in Wyalkatchem upon cold treatment, but not in Young flag leaves. Sugars and sugar alcohols play a role as osmo- and cryo-protectants (Loescher et al., 1992; Travert et al., 1997; Burg and Ferraris, 2008; Slama et al., 2015). The accumulation of these osmolytes indicates that Wyalkatchem is responding to water or dessication stress as a consequence of cold treatment. Repression of amino acid synthesis in Wyalkatchem may also contribute to this situation. None of these symptoms was observed in tolerant variety Young. Osmolytes can therefore serve as markers for chilling sensitivity; they may be indicative of water stress as a result of membrane damage caused by chilling and frost. But osmolytes point to a secondary effect of cold treatment and their accumulation is therefore not specific for low temperature stress. Osmolyte accumulation can be activated by other abiotic stresses as well (drought, heat, salinity; Beck et al., 2007). We did not observe many significant differences in phytohormone levels between Wyalkatchem and Young. Interestingly, the only phytohormone that showed significant differences between the two wheat varieties was salicylic acid. Trans-cinnamic acid (significant at TP2), one of the precursors of salicylic acid biosynthesis (Hayat et al., 2007), follows the same abundance profile as salicylic acid. Salicylic acid levels were consistently higher in Wyalkatchem compared to Young at both short and prolonged cold stress exposures. Salicylic acid is known for its role in plant pathogen responses, but also plays a role in abiotic stress in regulating stomatal closure under water stress. When applied to plants, salicylic acid was shown to reduce freezing tolerance and at high levels causes oxidative stress and increased stress sensitivity (Lissarre et al., 2010; Miura and Tada, 2014; Eremina et al., 2016).

Cold treatment of Wyalkatchem and Young flag leaves resulted in quantitative and qualitative changes in the lipid composition and the lipid changes outnumber those observed for the primary metabolites. The most prevalent changes in cold-stressed Wyalkatchem and Young

flag leaves were observed for the phospatidylcholine (PC) class of lipids. PCs are the most abundant plasma membrane lipids in plants and animals. Differences between Wyalkatchem and Young PC levels in response to cold may therefore contribute to changes in plasma membrane fluidity and permeability (Upchurch et al., 2008; van Meer et al., 2008). The saturated lipid species PC(34:0), monounsaturated species PC(34:1) and PC(35:1) increased in both wheat varieties after the first exposure to cold (TP_1) and then decreased after prolonged cold treatment (TP_3) (**Fig. I-2-5c**). However, the decrease of these PCs at TP_3 was faster in Young compared to Wyalkatchem and this may have contributed to a higher level of unsaturated lipids in Young compared to Wyalkatchem (**Fig. I-2-5c**). Even at TP_0, Young and Wyalketchem flag leaves show a different lipid saturation:unsaturation ratio and some lipid levels are marginally different, but become significantly different after the first night of cold treatment. This seems to indicate that Young is better adapted to cold from the beginning. The change in the unsaturated to saturated lipid ratio is the result of a change in relatively few lipid species and this may be the result of a modification in the expression of a small number of genes. The fact that Young and Wyalkatchem show a different lipid content before and after cold treatment may indicate that both lines are adapted differently to cold temperatures and this may be due to genetic variation in the regulation or function of lipid biosynthesis gene/genes. Using lipids as phenotyping markers may enable us to identify those genes using a mapping population. The superior ability of the tolerant variety Young to adjust and remodel its membrane composition may be the key factor to overcome prolonged cold exposure. We do not know to what extend the differences in lipid content between Young and Wyalkatchem flag leaves can protect against frost (temperature threshold) or whether the observed differences are sufficient to survive more severe frost conditions. But using lipidomics to screen wheat germplasm collections for varieties with higher lipid unsaturation levels than Young may hold the key to improving frost tolerance in wheat. Plants produce a large variety of lipid species in their chloroplasts and the fact that the spectrum of synthesised lipids depends significantly on the reigning environmental conditions (e.g., temperature) indicates that modification of membrane lipid composition is an important environmental adaption mechanism (Aid, 2018).

Phosphatidylglycerol lipids (PGs) are the main phospholipid class of thylakoid membranes in higher plants (Ren et al., 2014). PGs are the second largest lipid group that is affected by cold in wheat flag leaves. The saturated lipid PG(32:0) is lower in Young and higher in Wyalkatchem flag leaves after the prolonged cold stress (TP_3), indicating that this lipid species may also

contribute to the higher degree of lipid unsaturation in membranes of the tolerant variety Young. Phosphotidylinositol (PI) lipids are the third most abundant extraplastidic lipid. PIs are involved in membrane signalling under abiotic stress conditions such as osmotic stress (Munnik and Vermeer, 2010; Zheng et al., 2016). PIs increase by 50% after freezing in Arabidopsis and contribute to frost tolerance (Zheng et al., 2016). Significantly higher levels in Young compared to Wyalkatchem of polyunsaturated PI species such PI(36:4) at TP_1 may also contribute to better membrane protection for the tolerant variety during cold stress.

Plants respond with complex changes in lipid composition during cold acclimation to maintain membrane integrity (Uemura and Steponkus, 1994; Uemura et al., 1995; Degenkolbe et al., 2012). The amount of double bonds in unsaturated lipids improves membrane fluidity at lower temperatures. To maintain optimum membrane fluidity, unsaturation levels of lipids decreases at higher temperatures and increases at lower temperatures (Narayanan et al., 2016a, b; Zheng et al., 2016). The significant increase in the ratio of unsaturated to saturated lipids after prolonged cold treatment suggests that Young is better able to adapt its membrane composition to low temperatures. Failure of Wyalkatchem to modify lipid composition in favour of unsaturated to saturated lipids may lead to membrane damage, causing electrolyte leakage and water loss, leading to the osmotic stress response observed in this variety. The lipid changes we observed in Young and Wyalkatchem flag leaves are part of an acclimation response to cold; they are amplified during prolonged cold treatment, they are not subjected to diurnal fluctuations and they are specific for low temperature adaptation. Lipids are therefore suitable markers for chilling and frost tolerance phenotyping.

2.6 Conclusion

In conclusion, combined metabolome and lipidome analyses in flag leaves have shed light on important differences in cold acclimation between the cold-sensitive Wyalkatchem and cold-tolerant Young varieties. The main differences between the two wheat cultivars were the differential modification of membrane lipids in both varieties and the establishment of an osmotic stress-like response in the sensitive varieties Wyalkatchem. There is a gradual change in the ratio of unsaturated versus saturated lipids that favors higher levels of unsaturated lipids being incorporated in the tolerant variety Young. As a consequence, Young may acquire a superior ability to adapt membrane fluidity to cold conditions and avoid membrane damage. Diagnostic

metabolites, including sugars and lipids, can therefore serve as tools to improve the reliability of phenotyping for chilling and frost tolerance in wheat. Furthermore, metabolomics and lipidomics can be combined with transcriptome analysis and genomics approaches to identify the genetic mechanism driving the observed differences in metabolite accumulation and this could lead to future DNA marker-based approaches for frost tolerance breeding in wheat.

2.7 Acknowledgements

Cold treatments were carried out using growth chambers from the High- Resolution Plant Phenomics Centre in Canberra (HRPPC; https://www.plantphenomics.org.au/tag/high-resolution-plant-phenomics-centre/). The authors thank Mrs Cheka Kehelpannala from the School of BioSciences, Mrs Nirupama Jayasinghe, Mrs Himasha Mendis, Ms. Veronica Lui and Dr Siria Natera from Metabolomics Australia for the metabolite, lipid and phytohormone analyses. Metabolomics Australia (School of BioSciences, The University of Melbourne, Australia) is a National Collaborative Research Infrastructure Strategy initiative under Bioplatforms Australia Pty Ltd (http://www.bioplatforms.com/).

2.8 Author Contributions

BEC performed part of the metabolite, lipid and phytohormone experiments and analysed the data. WWHH and TWTR contributed to the data analysis. UR designed the metabolite analysis and contributed to data analysis, statistical analysis and manuscript writing. RD conceived the project, designed the experiments and contributed to the writing of the manuscript. RD, XW, and TR established the controlled environmental conditions for chilling treatments and harvested the plant tissue samples for metabolite analysis. BB provided advice on the wheat germplasm to best use in this study and provided field climatic information, as well as advice to establish the controlled environmental conditions most likely to provide discriminating damage based on field experience in phenotyping the same material. BEC, WWHH, TWTR and RD wrote the manuscript.

2.9 Funding

This research was supported by grants of the Australian Grains Research and Development Corporation (GRDC projects CSP00143 and CSP00202).

CHAPTER 2

(Part II)

2.10. The following work was published in *Cells* (2020) Volume 9: Article 1309 (DOI: 10.3390/cells9051309). The work presented in this chapter has been modified from the original published paper in which the numbering for each main section is modified to begin with **2.10.x.** Besides, all the numberings of the figures and tables are modified to begin with **II-2-x** (II represents Part II; 2 represents chapter 2; x represents number in sequence) and for supplemental data are begin with **II-S2-x** (S represents supplemental).

Title

Phenotyping the Chilling and Freezing Responses of Young Microspore Stage Wheat Spikes Using Targeted Metabolome and Lipidome Profiling

Bo Eng Cheong [1], Olive Onyemaobi [2], William Wing Ho Ho [1], Ben Biddulph [3], Thusitha W.T. Rupasinghe [1], Ute Roessner [1], Rudy Dolferus [2,*]

1 School of BioSciences, The University of Melbourne, Victoria 3010, Australia; cheongb@student.unimelb.edu.au (B.E.C.); whho@unimelb.edu.au (W.W.H.H.); tru@unimelb.edu.au (T.W.T.R.); u.roessner@unimelb.edu.au (U.R.)

2 CSIRO Agriculture & Food, GPO Box 1700, Canberra ACT 2601, Australia; Olive.Onyemaobi@csiro.au (O.O.); rudy.dolferus@csiro.au (R.D.)

3 Department of Primary Industries and Regional Development, 3 Baron Hay Court, South Perth, WA 6151, Australia; ben.biddulph@dpird.wa.gov.au (B.B.)

* Correspondence: rudy.dolferus@csiro.au; Tel.: +61-2-6246 5010 (R.D.)

2.10.1 Abstract

Chilling and frost conditions impose major yield restraints to wheat crops in Australia and other temperate climate regions. Unpredictability and variability of field frost events are major impediments for cold tolerance breeding. Metabolome and lipidome profiling were used to compare the cold response in spikes of cold-tolerant Young and sensitive variety Wyalkatchem at the young microspore (YM) stage of pollen development. We aimed to identify metabolite markers that can reliably distinguish cold-tolerant and sensitive wheat varieties for future cold-tolerance phenotyping applications. We scored changes in spike metabolites and lipids for both varieties during cold acclimation after initial and prolonged exposure to combined chilling and freezing cycles (1 and 4 days, respectively) using controlled environment conditions. The two contrasting wheat varieties showed qualitative and quantitative differences in primary metabolites involved in osmoprotection, but differences in lipid accumulation most distinctively separated the cold response of the two wheat lines. These results resemble what we previously observed in flag leaves of the same two wheat varieties. The fact that this response occurs in tissue types with very different functions indicates that chilling and freezing tolerance in these wheat lines is associated with re-modelling of membrane lipid composition to maintain membrane fluidity.

Keywords

wheat; spike; cold tolerance; phenotyping; reproductive development; metabolomics; lipidomics

2.10.2 Introduction

Frost events can cause major yield losses to cereal crops in many temperate climate regions in the world. Wheat crops in Australia are grown during winter and they flower in early spring to avoid the hot summers and to take advantage of available soil moisture. The sensitive stage of flowering is therefore frequently exposed to frost. The annual yield loss due to frost events to the Australian grains industry is estimated to be A$360 million (Paulsen and Heyne, 1983; Boer et al., 1993, Gu et al., 2008, Frederiks et al., 2015, Zheng et al., 2015). The problem is exacerbated by climate change. In China and Australia, spring frosts have become increasingly frequent since the 1960s and the length of the frost season has been extended by one month, leading to more frequent yield losses due to frost damage (Zheng et al., 2015; Li et al., 2014; Crimp et al., 2015; Li et al., 2015).

In field conditions, severity, occurrence and timing of frosts during plant development are highly variable, making screening and selection for wheat germplasm with higher frost tolerance very difficult. Using controlled environment experiments is complicated by the fact that radiative frost conditions are difficult to simulate (Marcellis et al., 1975; March et al., 2020; Frederiks et al., 2012; Single 1966). Phenology and flowering time play an important role in avoiding exposure of the sensitive reproductive structures, anthers in particular, to frosts (Zheng et al., 2015; Crimp et al., 2015; Fowler et al., 2001; Limin and Fowler, 2006). The increased frequency of frost occurrences in field environments indicates the need for wheat germplasm with improved tolerance to frost conditions.

Acclimation to non-freezing chilling conditions (above zero degrees, low temperatures) plays an important role in establishing tolerance to freezing (below zero degree) temperatures. Frosts occur when ice crystallization takes place in plant tissue due to a combination of freezing temperatures, humidity, and temperatures falling below the dew point (Marcellos and Single, 1975; Frederiks et al., 2015). Plants respond during the chilling period by mounting an acclimation response to protect macromolecules and cellular functions against reactive oxygen species (ROS) and to protect tissues against ensuing freezing and frost conditions (Mahajan and Tuteja, 2005; Wong and Shimamoto, 2009; Das and Roychoudhury, 2014; You and Chan, 2015). Low temperatures were shown to lead to accumulation of osmolytes (various sugars, polyols, betaines, amines and amino acids) that may act as cryo-protectants to protect the cells against freezing and associated water loss (Vagujfalvi et al., 1999; Uemura et al., 2003; Bouche et al., 2004; Burg and Ferraris, 2008; Nahar et al., 2016). Importantly, protection of membrane fluidity through changes

in unsaturated lipid levels in the membrane was also found to play an important role in protecting plant tissues against frost damage (Los and Murata, 2004; Upchurch 2008; Ruelland and Zachowski, 2010). However, it remains unclear how quantitative and qualitative differences in the accumulation of these compounds during the acclimation response correlates with differences in frost tolerance levels and information about physiological differences in cold-acclimation responses between cold-tolerant and sensitive germplasm is also missing.

Changes in metabolite composition provide a powerful tool to explore cold acclimation and potentially tolerance to chilling and frost conditions. Metabolomics is therefore a technology that can contribute to more accurate and reliable phenotyping of physiological changes in plant tissues (Keurentjes 2009; Weckwerth 2011; Radomiljac et al., 2013). Metabolite and lipidome analyses in wheat flag leaves revealed significant differences in the cold response to chilling of frost-tolerant and sensitive wheat lines: membrane fluidity was maintained mainly by increasing unsaturated lipid levels in cold-tolerant wheat. This response was absent in cold-sensitive wheat, where a water stress-type response was observed instead (Cheong et al., 2019).

The aim of this study was to use metabolomics and lipidomics profiling to investigate changes in cold acclimation in the reproductive tissues (spikes) of two wheat varieties with contrasting cold tolerance. Herein we used the same wheat varieties with our previous published paper, which are the cold-tolerant Young and cold-sensitive Wyalkatchem (Cheong et al., 2019). Metabolites that can reliably differentiate the response of a cold-tolerant and sensitive wheat line are useful as “diagnostic markers” in wheat cold-tolerance phenotyping. To achieve this, we will have to test the reliability of candidate metabolite markers identified in this study first on a wider range of wheat chilling/freezing tolerant and sensitive germplasm before using these markers in routine phenotyping tasks. We scored metabolite and lipidome changes during cold acclimation after initial exposure (1 day) and prolonged exposure to cold (4 days) in order to identify diagnostic metabolite markers that could reliably distinguish the cold-tolerant wheat variety from the cold-sensitive one. We then compared the cold acclimation response between spikes and flag leaves for the two wheat varieties to identify differences in cold acclimation and to determine which tissue is most suitable for cold tolerance phenotyping. Wheat spikes are physiologically different from flag leaves in that the former are actively developing sink tissues, while the latter are static photosynthetic source tissues. Comparison of the primary metabolite and lipid changes in response

to cold for both wheat varieties will enable us to distinguish which metabolites are critically important for cold acclimation.

Abiotic stresses such as cold affect sink source relationships and distribution of sugars in the plant (Lemoine et al., 2013). Source and sink tissues may therefore react differently to cold and reveal accumulation of different metabolites during cold acclimation. At the young microspore (YM) stage and during grain-filling, the reproductive structures in cereals represent the strongest sink strength of the plant. This is essential to attract sugars for reproductive development and grain filling. Sink strength is highest during pollen formation after meiosis and during grain development after fertilization (Zinselmeier et al, 1995a, 1995b; Clement et al., 1996, 1998; Reynolds et al., 2005; Castro and Clement 2007). Abiotic stresses such as cold and drought reduce sink strength in anthers of stress-sensitive lines, while stress tolerance was correlated with a higher potential to maintain sink strength (Oliver et al., 2005; Ji et al., 2010). In this study we demonstrate that cold acclimation in spikes and flag leaves shows some similarities in terms of accumulation of compounds involved in osmoprotection and defense against ROS. However, more importantly, both tissues share a similar mechanism in modifying their lipid composition by increasing the unsaturated to saturated lipid ratio in response to cold. These findings highlight the importance of preserving membrane fluidity in different plant tissues during cold acclimation in wheat. Metabolomics and lipidomics can be exploited as a phenotyping strategy to discriminate cold-tolerant from cold-sensitive wheat germplasm.

2.10.3 Materials and Methods

2.10.3.1 Controlled Environment for Wheat Growth, Cold Treatment and Tissue Sampling

Wheat varieties Wyalkatchem (cold-sensitive) and Young (cold-tolerant), plant growth and cold treatment conditions were as previously described (Cheong et al., 2019). Briefly, plants were grown in the glasshouse under natural lighting conditions and controlled temperature regime (24/16°C, L/D). When plants reached the young microspore (YM) stage of pollen development, YM-stage tillers were tagged and plants were transferred to a Conviron PGC 20 growth chamber (Conviron, Winnipeg, Canada) with the following settings (**Fig. II-2-1A**): 12h at 21°C (light period), 4h linear cooling gradient in the dark to -3°C, followed by 8h in the dark at constant -3°C (12/12 light/dark cycle, using 400µmol/m^2s^1 light intensity) as a cold cycle. The cold-treatment uses a simplified profile of a typical mid-August early morning chilling/frost event in the Southern

Australian wheat growing areas. The linear temperature decline in the profile allows induction of an acclimation response before a period of freezing temperatures. Despite the use of below-zero temperatures, this treatment does not cause ice crystal formation. Ice crystallization depends on humidity and dew point which is hard to control in controlled environments. Super-cooling above the canopy (Marcellos and Single, 1975) or treatments with ice-nucleating agents can cause ice crystallization but were avoided because of secondary effects and because ice formation is not essential for this study that focuses on varietal differences in acclimation to chilling conditions. YM-stage spike samples were harvested at the start of the treatment (TP_0, TP = time point), at the end of the first overnight cold cycle (TP_1), and six hours into the light cycle after the first cold treatment (TP_2). Samples TP_3 and TP_4 are equivalent to TP_1 and TP_2, but samples were harvested after the fourth consecutive cold treatment to study the effect of long-term cold treatment on the acclimation response (Cheong et al., 2019) (**Fig. II-2-1A**). Each sample used for metabolite measurements consisted of three spikes, harvested from different plants, and for each time point we collected three biological repeat samples for both the cold-tolerant and sensitive wheat varieties.

2.10.3.2 Analysis of Sugars, Organic Acids, Amino Acids and Amines

All chemicals and solvents for metabolite measurements were purchased from Sigma-Aldrich (Castle Hill, NSW, Australia) and were of analytical or mass spectrometry grades. For sugars, organic acids and amines, tissue extraction was performed as previously described (Cheong et al., 2019; Dias et al., 2015), with some modifications. Aliquots of 20mg of frozen spike material were weighed in Cryomill tubes (Precellys 24, Bertin Technologies, Rockville, MD, USA). To each sample, 500µL of methanol containing 4% of internal standards (from a stock solution containing 0.5mg/mL of $^{12}C_6$-sorbitol and 0.5mg/mL $^{13}C_5$-^{15}N-L-valine) was added, followed by vortexing for 30 sec and homogenization at -10°C using a Cryomill (3 x 45 sec at 6,100 rpm). The samples were then extracted for 15 mins at 30°C in a thermomixer at 850 rpm, and subsequently centrifuged for 15 mins at 4°C at 13,000 rpm. The supernatants were combined into new tubes and 500µL of 0.2% formic acid (in water) was added into the Cryomill tubes containing the previously ground tissue pellet. The samples were vortexed for 30 sec, and spun at 13,000 rpm for 15 mins at 4°C. The supernatants were then combined with the methanolic extracts from the previous centrifugation and stored at -80°C for subsequent analyses.

For the analyses of sugars and organic acids, an 80µL aliquot of the supernatants was transferred into new glass vial inserts and dried in vacuo without heating. Prior to the GC-QqQ-MS analysis, the dried extracts were derivatized with methoxyamine hydrochloride in pyridine and bis-(trimethylsilyl)-trifluoroacetamide (BFTFA) as previously described (Dias et al., 2015). Briefly, samples were re-dissolved in 20µL of 30mg/mL methoxyamine hydrochloride in pyridine and derivatized at 37°C for 120 mins with mixing at 500 rpm. After addition of 20µL N,O-bis-(trimethylsilyl)-trifluoroacetamide (BSTFA), the samples were incubated for 30 mins with mixing at 500 rpm at 37°C. Derivatized samples were allowed to equilibrate for 60 min and 1µL aliquots of each sample were injected into a GC-QqQ-MS system, consisting of a Gerstel 2.5.2 Autosampler, a 7890A Agilent gas chromatograph and a 7000 Agilent triple-quadruple MS (Agilent Technologies, Santa Clara, CA, USA) with an electron impact (EI) ion source. The instrument settings were the same as described previously (Cheong et al., 2019; Dias et al., 2015). For calibration and quantification of sugars and organic acids in the flag leaf samples, we used serial concentrations of calibration standards (**Table II-S2-1**). Standards included 24 sugars (sugars, sugar phosphates, sugar acids and sugar alcohols) and 19 organic acids, derivatized and subjected to GC-QqQ-MS analysis as described previously (Cheong et al., 2019; Dias et al., 2015).

For the amino acid and amine analyses with LC-QqQ-MS, 10µL of supernatants were transferred into new glass vial inserts. The amino acids and amines in the supernatants were then derivatized with 6-aminoquinolyl-N-hydrosysuccinimidyl carbamate (AQC) reagent (Cheong et al., 2019; Dias et al., 2015; Boughton et al., 2011). Briefly, 10µL samples were added to 70µL of borate buffer (200mM, pH 8.8 at 25°C) containing 10mM TCEP, 1mM ascorbic acid and 50µM 2-aminobutyrate. The resulting solution was vortexed before adding 20µL of 6-aminoquinolyl-N-hydrosysuccinimidyl carbamate (AQC) reagent [200 mM dissolved in 100% acetonitrile (ACN)] and then vortexed immediately. The samples were heated with shaking at 55°C for 10 mins and centrifuged at 13,000 rpm at room temperature and then transferred to HPLC vials containing inserts (Agilent, spring-less glass inserts, 250µL) prior to injection. Aliquots (1µL) of the derivatized samples were immediately injected into a LC-QqQ-MS system comprising of an Agilent 1200 LC-system coupled to an Agilent 6410 Electrospray Ionization-Triple Quadruple-MS. The settings of the LC-MS instrument were previously described [30, 40]. For calibration and quantification of amino acids and amines in the flag leaf samples, a series of concentrations of calibration authentic standards comprising of 29 amino acids and amines (**Table II-S2-1**), mixed

with a sulfur-containing compound solution, were prepared, derivatized and subjected to LC-QqQ-MS analysis same as previously described (Cheong et al., 2019; Dias et al., 2015).

2.10.3.3 Analysis of Lipids

The extraction of lipids was carried out as described previously (Cheong et al., 2019; Folch et al., 1957), with modifications. Briefly, 20mg freshly frozen spike samples were homogenized in 500µL of a 2:1 methanol:chloroform mixture using a Cryomill (Precellys 24, Bertin Technologies, Rockville, MD, USA) for 3x45 sec at 6,100 rpm (-10°C). The extracts were shaken at 750 rpm for 15 mins at 30°C and centrifuged at 13,000 rpm for 15 mins. The supernatants were transferred to new tubes, while 500µL of a 2:1 methanol:chloroform mixture was added again to the remaining residue. The tubes were vortexed and centrifuged again at 13,000 rpm for 15 mins. The supernatants were combined and dried down in vacuo and then re-constituted in 100µL of 1:1 butanol:methanol for the subsequent LC-QqQ-MS analysis using an Agilent 1200 LC-system coupled to an Agilent 6410 Electrospray Ionization-Triple Quadruple-MS system. An injection of 5µL of each total lipid extract was chromatographically separated on an Ascentis Express RP-Amide 50 X 2.1 mm, 2.7µm HPLC column (Sigma-Aldrich, Castle Hill, NSW) using an 8 mins gradient from 0% A to 100% B, which was then held for 2 mins and followed by a 4 mins column re-equilibration with a flow rate of 0.18 mL/min. The mobile phases were: A: 10mM ammonium formate in water:methanol:tetrahydrofuran (50:20:30, v:v:v); B: 10mM ammonium formate in water:methanol:tetrahydrofuran (5:20:75, v:v:v). Lipid species were identified and quantified based on multiple reaction monitoring (MRMs) established using external lipid standards and references from the LIPIDMATCH database (https://github.com/GarrettLab-UF/LipidMatch/releases/tag/v2.0.2) as listed in **Table II-S2-2**, with a 5-20 msec dwell time for the simultaneous measurements of up to 100 compounds. We used optimized parameters for capillary (4000V), fragmentor (60–160V) and collision voltages (20-40V). In all cases, the collision gas was nitrogen with a flow rate of 7L/min. The external lipid standards used were: lysophosphatidylcholine LPC(17:0), lysophophatidylglycerol LPG(16:0), phospatidylcholine PC(20:0) and PC(34:1), phosphatidylethanolamine PE(34:0), phosphatidylglycerol PG(34:1) and PG(36:0), phosphatidylinositol PI(34:2) and PI(36:2), and phosphatidylserine PS(34:0) (Table S2). Detected lipid species were annotated by lipid class designation, followed by the "total number of

carbon atoms in the fatty acid chains" and the "total number of double bonds in the fatty acid chains", separated by a colon sign.

2.10.3.4 Processing of Raw Data

Raw metabolite and lipid data were processed and analyzed using Quantitative Analysis MassHunter Workstation software for QQQ (Agilent Technologies, Santa Clara, CA, USA). The level of identification was carried out based on the Metabolomics Standards Initiative (MSI) requirements (Sumner et al., 2007). For all measured metabolites (sugars, organic acids, amino acids and amines), absolute concentrations were determined for all the metabolites except for fructose-6-phosphate and glucose-6-phophate as the linear standard curves for these two metabolites could not be generated for quantification due to very high abundance of these two metabolites in the spike samples. The concentration unit for all the metabolites was expressed as picomole/mg of fresh weight except responses normalized to mg of fresh weight for fructose-6-phosphate and glucose-6-phophate (**Table II-S2-3**). All the metabolites measured at MSI Level 1, as the identification was based on Multiple Reaction Monitoring (MRMs) established using authentic standards (**Table II-S2-1**). For lipids, responses were normalized to mg of fresh weight, FW (**Table II-S2-4**). Although single authentic lipid species were used for each of the phospholipid class, the identification of individual lipid species was based on both the MRM experiment and retention time and was therefore measured at MSI Level 2 (**Table II-S2-2**).

2.10.3.5 Statistical Analysis of Metabolite and Lipid Data

The statistical analysis for metabolite and lipid data was performed by using MetaboAnalyst v3.0 (Xia and Wishart, 2016). For normalization of metabolite data which already in absolute quantity (picomole/mg of fresh weight), the data was $\log_2$-transformed and mean-centered. For normalization of lipid data which in response/mg of fresh weight, the data was first normalized by median, $\log_2$-transformed, mean-centered and divided by the standard deviation of each variable. Next, for the statistical significance determination of metabolites and lipids in each variety or between varieties, the normalized data was subjected to one-way Analysis of Variance (ANOVA), with false discovery rate (FDR)-adjusted *p*-value of 0.05 as significance level (Benjamini and Hochberg, 1995). This was followed by the Tukey's honestly significant difference (HSD) *post-hoc* test to perform significant pair-wise comparisons performed using MetaboAnalyst 3.0 or

Graphpad Prism 7.0 (GraphPad Software, La Jolla California USA). In order to determine which metabolites or lipids responded specifically to short cold stress (TP_1), prolonged cold stress (TP_3), diurnal fluctuations when the spikes were exposed to normal day-time temperature of 21°C for 6h (TP_2 and TP_4), we performed pairwise comparisons of the selected two groups: TP_1 vs. TP_0 (for short cold stress), TP_3 vs. TP_1 (for prolonged cold stress), TP_2 vs. TP_1 and TP_4 vs. TP_3 (for recovery and the effect of diurnal fluctuations on metabolite levels) in each variety, and also comparisons at every time point between the two varieties (varietal differences) via Student's *t*-test using MetaboAnalyst and GraphPad Prism software. The Student's *t*-test for comparing the unsaturation to saturation lipid ratio (using the response/mg values) between Wyalkatchem and Young at different time points was performed in Microsoft-Excel. All plots shown in the results section were generated either using GraphPad Prism 7.0 software, MetaboAnalyst 3.0 software, and the Venn diagram webtool (http://bioinformatics.psb.ugent.be/webtools/Venn/).

2.10.4 Results

2.10.4.1 Metabolite and Lipid Profiling Using YM Stage Wheat Spikes

The spike tissues analyzed in this study were collected from the same plant material treated by the same controlled environment cold treatment as the previously analyzed flag leaf samples [30]. YM stage spikes are actively developing sink tissues inside the leaf sheaths of the wheat plant where they lack direct exposure to light (**Fig. II-2-1B**). This material needs to be destructively harvested (i.e., plants will not produce seeds) for metabolite analysis. The cold-tolerant wheat variety Young used in this study consistently performs better than the cold-sensitive variety Wyalkatchem in terms of spike grain yield in both field trials of the Australian National Frost Program (ANFP) and our controlled environment assays (Cheong et al., 2019). The aim of the time-course experiment was to capture changes in cold acclimation after a single night of exposure to cold ($TP_{1,2}$) and after a prolonged 4-day treatment ($TP_{3,4}$). To be able to measure the effect of daytime recovery and circadian rhythms, we also compared metabolite levels in samples harvested in the morning immediately after overnight cold treatment ($TP_{1,3}$) to the samples harvested after six hours of day-time recovery at normal temperatures following the respective cold treatments ($TP_{2,4}$). We quantified 58 primary metabolites, including 21 sugars/sugar phosphates/polyols, 13 organic acids and 24 amino acids (including amines). A total of 95 lipid species were detected and measured in the spikes of both varieties, including 86 phospholipids such as PCs (phosphotidylcholine), PEs

(phosphotidylethanolamine), PGs (phosphotidylglycerolipid), PIs (phosphoinositide) and lysophospholipids. In addition, we also quantified 9 galactosyl lipids (galactosyldiaclyglycerols) in the spikes: digalactosyldiacylglycerols (DGDG), monogalactosyldiacylglycerols (MGDG) and sulfoquinovosyl diacylglycerols (SQDG).

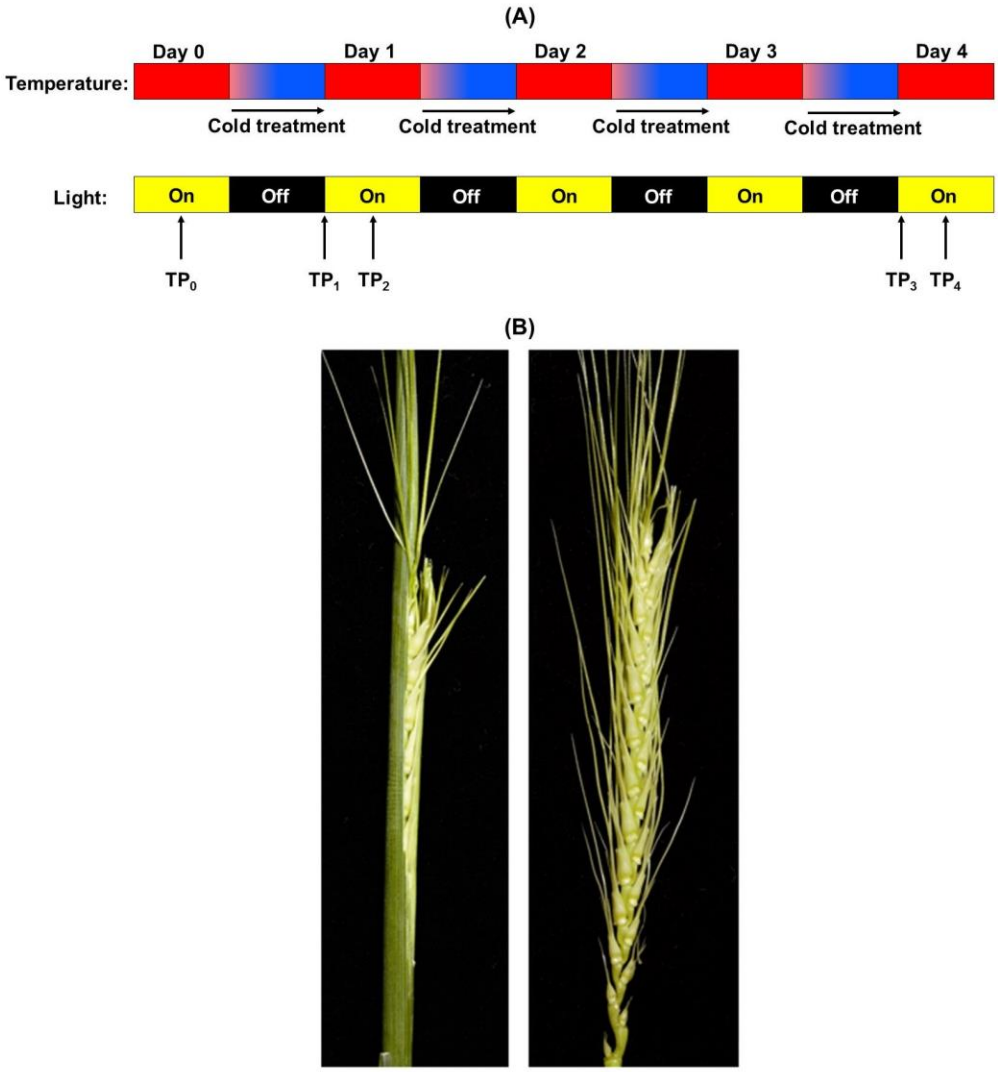


Figure II-2-1. **(A):** Schematic diagram showing the controlled environment design of the cold treatments and lighting conditions (see Materials & Methods section). Yellow bars show day-light conditions, dark bars dark conditions. Arrows labelled TPx indicate where samples were harvested from wheat plants. **(B):** Pictures showing the morphological stage of the young microspore (YM) stage wheat spikes used in this study. At the YM stage, wheat spikes have been shielded from light exposure by the surrounding leaf sheaths (left picture).

2.10.4.2 Cold Treatment Affects Spike Metabolites in Wyalkatchem More Than Young Spikes

A short overnight cold treatment (~12h) revealed that four primary metabolites and one lipid were significantly affected in Wyalkatchem spikes: maltose (+17.8-fold), fructose-6-phosphate (+4.2-fold), glucose-6-phosphate (+4.7-fold), beta-alanine (+2.0-fold) and the lipid PG(36:5) (+1.2-fold) were all significantly increased (TP_1 *vs*. TP_0; **Fig. II-2-2A**). In contrast, the comparison of TP_1 *vs*. TP_0 in Young showed no significant changes in primary metabolites and only one lipid, *i.e*. PC(37:5), was significantly reduced (–16.5-fold; **Fig. II-2-2B**). The TP_2 spike samples were harvested after 6 hours of day-light and normal temperatures (21°C) following the first night cold exposure (TP_1). Comparison of TP_2 to TP_1 in Wyalkatchem spikes showed that only two metabolites were significantly changed: rather than induced at TP_1, maltose was this time strongly repressed back to TP_0 levels (-20-fold) and levels stay the same at TP_2 and TP_4, while 2-oxoglutarate was induced (+3.1-fold). There were no significant changes in the lipids at TP_2 *vs*. TP_1, indicating that the observed change in PG(36:5) at TP_1 was maintained during day-time recovery (**Supplemental Fig. II-S2-1 and II-S2-2**). In Young spikes, maltose was also repressed compared to TP_1 (–10.7-fold) and we also found a significant increase in methionine levels at TP_2 (+2.1-fold). There were no significant changes in the lipids, again indicating that the PC(37:5) lipid change at TP_1 was maintained at TP_2 (**Supplemental Fig. II-S2-1 and II-S2-2**).

After a prolonged four-night cold treatment (TP_3 *vs*. TP_1 comparison), three primary metabolites changed significantly in Wyalkatchem spikes: raffinose (+1.9-fold), shikimate (–1.4-fold) and putrescine (+3.2-fold). Additionally, a series of saturated and unsaturated PC(36:x) lipids were significantly reduced at TP_3 compared to TP_1: PC(36:0) (–1.6-fold), PC(36:1) (–1.5-fold), PC(36:2) (–1.5-fold), PC(36:3) (–1.2-fold). Four PE lipid species were also significantly reduced: PE(34:0) (–1.4-fold), PE(34:1) (–1.4-fold), PE(38:4) (–1.2-fold) and PE(41:4) (–1.5-fold) (**Fig. II-2-2A**). In Young spikes, the prolonged cold treatment (TP_3) did not cause any significant changes in primary metabolites and lipids compared to TP_1 (**Fig. II-2-2B**). Comparing the prolonged cold treatment samples with their equivalent day-time samples (TP_4 *vs*. TP_3) showed the same significant reduction in maltose levels (-8.8-fold) as observed in Wyalkatchem spikes between TP_2 and TP_1, as well as an increase in quinate levels (+1.7-fold). There were no significant changes in lipid levels (**Supplementary Fig. II-S2-1 and II-S2-2**). In Young spikes, the TP_4 *vs*. TP_3 pairwise comparison did not reveal any significant changes in primary metabolites or lipids (**Supplemental**

Fig. II-S2-1 and II-S2-2). These data indicate that the cold treatment has a more drastic effect on spikes of the cold-sensitive line Wyalkatchem compared to the tolerant line Young.

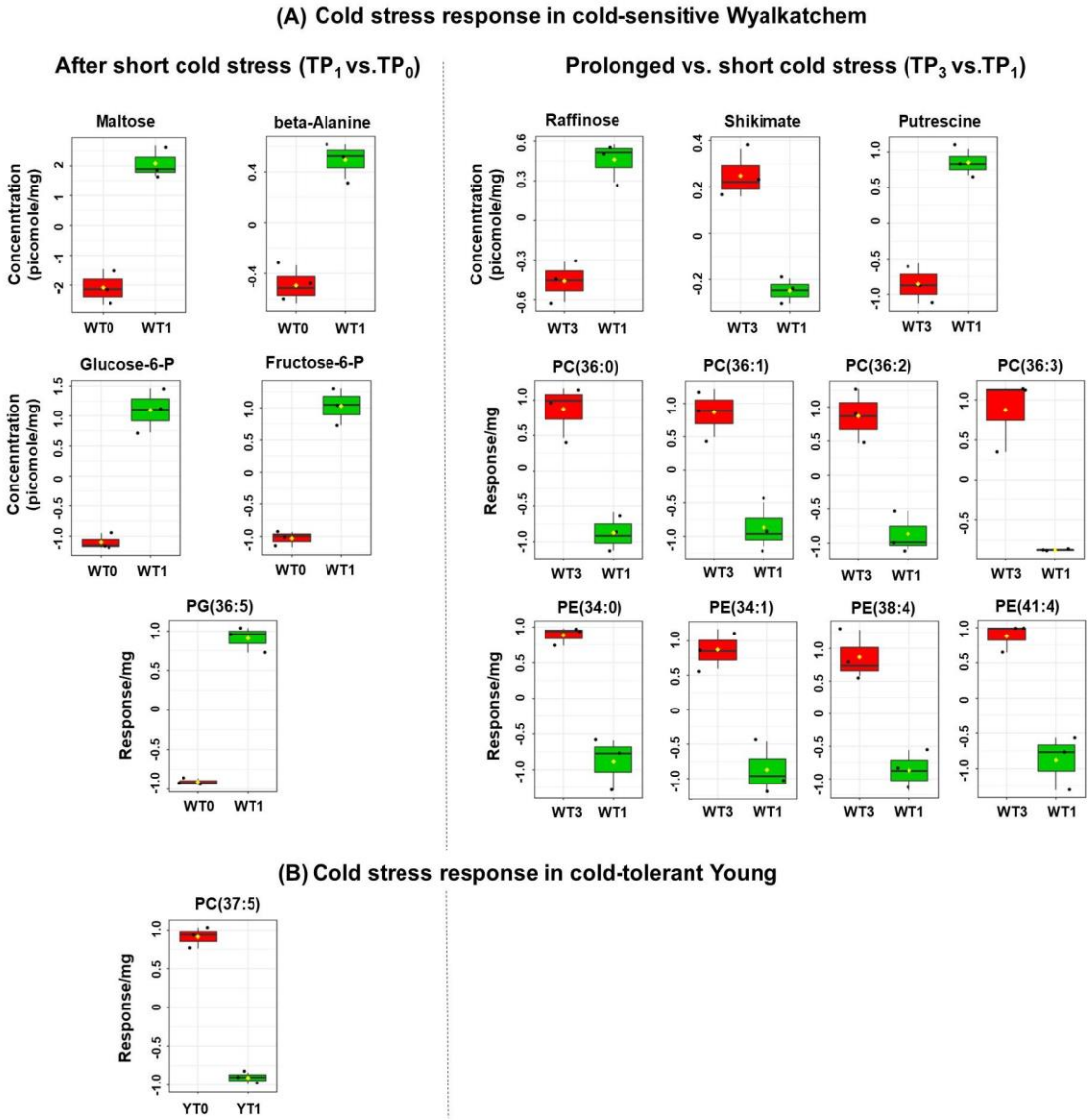


Figure II-2-2. Pairwise comparisons of normalized and log_2-transformed primary metabolites and lipids in the spikes of **(A)** cold-sensitive Wyalkatchem and **(B)** cold-tolerant Young after one night (TP_1 *vs*. TP_0) and prolonged (TP_3 *vs*. TP_1) of cold treatment. Metabolites and lipids shown are significantly different and the significance levels were determined using the Benjamini and Hochberg method (Benjamini and Hochberg, 1995) with a false discovery rate (FDR)-adjusted *p*-value of 0.05 as cut-off. There were three biological replicates (n=3) for all the measured metabolites and lipids. W = Wyalkatchem; Y = Young.

2.10.4.3 Varietal Differences in Metabolite and Lipid Levels Before and After Cold Treatment

Before the plants were subjected to cold stress (TP_0), there were already significant differences in the levels of primary metabolites and lipids in the spikes of cold-tolerant Young and cold-sensitive Wyalkatchem. Nine primary metabolites were significantly higher in Young compared to Wyalkatchem at TP_0: glucose (+1.4-fold), sucrose (+3.1-fold), trehalose (+2.5-fold), fructose-6-phosphate (+2.2-fold), glucose-6-phosphate (+1.8-fold), beta-alanine (+1.7-fold), glutamate (+1.4-fold), glycine (+1.3-fold) and proline (+1.9-fold). Two metabolites were significantly lower in Young compared to Wyalkatchem spikes: histidine (–2.8-fold) and phenethylamine (–2.9-fold) (**Fig. II-2-3**). Three unsaturated lipid species were significantly higher at TP_0 in Young spikes compared to Wyalkatchem: PC(37:5) (+12.9-fold), PC(39:4) (+2.2-fold) and PG(32:1) (+2.3-fold). In contrast, six unsaturated lipids were significantly lower at TP_0 in Young spikes compared to Wyalkatchem: LPC(18:2) (–9.2-fold), PC(33:1) (–1.2-fold), PC(35:5) (–1.3-fold), PE(33:1) (–1.7-fold), PE(35:3) (–1.7-fold) and PE(35:4) (–1.5-fold) (**Fig. II-2-4**). Before the start of the cold treatment, there was no significant difference in the overall unsaturated to saturated lipid ratio between the two varieties (**Fig. II-2-5A**).

After one night of cold exposure (TP_1), three metabolites were found to be significantly different between the two varieties. The osmolyte mannitol accumulated to significantly higher levels (+1.5-fold), while ribose (–1.5-fold) and shikimate (–2.1-fold) were significantly lower in Young compared to Wyalkatchem spikes (**Fig. II-2-3**). Two lysophosphatidylcholine lipids were significantly lower in Young spikes compared to Wyalkatchem: LPC(17:0) (–1.8-fold) and LPC(18:1) (–3.8-fold). Two lipids that contain two polyunsaturated acyl chains in their structures, PC(36:6) (+1.3-fold) and PE(36:6) (+1-3-fold), had significantly higher levels in Young spikes compared to Wyalkatchem at TP_1 (**Fig. II-2-4**). But again, at TP_1 there was no significant difference in the overall ratio of unsaturated to saturated lipids between the two varieties (**Fig. II-2-5A**).

When comparing the TP_2 day-time samples between the two varieties, seven metabolites were significantly higher in Young compared to Wyalkatchem spikes. All of them were either amino acids or amines: alanine (+1.7-fold), beta-alanine (+1.7-fold), GABA (+1.7-fold), glutamate (+1.3-fold), methionine (+1.8-fold), proline (+2.8-fold) and threonine (+1.2-fold). Three sugars (fucose, –1.5-fold; ribose, –1.6-fold; xylose, –1.6-fold), one organic acid (shikimate –2.3-fold)

and one amine (phenethylamine –2.3-fold) were significantly reduced at TP_2 in Young spikes compared to Wyalkatchem (**Fig. II-2-3**). There were no significant differences in the lipids between the two varieties at TP_2, but for the first time, Young spikes showed a significantly higher ratio in unsaturated to saturated lipids compared to the ratio in Wyalkatchem spikes (**Fig. II-2-5A**).

After prolonged cold exposure (TP_3), three metabolites were decreased significantly in Young spikes compared to Wyalkatchem: quinate (–1.8-fold), methionine (–2.2-fold) and putrescine (–3.8-fold) (**Fig. II-2-3**). The largest difference between both wheat varieties at TP_3 was in the lipid levels. Three lysophosphatidylcholines with a carbon backbone of 18 were significantly lower in Young spikes compared to Wyalkatchem: LPC(18:1) (–5.0-fold), LPC(18:2) (–7.3-fold) and LPC(18:3) (–3.6-fold). Coincidently, 25 lipids with a higher carbon backbone length of 36 and a higher poly-unsaturation level were increased significantly in Young spikes compared to Wyalkatchem (**Fig. II-2-4**). Interestingly, ten of these 25 lipid species were found to contain two polyunsaturated acyl chains in their structures: PC(36:5) (+1.3-fold), PC(36:6) (+1.6-fold), PC(38:5) (+1.3-fold), PC(38:6) (+1.3-fold), PE(36:6) (+1.6-fold), PE(38:6) (+1.2-fold), PG(36:6) (+1.1-fold), PG(36:7) (+2.4-fold), PI(36:6) (+1.9-fold) and DGDG(36:6) (+1.2-fold). This change in the lipid spectrum at TP_3 resulted in Young spikes showing a significantly higher unsaturated to saturated lipid ratio compared to Wyalkatchem (**Fig. II-2-5A**).

Comparison between Young and Wyalkatchem at the last day-time sampling point (TP_4) showed that there were no significant differences in primary metabolites between the two wheat varieties (**Fig. II-2-3**). In terms of lipids, three lysophosphatidylcholines were again significantly lower in Young compared to Wyalkatchem spikes: LPC(18:1) (–4.5-fold), LPC(18:2) (–7.6-fold) and LPC(18:3) (–5.9-fold). But two unsaturated phosphatidylethanolamine lipids species, PE(32:3) (+1.7-fold) and PE(36:6) (+1.5-fold), were significantly higher in Young spikes compared to Wyalkatchem (**Fig. II-2-4**). At TP_4, there was no significant difference in the unsaturated to saturated lipid ratio between the two varieties (**Fig. II-2-5A**).

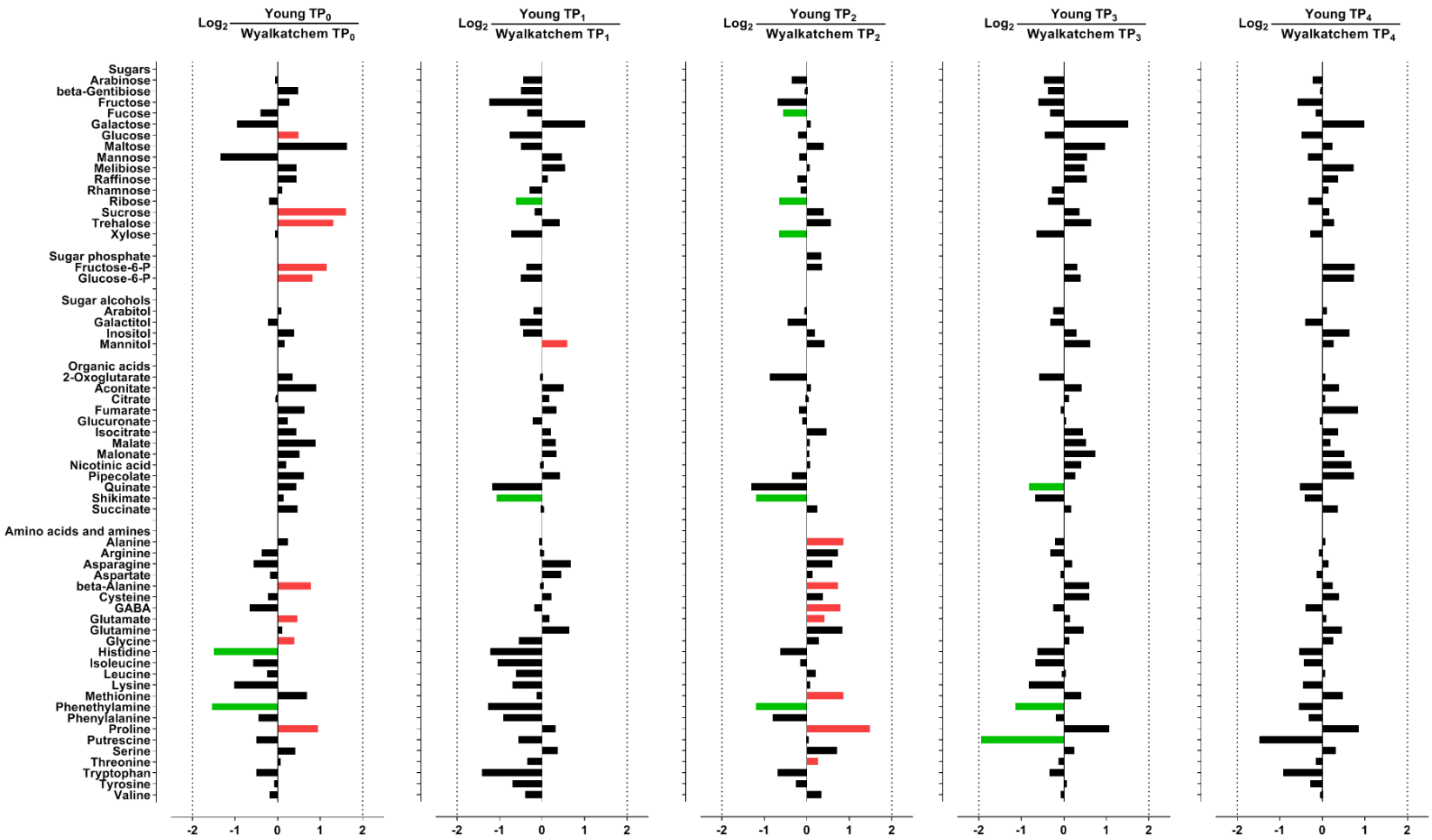


Figure II-2-3. Log_2-fold changes of primary metabolites in spikes of cold-tolerant Young (Y) compared to cold-sensitive Wyalkatchem (W) at each time point. Fold changes were calculated by dividing the concentration of Y to the concentration of W at that particular time point, followed by log_2-transformation. FDR-adjusted *p*-value of 0.05 was set as the cut-off. Green = significantly lower in Young, or higher in Wyalkatchem; Red = significantly higher in Young, or lower in Wyalkatchem. n=3.

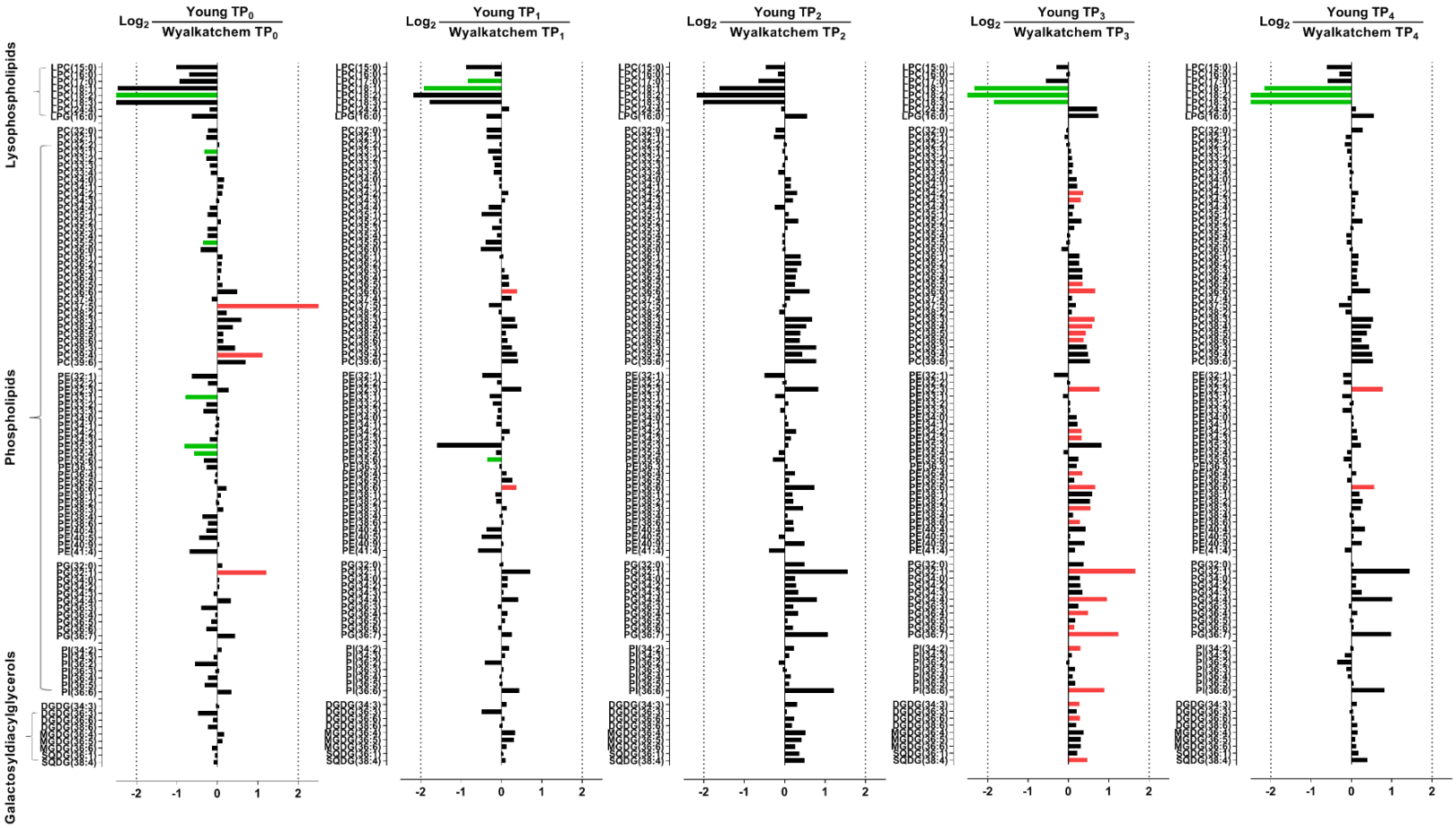


Figure II-2-4. Log_2-fold changes of lipids in the spikes of cold-tolerant Young (Y) compared to cold-sensitive Wyalkatchem (W) at each time point. Fold changes were calculated by dividing the concentration of Y to the concentration of W at that the particular time points, followed by log_2-transformation. FDR-adjusted *p*-value of 0.05 was set as the cut-off. Green = significantly lower in Young, or higher in Wyalkatchem; Red = significantly higher in Young, or lower in Wyalkatchem. n=3.

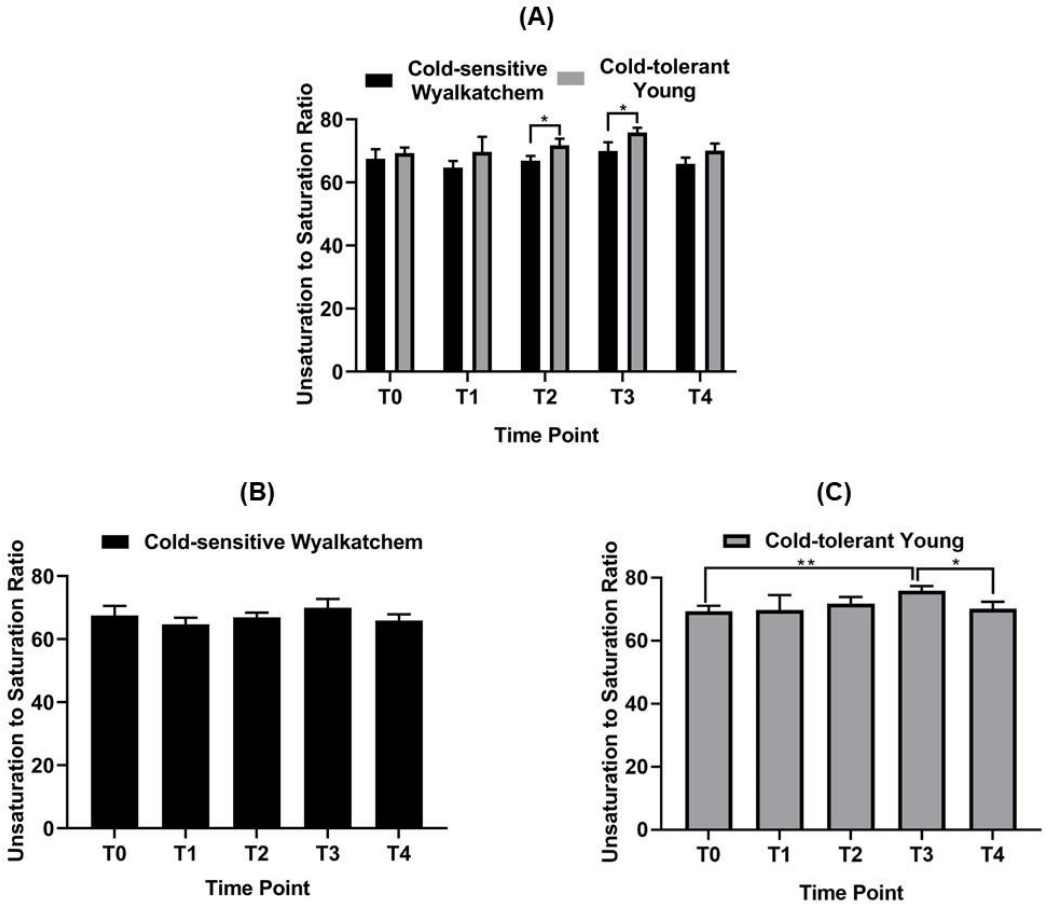


Figure II-2-5. (A) Comparison of unsaturated to saturated lipid ratio between Wyalkatchem and Young across the time points. **(B)** Comparison of unsaturated to saturated lipid ratio in Wyalkatchem across the time points. **(C)** Comparison of unsaturated to saturated lipid ratio in Young across the time points. Student's *t*-test was used to compare the ratio for a time point with its following time point. Error bars indicate the standard error mean (SEM) of three biological replicates (n=3). Significantly different ratios were labelled with an asterisk (*; $p < 0.05$, **; $p < 0.01$).

2.10.4.4 Differences in Primary Metabolite Levels between Spikes and Flag Leaves of Wyalkatchem and Young

The spikes and flag leaves of the two wheat varieties showed significant differences in sugars and organic acids that are part of glycolysis and tricarbosylic acid (TCA) cycle. Twelve amino acids, putrescine, gamma-aminobutyric acid (GABA) and two organic acids (quinate and shikimate) that are involved in amino acid metabolism, showed significant differences between the spikes and flag leaves of the two wheat varieties (**Fig. II-2-6 and II-2-7**; for one-way ANOVA results, see **Supplemental Table II-S2-10**). Of these sixteen metabolites, eight were found to be significantly higher in the spikes compared to the flag leaves over the 4-day cold treatment: tyrosine, phenylalanine, quinate, shikimate, proline, glutamine, beta-alanine and asparagine. Five amino acids (glutamate, aspartate, threonine, serine and cysteine) and GABA were significantly lower in the spikes compared to the flag leaves. Putrescine was slightly lower in the spikes compared to the flag leaves, especially in the cold-tolerant variety Young. Interestingly, the response of alanine increased significantly from TP_1 to TP_3 in spikes, while it decreased for the same time points in flag leaves for both varieties. The results in **Figs. II-2-6** and **II-2-7** reveal that the overall response of metabolites to cold is quantitatively stronger in the reproductive tissues (spikes) compared to the flag leaves for both the sensitive and tolerant wheat line.

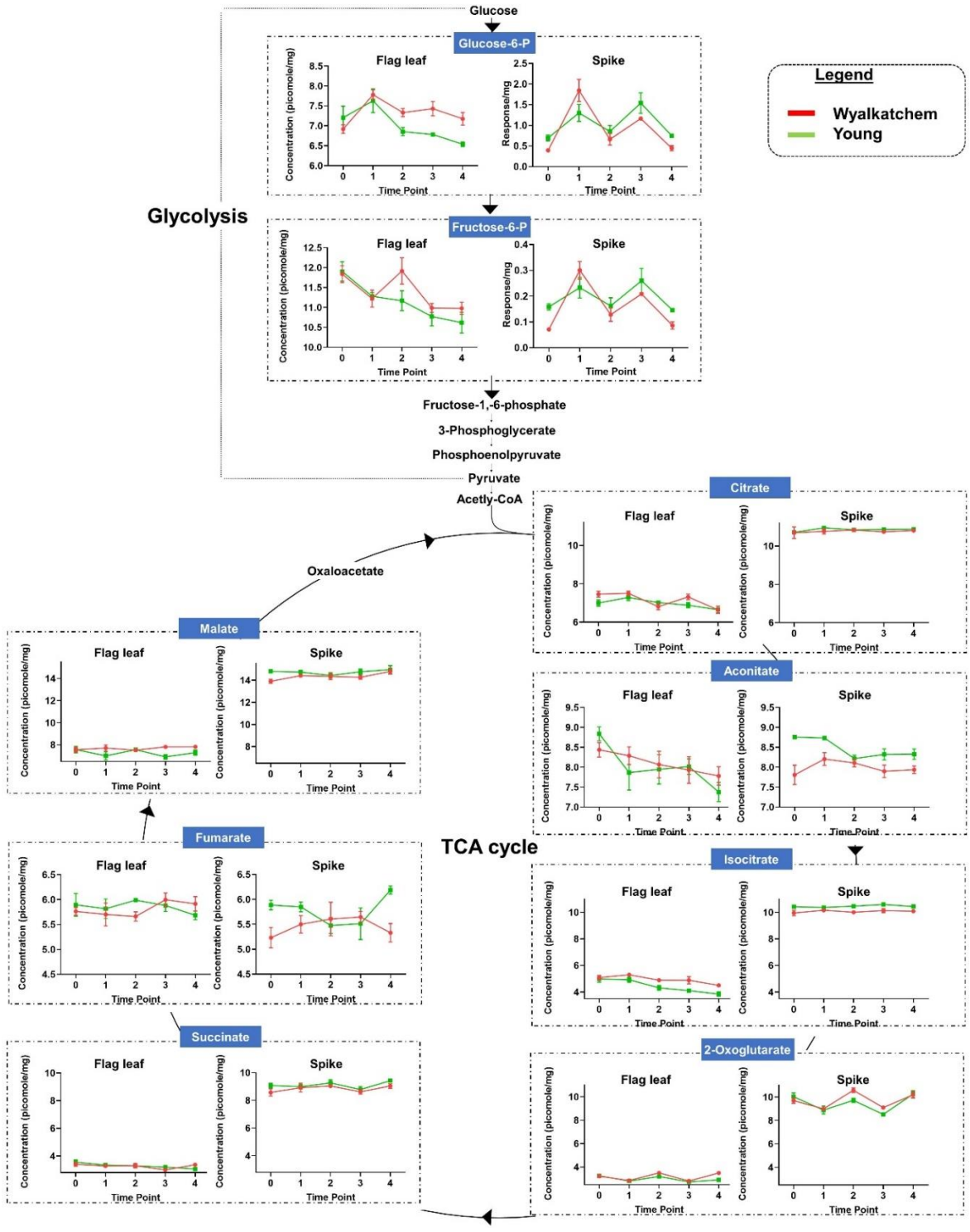


Figure II-2-6. Comparison of primary metabolites involved in glycolysis and the tricarboxylic acid (TCA) cycle, the two main energy-providing pathways of the cell. The graphs show differences in relevant primary metabolite concentrations (picomole/mg of fresh weight, $\log_2$-transformed) between flag leaf and spike metabolite data. For glucose-6-phosphate and fructose-6-phosphate, the spike data compare the response normalized per mg of fresh weight. The graphs reveal differences in accumulation levels of these metabolites in cold-tolerant Young and cold-sensitive Wyalkatchem spikes. n = 4 ± SEM for flag leaf, n = 3 ± SEM for spike.

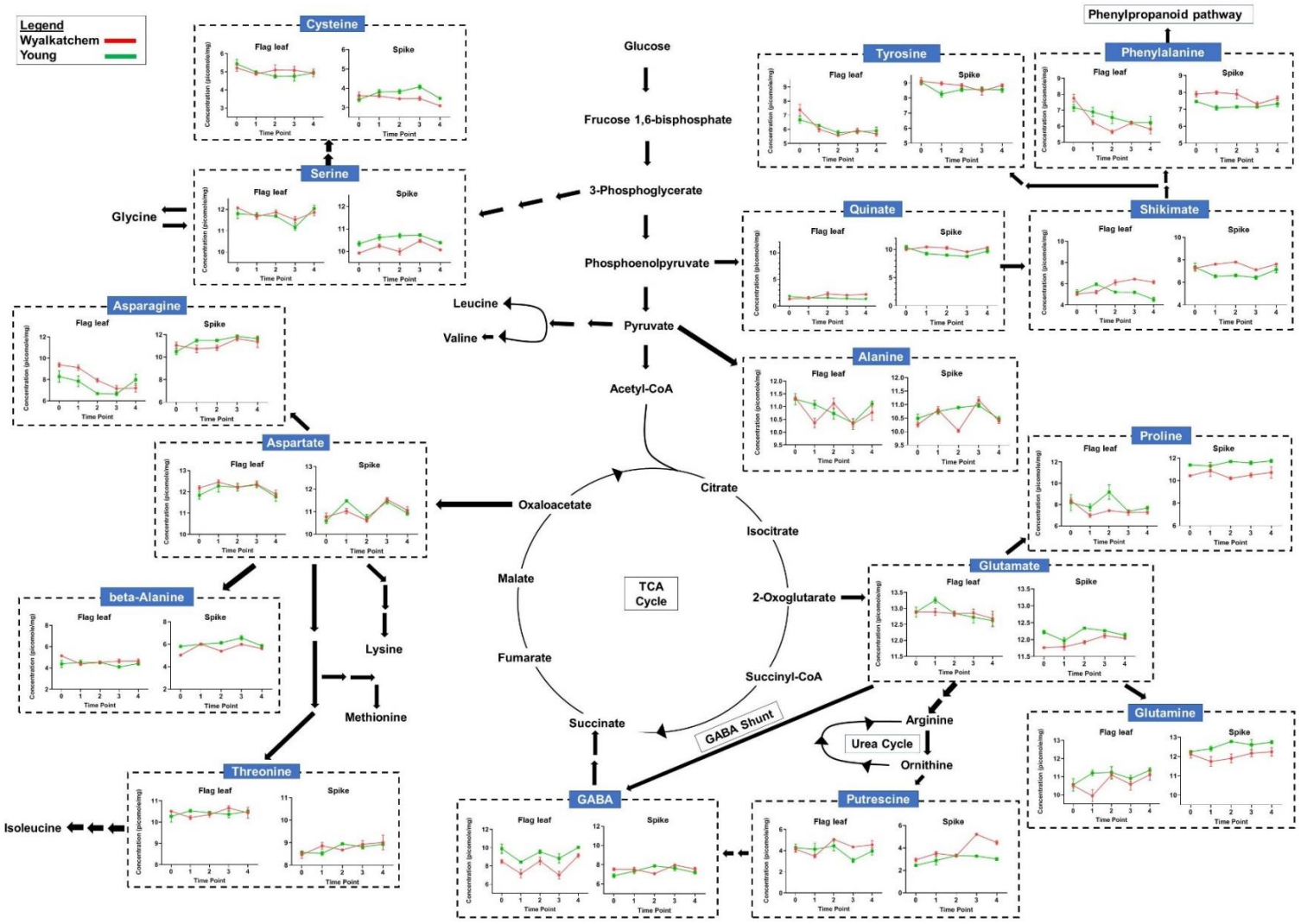


Figure II-2-7. Comparison of amino acid and amine levels (in concentration unit picomole/mg of fresh weight and log_2-transformed), as well as their relationship to the main energy providing pathways (glycolysis and TCA cycle). The graphs show differences in metabolite levels between flag leaf and spike metabolite data, as well as differences in accumulation levels of those metabolites in cold-tolerant Young and cold-sensitive Wyalkatchem spikes**.** n = 4 ± SEM for flag leaf, n = 3 ± SEM for spike.

2.10.4.5 Differences in Metabolite and Lipid Levels between Spikes and Flag Leaves of Wyalkatchem and Young

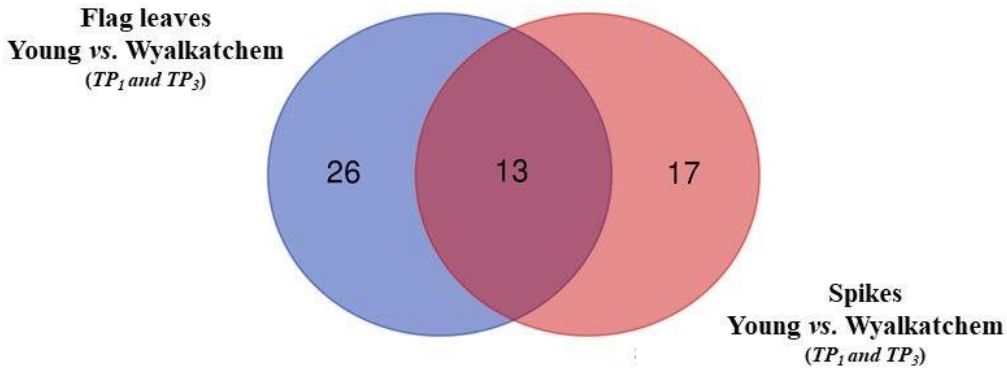
The most dramatic changes in primary metabolites and lipids occur at TP_1 and TP_3. We therefore compared the response at these time points between flag leaves and spikes for Young and Wyalkatchem. In terms of primary metabolites, cold treatment only affected ten and six primary metabolites in flag leaves and spikes, respectively, and only three of these metabolites were common to both tissues: putrescine, quinate and shikimate (**Supplemental Fig. II-2-S3**). Interestingly, all three of these overlapping metabolites were lower in both Young flag leaves and spikes compared to Wyalkatchem. We observed a larger number of changes in lipid composition for both wheat varieties at TP_1 and TP_3 (**Fig. II-2-8**). The results show that there were both similarities and differences in lipid accumulation between flag leaves and spikes (**Fig. II-2-8**). Thirteen lipids were found to overlap between the lipid species of flag leaves and spikes and all of them were polyunsaturated lipids. Of the common lipids, five were accumulating to higher levels in both spike and flag leaf tissues of cold-tolerant Young compared to cold-sensitive Wyalkatchem: PC(38:3), PE(34:2), PE(36:4), PE(38:3) and PG(36:4). Eight unsaturated lipids were found to be lower in Young flag leaves when compared to Wyalkatchem, but their levels were higher in Young spikes compared to Wyalkatchem spikes: PC(34:4), PC(36:6), PC(38:6), PE(34:3), PE(36:6), PE(38:6), PG(36:6) and PI(36:6). Interestingly, levels of all these thirteen polyunsaturated lipid species showed quantitatively higher levels in Young compared to Wyalkatchem spikes (Fig. 8). These results indicate that there are quantitative and qualitative differences in cold acclimation between sensitive variety Wyalkatchem and tolerant Young.

2.10.5 Discussion

2.10.5.1 Are Wheat Spikes or Flag Leaves Better for Cold Tolerance Phenotyping?

We have previously compared the effect of cold stress on metabolite levels during cold acclimation in flag leaves of cold-tolerant Young and cold-sensitive Wyalkatchem (Cheong et al., 2019). For the ultimate aim of phenotyping, flag leaves are easy to collect, especially on the field. The motivation to also study metabolite changes in wheat spikes during cold acclimation came from the fact that spikes are the organs of the wheat plant where grain yield is determined. Spike material at the stage of highest sensitivity to cold, the YM stage of pollen development (Cheong et al., 2019), is harder to collect. However, this tissue may provide metabolite information that is more

directly correlated with the cold tolerance/sensitivity mechanism. If we can prove that the metabolite changes in flag leaves and spikes show significant similarities, then we can be confident that flag leaf material suits our phenotyping needs.



Differences in expression behavior of 13 overlapping lipids between flag leaves and spikes of Young and Wyalkatchem (TP_1 and TP_3 samples)

Overlapped (13)	Higher in Young Flag leaves	Lower in Young Flag Leaves	Higher in Young Spikes	Lower in Young Spikes
PC(38:3)	√		√	
PE(34:2)	√		√	
PE(36:4)	√		√	
PE(38:3)	√		√	
PG(36:4)	√		√	
PC(34:3)		√	√	
PC(36:6)		√	√	
PC(38:6)		√	√	
PE(34:3)		√	√	
PE(36:6)		√	√	
PE(38:6)		√	√	
PG(36:6)		√	√	
PI(36:6)		√	√	

Figure II-2-8. Differences in differentially expressed lipid species between flag leaves and spikes of cold-tolerant Young and cold-sensitive Wyalkatchem. The Venn diagrams show the degree of overlap between differentially expressed cold-induced lipid species in flag leaves and spikes for Young and Wyalkatchem. Thirteen lipid species were commonly expressed in flag leaves and spikes at TP_1 and TP_3. The table below the diagram shows how these 13 lipid species are expressed differently in flag leaves and spikes of Wyalkatchem and Young.

An important difference between flag leaf and YM stage spike tissues is that the former is a static photosynthetic source tissue, whilst the latter is a young and actively growing tissue in need of sugar supply to drive reproductive development (sink tissue). YM stage spikes are shielded from daylight by the surrounding leaf sheaths and have a light-green appearance; there may be a low amount of chlorophyll and photosynthetically active chloroplasts in cells of the outside tissue layers of the florets (glumes, lemma and awns), but the anthers that produce pollen inside the florets are yellow and at the YM stage are non-photosynthetic sink tissues (Oliver et al., 2005; Ji et al., 2010). Sink strength is defined as the competitive ability of an organ to attract and store assimilates (Marcelis 1996). At the reproductive stage, developing wheat spikes need a strong sink strength to attract sugars for reproductive development and grain filling (Zinselmeier et al, 1995a and 1995b; Clement et al., 1996; Reynolds et al., 2005; Lemoine et al., 2013). In rice and wheat, cold and drought stress reduce sink strength in lines that are more sensitive to those stresses and stress tolerance correlates with a higher capability to maintain sink strength (Oliver et al., 2005; Thakur et al., 2010). The higher sugar levels in Young compared to Wyalkatchem spikes before cold exposure therefore indicate that Young spikes have a higher sink strength than Wyalkatchem spikes.

The spikes of the cold-tolerant variety Young did not show any significant primary metabolite changes upon short or prolonged exposure to cold, while cold-sensitive Wyalkatchem did show some metabolites that were significantly affected by cold. In the flag leaves there were more changes in primary metabolites in response to the same cold treatment (Cheong et al., 2019). It is possible that the cold treatment at the spike level is somewhat less stringent compared to the flag leaf. While the flag leaf is directly exposed to cold air, at the YM stage the spike is still protected inside the leaf sheath of the flag leaf and the penultimate leaf. However, spikes of both wheat varieties show a clear lipid response to cold, which is similar to that of the flag leaf (Cheong et al., 2019). This indicates that the YM stage spikes have experienced cold stress. Alternatively, they responded to a cold stress signal coming from the vegetative plant parts.

Most metabolites we detected are present at higher levels in actively growing spikes than in flag leaves and are therefore easier to detect in spike tissues. Despite quantitative and qualitative differences in the cold acclimation response between spike and flag leaves, the message we obtained in terms of metabolite profiles and differences in cold acclimation between the tolerant and sensitive wheat line is quite similar. This observation also strengthens the conclusion that the

response we observed is a true defensive acclimation response to the chilling/freezing treatment we imposed.

2.10.5.2 Spikes of Cold-Tolerant Young Are Potentially Better Prepared for Low Temperature Stress

Levels of important sugars (glucose, sucrose, trehalose, fructose-6-phosphate and glucose-6-phosphate) were significantly higher under unstressed conditions (TP_0) in spikes of cold-tolerant Young compared to cold-sensitive Wyalkatchem. Higher levels of these sugars may indicate that Young spikes have a higher sink strength and are more metabolically active than Wyalkatchem spikes under normal growth conditions. High sugar levels also play a role in osmotic adjustment and membrane protection during water and cold stress (Lokhande and Suprasanna, 2012). In addition, proline and ß-alanine levels were also significantly higher in Young spikes before cold stress treatment. Proline is an osmolyte with protective functions in plant tissues under a variety of stresses (drought, salinity, cold and heat) (Mayer et al., 1990; Ashraf and Fooland, 2007; Lehmann et al., 2010; Hayat et al., 2012; Liang et al., 2013). ß-Alanine in spikes of the sensitive variety Wyalkatchem is only increased after the first night of cold exposure. ß-Alanine is a non-proteinogenic amino acid that is increased during abiotic stress conditions (Mayer et al., 1990; Kaplan and Guy, 2004; Rizhsky et al., 2004); it is a coenzyme A precursor that is involved in the tricarboxylic acid cycle, as well as phospholipid and fatty acid metabolism (Broeckling et al., 2005). ß-Alanine serves also as a substrate for ß-alanine betaine synthesis, a quaternary ammonium compound with osmo-protective functions under stress conditions (Hanson et al, 1991, 1994; Rocha et al., 2010a and 2010b). The polyol sugar mannitol accumulates to higher levels in Young spikes after the first cold night (TP_1). Mannitol acts as a radical scavenger to protect against ROS under abiotic stress conditions (Morsy et al., 2007; Folgado et al., 2015; Llanes et al. 2013). The flag leaf study showed similar observations (Cheong et al., 2019).

Some other sugars with protective functions are mainly accumulating in spikes of the sensitive line Wyalkatchem. Maltose levels increase after the first night of cold stress exposure, but in Young the increase in maltose remained insignificant. Maltose is a transitory starch breakdown product and this breakdown is induced during the day under photorespiratory conditions. Maltose metabolism is regulated by the circadian clock, day-length and temperature (Lu and Sharkey, 2006). Maltose plays a role in stabilizing membranes and proteins (Wolfe and

Bryant, 1999; Ambroise et al., 2019). In Arabidopsis, maltose functions as a compatible solute and a stabilizing factor in the chloroplast stroma during temperature stress (Kaplan and Guy, 2004). *In vitro* assays indicate that maltose protects proteins, membranes and the photosynthetic electron transport chain during freezing stress. Increased maltose levels under cold stress could be caused by increased expression of β-amylase (Kaplan and Guy, 2004; Lu and Sharkey, 2006).

Spikes of the cold-sensitive variety Wyalkatchem also showed increased levels of putrescine and raffinose after prolonged cold stress (TP_3). Putrescine is a polyamine and amino acid breakdown product with growth-regulatory properties that plays a role in abiotic stresses (Giu and Tuteja, 2010; Shi and Chan, 2014). Raffinose is a soluble galactosyl-sucrose carbohydrate that plays a role in stabilizing photosystem II during freeze-thaw cycles in Arabidopsis (Knaupp et al., 2011). Raffinose acts as an antioxidant that can protect cells from oxidative stress damage by scavenging reactive oxygen species (ROS) (Morsy et al., 2007; Folgado et al., 2015; Llanes et al., 2013; Keunnen et al., 2013; Couee et al., 2006).

In contrast to Young, where a protection mechanism involving higher sink strength and accumulation of osmolytes (sugars, amino acids) appears to be constitutively present, Wyalkatchem activates primary metabolite changes after the first night and during prolonged cold exposure to cold. Spikes of cold-tolerant Young may therefore be better prepared against cold stress from the start. This knowledge can be exploited in phenotyping approaches for cold tolerance. The primary metabolite response in cold-sensitive Wyalkatchem is a true cold stress response. Being a sensitive variety, Wyalkatchem responds with osmolyte synthesis, possibly to control water loss caused by membrane damage, and with activation of a signature oxidative stress and ROS protection mechanism. The same type of response was also observed in Wyalkatchem flag leaves. Osmolytes can therefore be used as indicator for the secondary water stress response caused by cold-induced membrane damage (Cheong et al., 2019; Beck et al., 2007).

2.10.5.3 Lipid Remodeling is Critical for Cold Acclimation in Wheat Spikes

Modifying membrane lipid composition forms an important part of cold acclimation. Similar to what we found for flag leaves, in wheat spikes chilling stress also had a more drastic effect on lipids compared to primary metabolites. Under unstressed conditions, Young spikes showed higher levels of three unsaturated phospholipids, with PC(37:5) being the most prevalent one. Unstressed

Wyalkatchem spikes had higher levels of five different unsaturated phospholipids. Interestingly, in Young spikes the high level of PC(37:5) was reduced drastically after overnight cold stress. PC(37:5) was much lower in unstressed Wyalkatchem spikes, nor was the level of this lipid strongly repressed by overnight cold treatment. Instead, Wyalkatchem increased PG(36:5) levels upon cold exposure. PG(32:1) is higher in Young compared to Wyalkatchem at the unstressed and prolonged cold stress stage (TP_3). PG lipids are the main phospholipid class in thylakoid membranes of higher plants (Ren et al., 2014). Plant cells contain proplastids that can multiply and develop into specialised plastids such as chloroplasts. Plants increase the degree of fatty acid unsaturation and the content of phospholipids when they are exposed to low, non-freezing temperatures (Murata et al., 1992; Welti et al., 2007). PG lipids contain trans-Δ3-hexadecenoic acid (C16 :1t, a monounsaturated 16-carbon fatty acid with trans-double bond at position C-3); they are major fatty acid involved in decreasing the phase transition temperature of thylakoid PG and maintaining membrane fluidity at lower temperatures (Ren et al., 2014; Li et al., 2015; Williams and Harwood, 1997; Campos et al., 2003; Moon et al., 1995). The highly unsaturated PG(36:5) lipid in Wyalkatchem spikes consists of 18:2 and 18:3 acyl chains and may protect the plastidial/thylakoid membranes. Interestingly, this species was also found to increase significantly in the flag leaves of the same variety after overnight cold stress (TP_1) (Cheong et al., 2019).

After prolonged cold stress, a series of PC(36:x, with x = 0 to 3) lipids, as well as several saturated and polyunsaturated PE lipids, were decreased in cold-sensitive Wyalkatchem and not in cold-tolerant Young spikes. This may be a consequence of their utilization as substrates to produce PAs by phospholipases to trigger a further response against cold stress. Alternatively, the decrease in those PC and PE lipids in Wyalkatchem could be the consequence of membrane damage and/or lipid degradation.

In Young spikes, the first cold night increased the levels of the polyunsaturated lipids PC(36:6) and PE(36:6). The result is a net increase in the degree of fatty acid unsaturation and phospholipid content in Young spikes. In Arabidopsis, PC lipids are amongst a group of lipids that increased during cold acclimation (Welti et al., 2002). The higher lipid unsaturation to saturation ratio in Young compared to Wyalkatchem improves the ability to maintain membrane fluidity at low temperatures.

Under unstressed conditions, and particularly after prolonged exposure to cold, most short-chain lysophospholipids (LPC) were higher in Wyalkatchem spikes compared to Young. PCs and

PEs are the most abundant plasma membrane lipids in plants (Nakamura, 2017; Cheong et al., 2019). Plants can lower the ratio of PC to PE during cold stress via a hydrolysis reaction catalyzed by phospholipase D (PLDα). Hydrolysis of PC lipids at the sn-1 or sn-2 positions of the glycerol backbone results in formation of LPC and phosphatidic acid (PA), a signaling molecule involved in cold and ABA signaling (Zhang et al., 2013; Vance and Vance, 2008; Guschina and Harwood, 2006; Ruelland et al., 2002; Murata and Yamaya, 1984; Bargmann and Munnik, 2006; Testerink and Munnik, 2005; Guo et al., 2011; Bargbaglia and Hoffmann-Benning, 2016). LPC levels are generally higher in Wyalkatchem spikes at all time points, but most obviously after prolonged cold treatment ($TP_{3,4}$). This was not observed in flag leaves, where none of the LPC lipids were significantly different between Wyalkatchem and Young. In Young spikes, cold-induced PC(37:5) catabolism does not seem to impact LPC levels. PC(39:4) is also higher in unstressed Young spikes; this lipid does not seem to be reduced as dramatically as PC(37:5), but is also induced in Wyalkatchem to a level similar to Young after overnight cold exposure. Both PC(37:5) and PC(39:4) can serve as substrates for PLDα to produce the cold response signaling molecule PA (Bargmann and Munnik, 2006; Testerink and Munnik, 2005), so Young could initially benefit from higher levels of these lipids to produce PA and trigger a cold response quicker and more efficiently than Wyalkatchem. Higher levels of LPC(18:1), LPC(18:2) and LPC(18:3) in Wyalkatchem spikes after prolonged cold stress (TP_3 and TP_4) may indicate that prolonged cold stress has caused degradation of PC lipids, causing damage to the plasma membrane. This may then lead to water loss and electrolyte leakage.

Maintenance of plastid functionality during chilling conditions also requires changes in membrane lipid composition. The wheat spike consists of several tissue types (glumes, lemma, awns, anthers and ovule), most of which will become photosynthetically active when the spike extrudes from the leaf sheath of the flag leaf later on in development. As mentioned earlier, plant cells contain proplastids that can multiply and develop into specialised plastids such as chloroplasts. Light exposure leads to synthesis of photysynthetically active thylakoid membranes and differentiation into chloroplasts (Pyke 1999; Pogson et al., 2015; Vothknecht and Westhoff, 2001). The thylakoid membrane of chloroplasts is composed mainly of galactosylglycerolipids, consisting of 50% MGDG, 26% DGDG and 24% SQDG lipids, as well as other galactosylglycerolipid species and PG lipids (Dormann 2013). Low temperature acclimation can lead to an increased proportion of highly unsaturated fatty acids in galactolipids, such as linolenic

acid (C18:3) (Routaboul et al., 2000). Levels of DGDG(34:3), DGDG(36:6) and SQDG(38:4) in Young spikes after prolonged cold treatment (TP_3) may help this cold-tolerant variety to maintain better chloroplast functionality. Higher levels of DGDG improves ionic permeability of the chloroplasts and preserves activity of membrane proteins (Quartacci et al., 1995; Navari-Izzo et al., 1995). Experiments using desaturase enzyme mutants in Arabidopsis have illustrated the importance of glycerolipid composition and the degree of fatty acid desaturation in controlling membrane performance during cold stress (Li et al., 2015).

2.10.6 Conclusion

Profiling of primary metabolite and lipid changes in response to cold treatment of wheat spikes provided a better understanding about differences in cold acclimation of cold-tolerant Young and cold-sensitive Wyalkatchem. The changes in metabolomes and lipidomes of spikes were similar to those of flag leaves in many ways (Cheong et al., 2019), but there were clearly some interesting quantitative and qualitative differences in accumulation of osmolytes, ROS protective compounds and lipids. This means that both flag leaf and spike metabolite and lipidome analysis are complementary in terms of physiological information, and they can be used interchangeably for cold tolerance phenotyping in wheat. Flag leaf tissue is easier to collect, while spike tissue offers an advantage in terms of detectability because of the higher levels of some metabolites present in spikes. Both the flag leaf and spike datasets pointed out that remodeling of membrane lipids is critical for adaptation to low temperature stress. Controlling the unsaturated lipid levels to maintain membrane fluidity at low temperatures appears to be a distinguishing factor between cold-tolerant line Young and cold-sensitive Wyalkatchem. However, the changes in the ratio of saturated to unsaturated lipids is small. We do not know the biochemical structure of the lipid species that are affected by cold, nor do we know their exact role in controlling membrane functionality or which cellular membranes they are associated with. We identified some individual lipid species that stand out in the response of the cold-tolerant and sensitive wheat line, but for phenotyping purposes it is also important to study the changes of the entire lipid spectrum. Experiments are in progress to demonstrate whether lipid profiling proves to be reliable in a wider variety of cold-tolerant and sensitive wheat lines and whether the changes in lipid spectrum matches the ones observed in Young and Wyalkatchem. When lipid profiling proves to be reliable, we can deploy the technology in QTL mapping or genome-wide association studies (GWAS) to identify to identify genetic

markers that can be used to predict the cold tolerance phenotype. In addition, the data presented here have provided new avenues to investigate genes involved in metabolic and lipid biochemical processes using transcriptome analysis. Combination of metabolome and transcriptome analysis can further improve our understanding of how cold tolerance is controlled in wheat.

2.10.7 Author Contributions

B.E.C. performed part of the metabolite and lipid experiments and analyzed the data. B.E.C., O.O. and T.W.T.R. contributed to the data analysis. U.R., W.W.H.H., B.E.C. and R.D. designed the metabolite analysis and contributed to data analysis, statistical analysis and manuscript writing. R.D. conceptualized the project, designed the experiments and contributed to the writing of the manuscript. R.D. and O.O. established the controlled environmental conditions for chilling treatments and harvested the plant tissue samples for metabolite analysis. B.B. provided advice on the wheat germplasm to best use in this study and provided field climatic information, as well as advice to establish the controlled environmental conditions most likely to provide discriminating damage based on field experience in phenotyping the same material. B.E.C, O.O., W.W.H.H., U.R. and R.D. wrote and edited the manuscript. All authors have read and agreed to the published version of the manuscript.

2.10.8 Funding

This research was supported by grants of the Australian Grains Research and Development Corporation (GRDC projects CSP00143 and CSP00202).

2.10.9 Acknowledgments Cold treatments were carried out using growth chambers from the High- Resolution Plant Phenomics Centre in Canberra (HRPPC; https://www.plantphenomics.org.au/tag/high-resolution-plant-phenomics-centre/). The authors would like to thank Mrs. Xiaomei Wallace and Mrs. Tina Rathjen from CSIRO Agriculture and Food for excellent technical assistance. The authors also thank Mrs. Nirupama Jayasinghe, Mrs. Himasha Mendis, Ms. Veronica Lui and Dr. Siria Natera from Metabolomics Australia for the metabolite and lipid analyses. Metabolomics Australia (School of BioSciences, The University of

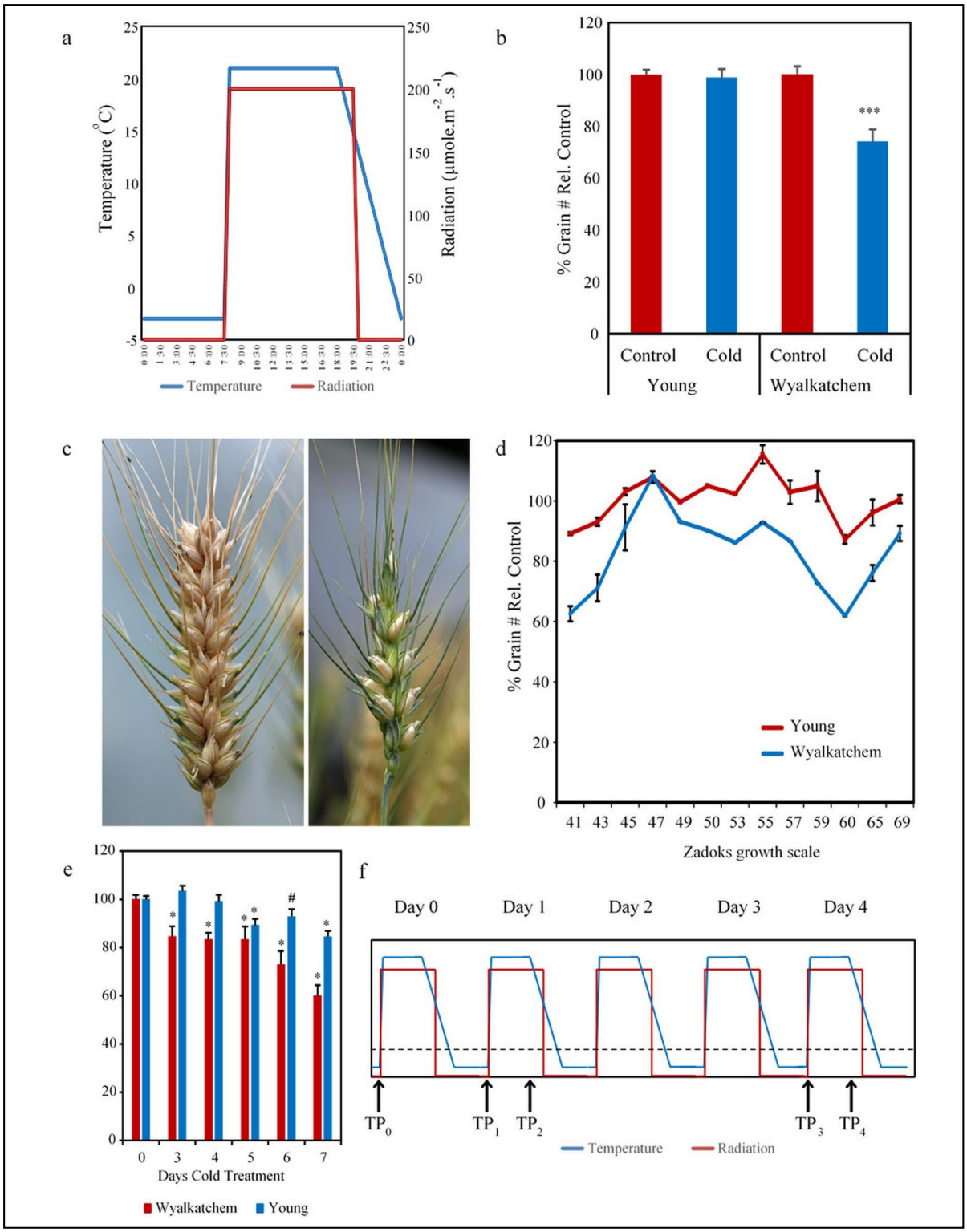
Melbourne, Australia) is a National Collaborative Research Infrastructure Strategy initiative under Bioplatforms Australia Pty Ltd (http://www.bioplatforms.com/).

2.10.10 Conflicts of Interest

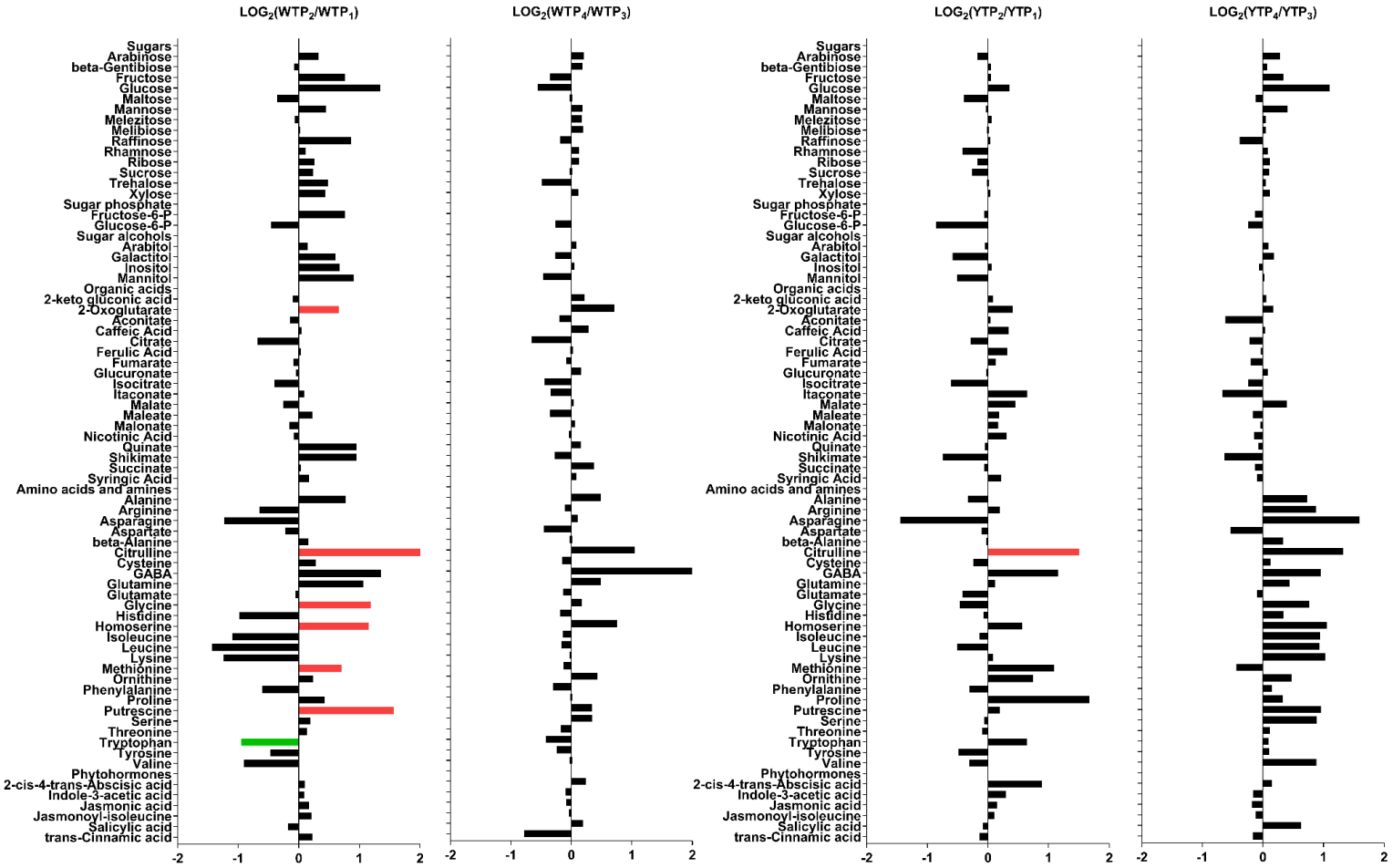
The authors declare no conflict of interest

2.10.11 Supplemental Figures

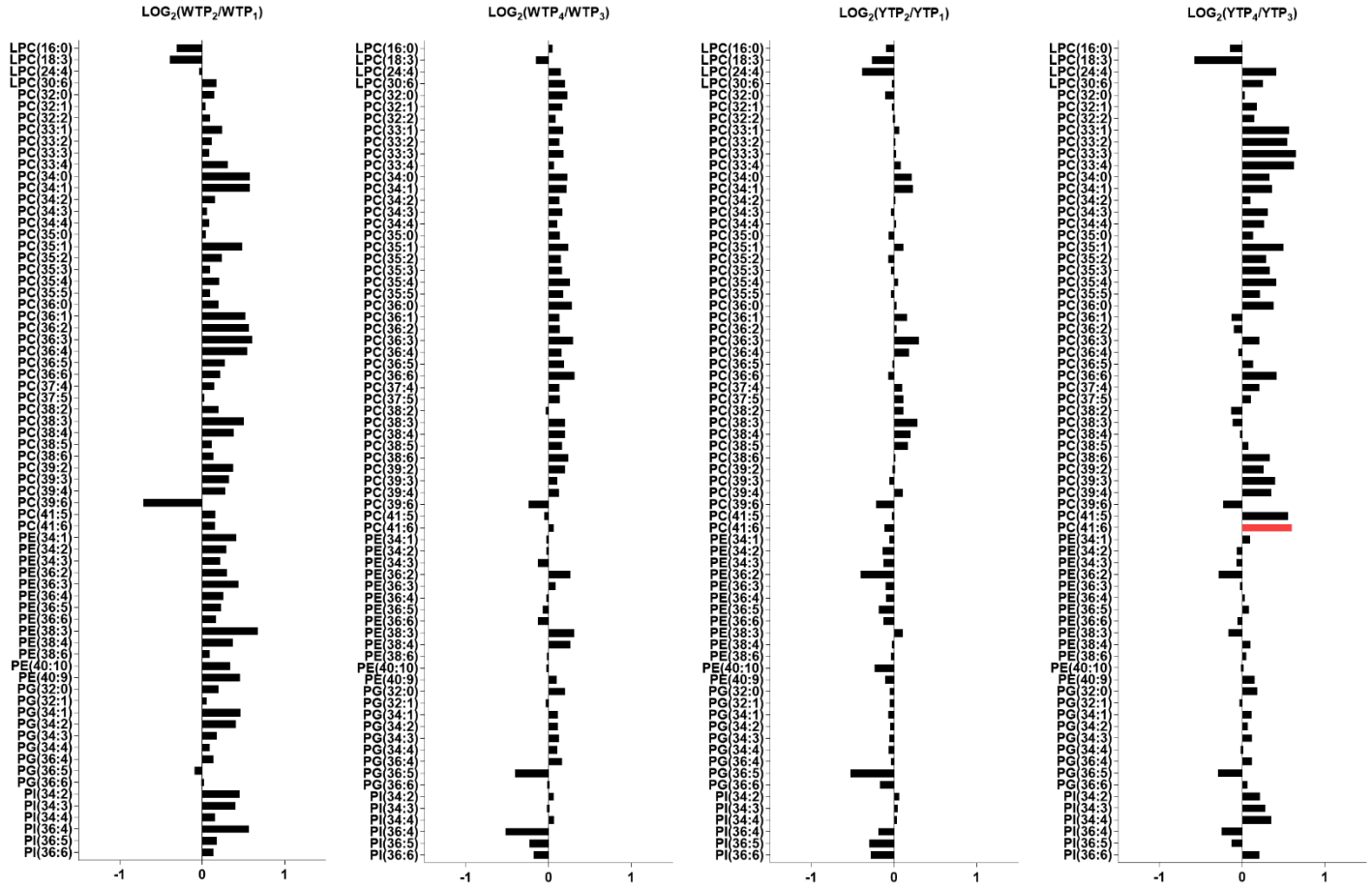
Supplemental Figures I-S2-1 to I-S2-3 and II-S2-1 to II-S2-3 are shown in this section, while the information for other Supplemental Data and Supplemental Tables can be found in the **Appendices**, **Appendix A: Supplemental Data and Figures for Chapter 2, Part I (page 278) and Part II (page 294) .**



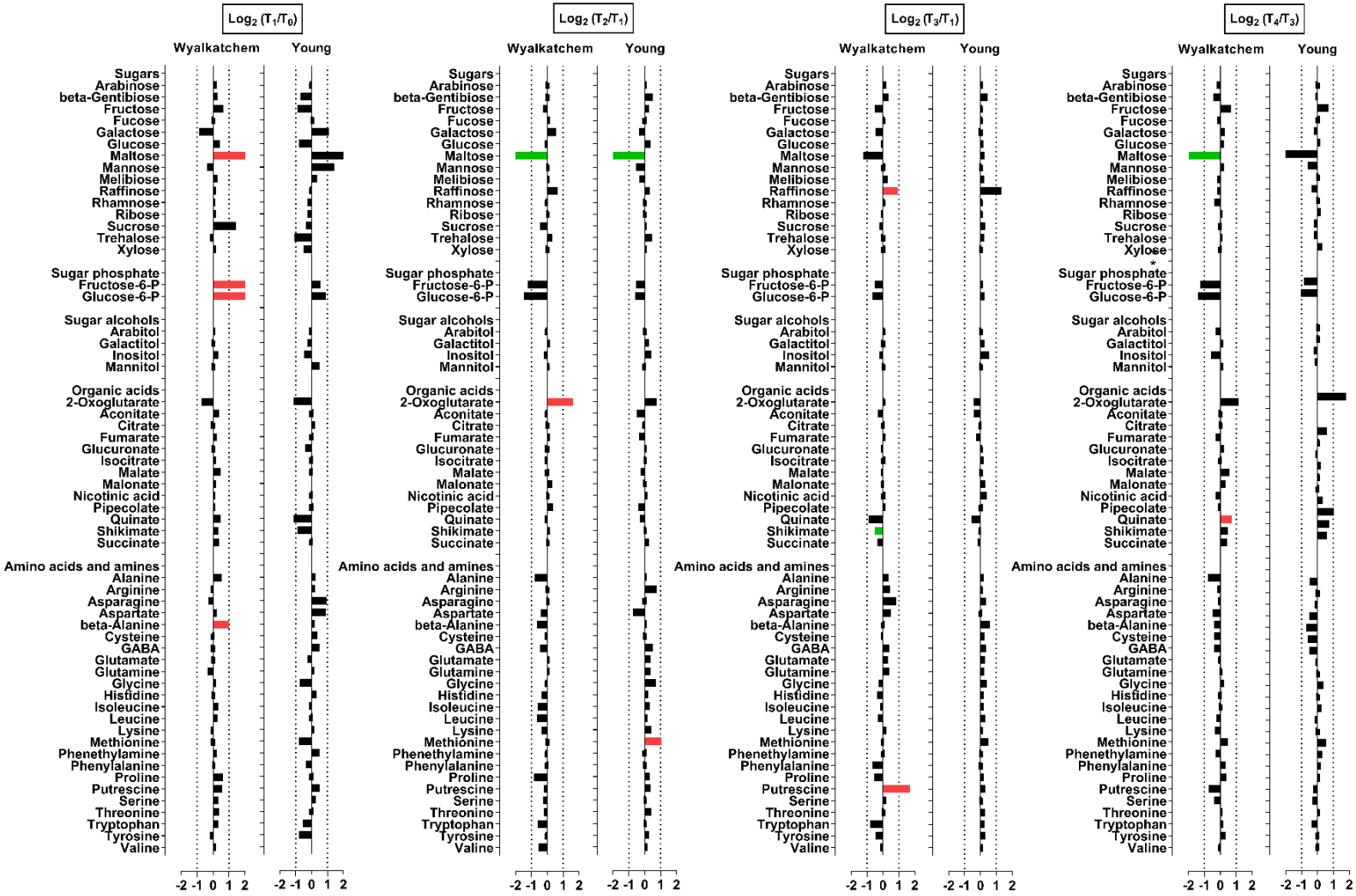
Supplemental Fig. I-S2-1. Schematic of the controlled environment chilling tolerance assay. **a.** Profile of temperature and lighting used in the controlled environment cabinets. **b.** Average spike grain number relative to unstressed control plants after a four-day chilling treatment at the YM stage in Young and Wyalkatchem. **c.** Larger grain size observed in fertile Wyalkatchem spikelets where spike grain number was reduced by four-day chilling treatment. **d.** Effect of cold treatment during different stages of flowering. Zadoks growth scale was used to determine flowering stages for the two cultivars Young and Wyalkatchem. A standard four-day cold treatment was applied. **e.** Time course experiment for cold treatment over seven days showing the effect of longer cold treatments on spike fertility for Young and Wyalkatchem. **f.** Graphic representation for the experimental design used for leaf harvesting and metabolite analysis.



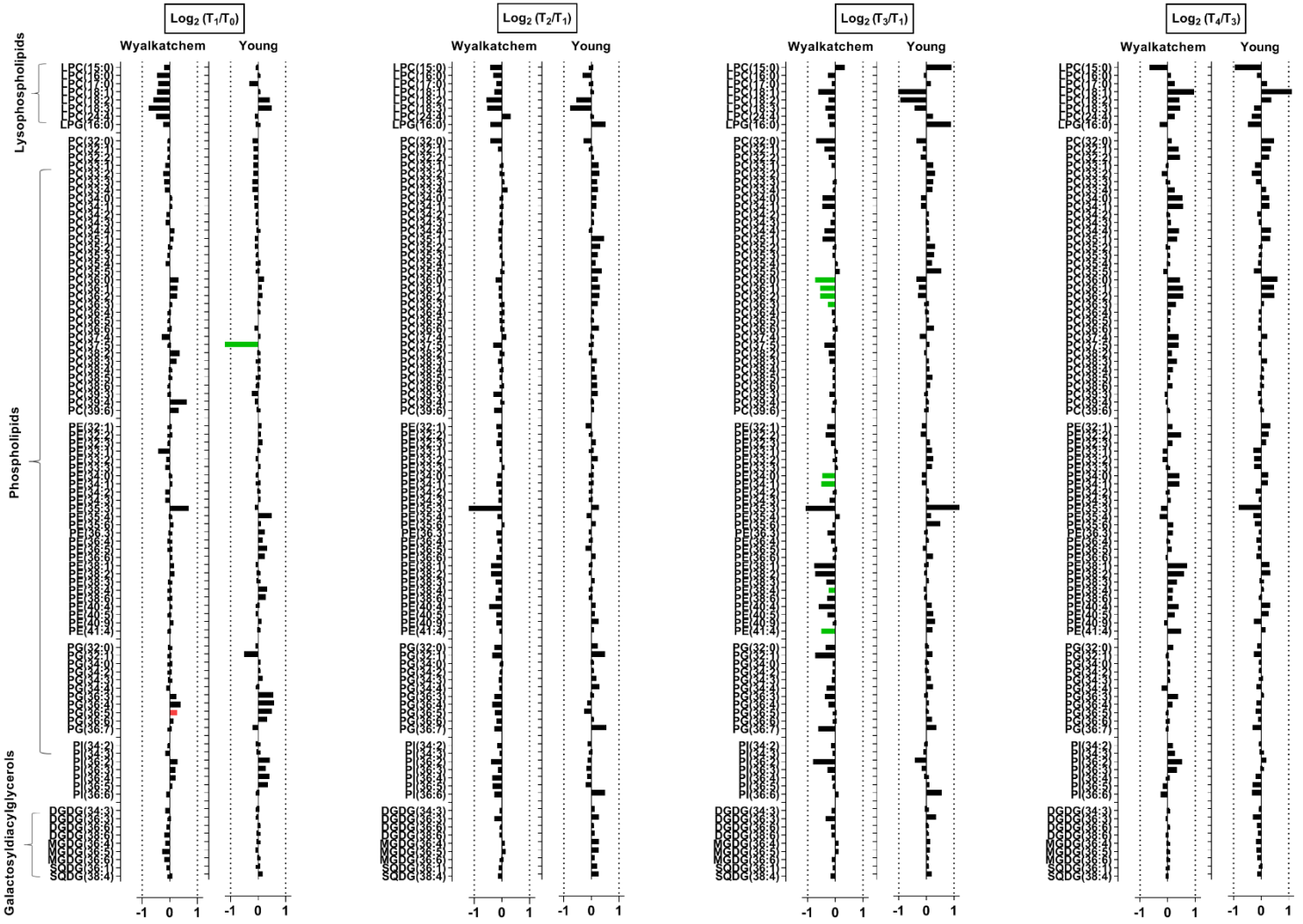
Supplemental Fig. I-S2-2. Log_2-fold changes of primary metabolite recoveries in the flag leaves of the cold-sensitive Wyalkatchem (W) and cold-tolerant Young (Y) after one night (TP_2 vs TP_1) and prolonged (TP_4 vs TP_3) of cold treatment. Fold changes were calculated by dividing the concentration of the variety at a time point (eg. TP_2) to the concentration of the variety at the previous time point (eg. TP_1), then Log_2-transformed. Significance of difference was determined by Benjamini and Hochberg method (Benjamini and Hochberg, 1995) with false discovery rate (FDR)-adjusted *p*-value of 0.05 as the cut-off. Green = significant decrease; Red = significant increase. There were four biological replicates (n=4) for all the measured metabolites, except phytohormones (n = 3).



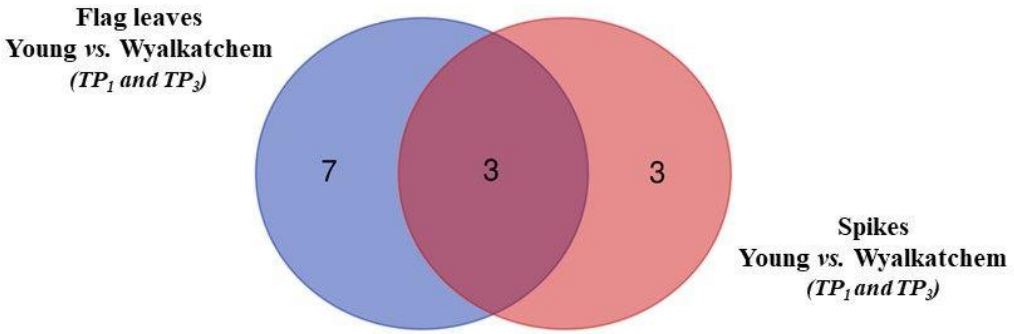
Supplemental Fig. I-S2-3. Log_2-fold changes of phospholipid recoveries in the flag leaves of the cold-sensitive Wyalkatchem (W) and cold-tolerant Young (Y) after one night (TP_2 vs TP_1) and prolonged (TP_4 vs TP_3) of cold treatment. Fold changes were calculated by dividing the normalized response of the variety at a time point (eg. TP_2) to the normalized response of that variety at the previous time point (eg. TP_1), then Log_2-transformed. Statistical method and cut-off are as stated in Fig. S2. Green = significant decrease; Red = significant increase. They were four biological replicates (n=4) for all the measured lipids.



Supplemental Fig. II-S2-1. Log_2-fold changes of primary metabolite concentrations in the spikes of cold-sensitive Wyalkatchem (W) and cold-tolerant Young (Y) after one night (TP_1 vs. TP_0) and prolonged (TP_3 vs. TP_1) exposure to cold, and the day-time recoveries after each of these cold treatments (TP_2 vs. TP_1 and TP_4 vs. TP_1). n =3.



Supplemental Fig. II-S2-2. Log_2-fold changes of lipid concentrations in the spikes of the cold-sensitive Wyalkatchem (W) and cold-tolerant Young (Y) after one night (TP_1 vs. TP_0) and prolonged (TP_3 vs. TP_1) exposure to cold, and the day-time recoveries after each of these cold treatments (TP_2 vs. TP_1 and TP_4 vs. TP_3). n = 3.



Differences in expression behavior of three overlapping metabolites between flag leaves and spikes of Young and Wyalkatchem (TP_1 and TP_3 samples)

Overlapped (3)	Higher in Young Flag leaves	Lower in Young Flag Leaves	Higher in Young Spikes	Lower in Young Spikes
Putrescine		√		√
Quinate		√		√
Shikimate		√		√

Supplemental Fig. II-S2-3. Differences in differentially expressed primary metabolites between flag leaves and spikes of cold-tolerant Young and cold-sensitive Wyalkatchem. The Venn diagrams show the degree of overlap between differentially expressed cold-induced metabolites in flag leaves and spikes for Young and Wyalkatchem. Three metabolites were commonly expressed in flag leaves and spikes at TP_1 and TP_3. The table below shows how these three metabolites are expressed differently in Wyalkatchem and Young flag leaves and spikes.

CHAPTER 3

The Effect of Cold Stress onto the Tissue-Specific Root Lipidome of Two Wheat Varieties with Contrasting Cold Tolerance

Preface to Chapter 3

This chapter describes the spatial root lipidome analysis of cold-stressed wheat varieties from Australia. Cold stress studies on plants have mostly been performed using the aerial plant parts, i.e. leaves and shoots. There are limited cold stress studies on whole roots or even rarely on the tissue-specific effects of cold stress on tissues such as the meristem and division zone, elongation zone, and maturation zone. In **Chapter 2**, the lipid profiling of cold-treated flag leaves and spikes indicates the involvement and importance of certain phosphoglycerolipids and galactosyl glycerolipids for cold tolerance in the aerial parts of wheat. This prompted us to further expand the study to investigate the lipid profiles in the roots of the two studied wheat varieties (cold-sensitive Wyalkatchem and cold-tolerant Young) subjected to cold stress. I therefore conducted a study to investigate the tissue-specific root lipidomes derived from young seedlings of Wyalkatchem and Young grown at optimal/unstressed temperature (21°C) and after subjected to chilling (4°C) and freezing (-3°C) stresses. The details of the study are described in the Materials and Methods, Results and Discussion parts of this chapter. I claim that I contributed to more than 80% of this work (experimental, data processing, data analysis, interpretation and writing) to this chapter.

3.1 Introduction

Wheat (*Triticum aestivum L.*) is the most widely cultivated crop on Earth, with production of 749 million tons in 2016. The production of wheat needs to increase by 60% to feed the projected 9.6 billion of world population by year 2050 (International Wheat Genome Sequencing Consortium, www.wheatgenome.org). A key challenge for wheat breeding is the improvement of varieties with tolerance to multiple biotic and abiotic stresses, while maintaining stable yields (Appels et al., 2018; Ortiz et al., 2008).

Low temperatures, such as chilling (0 – 12°C) and freezing (< 0°C), are one of the major yield-limitations to wheat productivity. The capacity to withstand cold temperatures in wheat may vary depending on the genetic background and variability. Some wheat varieties are cold tolerant, while others are more sensitive. Nonetheless, all of these varieties need to go through a similar process during the exposure to low, non-freezing temperatures to acquire freezing tolerance. This process is referred to as cold acclimation (Fowler and Gusta, 1979, Fowler et al., 1996b).

Induction of cold acclimation and freezing tolerance involves physiological and biochemical changes in plants (Wanner and Junttila, 1999). Plasma membranes are considered as the primary barrier between the organism and external environment, being the first to experience the injurious effects of stress. The plasma membrane transits from fluid state to rigid gel phase when exposed to low temperatures. In order to maintain the fluidity and re-stabilize the membrane at low temperatures, the cell increases the level of unsaturated lipids, alters the chain length and lipid class composition, and changes the membrane lipid:protein ratio. All these mechanisms lead to the remodeling of the membrane, which allow the cell to mechanically adapt to cold (Miquel et. al., 1993; Welti et al., 2002; Wang et al., 2006). In the cell, not only does the plasma membrane undergo such remodeling, but the endomembranes of other organelles such as the chloroplast, the endoplamic reticulum, the Golgi apparatus and the tonoplast also undergo similar remodeling when exposed to low temperature.

Plant membranes (plasma and endomembranes) are composed of three main categories of lipids: (1) glycerolipids such as phosphoglycerolipids, galactosyl glycerolipids and di/triacylglycerols, (2) sphingolipids and (3) sterols. Glycerolipids that contain phosphate groups in their structures are called phosphoglycerolipids, for example the phosphotidylcholines (PCs) and phophotidylethanoamines (PEs) which are the most abundant glycerolipids present in the extra plastidial membrane such as plasma membrane (Cacas et al., 2012). Glycerolipids that contain

galactose in their structures are called galactosyl glycerolipids. Galactosyl glycerolipids are present dominantly in the plastidial membrane such as the chloroplastic thylakoid membranes. The thylakoid membrane is composed mainly of 50% of monogalactosyldiacylglycerol lipids (MGDG), 26% of digalactosyldiacylglycerol lipids (DGDG), and the remaining are sulfoquinovosyldiacylglycerol lipids (SQDG) and phosphatidylglycerol lipids (PGs) (Dormann et al., 2013). There are also glycerolipids that do not contain any phosphate or sugar groups in their structures. For example, the diacylglycerols (DAGs) and triacylglycerols (TAG). DAGs are mainly used for membrane lipid assembly during vegetative growth to support cellular membrane biogenesis, expansion, and maintenance (Bates and Browse, 2012). Different from the first category of plant lipids glycerolipids, plant sphingolipids are structurally diverse molecules composed of three building blocks: a sphingoid long-chain base (LCB) backbone amide-linked to a fatty acid (FA), which is bonded to a polar head group (Hou et al., 2016). Sphingolipids compose an estimate 40% of plasma membrane lipids and are enriched in the outer leaflet where they influence membrane integrity and ion permeability (Sperling et al., 2005; Markham et al., 2013; Luttgeharm et al., 2016). The third category of plant lipids, sterols, fill the voids between sphingolipids to increase the packing of lipids and together with specific phosphoglycerolipids, they form membrane domains such as lipid rafts (Simon-Plas et al., 2011; Cacas et al., 2012; Yang et al., 2013). Besides of structural protection to the cell membranes and involvement of remodeling during cold stress, plant lipids also serve as signaling molecules when plants are exposed to low temperature. Lipid signaling molecules are low abundant (less than 1% of total lipids), accumulate transiently and have a fast turnover rate (Testerink and Munnik, 2005). Signaling lipids include phosphatidic acid (PA), phosphoinositides (PIs), sphingolipids, lysophospholipids, diacylglycerols (DAGs), oxylipins and others (Wang and Chapman, 2013; Xiong et al, 2002; Arisz et al., 2013; Bargmann and Munnik, 2006; Barbaglia et al., 2016; Guo et al., 2011; Dutilleul et al., 2012).

Considering these important roles of different lipid species in plants upon low temperature stress, it is therefore essential to investigate their profiles and changes in plants subjected to cold stress to understand the underlying mechanism in depth. Simple lipid profiling to complex lipidome studies have been conducted on plants exposed to cold stress, but are mainly in *Arabidopsis thaliana* (Miquel et al., 1993; Ruelland et al., 2002; Welti et al., 2002; Moellering et al., 2010; Degenkolbe et al., 2012; Arisz et al., 2013; Li et al., 2015; Barnes et al; 2016; Zheng et

al; 2016), rice (Zheng et al., 2016), maize (Gu et al., 2017; Noblet et al., 2017), and barley (Margutti et al., 2018 and 2019).

Several studies have reported on lipid profiling and lipidome analyses upon cold stress in wheat (Roche et al., 1972; Ashworth et al., 1981; Vigh et al, 1985; Kendall and McKerzie, 1989; Bohn et al., 2007; Li et al., 2013; Li et al., 2015; Cheong et al., 2019; Cheong et al., 2020). The materials used for the analyses were either the leaves, shoots, wheat seedlings, or whole seedling roots. Most of the lipid analyses reported only determined changes in fatty acids, certain glycerolipids, certain long-chain sphingoid bases, sterols, or a combination of those. To date, complex lipidome analysis of wheat upon low temperature stress have been reported only by Li et al. (2015) and Cheong et al. (2019 and 2020), in which leaves or spikes were used for glycerolipidome analysis. There are no reports on the effects of cold stress on the tissue specificity of lipid responses in roots. Sarabia et al. (2018, 2019) have recently managed to conduct comparative spatial lipidomics analyses on different developmental root zones of barley subjected to salt stress and revealed cellular lipid remodeling in different developmental zones of barley roots in response to salinity. Their successful study to include sphingolipids (ceramides and monohexosyl ceramides) and sterols in addition to glycerolipids encouraged us to apply a similar approach on our wheat roots upon cold stress.

Roots are vital to anchor the plant in soil and take up water and nutrients. Nielsen and Humphries (1966) have reported that root growth is generally more sensitive to temperature than that of above-ground plant parts and root growth may cease altogether if soil temperatures drop below 2°C (Petr, 1991). In the tip of a root, there are different developmental zones along the root's longitudinal axes. The root cap and meristemic (division) zone that contains active dividing cells, the elongation zone in which cells rapidly expand along the longitudinal axis, and the differentiation (maturation) zone in which cells differentiate to become functionally specialized (Somssich et al., 2016). In this study, we aimed to investigate the lipid profiles across the spatial root zones of two cold-stressed spring wheat varieties with contrasting cold-tolerance, Wyalkatchem being cold-sensitive and Young being cold-tolerant (Cheong et al., 2019 and 2020) using a comprehensive targeted lipidomics approach developed by Yu et al., (2018, 2020). Two days old germinated seedlings of the two wheat varieties were subjected to optimal (21°C), chilling (4°C) and freezing (-3°C) temperatures for six hours. The meristemic/division, elongation and maturation zones of the roots were harvested, lipids extracted and analysed. Using the modified

lipidomics approach from Yu et al. (2018, 2020), which is a targeted profiling using MS/MS data acquired from scheduled parallel reaction monitoring assays, we managed to profile 273 lipid species derived from 21 lipid classes, which revealed distinct lipidomes of the different root zones in each variety, as well as between the two varieties in response to chilling and freezing stresses. Together with the outcomes gained from the studies of flag leaf and spike in Chapter 2, the outcomes gained from this study (roots) may help us to better understand the mechanisms of wheat in response to cold, thus contributing to wheat breeding programs for the improvement of more cold-tolerant varieties in the future.

3.2 Materials and Methods

3.2.1 Chemicals and Reagents

All chemicals and solvents were purchased from Sigma-Aldrich (Australia) and were either of analytical or mass spectrometry grades. Lipid standards [PC(13:0/13:0), PE(12:0/12:0), PG(12:0/12:0), PS(12:0/12:0), PA(12:0/12:0), Cer(d18:1/12:0), LysoPC(13:0), Sitosterol, Cholesteryl-ester (9:0)] were purchased from Avanti Polar Lipids (Alabaster, Alabama, USA).

3.2.2 Lipid Nomenclature, Notation and Abbreviations

The nomenclature and notation for lipids present in this study were referred to LIPID MAPS (http://www.lipidmaps.org/data/classification/LM_classification_exp.php), Liebisch et al. (2013) and Yu et al. (2018, 2020). For example, the nomenclature of PC(16:1_18:2) indicates a PC species with two fatty acyl (FA) chains, 16:1 (16 carbons with one double bond) and 18:2 (18 carbons with two double bonds), but that the exact sn-position (sn-1 or sn-2) of the two esterified fatty acyl chains is unknown. The abbreviations for lipids measured in this study were (1) sterols such as ASG: acylated steryl glycoside; SG: steryl glycoside; SE: steryl ester and ST: steryl derivative; (2) sphingolipids such as Cer: ceramide and HexCer: monohexosyl ceramide; (3) DAG: diacylglycerol; (4) galactosyl glycerol lipids such as DGDG: digalactosyl diacylglycerol; DGMG: digalactosyl monoacylglycerol; MGDG: monogalactosyl diacylglycerol; MGMG: monogalactosyl monoacylglycerol; SQDG: sulfoquinovosyl diacylglycerol and SQMG: sulfoquinovosyl monoacylglycerol; (5) phosphoglycerolipids (including their lyso species) such as PC: phosphatidylcholine; PE: phosphatidylethanolamine; PG: phosphatidylglycerol; PI: phosphatidylinositol and PS: phosphatidylserine; (6) CL: cardiolipin.

3.2.3 Plant Material and Growth Conditions

The two wheat varieties used in this study, Wyalkatchem (cold-sensitive) and Young (cold-tolerant) were obtained via the National Frost Initiative, Australia (http://www.nvtonline.com.au/frost/). Seeds were sterilised and germinated according to Shelden et al. (2013), with some modifications. Briefly, seeds were surface-sterilised in 70% (v/v) ethanol for 1 min, followed by 1% (v/v) sodium hypochlorite (bleach) for 10 min and rinsed six times with sterile ultrapure water (Millipore, Billerica, MA, USA). The seeds were then imbibed in sterile ultrapure water for 16 hrs with aeration at room temperature in the dark. After that, the seeds were transferred to Whatman® Grade 50 filter papers (MERCK, Australia) pre-wetted with sterile ultrapure water in round petri dishes (100 mm X 20 mm, Greiner Bio-One, Germany; 10 seeds per plate; **Fig. S3-1A**). The seeds were allowed to germinate with the radical orientated downwards by placing the dishes at a 45° angle for 48 hrs at 21°C in the dark (covered with aluminium foil). Uniform germinated seedlings with the longest seminal root between 1.5 and 2.0 cm (**Fig. S3-1B**) were selected and transferred to square petri dishes (100 mm X 100 mm X 20 mm) containing nutrient agar medium with modified Hoaglands nutrient solution (Genc et al. 2007). Two seedlings were placed per plate and allowed to grow with the radical orientated downwards by placing the dishes at a 45° angle for another 48 hrs at 21°C in the dark (**Fig. S3-1C**).

3.2.4 Stress Treatment and Harvest of Root Samples

After 48 hrs grown at 21°C in the dark, the seedlings either remained at 21°C for 6 hrs in dark (control treatment), transferred to a cold chamber at 4°C for 6 hrs in the dark (chilling stress), or were transferred to a frost chamber at -3°C for 6 hrs in the dark (freezing stress). A total of 20 plates of seedlings (2 seedlings per plate x 20 plates = 40 seedlings) were treated as one biological replicate (n). There were four biological replicates (n = 4) for each condition (control, chilling and freezing). For the harvest of root samples, the apical region of the root was cut into three zones/sections measured from the root tip (**Figure 3-1**). From **Fig. 3-1**, DZ comprised the root cap and cell division zone (cut 1.5 mm from the root tip and labelled as DZ), EZ represented the elongation zone (after cutting 1.5 mm of the DZ, another 1.5 mm was cut and labelled as EZ), and MZ represented the maturation zone (after cutting the EZ, another 2.0 mm was cut and labelled as MZ). The root sections were cut with pre-chilled scalpel and immediately snap-frozen with liquid nitrogen. The

root samples were weighed and recorded (average = 40 mg) prior to being kept at -80°C for liquid extraction.

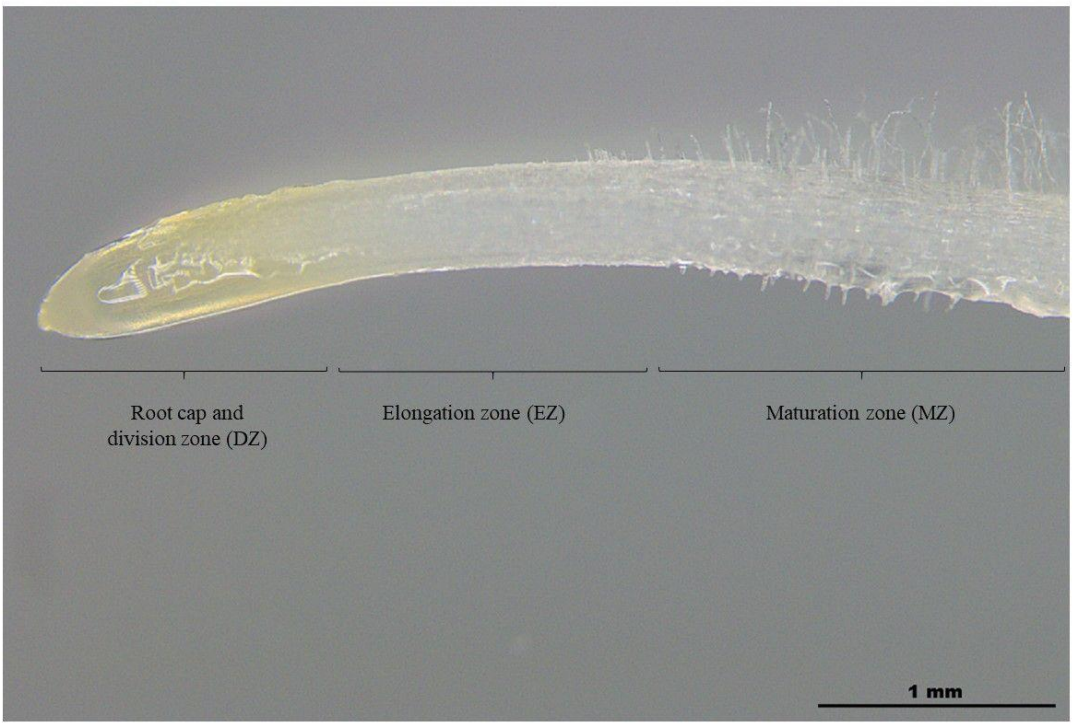


Figure 3-1. The three root zones analysed in this study. DZ = root cap and division zone, EZ = elongation zone, MZ = maturation zone.

3.2.5 Lipid Extraction

The extraction of lipids was carried out as described by Folch et al. (1957), with some modifications. Frozen root sections were transferred into Cryomill tubes (Precellys 24, Bertin Technologies). Subsequently, 500 µL of chloroform:methanol:water (1:3:1, v/v/v) and 5 µL of 1% butylated hydroxytoluene (BHT) was added to the samples, followed by vortexing for 30 secs and homogenization at -10°C using a Cryomill (3 × 45 secs at 6,100 rpm). The samples were then extracted for 30 mins at 25°C in a thermomixer at 1,400 rpm, and subsequently centrifuged for 10 mins at 4°C at 15,000 rpm. The supernatants were transferred into new tubes. 500 µL of the same extraction solvents and BHT were added into the remaining pellets for second extraction. The supernatants were collected and combined, vortexed for 30 secs, re-centrifuged for 10 mins at 15,000 rpm. A 200 µL aliquot of 0.1 M hydrochloric acid (HCl) was then added in, followed by

vortexing and centrifugation (10 mins, 15,000 rpm). The bottom layers of the supernatants (100 µL for each sample) were carefully transferred to new tubes and dried using SpeedVac at 40°C. The dried samples were kept at -80°C prior to lipid analysis.

3.2.6 LC-ESI-MS/MS Analysis

The samples were analysed using a LC-ESI-QqTOF system as decribed in Yu et al. (2018), with some modifications. The samples were first re-constituted with 150 µL of isopropanol:methanol:water (4:4:1, v/v/v). Internal standard mixtures of PC(13:0/13:0) and Cer(d18:1/12:0) were added into each sample in 1 µM final concentration prior to LC-MS analysis. An extra sample named pooled biological quality control (PBQC) sample was then produced by collecting 30 µL from each sample. Samples (10 uL each) were injected to an Agilent 1290 HPLC system (Santa Clara, CA, USA) coupled to a SCIEX TripleTOF^{TM} 6600 QqTOF mass spectrometer (Framingham, Massachusetts, USA). Separation of lipid species was carried out using an Agilent Poroshell EC-C18 column (100 mm × 2.1 mm, 2.7 µm) at a flow rate of 0.4 mL/min, and run in a linear gradient based on two mobile phases. Mobile phase A consisted of methanol and 20 mM ammonium acetate in 3:7 ratio (v/v), and mobile phase B consisted of 2-propanol:methanol:20 mM ammonium acetate in 6:3:1 ratio (v/v/v). Gradient started with 65% B for 2 min, increase to 100% B over 8 min, followed by 100% B for 6 min and then re-equilibrated to 65% B in 2 min. The PBQC sample was injected after every ten samples. During the run, the instrument was calibrated automatically every 20 samples to maintain the mass resolution of MS1 spectra at ~35,000 FWHM (full width at half maximum) and mass accuracy below 5 ppm, resolution of MS/MS spectra at ~20,000 FWHM and mass accuracy below 10 ppm. All the ESI and parallel reaction monitoring (PRM) parameters were set as according to Yu et al. (2018), except the collision energies (CEs). Lipids such as ASG, Cer, HexCer, DAG, SG, SE and ST were analysed with positive ion mode at CE -40 V. Meanwhile, lipids such as DGDG, DGMG, MGDG, MGMG, SQDG, SQMG, PC, PE, PG, PI, PS and CL were analysed with negative ion mode at a CE +60 V.

3.2.7 Data Processing

Each of the detected lipids using PRM transitions (MS/MS spectra) was identified using an in-house generated lipid database for barley (Yu et al., 2018), and the peak area of the identified lipid

was based on extracted ion count chromatogram (EICC) for one or multiple fragment ions analysed using MultiQuant software (SCIEX, Version 3.0.2). For phosphoglycerolipids, galactosyl glycerolipids as well as CLs detected in negative ion mode, peak area of all negative charged FA fragments was summed. For DAGs detected in positive ion mode, total peak area of all fragments resulting from neutral loss of a FA chain was used. For HexCer and Cer species detected in positive ion mode, the sum of peak area of positively charged long chain base (LCB) and its dehydrates from up to three dehydration processes were used. For sterols detected in positive ion mode, the dehydrated sterol backbone was the only fragment chosen. Peak picking for fragment ions was set to 100 ppm width. Integration settings were as follows: Noise percentage = 40%; Gaussian smooth width = 2 points. Peak area of each of the lipid species was then normalised to the intensity/responses of internal standards and sample weight. The responses of the PBQC samples for each lipid species were used to calculate the coefficient of variation (CoV). Only lipid species with CoV less than 20% were selected for further data analysis.

3.2.8 Statistical Analysis

Pairwise comparisons were performed first in each root zone of each variety under control versus chilling or control versus freezing stress. Then, pairwise comparisons were performed between the two varieties Young and Wyalkatchem for each root zone in control, chilling and freezing conditions. Statistical significance of differences observed between samples was evaluated using the Student's *t*-test using Excel with a false discovery rate (FDR)-adjusted *p*-value of 0.05 as cut-off (Benjamini and Hochberg, 1995). The pairwise comparisons of the data were presented as $\log_2$-transformed of the fold change values and plotted using Graph Pad Prism 7.0 software (GraphPad Software, La Jolla, CA, USA). The stacked bars were plotted using the same Graph Pad software and BioRender software (https://biorender.com/).

3.3 Results

3.3.1 Targeted Profiling Using Scheduled Parallel Reaction Monitoring Assays Enables the Profiling of the Complex Lipidome in Different Wheat Root Developmental Zones

Using the scheduled parallel reaction monitoring (PRM) assays, a total of 273 lipid species derived from 21 lipid classes that fall under the three lipid categories (glycerolipids, sphingolipids and sterols) were detected, measured and analysed in the three wheat root developmental zones (**Table**

3-1). The numbers of lipid species analysed for each class is summarized in **Table 3-1**. More details of the identities of all the analysed lipid species such as the total carbon numbers, fatty acyl chain length and double bond numbers can be found in **Supplementary Table S3-1**. Among the 21 classes of lipids summarized in **Table 3-1**, the sphingolipid monohexosyl ceramides (HexCer) contributed to the highest number of detected lipid species (41). This was followed by the glycerolipids such as phosphatidylethanolamines PE (36), diacylglycerols DAG (31) and phosphatidylcholines PC (22). The PRM assays also enabled the detection and measurement of ceramides Cer (21), phophatidylglycerol PG (20), phosphatidylinositide PI (12), digalactosyl diacylglycerols DGDG (12), sulfoquinovosyl diacylglycerol SQDG (11) and sterols such as acylated steryl glycoside ASG (10) (**Table 3-1**). Besides, it was also interesting to analyse and understand the distribution of these lipid classes in each of the specific root zone of the two wheat varieties before and after being subjected to cold stress. Therefore, results are further described in the next sections.

3.3.2 Comparisons of Measured Lipid Profiles of the Developmental Root Zones in Each Wheat Variety at the Unstressed Stage

It was important to understand the compositions of the measured 273 lipids of the different root zones of the two wheat varieties with contrasting cold-tolerance prior to any treatment. In this section, the compositions of measured 273 lipids in each of the root zone for each variety at the unstressed (control) stage were elaborated first, followed by the comparison of differences between the three root zones for each variety at the unstressed stage. For the following analysis, we calculated the proportion of each lipid class as percent of mass spectral intensity. **Figure 3-2** showed the distribution of the 21 lipid classes (in percentage of mass spectral inetnsity) in each specific root zone of cold-sensitive Wyalkatchem and cold-tolerant Young at the unstressed stage.

At the unstressed stage, in the division zone where cells are actively dividing, it was observed that phosphatidylethanolamine (PE) was the most abundant lipid class in Wyalkatchem (29.4%), followed by monohexosyl ceramides (HexCer) with 22.8%. This was opposite for Young, in which HexCer occupied the highest abundance in the DZ (31.6%), then was followed by PE with 22.8% (**Fig. 3-2**). Phosphatidylglycerol (PG) was the third abundant lipid class for Wyalkatchem (15.9%), followed by phosphatidylcholines (PC, 10.6%), diacylglycerols (DAG, 10.2%), lysophospholipids and other classes of lipids. This lipid distribution was slightly different

Table 3-1. Summary of the detected and measured 21 classes of lipids and the number of lipid species per class in the root developmental zones.

Three Categories of Lipids	21 Classes of Lipids Detected and Measured in this Study	Number of Lipid Species per Class
Glycerolipids	1. Lysophosphatidylcholine (LysoPC)	9
	2. Lysophosphatidylethanolamine (LysoPE)	9
	3. Lysophosphatidylglycerol (LysoPG)	4
	4. Lysophosphatidylinositide (LysoPI)	2
	5. Lysophosphatidylserine (LysoPS)	1
	6. Phosphatidylcholine (PC)	32
	7. Phosphatidylethanolamine (PE)	36
	8. Phosphatidylglycerol (PG)	20
	9. Phosphatidylinositide (PI)	12
	10. Phosphatidylserine (PS)	5
	11. Digalactosyl diacylglycerol (DGDG)	12
	12. Digalactosyl monoacylglycerol (DGMG)	4
	13. Monogalactosyl diacylglycerol (MGDG)	3
	14. Monogalactosyl monoacylglycerol (MGMG)	3
	15. Sulfoquinovosyl diacylglycerol (SQDG)	11
	16. Sulfoquinovosyl monoacylglycerol (SQMG)	4
	17. Diacylglycerol (DAG)	31
Sphingolipids	18. Ceramide (Cer)	21
	19. Monohexosyl ceramide (HexCer)	41
Sterols	20. Acylated steryl glycoside (ASG)	10
	21. Steryl glycoside (SG)	3
	Total number	273

in Young where DAG (10.8%) was the third abundant lipid class in this root zone (DZ), followed by PG (10%), PC (8.1%) and other classes of lipids (**Fig. 3-2**). In the elongation zone (EZ) were cells are expanding their sizes, both the wheat varieties showed the same patterns for lipid distributions. It was observed that HexCer was the most abundant class in both Wyalkatchem (34.8%) and Young (42.1%). This was followed by PE (25.8% in Wyalkatchem and 21.0% in Young), DAG (10.7% in Wyalkatchem and 10.2% in Young), PG (10.3% in Wyalkatchem and 7.0% in Young), PC (9.6% in Wyalkatchem and 7.0% in Young) and the remaining classes. In the maturation zone (MZ) were cells start to differentiate for specialized functions, it was observed that the lipid distributions in both the wheat varieties were similar. HexCer was the highest

abundant lipid class in both the wheat varieties with 43.3% in Wyalkatchem and 45.4% in Young, followed by PE (21.3% in Wyalkatchem and 20.1% in Young), DAG (12.1% in Wyalkatchem and 10.3% in Young), PG in Wyalkatchem (7.5%) in Wyalkatchem but PC in Young (6.2%), then PC in Wyalkatchem (7.2%) and PG in Young (6.2%), and the remaining classes of lipids (**Fig. 3-2**).

When comparing the compositions of measured lipids (in percentage of mass spectral intensity) among the three root zones, it was interesting to observe that the percentages for all phosphoglycerolipids (PE, PG, PC, PI, and their lyso species) decreased in the EZ compared to the DZ for both the wheat varieties. EZ of Wyalkatchem contained 47.6% of phosphoglycerolipids s compared to its DZ (59.9%), while EZ of Young contained 40.3% of phosphoglycerolipids compared to its DZ (50.9%). The phosphoglycerolipids were further decreased in the MZ of both the varieties compared to EZ or DZ, in which in Wyalkatchem was 37.5% and Young was 35.6% (**Fig. 3-2**). Interestingly, percentages for sphingolipids such as Cer and HexCer were observed to increase in EZ compared to the DZ in both the varieties. EZ of Wyalkatchem contained 37.0% of sphingolipids compared to its DZ (24.5%), while EZ of Young contained 43.8% of sphingolipids compared to its DZ (32.9%). The sphingolipids were further increased in the MZ for both the varieties compared to EZ or DZ, in which in Wyalkatchem was 45.9% and Young was 47.9%. DAG was observed to be higher in the MZ (12.1%) in Wyalkatchem compared to its DZ (10.2%) and EZ (10.7%), while there was no obvious difference of this lipid class among the three root zones in Young (**Fig. 3-2**). The sterols ASGs were observed to be slightly higher in the MZ of Young compared to its DZ and EZ, while there was no difference for this class of lipids in Wyalkatchem. Besides, there were not many differences of galactosyl glycerolipids among the three root zones at the unstressed stage for both the varieties (**Fig. 3-2**).

When comparing between the two varieties, it could be observed that overall Young has higher abundances of sphingolipids (Cer and HexCer) compared to Wyalkatchem in all the three root zones, while Wyalkatchem has higher abundances of phosphoglycerolipids (PE, PG, PE, PI and PS) compared to Young in the three root zones. Meanwhile, Young also has higher abundances of lysophospholipids compared to Wyalkatchem in the three root zones. There were not many differences of DAG between the two varieties in the DZ and EZ, but this class was higher in Wyalkatchem compared to Young in the MZ (**Fig. 3-2**).

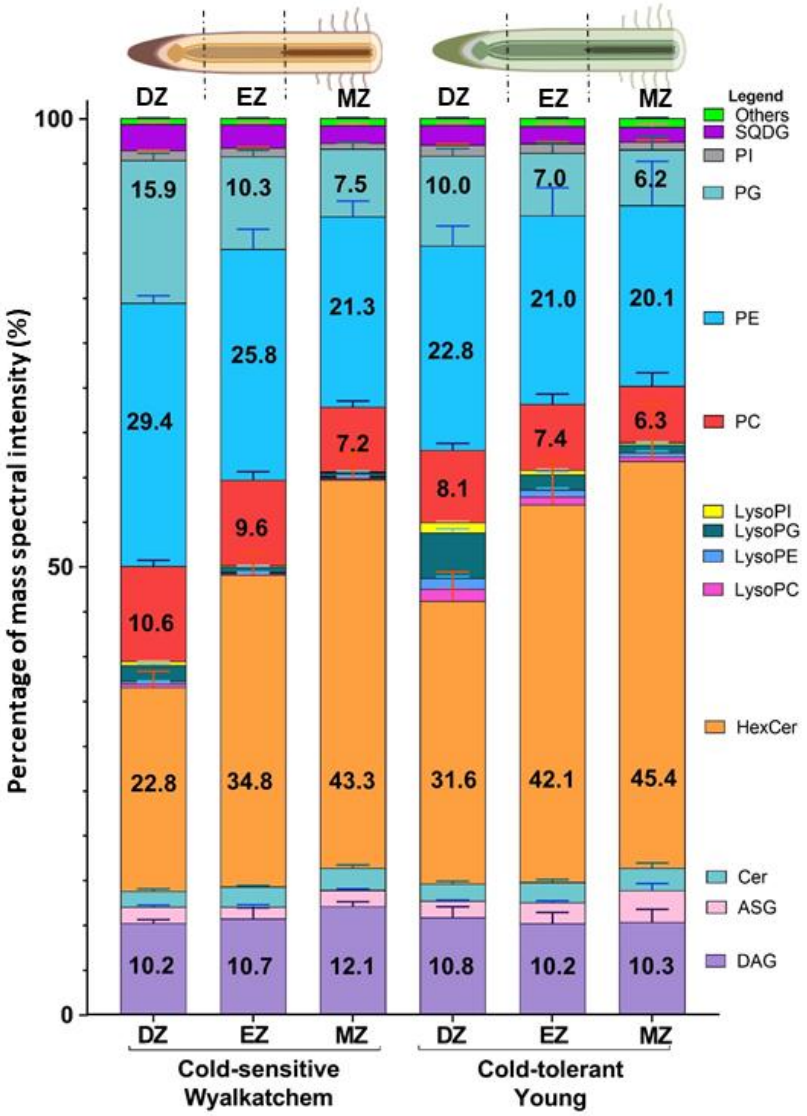


Figure 3-2. The distribution of the 21 measured lipid classes (based on percentage of mass spectral intensity, %) in each specific root zone of cold-sensitive Wyalkatchem and cold-tolerant Young at the unstressed stage. DZ = division zone, EZ = elongation zone, MZ = maturation zone. Others (light green colour) in the legend represent lipid classes PS, LysoPS, DGDG, DGMG, MGDG, MGMG, SQMG and SG that in total occupied less than or equal to 1% of the distribution.

3.3.3 Comparisons of Measured Lipid Profiles of the Developmental Root Zones in Each of the Wheat Variety Subjected to Chilling and Freezing Stresses

Next, in order to study the effects of cold stress (chilling and freezing) on the lipid composition of the three developmental root zones in each wheat variety, the distributions of the 21 classes of measured 273 lipids at the unstressed stage and after subjected to cold stress were compared (**Fig.**

3-3). Several interesting changes of lipids before and after cold stress were observed in the three root zones presented in **Fig. 3-3**. The first one was the increase of phosphoglycerolipids (PG, PE and PC) in all the three root zones of Wyalkatchem (**Fig. 3-3A**) and Young (**Fig. 3-3B**) after six hours of chilling (4°C) exposure. Like chilling stress, exposure of the roots to six hours of freezing temperature (-3°C) also caused the increase of phosphoglycerolipids in the DZ and EZ of both the varieties, but there was very slight or no changes in the MZ of both the varieties (**Fig. 3-3**). The second changes of lipids happened for the DAG class. Both six hours of chilling and freezing exposures caused the increase of this class of lipids in the EZ and MZ of Wyalkatchem and Young, but there was no effect in the DZ (**Fig. 3-3**). The third changes of lipids were observed for the sphingolipids HexCer and Cer classes. Chilling decreased these classes of lipids in all three root zones of both the varieties, but freezing only decreased these classes of lipids in the DZ and EZ of both the varieties with very slight decrease in MZ (**Fig. 3-3**).

As there were obvious cold effects of phosphoglycerolipids (PE, PC and PG), DAG and sphingolipids (HexCer and Cer) for the three different developmental root zones in Wyalkatchem and Young, it was important to know which respective lipid species caused these changes. Hence, $\log_2$-tranformed of fold changes of the lipid species obtained via the comparisons of cold (chilling or freezing) versus control for each variety on division zone (**Fig. 3-4** and **Fig. 3-5**), elongation zone (**Fig. 3-6** and **Fig. 3-7**) and maturation zone (**Fig. 3-8** and **Fig. 3-9**) were plotted for visualization and analysis. The significance of changes in individual lipid species was determined using Student *t*-test with False discovery rate (FDR)-adjusted *p*-value less than 0.05 (Benjamini-Hochberg, 1995) as cut-off. Lipid species that significantly increased after cold stress compared to control were coloured with red, while species that significantly decreased were coloured with green (**Fig. 3-4 to Fig. 3-9**). A large number of lipid species were found statistically significant as shown in Fig. 4 to Fig. 9, thus in the results below, only species that changed with equal to or more than –2.0-fold and +2.0-fold while also statistically significant were being described in the result sections.

Fig. 3-4 showed the chilling and freezing effects on the DZ of Wyalkatchem and Young for lipid species from the HexCer, Cer and DAG classes. In Wyalkatchem, after exposed to chilling stress, one DAG species, i.e. DAG(18:0_18:1) was decreased in the DZ with –2.7-fold. Meanwhile, DAG(18:2_24:1) and DAG(18:3_24:1) were increased with +3.4-fold and +2.7-fold, respectively (**Fig. 3-4A**). Compared to chilling, exposure to freezing stress caused more significant changes of

DAG species in DZ of Wyalkatchem (**Fig. 3-4B**). Four DAGs were observed to decrease in this zone, two of them were greater than –2.0-fold: DAG(18:0_18:1) with –2.3-fold and DAG(18:1_18:1) with –2.1-fold. Five DAGs were observed to increase after freezing stress in which four of them were greater than +2.0-fold: DAG(18:2_24:0) with +3.1-fold, DAG(18:2_24:1) with +4.1-fold, DAG(18:3_24:0) with +2.9-fold and DAG(18:3_24:1) with +3.3-fold (**Fig. 3-4B**). In Young, after exposed to chilling stress, nine DAG species were observed to decrease in the DZ, with three of them increased more than –2.0-fold. They were DAG(16:0_16:0) with –2.4-fold, DAG(16:0_18:0) with –2.0-fold and DAG(18:0_18:1) with –2.0-fold (**Fig. 3-4A**). Compared to chilling, exposure to freezing stress caused less significant changes of DAG species in DZ of Young (**Fig. 3-4B**). Four DAGs were observed to decrease in this zone but all less than –2.0-fold. Four DAGs were observed to increase more than 2.0-fold after freezing stress. They were DAG(18:2_24:0) with +3.5-fold, DAG(18:2_24:1) with +3.1-fold, DAG(18:3_24:0) with +2.7-fold and DAG(18:3_24:1) with +2.0-fold (**Fig. 3-4B**).

Chilling and freezing also caused significant decreases of sphingolipids (Cer and HexCer) in the DZ of Wyalkatchem and Young (**Fig. 3-4**). Chilling caused the decreased of four Cer species with a more than –2.0-fold change and no significant changes of HexCer species were found. The four Cer species were Cer(t18:0_22:0) with –3.0-fold, Cer(t18:0_24:0) with –3.7-fold, Cer(t18:0_24:1-OH) with –2.7-fold and Cer(t18:0_26:0) with –3.1-fold (**Fig. 3-4A**). Freezing caused an even stronger decrease of Cer species in the DZ of Wyalkatchem compared to chilling in which seven species were involved (**Fig. 3-4B**). Of these, six were decreased with greater than –2.0-fold. They were Cer(t18:0_24:0) with –3.1-fold, Cer(t18:0_24:1-OH) with –2.7-fold, Cer(t18:0_25:0-OH) with –2.0-fold, Cer(t18:0_25:1-OH) with –3.1-fold, Cer(t18:0_26:0) with –3.3-fold and Cer(t18:0_26:1) with –2.4-fold. One HexCer was decreased in this zone exposure to freezing stress, i.e. HexCer(d18:2_18:1-OH) but the decrease was less than –2.0-fold (i.e –1.6-fold) (**Fig. 3-4B**). On the other hand, chilling caused many significant decreases of Cer species (11) and HexCer species (21) in the DZ of Young (**Fig. 3-4A**). Of the eleven Cer species, eight were decreased greater than –2.0-fold. They were Cer(18:0_22:0) with –3.4-fold, Cer(t18:0_22:1-OH) with –3.3-fold, Cer(t18:0_24:0) with –4.0-fold, Cer(t18:0_24:1) with –2.0-fold, Cer(t18:0_24:1-OH) with –2.8-fold, Cer(t18:0_26:0) with –3.3-fold, Cer(t18:0_26:1-OH) with –2.4-fold and Cer(t18:1_24:0) with –2.1-fold. Of the 21 HexCer species, only six were decreased

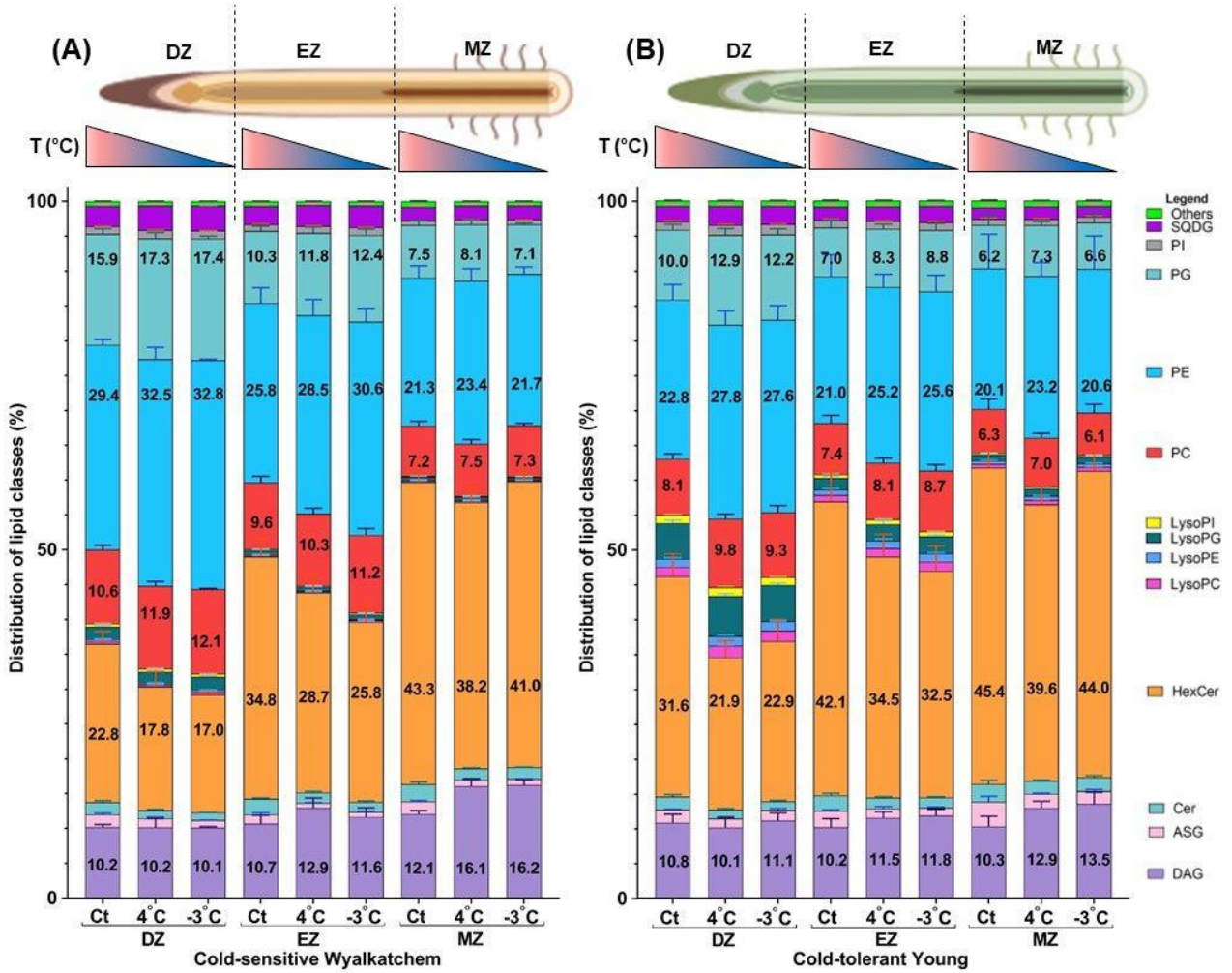


Figure 3-3. The distribution of the 21 measured lipid classes (in percentage of mass spectral intensity, %) in each specific root zone of **(A)** cold-sensitive Wyalkatchem and **(B)** cold-tolerant Young at the unstressed stage and after subjected to chilling (4°C) and freezing (-3°C) stress. DZ = division zone, EZ = elongation zone, MZ = maturation zone, Ct = control (21°C). Others (light green colour) in the legend represent lipid classes PS, LysoPS, DGDG, DGMG, MGDG, MGMG, SQMG and SG that in total occupied less than or equal to 1% of the distribution.

greater than –2.0-fold. They were HexCer(d18:1_16:0-OH) with –2.2-fold, HexCer(d18:2_16:0-OH) with –2.3-fold, HexCer(d18:2_18:0-OH) with –2.0-fold, HexCer(d18:2_18:1-OH) with –2.1-fold, HexCer(d18:2_20:1-OH) with –2.0-fold and HexCer(t18:1_18:0-OH) with –2.0-fold (**Fig. 3-4A**). Freezing caused lesser decreases of Cer and HexCer compared to chilling in the DZ of Young (**Fig. 3-4B**). Six Cer and five HexCer were significantly decreased in this root zone exposed to freezing stress. Of the six Cer species, five were decreased more than –2.0-fold. They were Cer(t18:0_24:1) with –3.4-fold, Cer(t18:0_24:1) with –2.0-fold, Cer(t18:0_24:1-OH) with –3.1-fold, Cer(t18:0_26:0) with –2.9-fold and Cer(t18:0_26:1) with –2.5-fold. Two HexCer decreased more than –2.0-fold: HexCer(t18:0_22:1-OH) with –3.1-fold and HexCer(t18:1_24:1-OH) with –2.3-fold (**Fig. 3-4B**).

On the other hand, both chilling and freezing did not cause many significant changes of phosphoglycerolipids (PC, PE and PG) in the DZ of Wyalkatchem and Young (**Fig. 3-5**). Chilling did not cause any significant changes of PC, PE or PG in both the varieties (**Fig. 3-5A**). Freezing, as shown in **Fig. 3-5B**, caused the decrease of only one PE in Wyalkatchem, which was PE(16:0_16:1) with –3.0-fold. In Young, freezing caused the decrease of two and increase of two PE species. The decreased species were PE(14:0_18:2) with –5.6-fold and PE(14:0_18:3) with –5.7-fold. The increase PE species were PE(16:0_16:0) with +3.3-fold and PE(16:1_16:1) with +4.6-fold. Freezing also caused the increase of two PG species in the DZ of Young, which were PG(16:0_16:0) with +3.3-fold and PG(16:1_16:1) with 4.8-fold (**Fig. 3-5B**).

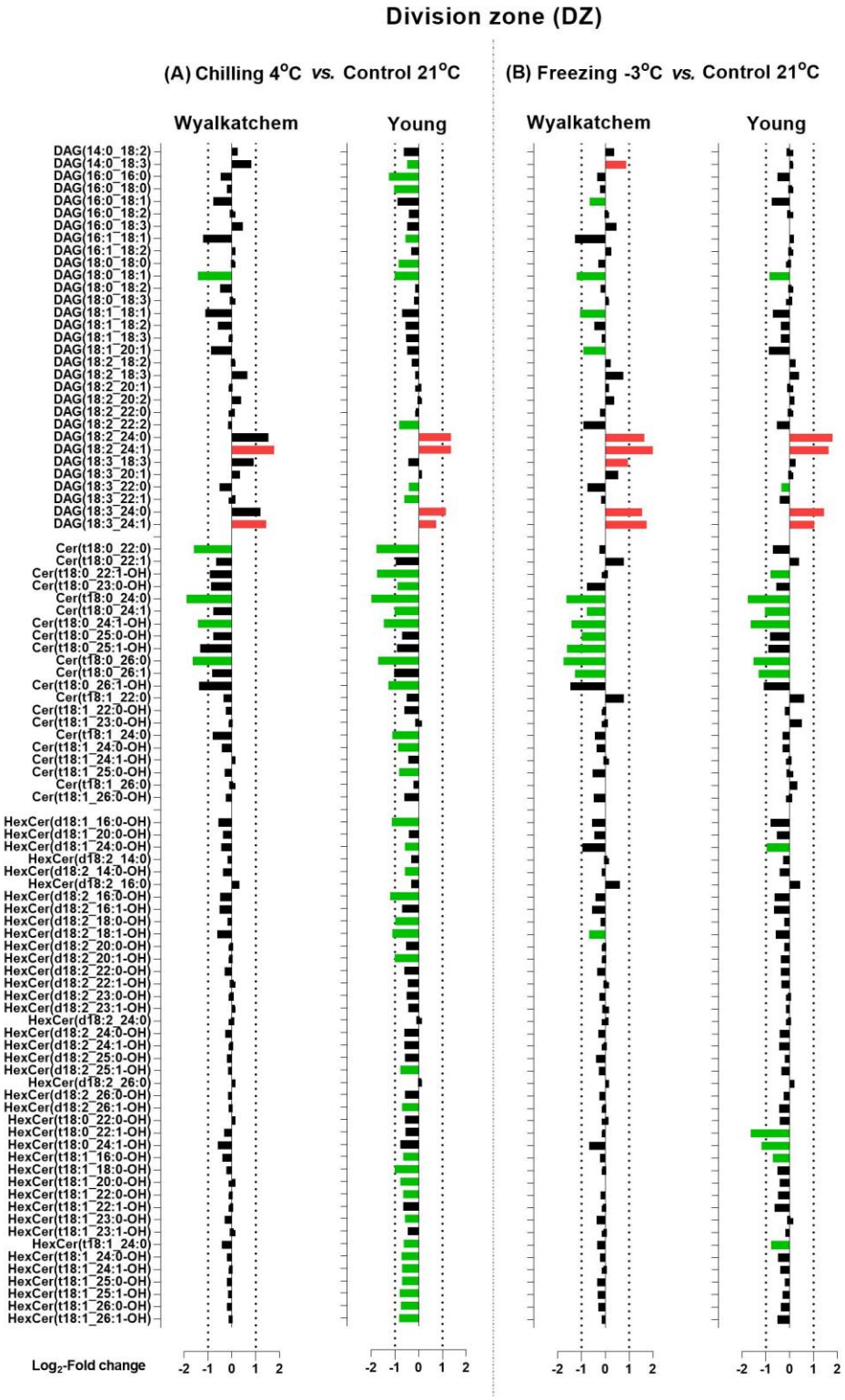


Figure 3-4. Log_2-fold changes of DAG, Cer and HexCer species in the division zone (DZ) of the cold-sensitive Wyalkatchem and cold-tolerant Young after exposed to **(A)** chilling and **(B)** freezing stresses. Statistical significance was determined using FDR-adjusted *p*-value of 0.05 as the cut-off. Green significant decrease, Red significant increase. n = 4.

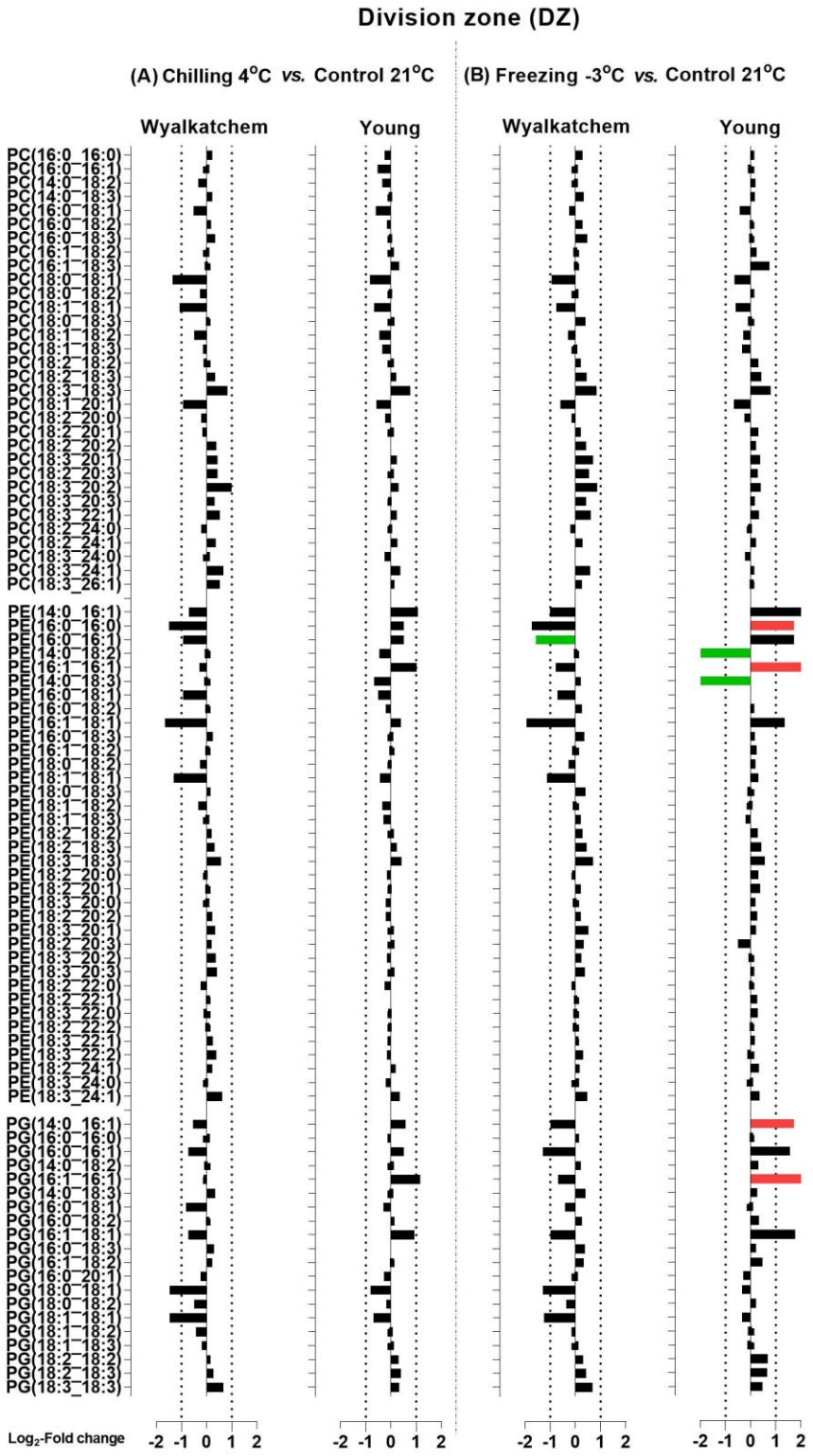


Figure 3-5. Log_2-fold changes of PC, PE and PG species in the division zone (DZ) of the cold-sensitive Wyalkatchem and cold-tolerant Young after exposed to **(A)** chilling and **(B)** freezing stresses. Statistical significance was determined using FDR-adjusted *p*-value of 0.05 as the cut-off. Green significant decrease, Red significant increase. n = 4.

Next, the chilling and freezing effects on the elongation zone (EZ) of Wyalkatchem and Young for lipid species from the HexCer, Cer and DAG classes are shown in **Fig. 3-6**, and for lipid species from PC, PE and PG classes are shown in **Fig. 3-7**. Chilling and freezing did not cause any significant changes of sphingolipids (Cer and HexCer) in the EZ of Wyalkatchem and Young (**Fig. 3-6**). Chilling and freezing also did also not cause any significant changes of DAG in the EZ of Wyalkatchem and Young, except only for two DAG species that were significantly increased after chilling exposure in Wyalkatchem (**Fig. 3-6A**). The DAG species were DAG(18:2_24:1) with +5.5-fold and DAG(18:3_24:1) with +4.9-fold.

The most obvious effects of chilling and freezing on EZ were observed in phosphoglycerolipids from PC, PE and PG classes in which many of the lipid species were significantly increased in the cold-sensitive Wyalkatchem after being subjected to cold stress. Chilling caused the increase of 16 PC species in Wyalkatchem, of which five of them were greater than +2.0-fold (**Fig. 3-7A**). The five PC species were PC(18:3_18:3) with +2.5-fold, PC(18:3_20:2) with +2.2-fold, PC(18:3_22:1) with +2.2-fold, PC(18:3_24:1) with +2.3-fold and PC(18:3_26:1) with +2.0-fold. Chilling also induced the increase of 18 PE species in EZ of Wyalkatchem, but only three among them were greater than +2.0-fold. The PE species were PE(18:3_18:3) with +2.4-fold, PE(18:3_20:3) with +2.0-fold and PE(18:3_24:1) with +2.3-fold. Nine PG species were also increased in EZ subjected to chilling, but only one PG(18:3_18:3) was increased with +2.2-fold (**Fig. 3-7A**). Freezing caused even more significant changes of PC, PE and PG species in the EZ of Wyalkatchem compared to chilling (**Fig. 3-7B**). A total of 24 PC species were significantly increased, with seven of them more than +2.0-fold. The PC species were PC(18:0_18:3) with +2.1-fold, PC(18:3_18:3) with +2.7-fold, PC(18:3_20:1) with +2.3-fold, PC(18:3_20:2) with +2.2-fold, PC(18:3_22:1) with +2.3-fold, PC(18:3_24:1) with +2.2-fold and PC(18:3_26:1) with +2.1-fold. Besides, 26 PE species were increased with ten of them more than +2.0-fold. The PE species were PE(18:0_18:3) with +2.2-fold, PE(18:1_18:3) with +2.0-fold, PE(18:2_18:3) with +2.0-fold, PE(18:3_18:3) with +2.7-fold, PE(18:3_20:1) with +2.3-fold, PE(18:2_20:3) with +3.8-fold, PE(18:3_22:0) with +2.0-fold, PE(18:3_22:1) with +2.1-fold, PE(18:3_24:0) with +2.0-fold and PE(18:3_24:1) with +2.5-fold. One PE species was significantly decreased in the EZ of Wyalkatchem subjected to freezing stress, i.e. PE (16:0_16:1) with –3.5-fold. For PG in EZ, ten species were increased after being subjected to freezing stress, but only two species were more than +2.0-fold. The species were PG(18:2_18:3) with +2.0-fold and

PG(18:3_18:3) with +2.5-fold. One PG specie was significantly decreased in this zone subjected to freezing stress, i.e. PG(16:0_16:1) with –3.0-fold (**Fig. 3-7B**). For the EZ of Young, chilling did not cause any significant changes of PC, PE and PG (**Fig. 3-7A**), but freezing did have some significant effects (**Fig. 3-7B**). Two PC species were significantly increased after freezing stress but the changes were less than +2.0-fold. Four PE species were significantly increased and only two of them were more than +2.0-fold. The PC species were PE(16:1_16:1) with +2.7-fold and PE(18:3_18:3) with +2.0-fold. One PG specie PG(18:3_18:3) was significantly increased in this root zone subjected to freezing, with a less than +2.0-fold change (+1.8-fold) (**Fig. 3-7B**).

In the third developmental root zone (maturation zone MZ), the effects of chilling and freezing for lipid species from the HexCer, Cer and DAG classes are shown in **Fig. 3-8**, and for lipid species from PC, PE and PG classes are shown in **Fig. 3-9**. As shown in **Fig. 3-8**, both chilling and freezing caused the increase of DAG species in the cold-sensitive Wyalkatchem, but no changes were observed for the cold-tolerant Young. A total of ten DAG species were observed to increase in the MZ of Wyalkatchem after exposure to chilling stress, all changing more than +2.0-fold (**Fig. 3-8A**). They were DAG(18:0_18:3) with +2.3-fold, DAG(18:1_18:3) with +2.0-fold, DAG(18:1_20:1) with +2.3-fold, DAG(18:2_20:1) with +2.5-fold, DAG(18:2_20:2) with +2.2-fold, DAG(18:2_24:0) with +5.2-fold, DAG(18:2_24:1) with +5.8-fold, DAG(18:3_20:1) with +2.9-fold, DAG(18:3_24:0) with +4.3-fold and DAG(18:3_24:1) with +4.8-fold. Compared to chilling stress, freezing stress caused an even greater number of DAG species to increase in the MZ of Wyalkatchem (**Fig. 3-8B**). A total of 18 DAG were increased more than +2.0-fold. They were DAG(16:0_18:1) with +2.6-fold, DAG(16:0_18:3) with +2.8-fold, DAG(18:0_18:2) with +2.8-fold, DAG(18:0_18:3) with +3.6-fold, DAG(18:1_18:1) with +2.7-fold, DAG(18:1_18:2) with +2.8-fold, DAG(18:1_18:3) with +3.4-fold, DAG(18:1_20:1) with +3.1-fold, DAG(18:2_18:3) with +2.6-fold, DAG(18:2_20:1) with +3.3-fold, DAG(18:2_20:2) with +2.4-fold, DAG(18:2_24:0) with +6.4-fold, DAG(18:2_24:1) with +7.2-fold, DAG(18:3_18:3) with +2.7-fold, DAG(18:3_20:1) with +4.2-fold, DAG(18:3_22:1) with +3.5-fold, DAG(18:3_24:0) with +6.4-fold and DAG(18:3_24:1) with +7.2-fold (**Fig. 3-8B).**

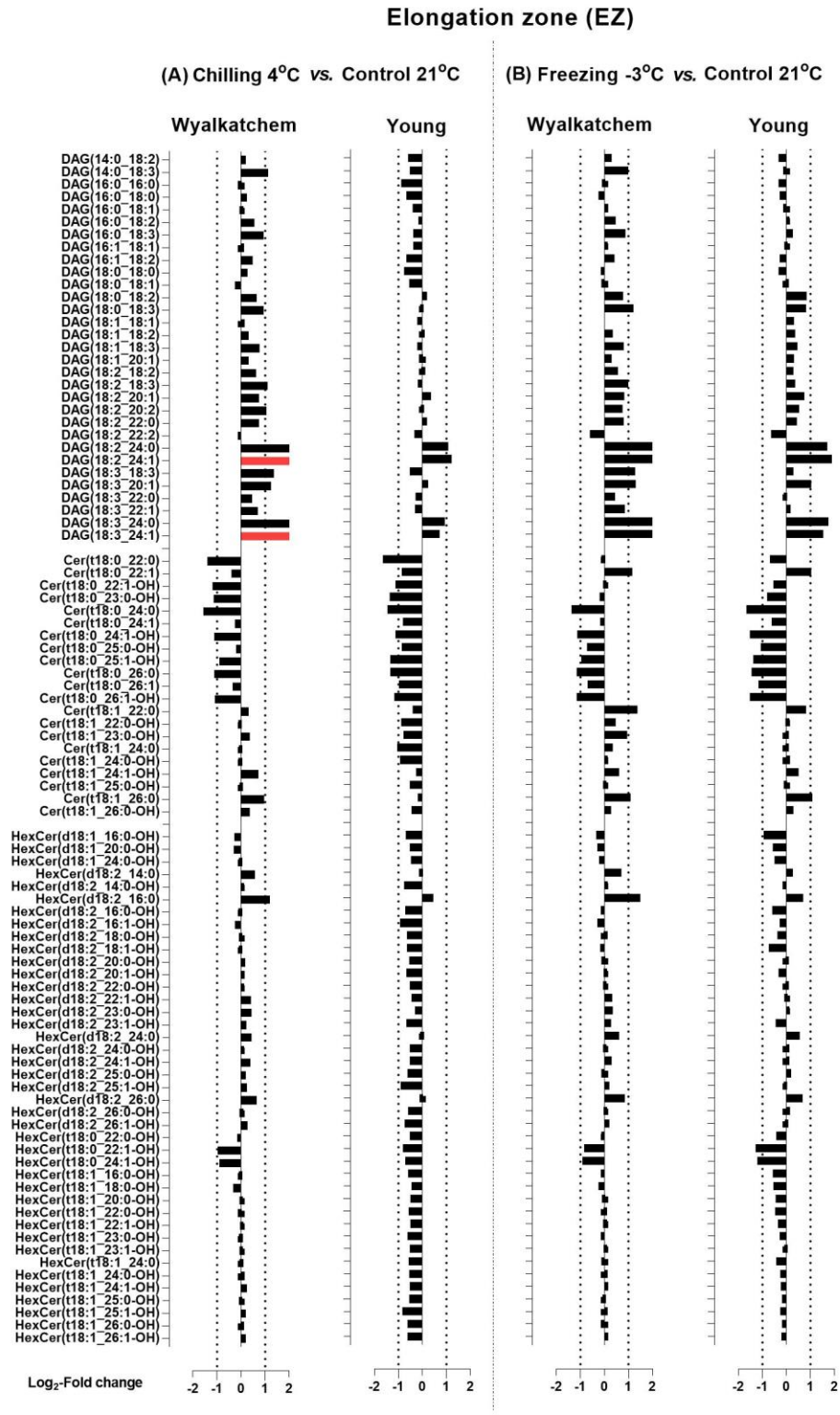


Figure 3-6. Log_2-fold changes of DAG, Cer and HexCer species in the elongation zone (EZ) of the cold-sensitive Wyalkatchem and cold-tolerant Young after exposed to **(A)** chilling and **(B)** freezing stresses. Statistical significance was determined using FDR-adjusted *p*-value of 0.05 as the cut-off. Green significant decrease, Red significant increase. n = 4.

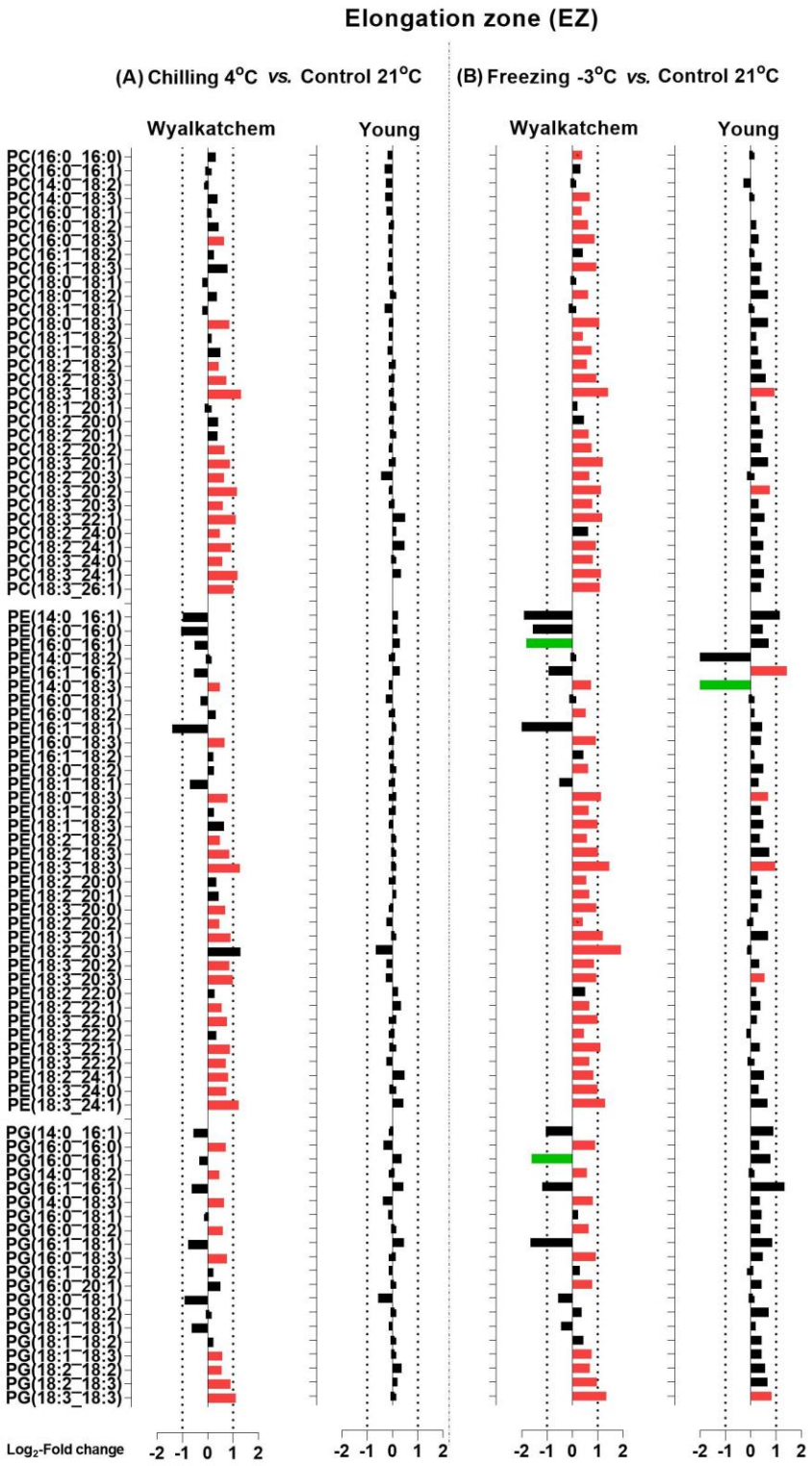


Figure 3-7. Log_2-fold changes of PC, PE and PG species in the elongation zone (EZ) of the cold-sensitive Wyalkatchem and cold-tolerant Young after exposed to **(A)** chilling and **(B)** freezing stresses. Statistical significance was determined using FDR-adjusted *p*-value of 0.05 as the cut-off. Green significant decrease, Red significant increase. n = 4.

On the other hand, chilling also caused the significant increase of two Cer but were less than +2.0-fold, and one HexCer(d18:2_26:0) with +2.1-fold in the MZ of Wyalkatchem (**Fig. 3-8A**). Compare to chilling stress, freezing stress again caused more increases of Cer and HexCer species in the MZ of Wyalkatchem (**Fig. 3-8B)**. Six Cer species were observed to increase with more than +2.0-fold. They were Cer(t18:0_22:1) with +3.2-fold, Cer(t18:1_22:0) with +5.0-fold, Cer(t18:1_22:0-OH) with +2.2-fold, Cer(t18:1_24:0) with +2.0-fold, Cer(t18:1_24:1-OH) with +2.6-fold and Cer(t18:1_26:0) with +3.1-fold. Opposite to Wyalkatchem, both chilling and freezing did not have significant effects on the MZ of Young, although a decrease of Cer and HexCer species was observed following chilling in this root zone in Young (**Fig. 3-8B).**

Similar to EZ, cold stress also caused the increase of phosphoglycerolipids in the MZ of the cold-sensitive Wyalkatchem, but not in the MZ of cold-tolerant Young (**Fig. 3-9**). As shown in **Fig. 3-9A**, chilling did not cause any significant changes of PC, but an increase of two PE and one PG species were observed in the MZ of Wyalkatchem. Among these three species, only one PC(18:3_24:1) was increased more than +2.0-fold (+2.1-fold). Compared to chilling stress, freezing stress caused even more increases of PC, PE and PG in the MZ of Wyalkatchem (**Fig. 3-9B**). A total of 18 PC were significantly increased due to freezing, but only 12 of them more than +2.0-fold. They were PC(18:0_18:3) with +2.1-fold, PC(18:1_18:2) with +2.0-fold, PC(18:1_18:3) with +2.2-fold, PC(18:1_20:1) with +2.0-fold, PC(18:2_20:1) with +2.0-fold, PC(18:3_20:1) with +2.5-fold, PC(18:3_20:2) with +2.4-fold, PC(18:3_22:1) with +2.5-fold, PC(18:2_24:1) with +2.0-fold, PC(18:3_24:0) with +2.2-fold, PC(18:3_24:1) with +2.4-fold and PC(18:3_26:1) with +2.0-fold. Eighteen PE species were significantly increased in the MZ of Wyalkatchem, with 16 of them more than +2.0-fold. The PE species were PE(14:0_18:3) with +22.5-fold, PE(16:0_18:3) with +2.0-fold, PE(18:0_18:3) with +2.7-fold, PE(18:1_18:2) with +2.2-fold, PE(18:1_18:3) with +2.6-fold, PE(18:2_18:3) with +2.3-fold, PE(18:3_18:3) with +3.0-fold, PE(18:2_20:1) with +2.0-fold, PE(18:3_20:0) with +2.3-fold, PE(18:3_20:1) with +2.7-fold, PE(18:2_22:1) with +2.1-fold, PE(18:3_22:0) with +2.3-fold, PE(18:3_22:1) with +2.5-fold, PE(18:2_24:1) with +2.1-fold, PE(18:3_24:0) with +2.3-fold and PE(18:3_24:1) with +3.1-fold. A total of six PG species were also increased due to freezing in this root zone in Wyalkatchem, with three more than +2.0-fold. They were PG(16:0_20:1) with +2.0-fold, PG(18:1_18:3) with +2.2-fold) and PG(18:3_18:3) with +2.0-fold (**Fig. 3-9B**).

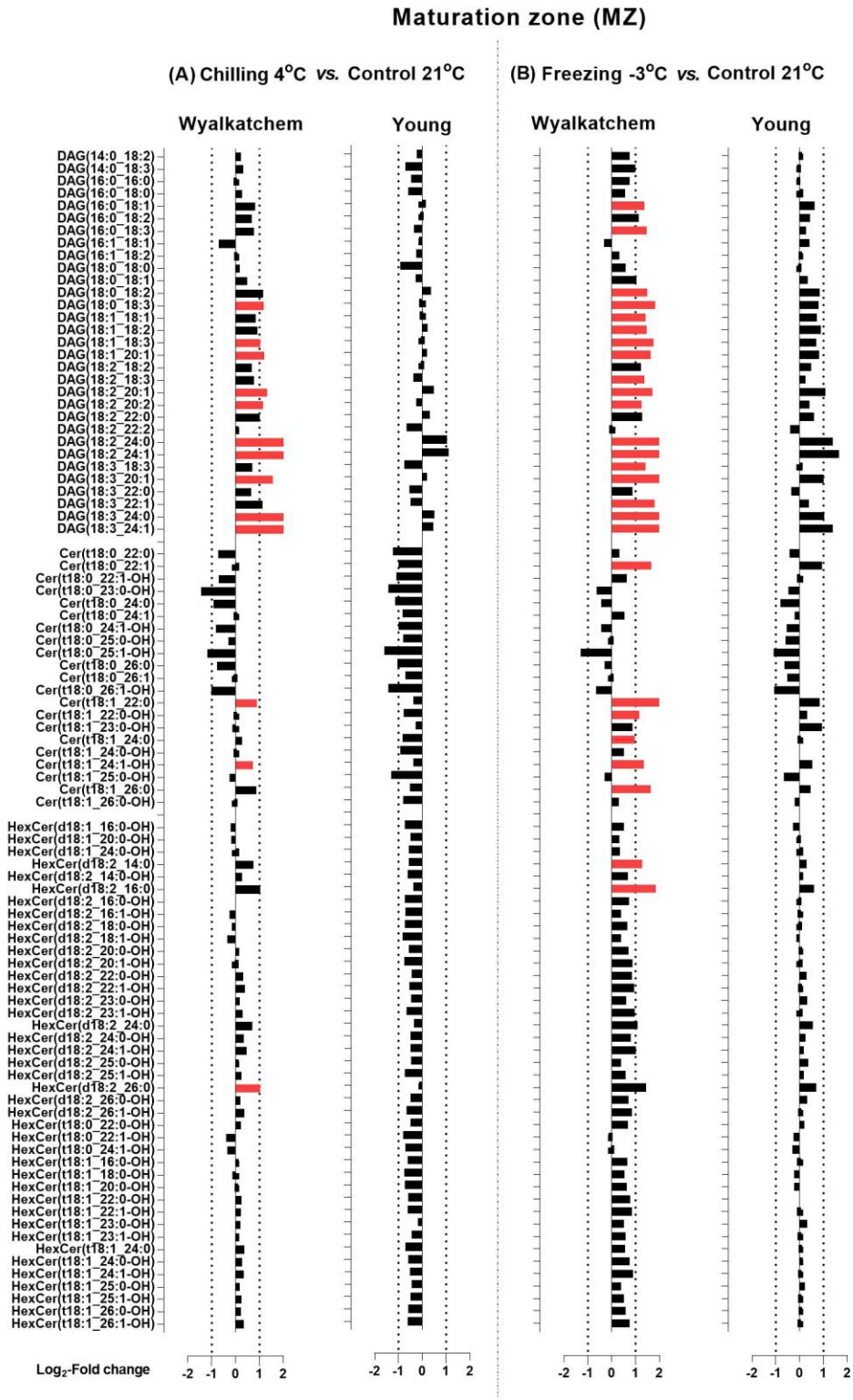


Figure 3-8. Log_2-fold changes of DAG, Cer and HexCer species in the maturation zone (MZ) of the cold-sensitive Wyalkatchem and cold-tolerant Young after exposed to **(A)** chilling and **(B)** freezing stresses. Statistical significance was determined using FDR-adjusted *p*-value of 0.05 as the cut-off. Green significant decrease, Red significant increase. n = 4.

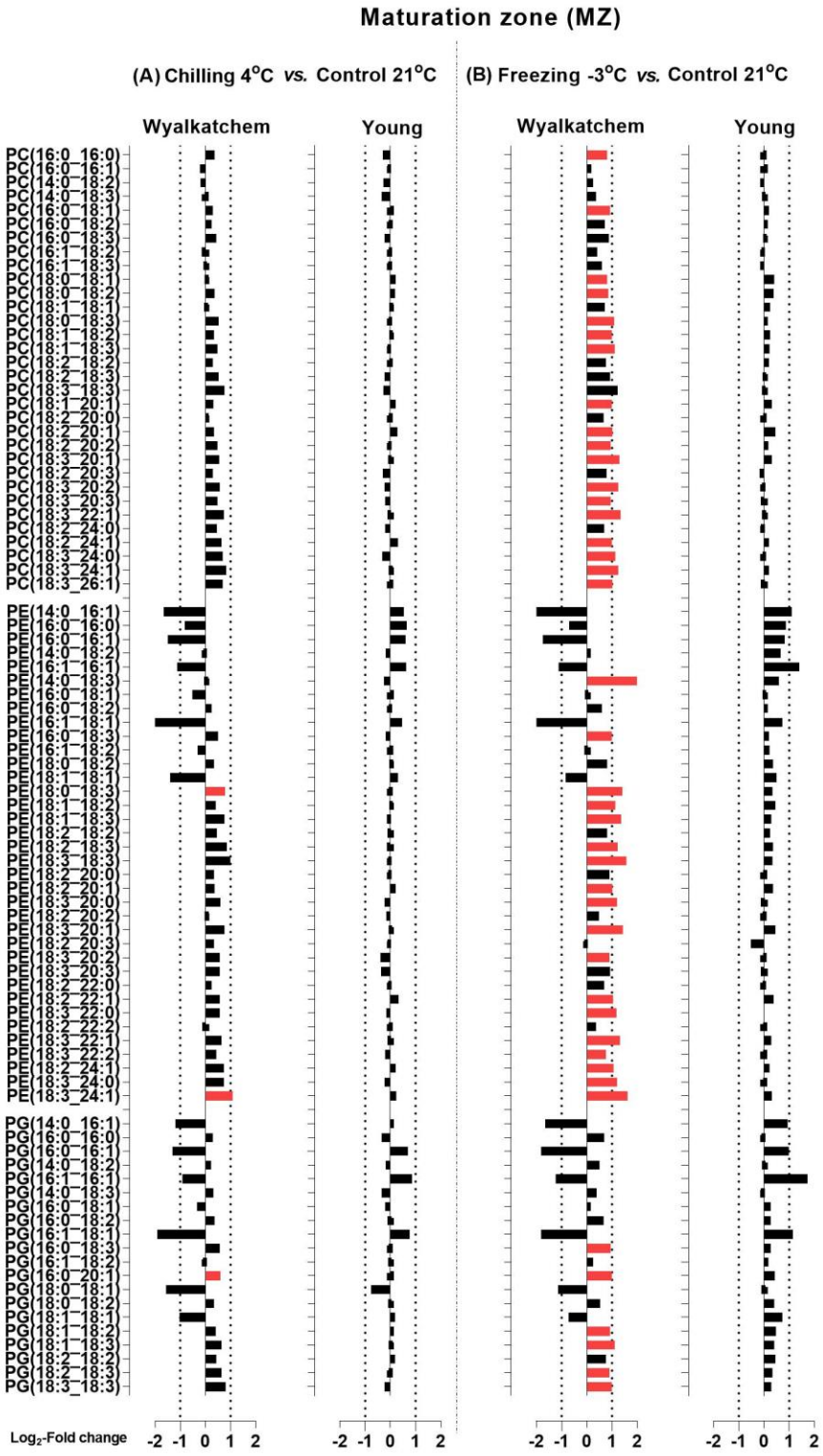


Figure 3-9. Log_2-fold changes of PC, PE and PG species in the maturation zone (MZ) of the cold-sensitive Wyalkatchem and cold-tolerant Young after exposed to **(A)** chilling and **(B)** freezing stresses. Statistical significance was determined using FDR-adjusted *p*-value of 0.05 as the cut-off. Green significant decrease, Red significant increase. n = 4.

3.3.4 Varietal Difference: Lipid Profiles of the Developmental Root Zones of Young and Wyalkatchem under Control, Chilling and Freezing Conditions

Besides of understanding the changes of lipid profiles in each of the root zone for each variety subjected to cold stress, it was also important to study the differences of lipid profiles between the cold-tolerant and cold-sensitive varieties in response to cold stress. Hence, the lipid profiles for each of the same root zone between cold-tolerant Young and cold-sensitive Wyalkatchem at the unstressed stage, after being subjected to chilling and freezing stresses were compared and summarized in **Table 3-2**. Overall, the main differences of lipid profiles for all the three developmental root zones between Wyalkatchem and Young were revealed by differences in phosphoglycerolipids such as lysophospholipids (lyso PC, lysoPE, lysoPG, lysoPS, lysoPI), PC, PE, PG, PI, PS and galactosyl glycerolipids such as DGDG, DGMG, MGDG, MGMG, SQDG and SQMG (**Table 3-2, Supplementary Table S3-1, Supplementary Fig. S3-2**). Lipid profiles of DAG, Cer and HexCer species also revealed differences between the two varieties, but were not as obvious compared to the phosphoglycerolipids and galactosyl glycerolipids (**Table 3-2, Table S3-1, Fig. S3-3**).

In the division zone (DZ), it was observed that the majority of the lysophospholipids, such as lysoPC, lysoPE, lysoPG, lysoPI and lysoPS species, were significantly higher in the cold-tolerant Young compared to cold-sensitive Wyalkatchem at the unstressed stage and after the cold exposures. Twenty-two out of a total of 25 lysophospholipids (phospholipids with single acyl chain in their structures) were higher in Young compared to Wyalkatchem at the unstressed stage, and the number increased to 23 and 25 (all species) after subjected to chilling and freezing stresses, respectively (**Table 3-2, Fig. S3-2, Table S3-1**). This phenomenon was opposite for the phospholipids with two acyl chains, in which the majority of the lipids were lower in Young compared to Wyalkatchem. For example, 11 of PC species were significantly lower in Young compared to Wyalkatchem at the unstressed stage, and the number increased to 24 and 26 after being subjected to chilling and freezing stresses, respectively (**Table 3-2**). The same was observed for PE, in which 16 species were significantly lower in Young compared to Wyalkatchem at the unstressed stage, and the number increased to 21 and 20 after being subjected to chilling and freezing stresses, respectively (**Table 3-2**). For other phospholipids such as PG, PI and PS, the majority of the species were also significantly lower in Young compared to Wyalkatchem (**Table 3-2**). For the galactosyl glycerolipid profiles, it was interesting to observe that the majority of the

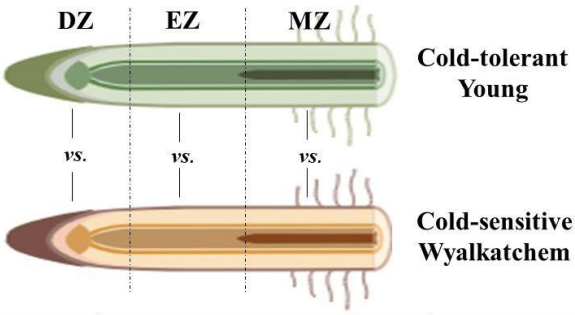
species that contained diacylglycerols in their structures such as DGDG (digalactosyl diacylglycerol), MGDG (monogalactosyl diacylglycerol) and SQDG (sulfoquinovosyl diacylglycerol) were significantly lower in Young compared to Wyalkatchem at the unstressed stage and after cold stress (**Table 3-2, Fig. S3-2**). Conversely, species that contained monoacylglycerol in their structures such as DGMG (digalactosyl monoacylglycerol), MGMG (monogalactosyl monoacylglycerol) and SQMG (sulfoquinovosyl monoacylglycerol) were significantly higher in Young compared to Wyalkatchem at the unstressed stage or after cold stress (**Table 3-2, Fig. S3-2**). For sphingolipids (Cer and HexCer) and sterols (ASG and SG), there were not many significant differences in this root zone between Young and Wyalkatchem. Only five Cer and four HexCer species were observed to be lower after being subjected to freezing stress in Young compared to Wyalkatchem (**Table 3-2, Fig. S3-3**). All the fold changes of the lipids that were significant different between Young and Wyalkatchem that have been mentioned here for DZ are listed in **Table S3-1**.

The patterns of phosphoglycerolipids and galactosyl lipids observed in the DZ were also found in the elongation zone (EZ). The majority of the lysophospholipids were significantly higher in Young compared to Wyalkatchem in this root zone (EZ) at the unstressed stage and after cold stress (**Table 3-2, Table S3-1, Fig. S3-2**). Meanwhile, the majority of the phospholipids (PC, PE, PG, PI and PS) were significantly lower in Young compared to Wyalkatchem at the unstressed stage and after cold stress. Interestingly, the numbers of PC and PE (two most abundant phospholipid classes in plant membranes) that were significantly lower in Young compared to Wyalkatchem were higher in this root zone compared to DZ (**Table 3-2**). Galactosyl glycerolipids such as DGDG, MGDG and SQDG were again lower in Young compared to Wyalkatchem in this root zone both in unstressed or cold-stressed conditions. Meanwhile, DGMG, MGMG and SQMG were again significantly higher in Young compared to Wyalkatchem in this root zone both in unstressed or cold-stressed conditions (**Table 3-2, Fig. S3-2**). It was interesting to observe significant differences of DAG, Cer and Hexcer species between the two varieties in this root zone, after being subjected to chilling stress. This phenomenon was not observed in the DZ. Twenty-one DAG, eight Cer and 15 HexCer were significantly lower in Young compared to Wyalkatchem after chilling stress. However, different from chilling stress, there were no significant differences of DAG, Cer and HexCer in this root zone (EZ) after the freezing stress (**Table 3-2, Fig. S3-3**).

All the fold changes of the lipids that significant different between Young and Wyalkatchem in EZ are listed in **Table S3-1**.

In the last developmental zone, which was the maturation zone (MZ), there were no significant differences of lysophospholipids between Young and Wyalkatchem at the unstressed stage. However, the majority of the lysophospholipids (PC, PE, PG, PI and PS) were significantly higher in Young compared to Wyalkatchem after exposure to chilling and freezing stresses (**Table 3-2, Table S3-2, Fig. S3-2**). There were also minor yet significant differences of phospholipids between the two varieties at the unstressed stage, in which only two PE and one PI species were significantly higher in Young compared to Wyalkatchem MZ tissue (**Table 3-2, Fig. S3-2**). However, after chilling and freezing stresses, the numbers of PC, PE and PG species that were significantly different between Young and Wyalkatchem increased. For example, 24 PC, 18 PE and 11 PG species were lower in Young compared to Wyalkatchem after chilling stress. Meanwhile, 24 PC, 15 PE and six PG species were lower in Young compared to Wyalkatchem after freezing stress (**Table 3-2, Fig. S3-2**). For the galactosyl glycerolipids, there were not many significant differences between the two varieties at the unstressed stage for this root zone as it was observed in the other two root zones. Only two DGMG species were significantly higher in Young compared to Wyalkatchem in MZ. However, after chilling and freezing stresses, DGDG, MGDG and SQDG were again lower (like in the other two root zones following cold stress) in Young compared to Wyalkatchem in MZ. Meanwhile, similar to other two root zones following freezing stress, DGMG, MGMG and SQMG were significantly higher in Young compared to Wyalkatchem in MZ (**Table 3-2, Fig. S3-2**). Also, similar to what was observed in following chilling stress, lipid species from the DAG, Cer and HexCer classes were significantly lower in Young compared to Wyalkatchem after cold stress (**Table 3-2, Fig. S3-3**). All the fold changes of the lipids that were significant different between Young and Wyalkatchem in MZ are listed in **Table S3-1**.

Table 3-2. Varietal Differences of the Lipid Profiles of Three Developmental Root Zones Under Control, Chilling and Freezing Conditions.

21 lipid classes (total number of lipid species per each class)									
	Division zone (DZ)			**Elongation zone (EZ)**			**Maturation zone (MZ)**		
	Control (21°C)	Chilling (4°)	Freezing (-3°)	Control (21°C)	Chilling (4°)	Freezing (-3°)	Control (21°C)	Chilling (4°)	Freezing (-3°)
LysoPC (9)	7↑	9↑	9↑	9↑	9↑	9↑	0	9↑	9↑
LysoPE (9)	8↑	9↑	9↑	8↑	9↑	9↑	0	9↑	9↑
LysoPG (4)	4↑	3↑	4↑	4↑	3↑	4↑	0	3↑	4↑
LysoPI (2)	2↑	1↑	2↑	2↑	1↑	2↑	0	1↑	2↑
LysoPS (1)	1↑	0	1↑	1↑	1↑	1↑	0	1↑	0
PC (32)	11↓	24↓	26↓	28↓	32↓	29↓	0	24↓	24↓
PE (36)	16↓ 2↑	21↓	20↓ 4↑	23↓ 1↑	25↓ 1↑	25↓ 3↑	2↑	18↓ 5↑	15↓ 6↑
PG (20)	16↓	17↓	15↓	16↓	17↓	14↓ 3↑	0	11↓ 2↑	6↓ 4↑
PI (12)	9↓ 1↑	10↓ 1↑	9↓ 1↑	9↓ 1↑	11↓ 1↑	11↓ 1↑	1↑	8↓ 1↑	8↓ 1↑
PS (5)	4↓	4↓	3↓	4↓	3↓	3↓	0	2↓	2↓
DGDG (12)	7↓	9↓	9↓	7↓	9↓	9↓	0	8↓ 1↑	8↓
DGMG (4)	4↑	3↑	3↑	4↑	3↑	3↑	2↑	3↑	4↑
MGDG (3)	2↓	1↓	1↓ 1↑	2↓	1↓	1↓ 1↑	0	1↓ 1↑	1↓ 1↑
MGMG (3)	2↑	1↓ 2↑	1↓ 2↑	2↑	1↓ 2↑	1↓ 2↑	0	1↓ 2↑	1↓ 2↑
SQDG (11)	5↓	8↓	10↓	12↓	12↓	12↓	0	11↓	9↓
SQMG (4)	4↑	4↑	4↑	4↑	3↑	4↑	0	3↑	3↑
DAG (31)	0	0	11↓	0	21↓	0	0	15↓	0
Cer (21)	0	0	5↓	0	8↓	0	0	5↓	0
HexCer (41)	1↓	0	4↓	0	15↓	0	0	5↓	0
ASG (10)	2↓	0	1↓	0	1↓	0	0	2↑	0
SG (3)	0	0	0	0	0	0	0	0	0

↑ significantly higher; ↓ significantly lower

3.4 Discussion

3.4.1 Lipid Composition at The Unstressed Stage Reveal Differences among The Three Developmental Root Zones in Each Wheat Variety

The root tip of a wheat seedling can be divided into three zones: a zone of cell division (DZ), a zone of elongation (EZ), and a zone of maturation or differentiation (MZ). The DZ is closest to the root tip and it is made up of actively dividing cells of the root meristem. The EZ is where the newly formed cells increase in length and thus lengthen the root (growth). Once the cells have reached their final size at the end of the EZ, they will enter the MZ, which is marked by the beginning of the first root hair where root cells begin to differentiate into special cell types (Somssich et al., 2016; https://courses.lumenlearning.com/ivytech-bio1-1/chapter/roots/). In the cold-sensitive Wyalkatchem and cold-tolerant Young, it was found that both the varieties shared similar patterns of lipid composition at the unstressed stage. phosphoglycerolipids such as PE, PG, PC and their lyso species occupied more than 50% of the total lipid composition in the DZ where cells are actively dividing. The percentage gradually decreased across the EZ and was the least for MZ among the three root zones. Conversely, sphingolipids such as HexCer and Cer were the least in DZ among the three root zones for both varieties, then gradually increased across EZ and became the biggest category of lipids in the MZ with more than 40% of total measured lipid (from 273 species) composition.

Phosphoglycerolipids, or more commonly known as phospholipids, are lipids containing two hydrophobic fatty acyl groups and a hydrophilic polar head group consisting a phosphate molecule attached to the glycerol backbone (**Fig. 3-10A**). Phospholipids that exist in plants are from the PC (phosphatidylcholine), PE (phosphatidylethanolamine), PG (phosphatidylglycerol), PI (phosphatidylinositol) and PS (phosphatidylserine) classes. Phospholipids are able to form a lipid bilayer due to their amphiphilic characteristic, thus they serve as the structural basis of cellular membranes. Among the five phospholipid classes, PC and PE are the two most abundant phospholipids that are present in plasma and extraplastidic membranes, while PG are most present in plastidic membranes (eg. thylakoid membranes) (Nakamura, 2017). The highest proportion of phospholipids found in the DZ compared to other two root zones may be due to the active cell division in this zone, in which large amounts of phospholipids are needed to build new plasma and endo-membranes of dividing cells.

In contrast to the prevalent glycerolipids that have glycerol in their structures, complex sphingolipids are composed of a sphingoid long-chain base (LCB, a kind of amino alcohol) having one amide-linked fatty acyl chain and a polar head group. The predominant sphingoid LCBs in plants are C18 amino alcohols, with the dihydroxy LCB sphinganine (d18:0; dihydrosphingosine) and the trihydroxy LCB 4-hydroxysphinganine (t18:0; phytosphingosine) are commonly found in plant tissues (**Fig. 3-10B**). The LCBs can be N-acylated with fatty acids to form ceramides (Cer) (**Fig. 3-10B**). The fatty-acyl chains of plant ceramides are predominantly α-hydroxy fatty acids varying in length from 16 to 26 carbons and are linked to the long-chain base by an amide bond. Ceramides can serve as precursors to more complex sphingolipids such as the monohexosyl ceramide (HexCer) and derivatives of inositolphosphorylceramide (IPC) in higher plants (Lynch 1993; Warnecke and Heinz, 2003; Lynch and Dunn, 2004; Lester and Dickson, 1993). They can also act as signal molecules in plants (Liang et al., 2003). Glucosylceramide (GlcCer) are the common HexCer found in plants, and the polar head group (glucose) is linked to C-1 of the N-acyl LCB (**Fig. 3-10B**). GlcCer are components of the plasma membrane and the tonoplast of plant cells (Merrill & Sweeley, 1996; Michaelson et al., 2016), and are thought to increase membrane stability, decrease membrane permeability, regulate ion permeability as a consequence of the associated very long (> C20) hydroxyl fatty-acyl chain and the intra- and intermolecular hydrogen bonding between amide and hydroxyl groups of the ceramide moiety (Boggs, 1987; Curatolo, 1987). Besides, the increased hydroxylation of the sphingolipid molecules has also been reported to be associated with increased stability and decreased permeability of membranes (Karlsson, 1982). Heavily hydroxylated species of GlcCer present in many plant tissues may contribute to the overall integrity of the plasma membrane and tonoplast, the two membranes most enriched in sphingolipids. These two membranes have critical and variable functions as barriers (Lynch and Dunn, 2004). Steponkus 1984 also reported the involvement of sphingolipids to regulate ion permeability and osmotic adaptation of cells to freezing and water deficit. Besides, ceramide and long-chain base metabolites have also been shown to regulate cellular processes including programmed cell death and G protein-mediated guard cell closure (Coursol et al., 2003, 2005). In this study, it was found that the proportion of sphingolipids (HexCer and Cer) was the highest in the MZ of both varieties. In MZ, cells differentiate for various important specialized functions, eg. some cells of the pericycle form lateral roots, epidermal cells may form root hairs, and the Casparian strip will develop between cells of the endodermis (Schiefelbein and Benfey, 1991).

The stability and integrity of those membranes in MZ hence need to have a different lipid composition and the high proportion of sphingolipids which function to regulate membrane permeability and overall integrity of the plasma membrane and tonoplast may be related to this.

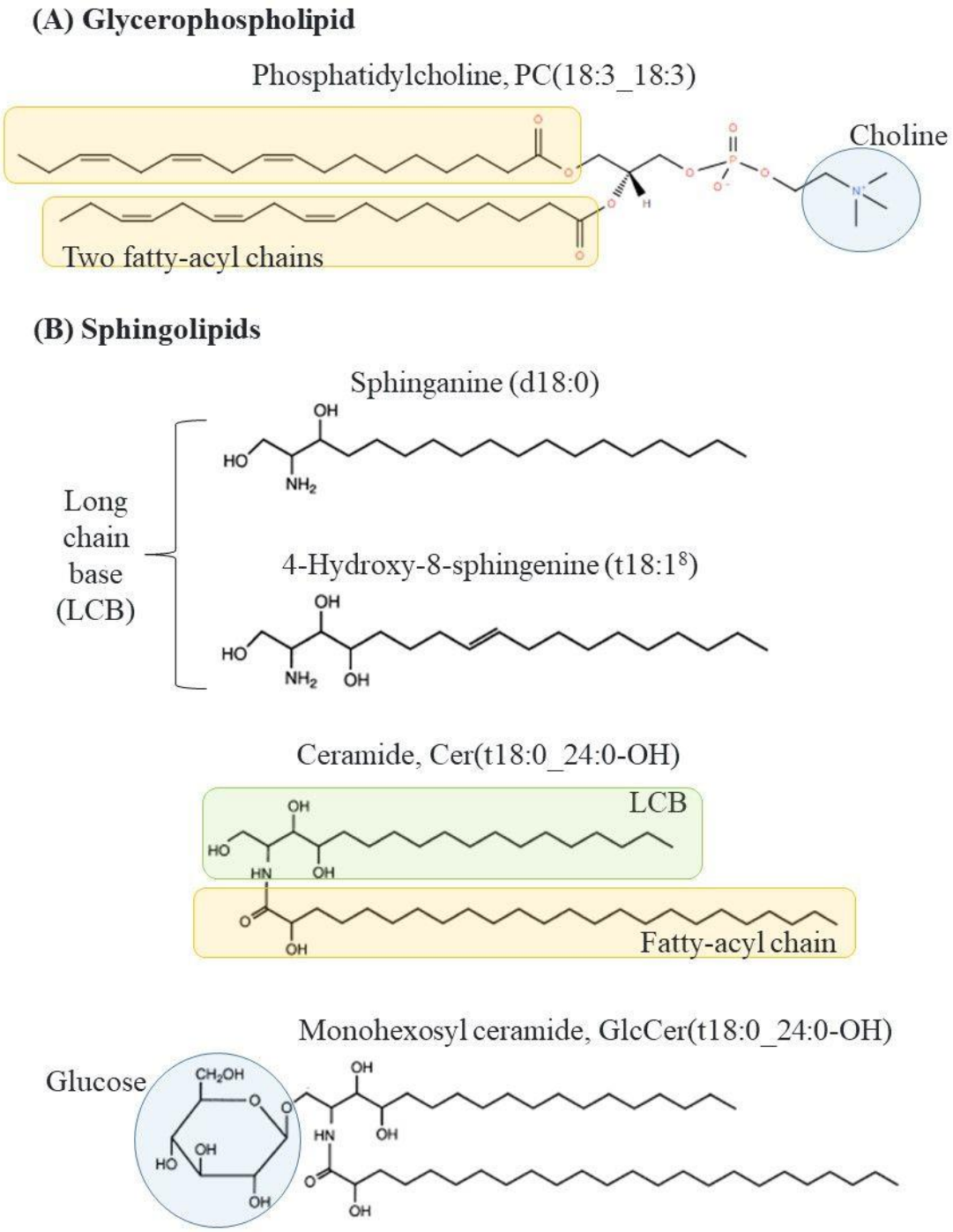


Figure 3-10. Examples of **(A)** phosphoglycerolipids and **(B)** sphingolipids analysed in this study. The figure is prepared based on the lipid structures taken from LIPIDMAPS (https://www.lipidmaps.org/), and Lynch and Dunn, 2004.

3.4.2 Cold Stress Mainly Alters the Glycerolipid and Sphingolipid Compositions of the Root Zones, which Also Reveals the Main Differences between the Cold-Sensitive and Cold-Tolerant Varieties

After the wheat seedlings were subjected to six hours of chilling (4°C) and freezing (-3°C), it was interesting to observe the increase of phospholipids in every root zone for both the wheat varieties. Uemura et al. (1995a & b) reported that when plants are exposed to low and non-freezing temperatures, the degree of fatty acid unsaturation and the content of phospholipids typically increase. These lipid changes are important to enhance membrane fluidity and reduce the propensity of cellular membranes to undergo freezing induced non-bilayer phase formation, thus maintaining the membrane integrity upon cold stress. Therefore, the increase of phospholipids in the three root zones of Wyalkatchem and Young subjected to chilling and freezing stress may indicate the involvement of these lipids in lipid remodeling of the root membranes to maintain the fluidity in cold condition. When comparing the phospholipids between the two wheat varieties, it was observed that phospholipids in Wyalkatchem were higher compared to Young subjected to chilling and freezing in this study (Fig. S3-2). This suggests that cold stress may have stronger effects on the membrane stability in the sensitive variety compared to the tolerant variety. It is therefore worth to further analyse and compare the degree of desaturation of the phospholipids (via unsaturation to saturation ratio) of the two varieties in the future.

Welti et al. (2007) also reported that cold exposure induces significant increases in specific lysoPC, lysoPE, and phosphatidic acid (PA) species. Lysophospholipids and PA are produced by enzymes phospholipase A and phospholipase D, which are activated during cold acclimation. Lysophospholipids and PA are minor phospholipids with potential regulatory functions, such as activation of target signaling proteins, regulation of cytoskeletal organization, and regulation of ion channel function. They may play both structural and regulatory roles in plant adaptation and survival during low temperature exposure (Wang et al., 2006). In this study, PA was not detected thus the results could not be inferred here. However, lysophospholipids such as lysoPC, lysoPE, lysoPG, lysoPI and lysoPS were measured in this study and observed to increase only in the EZ of both Wyalkatchem and Young upon freezing stress (Table S1). This may indicate the involvement of lysophospholipids for the adaptation and survival of the elongating tissues of wheat roots during freezing condition. Meanwhile, Young has shown higher amounts of lysophospholipids compared to Wyalkatchem in all the three root zones in all three conditions. The higher amounts of

lysophospholipids in Young compared to Wyalkatchem may indicate the potential of these lipid classes to have regulatory roles and thus confer greater cold tolerance in Young and its ability to adapt and survive in cold condition.

Cold stress also caused the significant increase of several DAG species in the DZ but had lesser effects on the EZ of both the varieties. The effects were greatest on the MZ of Wyalkatchem (highest numbers of significant increased lipids) but not on the MZ of Young. The accumulation of DAG under low temperature stress has been reported to may be due to two main mechanisms: (1) Involvement as lipid signaling molecules and (2) induced during freezing injury on the membrane (leakage). For (1), both Xiong et al. (2002) and Arisz et al. (2013) reported that under freezing condition, a fast induction of PA occurs through the phosphorylation of phosphoinositide (PtdIns) of the membrane to phosphatidylinositol 4,5-biphosphate, which is then further hydrolyzed by phospholipase C into the second messengers inositol 1,4,5-triphosphate (Ins(1,4,5)-P3) and DAG. The latter is then converted to PA by the action of diacylglycerol-kinases (DGK). For (2), Moellering et al. (2010) and Lu et al. (2020) reported that cellular dehydration increases the concentration of Mg^{2+} and cellular acidity during freezing stress. Mg^{2+} and protons are then transported into the chloroplast outer envelope membrane which activates the function of SENSITIVE TO FREEZING2 protein (SFR2). SFR2 then converts MGDG into oligogalactolipids and DAG. Oligogalactolipids are important to enhance membrane stability, whereas DAG reduces stability. The reason why the accumulation of DAG is adverse for the membrane is because it can be converted to PA via DGK enzyme. PA can bind and activate the enzyme NADPH oxidase (RbohD) and subsequently increases the production of reactive oxygen species (ROS) (Zhang et al., 2009). ROS can play a role as signal transduction molecules during stress response when the amount is low, but they are harmful when present excessively, leading to the oxidation of membrane lipids, and other molecules (Baxter, 2014). PA can also induce the formation of an unstable hexagonal II (H_{II})-type lipid phase with DAG or MGDG, which destabilizes the cell membrane (Webb and Green, 1991; Moellering et al., 2010; Barnes et al., 2016). To avoid the adverse effects brought by the excessive accumulation of DAG and PA, an enzyme called the diacylglycerol transferase (DGAT) converts DAG to TAG instead of PA. Evidence has shown that plants that better withstand freezing stress show an up-regulation of DGAT activity and accumulation of TAG upon cold stress (Arisz et al., 2018; Tan et al., 2018). Higher accumulation of DAG in Wyalkatchem's roots compared to Young's roots upon cold stress may cause the

molecules to be converted to PA via diacylglycerol kinase leading to lipid oxidation and damage of the membranes in this variety. Arisz et al. (2018) reported that plants that better withstand freezing stress show up-regulation of DGAT activity and accumulation of TAG upon cold stress. The lower amount of DAG in Young compared to Wyalkatchem upon cold stress may have relation with this enzyme and TAG content. Hence, the DGAT activity and TAG lipid profiles of both wheat varieties upon cold stress are worth being studied in the future to increase our understanding of these mechanisms. A thorough investigation of the effects on lipid oxidation will also be useful to conclude the interactions of PA, DAG and ROS.

In contrast to phosphoglycerolipids and DAG that were induced upon cold stress, decreases of sphingolipids (Cer and HexCer) in each of the root zone for both the wheat varieties were observed. Decreases in the proportion of GlcCer (glucosylceramide, a kind of HexCer) in plants subjected to low temperature stress and during the cold acclimation to acquire freezing tolerance has been reported. The proportion of GlcCer in plasma membranes of freezing-tolerant plants is reported to be lower than in freezing-sensitive plants (Lynch & Steponkus, 1987; Uemura & Steponkus, 1994; Uemura et al., 1995). The reduction of GlcCer composition during cold stress alters the membrane behavior during osmotic excursions and prevents dehydration-induced demixing of membrane lipid components (Steponkus et al., 1988; Steponkus et al.,1990). It has also been reported that trihydroxy-LCB having a cis double bond at the Δ8 position (eg. t18:1^{8}) are more prevalent in chilling resistant and freezing tolerant plants (Imai et al., 1997, Kawaguchi et al., 2000). Imai et. al (1995, 1997) and Imai (1998) also reported that monounsaturated hydroxy fatty acyl chains (especially h24:1, means a fatty acid chain with 24 carbons number, one double bond, and one hydroxyl group attached to one of the carbon which usually is carbon number two) are common in freezing-tolerant plants, whereas sensitive plants contain exclusively saturated hydroxy fatty-acyl chains (Imai et al., 1995; Imai, 1998). In this study, the decrease of HexCer (i.e. GlcCer) was observed in the three root zones of the cold-tolerant Young but not cold-sensitive Wyalkatchem upon cold stress, where the majority of the significant decreases occurred in the DZ. The lower amounts of HexCer in Young compared to Wyalkatchem upon cold stress may be one of the factors contributing to the cold tolerance of Young. This is one of the interesting findings in this study and a more in-depth study of this class of lipids such as how lipids are involved in remodeling the membranes in wheat upon cold stress is worth to be performed in future.

Wyalkatchem also showed different profiles for galactosyl glycerolipids compared to Young. All the galactosyl glycerolipids that have diacylglycerol in their structures such as DGDG, MGDG and SQDG are higher in Wyalkatchem compared to Young in all the three root zones at unstressed and cold stress conditions (Fig. S3-2). Conversely, all the galactosyl glycerolipids that have monoacylglycerol in their structures such as DGMG, MGMG and SQMG are higher in Young compared to Wyalkatchem (Fig. S3-2). Galactosyl glycerolipids are mainly abundant in the thylakoid membranes of plastids where 50% is MGDG, 26% is DGDG, and the remaining are sulfoquinovosyldiacylglycerol lipids (SQDG) and phosphatidylglycerol lipids (PGs) (Dormann et al., 2013). DGMG, MGMG and SQMG are scarce in the thylakoid membranes and are believed to be the hydrolysis products of DGDG, MGDG, and SQDG, respectively. For example, MGDG are synthesized in plants by galactosylation of DAG in the plastid envelope (Douce and Joyard, 1980). MGMG on the contrary have been thought to be principally formed by lipase hydrolysis of MGDG (McCarty and Jagendorf, 1965). The observation of higher MGMG, DGMG and SQMG in Young compared to Wyalkatchem is interesting. However, there is still lack of literature about the roles of those galactosyl monoacylglycerol lipids in plant cold stress response until today, especially in roots whose plastids are not fully developed as in leaves. More focus is paid to galactosyl diacylglycerol lipids in leaves (MGDG and DGDG) in plant cold stress response (Moellering et al., 2010; Moellering and Benning, 2011; Dormann 2013; Holzl and Dormann, 2019). Moellering et al. (2010) has reported that MGDG favours the formation of non-bilayer H_{II}-type structures brought by dehydration during freezing stress. The non-bilayer structures are formed at the interface of apposed membranes and are believed to initiate at the chloroplast envelope membranes during freezing, thus resulting in fusion between bilayers and damage the membranes. The authors also pointed to the importance of a protein called SENSITIVE TO FREEZING2 (SFR2) that converts MGDG into DGDG, oligogalactolipids and DAG during low temperature stress to reduce the formation of non-bilayer H_{II}-type structures (Moellering et al. 2010). The ratio of MGDG to DGDG has therefore been studied in plant cold stress response, however with a focus on leaf tissues. Besides, the potential for the formation of MGMG and DGMG in plants during stress via the acylation of (1) two MGDGs to acylated MGDG and MGMG, or (2) one MGDG plus DGDG to become acylated MGDG and DGMG has been reported (Vu et al., 2013). The observation of increase of MGMG and DGMG with decrease of MGDG and DGDG during chilling and freezing stresses of the two wheat cultivars in this study could be associated with the acylation response

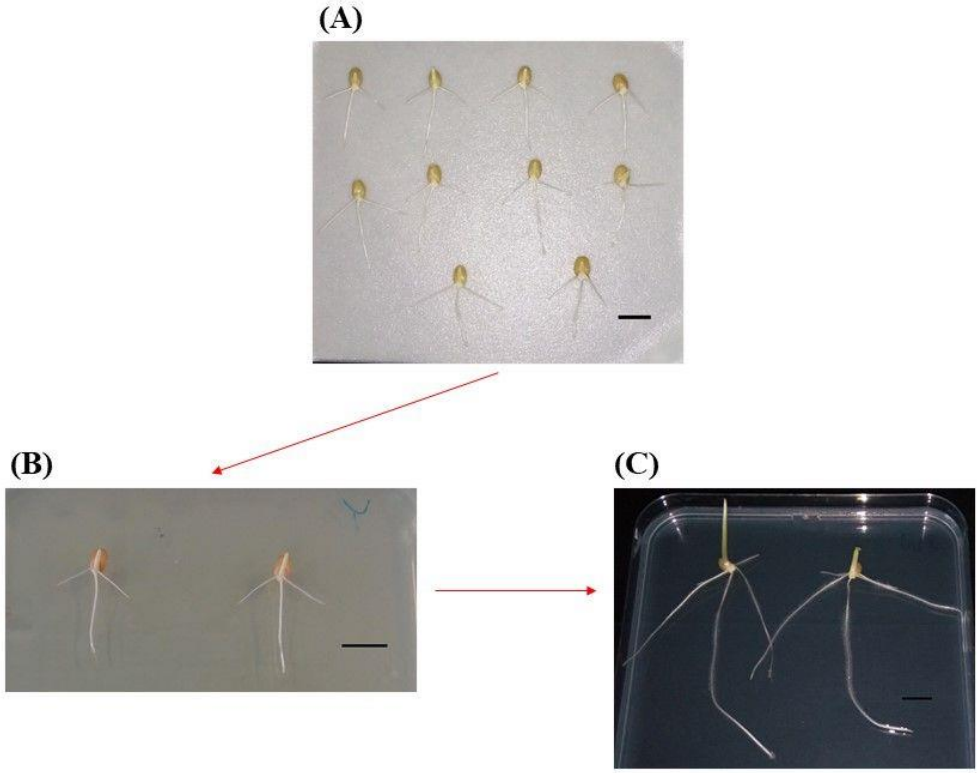
during cold stress. A further analysis of this phenomenon needs to be explored to conclude on potential differences in these mechanisms in Wyalkatchem and Young.

3.5 Conclusion

Using the modified lipidomics approach from Yu et al. (2018, 2020), a complex lipidome analysis of the developmental root zones of two wheat varieties with contrasting cold tolerance have been conducted in this study. A total of 273 lipid species derived from 21 lipid classes and three categories of lipids has been analysed. Chilling and freezing have effects mainly on the composition of phosphoglycerolipids, glycerolipids and sphingolipids composition in the root zones reveal main differences between the cold-sensitive Wyalkatchem and cold-tolerance varieties. Together with the outcomes gained from the studies of flag leaves and spikes in Chapter 2, the outcomes gained from this study (root) may help us to better understand the mechanisms of wheat in response to cold, thus contributing to wheat breeding program for the improvement of more cold-tolerant varieties in the future.

3.6 Supplemental Figures

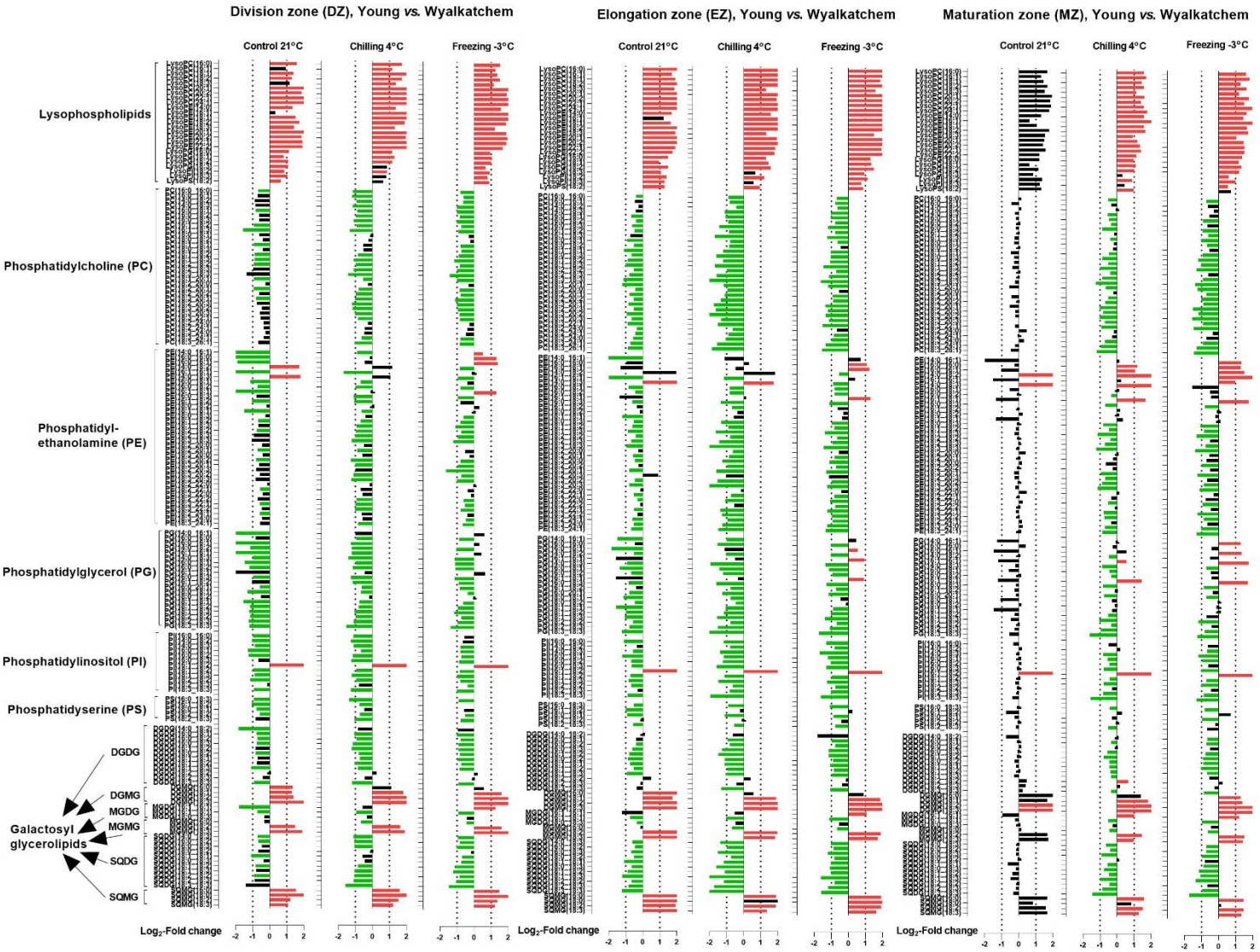
Supplemental Figures S3-1 to S3-3 are shown in this section, while the information for Supplemental Tables S3-1 can be found in the **Appendices**, **Appendix B: Supplemental Information for Chapter 3 (page 302).**



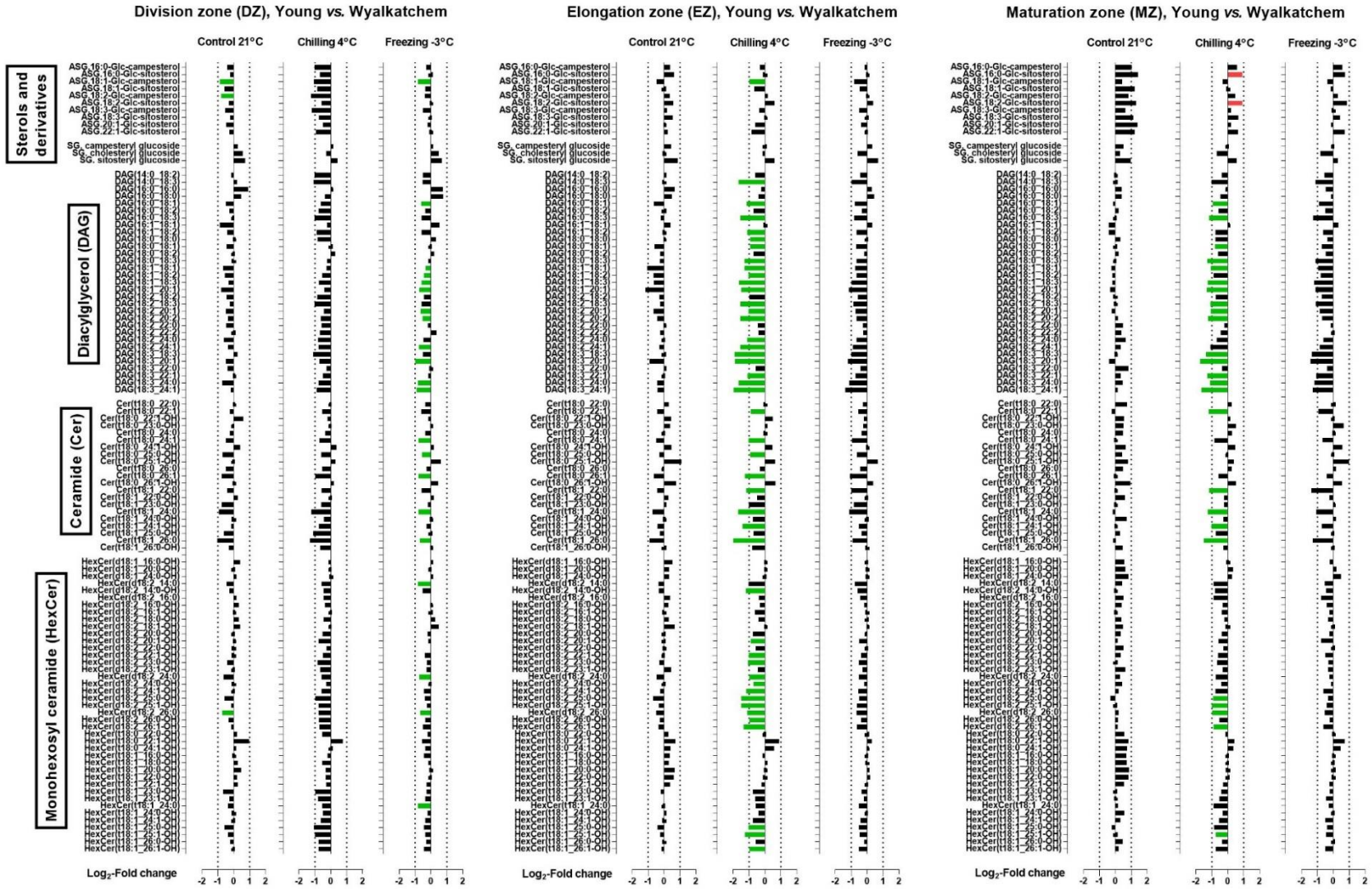
(D)

20 plates, the germinated seedlings	Date and time to put the plates into the 21°C chamber for 48 hrs of growth	Date and time to put into the cold chamber (eg. 4°C) for 6 hrs of treatment	Date and time to take out the plate from the cold chamber for root sectioning	The three root zones were immediately snap frozen with liquid nitrogen after sectioning.
Plate no. 1 and 2	Day 1, 8 am	Day 3, 8 am	Day 3, 2 pm	
Plate no. 3 and 4	Day 1, 8:10 am	Day 3, 8:10 am	Day 3, 2:10 pm	
Plate no. 5 and 6	Day 1, 8:20 am	Day 3, 8:20 am	Day 3, 2:20 pm	
Plate no. 7 and 8	Day 1, 8:30 am	Day 3, 8:30 am	Day 3, 2:30 pm	
Plate no. 9 and 10	Day 1, 8:40 am	Day 3, 8:40 am	Day 3, 2:40 pm	
Plate no. 11 and 12	Day 1, 8:50 am	Day 3, 8:50 am	Day 3, 2:50 pm	
Plate no. 13 and 14	Day 1, 9 am	Day 3, 9 am	Day 3, 3 pm	
Plate no. 15 and 16	Day 1, 9:10 am	Day 3, 9:10 am	Day 3, 3:10 pm	
Plate no. 17 and 18	Day 1, 9:20 am	Day 3, 9:20 am	Day 3, 3:20 pm	
Plate no. 19 and 20	Day 1, 9:30 am	Day 3, 9:30 am	Day 3, 3:30 pm	

Supplemental Fig. S3-1. Plant materials and growth conditions for the two wheat varieties used in this study. **(A)** Seeds were germinated on wetted filter paper in dark for 48 hrs at 21°. **(B)** Uniform germinated seedlings with the longest seminal root between 1.5 and 2.0 cm were selected and transferred to square petri dishes containing nutrient agar medium with modified Hoaglands nutrient solution. **(C)** Two seedlings were placed per plate and allowed to grow with the radical orientated downwards by placing the dishes at a 45° angle for another 48 hrs at 21°C in the dark. A biological replicate (n) was the pooled of roots from 20 plates (2 seedlings per plate x 20 plates = 40 seedlings). Only one biological replicate could be harvested or prepared per day. To ensure the cold-treated roots were still cold during the cutting into three root zones, the cold treatment and harvest of roots have to be done in a schedule/cycle as shown in (D). **(D)** A table listing an example of a harvesting schedule/cycle for one biological replicate (20 plates). Bars represent 1 cm.



Supplemental Fig. S3-2. Varietal differences of phosphoglycerolipids and galactosyl glycerolipids of the three developmental root zones at the control and after cold stress conditions.



Supplemental Fig. S3-3. Varietal differences of sterols, diacylglycerols (DAG) and sphingolipids (Cer and HexCer) of the three developmental root zones at the control and after cold stress conditions.

CHAPTER 4

Systemic Analysis of REIL Protein Function in Cold Acclimated *Arabidopsis thaliana* Roots

Preface to Chapter 4

The work presented in this chapter describes the systematic analysis of REIL protein functions in cold acclimated *Arabidopsis thaliana* roots. REIL proteins have been previously reported to be involved in late ribosomal biogenesis and to affect accumulation of 60S large subunits in *Arabidopsis thaliana* mature leaves and seedlings upon acclimation to low temperature. REIL proteins are therefore speculated to act as one of the cold acclimation factors in Arabidopsis plants. In order to validate these roles and discover more novel functions of REIL proteins in Arabidopsis, a comprehensive system analysis was conducted using the roots targeted at understanding the mechanism of late ribosome biogenesis, in which REIL proteins are involved. The results of this work are described and discussed in detailed in the following section. A manuscript reporting the outcomes from this chapter with title of "Arabidopsis REI-LIKE proteins activate ribosome biogenesis during cold acclimation" has been prepared and will be submitted to the journal *Scientific Reports* for consideration of publication. Therefore, this chapter is presented in form of publication-in-progress. I claim that I have contributed more than 70% of the experimental work of this chapter, including the laboratory experiments (plant growth, cold treatment, harvest, ribosomal profiling, transcript profiling), data processing, analysis and interpretation. I also have contributed more than 70% of the writing of this manuscript which has been proof-read and corrected by all other co-authors.

The manuscript presented in this chapter has been prepared and posted to bioRxiv (https://www.biorxiv.org/) with accession number 954396 and can also be accessed using doi: https://doi.org/10.1101/2020.02.18.954396. This manuscript has been submitted to the journal *Scientific Reports* for consideration of publication. This work is presented as publication-in-progress format in this chapter.

Title

Arabidopsis REI-LIKE Proteins Activate Ribosome Biogenesis during Cold Acclimation

Author Names and Affiliations

Bo Eng Cheong[a], Olga Beine-Golovchuk[b,c], Michal Gorka[b], William Wing Ho Ho[a], Federico Martinez-Seidel[a,b], Alexandre Augusto Pereira Firmino[b], Aleksandra Skirycz[b], Ute Roessner[a], Joachim Kopka[b, *]

a: School of BioSciences, The University of Melbourne, Victoria 3010, Australia

b: Max-Planck-Institute of Molecular Plant Physiology, Am Mühlenberg 1, D-14476 Potsdam-Golm, Germany

c: Heidelberg University, Biochemie-Zentrum, Nuclear Pore Complex and Ribosome Assembly, Im Neuenheimer Feld 328, 69120 Heidelberg, Germany

E-mail Address for Each Author

Bo Eng Cheong: cheongb@student.unimelb.edu.au

Olga Beine-Golovchuk: Beine@mpimp-golm.mpg.de; olga.beine@bzh.uni-heidelberg.de

Michal Gorka: Gorka@mpimp-golm.mpg.de, michal.gorka.ofc@gmail.com>

William Wing Ho Ho: whho@unimelb.edu.au

Federico Martinez-Seidel: MSeidel@mpimp-golm.mpg.de

Alexandre Augusto Pereira Firmino: Firmino@mpimp-golm.mpg.de

Aleksandra Skirycz: Skirycz@mpimp-golm.mpg.de

Ute Roessner: u.roessner@unimelb.edu.au

Joachim Kopka: Kopka@mpimp-golm.mpg.de

***Corresponding Author Details**

Joachim Kopka, Tel: +49 331 567 8262

4.1 Abstract

Arabidopsis REIL proteins are ribosomal 60S-biogenesis factors in cytosol. After shifting to 10°C, *reil* mutants deplete and slowly replenish non-translating eukaryotic ribosome complexes of root tissue, while tightly controlling the balance of non-translating 40S- and 60S-subunits. *Reil* mutations are compensated by hyper-accumulation of non-translating subunits at steady-state temperature; after cold-shift, a KCl-sensitive 80S sub-fraction remains depleted. We infer that the pre-existing non-translating ribosomes in Arabidopsis buffers the fluctuating translation before the temperature-induced demands were met by the *de novo* synthesis. *Reil1 reil2* double mutants accumulate 43S-preinitiation and pre-60S-maturation complexes and have altered paralog composition of ribosomal proteins in non-translating complexes. With few exceptions (e.g. RPL3B and RPL24C), these changes are not under transcriptional control. Our study suggests the requirement of *de novo* synthesis of specialized eukaryotic ribosomes for long-term cold acclimation, feedback control of *NUC2* and *eIF3C2* transcription, and links new proteins (AT1G03250 and AT5G60530) to plant ribosome biogenesis. In conclusion, REIL proteins are confirmed to act as cold acclimation factor in Arabidopsis in which they are required for ribosomal biogenesis and also involved in the translational machinery during cold acclimation.

Key words (6-10, in alphabetical order)

abiotic stress, Arabidopsis, cold acclimation, proteomics, REI-LIKE proteins, ribosome biogenesis, roots, system analysis, transcriptomics

4.2 Introduction

The *Arabidopsis thaliana* Col-0 (Arabidopsis) REI1-LIKE (REIL) proteins, REIL1 (At4g31420) and REIL2 (At2g24500) are homologs of the yeast Rei1 (YBR267W) and the paralog Reh1 (YLR387C) proteins. In yeast, both the Rei1 and Reh1 proteins function as ribosome biogenesis factors that participate either in parallel or sequentially in the late ribosome biogenesis step of cytoplasmic 60S ribosomal subunit maturation (Greber et al., 2012; Greber et al., 2016). Aside from this function, these proteins are required to maintain growth at suboptimal or cold temperatures. The *Δrei1* mutant is cold sensitive already at moderately suboptimal temperatures of yeast. The *Δrei1 Δreh1* double mutant is even more cold sensitive, while the yeast Δreh1 mutation alone has no effect on growth in the cold (Iwase and Toh-e, 2004; Lebreton et al., 2006; Parnell and Bass, 2009). Heterologous expression of Arabidopsis REIL1, but not of REIL2 partly complements the cold sensitivity of the yeast *Δrei1* mutant (Schmidt et al., 2013). The Arabidopsis REIL paralogs differ in structure from their yeast homologs. REIL1 and REIL2 are four zinc finger proteins with C2H2 zinc finger domains arranged in two pairs, namely ZF1/ZF2 at the N-terminus and ZF3/ZF4 in the middle of the primary structure (Schmidt et al., 2013). In contrast, both yeast paralogs contain only three canonical zinc fingers (Iwase and Toh-e, 2004; Greber et al., 2012). This observation is in line with a preliminary phylogenic study (Schmidt et al., 2013), as both analyses indicate that the duplications of the yeast and Arabidopsis REIL paralogs are evolutionary independent (Schmidt et al., 2013).

Intriguingly, transfer-DNA (T-DNA) mutants of the Arabidopsis *REIL1* and *REIL2* genes, *reil1-1*, and allelic *reil2-1* or *reil2-2*, and the yeast *Δrei1* and *Δreh1* mutants have convergent growth responses at suboptimal temperature (Schmidt et al., 2013; Schmidt et al., 2014). Arabidopsis REIL paralogs are required specifically for plants to grow in the cold, e.g. at 4°C or at 10°C, but not for growth at optimized 20°C temperature (Schmidt et al., 2013; Beine-Golovchuk et al., 2018). In agreement with these findings, identical T-DNA insertion mutants of *reil2* were recently discovered in a screen for chilling sensitive Arabidopsis mutants (Yu et al. 2020), namely *reil2.1/ stch4-2* (GK_166C10) and *reil2.2/ stch4-1* (SALK_040068). The *reil1-1 reil2-1* double mutant has a more severe cold phenotype and all but stops development after germination at 10°C prior to the emergence of the first rosette leaf (Schmidt et al., 2013; Beine-Golovchuk et al., 2018). The double mutation is, however, non-lethal and a valid system for the investigation of REIL functions in plants. The double mutant maintains cellular integrity and acquires freezing tolerance

after shifts from 20°C to 4°C or 10°C cold (Beine-Golovchuk et al., 2018). Expression of amino terminal FLUORESCENT PROTEIN (FP)-REIL fusion proteins driven by the UBIQUITIN10 promoter rescue the mutant phenotypes (Beine-Golovchuk et al., 2018). The two allelic *reil2-1* and *reil2-2* mutants are both growth retarded and form small spoon-shaped leaves at 10°C (Schmidt et al., 2013; Yu et al., 2020). This phenomenon reverted after shift from cold to optimal 20°C. Except for slightly delayed germination, the *reil1-1* mutant, similar to yeast *Δreh1*, has no growth phenotype under the tested low temperature conditions (Schmidt et al., 2013; Beine-Golovchuk et al., 2018).

Previous functional analyses of Arabidopsis REIL proteins focused on vegetative photoautotrophic plant rosettes that were cultivated on soil and acclimated to 10°C temperature. Conserved functions of the Arabidopsis REIL proteins and new functions that evolved on the path towards multicellular embryophyte plants became apparent (Beine-Golovchuk et al., 2018). As was expected in analogy to yeast, FP-REIL1 and FP-REIL2 fusion proteins localize to the cytosol (Beine-Golovchuk et al., 2018; Yu et al., 2020) and the REIL1 protein appears to interact with ribosome complexes containing the 60S large ribosome subunit (LSU). Based on immunoprecipitation-mass spectrometry, REIL2 associates with the eukaryotic ribosome (Yu et al., 2020). Our current study locates REIL2 to the non-translating 60S fraction of Col-0 wild type. In rosette leaves, REIL proteins accelerate 10°C cold induced accumulation of cytosolic ribosome subunits and of cytosolic ribosomal RNA (rRNA). After cold shift, they enhance gene expression of structural proteins of cytosolic ribosomes, ribosome biogenesis factors, and cytosolic translation initiation or elongation factors (Beine-Golovchuk et al., 2018). The acclimation responses occur within the first week after cold shift, while Arabidopsis wild type plants pass through a lag-phase before resuming growth. All of these processes lag behind in the *reil1-1 reil2-1* mutant that does not resume growth in the cold (Schmidt et al., 2013). Our current study confirms these observations in roots and provides mechanistic insights far beyond.

Besides an influence on cold-induced plant ribosome remodeling and on the accumulation of cytosolic ribosome subunits after cold shift, Arabidopsis REIL proteins are apparently involved in plant-specific processes. For example, the *reil1-1 reil2-1* mutant does not activate FLOWERING LOCUS T gene expression in mature leaves after the cold shift and exhibits plant cold-acclimation responses at the 20°C non acclimated state, including premature activation of the C-REPEAT/DRE BINDING FACTOR1/ DEHYDRATION-RESPONSIVE ELEMENT

BINDING (CBF/ DREB) regulon (Beine-Golovchuk et al., 2018). Analyses of the single paralog *reil2/ stch4* mutants confirmed the interaction of *reil2* function with the CBF/ DREB regulon, e.g. (Cook et al., 2004; Maruyama et al., 2004; Van Buskirk and Thomashow 2006), with REIL2 deficiency delaying CBF/ DREB regulon activation and reducing CBF/ DREB protein accumulation in the cold. Ectopic overexpression of REIL2 under control of the 35S promoter conveyed enhanced chilling and freezing tolerance under mixotrophic *in vitro* conditions, i.e. in the presence half-strength Murashige and Skoog (MS) medium (Yu et al., 2020).

To reveal organ-independent and likely direct or primary functions of Arabidopsis REIL proteins from more indirectly associated responses to REIL deficiency, we analyzed the root system of Arabidopsis Col-0 wild type and of reil mutant plants under 20°C to 10°C cold shift conditions and compared these results to previous analyses of mutant and wild type Arabidopsis rosette leaves. To obtain sufficient amounts of root material for multi-level systems analyses, we changed our experimental conditions from soil-grown plants (Beine-Golovchuk et al., 2018) to a mixotrophic hydroponic system that meets these demands. In this cultivation system, reil mutants retain reduced growth, but attenuate the previously reported strong growth and developmental phenotypes. For our current study, we did not adjust the growth conditions to reveal stronger phenotypes. By analyzing *reil* mutants under conditions that cause small, but still noticeable phenotypes, we hope to reveal the mutant effects that otherwise may be obscured by pleiotropic and secondary responses. For the purposes of: (1) identifying and understanding the mechanism of ribosome biogenesis in which Arabidopsis REIL proteins are involved and; (2) discovering alternative roles of REIL proteins, we analyzed ribosomal complexes and applied transcriptome and proteome profiling methods. In addition to the previously reported double mutant *reil1-1 reil2-1* (Schmidt et al., 2013; Schmidt et al., 2014; Beine-Golovchuk et al., 2018), we introduce a second double mutant, *reil1-1 reil2-2*, to our studies and analyzed abundances of ribosomal complexes from the single-paralog mutant lines, *reil1-1*, *reil2-1* and *reil2-2*, from which the double mutants originate.

4.3 Materials and Methods

4.3.1 Plant Materials

The single-paralog mutants, *reil1-1*, *reil2-1*, and *reil2-2* lines, with T-DNA insertions in exon 2 at base pairs 475, 733, and 731, respectively, were selected to investigate the role of REIL proteins

for the plant growth in suboptimal temperature condition. All T-DNA insertions were characterized previously by sequencing of the left border of insertion sites (Schmidt et al., 2013). The double homozygous *reil1-1 reil2-1* (*DKO1*) mutant (Schmidt et al., 2013) was created by crossing the T-DNA insertion mutant SALK_090487 (*reil1-1*) that was obtained through the Nottingham Arabidopsis Stock Centre (Scholl et al., 2000) and GK_166C10 (*reil2-1*) of the GABI-Kat program (Rosso et al., 2003). The second allelic double homozygous *reil1-1 reil2-2* (*DKO2*) mutant was created in this study by crossing the T-DNA insertion mutant SALK_090487 (*reil1-1*) and *reil2-2* (SALK_040068). Homozygosity of the insertion sites was verified by PCR amplification of genomic DNA with the previously described T-DNA- and *reil1*- and *reil2*-specific oligonucleotides (Schmidt et al., 2013). All system-profiling analyses were performed with the two double mutants and controls of the ecotype *Arabidopsis thaliana* Col-0 (wild type), the common genetic background of all mutants in this study. The three single-paralog *reil* mutants, *reil1-1*, *reil2-1* and *reil2-2*, were subjected to comparative analysis of ribosome complexes.

4.3.2 Photographic Documentation

The Arabidopsis shoot and root systems were digitally photographed at 300 dpi horizontal and vertical resolution using a Nikon D5100 camera with up to 4,928 x 3,264 pixels or a NIKON D850 camera with up to 8,256 x 5,504 pixels. Photographs were cropped to size and resolution reduced to meet size limitations of composite figures using Adobe Photoshop CS5 Extended (Version 12.0.4 x64). The scale bars were manually added using external documentation of scale and magnification.

4.3.3 Hydroponic System for Growth, Controlled Temperature Shift and Sampling of Arabidopsis Root Materials

Generation of seed batches, storage, sterilization, and in vitro pre-cultivation were as described previously (Schmidt et al., 2013). The hydroponic growth system for Arabidopsis plants used circular white glass containers with glass lids. The containers had a slightly tapered bottom with 10.0 cm top diameter and 7.5 cm bottom diameter (**Supplemental Fig. S4-1**). The containers had a total volume of ~ 580 mL. Each glass contained 250 mL of liquid MS media with 2% sucrose (w/v) adjusted to pH 5.7 (Murashige and Skoog, 1962). Sucrose addition reduced developmental and growth-differences between mutants and Col-0 wild type. The liquid was first poured into the

jar, then a sterilized stainless steel wire mesh insert of 9 cm diameter, with mesh size 1.40 mm and wire thickness 0.25 mm was adjusted level with the top of the liquid (**Supplementary Fig. S4-1**). Four small ~ 1 cm^3-blocks of solid MS media that contained 0.8 % (w/v) agar were placed on top of the mesh before applying single sterilized Arabidopsis seeds to each block. Four plants were routinely cultivated per container. The containers were closed tightly, but not airtight. Glass lids were fixed to the container by stainless steel clamps before transfer to a controlled-environment chamber for growth. The seeds were allowed to germinate and grow under sterile conditions in a long day photoperiod with a 16h/8h - day/night cycle. External temperature settings of the chamber were controlled. External light intensity was 100 - 150 µmol photons m^{-2} s^{-1}. External relative humidity was 60% - 70%. The standard temperature regime was 20°C during the day and 18°C during night (Supplementary Fig. S1).

4.3.4 Temperature Shift Experiments and Root Harvests

Plants were pre-cultivated at 20°C standard conditions to developmental stage ~1.10 (Boyes et al. 2001). At this stage, the plants were transferred carefully within their hydroponic containers from standard conditions to a second controlled-environment chamber with 10°C temperature during the day and 8°C during the night, but otherwise equal external light cycle, light intensity, and relative humidity settings (**Supplemental Fig. S4-2**). Non-cold shifted roots were harvested immediately before temperature shift and are in the following denoted non-acclimated or 0 day samples. Subsequently, samples were harvested after one day, three days, one week, and three weeks after cold shift (**Supplemental Fig. S4-3**). Each harvested biological replicate was the pool of total root material from four plants of a single container. Three biological replicates, n = 3, were harvested for microarray based transcriptome analyses. Five replicates per experimental condition, ~20 individual root systems, were pooled into single samples for the analysis of ribosome complexes using sucrose density gradients.

4.3.5 Sucrose Density Gradient Analysis of Ribosome Preparations from Arabidopsis Root Tissue

Ribosome fractions from Arabidopsis Col-0 wild type and *reil* mutants were prepared from pools of hydroponically grown root systems as described previously (Beine-Golovchuk et al., 2018). Due to the complex procedure, single pools of non-acclimated roots and roots at 1 day, 3 days, 7

days, and 21 days after cold-shift were analyzed per genotype for qualitative analyses. Briefly, per sample 100 - 102 mg fresh weight (FW) of frozen root tissue was homogenized 30 min on ice with 0.5 mL polysome extraction buffer (PEB) in horizontal tubes on an orbital shaker set to 400 rotations per minute. The final PEB buffer composition was 200 mM Tris-HCl adjusted to pH 9, 200 mM KCl, 25 mM EGTA, 36 mM MgCl2, 5 mM DTT, 50 μg mL^{-1} cycloheximide (CHX), 50 μg mL^{-1} chloramphenicol (CHL), 1.0 mg mL^{-1} heparin, 1 % (v/v) Triton X-100, 1 % (v/v) Tween 20, 1 % (w/v) Brij-35, 1 % (v/v) IGEPAL CA-630, 1 % (v/v) polyoxyethylene, 1 % (w/v) deoxycholic acid, 1 mM phenylmethylsulfonylfluoride (PMSF), and the equivalent of 0.002 tablets mL^{-1} cOmpleteTM protease inhibitor mixture. All chemicals were obtained from Sigma-Aldrich (Taufkirchen, Germany). The following procedures were carried out at 4°C. After initial centrifugation at 14,000 g for 10 min, the extract with remaining debris was placed on top a QIAshredder spin column of the RNeasy Plant Mini Kit (Qiagen, Hilden, Germany) and centrifuged again at 14,000 g for 1 min to remove all cell debris. Volumes of 0.5 mL of extract were loaded onto 9 mL of a 15% (w/v) to 60% (w/v) sucrose gradient that was prepared in PEB without detergents, heparin and protease inhibitors. The loaded density gradients were centrifuged at 33,000 g for 14.5 h at 4°C using a six-position SW41 Ti rotor (Beckman Coulter, Kerfeld, Germany). The positions of ribosome complexes varied slightly with each centrifugation run that comprised a set of six samples. In each centrifugation run, a non-sample control gradient was loaded with 0.5 mL PEB and used for photometric base line subtraction. The five remaining positions were used for root samples and included an Arabidopsis Col-0 sample for the estimation of relative abundances of ribosome complexes. Five centrifugation runs contained samples that were harvested at the same experimental time point. In the sixth centrifugation run, a randomly selected mutant of each time point was analyzed. The sucrose density gradients were separated into ~ 40 fractions of approximately 250 μL per fraction using a programmable density gradient fractionation system (Teledyne Isco Inc., NE, USA). An absorbance profile was recorded continuously at 254 nm wavelength using a 15% (w/v) sucrose solution in PEB without detergents, heparin and protease inhibitors, prior to each gradient recording to calibrate the absorbance minimum (0% $absorbance_{254nm}$). The absorbance profiles were exported from the acquisition system and background subtracted by the profile of blank sample of each centrifugation run and identically scaled. Abundances of ribosome fractions were measured as background subtracted peak areas (**Supplemental Table S4-1**). Peak areas and the total sum of all peak areas including

the 40S, 60S, 80S and polysome fractions, were determined by Chromas Lite 2.1 software (http://chromas-lite.software.informer.com/2.1/).

4.3.6 KCl-Sensitivity Test of Ribosome Complexes

Exemplary in vitro KCl-sensitivity of translating ribosome complexes was performed with wild type root tissue compared the *reil1-1 reil2-1* double mutant at 21 days after cold shift as a compromise between immediate and prolonged cold exposure. A pooled root sample of each simple type was split into two technical replicates of 100 mg FW each. Each of the replicates was extracted with 0.5 mL PEB that either contained regular 200 mM KCl or elevated 400 mM KCl. After 30 min incubation on ice all samples were fractionated by 15% - 60% sucrose density gradients. All samples were centrifuged in a single 2 h run with sedimentation at 50,000 g and 4°C using small 13 x 51 mm ultracentrifugation tubes in SW55 Ti rotor (Beckman Coulter, Krefeld, Germany). These centrifugation settings were optimized for polysome and monosome separations. Abundance analysis of the separated ribosome complexes was as described above omitting fraction collection.

4.3.7 Transcriptome Analysis

Twenty-seven root samples, 3 experimental conditions x 3 genotypes x 3 biological replicates, of non-acclimated and 1 day or 7 days cold acclimating Col-0, reil1-1 reil2-1, reil1-1 reil2-2 were analyzed. Liquid nitrogen frozen samples of 25.1 - 26.8 mg fresh weight were ground to fine powder. Total RNA was extracted from frozen powder using the RNeasy Plant Mini Kit and RNase-free DNase (Qiagen, Limburg, Netherlands) according to the manufacturer's instructions as was described previously (Beine-Golovchuk et al., 2018) with down-scaling modifications. Briefly, 110 µL RNA extraction buffer was used and 30 µL of RNase-free water for RNA elution. Total RNA was quantified by NanoDrop™ spectrophotometer (ThermoFisher Scientific, Germany) using absorbance wavelength 260 nm. RNA quality was evaluated by formaldehyde agarose gel electrophoresis and OD260/280 and OD260/230 ratios. The RNA integrity number (RIN) of RNA samples was assessed using an Agilent 2100 Bioanalyzer (Agilent Technologies, Germany). RNA samples of 10-15 µL per sample with RIN > 8 were processed by ATLAS Biolabs GmbH (Berlin, Germany) using Agilent Feature Extraction software (v10.7). The obtained gene expression data sets were quantile normalized using the normalize.quantile routine of the preprocessCore R

statistical computing and graphics package (https://www.r-project.org/). The obtained 4X44K Agilent microarray data comprise variable numbers of redundant gene probes. The expression data sets are available from the Gene Expression Omnibus (https://www.ncbi.nlm.nih.gov/geo/) through accession GSE144916. Gene expression information of redundant probes was averaged to reduce bias for functional enrichment analyses. Gene expression information was normalized per gene model to the average expression value from non-acclimated Col-0. Alternatively, the differential gene expression of mutants over Col-0 was calculated at each time point. Averaged log_2-transformed ratios of differential gene expression, standard errors and statistical test results are reported in **Supplemental Table S4-2**.

4.3.8 Functional Enrichment Analyses of Gene Expression Data

Functional enrichment analysis of differential gene expression was carried out by parametric analysis of gene set enrichment (Du et al., 2010; Tian et al., 2017) using the agriGOv2.0 web-service at http://systemsbiology.cau.edu.cn/agriGOv2/. The parametric analysis of gene set enrichment processes lists of genes with log_2-transformed numerical differential gene expression values from one or more experimental conditions and provides information on the enrichment of expression increases or decreases across gene sets of at least 10 gene entries that are defined by 2,145 GO gene ontology (GO) terms. Enrichment of mean log2-fold changes (log_2-FC) were evaluated by z-scores, and by false discovery rate (FDR)-adjusted *p*-values (Benjamini and Hochberg, 1995) applying a $p < 0.05$ thresholds (**Supplemental Table S4-3**).

4.3.9 Proteome Analysis of Ribosome Preparations from Arabidopsis Root Tissue

We performed two complex experiments of ribosome fraction preparation and shotgun ribo-proteome analysis that resulted in data sets DS1 and DS2, respectively. Each data set contained a pooled Arabidopsis Col-0 root sample and a pooled double mutant root sample either of *reil1-1 reil2-2* (DS1) or of *reil1-1 reil2-1* (DS2). Samples prior to temperature shift and samples prepared at 7 days after 10°C cold shift were analyzed.

Sucrose density fractionation and subsequent proteomic analysis were performed with approximately equal amounts of 100 mg FW. Tryptic peptides were prepared from up to five non-translating ribosome fractions and a low-oligomer polysome fraction by filter aided sample preparation (Erde et al., 2014; Swart et al., 2018). Sucrose density gradient fractions were washed

repeatedly with 500 µL of 0.04 M Tris-HCL buffer (pH 8.4) with 0.2 M KCl and 0.1 M $MgCl_2$ using regenerated cellulose membranes, Amicon Ultra-0.5 centrifugal filter units, with a 3 kDa molecular size cutoff (Merck, Kenilworth, New Jersey, USA). Removal of sucrose was considered complete, when the 500µL volume decreased to below 100 µL within 10 minutes of centrifugation at 5000-7000 rpm and 4°C.

Shotgun proteome analysis of recovered peptides was performed by liquid chromatography - tandem mass spectrometry (LC-MS/MS) with an ACQUITY UPLC M-Class system (Waters Corporation, Milford, MA, USA) hyphenated to a Q-Exactive HF high-resolution mass spectrometer (Thermo Fisher Scientific, Waltham, MA, USA). Samples were separated by reverse phase nano-liquid chromatography using a 125/ 132 min (DS1/ DS2) 3% to 85% (v:v) acetonitrile (ACN) gradient. Mass spectrometric data acquisition was performed by data dependent top-N tandem mass spectrometry (dd-MS2). This acquisition mode fragmented the top 10/ 15 (DS1/ DS2) most intense ions per full scan. Full scans were acquired at a resolution of 120,000/ 60,000 (DS1/ DS2) with automatic gain control (AGC) target set to 3e6/ 1e6 (DS1/ DS2), maximum injection time 100/ 75 ms (DS1/ DS2), and scan range 300 to 1600 m/z in profile mode. Each dd-MS2 scan was recorded in profile mode at a resolution of 15,000/ 30,000 (DS1/ DS2) with AGC target set to 1e5, maximum injection time 150 ms, isolation window of 1.2/ 1.4 m/z (DS1/ DS2), normalized collision energy 27 eV and dynamic exclusion of 30 sec. The LC-MS/MS files were analysed by using the MaxQuant software (Version 1.6.0.16) available in the website http://www.coxdocs.org/doku.php?id=maxquant:common:download_and_installation.

Then, *Arabidopsis thaliana* FASTA files of the reviewed Swiss-Prot compendium in the UniProt database (The UniProt Consortium, 2017) were served for peptide annotation. All peptides, including unique peptides and non-specific peptides of highly similar or identical paralogs of structural cytosolic ribosome proteins were analyzed by label-free quantification, LFQ (Zhang et al., 2012). The proteomics data set, identifier PXD016292, and detailed experimental settings are available via the ProteomeXchange Consortium at the PRIDE partner repository, https://www.ebi.ac.uk/pride/archive/login, (Perez-Riverol et al., 2019). Proteins were annotated according to majority peptide identification. 336 Specificity of detected peptides for cytosolic RP paralogs and ribosome-associated proteins (RAPs) was analyzed including potential non-specificity by minority peptide calls. **Supplemental Table S4-4** reports proteomic fraction characterization and the subset of samples from Pride data set PXD016292 used in this study. We

identified the 40S and 60S RPs, and the organelle 30S and 50S RPs according to previous publications (Barakat et al., 2001; Hummel et al. 2015; Sormani et al., 2011; Waltz et al., 2019; Rugen et al., 2019). Due to the differences of cytosolic ribosome subunits in each fraction, and to account for the variation between sample types, we normalized protein LFQ-abundances in fractions that contained 60S RPs to the sum of LFQ-abundances of all detected 60S proteins in each of the respective fractions. This procedure allowed analysis of compositional changes of 60S ribosome complexes, but may create false positives of components due to co-purified organelle RPs or other proteins. For this reason, we only considered changes relevant, if the non-normalized LFQ abundance had a maximum in the 60S or 60S/80S fractions and not in the 30S/40S or 50S fraction. We excluded all 40S RPs from the compositional analysis of the non-translating 60S fractions. To assess compositional changes of non-translating 40S complexes we normalized to the sum of all 40S RPs in each fraction. We excluded all 60S RPs and only considered proteins that we more abundant in the 30S/40S fraction relative to the 60S fraction. Due to the overall experimental design, we did not apply statistical analyses for feature selection. Instead, we selected for changes that were shared between the *reil1 reil2* double mutants at 10°C. In a more stringent analysis, we selected the respectively shared changes at both temperatures 10°C and 20°C.

4.3.10 Association Analysis of Changes in Transcript and Relative Protein Abundance

The differential transcript levels of the *reil1 reil2* mutants relative to *Arabidopsis thaliana* Col-0 wild type were compared to changes of relative protein abundance in the non-translating 40S and 60S plus 60S/80S fractions of the proteome analysis (**Supplemental Fig. S4-9**). For this purpose, we correlated the differential accumulation of cytosolic RPs and RAPs in non-translating ribosome fractions reported in **Supplemental Table S4-6** to differential gene expression (**Supplemental Table S4-2**, columns X to AC). We merged transcript and protein information according to the reported gene model information of the transcriptome and proteome analyses (Pride data set PXD016292). Note that the transcript information was in part splice variant specific. The proteome analyses in many cases did not distinguish splice variants and contained non-specific information due to peptides of proteins from the highly similar or in part identical ribosome protein families (**Supplemental Table S4-6**).

4.3.11 Statistical Analyses and Data Visualizations

Quantile-normalized log_2-transformed ratios of DEGs (differentially expressed genes) or log_2-transformed of differential protein abundances were analyzed, correlated and visualized by Microsoft Excel software of the Office Professional Plus 2010 package (Microsoft) and the Multiple Experiment Viewer version 4.9.0 (http://www.mybiosoftware.com/mev-4-62-multiple-experiment-viewer.html). Significance thresholds (p) of statistical analyses, e.g. one- or two-way analyses of variance (ANOVA), and two-group comparisons by heteroscedastic Student's t test, were routinely $p < 0.05$ if not mentioned otherwise. Details of the data analysis and visualization methods are reported in the legends of figures and tables.

4.4 Results

4.4.1 Hydroponic Growth of *reil* Mutant Plants Compared to the Arabidopsis Col-0 Wild Type

The established hydroponic system enabled sterile photomixotrophic cultivation of up to four Arabidopsis Col-0 wild type or mutant plants within a single container with 2% (w/v) sucrose in liquid growth medium (Murashige and Skoog, 1962). Attempts of photoautotrophic cultivation without sucrose caused slow plant growth and generated dwarfed and early flowering *reil1 reil2 double mutants* (DKOs) with minimal root systems. In the presence of 2% (w/v) sucrose, the Arabidopsis wild type reached the 10-leaf stage, i.e. Arabidopsis stage 1.10 (Boyes et al., 2001), after approximately 4 weeks under standard long-day photoperiod conditions with external temperatures set to 20°C during the day and 18°C during night (**Supplemental Fig. S4-1**). Morphology of Arabidopsis rosettes differed from soil-grown plants. The leaf petioles were elongated and leaf laminae smaller than on soil, e.g. (Schmidt et al., 2013; Beine-Golovchuk et al., 2018). Leaves of individual stage 1.10 plants overlapped minimally. From this stage onward, the single root systems entangled with each other and in part with the mesh. Only rapid harvests of the complete root systems from four plants of a single container were feasible (**Supplemental Fig. S4-2**). For this reason, all biological replicates were pooled root samples of at least four plants from single growth containers or of more plants from multiple containers.

Root and shoot growth of the Arabidopsis wild type continued after cold shift at stage 1.10 plants to 10°C during the day and 8°C during night under otherwise constant conditions. Plants phase-shifted to the generative phase and produced small inflorescences at 7 to 21 days after

exposure to cold (**Supplemental Fig. S4-2**). Photomixotrophic cultivation did not fully abolish differential growth of mutants and Col-0. Growth and development of the *reil1-1* mutant was, however, similar to wild type. Shoots of the mutants, *reil2-1*, *reil2-2*, and the double mutants, *reil1-1 reil2-1* (*DKO1*) and *reil1-1 reil2-2* (*DKO2*) remained slightly smaller than wild type after cold shift, but all mutants continued to grow and developed inflorescences (**Supplemental Fig. S4-2**). Shift to low temperature induced spoon-shaped leaf morphology of *reil2* mutants, but this phenotype was strongly attenuated compared with soil-grown *reil2* mutants (Schmidt et al. 2013). Similarly, the double mutants were not fully growth arrested after 10°C cold shift in our hydroponic growth system and continued to grow in contrast to soil cultivation (Beine-Golovchuk et al., 2018).

A preliminary study of mutant root systems from single plants of our cultivation system (**Supplemental Fig. S4-3**) showed delayed root growth and a shortened acropetal part of the primary root of the double mutants compared with the wild type. These observations became apparent 7 to 21 days after cold shift. In addition, at 21 days after cold shift, the double mutants and *reil1-1* appeared to be less branched, indicative of an altered root branching pattern compared to the wild type (**Supplemental Fig. S4-3**). Attempts to further characterize altered root growth and branching pattern without wounding failed in our current cultivation system because it was inadequate to quantify altered root architectures of single plants at stage 1.10 and later. For this reason, we did not perform morphometric analyses of mutant root systems in this study. In the following, we performed standardized temperature shift experiments that were similar in experimental design to previous experiments with soil-grown plants (Schmidt et al., 2013; Beine-Golovchuk et al., 2018). We analyzed pools of whole root systems and started experiments at developmental stage 1.10 with samples taken in the non-acclimated state followed by sampling at 1, 3, 7, and 21 days after shift to 10°C cold.

4.4.2 Analyses of Ribosome Complex Abundances from Roots Confirms Association of REIL Deficiency with Delayed 60S LSU Accumulation After Cold Shift

Previous analyses of cytosolic ribosome complexes from Arabidopsis showed activation of cytosolic rRNA expression and concerted accumulation of transcripts coding for cytosolic ribosomal proteins (RPs) after a 10°C cold shift from optimized temperatures (Beine-Golovchuk et al., 2018). The *reil1-1 reil2-1* mutant delayed these responses and the accumulation of the 60S

LSU fraction compared to wild type. In these studies, we analyzed leaf material of soil-cultivated rosette plants. The presence of chloroplast ribosomes interfered in parts with the analysis of cytosolic ribosome complexes. We succeeded to separate a 60S LSU fraction from the chloroplast 50S LSU and chloroplast 70S from 80S monosomes, but the chloroplast 30S and cytosolic 40S small subunits (SSUs) remained non-resolved and the polysome fraction was mixed. For this reason, we did not investigate previously, an indicated concerted regulation of cytosolic 60S LSU with the abundances of other cytosolic ribosomes complexes, such as the 40S SSUs.

To overcome this limitation and to extend and validate our analyses of the delayed accumulation of the 60S LSU in REIL deficient mutants, we focused on root material that became available in sufficient amounts, ~ 100 mg fresh weight per analysis, by hydroponic cultivation. As we expected, plastid ribosome complexes, 30S, 50S, and 70S, were negligible in this material and much less abundant than cytosolic ribosomes. We obtained improved separation and purity of 40S SSU, 60S LSU, 80S ribosome fractions and analyzed the abundance of these fractions in wild type compared to the double mutants, *reil1-1 reil2-1* and *reil1-1 reil2-2*, and the respective single 446 paralog mutants, *reil1-1*, *reil2-1*, and *reil2-2* (**Fig. 4-1**). Based on the equal amounts of root fresh weight Arabidopsis wild type accumulated cytosolic ribosome complexes, especially the 80S fraction, at 1, 3, 7, and 21 days after shift to 10°C. Profiles of ribosome complexes from both, the *reil1-1 reil2-1* and the *reil1-1 reil2-2* mutant, were distinct from wild type. The abundance of the 60S LSU fraction of both double mutants approximately equaled the 80S fraction already in the non-acclimated state. This difference to wild type persisted throughout cold acclimation (**Fig. 4-1**). In agreement with previous observations from leaf material, 60S LSU accumulation after cold shift lagged behind wild type in both *reil* double mutants.

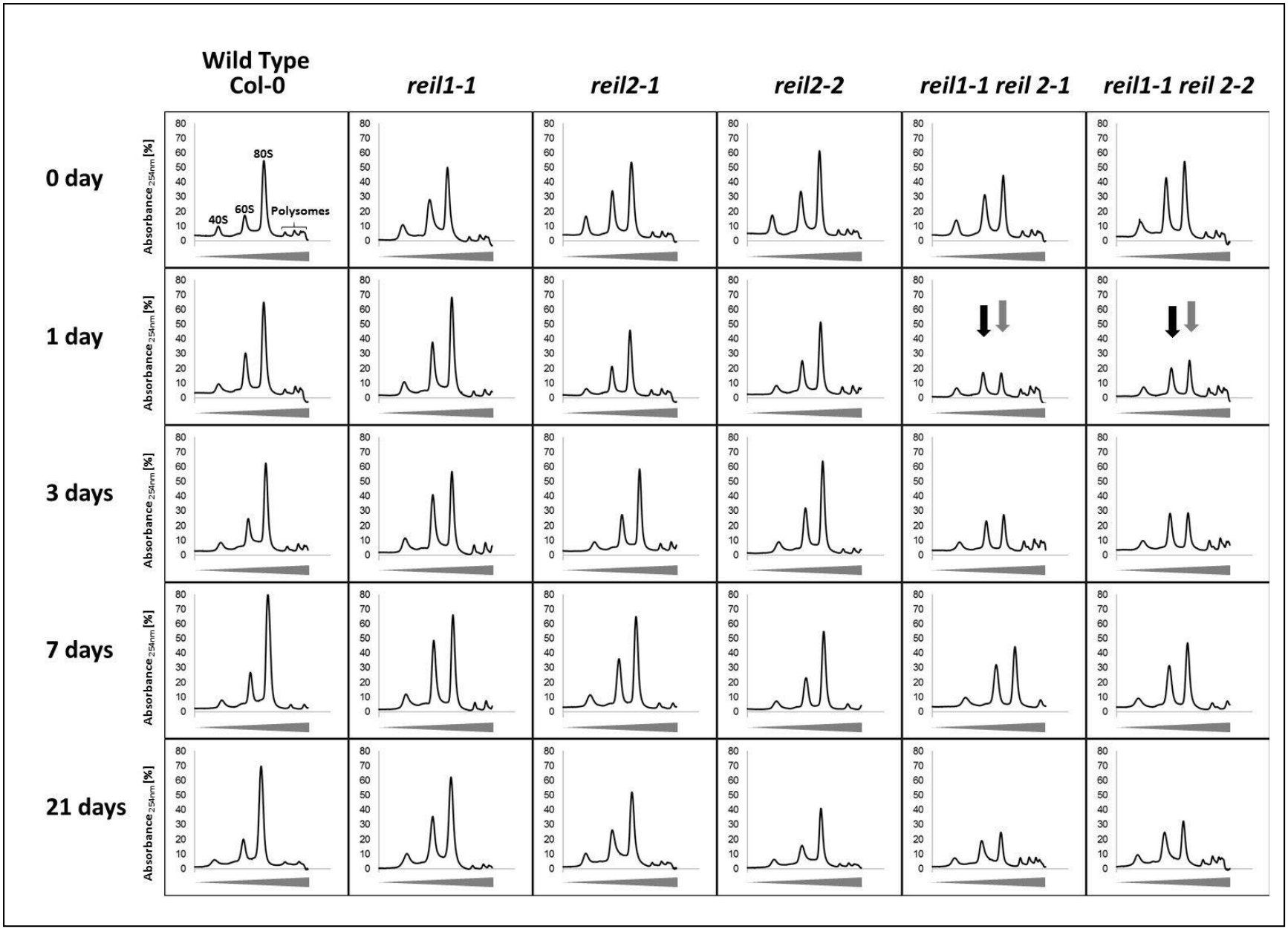

Wild Type
Col-0
reil1-1
reil2-1
reil2-2
reil1-1 reil 2-1
reil1-1 reil 2-2
0 day
1 day
3 days
7 days
21 days
Absorbance 254nm [%]
40S
60S
80S
Polysomes

Figure 4-1. Sucrose density gradient analyses of ribosome complexes from equal fresh weight amounts of hydroponically grown total root material before (0 day) and at 1, 3, 7, or 21 days after shift from 20°C (day)/ 18°C (night) to 10°C (day) and 8°C (night). The *Arabidopsis thaliana* wild type (Col-0) was compared to the single paralog mutants, *reil1-1*, *reil2-1*, *reil2-2*, and to the double mutants, *reil1-1 reil2-1* and *reil1-1 reil2-2*. Absorbance at wavelength 254 nm (y-axis) was recorded continuously during fractionation of 15 – 60 % sucrose density gradients (x-axis, tapered bars indicate the gradient) and background corrected by a non-sample control. This is a composite figure of multiple centrifugation runs that each contained a non-sample control. Gradients varied slightly with each centrifugation run. Note the altered abundance pattern of ribosome complexes from the *reil1-1 reil2-1* and *reil1-1 reil2-2* double mutants in non-acclimated and acclimating states and the delay relative to Col-0 of 60S LSU (black arrows) and 80S monosome (grey arrows) accumulation after cold shift. Inserts into the day 3 analyses magnify the low-oligomer polysome region and demonstrate accumulation of half-mer polysomes in the double mutants early after cold shift.

4.4.3 Changes of Ribosome Complex Abundances Reveal Inter-Complex Correlations and Compensation Responses to REIL Deficiency

This observation and associated effects of other ribosome fractions became apparent by analyzing $\log_2$-transformed ratios of ribosome complex abundances of mutants compared to wild type at each time point of our temperature shift experiment (**Fig. 4-2, Supplemental Table S4-1**). In the non-acclimated state, all *reil* mutants increased the 60S LSU and the 40S SSU fractions ~ two-fold relative to wild type (**Fig. 4-2A-B**), but 80S monosomes had wild type levels (**Fig. 4-2C**). These observations in the non-acclimated state coincided with a slight increase of sum of all detected ribosome complexes (**Fig. 4-2D**). At one day after cold shift, all *reil* mutants except *reil1-1* reduced the 60S LSU and the 40S SSU fractions to approximate wild type levels (**Fig. 4-2A-B**). Reductions 465 of these fractions were only marginal in the *reil1-1* mutant. All mutants subsequently returned to at least wild type levels and in most cases approximated the initial over-accumulation of 60S LSUs and 40S SSUs. The *reil1-1 reil2-1* and the *reil1-1 reil2-2* double mutants reduced the abundance of the 80S fraction up to four-fold relative to wild type upon cold shift (**Fig. 4-2C**). This phenomenon occurred at 1 day after cold shift and continued during prolonged cold exposure. In the *reil2* single paralog mutants, the relative abundances of the 80S fraction were similar, but less affected. The sum of all ribosome complexes in the double mutant changed only marginally, but was reduced at day 1 and 21 after cold shift in the double mutants and in part in the single mutants (**Fig. 4-2D**). The changes of 60S LSU and the 40S SSU abundances correlated with a Pearson´s correlation coefficient of r = 0.945 across all measurements of our experiment (**Fig. 4-3A**). The relative abundances of the 60S LSU and 80S monosome fractions, however, correlated less stringently, r = 0.607 (**Fig. 4-3B**).

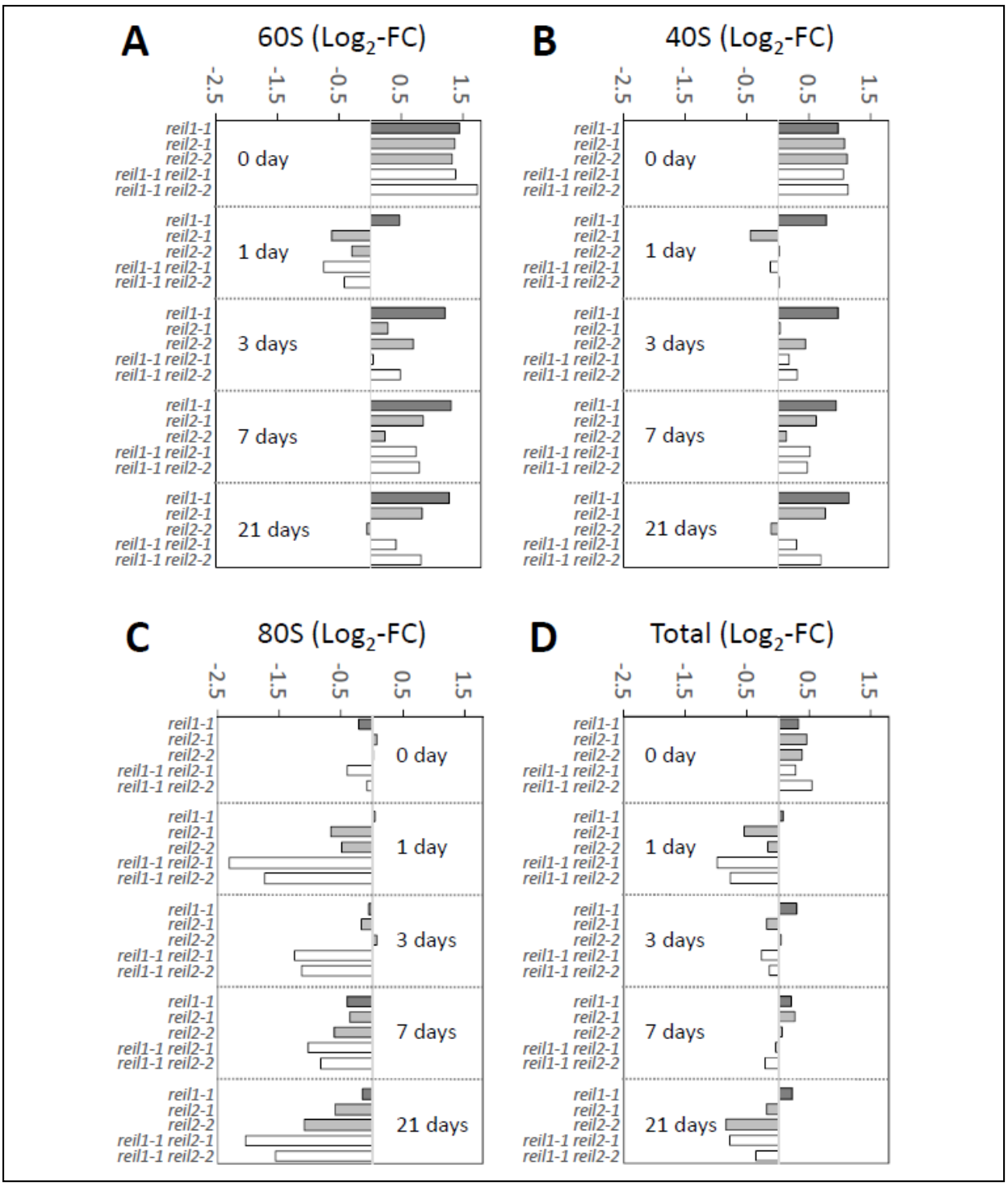


Figure 4-2. Relative quantification of abundances of ribosome complexes from non-acclimated (0 day) and 10°C cold acclimating *reil* mutants at 1, 3, 7, or 21 days after shift (cf. **Fig. 4-1**). Baseline corrected peak areas of ribosome complexes were integrated and $\log_2$-transformed ratios calculated relative to the respective wild type fractions at each time point, i.e. Log_2-fold change (FC). The 60S LSU **(A)**, 40S SSU **(B)**, 80S monosomes **(C)** and the sum ("total") of all ribosome complexes **(D)** were analyzed (dark grey: *reil1-1*, light grey: *reil2-1* and *reil2-2*, white: double mutants, *reil1-1 reil2-1* and *reil1-1 reil2-2*).

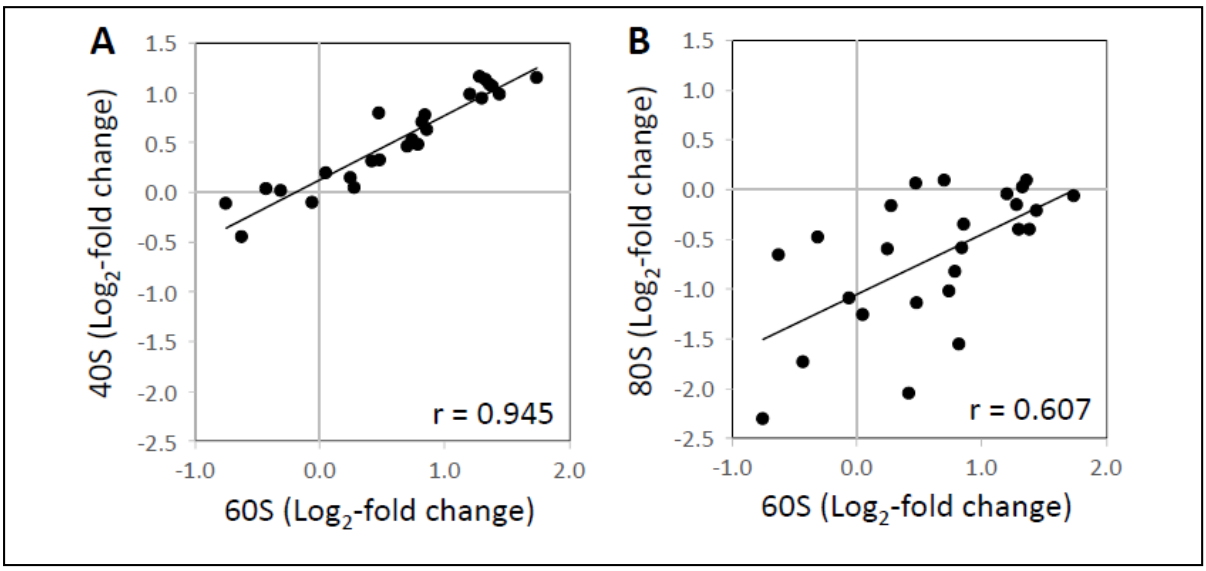


Figure 4-3. Correlation analyses of log_2-transformed ratios of ribosome complex abundances comparing the cold induced changes of abundances relative to wild type of the 40S SSU **(A)** and of the 80S monosome fractions **(B)** to the changes of the 60S LSU fraction across all *reil* mutants (cf. **Fig. 4-2**). Inserts are the Pearson´s correlation coefficients (r) assuming a linear trend.

The double mutant effect on the 80S fraction was the largest and most consistent among the observed changes of cytosolic ribosome complexes. We exemplarily tested the 80S fractions of wild type and the *reil1-1 reil2-1* mutant for previously described heterogeneity (Martin and Hartwell, 1970; Zylber and Penman, 1970) using a sucrose sedimentation gradient tuned to separate translating ribosome fractions, specifically the 80S monosomes from the polysomes. Translating yeast or mammalian ribosomes are stable at high ionic strength. A sub-fraction of monosomes that are thought to be non-translating can be dissociated in vitro by elevating KCl levels during preparation (Martin and Hartwell, 1970; Zylber and Penman, 1970). Like in yeast and mammals, the 80S monosomes of plant roots partitioned into a KCl-sensitive and a stable fraction (**Fig. 4-4**). KCl concentrations that were elevated from regular 200 mM to 400 mM did not affect the root polysome fraction. In contrast, the 80S fraction that accumulated in Arabidopsis wild type roots at 21 days after cold shift was to a large extend KCl-sensitive as was indicated by associated decreases of 80S monosomes and increases of the 60S LSU and 40S SSU fractions (**Fig. 4-4A**). The 80S fraction of the *reil1-1 reil2-1* mutant contained only a minor amount of KCl-sensitive 80S monosomes (**Fig. 4-4B**). Like wild type, the polysome fraction of the *reil1-1 reil2-1* mutant was not KCl-sensitive. Polysome abundance was unchanged or slightly increased relative to wild type. We conclude that the failure of the double mutants to accumulate the 80S monosome

fraction is likely a deficiency of accumulating the non-translating 80S sub-fraction. In summary, *reil* mutants appear to compensate deficiency of cytosolic ribosome biogenesis by over accumulation of free 60S LSU and 40S SSU and in the case of the double mutants by recruiting non-translating monosomes.

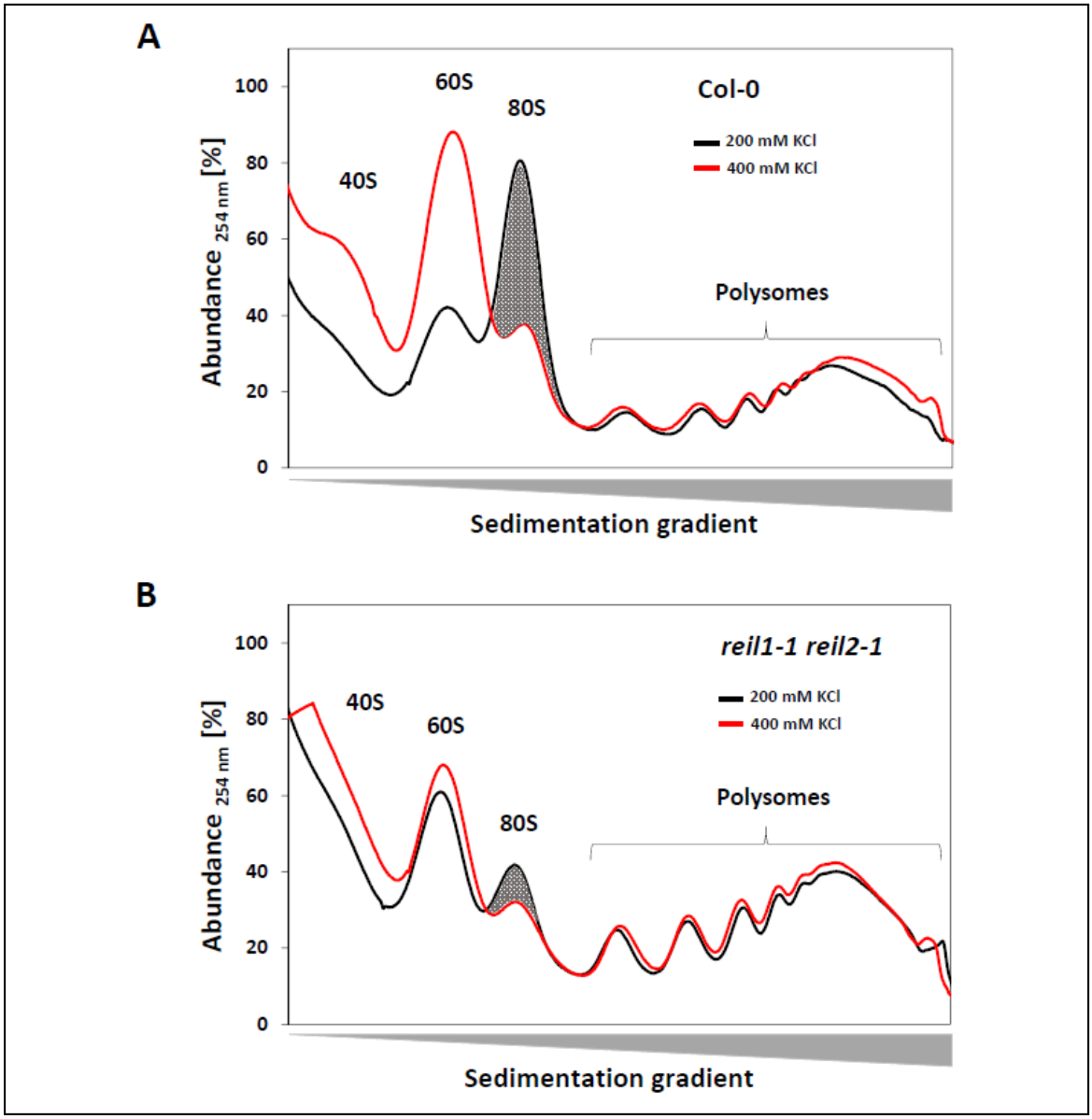


Figure 4-4. *In vitro* KCl-sensitivity test of monosomes and polysomes that were prepared from roots sampled at 21 days after start of 10°C cold-acclimation. Arabidopsis Col-0 wild type **(A)** was compared to the *reil1-1 reil2-1* double mutant **(B)**. Initial samples were homogenized and split into equal technical replicates. These replicates were extracted with PEB that either contained a normal KCl concentration (200 mM, black) or an elevated KCl concentration (400 mM, red). Note that the acclimated wild type accumulated a large fraction of KCl-sensitive monosomes, whereas KCl-sensitive monosomes were almost absent from cold acclimated *reil1-1 reil2-1* preparation.

4.4.4 REIL Deficiency Deregulates Transcriptional Temperature Acclimation Responses in Roots

In the following, we focused on the two double mutants, *reil1-1 reil2-1* and *reil1-1 reil2-2*, and compared non-acclimated (0 day) and the early cold-acclimating states at 1 day or at 7 days after cold-shift to Col-0 wild type. We chose the early cold-acclimating states according to our previous observations of a growth arrest after cold-shift that extended up to 7 day before Col-0 resumed growth in the cold (Beine-Golovchuk et al., 2018). Thereby, we aimed to avoid pleiotropic mutant effects that result from differential growth of the *reil* mutants at later time points. We aimed to reveal at transcriptional level, potential mechanisms that may regulate ribosome complex abundance or may take part in compensation responses to *reil* deficiency (**Supplemental Table S4-2**). Col-0 and reil double mutant roots responded in our axenic, photomixotrophic, hydroponic growth system to 10°C cold shift by expected functional enrichment of transcript changes that relate to cold stress. Expression of genes belonging to the GOs, cold acclimation (GO:0009631) or cold response (GO:0009409), increased over time (**Fig. 4-5A, Supplemental Table S4-3**). Marker genes of cold acclimation and response, e.g. *CBF1, CBF2, CBF3, KIN1, KIN2, VIN3, COR15A* or *COR15B*, changed accordingly (**Supplemental Fig. S4-4**). Inversely to the cold response, expression of heat response genes (GO:0009408) significantly decreased (**Fig. 4-5A**). This observation differed compared to our previous experiments with soil cultivated rosette leaves (Fig. 8A of Beine-Golovchuk et al., 2018) and was accompanied by similar high light intensity (GO:0009644), hydrogen peroxide (GO:0042542) and reactive oxygen species (GO:0000302) responses. Together these observations indicated that the roots of Col-0 and those of the *reil* double mutants were stressed already at 20°C (**Fig. 4-5A**). This stress likely arose due to the artificial, light exposed hydroponic cultivation of roots in this study. Across the complete observation period, the *reil1-1 reil2-1* and *reil1-1 reil2-2* mutants shared constitutive reduction of expression of both *reil* genes in roots (**Supplemental Fig. S4-5**). The reduced gene expression in roots was similar to or in the case of residual *reil2* expression exceeded previous observations of *reil2* silencing in *reil1-1 reil2-1* leaves (Supplemental Table S2 of Beine-Golovchuk et al., 2018).

Our previous study showed that mature leaves of *reil1-1 reil2-1* are prematurely cold acclimated at 20°C (Beine-Golovchuk et al., 2018). In our current study, we selected GOs that had significant enrichment of log2-FC in non-acclimated reil double mutant roots at 20°C compared to non-acclimated wild type at 20°C and of $\log_2$-FC in wild type that acclimated 7 days to 10°C

compared to non-acclimated wild type at 20°C. We applied the threshold of FDR-adjusted $P < 0.05$ to each selection criterion (**Fig. 4-5B-C**). The mean $\log_2$-FCs of genes from the selected GOs of the non-acclimated *reil* double mutants appeared to correlate to the mean $\log_2$-FCs of the cold acclimated wild type. However, part of the cold responsive GOs responded inversely (**Fig. 4-5B-C**). The overlay of both, positively and negatively correlated gene expression in non-acclimated mutant roots compared to cold acclimated Col-0 wild type was even more obvious at single gene level (**Fig. 4-5D-E**). In all of our four correlation analyses, namely the two double mutants at significant thresholds $p < 0.05$ and $p < 0.01$, respectively, the assumption of linear correlations did not apply. Therefore, correlation coefficients were not calculated. We concluded that *reil* double mutant roots deregulate transcriptional cold acclimation at 20°C in our growth system, with two subsets of genes, which either prematurely activate or prematurely deactivate. This response differs from premature cold acclimation as was indicated by transcription factors that control cold acclimation, e.g. *CBF1*, *CBF2* and *CBF3*. Transcripts of these factors did not consistently accumulate prematurely and expression of cold response marker genes, e.g. *KIN1*, *KIN2*, *VIN3*, *COR15A*, and *COR15B*, was reduced (**Supplemental Fig. S4-4**).

4.4.5 REIL Deficiency Affects Transcription of Root Morphogenesis Genes and Activates Expression of Cytosolic Ribosome and Translation Related Genes

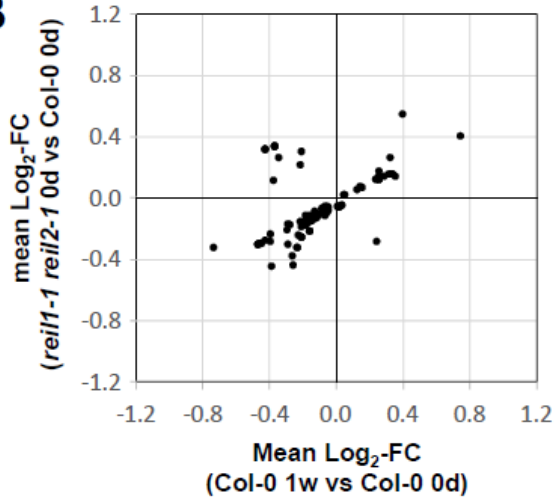
Transcription of 34 GO terms had significant (FDR-adjusted $p < 0.05$) enrichment in both *reil* mutants at every time point of our study relative to non-acclimated Col-0 (**Supplemental Table S4-3**). These GO terms comprised the four previously mentioned stress stimuli (**Fig. 4-5A**) and two miscellaneous GOs, manganese ion binding, GO:0030145, and glycoside metabolic processes, GO:0016137 (**Supplemental Fig. S4-6**). A major mutant response pattern supported our observation of altered mutant root morphology (**Supplemental Fig. S4-3**). Twelve GO terms had constitutive reduced expression. These GOs were related to developmental processes, e.g. GO:0021700, root and root hair morphogenesis, e.g. GO:0010015 and GO:0010054, and cell wall organization and biogenesis, e.g. GO:0071554 (**Supplemental Fig. S4-6A**).

Eight of the remaining GO terms were related to translation or ribosomes, specifically to both subunits of cytosolic ribosomes (**Fig. 4-6A-B**). Col-0 transiently activated gene expression of cytosolic ribosomal proteins (RPs). *Reil1-1 reil2-1* and *reil1-1 reil2-2* consistently activated expression of cytosolic RP genes at 1day and 7 days after the cold shift. Expression of organelle

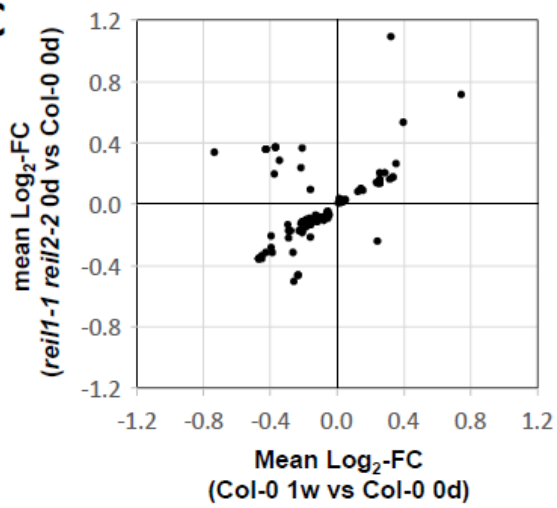
A

GO (Onthology)		Description	Genes	Col-0			*reil1-1 reil2-1*			*reil1-1 reil*	
				0 d	1 d	1 w	0 d	1 d	1 w	0 d	1 d
GO:0009631	P	cold acclimation	22		0.43 *	0.70 *	-0.04	0.20	0.67 *	-0.25	0.46 *
GO:0009409	P	response to cold	263		0.08 *	0.12 *	-0.03	0.05	0.10 *	0.03	0.13 *
GO:0009266	P	response to temperature stimulus	395		-0.04	-0.04	0.02	-0.06	-0.10 *	0.09 *	-0.03
GO:0010286	P	heat acclimation	16		-0.10	-0.02	0.26	-0.04	-0.03	0.06	-0.17
GO:0009408	P	response to heat	138		-0.26 *	-0.38 *	0.12 *	-0.24 *	-0.48 *	0.20 *	-0.32 *
GO:0009644	P	response to high light intensity	47		-0.31 *	-0.21 *	0.31 *	-0.47 *	-0.44 *	0.37 *	-0.41 *
GO:0042542	P	response to hydrogen peroxide	43		-0.38 *	-0.35 *	0.27 *	-0.45 *	-0.53 *	0.29 *	-0.50 *
GO:0000302	P	response to reactive oxygen species	69		-0.26 *	-0.22 *	0.22 *	-0.30 *	-0.33 *	0.24 *	-0.32 *

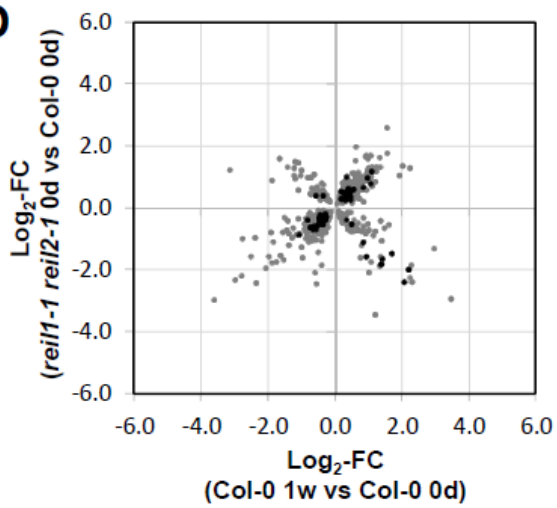
B



C



D



E

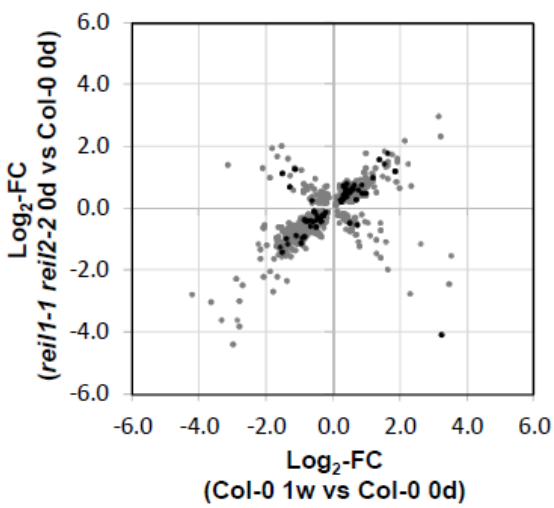


Figure 4-5. Functional enrichment and transcript correlation analyses of differential gene expression in the roots of Col-0, and the *reil1-1 reil2-1* and *reil1-1 reil2-2* double mutants at the non-acclimated state (0 day, 20°C) and shifted to 10°C cold for 1 day or 1 week. Differential gene expression was determined relative to non-acclimated Col-0 at optimized temperature 20°C.
(A) Mean log_2-fold changes (FC) of temperature related GO terms (P = biological process). Significant positive or negative functional enrichments, i.e. FDR-adjusted *p*-values < 0.05, are indicated by asterisks. The heat map color scale ranges from log_2-FC +1.5 (red) to -1.5 (blue). Mean log_2-FC, z-scores, and FDR-adjusted *p*-values of gene sets from 2145 GO terms were calculated by parametric analysis of gene set enrichment (PAGE; Tian et al., 2017; Supplemental Table S3).
(B) Mean log_2-FC of shared significantly enriched GO terms from the non-acclimated *reil1-1 reil2-1* mutant (0 d) compared to acclimated Col-0 at 1 week after shift.
(C) Mean log_2-FC of shared significantly enriched GO terms from the non-acclimated *reil1-1 reil2-2* mutant (0 d) compared to acclimated Col-0 at 1 week after shift. Note that both double mutants and cold acclimated Col-0 shared 100 GO terms of 2145 (FDR-adjusted $p < 0.05$).
(D) Significant changed transcripts of non-acclimated *reil1-1 reil2-1* relative to non-acclimated Col-0 compared to significantly cold-responsive transcripts of Col-0 at 1 week after cold shift ($p < 0.05$, gray, $p < 0.01$ black).
(E) Significant changed transcripts of non-acclimated *reil1-1 reil2-2* relative to non-acclimated Col-0 compared to significantly cold-responsive transcripts of Col-0 at 1 week after cold shift ($p < 0.05$, gray, $p < 0.01$ black).
Note that correlation coefficients were not calculated because assumptions of linear correlation did not apply to the full set of observations.

ribosomal protein (RP) genes did not significantly change in both mutants (**Fig. 4-6A**). The GO terms translation (GO:0006412) and the GO terms containing cytosolic RP genes (GO:0022625 - GO:0022627) responded similarly. Translation was specifically affected in translation initiation (GO:0003743) and eukaryotic translation initiation factor 3 (eIF3, GO:0005852) (**Fig. 4-6B**). The activation of cytosolic ribosome and translation related gene expression in mutant roots mirrored the effects in *reil1-1 reil2-1* leaves (Beine-Golovchuk et al., 2018). Kinetics of cold-induced gene expression appeared accelerated and reduced in amplitude in Col-0 roots compared to the rosette leaves analyzed in our previous study. In addition, expression of ribonucleoprotein (RNP) complexes (GO:0030529) and RNP biogenesis (GO:0022613) was activated in the cold. Expression of small nuclear RNP complexes (GO:0030532) that take part in splicing processes was constitutively activated in both mutants (**Fig. 4-6C**). Finally, five large biosynthesis and cytosol related GOs responded in a pattern that was similar to cytosolic ribosomes (**Supplemental Fig. S4-6B, Supplemental Table S4-3**).

A more detailed study of 40S SSU (104 transcripts covered by our current study) and 60S LSU (159 transcripts) RP gene expression compared to plastid 30S (30 transcripts) and 50S (41 transcripts) RPs revealed in part opposing effects of *reil* deficiency on structural cytosolic and plastid RPs (**Fig. 4-7**). At 10°C, expression of 40S and 60S RPs coordinately increased in both mutants relative to Col-0 at each time point. In the non-acclimated state, *reil1-1 reil2-1* roots reduced cytosolic RP expression whereas *reil1-1 reil2-2* roots had increased cytosolic RP

transcripts (**Fig. 4-7A**). Expression of plastid RPs inversely increased in the non-acclimated state and decreased after shift to cold (**Fig. 4-7A**).

A

GO (Onthology)		Description	Genes	Col-0			*reil1-1 reil2-1*			*reil1-1 reil2-2*		
				0 d	1 d	1 w	0 d	1 d	1 w	0 d	1 d	1 w
GO:0042254	P	ribosome biogenesis	151		0.27 *	0.07	-0.12 *	0.38 *	0.15 *	0.13 *	0.33 *	0.19 *
GO:0005840	C	ribosome	428		0.20 *	-0.02	-0.14 *	0.29 *	0.10 *	0.09 *	0.23 *	0.15 *
GO:0022626	C	cytosolic ribosome	277		0.23 *	-0.04	-0.22 *	0.37 *	0.11 *	0.11 *	0.33 *	0.20 *
GO:0022625	C	cytosolic large ribosomal subunit	133		0.27 *	-0.01	-0.22 *	0.42 *	0.15 *	0.13 *	0.36 *	0.23 *
GO:0022627	C	cytosolic small ribosomal subunit	109		0.22 *	-0.06	-0.24 *	0.37 *	0.11 *	0.07	0.32 *	0.18 *
GO:0000313	C	organellar ribosome	42		0.13	0.09	0.15	0.05	0.13	0.04	-0.17	0.04
GO:0000315	C	organellar large ribosomal subunit	20		0.10	0.12	0.23	0.01	0.11	0.05	-0.21	0.06
GO:0000314	C	organellar small ribosomal subunit	21		0.15	0.05	0.09	0.08	0.15	0.01	-0.14	0.02
GO:0009547	C	plastid ribosome	30		0.20 *	0.17	0.29 *	0.12	0.23 *	0.13	-0.15	0.08
GO:0000311	C	plastid large ribosomal subunit	16		0.18	0.19	0.35 *	0.11	0.19	0.18	-0.13	0.10
GO:0000312	C	plastid small ribosomal subunit	14		0.22	0.14	0.23	0.13	0.28	0.08	-0.17	0.05
GO:0005761	C	mitochondrial ribosome	12		-0.04	-0.09	-0.20	-0.11	-0.12	-0.19	-0.21	-0.05

B

GO (Onthology)		Description	Genes	Col-0			*reil1-1 reil2-1*			*reil1-1 reil2-2*		
				0 d	1 d	1 w	0 d	1 d	1 w	0 d	1 d	1 w
GO:0006412	P	translation	620		0.19 *	0.00	-0.07 *	0.28 *	0.10 *	0.07 *	0.19 *	0.12 *
GO:0008135	F	translation factor activity	145		0.15 *	0.02	0.03	0.24 *	0.08	0.09 *	0.11 *	0.02
GO:0003743	F	translation initiation factor (IF) activity	95		0.16 *	0.02	0.04	0.24 *	0.09	0.10	0.14 *	0.04
GO:0005852	C	eukaryotic translation IF3 complex	10		0.33 *	0.11	0.18	0.64 *	0.56 *	0.26	0.52 *	0.46 *
GO:0003746	F	translation elongation factor activity	33		0.19 *	0.02	-0.06	0.24 *	0.01	0.07	0.09	-0.01
GO:0003747	F	translation release factor activity	13		0.01	0.06	0.11	0.01	0.06	0.05	-0.17	-0.08
GO:0006418	P	tRNA aminoacylation for translation	69		0.14 *	0.03	0.04	0.20 *	0.00	-0.01	0.04	0.03

C

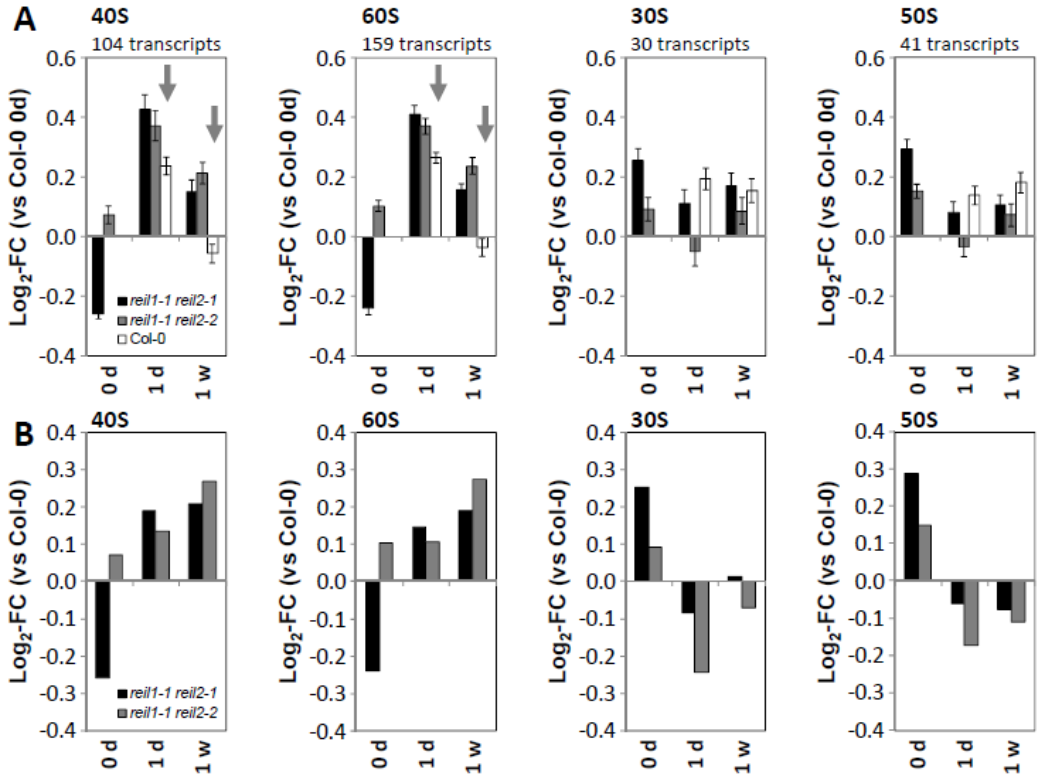
GO (Onthology)		Description	Genes	Col-0			*reil1-1 reil2-1*			*reil1-1 reil2-2*		
				0 d	1 d	1 w	0 d	1 d	1 w	0 d	1 d	1 w
GO:0030529	C	ribonucleoprotein (RNP) complex	514		0.21 *	0.02	-0.10 *	0.28 *	0.12 *	0.11 *	0.24 *	0.16 *
GO:0022613	P	RNP complex biogenesis	159		0.26 *	0.06	-0.12 *	0.36 *	0.13 *	0.13 *	0.30 *	0.17 *
GO:0022618	P	RNP complex assembly	12		0.07	-0.08	-0.10	0.09	0.02	0.12	-0.06	-0.11
GO:0005732	C	small nucleolar RNP complex	30		0.26 *	0.16	-0.09	0.28 *	0.17	0.14	0.33 *	0.21 *
GO:0030532	C	small nuclear RNP complex	13		0.65 *	0.74 *	0.41 *	0.53 *	0.87 *	0.72 *	0.90 *	0.83 *

Figure 4-6. Functional enrichment analyses of differential gene expression in roots of Col-0, and the *reil1-1 reil2-1* and *reil1-1 reil2-2* double mutants at the non-acclimated state (0 day, 20°C) and shifted to 10°C cold for 1 day or 1 week. Differential gene expression was determined relative to non-acclimated Col-0 at optimized temperature 20°C.
(A) Mean log_2-fold changes (FC) of selected ribosome biogenesis and ribosome related GO terms. Note the prolonged and stronger activation of cytosolic ribosome related genes.
(B) Mean log_2-FCs of selected translation related GO terms.
(C) Mean log_2-FCs of selected ribonucleoprotein related GO terms.
(C = cellular component, P = biological process, F = molecular function). Significant positive or negative functional enrichments, i.e. FDR-adjusted *p*-values < 0.05, are indicated by asterisks. The heat map color scale ranges from log_2-FC +1.5 (red) to -1.5 (blue). Mean log_2-FC, z-scores, and FDR-adjusted *P*-values of gene sets from 2145 GO terms were calculated by parametric analysis of gene set enrichment (PAGE; Tian et al., 2017). The full data set is listed in Supplemental Table S4-3.

Analysis of cytosolic RP transcripts by pair wise comparisons at each time point and by two factorial analyses of variance (ANOVA) that tested for the influence of the factors, mutant genotype and time of cold exposure, indicated heterogeneity of RP gene expression at single gene levels (**Fig. 4-7B, Supplemental Table S4-2**). RP gene families comprised members with only a significant effect of either cold exposure or of genotype on their gene expression. We also observed RP paralogs with significant interactions between genotype and cold exposure or no significant change (**Fig. 4-7B**). In summary, *reil* deficiency globally activates cytosolic RP expression with inverse side effects in roots on plastid RP gene expression. *Reil* deficiency may affect gene expression of paralogs from one family synergistically, e.g. RPL4A and RPL4D (**Fig. 4-7B**). Alternately, the lack of REIL proteins can cause strong differential changes of gene expression of specific paralogs from 40S and 60S RP families, for example of the *RPL3*, *RPP2* or *RPP3*, and of the *RPS23*, and *RPS27* gene families (**Fig. 4-7B**). We conclude that differential regulation of RP gene transcription may contribute to the compensation of delayed cytosolic ribosome accumulation in the cold, but is likely not a compensation mechanism in the non-acclimated state.

4.4.6 Constitutive Transcriptional Compensation Responses to REIL Deficiency Indicate Interaction of Cytosolic Ribosome Maturation with Nucleolar rRNA Biogenesis and Translation Initiation

Several observations of GO enrichment among the differential transcript responses indicated constitutive transcriptional changes before and after cold acclimation, e.g. of the eIF3 complex (**Fig. 4-6B**). A detailed analysis of the ten members of GO:0005852 and the complete set of 13 subunits and in total 21 partly paralog genes constituting plant eIF3 (Burkes et al., 2001; Browning and Bailey-Serres, 2015) revealed a single gene, namely *eIF3C-2* (AT3G22860), that was highly and constitutively activated 604 (**Fig. 4-8**). This activation was in contrast to its paralog, *eIF3C-1* (AT3G56150), and other eIF3 components, such as *eIF3G-2* (AT5G06000), that mostly mirrored cytosolic RP expression (**Fig. 4-8**). Applying the stringent criterion of significant constitutive changes relative to Col-0 in both mutants, at all non-acclimated and cold acclimating states, with $p < 0.05$ of each pairwise comparison (heteroscedastic T-tests), we discovered five additional constitutively accumulated transcripts. Next to two only marginally characterized F-box proteins (AT1G64540 and AT3G44120) and a MATH domain protein (AT3G29580) we found PISTILLATA (AT5G20240) and NUCLEOLIN 2 (NUC2, AT3G18610). PISTILLATA is a floral



C

RP Name	RP Class	Gene Symbol	Log$_2$-FC (*reil1-1 reli2-1* /Col-0) 0 d	1 d	1 w	Log$_2$-FC (*reil1-1 reil2-2* /Col-0) 0 d	1 d	1 w	ANOVA *P* (genotype)	*P* (time)	*P* (interaction)
60S LSU											
RPL3A	uL3	AT1G43170.1	-0.302	0.097	0.167	-0.020	-0.140	0.189	9E-01	8E-06	8E-03
RPL3B	uL3	AT1G61580.1	-1.622	-1.328	-0.743	-0.727	-0.942	-0.788	1E-07	2E-04	6E-02
RPL4A	uL4	AT3G09630.1	-0.224	0.316	0.247	0.073	-0.029	0.332	3E-01	9E-06	3E-02
RPL4D	uL4	AT5G02870.1	-0.315	0.248	0.394	-0.084	0.091	0.497	5E-02	6E-05	1E-03
RPP2A	P1/P2	AT2G27720.1	-0.196	0.009	-0.001	0.040	0.050	0.121	4E-01	2E-04	9E-01
RPP2B	P1/P2	AT2G27710.3	-0.372	0.143	0.284	-0.032	0.017	0.376	4E-01	1E-03	4E-02
RPP2C	P1/P2	AT3G28500.1	0.745	2.104	2.720	0.269	0.899	2.590	1E-03	6E-01	2E-01
RPP2D	P1/P2	AT3G44590.1	-0.289	0.064	0.268	0.205	0.169	0.323	1E-01	1E-01	4E-01
RPP2E	P1/P2	AT5G40040.1	-2.382	0.315	2.035	-0.603	0.200	2.420	5E-02	2E-02	1E-04
RPP3A	P1/P2	AT4G25890.1	-0.320	0.147	0.510	-0.232	0.381	0.590	2E-01	6E-03	1E-01
RPP3B	P1/P2	AT5G57290.1	0.109	0.430	0.479	0.252	0.466	0.480	4E-04	2E-03	5E-01
40S LSU											
RPS23A	uS12	AT3G09680.1	-0.077	0.975	1.819	1.217	1.274	1.875	4E-06	4E-04	2E-02
RPS23B	uS12	AT5G02960.1	-0.293	0.149	0.180	0.030	0.131	0.205	2E-01	6E-03	8E-02
RPS27A	eS27	AT2G45710.1	-0.208	0.510	0.268	0.072	0.675	0.459	8E-04	5E-06	3E-02
RPS27B	eS27	AT3G61110.1	-0.083	0.067	0.320	-0.050	-0.127	0.104	3E-01	8E-05	3E-01
RPS27C	eS27	AT3G61111.1	0.001	4.179	2.839	0.257	4.034	1.859	4E-09	8E-10	2E-06
RPS27D	eS27	AT5G47930.1	-0.375	0.123	0.023	-0.208	0.055	0.210	5E-01	1E-03	2E-01

Figure 4-7. Differential expression of cytosolic and plastid ribosome genes in *reil1-1 reil2-1* and *reil1-1 reil2-2* double mutant roots at the non-acclimated state (0 day, 20°C) and shifted to 10°C cold for 1 day or 7 days.
(A) Average log_2-fold change (FC, means +/- standard error) relative to non-acclimated Col-0 (0 day) of transcripts coding for ribosome proteins (RPs) from the cytosolic 40S and 60S subunits and from the plastid 30S and 50S subunits. Grey arrows indicate transcript accumulation of the mutants in the cold.
(B) Average log_2-fold changes relative to Col-0 at each time point calculated form the means of the data from (A).
(C) Log_2-fold changes relative to Col-0 at each time point of selected cytosolic RP families. Two-factorial analysis of variance (ANOVA) indicates differential effects of the genotype, cold exposure (time) or the interaction of both on the expression of paralogous RPs from the 60S and the 40S subunits in the mutants.
The three-color scale of the log_2-FC heat map ranges from -3.0 (blue) to 0.0 (yellow) to $\geqslant$ +3.0 (red). The two-color significance scale ranges from $p \leqslant 1.0 \times 10\text{-}10$ (dark green) to $p < 0.05$ (light green), $p \geqslant 0.05$ (white).

homeotic protein, and probable transcription factor involved in the control of petal and stamen development. PISTILLATA is in addition highly expressed in and near root quiescent centers (Lee et al., 2006; Brady et al. 2007). PISTILLATA appears to serve a yet elusive function in root development. Contrary to this enigmatic finding, function of NUC2 and of its paralog NUC1 provide a link to ribosome biogenesis (Durut et al., 2014). NUC1 and NUC2 nucleolins have antagonistic roles in rRNA gene expression. Both are required for plant growth (Sáez-Vásquez and Delseny, 2019). Similar to *eIF3C2* and *eIF3G2*, the *reil* double mutants constitutively activate *NUC2* expression whereas *NUC1* expression mirrored cytosolic RP gene expression. Contrary to NUC1, NUC2 maintains or induces a repressive state of rDNA chromatin (Durut et al., 2014).

In a meta-analysis, we compared constitutively changed root gene expression to non-acclimated and cold acclimating *reil1-1 reil2-1* rosette leaves at 1 day, 7 days, and 3 weeks after cold shift (Supplemental Table S2 of Beine-Golovchuk et al., 2018). Transcripts of *eIF3C2* (AT3G22860) and *NUC2* (AT3G18610) are constitutively and significantly increased in *reil1-1 reil2-1* mutant leaves with $p < 0.05$ (heteroscedastic T-tests) of each pairwise comparison to Col-0. Transcripts of the F-box proteins, AT1G64540 and AT3G44120, increase significantly using the same significance threshold in mutant leaves only at two or three of the compared time points, respectively. PISTILLATA and the MATH domain protein do not significantly change gene expression in *reil1-1 reil2-1* mutant leaves.

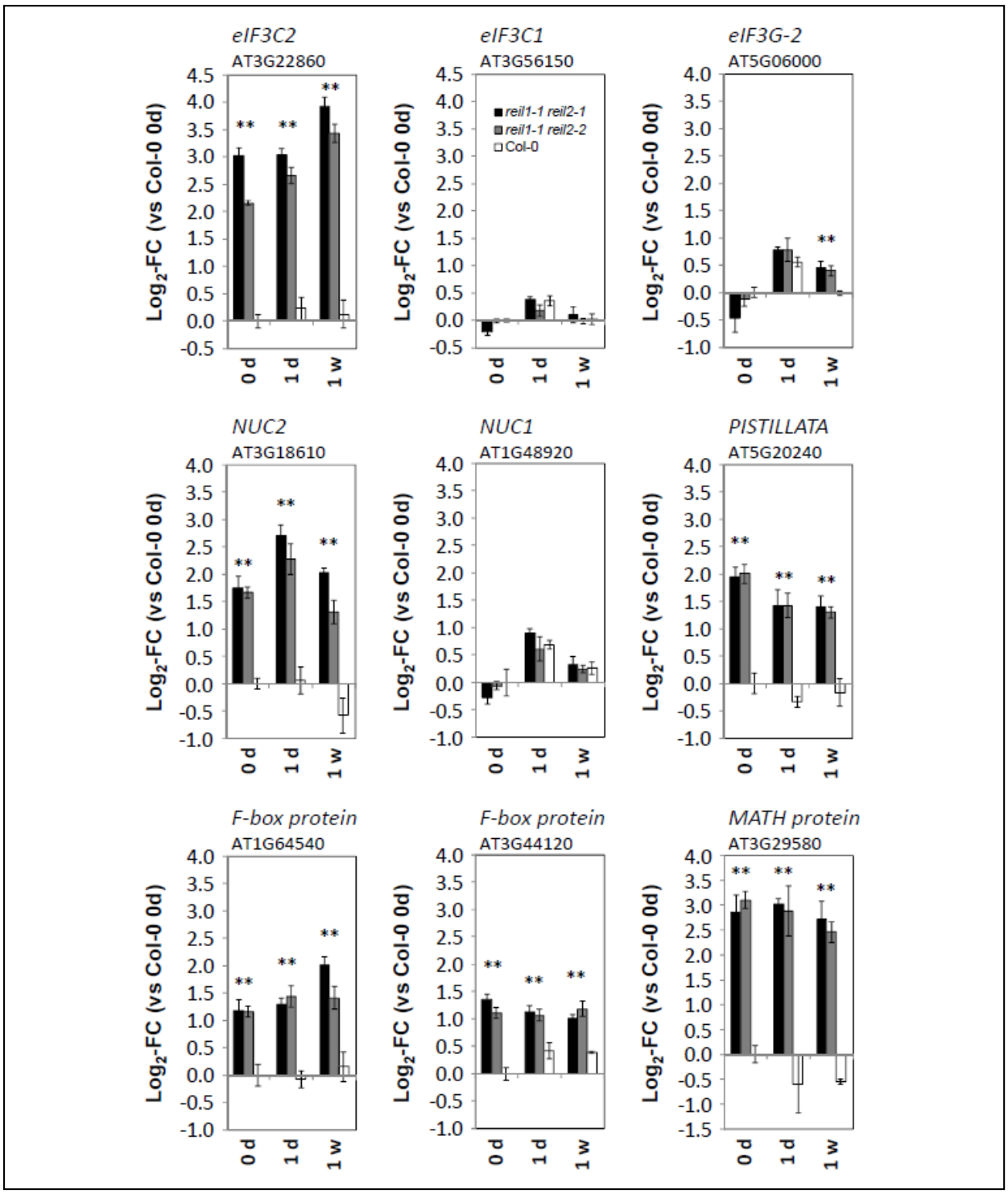


Figure 4-8. Differential expression of six genes that accumulate constitutively in *reil1-1 reil2-1* and *reil1-1 reil2-2* double mutant roots (means +/- standard error, n = 3). *eIF3C2*, *eIF3C1* and *eIF3G2* code for paralogs of the eukaryotic translation initiation factor 3 multi-protein complex. NUC1 and NUC2 are plant nucleolins. Asterisks indicate $p < 0.05$ (heteroscedastic Student´s *t*-test) of comparisons to Col-0 at the same time point. *NUC1*, *eIF3C1* and *eIF3G2* were added to this figure to demonstrate the specific mutant effect on paralog transcription.

4.4.7 Proteome Analysis of Ribosome Preparations from Arabidopsis Root Tissue

For comparative proteome analysis of ribosome complexes, we selected Col-0 wild type and the two double mutants, *reil1-1 reil2-1* and *reil1-1 reil2-2*. We performed two independent experiments each comparing pools of whole root systems from Col-0 wild type to pools of one of the two double mutants, DS1 (*reil1-1 reil2-2*) and DS2 (*reil1-1 reil2-1*). We analyzed the non-acclimated ribo-proteomes at day 0 to preparations obtained 7 days after shift to 10°C and sampled up to five non-translating ribosome complexes and the low-oligomer polysome fraction from sucrose density gradients. In this study, we avoided the period of reduced non-translating subunit abundance of the mutants at day 1 after cold shift and focused on the recovering ribo-proteome (**Fig. 4-1 and 4-2**).

We first analyzed the RP composition of each fraction to identify and align the ribosome fractions between experiments that may differ slightly in the position, but not the sequence of ribosome complexes with the sucrose gradient. For alignment of fractions, we used the sums of abundances of all detected 40S and 60S RPs, the plastid and mitochondrial 30S and 50S RPs, as well as the abundances of Arabidopsis EUKARYOTIC TRANSLATION INITIATION FACTOR 6, eIF6A (AT3G55620), and NONSENSE-MEDIATED mRNA DECAY 3 protein, NMD3 (AT2G03820) (**Supplemental Table S4-4**). eIF6A and NMD3 are homologs of the yeast cytosolic 60S maturation factors, TIF6 (Basu et al., 2001) and NMD3 (Ho et al., 2000). NMD3 and TIF6 are bound to translationally inactive pre-60S ribosome complexes (Lo et al., 2010; Greber et al., 2016) and in the case of TIF6 also indicate the position of NOP7-affinity purified 66S pre-ribosomes (Harnpicharnchai et al., 2001). Next to the polysome fraction, we obtained from both experiments a fraction enriched in 40S and organelle 30S RPs, designated 30S/40S fraction, a fraction of organelle 50S RPs (50S), a fraction that contained predominantly 60S RPs (60S) and a mixed fraction of 80S and 60S complexes (60S/80S) (**Supplemental Fig. S4-7**). In our current experiment, we did not reproducibly obtain proteome profiles of 80S fractions. For this reason, and because the 80S fraction is a difficult to interpret mixture of KCl-sensitive, non-translating and non KCl-sensitive, translating subpopulations (**Fig. 4-4**), we omitted 80S fractions from the current analyses. Both, the 60S and the 60S/80S fractions of experiments DS1 and DS2 contained eIF6A and NMD3 indicative of plant equivalents of 60S or 66S pre-ribosome complexes. In DS1, REIL proteins were detected only by few peptides and a sequence coverage of < 8.0 %. Therefore, we did not analyze the abundance of REIL proteins in DS1. In DS2, however, the 60S and 60S/80S

fractions of the Col-0 wild type contained the REIL2 protein. Identification of REIL2 was supported by up to six peptides and 22.3 % sequence coverage.

The variation of cytosolic, plastid, and mitochondrial RP abundances among the four sample pools and resulting fractions of our proteomics experiments (**Supplemental Fig. S4-7**) prompted us to investigate total RP abundances added up across all ribosome fractions of each of the samples (**Supplemental Table S4-5**). The *reil1-1 reil2-1* sample of DS2 fully recovered after 7 days in the cold in terms of total 40S and 60S abundances. At the same time after cold shift, the *reil1-1 reil2-2* sample of DS1 still lacked in total 40S and 60S abundance. This observation was in agreement with our previous spectrophotometric analysis of the sedimentation profiles at seven days after cold shift **(Fig. 4-2D**). The two mutant samples also differed in organelle RPs. *Reil1-1 reil2-1* roots decreased organelle RPs especially plastid and mitochondrial 50S RPs, both before and after cold shift. Inversely, *reil1-1 reil2-2* accumulated 50S RPs (**Supplemental Table S4-5**).

For our subsequent datamining, we focused on common responses of both mutants and searched for proteins that consistently accumulated or decreased relative to Col-0 wild type. We analyzed the non-translating fractions, namely the 60S and 60S/80S fractions in combination and separately the 30/40S fraction. Given the cold sensitivity of the *reil* mutants we looked for common changes of the two *reil* double mutants relative to Col-0 wild type in the cold and subsequently extracted the subset of common changes that were also present prior to the cold shift at 20°C. We decided to take into account the obvious variation 40S SSU and 60S LSU abundances among the ribosome fractions and among the four analyzed sample pools. To normalize the 60S and 60/80S fractions, we divided the abundance of the single observed proteins in each fraction to the abundance sum of all 60S RPs from the respective fraction. The 30S/40S fractions were normalized separately by the sum of all detected 40S RPs. The normalization enabled analyses of compositional changes of cytosolic RPs and co-purified non-ribosomal proteins in the non-translating SSU and LSU fractions. We analyzed increases and decreases in the mutants relative to the Col-0 wild type by $\log_2$-fold changes ($\log_2$-FC) (**Fig. 4-9 to 4-11**). The presence of a protein in a mutant sample and absence in corresponding Col-0 wild type rated as accumulation (+), absence in the mutant and presence in Col-0 as decrease (-).

As to general observations, DS1 and DS2 differed in complexity. DS1 yielded a more complex data set with 2820 compared to 1675 detected proteins in DS2 (**Supplemental Table S4-5**). The number of detected cytosolic RPs and RP paralogs was, however, almost equal, 175 in

DS1 and 174 in DS2 (**Supplemental Table S4-6**). The experiments shared 162 cytosolic RPs and RP paralogs of in total 1485 common proteins. The detection of cytosolic RPs was mostly paralog specific or represented RP families with identical amino acid sequences. Twenty-six (DS1) and 21 (DS2) cytosolic RPs lacked paralog specificity (**Supplemental Table S4-6**). Our analysis did not differentiate splice variants. In agreement with the cold-sensitivity of the mutants, we found more shared changes of normalized protein abundances in the cold than prior to cold shift. Most of the observed changes were larger in magnitude in DS1 (*reil1-1 reil2-2*) than in DS2 (*reil1-1 reil2-1*). The current experiments, however, do not allow attributing these observations to differences between the two mutants or to a potential slight difference between their respective recovery kinetics after cold shift (**Fig. 4-2**).

4.4.8 60S RPs and RP Paralogs Differentially Accumulate in Non-Translating 60S Fractions of *reil* Double Mutants

We selected 61 proteins with shared increases (36) or decreases (25) at 10°C in the non-translating 60S fractions of *reil* double mutants (**Supplemental Table S4-7A**). Co-purified proteins with an abundance maximum in the 50S fraction were removed from our selection of 60S compositional changes. Most observed changes were below 2-fold. Eight proteins increased consistently at 10°C and 20°C, seven decreased. The remaining 46 proteins changed in part inversely at 20°C in both *reil* double mutants (15), were not detectable at optimized temperature or differed at optimized temperature between mutants (**Supplemental Table S4-7A**).

The majority of the selected proteins were structural cytosolic RPs (45) that either increased (20) or decreased (25) relative to the sum of abundances of all detected 60S RPs. RPL3A (AT1G43170), RPL10aB (AT2G27530), RPL12C (AT5G60670), and RPL30C (AT3G18740) increased consistently in the *reil* double mutants, RPL3B (AT1G61580), RPL7aB (AT3G62870), RPL13aD (AT5G48760), RPL24B (AT3G53020), RPL26A (AT3G49910), RPL37aC (AT3G60245) decreased (**Fig. 4-9**). The 61 changes comprised cytosolic RPs that are assembled in the nucleus and RPs that are added or exchanged within the cytosol, such as, already mentioned RPL24B (AT3G53020) of the eL24 family and RPL10A (AT1G14320) and RPL10C (AT3G11250) of the uL16 family, RPP0B (AT3G09200) and RPP0C (AT3G11250) of the uL10 P-stalk family or RPP1A (AT1G01100), RPP1B (AT4G00810), RPP1C (AT5G47700), RPP2D (AT3G44590) of the P1/P2 P-stalk protein family (**Fig. 4-9, Supplemental Fig. S4-8,**

Supplemental Table S4-7A). RPP1A, RPP1B, RPP1C and RPP0B decreased at 10°C and increased at 20°C relative to wild type (**Fig. 4-9, Supplemental Fig. S4-8**).

Gene code	RP Name	RP Family	log_2 (*reil1.1 reil2.1* /Col-0) 10°C (DS2)	log_2(*reil1.1 reil2.2* /Col-0) 10°C (DS1)	log_2(*reil1.1 reil2.1* /Col-0) 20°C (DS2)	log_2(*reil1.1 reil2.2* /Col-0) 20°C (DS1)
60S LSU						
AT4G27090	RPL14B	eL14	0.47	0.22	-0.74	-0.40
AT3G14600	RPL18aC	eL20	-1.27	-0.36	0.13	0.24
AT3G53020	RPL24B	eL24	-0.54	-1.04	-0.64	-1.25
AT3G18740	RPL30C	eL30	1.06	0.68	0.51	0.39
AT1G41880	RPL35aB	eL33	-0.21	-0.76	0.66	1.40
AT3G60245	RPL37aC	eL43	-1.46	-0.32	-0.58	-0.40
AT3G62870	RPL7aB	eL8	-0.80	-0.45	-0.12	-0.45
AT1G01100	RPP1A	**P1/P2**	-0.22	-0.52	0.51	0.60
AT5G47700	RPP1C	**P1/P2**	-0.73	-0.49	0.16	0.63
AT4G00810	RPP1B	**P1/P2**	-0.19	-0.33	+	0.10
AT2G27530	RPL10aB	**uL1**	0.26	0.60	0.13	0.13
AT1G08360	RPL10aA	**uL1**	0.58	1.72	-0.31	-0.85
AT5G22440	RPL10aC	**uL1**	-0.30	-0.81	0.15	0.06
AT3G09200	RPP0B	uL10	-0.32	-1.10	0.63	0.82
AT5G60670	RPL12C	uL11	0.90	1.09	0.37	0.22
AT5G48760	RPL13aD	uL13	-0.30	-0.78	-0.37	-0.15
AT3G25520	RPL5A	uL18	0.32	1.09	-0.03	-0.22
AT5G67510	RPL26B	**uL24**	0.47	+	-1.43	-0.71
AT3G49910	RPL26A	**uL24**	-0.28	-0.37	-0.12	-0.08
AT1G43170	RPL3A	**uL3**	0.17	0.23	0.26	0.02
AT1G61580	RPL3B	**uL3**	-	-2.03	-1.44	-0.92
AT2G01250	RPL7B	**uL30**	-0.09	-0.11	0.49	0.18
AT2G44120	RPL7C	**uL30**	-0.56	-0.90	0.48	0.23
AT4G10450	RPL9D	uL6	-0.92	-0.40	0.09	0.62
40S SSU						
AT5G61170	RPS19C	**eS19**	-1.34	-0.12	0.70	0.36
AT3G02080	RPS19A	**eS19**	0.53	2.00	0.42	1.16
AT3G53890	RPS21B	eS21	-0.09	-1.80	-0.41	-0.23
AT3G04920	RPS24A	eS24	0.52	0.55	0.24	0.49
AT2G21580	RPS25B	**eS25**	0.50	+	-0.30	-1.03
AT4G39200	RPS25E	**eS25**	0.56	+	0.07	0.34
AT5G03850	RPS28B	eS28	0.62	+	-0.92	-0.41
AT5G02960	RPS23B	uS12	-0.15	-0.31	0.88	1.08
AT4G09800	RPS18C	uS13	0.32	0.71	-0.04	-0.15
AT1G04270	RPS15A	uS19	0.48	+	+	0.26
AT1G72370	RPSaA	uS2	0.03	1.78	-0.90	-0.38

Figure 4-9. Changes of RP composition in the non-translating 60S LSU and 40S SSU fractions of the *reil1 reil2* double mutants 7 days after shift to 10°C and prior to cold shift at 20°C. This selection shows RPs with responses shared between *reil1-1 reil2-1* (DS2) and *reil1-1 reil2-2* (DS1) at 10°C and 20°. Log_2-fold changes between mutants and Col-0 wild type were calculated after normalization of RP LFQ-abundances by the abundance sums of all detected 60S RPs in the respective fraction and combined across the 60S and 60S/80S fractions (top) or by the abundance sums of all detected 40S RPs in the 30S/40S fractions (bottom). Presence relative to absence in Col-0 and log_2-fold increases > 1 are color-coded red, increases < 1 are coded light red. Absence relative to presence in Col-0 and log_2-fold decreases < -1 are color-coded blue, decreases > -1 are coded light blue.

4.4.9 Homologs of Yeast 66S Pre-Ribosome Constituents and 60S Biogenesis Factors Accumulate in Non-Translating 60S Fractions of *reil* Double Mutants

The sixteen non-structural cytosolic RPs among the set of 61 differentially accumulating proteins were with two exceptions, namely a root tip expressed LEA protein (AT5G60530) and a R3H domain protein (AT1G03250), homologs of yeast 60S biogenesis factors and 66S pre-ribosome constituents (**Fig. 4-10**). We found the homologs of yeast TIF6, NMD3, RLP24, NOP7, NOG1, NOG2 (alias NUG2), RPF2, NSA2, MAK16, RSA4, CIC1 (alias NSA3), EBP2, HAS1 and YTM1. All accumulated in the non-translating 60S fractions at 10°C. The TIF6-, NMD3- and RLP24-homologs and the R3H domain protein accumulated in addition at 20°C. Next to yeast NOP7, the biogenesis factors, yeast TIF6, NOG1, MAK16, HAS1, EBP2, NSA2, CIC1, YTM1 and RLP24 are non-ribosomal proteins that are associated with 66S pre-ribosomes that can be NOP7 affinity-purified (Harnpicharnchai et al., 2001; Kater et al., 2017). The remaining NMD3, NOG2, RPF2, RSA4 are part of other pre-60S ribosome complexes. In detail and again assuming basic homology of plant and yeast 60S biogenesis, NMD3 is a nuclear export adaptor of pre-60S subunits that is part of a pre-60S ribosome carrying TIF6, LSG1 and the yeast REI-homolog, REH1 (Ma et al., 2017). Like TIF6, RLP24 and NOG1, NMD3 is released from pre-60S ribosomes in the final cytosolic maturation steps and recycled (Ho et al., 2000, Greber et al., 2016). NOG2 (alias NUG2) precedes NMD3 binding to pre-60S ribosomes at overlapping binding sites prior to nuclear export (Matsuo et al., 2014). RSA4 is present on NOG2 associated particles and co-substrate of the REA1 remodeling factor that is required for NOG2 release from pre-60S ribosomes (Matsuo et al., 2014). Finally, NOG2 (Gamalinda et al., 2013) associates with pre-60S ribosomes already in the nucleolus and together with NSA2 is thought to be part of a 66SB pre-ribosome and required for 27SB pre-rRNA processing into 25S rRNA (Gamalinda et al., 2013). Similarly, RFP2 (Morita et al., 2002) predominantly localizes to the nucleolus, associates with 66S pre-ribosomes by an alternative recruiting pathway and is also required for 27SB pre-rRNA processing (Gamalinda et al., 2013). HAS1 is RNA helicase that takes part in both small and large ribosomal subunit biogenesis (Gnanasundram et al., 2019). HAS1 is present in yeast 90S pre-ribosomes and has multiple binding sites in the 18S rRNA and the 5.8S and 25S rRNAs and remains associated with pre-40S and pre-60S complexes (Gnanasundram et al., 2019). We, however, detected the plant homolog of HAS1 only in non-translating 60S fractions of the cold-exposed *reil* double mutants (**Supplemental Table S4-7A**).

A

Gene code	Yeast homolog	Name	log_2 (*reil1.1 reil2.1* /Col-0) 10°C (DS2)	log_2(*reil1.1 reil2.2* /Col-0) 10°C (DS1)	log_2(*reil1.1 reil2.1* /Col-0) 20°C (DS2)	log_2(*reil1.1 reil2.2* /Col-0) 20°C (DS1)
AT2G24500	REI1/REH1	REIL2	-	NA	-	NA
AT2G03820	NMD3	NMD3	1.44	0.66	1.01	2.60
AT3G55620	TIF6	eIF6A	0.11	1.81	0.34	0.72
AT2G44860	RLP24	RPL24C	2.51	3.91	3.11	+
AT5G15550	YTM1	ATPEP2	+	1.35	NA	+
AT3G58660	CIC1 (alias NSA3)	-	0.82	1.64	NA	+
AT3G23620	RPF2	ARPF2	0.43	1.81	-1.02	3.56
AT5G06360	NSA2	-	0.62	1.95	-0.96	+
AT5G14520	NOP7	PES	1.14	2.36	-	+
AT1G50920	NOG1	ATNOG1-1	1.93	2.43	-0.72	3.81
AT1G52980	NOG2 (alias NUG2)	ATNUG2	0.26	2.76	NA	3.51
AT5G52820	RSA4	ATNLE1	+	3.10	NA	+
AT1G23280	MAK16	MAK16-related	+	4.06	NA	+
AT3G22660	EBP2	EBP2	+	+	NA	+
AT3G18600	HAS1	-	+	+	NA	NA
AT1G03250	-	R3H-protein	2.55	+	+	+
AT5G60530	-	LEA-protein	+	+	NA	NA

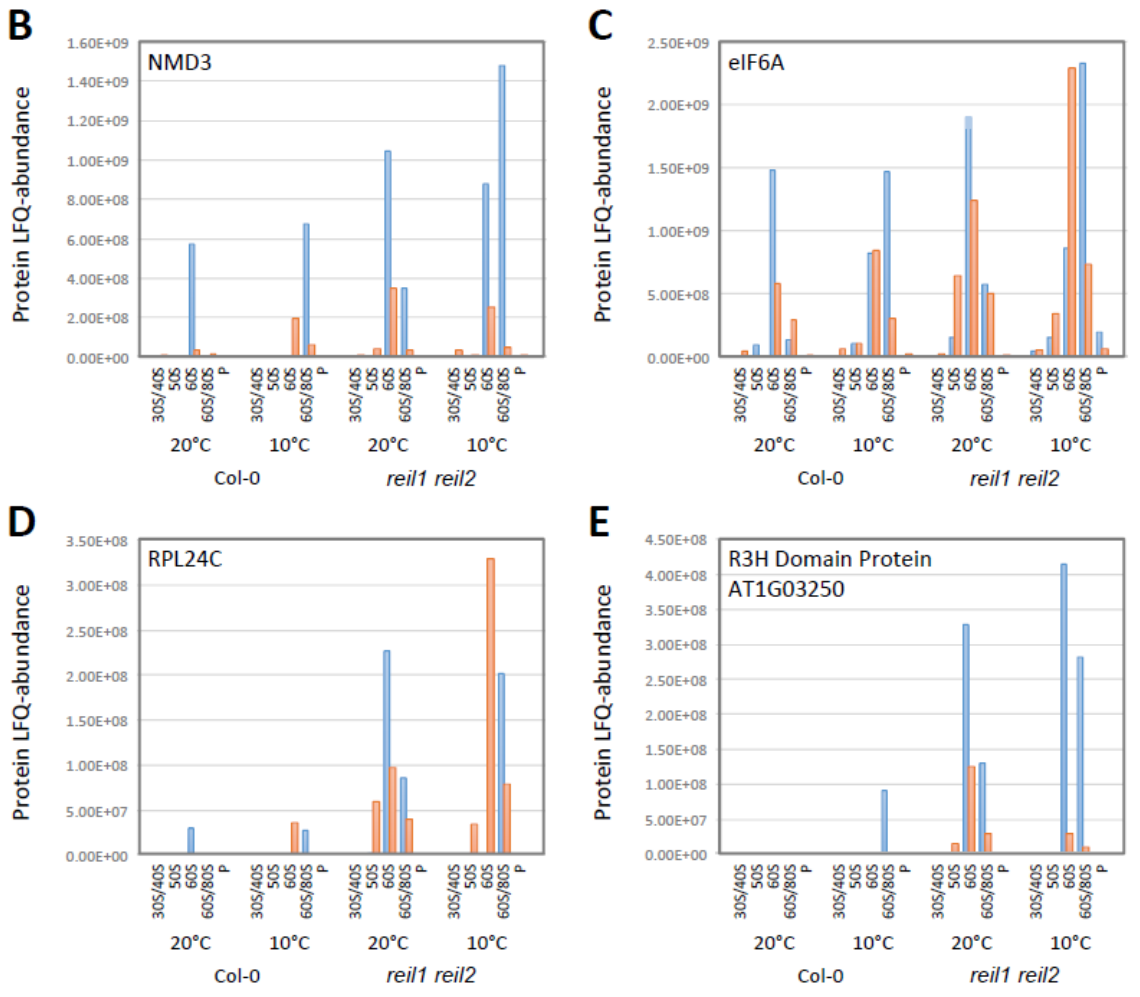
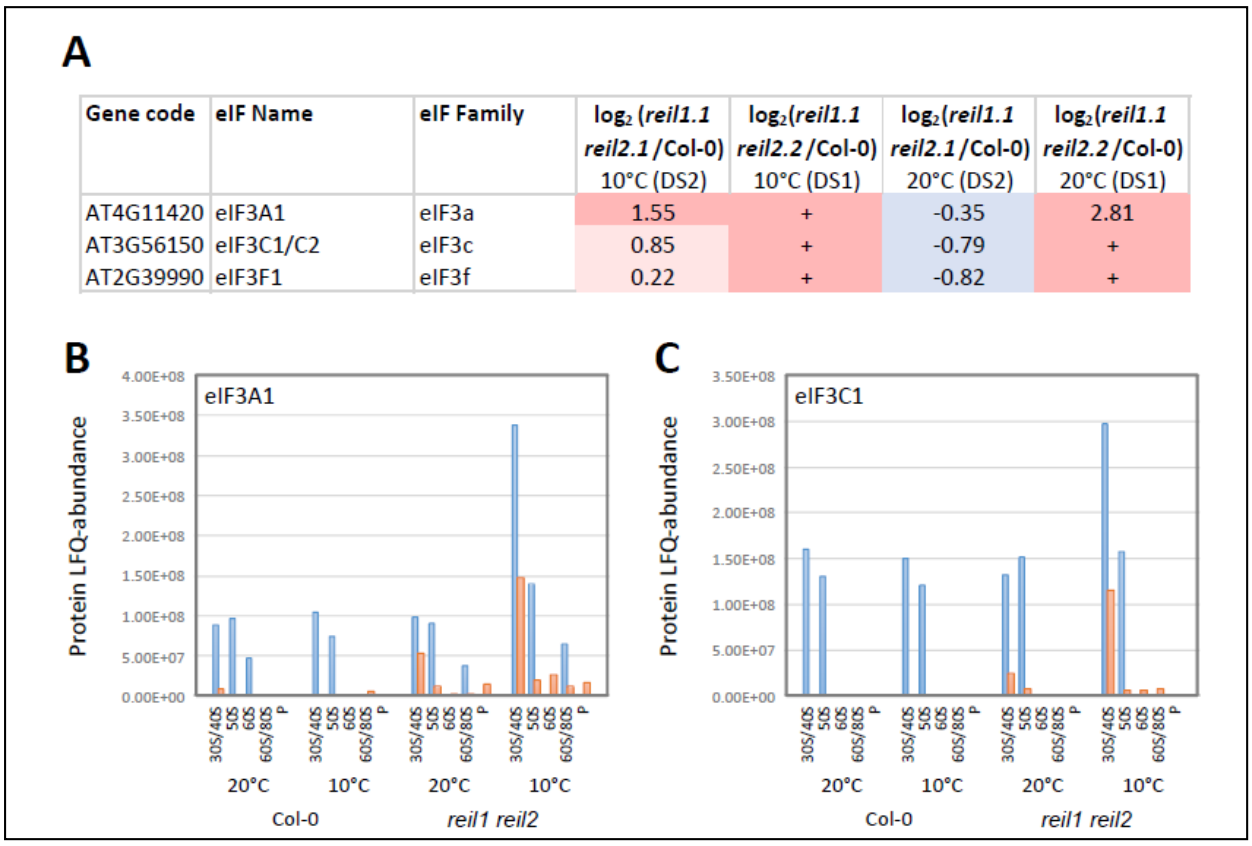


Figure 4-10. Changes of the composition of ribosome associated proteins in the non-translating 60S fractions of the *reil1 reil2* double mutants 7 days after shift to 10°C and prior to cold shift at 20°C.
(A) REIL2 and the shared changes at 10°C between *reil1-1 reil2-1* (DS2) and *reil1-1 reil2-2* (DS1). Log_2-fold changes between mutants and Col-0 wild type were calculated after normalization of protein LFQ-abundances by abundance sums of all detected 60S RPs and combined across the 60S and 60S/80S fractions. Presence in mutants relative to absence in Col-0 and log_2-fold increases > 1 are color-coded red, increases < 1 are light red. Absence relative to presence in Col-0 and log_2-fold decreases < - 1 are color-coded blue, decreases > -1 are light blue. Absence in both mutant and Col-0 is color-coded grey and indicated by NA (not available).
(B, C, D, E) LFQ-abundance distributions of NMD3, eIF6A, RPL24C, and R3H domain Protein AT1G03250 across the sampled ribosome fractions and analyzed conditions, DS1 orange, DS2 blue. Note the abundance maxima of the proteins in the non-translating 60S and 60/80S fractions.

4.4.10 40S RPs and Eukaryotic Translation Initiation Factors Differentially Accumulate in Non-Translating 40S Fractions of *reil* Double Mutants

In comparison to the moderate number of highly specific ribosome and ribosome associated proteins (RAPs) that differentially accumulated in non-translating 60S fractions, we detected 146 proteins with shared increases (135) or decreases (11) at 10°C in the non-translating 40S fractions of the *reil* double mutants (**Supplemental Table S4-7B**). Only 21 of the selected proteins were structural cytosolic RPs that either increased (12) or decreased (9) relative to the sum of abundances of detected 40S RPs. The majority of selected proteins were co-purified proteins, e.g. 2 organelle 30S RPs, 3 nitrilases, 4 heat shock proteins, 6 components of the proteasome, 10 components of ATP synthases and a multitude of enzymes. We concluded that these observations may be relevant, but are likely not linked to the non-translating 40S fraction. RPS24A (AT3G04920), RPS19A (AT3G02080), RPS25E (AT4G39200), and RPS15A (AT1G04270) increased consistently in the *reil* double mutants, RPS21B (AT3G53890) decreased (Fig. 9). Six additional 40S RPs changed inversely. Besides changes of structural 40S RPs, we found, at 10°C, accumulation of eIF3A1 (AT4G11420), eIF3C1 (AT3G56150), and eIF3F1 (AT2G39990) in the non-translating 40S fraction of both double mutants (**Fig. 4-11**). Detection of eIF3C1 (AT3G56150) included minority contribution by two of 16 (DS1) or one of 22 peptides (DS2) of eIF3C2 (At3g22860) (**Supplemental Table S4-6**). These selected translation initiation factors are a subset of the ten detected components of the 13-subunit plant eukaryotic translation initiation factor 3 (eIF3) (Browning et al., 2001). eIF3 is part of the 43S and 48S pre-initiation complexes and exits upon joining of the 60S subunit (Browning and Bailey-Serres, 2015).



Gene code	eIF Name	eIF Family	log₂ (*reil1.1 reil2.1* /Col-0) 10°C (DS2)	log₂(*reil1.1 reil2.2* /Col-0) 10°C (DS1)	log₂(*reil1.1 reil2.1* /Col-0) 20°C (DS2)	log₂(*reil1.1 reil2.2* /Col-0) 20°C (DS1)
AT4G11420	eIF3A1	eIF3a	1.55	+	-0.35	2.81
AT3G56150	eIF3C1/C2	eIF3c	0.85	+	-0.79	+
AT2G39990	eIF3F1	eIF3f	0.22	+	-0.82	+

Figure 4-11. Changes of the composition of translation initiation factor 3 proteins in the non-translating 40S fraction of the *reil1 reil2* double mutants 7 days after shift to 10°C and prior to cold shift at 20°C.
(A) Shared changes at 10°C between *reil1-1 reil2-1* (DS2) and *reil1-1 reil2-2* (DS1). Log_2-fold changes between mutants and Col-0 wild type in the 30S/40S fractions were calculated after normalization of protein LFQ-abundances by abundance sums of all detected 40S RPs. Presence in mutants relative to absence in Col-0 and log_2-fold increases > 1 are color-coded red, increases < 1 are light red. Absence relative to presence in Col-0 and log_2-fold decreases < -1 are color-coded blue, decreases > -1 are light blue.
(B) Distribution of eIF3A1 LFQ-abundances across the sampled ribosome fractions and analyzed conditions, DS1 orange, DS2 blue.
(C) Distribution of eIF3C1 LFQ-abundances across the sampled ribosome fractions and analyzed conditions, DS1 orange, DS2 blue.
Note the abundance maxima in the 30/40S fractions that may contain 40S subunits and 43S pre-initiation complexes.

4.4.11 Association of Differential Accumulation of RPs and RAPs in Non-Translating 40S and 60S Fractions of *reil* Double Mutants with Differential Gene Expression

With few exceptions, the differential accumulation of RPs in non-translating 40S and 60S fractions and the changes of ribosome biogenesis factors or eIF3 components in these fractions did not correlate with respective changes in transcript levels. We attempted to correlate differential accumulation of RPs in non-translating 40S and 60S fractions of *reil* double mutants from experiments DS1 and DS2 with differential accumulation of their transcripts at 20°C prior to cold

shift and at 7 days after shift to 10°C (**Supplemental Fig. S4-9A-B, E-F**). In addition, we tested for time-shifted correlation of differential protein accumulation at 7 days after cold shift with preceding differential gene expression at 1 day after the shift (**Supplemental Fig. S4-9C-D**). With few exceptions, differential protein accumulation was not generally associated with changes of gene expression. However, the consistent decrease of RPL3B (AT1G61580) gene expression (**Fig. 4-7C**) before and after cold shift, average $\log_2$-FC = -1.03, $P = 1.15\ 10^{-7}$ (genotype effect of 2-way ANOVA), matched to consistent reduction of RPL3B protein in the non-translating 60S fraction of the two *reil* double mutants, experiments DS1 and DS2 (**Fig. 4-9**). In addition, consistent slight increase of RPL24C (AT2G44860) gene expression, average $\log_2$-FC = 0.24, $p = 1.43x10^{-2}$ (genotype effect of 2-way ANOVA), matched to consistent increase of RPL24C protein in the non-translating 60S fraction of the two *reil* double mutants.

4.5 Discussion

4.5.1 The Mixotrophic *in vitro* Cultivation System: Requirements and Biases

We validated through this study the function of Arabidopsis REIL proteins as ribosome biogenesis factors of eukaryotic plant ribosomes. Our previous studies of REIL function in rosette leaves (Beine-Golovchuk et al., 2018) indicated that analyses of eukaryote ribosome complexes from leaf material were in part masked by almost equally abundant chloroplast ribosomes. Using root material, the organelle interference of UV-absorbance traces from density gradient separations of plant ribosome complexes was negligible (**Fig. 4-1**). Plastid and mitochondrial ribosomes co-purified from root material, but the prokaryote-type ribosome complexes were according to our proteome analyses on average more than 100-fold less abundant than eukaryote ribosome complexes (**Supplemental Fig. S4-7**, **Supplemental Table S4-5**). The choice of root material thus enabled relative and correlative quantification of eukaryote ribosome complexes (**Fig. 4-2** and **4-3**). These analyses were not possible previously using leaf material (Beine-Golovchuk et al., 2018). Analyses of ribosomes complexes required amounts of ~100 mg (FW) tissue (Beine-Golovchuk et al., 2018). Our axenic in vitro cultivation system (**Supplemental Fig. S4-1**) delivered required amounts of root tissue from plants that had developmental stage, ~1.10 (Boyes et al., 2001). Our current study confirmed *reil* gene expression in Col-0 wild type roots under our mixotrophic hydroponic cultivation conditions and strong reduction of expression of both genes in *reil* double mutants (**Supplemental Fig. S4-5**). Recent promoter GUS studies confirmed constitutive *reil2*

expression throughout Arabidopsis seedlings under similar in vitro conditions and revealed relevance of REIL2 in the root organ by demonstrating high expression in the root tip (Yu et al., 2020).

The previously reported delay of *reil* mutant development and growth in the cold attenuated using our cultivation system (**Supplemental Fig. S4-2** and **S4-3**). We did not adjust temperature settings to achieve previous phenotypic strength. Instead, we used the phenotype-attenuating settings to minimize pleiotropic effects that may arise due to differential development of mutants and wild type (**Supplemental Fig. S4-2**). We maintained comparability with our previous analyses of soil grown Arabidopsis rosettes (Schmidt et al., 2013; Beine-Golovchuk et al., 2018) by selecting stage ~ 1.10 plants to perform temperature shift experiments.

We did not succeed, however, in avoiding the bias of mixotrophic cultivation. Mutant plants stayed dwarfed and flowered early even at optimized temperature without addition of sucrose to the liquid cultivation medium. As consequence, we cultivated in the presence of sucrose, but need to consider that the sucrose supply will mask or distort endogenous carbohydrate dependent signals. In addition, the illumination of the root system and the high humidity of hydroponic cultivation may affect transcriptional responses, for example, the observations linked to high light and reactive oxygen species that we report (**Fig. 4-5A**).

We discovered a further potential developmental bias of our study. *Reil* mutations affected root architecture (**Supplemental Fig. S4-3**). The branching pattern of hydroponic root systems in *reil* single and *reil1 reil2* double mutants appeared changed. The functional link of REIL proteins to root development or root system architecture (Jung and McCouch, 2013) was supported further by functional enrichment analyses of differential gene expression. The *reil1 reil2* double mutants had altered transcript levels of genes belonging to developmental growth ontologies, specifically root morphogenesis, epidermis and trichoblast differentiation (**Supplemental Fig. S4-6**). These transcript changes between mutants and wild type became apparent already at optimizedcultivation conditions and preceded cold induced responses. Because our current cultivation system was not suited for detailed root morphology or root patterning studies, we did not pursue this aspect further and considered this effect negligible for our current study.

We previously reported premature transcriptional cold acclimation responses at optimized temperature of *reil1-1 reil2-1* rosette leaves from soil-cultivated plants (Beine-Golovchuk et al., 2018). An initial global differential gene expression analysis of shared significantly enriched GOs

between the non-acclimated *reil1 reil2* mutants and 7-days cold acclimated Col-0 appeared to confirm the triggering of premature transcriptional cold responses (**Fig. 4-5B-C**). The same comparison at single gene level, however, revealed an overlay of positively and negatively correlated transcriptional responses (**Fig. 4-5D-E**). Globally, premature responses to heat among the 138 genes of this ontology appeared to dominate over the cold responses of 263 genes, respectively, but neither cold acclimation nor heat acclimation responses were significantly enriched in the *reil1 reil2* double mutants prior to cold shift (**Fig. 4-5A**). Selected marker genes of cold acclimation and cold response were either not prematurely changed, e.g. *C-REPEAT/DRE BINDING FACTOR1/ DEHYDRATION-RESPONSIVE ELEMENT BINDING PROTEIN1B (CBF1/DREB1B), CBF2/DREB1C, CBF3/DREB1A, and VERNALIZATION INSENSITIVE 3 (VIN3),* or had reduced expression prior to cold shift, e.g. *COLD-INDUCED1 (KIN1)* and *KIN2* or *COLD-REGULATED15A (COR15A)* and *COR15BA* (**Supplemental Fig. S4-4**). Cold acclimation of Arabidopsis has a well characterized carbohydrate component, where acclimating plants accumulate, e.g. (Kaplan et al., 2004; Kaplan et al., 2007) and deacclimating plants rapidly reduce endogenous sugar levels (Pagter et al., 2017). Adaptations in photosynthetic carbon metabolism provide signals that are integral part of Arabidopsis cold acclimation, including post transcriptional and transcriptional changes to sucrose metabolism (Stitt and Hurry, 2002). In addition, photosynthesis-derived glucose is a regulator of TARGET OF RAPAMYCIN (TOR) signaling that is a component of Arabidopsis cold acclimation, e.g. (Xiong et al., 2013; Dong et al., 2019). Considering the biases of our root cultivation system and especially the masking of carbohydrate signals, we cautiously conclude that the *reil1 reil2* double mutants deregulate temperature responses in mixotrophic roots at optimized temperature.

4.5.2 REIL Deficiency Reveals Requirement for *de novo* Synthesis of Eukaryote Ribosomes After Cold Shift

Our current study confirmed and extended our previous observation that reil mutants delay accumulation of non-translating 60S LSUs after cold shift (Beine-Golovchuk et al., 2018). We demonstrated that the delay affects both, the non-translating 60S LSUs and 40S SSUs (Fig. 1-2). Shortage of non-translating free ribosome subunits was clearly transient and the balance of the abundances of non-translating large and small eukaryotic ribosome subunits was under tight control in plants (**Fig. 4-3**). We currently do not have evidence that control of this balance is

dependent on REIL function in Arabidopsis. Our observation of concomitant decrease of 40S SSUs in *reil* double mutants was unexpected, as the 40S SSU fraction increases in yeast *Δrei1* mutants, e.g. (Lebreton et al., 2006; Greber et al., 2016). Arabidopsis apparently has different control mechanisms to balance non-translating 40S and 60S subunits. However, our finding agrees with yeast data that show concomitant decreases of 40S SSUs and 60S LSUs in mutants that are defective in 60S structural RPs, whereas mutants defective in 40S structural RPs may accumulate high levels of 60S LSUs (Cheng et al. 2019).

We observed compensation responses of REIL deficiency that act both, before cold shift and after extended periods of cold (**Fig. 4-2** to **4-4**). All *reil* mutants over-accumulated baseline pools of non-translating 60S LSUs and 40S SSUs, when not immediately responding to cold shift. Mutants containing a defective reil2 gene depleted in addition the 80S fraction in the cold. In Arabidopsis, the 80S fraction, similar to yeast (Martin and Hartwell, 1970; Zylber and Penman, 1970), appears to be composed of translating and non-translating 80S ribosome monomers. Our KCl-sensitivity tests of the Arabidopsis 80S fraction and the poor correlation between 80S and non-translating 60S fractions indicated the heterogeneous nature of the 80S fraction (**Fig. 4-3** and **4-4**). Mainly for this reason, we did not analyze the ribo-proteome of the 80S fraction in this study.

The function of the two REIL paralogs was clearly not fully redundant. REIL1 deficiency can be compensated successfully under both optimized and low temperature conditions, but a compensation by over-accumulation of free subunits and slight deficiency after cold shift was observable (**Fig. 4-2A-D**). In contrast, REIL2 deficiency was compensated at optimized temperature, but compensation apparently failed in the cold. This was indicated by persistent depletion of the 80S fraction both in the *reil2* single mutants and in the *reil1 reil2* double mutants (**Fig. 4-2C).**

The requirement of *de novo* synthesis 902 in the cold is evident by slow recovery of ribosome complex abundances in the *reil* mutants. The time scale of 3-7 days after the shift is in agreement with previous reports of ribosome protein turnover in Arabidopsis (Li et al. 2017; Salih et al., 2019), where half-life of the ribosome population was approximately 3-4 days. Only RPP0D and the RACK1B and 1C paralogs were shorter lived with half-lives between 0.5 and 1.5 days (Salih et al., 2019). Induction of 40S and 60S RP transcripts after cold shift in the Col-0 wild type and compensatory enhanced and prolonged expression of these genes in *reil1 reil2* double mutants

indicate that Arabidopsis roots (**Figs. 4-6**, **4-7A**, **4-7B**) are prepared by transcript availability for ribosome *de novo* synthesis after cold shift. Rosette leaves provided similar observations, however, at larger amplitude (Beine-Golovchuk et al., 2018).

Compensational depletion of non-translating ribosome complexes in the *reil* mutants cannot be explained alone by 60S subunit shortage and deficient de novo ribosome biosynthesis. We propose that Arabidopsis maintains and controls pools of non-translating free 60S LSUs and 40S SSUs, likely under a tight and common control (**Fig. 4-3**) and in addition a pool of assembled, but non-translating 80S ribosomes. These translationally inactive pools of ribosome complexes recycle ribosome complexes and may serve as buffers that respond to changing translation demands (Uesono and Toh-e, 2002; Krokowski et al., 2011; van den Elzen et al., 2014). Such pools may save energy by harboring surplus extant ribosomes instead of initiating wasteful premature degradation. Such pools may fill, when translation demands are low and prepare for rapid responses to environmental cues without immediate need of comparatively slow de novo ribosome biosynthesis and assembly. Fluctuating temperature cues, such as investigated in this study, obviously alter translation demands.

4.5.3 Effects of REIL Deficiency on Translation Initiation

In yeast cells, Rei1 deficiency, similar to other mutations that limit the amount of 60S LSU subunits, is associated to the hallmark observation of so-called half-mer polysomes, e.g. (Parnell and Bass, 2009; Greber et al., 2016). Half-mers are polysome complexes with a stalled 40S preinitiation complex and one or more fully assembled translating 80S ribosomes bound to a single mRNA. Stalling of the preinitiation complex finds an obvious explanation through the lack of translationally competent 60S LSUs for translating 80S monomer assembly. Half-mer polysomesof yeast have 932 been detected by sucrose density gradient centrifugation (Parnell and Bass, 2009; Greber et al., 2016). In our sucrose gradient analyses, we found indications of accumulating half-mer polysomes in the *reil1 reil2* double mutants at 1-3 days after cold shift (**Fig. 4-1**), but this phenomenon did not persist after prolonged cold exposure (**Fig. 4-1**, **4-4**). Proteomic analysis demonstrated the presence of components of the eIF3 multi-protein complex (Burks et al., 2001) in the non-translating 40S fraction and in a subsequent fraction enriched for organelle 50S RPs. These observations likely indicate the presence of co-purified plant 43S and 48S preinitiation

complexes, respectively (**Fig. 4-11B-C**). Accumulation of eIF3 components in both cold acclimating *reil1 reil2* double mutants indicated accumulation mostly of stalled 43S preinitiation complexes after cold shift (**Fig. 4-11A-C**). The existence of half-mer polysome complexes in cold exposed *reil* double mutants were supported by the presence of eIF3A1 in the mutant low-oligomer polysome fraction in one of our analyses (**Fig. 4-11B**). We conclude that REIL protein deficiency can cause accumulation of Arabidopsis 43S preinitiation complexes and that half-mer polysomes can accumulate. These observations prove REIL function as a ribosome biogenesis factor by indicating lack of translationally competent 60S subunits in the cold.

At transcriptome level, we found evidence that reil deficiency feeds back constitutively onto gene expression of the eIF3C2 paralog. REIL deficiency specifically released the suppression eIF3C2 expression (**Fig. 4-8**) and largely did not affect expression of other constituents of the eIF3 complex. In our current study, the eIF3C2 protein was not selectively detectable with one of 22 or two of 16 detected peptides shared between the eIF3C1 and eIF3C2 paralogs (**Supplemental Table S4-6**). The amino acid eIF3C2 protein has an internally shortened N-terminal domain and lacks a large part of the C-terminus compared to the amino acid eIF3C1 paralog (Burks et al., 2001). It may be allowed to speculate that the eIF3C2 paralog competes with eIF3C1 in plant eIF3 complexes and/ or may have an inhibitory regulatory role that adjusts eIF3 abundance to availability of translationally competent 60S LSUs. Such a function may cause a sub-fraction of eIF3 not to bind to ribosomes, but a mechanistic explanation must currently remain elusive.

4.5.4 Effects of REIL Deficiency On Ribosome Biogenesis

The *reil1 reil2* mutants accumulate Arabidopsis homologs of yeast 60S and 66S ribosome biogenesis factors in the non-translating 60S fraction. Homologs of cytosolic biogenesis factors, NMD3, TIF6, RLP24 that are assembled within the nucleus and released in the cytosol before the 60S LSU becomes translationally competent accumulate before and after temperature shift (**Fig. 4-10A-E**). Nuclear ribosome biogenesis factors associate predominantly with the 66S pre-ribosome. These factors include proteins that block positions in the 66S complex which are later occupied by the cytosolic biogenesis factors in the 60S pre-ribosome. Nuclear ribosome biogenesis factors accumulated in the cold in both *reil* double mutants and only in one double mutant, *reil1-1 reil2-2* before cold shift (**Fig. 4-10A**). These observations indicate a heterogeneity between the

reil2 alleles that we currently have available or a non-controlled variation in our cultivation system at optimized temperature that currently eludes us.

We therefore conclude that REIL deficiency inhibits the release of Arabidopsis NMD3-, TIF6-, and RLP24-homologs and thereby slows down biogenesis of translationally competent 60S LSUs. We interpret accumulation of nuclear ribosome biogenesis factors as pile-up of precursor complexes caused by blocked cytosolic 60S maturation. We observe that the block of 60S maturation intensifies at low temperature (**Fig. 4-10**). Taken together the observations prove conserved REIL function as a cytosolic 60S biogenesis factors. In addition, we imply previously non-described plant proteins, namely a R3H-domain protein and a LEA-like protein that do not have apparent homology in yeast or humans beyond the conserved R3H-domain, to contribute to plant specific aspects of 60S biogenesis.

At transcriptome level, we find *NUC2*, but not *NUC1* gene expression constitutively activated. *NUC2* codes for one of the two antagonistic plant nucleolins and thereby provide a functional link to eukaryote ribosome biogenesis. Both, *NUC2* and *NUC1* expression is required for plant growth. NUC2 and NUC1 act as histone chaperons early in eukaryotic ribosome biogenesis. The nucleolins control rDNA variant expression by modulation of 45S rRNA transcription and/ or processing (Durut et al., 2014; Sáez-Vásquez and Delseny, 2019). *NUC2* expression is high in the root apical meristem, similar to our still enigmatic finding of *reil* dependent PISTILLATA deregulation in roots. Both nucleolins are expressed in root and leaf tissues, but *NUC2* transcripts accumulate more in root than in leaf and shoot tissue (Durut et al., 2014). Durut and co-authors (2014) conclude that NUC2 might bind nucleosomes to induce and/or maintain a repressive rDNA chromatin state. Building on the hypothesis that *NUC2* may act as a repressor (Sáez-Vásquez and Delseny, 2019), we may naively interpret our observation of deregulated *NUC2* expression as indication of feedback repression of the primary step of rRNA transcription in response to blocked 60S maturation. However, studies on *reil2* single paralog mutants suggest that the control of rRNA transcription may be negligible compared to feed back control of rRNA processing exerted downstream of the 35S rRNA precursor (Yu et al., 2020). Obviously, this control affected both of the two parallel terminal plant pre-rRNA processing pathways (Weis et al., 2015). Accumulation of pre-60S maturation factors confirmed stalling of nuclear 66S maturation complexes that contain partially processed rRNA.

4.5.5 REIL Deficiency Affects the RP Paralog Composition of Non-Translating 40S SSU and 60S LSU fractions

We discovered that REIL deficiency affects the paralog composition of non-translating ribosome subunits. Most of our observations are less than 2-fold changes (**Fig. 4-9**). Considering the composite nature of the 40S SSU and 60S LSU fractions that may contain both, recycled ribosome populations that were synthesized prior to cold shift and ribosome populations that are *de novo* synthesized in the cold, we were surprised by these observations that were consistent between the two *reil* double mutants.

One of the more obvious observations was the consistent decrease of RPL24B of the eL24 RP family in the non-translating 60S fractions of the *reil1 reil2* double mutants (**Fig. 4-9**). This phenomenon can be linked directly to the concomitant accumulation of the RPL24C (**Fig. 4-10**), the Arabidopsis homolog of the yeast RLP24 maturation factor that is a placeholder during pre-60S complex assembly and replaced in the cytosol to form translationally competent 60S LSUs (Greber et al., 2016). Competent 60S LSUs of yeast contain either yeast RPL24A or RPL24B. Similar to yeast, Arabidopsis REIL proteins appear to be required to facilitate or accelerate this exchange.

Two other 60S RP families are assembled onto the 60S subunit in the cytosol, uL10 and uL16 (Greber et al., 2016). Of these, we find RPP0B, uL10 family, to be consistently decreased at 10°C and inversely increased at 20°C in both *reil* double mutants (Fig. 4-9). RPP0B is one of the Arabidopsis paralogs that code for the P-stalk protein P0 that anchors the P-stalk to the ribosome (Krokowski et al., 2005; Krokowski et al., 2006; Mitroshin et al., 2016; Liljas and Sanyal, 2018). P0 interacts as a scaffold with other P-stalk proteins of the P1/P2 family, here represented by consistent abundance changes of Arabidopsis RPP1A, RPP1B and RPP1C (**Fig. 4-9**) and likely overall reduced abundance of RPP2D in the *reil* double mutants (**Supplemental Fig. S4-8A**). The fully assembled and active P-stalk substructure interacts with translation elongation factors and is required for translation.

Besides these changes of ribosome subunit composition that may be explained by lack of direct functions of the REIL biogenesis factors in the cytosol, we found temperature dependent and independent effects on the composition of structural ribosome proteins within the non-translating 40S SSU and 60S LSU (**Fig. 4-9**). Such composition changes must involve either an indirect REIL function that affects *de novo* subunit assembly in the nucleus or may involve RP

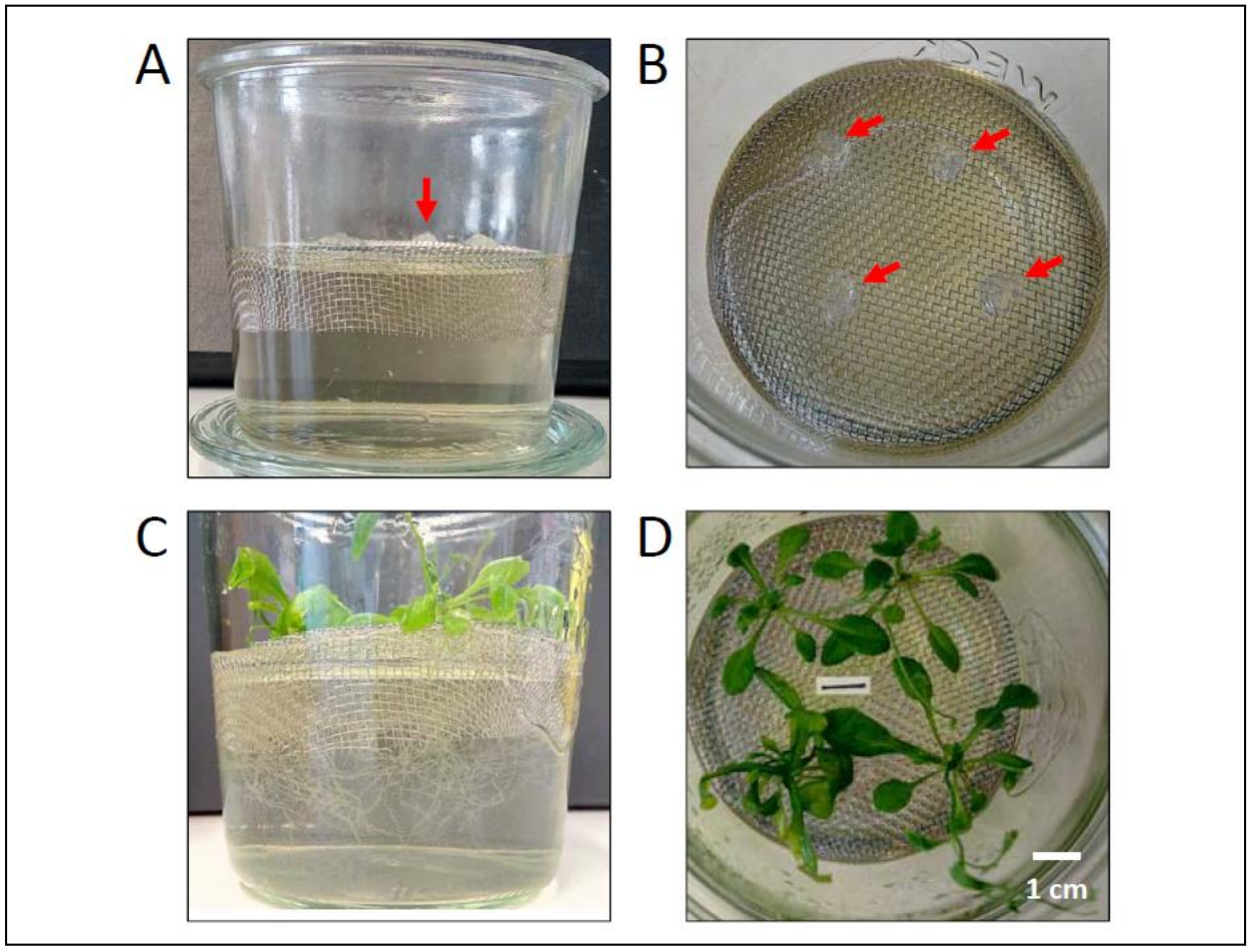
paralog exchange in assembled ribosome that pre-exist in the cytosol. Such a mechanism was previously proposed for *in situ* ribosome repair (Holt and Schuman, 2013). Among the many observations of compositional changes, we would like to highlight the effect on the uL3 family that is part of 60S LSUs (Kim et al., 1990). REIL proteins apparently are required to accumulate RPL3B paralogs in non-translating 60S fractions (**Fig. 4-9**). The slight accumulation of abundant RPL3A, an essential gene for Arabidopsis (Meinke, 2019), appears to compensate reduction of RPL3B in our study. In addition, RPL3B decrease in the absence of REIL proteins has a transcriptional component, as the reduction of RPL3B transcript is one of the rare observations of otherwise absent associations between transcriptome and proteome changes of non-translating fractions (**Supplemental Fig. S4-9**).

4.6 Conclusion

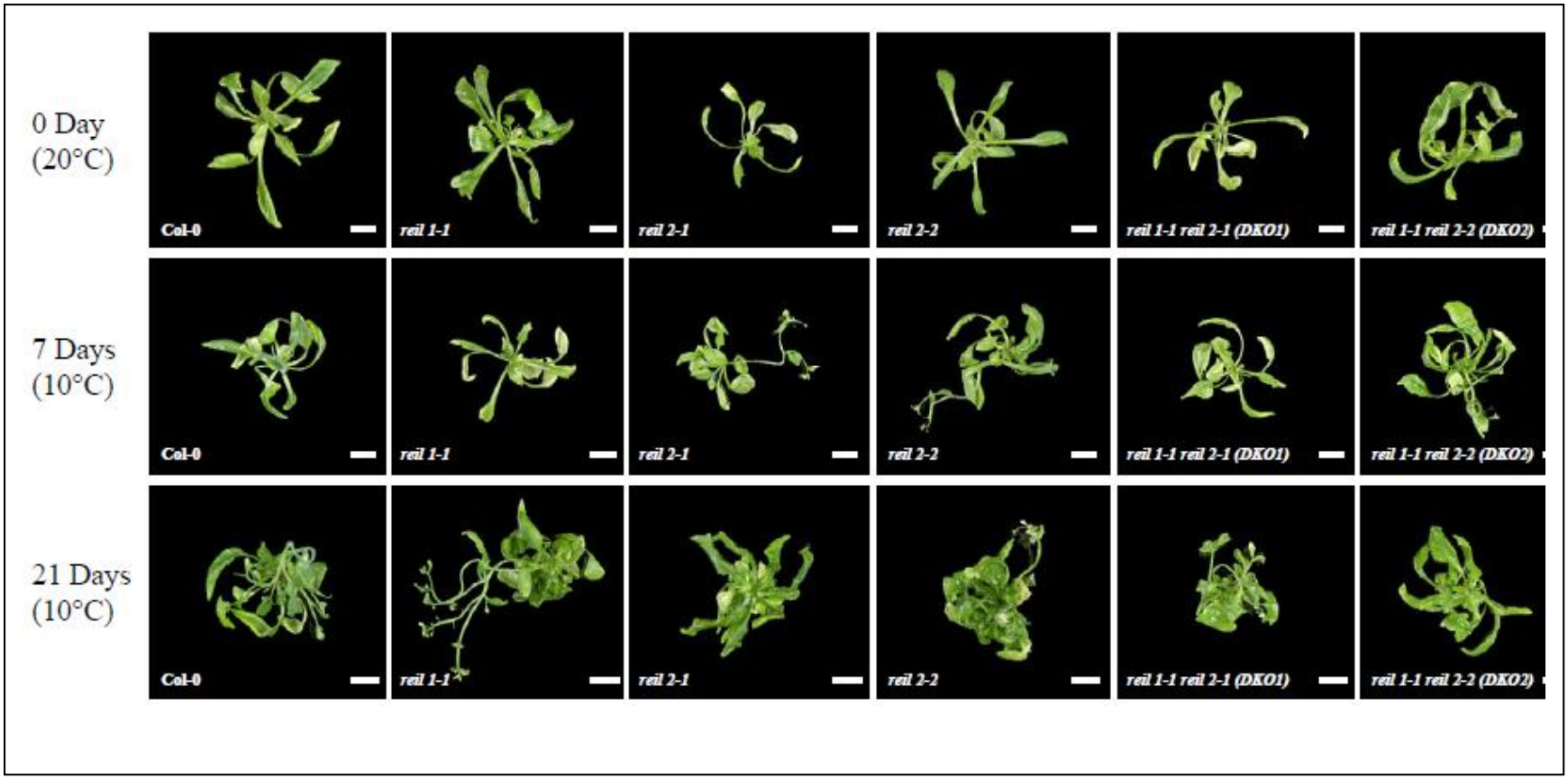
Our study proves that Arabidopsis REIL proteins function as cytosolic ribosome biogenesis factors and supports their role of accelerating ribosome *de novo* synthesis in the cold. Arabidopsis compensates for the lack of REIL function at optimized temperature, but cannot fully compensate in the cold. The compensation mechanisms accumulate non-translating pools of ribosome complexes and appear to activate pre-existing pools upon cold-shift. We hypothesize, that Arabidopsis controls non-translating ribosome complexes to buffer fluctuating demands on translation. Thereby Arabidopsis may limit the demand for de novo ribosome synthesis under rapidly changing environmental conditions. REIL function is mostly post-transcriptional, however, with a few obvious transcriptional components. REIL function feeds forward onto formation of 43S initiation complexes likely in a passive mode by modulating 60S LSU availability or more actively via *eIF3C2*, *NUC2* or RP gene expression and feedback onto nuclear pre-60S subunit assembly. Through disturbance of *de novo* ribosome biosynthesis and translation initiation, *reil* mutants allow the study of these processes and their control in plants. Unexpectedly, REIL function in Arabidopsis appears to control the paralog composition of non-translating 40S and 60S subunits. Considering paralog composition as one mechanism that may create heterogeneous functional ribosome populations (Xue and Barna, 2012; Simsek et al., 2017; Shi et al., 2017; Genuth and Barna, 2018), we propose that *reil* mutants and temperature acclimation cues may provide feasible and highly relevant experimental systems to study ribosome heterogeneity in plants.

4.7 Supplemental Figures

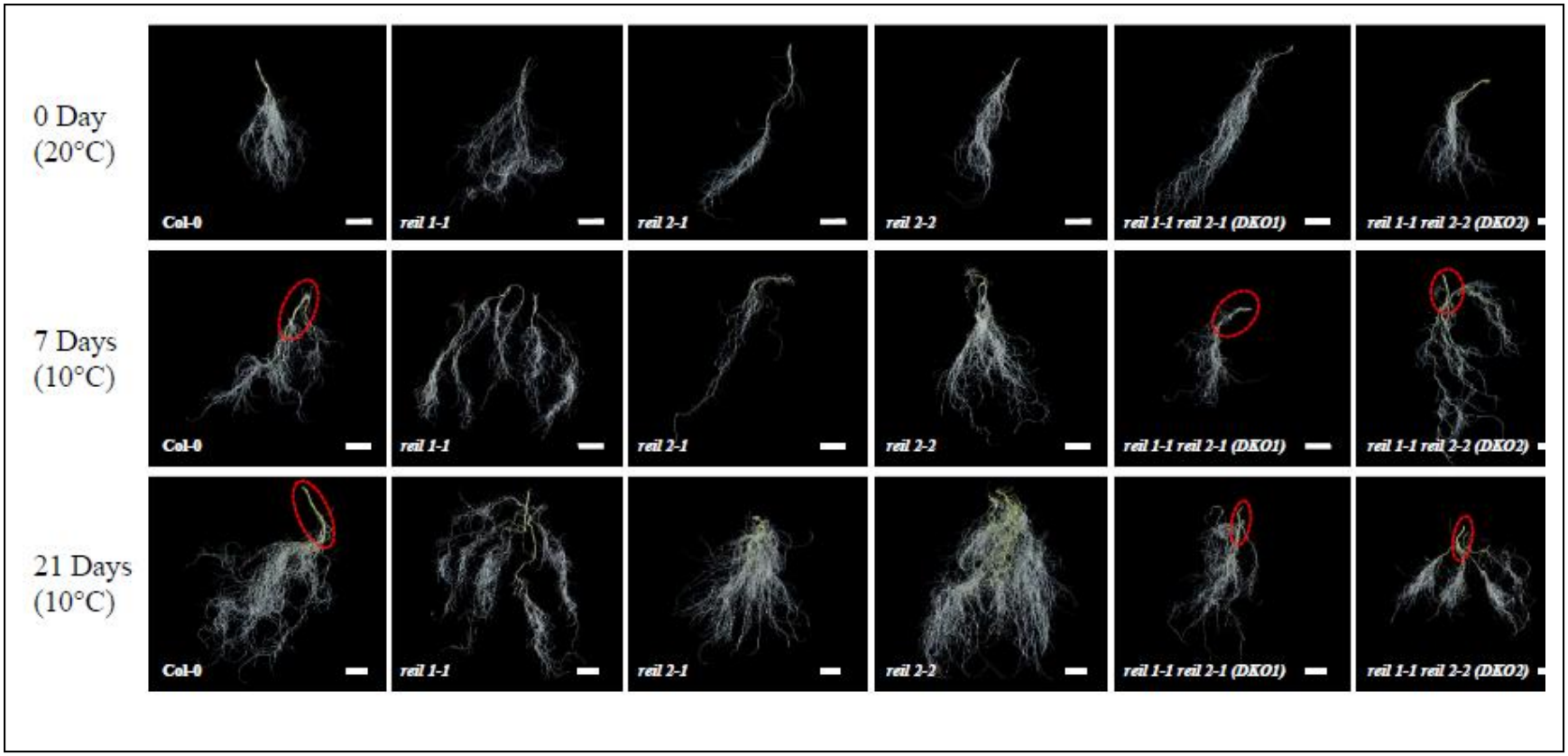
Supplemental Figures S4-1 to S4-9 are shown in this section, while the information for Supplemental Tables S4-1 to S4-7 can be found in the **Appendices**, **Appendix C: Supplemental Information for Chapter 4 (page 312).**



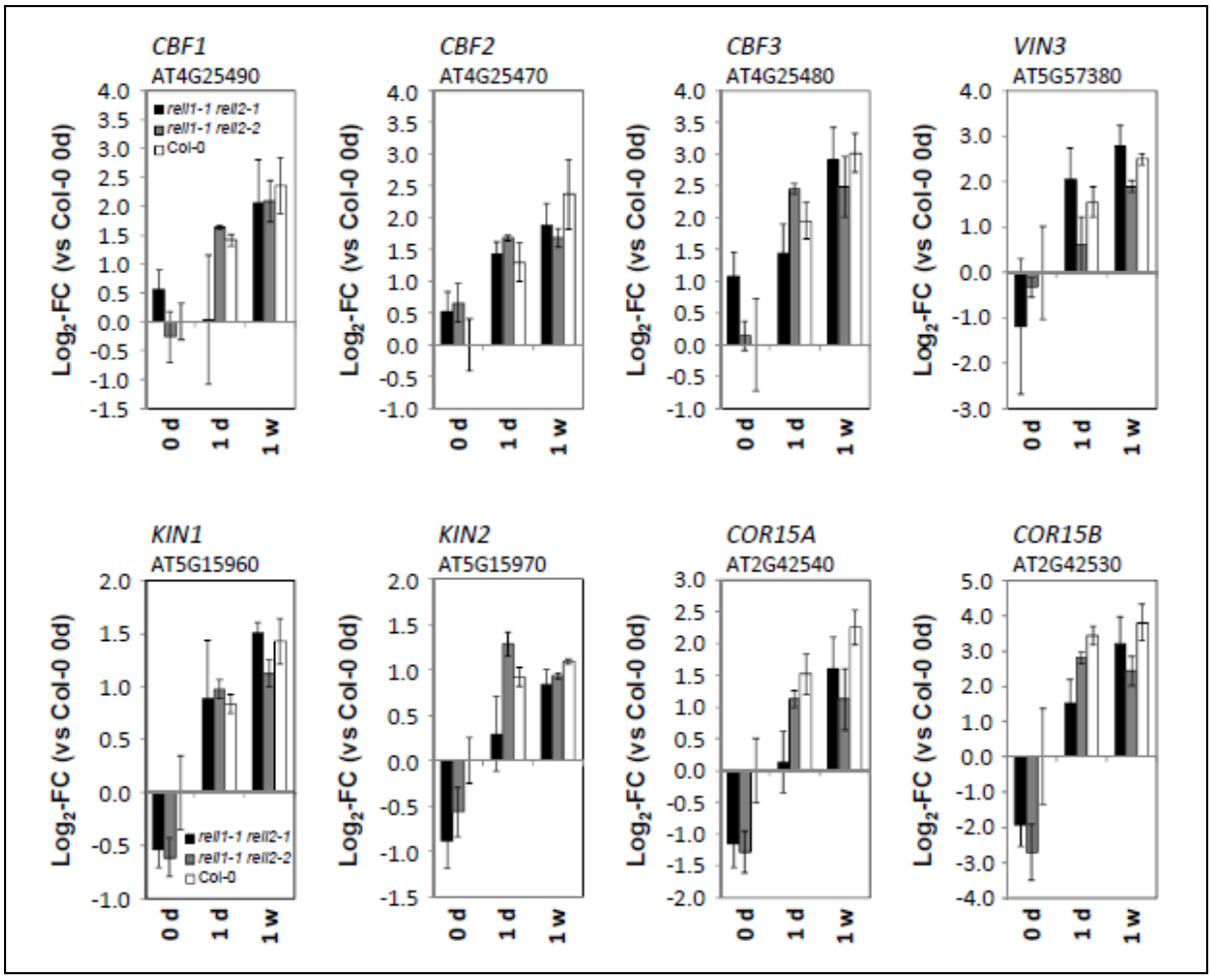
Supplemental Fig. S4-1. Hydroponic growth system of Arabidopsis thaliana Col-0 wild type and mutants. The system was feasible for temperature shift experiments in the vegetative phase and for rapid sampling of pooled material of whole root or shoot systems.
(A) Assembled growth system with stainless steel mesh adjusted level with the surface of ~ 250 mL liquid Murashige and Skoog-medium with 2% sucrose. One of the four agar blocks for seed germination is indicated (red arrow, view from the side).
(B) Assembled growth system with stainless steel mesh adjusted level with the surface of the liquid. The four agar blocks for seed germination are indicated (red arrows, view from the top). Each block contains a single seed.
(C) Assembled growth system with *Arabidopsis thaliana* Col-0 wild type plants at approximate ten-leaf stage after 4 weeks in 16 h/ 8 h long day conditions at 20°C during the day and 18°C during the night (view from the side).
(D) Assembled growth system with *Arabidopsis thaliana* Col-0 wild type plants at approximately ten-leaf stage (view from the top).
The clamped-on glass lids were opened and sterile conditions compromised for the photographs.



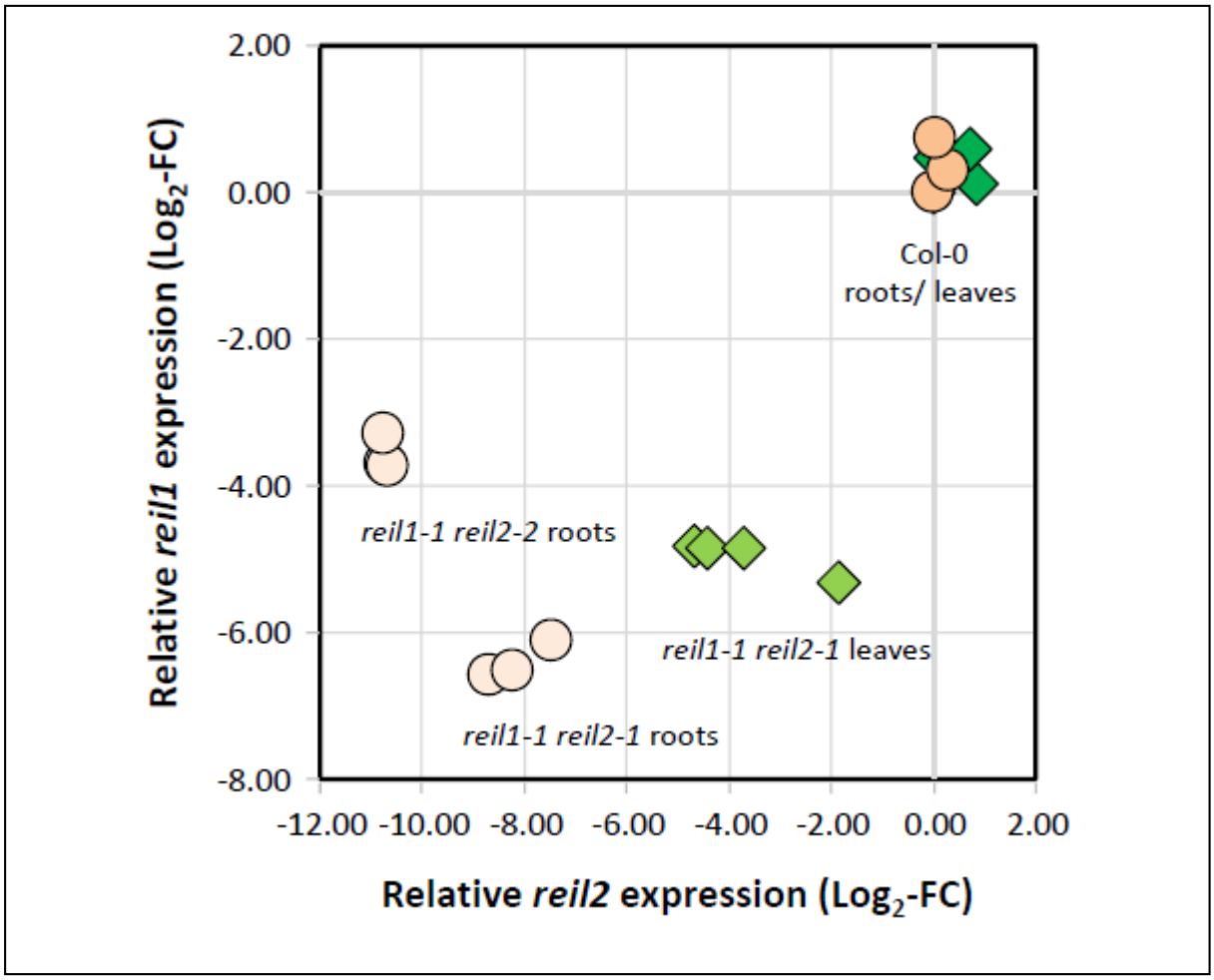
Supplemental Fig. S4-2. Exemplary documentation of shoot systems of hydroponically cultivated *Arabidopsis thaliana* wild type (Col-0), of the single mutants, *reil1-1*, *reil2-1*, *reil2-2*, and of the double mutants, *reil1-1 reil2-1* (DKO1) and *reil1-1 reil2-2* (DKO2), before (0 day) and 7 or 21 days after shift from 20°C (day)/ 18°C (night) to 10°C (day) and 8°C (night).
Note that at 21 days after cold shift shoots and inflorescences of *reil2-1*, *reil2-2*, and the double mutants, *reil1-1 reil2-1* (DKO1) and *reil1-1 reil2-2* (DKO2), are smaller than wild type and the *reil1-1* mutant. Growth of the double mutants did not arrest under the conditions of this hydroponic system. Cultivation was in liquid MS media with 2% sucrose (w/v) adjusted to pH 5.7 (Murashige and Skoog, 1962). All photographs were taken separately as indicated by vertical white bars. In parts, black background was added to the single sections of the graph for a regular and centered display of the shoot systems. All bars are 1 cm and indicate the slightly varying scales of single photographs.



Supplemental Fig. S4-3. Exemplary documentation of hydroponic root systems of *Arabidopsis thaliana* wild type (Col-0), of the single mutants, *reil1-1*, *reil2-1*, *reil2-2*, and of the double mutants, *reil1-1 reil2-1* (*DKO1*) and *reil1-1 reil2-2* (*DKO2*), before (0 day) and 7 or 21 days after shift from 20°C (day)/ 18°C (night) to 10°C (day) and 8°C (night). Roots were cut at the hypocotyl to root transition. Root systems of single plants were carefully prepared with minimal wounding from joined cultivations of four plants in single containers. Preparation of complete root systems from single plants was not possible. Photographs may therefore show in parts incomplete root systems. Note the shortened primary root of both double mutants at 7 and 21 days after cold shift compared to wild type (red circles). At 21 days after cold shift, the double mutants and *reil1-1* appeared less branched indicative of a possibly altered root branching pattern. Cultivation was in liquid MS media with 2% sucrose (w/v) adjusted to pH 5.7 (Murashige and Skoog, 1962). All photographs were taken separately as indicated by vertical white bars. In parts, black background was added to the single section of the graph for a regular and centered display of the root systems. All bars are 1 cm and indicate the slightly varying scales of single photographs.



Supplemental Fig. S4-4. Differential expression of selected cold responsive genes in the roots of Col-0, and the *reil1-1 reil2-1* and *reil1-1 reil2-2* double mutants at the non-acclimated state (0 day, 20°C) and shifted to 10°C cold for 1107 1 day or 7 days. Differential gene expression was determined relative to non-acclimated Col-0 at optimal temperature 20°C (means +/- standard error, n = 3). The genes belonged to GO term GO:0009409, response to cold, and in part to GO term GO:0009631, cold acclimation. Note that the marker genes indicate deregulation of cold marker gene expression in non-cold acclimated *reil* double mutant roots. Analysis of variance of each of the examples indicated a significant temperature effect ($p < 0.001$, 2 way-ANOVA) and no significant interaction with the mutant effect. The mutant effect was significant ($p < 0.05$, 2 way-ANOVA) in the cases of *KIN2*, *COR15A*, and *COR15B*.



Supplemental Fig. S4-5. Reduced transcript levels of the *reil 1* and *reil2* genes in the *reil1-1 reil2-1* and *reil1-1 reil2-2* double mutants. Root transcript data are of this study (Supplemental Table S4-2). Leaf transcript data are from soil grown rosette plants of *reil1-1 reil2-1* from a previous study (Supplemental Table S2 of Beine-Golovchuk et al., 2018). Log_2-transformed transcript data were normalized to the non-acclimated Col-0 wild type, i.e. log_2-fold changes (FC), of each transcriptome experiment, respectively. Roots (circles), leaves (diamonds).

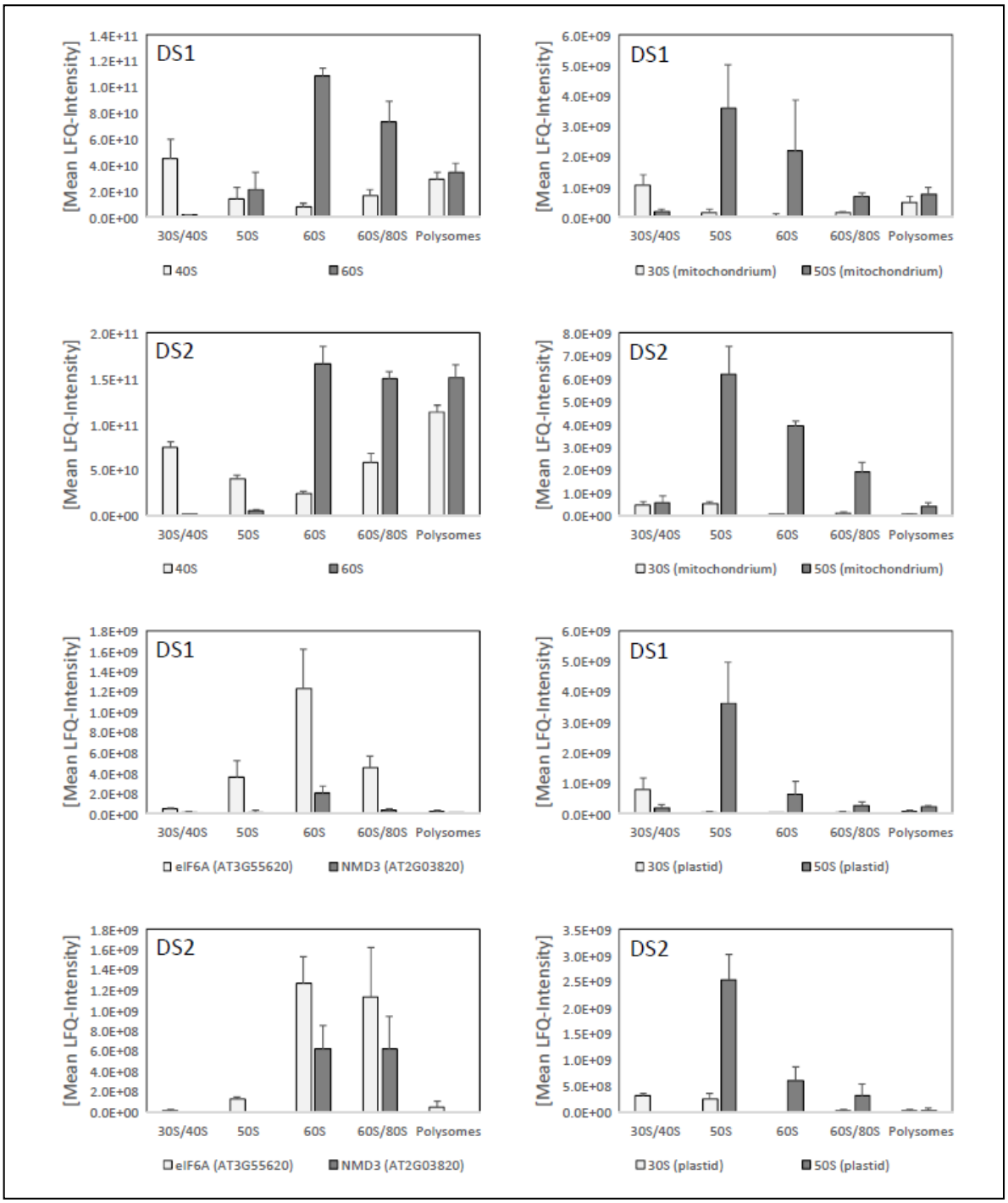
A

GO (Onthology)		Description	Genes	Col-0			*reil1-1 reil2-1*			*reil1-1 reil2-2*		
				0 d	1 d	1 w	0 d	1 d	1 w	0 d	1 d	1 w
GO:0048589	P	developmental growth	211		-0.08 *	-0.21 *	-0.18 *	-0.13 *	-0.20 *	-0.11 *	-0.12 *	-0.11 *
GO:0048468	P	cell development	158		-0.06	-0.22 *	-0.15 *	-0.16 *	-0.24 *	-0.12 *	-0.16 *	-0.13 *
GO:0021700	P	developmental maturation	47		-0.20 *	-0.40 *	-0.23 *	-0.29 *	-0.38 *	-0.28 *	-0.36 *	-0.26 *
GO:0048469	P	cell maturation	36		-0.23 *	-0.47 *	-0.30 *	-0.31 *	-0.45 *	-0.35 *	-0.39 *	-0.30 *
GO:0010015	P	root morphogenesis	91		-0.11	-0.28 *	-0.17 *	-0.18 *	-0.28 *	-0.17 *	-0.20 *	-0.15 *
GO:0010053	P	root epidermal cell differentiation	49		-0.21 *	-0.45 *	-0.29 *	-0.33 *	-0.45 *	-0.33 *	-0.38 *	-0.26 *
GO:0048765	P	root hair cell differentiation	36		-0.23 *	-0.47 *	-0.30 *	-0.31 *	-0.45 *	-0.35 *	-0.39 *	-0.30 *
GO:0010054	P	trichoblast differentiation	43		-0.19 *	-0.45 *	-0.29 *	-0.30 *	-0.45 *	-0.35 *	-0.37 *	-0.25 *
GO:0048764	P	trichoblast maturation	36		-0.23 *	-0.47 *	-0.30 *	-0.31 *	-0.45 *	-0.35 *	-0.39 *	-0.30 *
GO:0071554	P	cell wall organization or biogenesis	233		-0.22 *	-0.30 *	-0.20 *	-0.24 *	-0.29 *	-0.13 *	-0.10 *	-0.15 *
GO:0016757	F	transferase activity, transferring glycosyl	484		-0.10 *	-0.12 *	-0.12 *	-0.10 *	-0.10 *	-0.08 *	-0.08 *	-0.09 *
GO:0016758	F	transferase activity, transferring hexosyl	303		-0.13 *	-0.13 *	-0.13 *	-0.12 *	-0.12 *	-0.11 *	-0.11 *	-0.13 *

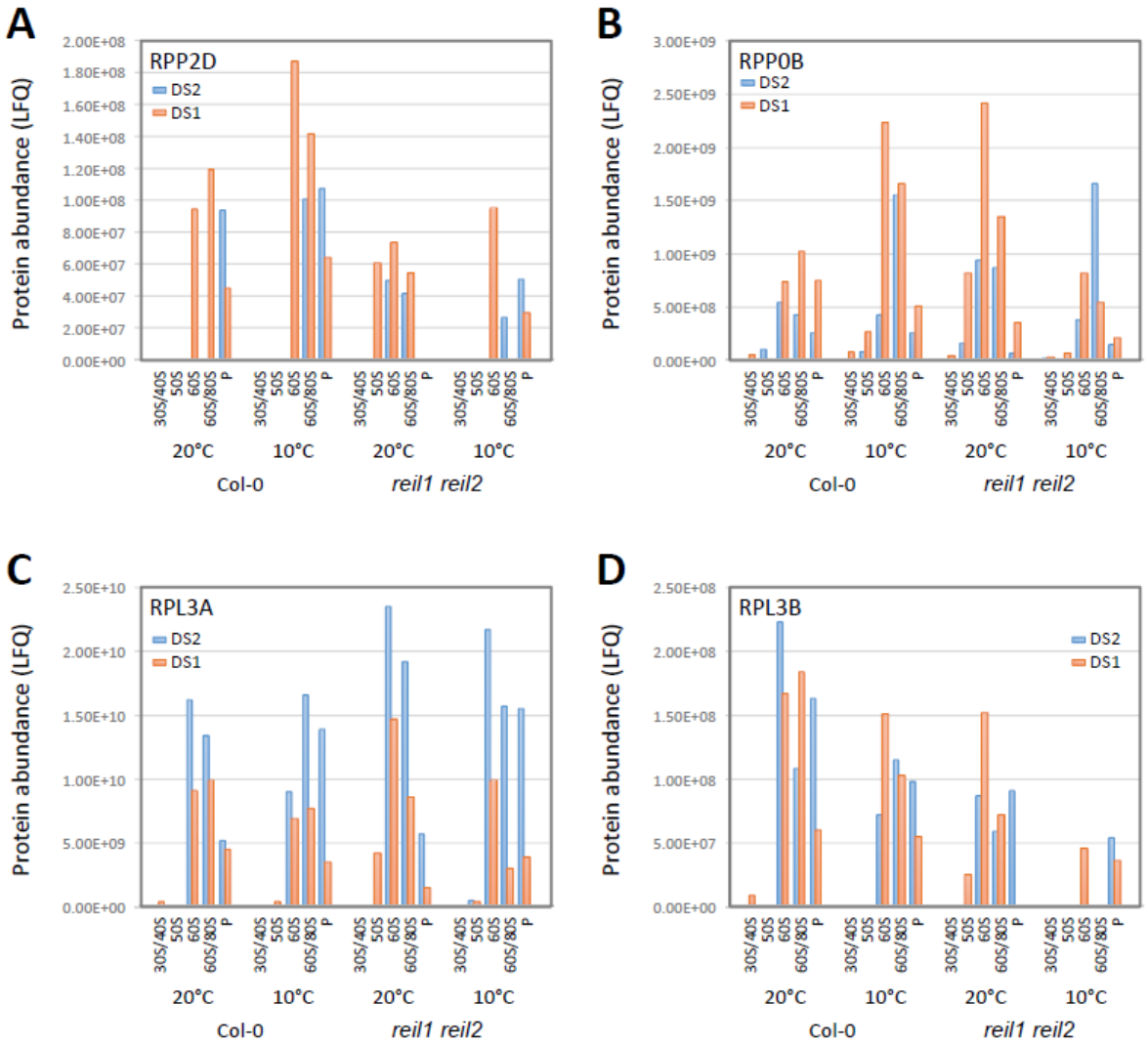
B

GO (Onthology)		Description	Genes	Col-0			*reil1-1 reil2-1*			*reil1-1 reil2-2*		
				0 d	1 d	1 w	0 d	1 d	1 w	0 d	1 d	1 w
GO:0009058	P	biosynthetic process	3716		0.04 *	0.01 *	-0.05 *	0.05 *	0.02 *	0.01 *	0.03 *	0.01 *
GO:0009059	P	macromolecule biosynthetic process	2505		0.06 *	0.03 *	-0.04 *	0.07 *	0.04 *	0.02 *	0.05 *	0.03 *
GO:0034645	P	cellular macromolecule biosynthetic pro	2483		0.07 *	0.03 *	-0.04 *	0.07 *	0.04 *	0.02 *	0.05 *	0.04 *
GO:0044249	P	cellular biosynthetic process	3536		0.05 *	0.02 *	-0.05 *	0.06 *	0.02 *	0.01 *	0.04 *	0.02 *
GO:0016137	P	glycoside metabolic process	86		0.01	-0.04	0.17 *	0.25 *	0.17 *	0.24 *	0.21 *	0.13 *
GO:0030145	F	manganese ion binding	30		0.04	0.00	-0.56 *	0.29 *	0.27 *	-0.41 *	0.47 *	0.22 *

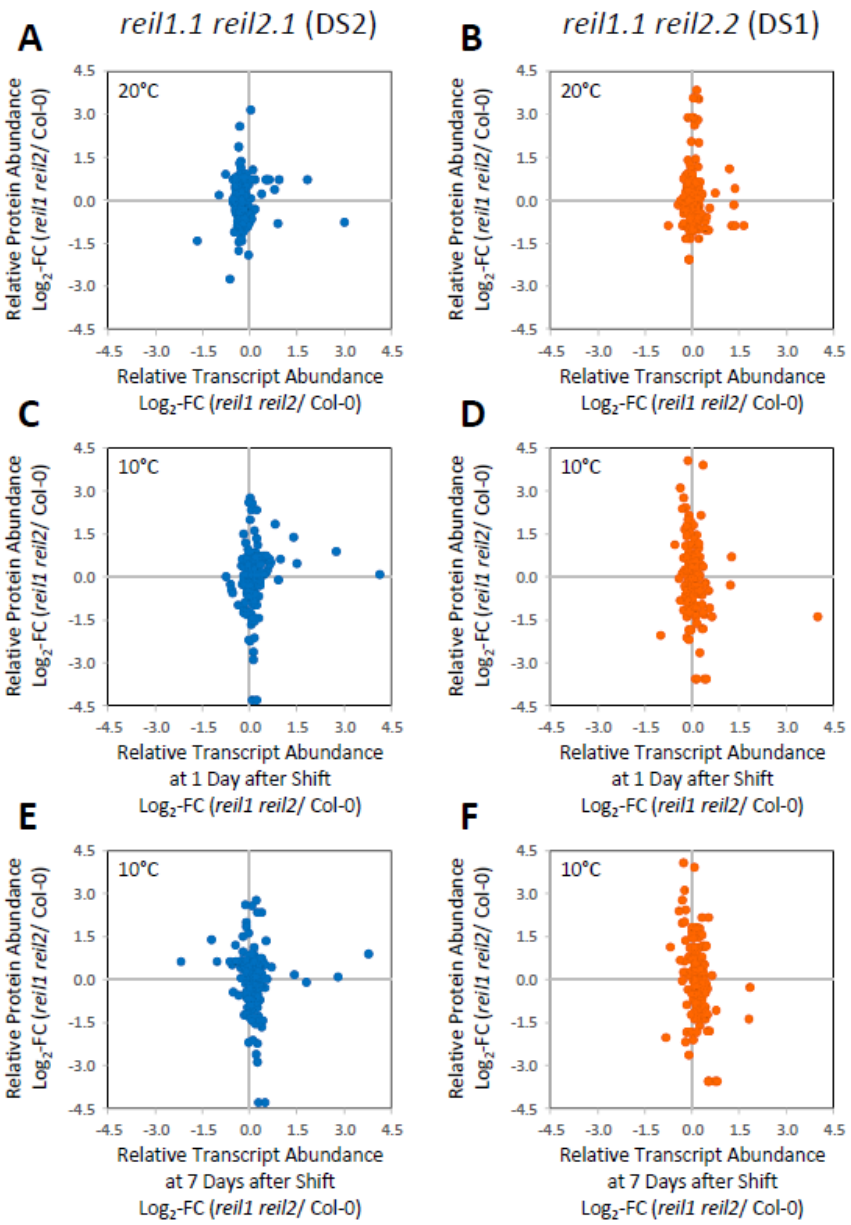
Supplemental Fig. S4-6. Functional enrichment analyses of differential gene expression in the roots of Col-0, and the *reil1-1 reil2-1* and *reil1-1 reil2-2* double mutants at the non-acclimated state (0 day, 20°C) and shifted to 10°C cold for 1 day or 7 days. Differential gene expression was determined relative to non-acclimated Col-0 at optimized temperature 20°C.
(A) Mean log2-FCs of developmental, cell wall, and root related GO terms.
(B) Mean log2-FCs of large biosynthesis related and miscellaneous GO terms.
(C = cellular component, P = biological process, F = molecular function). Significant positive or negative functional enrichments, i.e. FDR-adjusted $p < 0.05$, are indicated by asterisks, heat map color scale of $\log_2$-FC +1.0 (red) to -1.0 (blue). Mean $\log_2$-FC, z-scores, and FDR-adjusted p values of gene sets from 2145 GO terms were calculated by parametric analysis of gene set enrichment (PAGE; Tian et al., 2017). The full data set is listed in Supplemental Table S4-3.



Supplemental Fig. S4-7. Proteomic characterization of ribosome preparations obtained from root material by sucrose density gradient fractionation experiments DS1 and DS2, i.e. the root subset of Pride repository data set PXD016292. Ribosome complexes are represented by sums of label-free quantification (LFQ)-intensities of all detected RPs of 40S, 60S, and mitochondrial or plastid 30S and 50S subunits within each fraction. Non-translating immature 60S subunits are assessed by Arabidopsis homologs eIF6A and NMD3 of yeast cytosolic 60S maturation factors, means +/- standard error of the four fractionations of DS1 or DS2 (Supplemental Table S4-4).



Supplemental Fig. S4-8. Distribution analysis of RPP2D **(A)**, RPP0B **(B)**, RPL3A **(C)**, and RPL3B **(D)** across the sampled ribosome fractions and analyzed conditions, DS1 orange, DS2 blue.



Supplemental Fig. S4-9. Association analysis of changes in root transcript abundance and relative protein abundance in non-translating 40S and 60S (60S/80S) fractions of *reil1 reil2* mutants compared to *Arabidopsis thaliana* Col-0 wild type. DS2 (*reil1-1 reil2-1*) blue **(A, C, E)**, DS1 (*reil1-1 reil2-2*) orange **(B, D, F)**. (A, B) relative protein and transcript abundance determined at 20°C, i.e. at day 0, prior to cold shift; (C, D) relative protein abundance determined at 7 days after shift to 10°C, transcript abundance at 1 day after shift to 10°C; (E, F) relative protein and transcript abundance determined at 7 days after shift to 10°C.
Note that differential accumulation of cytosolic RPs and ribosome associated proteins in non-translating ribosome fractions (Supplemental Table S6) was matched to differential gene expression (Supplemental Table S4-2 columns X to AC) according to the gene model information of the transcriptome and proteome analyses (Pride data set PXD016292). Transcript information was in part splice variant specific. The proteome analyses contained in part non-specific information due to peptides that represented multiple splice variants, and proteins of highly similar or identical protein families (Supplemental Table S4-6).

CHAPTER 5

Evaluation of REIL as Potential Cold Acclimation Factor in Wheat

Preface to Chapter 5

This chapter describes the investigation and evaluation of REIL as a potential cold acclimation factor in wheat. Results from **Chapter 4** substantiate the role of REIL proteins as potential cold acclimation factors in *Arabidopsis*. It is therefore important to investigate if this protein may also be required for wheat to adapt to cold conditions. To this end, I examined the presence of *REIL* homologs in wheat by referring to the wheat genome available in Ensembl Plants database (https://plants.ensembl.org/Triticum_aestivum/Info/Index). I also evaluated the *REIL* expressions in wheat subjected to cold, drought and heat stress by re-analyzing published transcriptomics data from other researchers. Besides, I also conducted real-time PCR to evaluate the *REIL* expression in the two wheat varieties (Wyalkatchem and Young) that I used to study in Chapter 2. The details of the study are described in the Materials and Methods, Results and Discussion parts of this chapter. I claim that I contributed to more than 80% of this work (experimental, data processing, data analysis, interpretation and writing) to this chapter.

5.1 Introduction

The results obtained in Chapter 4 suggest the role of REIL proteins as potential cold acclimation factors in *Arabidopsis*. REIL proteins are required by the plant ribosomal biogenesis and involved in the translational machinery during cold acclimation. Therefore, this study aimed to investigate whether the *REIL* homologs are present in wheat, and whether the cold acclimation function is conserved in wheat.

First, I used the two *Arabidopsis thaliana REIL* sequences to search against the Chinese Spring wheat reference genome (Appels et al., 2018) available in Ensembl Plants website using the BLAST-search tool (https://plants.ensembl.org/Triticum_aestivum/Tools/Blast). Ensembl Plants is a genome-centric portal for plant species of scientific interest. I also carried out the topologic and phylogenetic analyses of the two *Arabidopsis* REIL proteins with various wheat REILs retrieved from available databases such as Wheat Expression Browser (http://www.wheat-expression.com/) to investigate the sequence conservation of the REIL proteins.

Next, to evaluate the potential of wheat REIL proteins to serve as cold acclimation factors, the expression of *REIL* genes in wheat under cold, drought and heat stress was evaluated by re-analyses of available transcriptomics data published by other researchers. Two sets of transcriptomics data were chosen for this purpose. The first set of transcriptomics data was obtained from Li, et al. (2015a). Their study focused on the lipidome and transcript profiling of three plant species (*Arabidopsis thaliana*, *Atriplex lentiformis* and *Triticum aestivum*) under various temperature stresses. As my focus was on wheat, I therefore extracted only the *Triticum aestivum* (wheat) transcriptomics data (accession number GSE58805) for my re-analyses. In Li, et al. (2015a), the wheat variety used was the cold-sensitive spring wheat variety Manitou. The varieties were grown in soil at 23°C for 2 weeks (three-leaf stage) after germination, and then half of the plants were moved to 4°C for cold treatment for another 2 weeks (three leaf stage). The leaves were harvested for RNA extraction and cDNA library construction and sent for paired-end sequencing using the Illumina HiSeq2500 platform (Illumina, San Diego, USA).

Another transcriptomics data set I chosen for my re-analysis was from Liu et al. (2015). Liu et al. focused on exploring the transcriptional response of wheat seedlings from the wheat variety TAM107 (a heat- and drought- tolerant variety) subjected individually to heat, drought and combined stresses for one and six hours. The extracted RNA samples were sent for paired-end sequencing using the Illumina HiSeq2000 platform (Illumina, San Diego, USA).

Besides re-analysing the published transcriptomics data, I also studied the expression of *REIL* genes in wheat subjected to cold stress by using real-time or quantitative polymerase chain reaction (qRT-PCR). The experiment was conducted in Commonwealth Scientific and Industrial Research Organisation (CSIRO) in Canberra with the assistance from Dr. Rudy Dolferus and his team. The same wheat varieties mentioned in Chapter 2 and 3, i.e. cold-sensitive Wyalkatchem and cold-tolerant Young, were used for this study.

5.2 Materials and Methods

5.2.1 Analysis of the Topology of Wheat (cv. Chinese Spring) *REIL* Gene Sequences Retrieved from Ensembl Plants

The two *Arabidopsis thaliana REIL* coding sequences, *REIL1* (gene code AT4G31420) and *REIL2* (gene code AT2G24500) (**Supplemental Data S5-1**), were uploaded to the wheat reference genome database (using wheat variety Chinese Spring) in Ensembl Plants (https://plants.ensembl.org/Triticum_aestivum/) and searched using the BLAST tool (BLASTX) for the presence of *REIL* gene(s) in wheat. Three homologs of *REIL* genes were found to be present in the wheat chromosome number 7A, 7B and 7D. Details of each *REIL* gene such as location/locus in Chromosome 7, transcript identity (ID), total exon numbers, transcript length, translation length/amino acid numbers were downloaded and are shown in **Figure 5-1**. The obtained wheat *REIL* sequences were aligned and compared with the two *Arabidopsis thaliana REIL* sequences for similarity study using the Clustal Omega program (https://www.ebi.ac.uk/Tools/msa/clustalo/).

5.2.2 Evaluation of *REIL* Expression in Wheat Subjected to Cold, Drought or Heat Stress using Published Transcriptomics Data from Li et al. (2015) and Liu et al. (2015)

5.2.2.1 Reprocessing of Reads and Re-mapping to the Latest Wheat Genome Released by International Wheat Genome Sequencing Consortium (IWGSC)

The RNA-Seq short reads for Li et al. (Plant Cell, Volume 27, Page 86-103, Year 2015a, Title: Understanding the biochemical basis of temperature-induced lipid pathway adjustments in plants) were retrieved from the Gene Expression Omnibus (https://www.ncbi.nlm.nih.gov/geo/) (accession number: GSE58805). The RNA-Seq short reads for Liu et al. (BMC Plant Biology, Volume 15, Article no. 152, Year 2015, Title: Temporal transcriptome profiling reveals expression partitioning of homeologous genes contributing to heat and drought acclimation in wheat (*Triticum aestivum* L) were retrieved from the Short Read Archive of the National

Center for Biotechnology Information (http://www.ncbi.nlm.nih.gov/sra/) (accession number: SRP045409). The raw reads were preprocessed and analyzed using the tools available in the Galaxy Australia platform (https://usegalaxy.org.au/). First of all, the raw reads were groomed and the quality of the reads were checked using fast quality control (FastQC) tool (Andrew, 2010). The reads were then filtered by using the Trimmomatic tool (Bolger et al., 2014), in which ten bases (adapter sequences) were removed from start of the reads because they are below the conventional Phred score cutoff, and reads with Phred quality score of more than 20 were retained for further use. The clean reads were groomed and checked for quality again before performing the alignment to wheat reference genome sequences released by the International Wheat Genome Sequencing Consortium (IWGSC) in August 2018 (https://urgi.versailles.inra.fr/download/iwgsc/IWGSC_RefSeq_Assemblies/v1.0/) using the HISAT2 tool (Kim et al., 2015). Due to the restricted computational resource (both memory and disc quota) provided to new users of the GALAXY Australia, here we have to re-structure the genomic scaffold of the wheat genomes by command lines and divide each of its chromosome 7A, 7B, and 7D in shorter chunks for alignment of reads.

5.2.2.2 Differential Gene Expression (DGE) Analysis of *REILs* in Wheat Subjected to Cold, Drought and Heat Stress

The DGE analysis was performed in the Galaxy Australia platform. The aligned reads in BAM format from part 5.2.2.1 were further converted to SAM format first, and used to generate the counting matrix file by referring to the annotation file IWGSC_v1.1_HC_20170706.gff3 (https://urgi.versailles.inra.fr/download/iwgsc/IWGSC_RefSeq_Annotations/v1.1/). DGEs of *REIL* genes between the control and treated samples were calculated using the counting matrix file and limma/VOOM package (Ritchie et al., 2015) from BioConductor available in Galaxy Australia. We identified differentially expressed transcripts with a significance of FDR corrected *p*-value of 0.05 (Benjamini-Hochberg, 1995) as cutoff.

5.2.3 Evaluation of *REIL* Expression in Wheat Subjected to Cold Stress Using Quantitative Real Time Polymerase Chain Reaction (PCR)

5.2.3.1 Controlled Environment for Wheat Growing, Cold Treatment and Sample Collection

The wheat varieties used for this study were Wyalkatchem (cold-sensitive) and Young (cold-tolerant) obtained from the National Frost Initiative, Australia (http://www.nvton line.

com.au/frost /). Seeds were sown in trays (36 × 25 × 13 cm, L × W × H; 15 plants/tray) filled with soil (100% composted soil, containing 1 g l−1 fertilizer: 14.4% N/6.6% P/5% K). Plants were grown in the glasshouse under natural lighting conditions and controlled temperature regime (24/16 °C, L/D) and water daily. Cold treatment was carried out at the young microspore (YM) stage of pollen development, which was determined using auricle distance (AD) measurements (Ji et al. 2010; Dolferus et al. 2013). Plants at YM stage were tagged, removed from the glasshouse and placed in a Conviron PGC 20 growth chamber for cold treatment. The treatment cycle consisted of 12 h incubation at 21°C in the light, followed by a linear cooling gradient descending from 21°C to – 2.5 °C over a period of 2 h, then followed by a continuous cold period at – 2.5 °C over a period of 8 h in the dark (12/12 light/dark cycle, using 400 μmol m^{-2} s^{-1} light intensity; see **Fig. 5-1**). The whole experiment was run over two consecutive nights and samples (flag leaves) were harvested in the morning after the cold treatment. Three flag leaves were harvested from three different tagged plants before cold treatment (control) and pooled as one biological replicate. This step was repeated for the cold-treated samples. For each variety, there were two biological replicates (n =2) for the control and cold-treated samples.

5.2.3.2 Extraction of Total RNA

The extraction of total RNA from flag leaf samples was performed using Maxwell® RSC Plant RNA Kit (PROMEGA, Australia), according to the manufacturer's instruction. Plant material was ground to a fine powder in liquid nitrogen with a mortar and pestle; 20–100 mg of the plant tissue powder was transferred into pre-chilled Eppendorf sample tubes on dry ice. Six hundred (600) µL of homogenization solution was added into each sample tube and the sample was pulse-spun at maximum speed (13,000 rpm) in a microcentrifuge. The homogenate was kept on ice to avoid RNA degradation. A 400 µL of homogenate was then transferred into a new 1.8 mL microcentrifuge tube, followed by the addition of 200 µL lysis buffer and vortexed vigorously for 15 s. The mixture was incubated for 10 mins at room temperature and then centrifuged at 13,000 rpm for 2 min. The supernatant was carefully taken out (without any debris) and transferred into the Maxwell® RSC Plant RNA plunger (first well position) which had already 5 µL of DNaseI (fourth well position) pre-added and 50 µL of nuclease-free water (elution tube position). The plunger was then attached to the RSC Plant RNA cartridge and put into the Maxwell® Instrument for RNA extraction. The eluted RNA samples were checked for concentration and purity using a NanoDrop™ 2000/2000c Spectrophotometer (Thermo Fisher Scientific, Waltham, MA, USA).

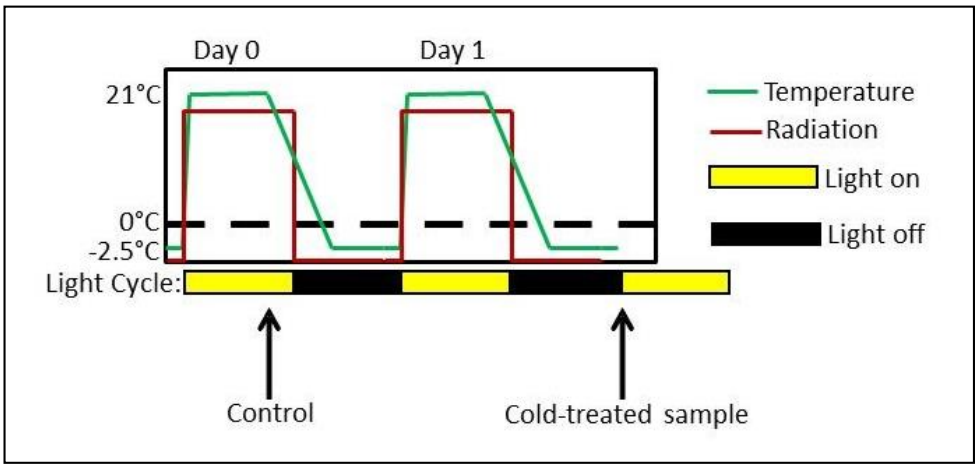


Figure 5-1. Graphic representation for the experimental design and cold treatment of Wyalkatchem and Young in controlled environment. The cold treatment was set for consecutive of two days, instead of four days like have been described in Chapter 2.

5.2.3.3 Reverse Transcription of Total RNA to Synthesize First Strand cDNA

The reverse transcription of total RNA to synthesize first strand cDNA was performed using Thermo Scientific™ Maxima H Minus Reverse Transcriptase with oligo (dT) to prime mRNA and 3 µg total RNA according to the manufacturer's instruction. A reaction mixture for each of the sample was prepared according to **Table 5-1**.

The reaction mixture was gently mixed, spun and incubated at 65°C for 5 min using a PCR thermal cycler and chilled on ice. Then, 4 µL of 5X RT buffer, 0.5 µL of Ribolock RNase inhibitor (Thermo Scientific, USA), 1 µL of Maxima™ H Minus reverse transcriptase were added to the reaction mixture to make up a final volume of 20 µL solution. The new reaction mixture was mixed gently, given a quick spin and PCR was performed for cDNA synthesis with the conditions: 60°C for 30 min followed by 85°C for 5 min, and cooled down to 4°C. The synthesized cDNAs were kept at -20°C prior to the next step.

Table 5-1. Reaction mixture recipe for each sample

Template RNA used:	Total RNA	3 µg
Primer used:	Oligo (dT) $_{18}$ primer	1 µL (or 100 pmol)
dNTP mixture, 10 mM each:		1 µL (or 0.5 mM final concentration)
Nuclease free water:		Top up to 14.5 µL

5.2.3.4 Quantitative Real Time PCR Analysis

The synthesized cDNA was diluted 20-fold and 5 µL of diluted cDNA was used in each qPCR reaction. A 10 µL of reaction mixture and 5 µL of primer mixture were added into the strip tube, followed by gentle mixing and tapping of the strip tubes make sure samples were at the bottom of the tubes. The preparation for the reaction and primer mixtures were performed according to **Table 5-2**. qPCR was performed on the final sample mix using a Rotor-Gene Q (Qiagen, Australia) and the cycling conditions were as follows: 95°C for 5 mins; 45 cycles of 95°C for 20 s, 60°C for 20 s; 72°C for 30s; 72°C for 10 mins. The qPCR products were analyzed using Rotor-Gene Q Series software. The Ubiquitin gene was used as the reference gene and gene expression data for each sample were normalised against Ubiquitin. Averages of three technical replicates were used to determine absolute quantification values for the biological replicates (**Supplemental Table S5-2**). Error bars represent standard error. All the primers used in this study were designed using the Primer3 software (http://bioinfo.ut.ee/primer3-0.4.0/) and are listed in **Supplemental Table S5-1**.

Table 5-2. Reaction mixture and primer mixture recipes for each sample

Reaction mixture (µL)		Primer mixture (µL)	
10X buffer	2	Primer (forward) 100 µM	0.2
$MgCl_2$ 50mM	1.4	Primer (reverse) 100 µM	0.2
dNTPs (5 mM)	0.8	Nuclease free water	Top up to 5 µL
SyberGreen	1		
Taq enzyme	0.1		
Nuclease free water	Top up to 10 µL		

5.2.4 Phylogenetic Analysis of REIL Proteins in Wheat and *Arabidopsis thaliana*

The coding sequences of three *REIL* genes for each wheat variety, including Manitou (Li et al., 2015a), TAM107 (Liu et al., 2015), Halberd (Browne et al., 2018) and Aegilops (Luo et al., 2017) were retrieved by alignment with the Chinese Spring wheat genome (chromosome 7) using Galaxy Australia. Meanwhile, the coding sequences of three *REIL* genes for wheat varieties Wyalkatchem and Young were provided by Dr. Rudy Dolferus from CSIRO, Canberra, Australia. All the coding sequences of *REILs* from wheat and *Arabidopsis thaliana*

used for phylogenetic tree building were first translated to amino acid sequences using the EMBOSS Transeq tool (https://www.ebi.ac.uk/Tools/st/emboss_transeq/) and are listed in **Supplemental Data S5-2**. Multiple sequence alignments of REIL amino acid sequences for phylogenic tree construction were generated by ClustalW tool in MEGA X software (https://www.megasoftware.net/) (Kumar et al., 2018) with gap-opening penalty set to 15 and gap extension set to 0.3. The phylogenetic tree was constructed and the evolutionary history was inferred by using the same software, in which Maximum Likelihood method based on the JTT matrix-based model (Jones et al., 1992) was used.

5.3 Results

5.3.1 Analysis of the Topology of Wheat (cv. Chinese Spring) *REIL* Gene Sequences Retrieved from Ensembl Plants

The search for the presence of *REIL* gene in Chinese Spring wheat reference genome database in Ensembl Plants using the two *Arabidopsis thaliana REIL* sequences yielded three homologs in wheat. The E-values for the three top hits were: 5.6E-129 for transcript with identity (ID) TraesCS7B02G332300.1 (% ID = 75.7%), 1.0E-128 for transcript with identity TraesCS7A02G432100.1 (% ID = 75.7%), and 1.0E-128 for transcript with identity TraesCS7D02G423800.1 (% ID = 75.7%). As shown in **Fig. 5-2A** and **5-2C**, the three wheat *REIL* homologs were located at the Chromosome 7A (locus: 625,742,700 – 625,745,964), Chromosome 7B (587,914,675 – 587,918,268) and Chromosome 7D (locus: 544,472,329 – 544,475,518). The transcript identity for *REIL* genes at Chromosome 7A was TraesCS7A02G432100 (with 1,698 base pairs), for *REIL* gene at Chromosome 7B was TraesCS7B02G332300 (with 2,068 base pairs), and for *REIL* gene at Chromosome 7D was TraesCS7D02G423800 (with 1,662 base pairs) (**Fig. 5-2C**). Similar to the *Arabidopsis thaliana REIL* genes, the wheat *REIL* genes have five exons (**Fig. 5-2B**), which encoded for REIL7A protein (400 a.a.), REIL7B protein (402 a.a.) and REIL7D protein (400 a.a.). The coding sequence length for each exon in the *REIL* gene is shown in **Fig. 5-2C**. When comparing the similarities of the open reading frame (ORF) of the *A. thaliana* and wheat *REIL* sequences, wheat *REIL7A* and *REIL7B* were found to share 65% similarities with the *A. thaliana REIL1*, while wheat *REIL7D* shared 63% similarity with *A. thaliana REIL1*. All the three wheat *REIL* homologs also shared 64% of similarity with *A. thaliana REIL2*.

Similar to *Arabidopsis thaliana* REIL proteins, the Chinese Spring wheat REIL proteins also possessed four zinc finger domains which were positioned in two pairs, ZF1/ZF2 at the N terminus and ZF3/ZF4 in the center of the sequence (**Supplemental Data S3**). All these four

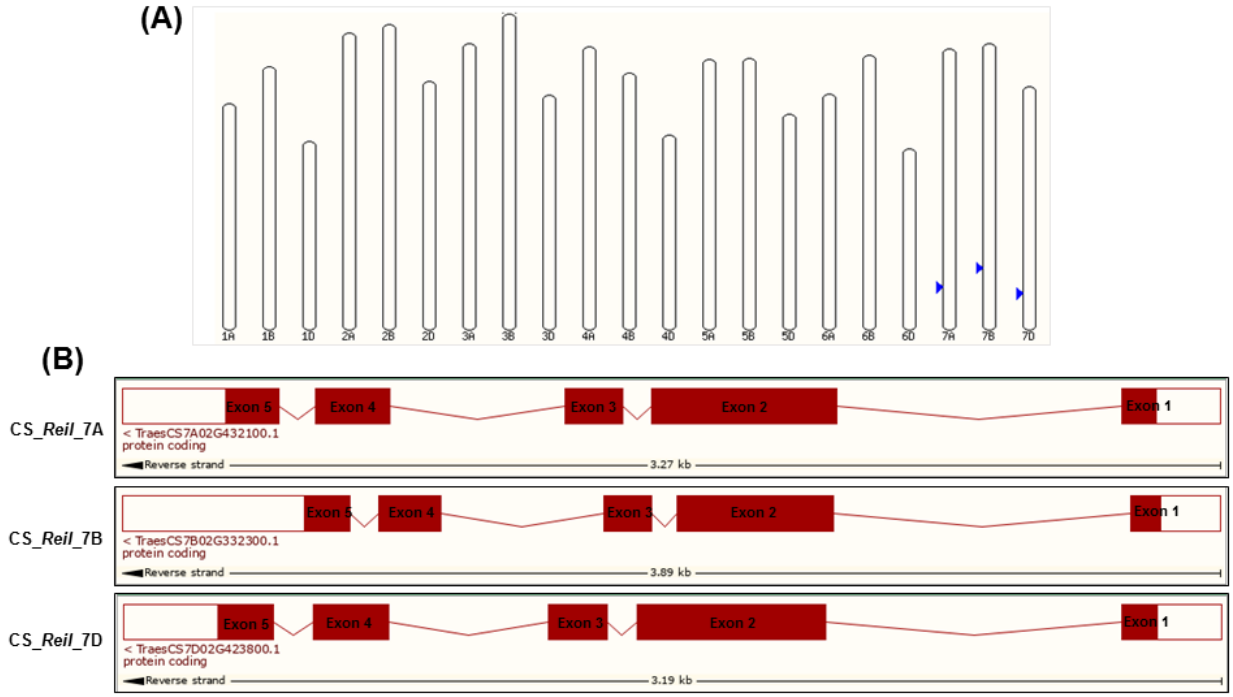
domains were highly conserved among the wheat and *A. thaliana* REIL proteins. The two conserved domains found in *Arabiodpsis thaliana* REIL proteins termed CD1 and CD2 that are located near the C terminus, were also found in the three wheat REIL homolog proteins and were highly conserved (**Supplemental Data S3**). All the three REIL amino acid sequences also shared 64% and 58% of similarities with the *A. thaliana* REIL1 and REIL2 amino acid sequences, respectively.

5.3.2 Evaluation of *REIL* Expression in Wheat Subjected to Cold, Drought or Heat Stress Using Published Transcriptomics Data from Li et al. (2015) and Liu et al. (2015)

For the evaluation of *REIL* gene expressions in the spring wheat variety 'Manitou' that was subjected to two weeks of cold stress (Li et al., 2015a), the exposure of the three-leaf stage plants to two weeks of cold at 4°C was found to significantly induce the expression of *REIL7B* gene (FDR-corrected *p* value < 0.05*), but the increase was slight and less than two folds (**Table 5-3**). On the other hand, for the evaluation of *REIL* gene expressions in the heat- and drought- tolerant winter wheat variety 'TAM107' (Liu et al., 2015), exposure of the wheat seedlings to heat-, drought- and combination of these two stresses for one and six hour(s) was found to significantly induce the expression of *REIL7A*, *REIL7B* and *REIL7D* genes, with majority of the FDR-corrected *p* values of the *REIL* genes were less than 0.05 (**Table 5-3**). However, none of the increases of the *REIL* genes upon heat- or drought stress were more than 2-fold. Combination of the two stresses independent of exposure time resulted in the strongest impact on *REIL* expressions, in which all the FDR-corrected *p* values were less than 0.001 (**Table 5-3**).

5.3.3 Evaluation of *REIL* Expression in Wheat Subjected to Cold Stress Using Quantitative Real Time Polymerase Chain Reaction (qRT-PCR)

Relative expression levels of *REIL7A*, *REIL7B* and *REIL7D* genes were measured using the YM stage flag leaves of Wyalkatchem and Young subjected to two consecutive nights of cold (**Fig. 5-1**) via qRT-PCR. As shown in **Fig. 5-3** and **Table 5-4**, cold exposure was found to very slightly increase the expression of *REIL7A* and *REIL7D* in Wyalkatchem, *REIL7B* in Wyalkatchem and Young. All the increases of *REIL* expression upon cold stress were less than +1.4-fold. However, all the increases were insignificant (both the raw and FDR-adjusted *p* values were more than 0.05) (**Table 5-4**).



(C)

Reil gene in Chinese spring variety	Transcript ID	Location at chromosome	Protein (amino acid number)	Coding sequence length (bp)	Sequence length for Exon 1 (bp)	Sequence length for Exon 2 (bp)	Sequence length for Exon 3 (bp)	Sequence length for Exon 4 (bp)	Sequence length for Exon 5 (bp)
CS_*Reil*_7A	TraesCS7A02G 432100	7A: 625,742,700 – 625,745,964	400	1,698	292	549	170	219	468
CS_*Reil*_7B	TraesCS7B02G 332300	7B: 587,914,675 – 587,918,268	402	2,068	316	555	170	219	808
CS_Reil_7D	TraesCS7D02G 423800	7D: 544,472,329 – 544,475,518	400	1,662	289	549	170	219	435

Figure 5-2. The Genomic Sequence Topology of the REIL Proteins from *Triticum aestivum* (wheat, Chinese Spring variety). **(A)** The three wheat *REIL* homologs are located at the Chromosome 7A, 7B and 7D of wheat genome. **(B)** Schematic representation of the intron-exon structure of wheat *REIL* genes. **(C)** The wheat *REIL* transcript identities, locus at Chromosome 7, exon lengths, and REIL amino acid lengths.

5.3.4 Phylogenetic Analysis of REIL Proteins in Wheat and *Arabidopsis thaliana*

Two REIL proteins from *A. thaliana*; and *REIL7A*, *REIL7B* and *REIL7D* proteins from spring wheat varieties Chinese Spring (CS), Wyalkatchem, Young, Halberd, Manitou, from winter wheat variety TAM107 and REIL protein from *Aegilops tauschii* (the D-genome donor) were aligned (**Supplemental Data S5-3**) and used to build a phylogenetic tree using the maximum-likelihood inference. The bootstrap values supporting each of the nodes were high with more than 79% (**Fig. 5-4**). Phylogenetic analysis of *A. thaliana* and wheat REIL proteins revealed that both the *A. thaliana* REIL1 and REIL2 proteins were quite different from the wheat REIL proteins, where these two proteins formed a separate clade from the other proteins (blue box in

Fig. 5-4). All the wheat REIL proteins showed closer phylogenetic relationship with each other (red dotted box in **Fig. 5-4**). For example, REIL7B proteins from the four spring wheat varieties, i.e. Chinese Spring, Manitou, Wyalkatchem and Young formed a clade (yellow box in **Fig. 5-4**). Interestingly, all the three REIL proteins from the winter wheat variety TAM107 were close to each other as another clade (green box in **Fig. 5-4**). REIL protein from *Aegilops tauschii* (the D-genome donor) were found to be closest to the Wyalkatchem and Young REIL7D proteins in another clade (pink box in **Fig. 5-4**). The four zinc finger domains and two conserved domains of all the wheat REIL proteins were also found to be highly identical among each other (**Supplemental Data S5-3**).

Table 5-3. Differential gene expression (DGE) analysis of *REIL* genes in wheat variety TAM107 subjected to subjected to heat, drought or combination of the two stress; and in wheat variety Manitou subjected to cold stress.

	TAM107 variety, subjected to heat, drought and combination of heat and drought stress (Liu et al., 2015)						Manitou variety, subjected to cold stress (Li et al., 2015)
	Heat _1hr	Heat _6hr	Drought _1hr	Drought _6hr	Heat & Drought _1hr	Heat & Drought _6hr	Cold_2 weeks
	Fold change (*vs.* control)	Fold change (*vs.* control)	Fold change (*vs.* control)	Fold change (*vs.* control)	Fold change (*vs.* control)	Fold change (*vs.* control)	Fold change (*vs.* control)
REIL 7A	1.7**	1.7***	1.0	1.3*	1.8***	1.6***	-1.2
REIL 7B	1.9**	1.9***	1.2	1.6**	1.6***	1.8***	1.3*
*REIL*7D	1.8**	1.5**	1.1	1.3*	2.0***	1.4***	1.2

FDR-corrected p value < 0.05*, p < 0.01**, p < 0.001***

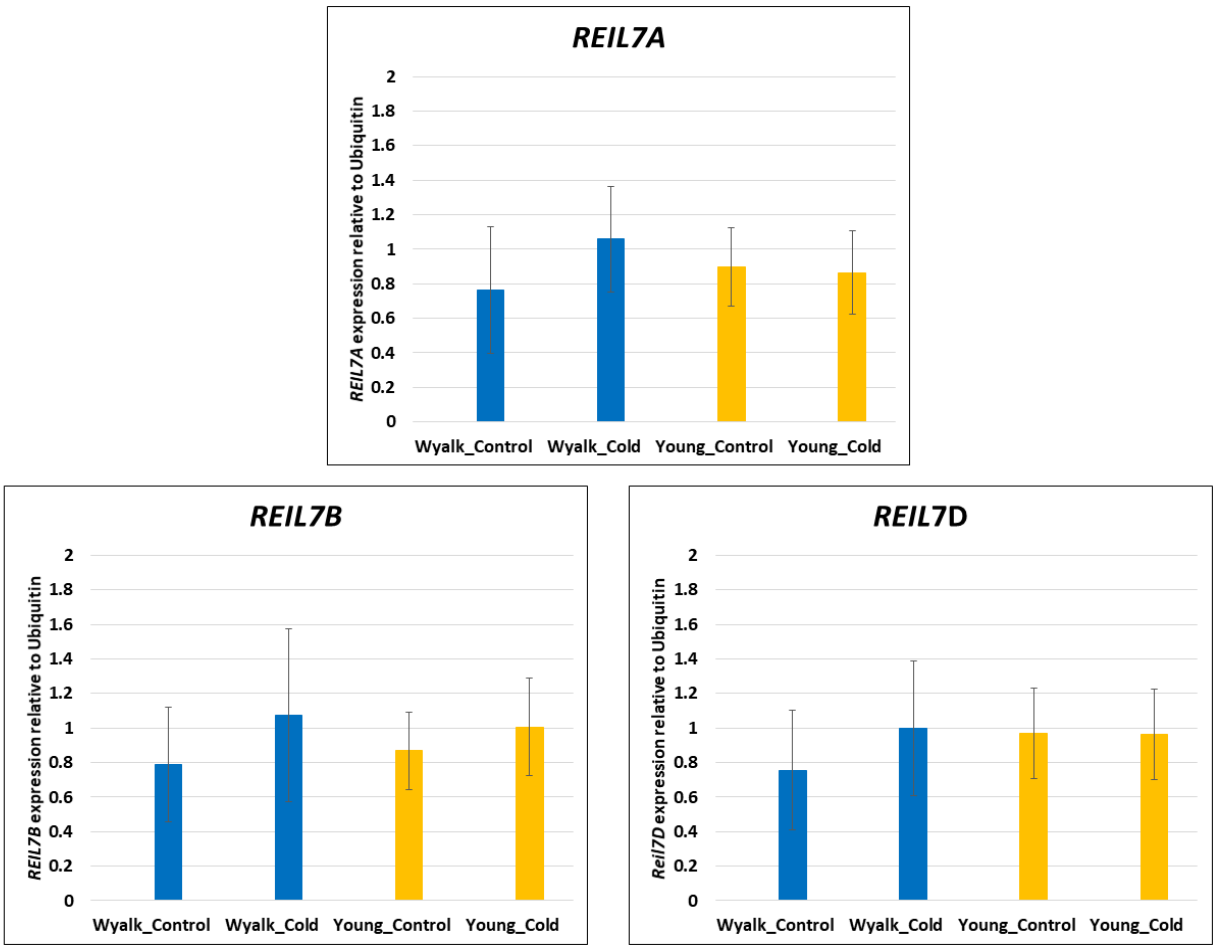


Figure 5-3. The relative expression of *REIL7A*, *REIL7B* and *REIL7D* to Ubiquitin genes in the flag leaves of Wyalkatchem and Young before and after cold treatment. Each sample was the averaged value from two biological replicates (n), in which each biological replicate was the averaged value from three technical replicates. n = 2 ± sem.

Table 5-4. Expression changes (in fold-change) of *REIL* genes in the flag leaves of Wyalkatchem and Young in response to cold stress. Statistical significant differences ($p < 0.05$) between the control and cold-treated samples were analyzed by using Student's *t*-test.

***REIL* gene**	**Wheat Variety**	**Cold vs. Control**			
		Raw *p* value	**FDR-adjusted *p* value**	**Significance (if $p < 0.05$)**	**Fold-change**
7A	Wyalkatchem	0.5971	0.9833	No	1.4
	Young	0.9231	0.9833	No	1.0
7B	Wyalkatchem	0.6795	0.9833	No	1.4
	Young	0.7394	0.9833	No	1.2
7D	Wyalkatchem	0.6860	0.9833	No	1.3
	Young	0.9833	0.9833	No	1.0

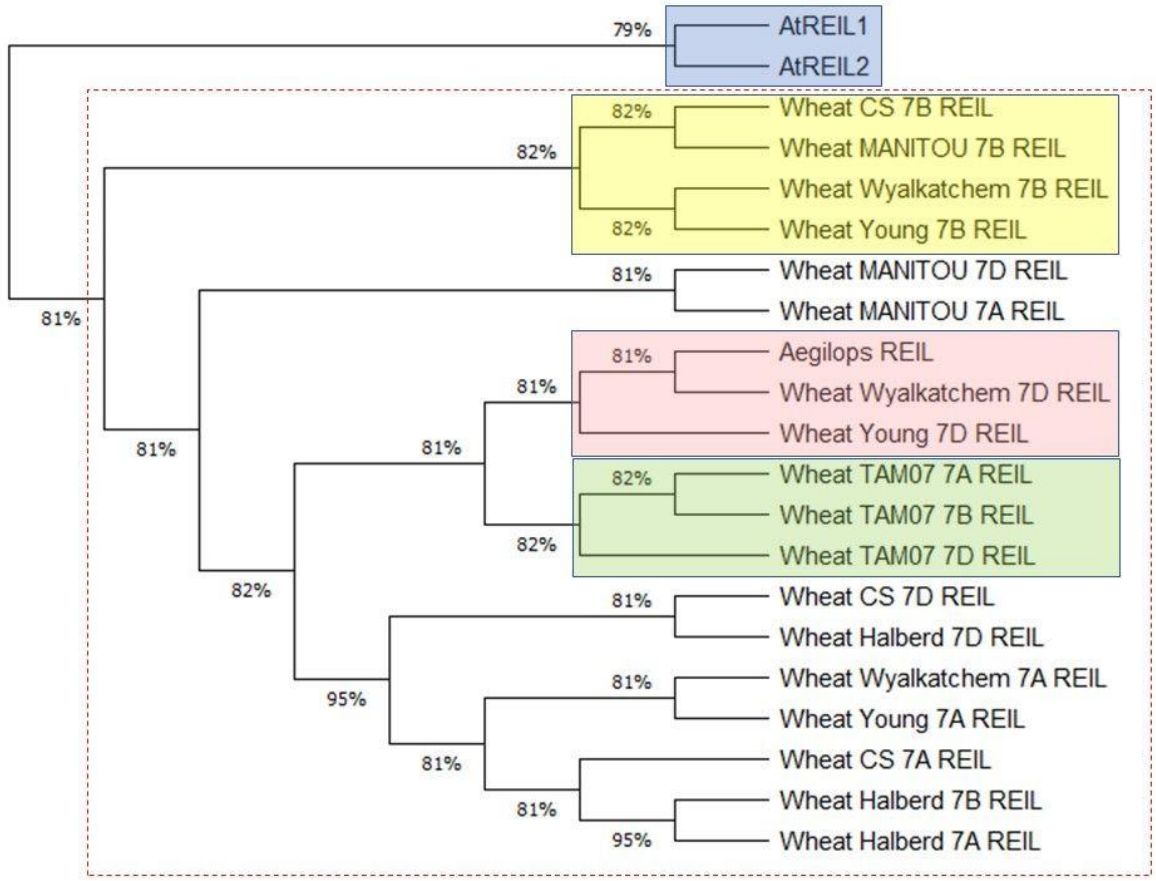


Figure 5-4. Molecular phylogenetic analysis of *Arabidopsis thaliana* and wheat REIL proteins by Maximum Likelihood method. The evolutionary history was inferred by using the Maximum Likelihood method based on the JTT matrix-based model (Jones et al., 1992). The tree with the highest log likelihood (-3349.70) is shown. Initial tree(s) for the heuristic search were obtained automatically by applying Neighbor-Join and BioNJ algorithms to a matrix of pairwise distances estimated using a JTT model, and then selecting the topology with superior log likelihood value. The tree is drawn to scale, with branch lengths measured in the number of substitutions per site. The analysis involved 21 amino acid sequences. There were a total of 490 positions in the final dataset. Data coverage for internal nodes (bootstrap values) were displayed as percentage (%). Evolutionary analyses were conducted in MEGA X (Kumar et la., 2008). At = *Arabidopsis thaliana*; CS = Chinese Spring.

5.4 Discussion

The outcomes from Chapter 4 suggest the role of REIL proteins as potential cold acclimation factors in *Arabidopsis thaliana*. REIL proteins are required by the plant for ribosome biogenesis (by speeding up accumulation of 60S large ribosomal subunit) and they are involved in the translational machinery to assist the plant to acclimate in cold temperature. It therefore

led us to evaluate if *REIL* homologs are present in wheat, and if they can act as potential cold acclimation factor in monocot.

According to the studies reported by Schmidt et al. (2013), the plant *REIL* genes underwent gene duplications, which occurred independently in several plant phylae. The REIL1 and the REIL2 paralogs in dicots, such as *A. thaliana*, originated from gene duplication during the speciation of the Brassicales. They also reported that plants, except for monocots, tend to have independent gene duplications of the *REIL*. For example, duplication of *REIL* genes were found in eudicot plants such as *Populus trichocarpa* (black cottonwood), *Malus domestica* (apple), *Brassica rapa* (field mustard) and many more. Interestingly, they reported there is only one copy of REIL gene in monocot plants such as *Zea mays* (maize), *Triticum aestivum* (wheat), *Oryza sativa* (rice) and *Hordeum vulgare* (barley).

In this study, I found three potential homologs of *REIL* genes in wheat, i.e. *REIL* from chromosome 7A, 7B and 7D. As described in Chapter 1 (Literature review), bread wheat is hexaploid (AABBDD), with a genome size estimated at ~17 Gb, composed of three closely-related and independently maintained genomes (wheat A, B and D, each comprising 7 chromosomes) that are the result of a series of naturally occurring hybridization events. The ancestral progenitor genomes are considered to be *Triticum urartu* (the A-genome donor) and an unknown grass thought to be related to *Aegilops speltoides* (the B-genome donor). This first hybridization event produced tetraploid emmer wheat (AABB, *T. dicoccoides*) which hybridized again with *Aegilops tauschii* (the D-genome donor) to produce modern bread wheat (http://plants.ensembl.org/Triticum_aestivum/Info/Index). The three *REIL* homologs found in wheat are therefore believed to be contributed by the sub-genome independently, and not the results of the duplication of REIL genes as observed in dicot plants such as *A. thaliana*.

Meanwhile, I also performed preliminary analyses of *REIL* gene expressions in wheat subjected to cold, drought (water dehydration stress is related to cold stress) and heat stress. The analyses of transcriptome data from published works (Liu et al., 2015; Li et al., 2015a) showed that there is significant increase in *REIL* expression when plants were subjected to heat, drought or cold stress, though the fold-change was less than 2-fold. However, the results obtained from the quantitative polymerase chain reaction (qRT-PCR) performed using the varieties Wyalkatchem and Young showed a slight increase though not statistically significant of *REIL* genes upon cold stress. This may be due to the duration of cold stress applied (two consecutive nights) which may have been insufficient to induce expression in the two varieties, or the tissue of study (flag leaves at the young microspore stage) doesn't show any changes in gene expression. Also, samples were collected from flag leaves at young microspore stage that

differed from the mature leaves at three-leaf-stage used in Li et al. (2015) may also account for the difference observed. Due to the time constraint of my PhD study, unfortunately, the experimental workflow of the qRT-PCR could not be optimized and repeated in a larger number of biological replicates.

5.5 Conclusion

In summary, my preliminary study presented in this chapter revealed that *REIL* homologs are present and expressed in wheat. However, it is unclear whether the cold acclimation function of REIL may be conserved among the dicots (*Arabidopsis thaliana*) and the monocots (wheat), thus further investigation is required. More in-depth studies such as overexpression or silencing of the *REIL* expression in the Australian spring wheat varieties will support the investigation of the function and potential of this protein as a cold acclimation factor in monocots.

5.6 Supplemental Information

The Supplemental Data S5-1 to S5-3, and Supplemental Tables S5-1 and S5-2 can be found in the **Appendices**, **Appendix D: Supplemental Information for Chapter 5 (page 314).**

CHAPTER 6

Conclusions and Future Directions

Frost events can cause major yield losses to cereal crops in many temperate climate regions in the world. Wheat crops in Australia are grown during winter and they flower in early spring to avoid the hot summers and to take advantage of available soil moisture. The sensitive stage of flowering is therefore frequently exposed to spring frost. The annual yield loss due to frost events to the Australian grains industry is estimated to be A$360 million (Paulsen and Heyne, 1983; Boer et al., 1993; Gu et al., 2007; Frederiks et al. 2015; Zheng et al., 2015). Minimising the loss caused by chilling and frost events is therefore critical for breeders in Australia. One of the solutions is via the development of more frost-tolerant wheat varieties. To achieve this goal, we first need to understand the underlying molecular mechanisms of cold responses of Australian wheat subjected to cold stress. In this study, I employed targeted metabolomics and lipidomics approaches to understand the metabolic traits involved in the cold acclimation potential of two Australian wheat varieties with contrasting cold tolerance. The varieties used were the cold-sensitive Wyalkatchem and cold-tolerant Young. Besides of analyzing the metabolome and lipidome of the wheat aerial parts (i.e. flag leaf and spike in **Chapter 2**) upon cold stress, I also expanded the lipidome analysis to the roots, the organ where there is has no such study reported yet on cold stress responses (**Chapter 3**). Through the targeted metabolomics and lipidomics approaches, we gained a better understanding of the cold responses of the two Australian wheat varieties subjected to cold stress. I also identifed several potential metabolite and lipid markers responsible for chilling tolerance in the tolerant wheat variety through the targeted approaches. In addition of taking a metabolomics approach to understand plant responses to cold, another approach to develop more frost-tolerant wheat varieties could be achieved via the bioengineering of cold responsive gene into wheat. The target gene of our study is *REIL* which encodes for REIL (**Re**quired for **i**sotopic bud growth 1 - **l**ike) protein. REIL proteins (REIL1 and REIL2) function as ribosome biogenesis factors by participating in the late maturation of the 60S subunit in *Arabidopsis thaliana* (Schmidt et al., 2013, 2014; Beine-Golovchuk et al., 2018). It has been reported that REIL proteins are required for the growth of the mature leaves of *A. thaliana* in cold conditions (10°C), but not at optimal temperatures (20°C) (Schmidt et al., 2013, Beine-Golovchuk et al., 2018). REIL therefore has been postulated to act as a cold acclimation factor in *A. thaliana*. In order to validate this role prior to studying these genes in wheat, here I performed a comprehensive systematic analysis (ribosomal profiling, ribo-proteomics, transcriptomics) was conducted using roots of *A. thaliana* (**Chapter 4**). The results confirmed REIL as cold acclimation factor in *A. thaliana*

and proposed that *A. thaliana* requires the biosynthesis of specialized ribosomes for cold acclimation. Next, I was interested to determine if REIL may also act as a cold acclimation factor in wheat. Therefore, the potential role of REIL as a cold acclimation factor in wheat was evaluated (**Chapter 5**). While there are two homologs of REIL in *A. thaliana*, three REIL homologs were found to be present in wheat. The *REIL* expressions in wheat subjected to cold, drought and heat stress were re-analysed using published transcriptomics data from other researchers. In addition, the *REIL* expression in the two wheat varieties used in Chapter 2 and 3 (Wyalkatchem and Young) upon cold stress was also evaluated using real-time PCR. While there was up-regulation of the *REIL* genes subjected to cold, drought and heat stress revealed by the re-analyses of published transcriptomics, there were no significant changes of *REIL* expression in Wyalkatchem or Young upon cold stress. The preliminary evaluation of wheat REIL did not yet allow definite conclusions on conserved functions with Arabidopsis, and more in-depth studies such as overexpression or silencing of the genes in wheat are needed in the future. The key results obtained from each research chapter (Chapter 2 to 5) are summarized and the future directions for further research are discussed in the next section.

6.1 Summary of Key Results from this Research and Future Directions

Chapter 2 describes the investigation of the cold acclimation potential of two Australian wheat varieties with contrasting cold tolerance using targeted metabolomics and lipidomics approaches. The selected cold-sensitive spring wheat variety used in this study was Wyalkatchem and the selected cold-tolerant spring wheat variety was Young. Wheat is known to be susceptible to cold stress at their reproductive or flowering stage. Therefore, wheat tissues from the aerial part of the plants (i.e. flag leaves and spikes) at the young microspore (male reproductive development) stage were chosen for this study. Wheat flag leaves are physiologically different from spikes in that the former are static photosynthetic source tissues, while the latter are actively developing sink tissues (grains). In this study, a comprehensive analysis of metabolites (sugars and derivatives, organic acids, amino acids, amines and/or phytohormones) and glycerolipids of the harvested flag leaf and spike tissues subjected to cold stress was performed using GC and LC coupled to triple quadruple (QqQ) mass spectrometry. The cold stress experiment was conducted in a controlled environment. The metabolite and lipidome changes during cold acclimation after initial exposure (1 day) and prolonged exposure to cold (4 days) were analysed in order to first identify metabolites and lipids that are responsive

to cold stress, followed by identification of potential metabolite/lipid markers that could distinguish the cold-tolerant wheat variety from the cold-sensitive one.

Due to the datasets obtained from the flag leaf and spike analysis, I firstly analysed the flag leaf dataset in detail and organized the outputs as the first part of Chapter 2, followed by the analysis of the spike dataset and organized the outputs as the second part of Chapter 2. For the flag leaf dataset, a total of 70 metabolites (sugars and derivatives, organic acids, amino acids, amines, phytohormones) and 70 phosphoglycerolipids were identified and quantified. It was discovered that the sensitive variety Wyalkatchem showed a strong reduction in amino acids after the first cold night, followed by accumulation of osmolytes such as fructose, glucose, putrescine and shikimate over a 4-day period. Accumulation of osmolytes is indicative of acclimation to water stress in Wyalkatchem. This response was not observed in the tolerant variety Young. The two varieties also displayed significant differences in lipid accumulation. Variation in two lipid clusters, resulted in a higher unsaturated to saturated lipid ratio in Young after 4 days cold treatment and the lipids PC(34:0), PC(34:1), PC(35:1), PC(38:3), and PI(36:4) were the main potential contributors to the unsaturated to saturated ratio change. This indicates that Young may have superior ability to maintain membrane fluidity following cold exposure, thereby avoiding membrane damage and water stress as observed for Wyalkatchem. The results suggest that metabolomics and lipidomics could be used as an alternative phenotyping method to discriminate wheat varieties with differences in cold acclimation. The work on the flag leaf has been published in the journal *Metabolomics* (Cheong et al. 2019). Also, the results from flag leaves has also been presented as a poster in the *Australian Society of Plant Scientists (ASPS) 2019 – Bring Plant Science Together Conference* for which I won the first prize for the ASPS Student Poster Competition. I was delighted with this achievement and was invited to write a report about this to be published in the online *Phytogen June 2020 issue* (https://www.asps.org.au/archives/6002).

The spike analysis resulted in a total of 58 metabolites (sugars, organic acids, amino acids and amines) and 95 phosphoglycerolipids and galactosyl lipids being identified and quantified. Phytohormones were not analysed as the detection limit of the methodology was unfortunately too low for this tissue. The spikes of the two contrasting wheat varieties showed qualitative and quantitative differences in primary metabolites involved in osmoprotection and lipids involved in membrane remodeling upon cold stress. Cold treatment affected more changes of metabolites and lipids in Wyalkatchem's spikes compared to Young's spikes. Maltose, fructose-6-phosphate, glucose-6-phosphate, beta-alanine, and the lipid PG(36:5) were significantly induced in the sensitive Wyalkatchem after short cold stress, while there were no

changes of metabolites and only one lipid species (PC(37:5)) was reduced in Young after the short cold stress. More metabolites and lipids were affected in the Wyalkatchem after prolonged cold stress compared to the short treatment, eg. raffinose and putrescine were induced, shikimate was reduced, a series of PC(36:x, x = 0 to 3) lipids and several other lipids ((PE (34:0), PE (34:1), PE(38:4), and PE(41:4)) were reduced. Conversely, prolonged cold stress did not significantly change the metabolites and lipids in Young. When comparing the lipid compositions between the two varieties, it was discovered that Young contained higher amounts of polyunsaturated species with two polyunsaturated fatty acyl chains in their structures when compared to Wyalkatchem upon cold stress, eg. PC(36:6), PE(36:6), PG(36:6), PI(36:6) and DGDG(36:6). Welti et al. (2002) has reported that PC, PE, PG and MGDG species containing two polyunsaturated acyl species, including 36:5 (18:2/18:3) and 36:6 (di-18:3), increased during cold acclimation in Arabidopsis. They also reported that plants tend to increase the degree of fatty acid unsaturation and the content of phospholipids when they are exposed to low, non-freezing temperatures (Welti et al. 2007). Similar to the flag leaf results, Young's spikes also had higher unsaturation to saturation ratio compared to Wyalkatchem's spikes upon cold stress. This indicates that differences in lipid accumulation most distinctively separated the cold response of the two wheat varieties, and the chilling and freezing tolerance of Young could be associated with better capability of the variety to remodel its membrane lipid composition to maintain membrane fluidity in cold condition compared to Wyalkatchem. The results from the spike analyses has been published in the journal *Cells* (Cheong et al. 2020).

In conclusion, profiling of primary metabolite and lipid changes in response to cold treatment of wheat flag leaves and spikes provided a better understanding about differences in cold acclimation of cold-tolerant Young and cold-sensitive Wyalkatchem. The changes in metabolomes and lipidomes of spikes were similar to those of flag leaves in many ways, but there were also some interesting differences in the accumulation of osmolytes, ROS protective compounds, and lipids between the two tissues. This means that both flag leaf and spike metabolite and lipidome analysis are complementary in terms of physiological information, and they can be used interchangeably for cold tolerance phenotyping in wheat in the future. Flag leaf tissue is easier to collect, while spike tissue offers an advantage in terms of detectability because of the presence of higher levels of some of the metabolites. Both the flag leaf and spike datasets pointed out that remodeling of membrane lipids is critical for adaptation to low temperature stress. Controlling the unsaturated lipid levels to maintain membrane fluidity at low temperatures appears to be a distinguishing factor between cold-tolerant line Young and cold-sensitive Wyalkatchem. Some potential lipid species that stand out in the

response of the cold-tolerant and sensitive wheat varieties were identified, but for phenotyping purposes the determination of the changes of the entire lipid spectrum of each variety upon cold stress is also necessary. Experiments are in progress to demonstrate whether lipid profiling proves to be reliable in a wider germplasm of cold-tolerant and sensitive wheat lines and whether the changes in lipid spectrum correlate to the ones observed in Young and Wyalkatchem. When lipid profiling proves to be reliable, technology such as QTL mapping or genome-wide association studies (GWAS) can be deployed to identify genetic markers that can be used to predict the cold tolerance phenotype. In addition, the data presented here have provided new avenues to investigate genes involved in metabolic and lipid biochemical processes using transcriptome analysis. Combination of metabolome and transcriptome analysis can further improve our understanding of how cold tolerance is controlled in wheat.

Chapter 3 describes the spatial root lipidome analysis of cold-stressed wheat varieties from Australia. Cold stress studies on wheat have thus far been performed mostly on aerial plant parts, i.e. leaves and spikes. There are limited cold stress studies on whole roots or even more rarely on the specific root tissues such as the tissues derived from the developmental root zones consisting of the meristem and cell division zone (DZ) in which cells are actively dividing, the elongation zone (EZ) in which cells are growing and expanding their sizes, and the maturation zone (MZ) in which cells differentiate to perform specific functions. In **Chapter 2**, the lipid profiling of cold-treated flag leaves and spikes indicated the involvement and importance of certain phospholipids and galactosyl lipids for cold tolerance in the aerial parts of wheat. This prompted me to also investigate the tissue-specific lipidomes of roots of the two studied wheat varieties (Wyalkatchem and Young) subjected to cold stress. Therefore, the lipid profiles of the spatial root zones derived from young seedlings of Wyalkatchem and Young grown at optimal temperature (21°C) and subjected to chilling (4°C) and freezing (-3°C) stresses were investigated in this chapter. The harvested samples were analysed with a high resolution high performance liquid chromatography (HR-HPLC) coupled with quadruple-time-of-flight (QqTOF) platform via modified parallel reaction monitoring (PRM) methods derived from Yu et al. (2018, 2020).

The analysis resulted in a total of 273 lipid species derived from 21 lipid classes to be detected and analysed. Analysis of the lipid composition at the unstressed stage revealed that there were differences among the three developmental root zones in each wheat variety. For example, phosphoglycerolipids (PE, PG, PC and their lyso species) were the main components of lipids in the DZ (occupied more than 50%) where cells are actively dividing thus requiring

large amounts of phospholipids to build the membrane structures. The content of phosphoglycerolipids gradually decreased across the EZ and MZ. Conversely, sphingolipids such as HexCer and Cer were present at highest quantities in the MZ (accounting for more than 40% of the mass spectral intensity from lipids) compared to the other two root zones. MZ is a root zone where root cells differentiate to specialized functions and the high proportion of sphingolipids observed in this zone could be related to their roles to regulate membrane permeability and overall integrity of the plasma membrane and tonoplast of the specialized cells.

After being subjected to cold stress, both chilling and freezing were found to alter mainly the glycerolipid and sphingolipid compositions of the root zones, which also revealed the main differences between the cold-sensitive and cold-tolerant varieties. For example, phospholipids (PE, PC, PG, PI and PS) were observed to increase in every root zone for both the wheat varieties. Plants tend to increase the degree of fatty acid unsaturation and the content of phospholipids in order to enhance membrane fluidity during low temperature stress Uemura et al. (1995). The increase of phospholipids observed in all root zones of both varieties upon cold stress may indicate the involvement of these lipids in lipid remodeling of the root membranes to maintain the fluidity in cold condition. When comparing the phospholipids between the two wheat varieties, it was observed that phospholipids in cold-sensitive Wyalkatchem were higher compared to tolerant Young upon cold stress. This suggests that cold stress may have stronger effects on the membrane stability in the sensitive variety compared to the tolerant variety. It is therefore worth to further analyse and compare the degree of desaturation of the phospholipids (via unsaturation to saturation ratio) of the two varieties in the future.

Wyalkatchem's roots were also observed to contain higher amounts of DAG compared to roots of Young upon cold stress. The excessive accumulation of DAG could be adverse for the membrane because it can be converted to phosphatidic acid (PA) via diacylglycerol kinase. PA can activate the enzyme NADPH oxidase and subsequently increases the production of reactive oxygen species (ROS) which if present excessively in cells may lead to the oxidation of membrane lipids (Zhang et al., 2009; Baxter et al., 2014). Higher accumulation of DAG observed in Wyalkatchem compared to Young upon cold stress therefore may indicate the potential of these lipids being converted to PA which subsequently produce ROS that may damage the membrane of the cold sensitive variety. To cope with the excessive DAG produced during cold stress, plants that withstand freezing better have been reported to show up-regulation of the diacylglycerol acyl transferase (DGAT) activity to convert the DAG to the

non-polar TAG (triacylglycerol) (Arisz et al., 2018). The cold tolerant Young, which has lower DAG contents compared to Wyalkatchem upon cold stress, may possess higher activity of this enzyme and TAG content. In the future, a thorough investigation of the DGAT activity, DAG and TAG contents, oxidized lipids and ROS profiles of the wheat varieties subjected to cold stress is necessary to help us to increase the understanding of these mechanisms and how they are interrelated to each other.

On the other hand, the cold-tolerant Young also showed lower accumulation of HexCer (i.e. GlcCer) compared to the cold-sensitive Wyalkatchem in all the three root zones upon cold stress. It has been reported that freezing-tolerant plants have a lower proportion of GlcCer in their plasma membranes compared to the freezing-sensitive plants. The reduction of GlcCer contents during cold stress is important for the plants to adjust membranes during osmotic stress and prevent dehydration-induced demixing of membrane lipid components (Lynch & Steponkus, 1987; Steponkus et al., 1988; Steponkus et al.,1990; Uemura & Steponkus, 1994; Uemura et al., 1995). The lower amounts of HexCer in Young compared to Wyalkatchem as observed in this study could be one of the key factors contributing to the cold tolerance of Young. Therefore, more in-depth attention should be paid to sphingolipids to determine their involvement in membrane remodeling upon cold stress.

Together with the outcomes gained from the studies of flag leaves and spikes in Chapter 2, the outcomes obtained from this study (roots) may help us to gain a more comprehensive understanding of lipid metabolisms of wheat in response to cold. A wider variety of tolerant and sensitive wheat lines subjected to cold stress should be used for the next study with focus given to glycerolipids (phosphoglycerolipids, galactosyl glycerolipids, DAG) and sphingolipids (Cer and HexCer) but also including lipid species from other classes not studies here such as TAG.

Chapter 4 describes the systematic analysis of REIL protein functions in cold acclimated *Arabidopsis thaliana* roots. REIL proteins have been reported to act as potential cold acclimation factor in *A. thaliana* leaves. They were shown to be involve in late ribosomal biogenesis and to affect accumulation of 60S large subunits in *A. thaliana* mature leaves and seedlings upon acclimation to low temperature (Schmidt et al., 2013. 2014; Beine-Golovchuk et al., 2018). In order to discover and validate these roles of REIL proteins, a comprehensive systematic analysis was conducted targeted at understanding the mechanisms of late ribosome biogenesis in which REIL proteins are involved. Previous work described these mechanisms in leaves (REFs), thus in my study I focused on roots. The roots grown at optimized temperature

and at different times after shift to suboptimal/low temperatures were analysed. Like the reported analysis on mature leaves, root phenotyping of *reil* mutants, namely the single gene mutants *reil1-1*, *reil2-1*, *reil2-2* and the double mutants *reil1-2 reil2-1*, *reil1-1 reil2-2*, indicated effects on growth, metabolic stress responses and transcriptomic reactions that were strongly connected to ribosomal biogenesis and translation. Ribosomal profiling analyses confirmed the requirement of REILs for the rapid accumulation of 60S large subunit after cold shift and revealed effects on 80S monosome levels at prolonged cold conditions. Proteome analysis of ribosome complexes based on sucrose density sedimentation profiles indicated that REIL proteins were required to maintain the 80S monosome levels in the cold. Non-translating 60S subunit levels were highly correlated to non-translating 40S levels. Transcript profiling results confirmed the associated regulation of 60S and 40S gene expression and indicated that REIL may have relationships with both 40S small subunit and 60S large subunit accumulation in cold environments. In the absence of REILs in the double mutants, Arabidopsis homologs of yeast 60S ribosome biogenesis factors accumulated in the non-translating 60S fraction and translation initiation factor 3 (eIF3) components accumulated in the non-translating 40S fraction. An interaction of REIL function with translation initiation was further supported by constitutive increase of transcripts coding for eukaryotic translation initiation factor 3 subunit C2 (eIF3C2). *eIF3C2* was highly expressed in both double mutants compared to the wild type before and after cold-shift. In this study, the requirement of REIL proteins for the ribosomal biogenesis at low temperature and their roles in accelerating ribosome *de novo* synthesis were confirmed. The first mechanistic insights into the potential roles of REIL proteins in plants upon cold stress were revealed. It is concluded that REIL could act as a potential cold acclimation factor in *Arabidopsis thaliana*. Unexpectedly, REIL function in Arabidopsis appeared to control the paralog composition (composition of the paralog ribosomal proteins) of non-translating ribosomal 40S and 60S subunits. Considering paralog composition as one mechanism that may create heterogeneous functional ribosome populations (Xue and Barna, 2012; Simsek et al., 2017; Shi et al., 2017; Genuth and Barna, 2018), this study also proposed that *reil* mutants and temperature acclimation cues may provide feasible and highly relevant experimental systems to study ribosome heterogeneity in plants exposed to low temperature stress.

Chapter 5 describes the evaluation of REIL as a potential cold acclimation factor in wheat. The outcomes from **Chapter 4** substantiated the role of REIL proteins as potential cold acclimation factors in Arabidopsis. REIL proteins are required by the plant for ribosome

biogenesis (by enhancing accumulation of 60S large ribosomal subunit) and they are involved in the translational machinery to assist the plant to acclimate in cold temperature. It therefore led me to evaluate if REIL homologs are present in wheat, and if so, to investigate if this protein is required for wheat to adapt to cold conditions. I first examined the presence of REIL homologs in wheat by referring to the wheat genome available in Ensembl Plants database (https://plants.ensembl.org/Triticum_aestivum/Info/Index). As a result, three homologs of *REIL* genes were found to be present in the wheat chromosome number 7A, 7B and 7D. The phylogeny studies of the wheat REIL sequences showed that the Arabidopsis duplication into REIL1 and REIL2 is independent of the wheat isoforms. I also evaluated the *REIL* expressions in wheat subjected to cold, drought and heat stress by re-analyzing published transcriptomics data (Li et al., 2015; Liu et al., 2015). The results showed that there appeared to be a cold temperature responsiveness of *REILs*, but also in response to heat or combined heat/drought stresses A real-time PCR analysis was then performed to evaluate the *REIL* expression in the two wheat varieties used in Chapter 2 and 3 (i.e. Wyalkatchem and Young) subjected to cold stress. The results showed that there were no statistically significant changes of *REIL* gene expression in Wyalkatchem or Young upon cold stress. This may be due to the duration of cold stress applied (two consecutive nights) which may have been insufficient to induce expression in the two varieties. Also, samples were collected from flag leaves at young microspore stage that differed from the mature leaves at three-leaf-stage used in Li et al. (2015) which may also account for the difference observed. Due to the time constraint of my PhD study, unfortunately, the experimental workflow of the qRT-PCR could not be optimized and repeated in a larger number of biological replicates. Thus it would be important in the future to perform more in depth studies of the function of REIL in wheat upon cold stress, e.g. overexpression or silencing of this protein is clearly necessary to further evaluate the potential of REIL as a cold acclimation factor in wheat.

6.2 Concluding Remarks

In conclusion, targeted metabolomics and lipidomics are proven to be useful as an alternative phenotyping method to understand the cold response of wheat, and useful to discriminate wheat varieties with differences in cold acclimation. The outcomes gained from my studies may help us to better understand the mechanisms of wheat in response to cold, thus contributing to wheat breeding programs for the improvement of more cold-tolerant varieties in the future. On the other hand, REIL proteins have been confirmed to act as potential cold acclimation factors in

Arabidopsis. My preliminary study revealed that *REIL* homologs are present and expressed in wheat. However, it is unclear whether the cold acclimation function of REIL may be conserved among the dicots (*Arabidopsis thaliana*) and the monocots (wheat), thus further investigation is required. More in-depth studies such as overexpression or silencing of the *REIL* expression in Australian spring wheat varieties will support the investigation of the function and potential of this protein as a cold acclimation factor in monocots in the future.

References

Afgan, E., Sloggett, C., Goonasekera, N., Makunin, I., Benson, D., Crowe, M., Gladman, S., Kowsar, Y., Pheasant, M., Horst, R., & Lonie, A. (2015). Genomics Virtual Laboratory: A Practical Bioinformatics Workbench for the Cloud. *PLoS One* **10**(10)**:** e0140829.

Aid, F. (2019). Plant Lipid Metabolism. *In Lipid Metabolism* (Baez, R.V. ed), IntechOpen.

Akashi, K., Miyake, C., & Yokota, A. (2001). Citrulline, a novel compatible solute in drought-tolerant wild watermelon leaves, is an efficient hydroxyl radical scavenger. *FEBS Letters* **508**(3)**:** 438-442.

Ambroise, V., Legay, S., Guerriero, G., Hausman, J.-F., Cuypers, A., & Sergeant, K. (2019). The roots of plant frost hardiness and tolerance. *Plant Cell Physiol.* **61:** 3–20.

Andrews, S. (2010). FastQC: a quality control tool for high throughput sequence data. Available online at: http://www.bioinformatics.babraham.ac.uk/projects/fastqc.

Appels, R. et al. (2018). Shifting the limits in wheat research and breeding using a fully annotated reference genome. *Science* **361:** DOI: 10.1126/science.aar7191.

Arbona, V., Manzi, M., de Ollas, C., & Gomez-Cadenaz, A. (2013). Metabolomics as a tool to investigate abiotic stress tolerance in plants. *Int. J. Mol. Sci.* **14:** 4885-4911.

Argiolas, A., Puleo, G.L., Sinibaldi, E., & Mazzolai, B. (2016). Osmolyte cooperation affects turgor dynamics in plants. *Scientific Reports* **6:** Article 30139.

Arisz, S.A., van Wijk, R., Roels, W., Zhu, J.K., Haring, M.A., & Munnik, T. (2013). Rapid phosphatidic acid accumulation in response to low temperature stress in Arabidopsis is generated through diacylglycerol kinase. *Frontiers in Plant Science* **4:** Article 1.

Arisz, S.A., Heo, J., Koevoets, I.T., Zhao, T., van Egmond, P., Meyer, A.J., Zeng, W., Niu, X., Wang, B., Mitchell-Olds, T., Schranz, M.E., & Testerink, C. (2018). Diacylglycerol acyltransferase1 contributes to freezing tolerance. *Plant Physiology* **177:** 1410-1424.

Ashraf, M., & Foolad, M.R. (2007). Roles of glycine betaine and proline in improving plant abiotic stress resistance. *Environmental and Experimental Botany* **59**(2)**:** 206-216.

Ashworth, E.N., Christiansen, M.N., St. John, J.B., & Patterson, G.W. (1981). Effect of temperature and BASF 13 338 on the lipid composition and respiration of wheat roots. *Plant Physiology* **67:** 711-715.

Bakht, J., Bano, A., & Dominy P. (2006). The role of abscisic acid and low temperature in chickpea (*Cicer arietinum*) cold tolerance. II. Effects on plasma membrane structure and function. *Journal of Experimental Botany* **57:** 3707–3715

Barakat, A., Szick-Miranda, K., Chang, I.F., Guyot, R., Blanc, G., Cooke, R., Delseny, M.,& Bailey-Serres, J. (2001). The organization of cytoplasmic ribosomal protein genes in the Arabidopsis genome. *Plant Physiology* **127:** 398–415.

Barbaglia, A.M., & Hoffmann-Benning, S. (2016). Long-distance lipid signaling and its role in plant development and stress response. *Subcell Biochem.* **86:** 339–361.

Bargmann, B.O., & Munnik, T. (2006). The role of phospholipase D in plant stress responses. *Curr. Opin. Plant Biol.* **9:** 515–522.

Barlow, K.M., Christy, B.P., O'Leary, G.J., Riffkin, P.A., & Nuttall, J.G. (2015). Simulating the impact of extreme heat and frost events on wheat crop production: A review. *Field Crops Research* **171:** 109-119.

Barnes, A.C., Benning, C., & Roston, R.L. (2016). Chloroplast membrane remodeling during freezing stress is accompanied by cytoplasmic acidification activating SENSITIVE TO FREEZING2. *Plant Physiol.* **171:** 2140–2149.

Barrero-Sicilia, C., Silvestre, S., Haslam, R.P., & Michaelson, L.V. (2017). Lipid remodelling: Unravelling the response to cold stress in Arabidopsis and its extremophile relative *Eutrema salsugineum*. *Plant Science* **263:** 194-200.

Basu, U., Si, K., Warner, J.R., & Maitra, U. (2001). The Saccharomyces cerevisiae TIF6 gene encoding translation initiation factor 6 is required for 60S ribosomal subunit biogenesis. *Mol Cell Biol* **21:** 1453–1462.

Bates, P.D., & Browse, J. (2012). The significance of different diacylglycerol synthesis pathways on plant oil composition and bioengineering. *Frontiers in Plant Science* **3:** Article 147.

Baxter, A., Mittler, R., & Suzuki, N. (2014). ROS as key players in plant stress signalling. *J. Exp. Bot.* **65:** 1229–1240.

Beck, E.H., Fettig, S., Knake, C., Hartig, K., & Bhattarai, T. (2007). Specific and unspecific responses of plants to cold and drought stress. *J. Biosci.* **32**: 501–510.

Beine-Golovchuk, O., Firmino, A.A.P., Dabroska, A., Schmidt, S., Erban, A., Walter, D., Zuther, E., Hincha, D.K., Kopka, J. (2018). Plant temperature acclimation and growth rely on cytosolic ribosome factor homologs. *Plant Physiology* **176:** 2251-2276.

Benjamini, Y., & Hochberg, Y. (1995). Controlling the false discovery rate: a practical and powerful approach to multiple testing. *Journal of the Royal Statistical Society (Series B)* **57**(1)**:** 289-300.

Boer, R., Campbell, L.C., & Fletcher, D.J. (1983). Characteristics of frost in a major wheat-growing region of Australia. *Aust. J. Agric. Res.* **44:** 1731–1743.

Boggs, J. (1987). Lipid intermolecular hydrogen bonding: influence on structural organization and membrane function. *Biochimica et Biophysica Acta* **906:** 353–404.

Bohn, M., Luthje, S., Sperling, P., Heinz, E., & Dorffling, K. (2007). Plasma membrane lipid alterations induced by cold acclimation and abscisic acid treatment of winter wheat seedlings differing in frost resistance. *Journal of Plant Physiology* **164**(2)**:** 146-156.

Bolger, A.M., Lohse, M., & Usadel, B. (2014). Trimmomatic: a flexible trimmer for Illumina sequence data. *Bioinformatics* **30:** 2114-2120.

Bouche, N., & Fromm, H. (2004). GABA in plants: just a metabolite? *Trends in Plant Science* **9**(3)**:** 110-115.

Bouche, N., Fait, A., Zik, M., & Fromm, H. (2004). The root-specific glutamate decarboxylase (GAD1) is essential for sustaining GABA levels in Arabidopsis. *Plant Mol. Biol.* **55:** 315–325.

Boughton, B.A., Callahan, D.L., Silva, C., Bowne, J., Nahid, A., Rupasinghe, T., Tull, D.L., McConville, M.J., Bacic, A., & Roessner, U. (2011). Comprehensive profiling and quantitation of amine group containing metabolites. *Anal. Chem.* **83:** 7523–7530.

Bowne, J.B., Erwin, T.A., Juttner, J., Schnurbusch, T., Langridge, P., Bacic, A., & Roessner, U. (2012). Drought responses of leaf tissues from wheat cultivars of differing drought tolerance at the metabolite level. *Molecular Plant* **5**(2)**:** 418-429.

Boyes, D.C., Zayed, A.M., Ascenzi, R., McCaskill, A.J., Hoffman, N.E., Davis, K.R., & Gorlach, J. (2001). Growth stage-based phenotypic analysis of Arabidopsis: a model for high-throughput functional genomics in plants. *Plant Cell* **13:** 1499-1510.

Brady, S.M., Orlando, D.A., Lee, J-Y., Wang, J.Y., Koch, J., Dinneny, J.R., Mace, D. et al. (2007). A high-resolution root spatiotemporal map reveals dominant expression patterns. *Science* **318:** 801-806.

Broeckling, C.D., Huhman, D.V., Farag, M.A., Smith, J.T., May, G.D., Mendes, P., Dixon, R.A., Sumner, L.W. (2005). Metabolic profiling of *Medicago truncatula* cell cultures reveals the effects of biotic and abiotic elicitors on metabolism. *J. Exp. Bot.* **56:** 323–336.

Browne, R.G., Iacuone, S., Li, S.F., Dolferus, R., & Parish, R.W. (2018). Anther morphological development and stage determination in *Triticum aestivum. Frontiers in Plant Science* **9:** Article 228.

Browning, K.S., & Bailey-Serres, J. (2015). Mechanism of cytoplasmic mRNA translation. *Arabidopsis Book* **13:** e0176

Browning, K.S., Gallie, D.R., Hershey, J.W., Hinnebusch, A.G., Maitra, U., Merrick, W.C., Norbury, C. (2001). Unified nomenclature for the subunits of eukaryotic initiation factor 3. *Trends Biochem. Sci.* **26:** Article 284.

Browse, J., Warwick, N., Somerville, C.R., & Slack, C.R. (1986). Fluxes through the prokaryotic and eukaryotic pathways of lipid synthesis in the '16:3' plant *Arabidopsis thaliana*. *Biochem. J.* **235:** 25–31.

Buchanan, B., Gruissem, W., & Jones, R. (2002). *Biochemistry & Molecular Biology of Plants*, pp. 456–527. John Wiley & Sons, Rockville, MD, USA.

Burg, M.B., & Ferraris, J.D. (2008). Intracellular organic osmolytes: function and regulation. *Journal of Biological Chemistry* **283**(12)**:** 7309-7313.

Burks, E.A., Bezerra, P.P., Le, H., Gallie, D.R., & Browning, K.S. (2001). Plant initiation factor 3 subunit composition resembles mammalian initiation factor 3 and has a novel subunit. *Journal of Biological Chemistry* **276:** 2122-2131.

Buskirk, H.A.V., & Thomashow, M.F. (2006). Arabidopsis transcription factors regulating cold acclimation. *Physiologia Plantarum* **126:** 72-80.

Cacas, J-L., Furt, F., Le Guedard, M., Schmitter, J-M., Bure, C., Gerbeau-Pissot, P., Moreau, P., Bessoule, J-J., Simon-Plas, F., Mongrand, S. (2012). Lipids of plant membrane rafts. *Prog. Lipid Res.* **51:** 272–299.

Campos, P., Quartin, V., Ramalho, J., & Nunes, M. (2003). Electrolyte leakage and lipid degradation account for cold sensitivity in leaves of *Coffea* sp. plants. *J. Plant Physiol.* **160:** 283–292.

Cao, D., Lutz, A., Hill, C.B., Callahan, D.L., & Roessner, U. (2017). A quantitative profiling method of phytohormones and other metabolites applied to barley roots subjected to salinity stress. *Frontiers in Plant Science* **7:** Article 2070.

Castro, A.J., & Clément, C. (2007). Sucrose and starch catabolism in the anther of *Lilium* during its development: A comparative study among the anther wall, locular fluid and microspore/pollen fractions. *Planta* **225:** 1573–1582.

Chakrabarti, B., Singh, S.D., Nagarajan, S., & Aggarwal, P.K. (2011). Impact of temperature on phenology and pollen sterility of wheat varieties. *Australian Journal of Crop Science* **5**(8)**:** 1039-1043.

Chen, Y., Jiang, J., Chang, Q., Gu, C., Song, A., Chen, S., Dong, B., & Chen F. (2014). Cold acclimation induces freezing tolerance via antioxidative enzymes, proline metabolism and gene expression changes in two *Chrysanthemum* species. *Molecular Biology Reports* **41**(2)**:** 815-822.

Cheng, Z., Mugler, C.F., Keskin, A., Hodapp, S., Chan, L.Y.L., Weis, K., Mertins, P., Regev, A., Jovanovic, M., & Brar, G.A. (2019). Small and large ribosomal subunit deficiencies lead to distinct gene expression signatures that reflect cellular growth rate. *Molecular Cell* **73:** 36-47.

Cheong, B.E., Ho, W.W.H., Biddulph, B., Wallace, X., Rathjen, T., Rupasinghe, T.W.T., Roessner, U., & Dolferus, R. (2019). Phenotyping reproductive stage chilling and frost tolerance in wheat using targeted metabolome and lipidome profiling. *Metabolomics* **15:** Article 144.

Cheong, B.E., Onyemaobi, O., Ho, W.W.H., Biddulph, B., Rupasinghe, T.W.T., Roessner, U., & Dolferus, R. (2020). Phenotyping the chilling and freezing responses of young microspore stage Wheat spikes using targeted metabolome and lipidome profiling. *Cells* **9:** Article 1309.

Chinnusamy, V., Zhu, J. & Zhu, J.K. (2006). Gene regulation during cold acclimation in plants. *Trends in Plant Science* **12:** 444-451.

Ciftci-Yilmaz, S., & Mittler, R. (2008). The zinc finger network of plants. *Cell Mol. Life Sci.* **65:** 1150-1160.

Clément, C., Burrus, M., & Audran, J.-C. (1996). Floral organ growth and carbohydrate content during pollen development in *Lilium*. *Am. J. Bot.* **83:** 459–469.

Clément, C., Laporte, P., & Audran, J.C. (1998). The loculus content and tapetum during pollen development in *Lilium*. *Sex. Plant Reprod.* **11:** 94–106.

Cook, D., Fowler, S., Fiehn, O., & Thomashow, M.F. (2004). A prominent role for the CBF. *Proc Natl Acad Sci USA* **101:** 15243-15248.

Couée, I., Sulmon, C., Gouesbet, G., & El Amrani, A. (2006). Involvement of soluble sugars in reactive oxygen species balance and responses to oxidative stress in plants. *J. Exp. Bot.* **57:** 449–459.

Coursol, S., Fan, L.M., Le Stunff, H., Spiegel, S., Gilroy, S., & Assmann, S.M. (2003). Sphingolipid signalling in Arabidopsis guard cells involves heterotrimeric G proteins. *Nature* **423:** 651–654.

Coursol, S., Le Stunff, H., Lynch, D.V., Gilroy, S., Assmann, S.M. and Spiegel, S. (2005). Arabidopsis sphingosine kinase and the effects of phytosphingosine-1-phosphate on stomatal aperture. *Plant Physiol.* **137:** 724–737.

Criddle, R.S., Smith, B.N., & Hansen, L.D. (1997). A respiration based description of plant growth rate responses to temperature. *Planta* **201:** 441-445.

Crimp, S., Bakar, K.S., Kokic, P., Jin, H., Nicholls, N., & Howden, M. (2015). Bayesian space-time model to analyse frost risk for agriculture in Southeast Australia. *International Journal of Climatology* **35**(8)**:** 2092-2108.

Curatolo W. (1987). The physical properties of glycolipids. *Biochimica et Biophysica Acta* **906:** 111–136.

Das, K., & Roychoudhury, A. (2014). Reactive oxygen species (ROS) and response of antioxidants as ROS-scavengers during environmental stress in plants. *Frontiers in Environmental Science* **2:** Article 53.

Degenkolbe, T., Giavalisco, P., Zuther, E., Seiwert, B., Hincha, D.K., & Willmitzer, L. (2012). Differential remodeling of the lipidome during cold acclimation in natural accessions of *Arabidopsis thaliana*. *Plant Journal* **72**(6)**:** 972-982.

Demotes-Mainard, S., Doussinault, G., Meynard, J.M., & Gate, P. (1996). Is it possible to diagnose at harvest a problem of pollen sterility in wheat? *European Journal of Agronomy* **5**(3-4)**:** 169-180.

Dias, D.A., Hill, C.B., Jayasinghe, N.S., Atieno, J., Sutton, T., Roessner, U. (2015). Quantitative profiling of polar primary metabolites of two chickpea cultivars with constrasting responses to salinity. *Journal of Chromatography B* **1000:** 1-13.

Dolferus, R., Powell, N., Ji, X., Ravash, R., Edlington, J., Oliver, S., Van Dongen, J.T., & Shiran, B. (2013). The physiology of reproductive-stage abiotic stress tolerance in cereals. In Rout G., Das A. (eds), *Molecular Stress Physiology of Plants* (pp 193-216). India: Springer.

Dong Y., Teleman, A.A., Jedmowski, C., Wirtz, M., & Hell, R. (2019). The Arabidopsis THADA homologue modulates TOR activity and cold acclimation. *Plant Biology* **21:** 77–83.

Dormann, P. (2013). Galactolipids in plant membranes, in *eLS* (Chichester: John Wiley and Son, Ltd), 1-6. Doi: 10.1002/9780470015902.a0020100.pub2.

Douce, R., & Joyard, J. (1980). Plant galactolipids. *Lipids: Structure and Function* Pages 321-362.

Douglas, D.J. (2009). Linear quadruples in mass spectrometry. *Mass Spectrometry Reviews* **28:** 937-960.

Du, Z., Zhou, X., Ling, Y., Zhang, Z., Su, Z. (2010). AgriGO: a GO analysis toolkit for the agricultural community. *Nucleic Acids Research* **38:** W64–W70.

Dubacq, J., Drapier, D., & Tremoliesres, A. (1983). Polyunsaturated fatty acid synthesis by a mixture of chloroplast and microsomes from spinach leaves: evidence for two distinct pathways of the biosynthesis of trienoic acids. *Plant and Cell Physiology* **24:** 1-9.

Dubcovsky, J., Loukoianov, A., Fu, D, Valarik, M., Sanchez, A., & Yan, L. (2005). Effect of the photoperiod on the regulation of wheat vernalization genes VRN1 and VRN2. *Plant Molecular Biology* **60:** 469-480.

Dubouzet, J.G., Sakuma, Y., Ito, Y., Kasuga, M., Dubouzet, E.G., Miura, S., Seki, M., Shinozaki, K., Yamaguchi-Shinozaki, K. (2003). OsDREB genes in rice, *Oryza sativa L.,* encode transcription activators that function in drought-, high-salt- and cold-responsive gene expression. *Plant J.* **33:** 751–763.

Durut, N., Abou-Ellail M., Pontvianne, F., Das, S., Kojima, H., Ukai, S., de Bures, P. et al. (2014). A duplicated NUCLEOLIN gene with antagonistic activity is required for chromatin organization of silent 45D rDNA in Arabidopsis. *Plant Cell* **26:** 1330-1344.

Dutilleul, C., Benhassaine-Kesri, G., Demandre, C., Reze, N., Launay, A., Pelletier, S., Renou, J-P., Zachowski, A., Baudouin, E., & Guillas, I. (2012). Phytosphingosine-phosphate is a signal for AtMPK6 activation and Arabidopsis response to chilling. *New Phytologist* **194:** 181–191.

Edwards, D. et al. (2012). Bread matters: a national initiative to profile the genetic diversity of Australian wheat. *Plant Biotechnology Journal* **10:** 703-708.

Englbrecht, C.C., Schoof, H., Bohm, S. (2004). Conservation, diversification and expansion of C2H2 zinc finger proteins in the *Arabidopsis thaliana* genome. *BMC Genomics* **5:** 39.

Equiza, M., Mirave, J., & Tognetti, J. (2001). Morphological, anatomical and physiological responses related to differential shoot vs. root growth inhibition at low temperature in spring and winter wheat. *Annals of Botany* **87:** 67-76.

Equiza, M., Mirave, J., Tognetti, J. (1997). Differential inhibition of shoot vs. root growth at low temperature and its relationship with carbohydrate accumulation in different wheat cultivars. *Annals of Botany* **80**(5)**:** 657-663.

Erde, J., Rachel, R., Ogorzalek, L., & Joseph A. L. (2014). Enhanced FASP (eFASP) to increase proteome coverage and sample recovery for quantitative proteomic experiments. *Journal of Proteome Research* **13:** 1885-1895.

Eremina, M., Rozhon, W., & Poppenberger, B. (2016). Hormonal control of cold stress responses in plants. *Cellular and Molecular Life Sciences* **73**(4)**:** 797-810.

Espinoza, C., Degenkolbe, T., Caldana, C., Zuther, E., Leisse, A., Willmitzer, L., Hincha, D.K., & Hannah, M.A. (2010). Interaction with diurnal and circadian regulation results in dynamic metabolic and transcriptional changes during cold acclimation in Arabidopsis. *PLoS One* **5**(11)**:** e14101.

Farrell, G. (2018). Australia: Grain and feed annual report. United States Department of Agriculture (USDA), *Foreign Agricultural Service.* (https://www.fas.usda.gov/data/australia-grain-and-feed-annual-2).

Fiebelkorn, D., & Rahman, M. (2016). Development of a protocol for frost-tolerance evaluation in rapeseed/canola (*Brassica napus* L). *Crop Journal* **4**(2)**:** 147-152.

Fleury, D., Jefferies, S., Kuchel, H., & Langridge, P. (2010). Genetic and genomic tools to improve drought tolerance in wheat. *Journal of Experimental Botany* **61**(12)**:** 3211-3222.

Folch, J., Lees, M., & Sloane Stanley, G.H. (1957). A simple method for the isolation and purification of total lipids from animal tissues. *J. Biol. Chem.* **226:** 497–509.

Folgado, R., Panis, B., Sergeant, K., Renaut, J., Swennen, R., & Hausman, J.F. (2015). Unravelling the effect of sucrose and cold pretreatment on cryopreservation of potato through sugar analysis and proteomics. *Cryobiology* **71:** 432–441.

Fowler, D.B. (2008). Cold acclimation threshold induction temperatures in cereals. *Crop Science* **48**(3)**:** 1147-1154.

Fowler, D.B., & Gusta, L.V. (1979). Selection for winter hardiness in wheat . I. Identification of genotypic variability. *Crop Sci.* **19:** 769–772.

Fowler, D.B., Breton, G., Limin, A.E., Mahfoozi, S., & Sarhan, F. (2001). Photoperiod and temperature interactions regulate low-temperature-induced gene expression in barley. *Plant Physiology* **127**(4)**:** 1676-1681.

Fowler, D.B., Limin, A.E., Wang, S., & Ward, R.W. (1996a). Relationship between low-temperature tolerance and vernalization response in wheat and rye. *Canadian Journal of Plant Science* **76:** 37-42.

Fowler, D.B., Chauvin, L.P., Limin, A.E., & Sarhan, F. (1996b). The regulatory role of vernalization in the expression of low-temperature-induced genes in wheat and rye. *Theor Appl Genet* **93:** 554-559.

Fowler, S., & Thomashow, M.F. (2002). Arabidopsis transcriptome profiling indicates that multiple regulatory pathways are activated during cold acclimation in addition to the CBF response pathway. *Plant Cell* **14:** 1675-1690.

Francia, E., Barabaschi, D., Tondelli, A., Laidò, G., Rizza, F., Stanca, A., Busconi, M., Fogher, C., Stockinger, E., & Pecchioni, N. (2007). Fine mapping of a HvCBF gene cluster at the frost resistance locus Fr-H2 in barley. *Theor. Appl. Genet.* **115:** 1083–1091.

Frederiks, T.M., Christopher, J.T., Fletcher, S.E.H., & Borrell, A.K. (2011). Post head-emergence frost resistance of barley genotypes in the northern grain region of Australia. *Crop and Pasture Science* **62**(9)**:** 736-745.

Frederiks, T.M., Christopher, J.T., Harvey, G.L., Sutherland, M.W., & Borrell, A.K. (2012). Current and emerging screening methods to identify post-head-emergence frost adaptation in wheat and barley. *Journal of Experimental Botany* **63**(15)**:** 5405-5416.

Frederiks, T.M., Christopher, J.T., Sutherland, M.W., & Borrell, A.K. (2015). Post-head-emergence frost in wheat and barley: Defining the problem, assessing the damage, and identifying resistance. *J. Exp. Bot.* **66:** 3487–3498.

Gamalinda, M., Jakovljevic, J., Babiano, R., Talkish, J., de la Cruz, J., & Woolford, J.L. (2013). Yeast polypeptide exit tunnel ribosomal proteins L17, L35 and L37 are necessary to recruit late-assembling factors required for 27SB pre-rRNA processing. *Nucleic Acids Research* **41:** 1965-1983.

Gnanasundram, S.V., Kos-Braun, I.C., & Kŏs, M. (2019). At least two molecules of the RNA helicase Has1 are simultaneously present in pre-ribosomes during ribosome biogenesis. *Nucleic Acids Research* **47:** 10852 - 10864.

Garg, A.K., Kim, J., Owens, T.G., Ranwala, A.P., Choi, Y.D., Kochian, L.V., & Wu, R.J. (2002). Trehalose accumulation in rice plants confers high tolerance levels to different abiotic stresses. *Proceedings of the National Academy of Sciences of the United States of America* **99:** 15898-15903.

Genuth, N. R., & Barna, M. (2018). Heterogeneity and specialized functions of translation machinery: from genes to organisms. *Nature Reviews Genetics* **19:** 431-452.

Gill, S.S., & Tuteja, N. (2010). Polyamines and abiotic stress tolerance in plants. *Plant Signaling & Behavior* **5:** 26-33.

Gilmour, S.J., Zarka, D.G., Stockinger, E.J., Salazar, M.P., Houghton, J.M., & Thomashow, M.F. (1998). Low temperature regulation of the Arabidopsis CBF family of AP2 transcriptional activators as an early step in cold-induced COR gene expression. *Plant J* **16:** 433–442.

Gilmour, S.J., Sebolt, A.M., Salazar, M.P., Everard, J.D., & Thomashow, M.F. (2000). Overexpression of the Arabidopsis CBF3 transcriptional activator mimics multiple biochemical changes associated with cold acclimation. *Plant Physiol* **124:** 1854–1865.

Gilmour, S.J., Fowler, S.G., & Thomashow, M.F. (2004). Arabidopsis transcriptional activators CBF1, CBF2, and CBF3 have matching functional activities. *Plant Mol Biol* **54:** 767–781.

Grant, O.M., Brennan, D.P., Salas, C.D.M., & Dix, P.J. (2014). Impact of enhanced capacity to scavenge reactive oxygen species on cold tolerance of tobacco. *International Journal of Plant Sciences* **175**(5)**:** 544-554.

Gray, G.R., Chauvin, L-P., Sarhan, F., & Huner, N.P. (1997). Cold acclimation and freezing tolerance (a complex interaction of light and temperature). *Plant Physiology* **114:** 467-474.

Greber, B.J., Boehringer, D., Montellese, C., & Ban, N. (2012). Cryo-EM structures of Arx1 and maturation factors Rei1 and Jjj1 bound to the 60S ribosomal subunit. *Nat. Struct. Mol. Biol.* **19:** 1228–1233.

Greber, B.J., Gethardy, S., Leitner, A., et al. (2016). Insertion of the biogenesis factor Rei1 probes the ribosomal tunnel during 60S maturation. *Cell* **164:** 91-102.

Gu, L., Hanson, P.J., Post, W.M., Kaiser, D.P., Yang, B., Nemani, R., Pallardy, S.G., & Meyers, T. (2008). The 2007 Eastern US spring freeze: Increased cold damage in a warming world? *BioScience* **58:** 253–262.

Gu, Y., He, L., Zhao, C., Wang, F., Yan, B., Gao, Y., Li, Z., Yang, K., & Xu, J. (2017). Biochemical and transcriptional regulation of membrane lipid metabolism in maize leaves under low temperature. *Frontiers in Plant Science* **8:** Article 2053.

Gulick, P.J., Drouin, S., Yu, Z.H., Danyluk, J., Poisson, G., Monroy, A.F., & Sarhan, F. (2005). Transcriptome comparison of winter and spring wheat responding to low temperature. *Genome* **48:** 913-923.

Guo, J., Carrington, Y., Alber, A., & Ehlting, J. (2014). Molecular characterization of quinate and shikimate metabolism in *Populus trichocarpa*. *Journal of Biological Chemistry* **289:** 23846-23858.

Guo, L., Mishra, G., Taylor, K., & Wang, X. (2011). Phosphatidic acid binds and stimulates Arabidopsis sphingosine kinases. *J. Biol. Chem.* **286:** 13336–13345.

Guschina, I.A., & Harwood, J.L. (2006). Mechanisms of temperature adaptation in poikilotherms. *FEBS Lett.* **580:** 5477–5483.

Guy, C. (1999). Molecular responses of plants to cold shock and cold acclimation. *Journal of Molecular Microbiology Biotechnology* **1**(2)**:** 231-242.

Guy, C., Kaplan, F., Kopka, J., Selbig, J., & Hincha, D.K. (2008). Metabolomics of temperature stress. *Physiologia Plantarum* **132:** 220-235.

Guy, C.L. (1990). Cold acclimation and freezing stress tolerance: role of protein metabolism. *Annual Review of Plant Physiology and Plant Molecular Biology* **41:** 187-223.

Hall, R.D. (2005). Plant metabolomics: from holistic hope, to hype, to hot topic. *New Phytologist* **169:** 453-468.

Hanson, A.D., Rathinasabapathi, B., Chamberlin, B., & Gage, D.A. (1991). Comparative physiological evidence that β-alanine betaine and choline-O-sulfate act as compatible osmolytes in halophytic *Limonium* species. *Plant Physiol.* **97:** 1199–1205.

Hanson, A.D., Rathinasabapathi, B., Rivoal, J., Burnet, M., Dillon, M.O., & Gage, D.A. (1994). Osmoprotective compounds in the Plumbaginaceae: A natural experiment in metabolic engineering of stress tolerance. *Proc. Natl. Acad. Sci. USA* **91:** 306–310.

Hao, X., Chen, M., Xu, H., Gao, S., Chen, X., Li, L., Du, L., Ye, X., & Ma, Y. (2005). Obtaining of transgenic wheats with GHDREB gene and their physiological index analysis on drought tolerance. *Southwest China J. Agric. Sci.* **18:** 616–620.

Harnpicharnchai, P., Jakovljevic, J., Horsey, E., Miles, T., Roman, J., Rout, M., Meagher, D., Imai, B., Guo, Y., Brame, C.J., Shabanowitz, J., Hunt, D.F., & Woolford, J.L. Jr. (2001). Composition and functional characterization of yeast 66S ribosome assembly intermediates. *Molecular Cell* **8:** 505-515.

Harrigan, G.G., Martino-Catt, S., Glenn, K.C. (2007). Metabolomics, metabolic diversity and genetic variation in crops. *Metabolomics* **3:** 259-272.

Harwood, J.L. (1998). Plant Lipid Biosynthesis: Fundamentals and Agricultural Applications, pp. 95–110. Cambridge Unviersity Press, New York, USA.

Hasdai, M., Weiss, B., Levi, A., Samach, A., & Porat, R. (2006). Differential responses of Arabidopsis ecotypes to cold, chilling and freezing temperatures. *Annals of Applied Biology* **148:** 113-120.

Hayase, H., Satake, T., Nashiyama, I., & Ito, N. (1969). Male sterility caused by cooling treatment at the meiotic stage in rice plants. II. The most sensitive stage to cooling and fertilizing ability of pistils. *Proceedings of the Crop Science. Society of Japan* **38:** 706-711.

Hayat, S., Ali, B., & Ahmad, A. (2007). Salicylic acid: biosynthesis, metabolism and physiological role in plants. In Hayat S., Ahmad A., (eds), *Salicylic Acid: A plant hormone* (pp. 1-14) Dordrecht: Springer.

Hayat, S., Hayat, Q., Alyemeni, M.N., Wani, A.S., Pichtel, J., & Ahmad, A. (2012). Role of proline under changing environments: a review. *Plant Signaling & Behavior* **7**(11)**:** 1456-1466.

Hill, C.B., Taylor, J.D., Edwards, J., Mather, D., Bacic, A., Langridge, P., & Roessner, U. (2013). Whole-genome mapping of agronomic and metabolic traits to identify novel quantitative trait loci in bread wheat grown in a water-limited environment. *Plant Physiology* **162:** 1266-1281.

Hincha, D.K., Höfner, R., Schwab, K.B., Heber, U., & Schmitt, J.M. (1987). Membrane rupture is the common cause of damage to chloroplast membranes in leaves injured by freezing or excessive wilting. *Plant Physiology* **83**: 251-253.

Ho, J.H., Kallstrom, G., & Johnson, A.W. (2000). Nmd3p is a Crm1p-dependent adapter protein for nuclear export of the large ribosomal subunit. *J. Cell Biol.* **151:** 1057-1066.

Holt, C.E., & Schuman, & E.M. (2013). The central dogma decentralized: new perspectives on RNA function and local translation in neurons. *Neuron* **80:** 648-657.

Holzl, G., & Dormann, P. (2019). Chloroplast lipids and their biosynthesis. *Annual Review of Plant Biology* **70:** 51-81.

Horiguchi, G., Van Lijsebettens, M., Candela, H., Micol, J.L., & Tsukaya, H. (2012). Ribosomes and translation in plant developmental control. *Plant Science* **191192:** 24–34.

Horn, P., & Chapman, K.D. (2014). Lipidomics in situ: Insights into plant lipid metabolism from high resolution spatial maps of metabolites. *Progress in Lipid Research* **54:** 32-52.

Horvath, E., Szalai, G., & Janda, T. (2007). Induction of abiotic stress tolerance by salicylic acid signaling. *Journal of Plant Growth Regulation* **26**(3)**:** 290-300.

Hou, Q., Ufer, G., & Bartels, D. (2016). Lipid signalling in plant responses to abiotic stress. *Plant, Cell and Environment* **39:** 1029-1048.

Hsieh, T., Lee, J., Yang, P.T., Chiu, L.H., Charng, Y., Wang, Y., & Chan, M. (2002). Heterology expression of the Arabidopsis C-repeat/dehydration response element binding factor 1 gene confers elevated tolerance to chilling and oxidative stresses in transgenic tomato. *Plant Physiol.* **129:** 1086–1094.

Hu, Y., Jiang, L., Wang, F., & Yu, D. (2013). Jasmonate regulates the inducer of CBF expression-C-repeat binding factor/DRE binding factor1 cascade and feezing tolerance in Arabidopsis. *Plant Cell* **25:** 2907-2924.

Hummel, M., Dobrenel, T., Cordewener, J. J. H. G., Davanture, M., Meyer, C., Smeekens, S. J. C. M., Bailey-Serres, J., America, T.A., & Hanson, J. (2015). Proteomic LC-MS analysis of Arabidopsis cytosolic ribosomes: Identification of ribosomal protein paralogs and re-annotation of the ribosomal protein genes. *J. Proteomics* **128:** 436–449.

Hurry, V.M., & Huner, N.P. (1991). Low growth temperature effects a differential inhibition of photosynthesis in spring and winter wheat. *Plant Physiology* **96:** 491-497.

Hurry, V., & Norman P. A. H. (1992). Effect of cold hardening on sensitivity of winter and spring wheat leaves to short-term photoinhibition and recovery of photosynthesis. *Plant Physiology* **100**(3)**:** 1283-1290.

Hurry, V.M., Strand, A., Tobiaeson, M., Gardestrom, P., & Oquist, G. (1995). Cold hardening of spring and winter wheat and rape results in differential effects on growth, carbon metabolism, and carbohydrate content. *Plant Physiology* **109:** 697-706.

Ianutsevich, E.A., Danilova, O.A., Groza, N.V., & Tereshina, V.M. (2016). Membrane lipids and cytosol carbohydrates in *Aspergillus niger* under osmotic, oxidative, and cold impact. *Microbiology* **85**(3)**:** 302-310.

Imai, H., Ohnishi, M., Kinishita, M., Kojima, M., Ito, S. (1995). Structure and distribution of cerebroside containing unsaturated hydroxy fatty acids in plant leaves. *Bioscience, Biotechnology and Biochemistry* **59:** 1309–1313.

Imai, H., Ohnishi, M., Hotsubo, K., Kojima, M., Ito, S. (1997). Sphingoid base composition of cerebrosides from plant leaves. *Bioscience, Biotechnology and Biochemistry* **61:** 351–353.

Imai H. 1998. Glucocerebrosides containing unsaturated hydroxy fatty acids in *Arabidopsis thaliana*. In: Sanchez J, Cerda-Olmedo E, Martinez-Force E, eds. *Advances in plant lipid research.* Seville, Spain: University of Seville Publications, 38–40.

Ito, Y., Katsura, K., Maruyama, K., Taji, T., Kobayashi, M., Seki, M., Shinozaki, K., & Yamaguchi-Shinozaki, K. (2006). Functional analysis of rice DREB1/CBF-type transcription factors involved in cold-responsive gene expression in transgenic rice. *Plant Cell Physiol*. **47:** 141–153.

Iwase, M., & Toh-e, A. (2004). Ybr267w is a new cytoplasmic protein belonging to the mitotic signaling network of *Saccharomyces cerevisiae*. *Cell Structure and Function* **29:** 1-15.

Kackson, M.W., Stinchcombe, J.R., Korves, T.M., & Schmitt J. (2004). Costs and benefits of cold tolerance in transgenic *Arabidopsis thaliana. Molecular Ecology* **13:** 3609-3615.

Karlsson, K-A. (1982). Glycosphingolipids and surface membranes. In: Chapman D, ed. *Biological membranes*. Pages 1-74, Academic Press, New York, NY, USA.

Kater, L., Thoms, M., Barrio-Garcia, C., Cheng, J., Ismail, S., Ahmed, Y. L., Bange, G., Kressler, D., Berninghausen, O., Sinning, I., Hurt, E., & Beckmann, R. (2017). Visualizing the assembly pathway of nucleolar pre-60S ribosomes. *Cell* **171:** 1599 - 1610.

Kim, Y., Zhang, H., & Scholl, R.L. (1990). Two evolutionarily divergent genes encode a cytoplasmic ribosomal protein of *Arabidopsis thaliana*. *Gene* **93:** 177-182.

Krokowski, D., Tchórzewski, M., Boguszewska, A., & Grankowski, N. (2005). Acquisition of a stable structure by yeast ribosomal P0 protein requires binding of P1A1486 P2B complex: *in vitro* formation of the stalk structure. *Biochim. Biophys. Acta* **1724:** 59-70.

Krokowski, D., Boguszewska, A., Abramczyk, D., Liljas, A., Tchórzewski, M., & Grankowski, N. (2006). Yeast ribosomal P0 protein has two separate binding sites for P1/P2 proteins. *Mol. Microbiol.* **60:** 386-400.

Krokowski, D., Gaccioli, F., Majumder, M., Mullins, M.R., & Yuan, C.L., Papadopoulou, B., Merrick, W.C., Komar, A.A., Taylor, D., & Hatzoglou, M. (2011). Characterization of hibernating ribosomes in mammalian cells. *Cell Cycle* **10:** 2691-2702.

Jaglo, K.R., Kleff, S., Amundsen, K.L., Zhang, X., Haake, V., Zhang, J.Z., Deits, T., & Thomashow, M.F. (2001). Components of the Arabidopsis C-repeat/dehydration-responsive element binding factor cold-response pathway are conserved in *Brassica napus* and other plant species, *Plant Physiol.* **127:** 910–917.

Jaglo-Ottosen, K.R., Gilmour, S.J., Zarka, D.G., Schabenberger, O., & Thomashow, M.F. (1998). Arabidopsis CBF1 overexpression induces COR genes and enhances freezing tolerance. *Science* **280:** 104–106.

Janmohammadi, M. (2012). Metabolomic analysis of low temperature responses in plants. *Current Opinion in Agriculture* **1:** 1-6.

Javadian, N., Karimzadeh, G., Mahfoozi, S., & Ghanati, F. (2010). Cold-induced changes of enzymes, proline, carbohydrates, and chlorophyll in wheat. *Russian Journal of Plant Physiology* **57**(4)**:** 540-547.

Ji, X., Shiran, B., Wan, J., Lewis, D.C., Jenkins, C.L.D., Condon, A.G., Richards, R.A., & Dolferus, R. 2010. Importance of pre-anthesis anther sink strength for maintenance of grain number during reproductive stage water stress in wheat. *Plant, Cell and Environment* **33**(6)**:** 926-942.

Johnson, K.L. (2018). Baby, it's cold inside: maintaining membrane integrity during freezing. *Plant Physiology* **177:** 1350-1351.

Jones, D.T., Taylor, W.R., & Thornton, J.M. (1992). The rapid generation of mutation data matrices from protein sequences. *Computer Applications in the Biosciences* **8:** 275-282.

Jorge, T.F., Rodrigues, J.A., Caldana, C., Schmist, R., van Dongen, J.T., Thomas-Oates, J., Antonio, C. (2016). Mass spectrometry-based plant metabolomics: metabolite responses to abiotic stress. *Mass Spectrometry Reviews* **35:** 620-349.

Juhasz, Z., Boldizsar, A., Kocsy, G., Marincs, F., Galiba, G., & Banfalvi, Z. (2015). Pleiotropic effect of chromosome 5A and the mvp mutation on the metabolite profile during cold acclimation and the vegetative/generative transition in wheat. *BMC Plant Biology* **15:** 57.

Jung, J.K.H., & McCouch, S. (2013). Getting to the roots of it: genetic and hormonal control of root architecture. *Frontiers in Plant Science* **4:** Article 186.

Kalberer, S.R., Wisniewski, M., & Arora, R. (2006). Deacclimation and reacclimation of cold-hardy plants: Current understanding and emerging concepts. *Plant Science* **171**(1)**:** 3-16.

Kaplan, F., Guy, & C.L. (2004). beta-Amylase induction and the protective role of maltose during temperature shock. *Plant Physiol.* **135:** 1674–1684.

Kaplan, F., Kopka, J., Haskell, D.W., Zhao, W., Schiller, K.C., Gatzke, N., Sung, D.Y., & Guy, C.L. (2004). Exploring the temperature-stress metabolome of Arabidopsis. *Plant Physiology* **136:** 4159-4168.

Kaplan, F., Kopka, J., Sung, D.Y., Zhao, W., Popp, M., Porat, R., & Guy, C.L. (2007). Transcript and metabolite profiling during cold acclimation of Arabidopsis reveals an intricate relationship of cold-regulated gene expression with modifications in metabolite content. *The Plant Journal* **50:** 967-981.

Kasai, K., Kanno, T., Akita, M., Ikejiri-Kanno, Y., Wakasa, K., & Tozawa, Y. (2005). Identification of three shikimate kinase genes in rice: characterization of their differential expression during panicle development and of the enzymatic activities of the encoded proteins. *Planta* **222**(3)**:** 438-447.

Kasuga, M., Liu, Q., Miura, S., Yamaguchi-Shinozaki, K., & Shinozaki, K. (1999). Improving plant drought, salt, and freezing tolerance by gene transfer of a single stress-inducible transcription factor. *Nat Biotechnol* **17:** 287–291.

Kasuga, M., Miura, S., Shinozaki, K., Yamaguchi-Shinozaki, K. (2004). A combination of the Arabidopsis DREB1A gene and stress-inducible rd29A promoter improved drought- and low-temperature stress tolerance in tobacco by gene transfer. *Plant Cell Physiol.* **45:** 346–350.

Kawaguchi, M., Imai, H., Naoe, M., Yasui, Y., Ohnishi, M. (2000). Cerebrosides in grapevine leaves: distinct composition of sphingoid bases among the grapevine species having different tolerances to freezing temperature. *Bioscience, Biotechnology and Biochemistry* **64:** 1271–1273.

Kawasaki, S., Miyake, C., Kohchi, T., Fujii, S., Uchida, M., & Yokota, A. (2000). Responses of wild watermelon to drought stress: accumulation of an ArgE homologue and citrulline in leaves during water deficits. *Plant & Cell Physiology* **41**(7)**:** 864-873.

Kendall, E.J., & McKersie, B.D. (1989). Free radical and freezing injury to cell membranes of winter wheat. *Physiologia Plantarum* **76:** 86-94.

Keunen, E., Peshev, D., Vangronsveld, J., Van Den Ende, W., & Cuypers, A. (2013). Plant sugars are crucial players in the oxidative challenge during abiotic stress: Extending the traditional concept. *Plant Cell Environ.* **36:** 1242–1255.

Keurentjes, J.J. (2009). Genetical metabolomics: Closing in on phenotypes. *Curr. Opin. Plant Biol.* **12:** 223–230.

Kim, D., Langmead, B., & Salzberg, S.L. (2015). HISAT: a fast spliced aligner with low memory requirements. *Nature Methods* **12:** 357--360.

Kim, Y., Zhang, H., & Scholl, R.L. (1990). Two evolutionarily divergent genes encode a cytoplasmic ribosomal protein of *Arabidopsis thaliana. Gene* **93:** 177-182.

Kizis, D., & Pagès, M. (2002). Maize DRE-binding proteins DBF1 and DBF2 are involved in rab17 regulation through the drought-responsive element in an ABA-dependent pathway. *Plant Journal* **30:** 679–689.

Knaupp, M., Mishra, K.B., Nedbal, L., & Heyer, A.G. (2011). Evidence for a role of raffinose in stabilizing photosystem II during freeze-thaw cycles. *Planta* **234:** 477–486.

Knox, A.K., Li, C., Vágújfalvi, A., Galiba, G., Stockinger, E.J., & Dubcovsky, J. (2008). Identification of candidate CBF genes for the frost tolerance locus Fr-Am2 in *Triticum monococcum*. *Plant Mol. Biol.* **67:** 257–270.

Koornneef, M., & Meinke, D. (2010). The development of Arabidopsis as a model plant. *The Plant Journal* **61:** 909–921.

Kosova, K., Prasil, I.T., Vitamvas, P., Dobrev, P., Motyka, V., Flokova, K. et al. (2012). Complex phytohormone responses during the cold acclimation of two wheat cultivars differing in cold tolerance, winter Samanta and spring Sandra. *Journal of Plant Physiology* **169:** 567-576.

Kramer, U. (2015). Planting molecular functions in an ecological context with *Arabidopsis thaliana*. *eLife* **4:** e06100. DOI: 10.7554/eLife.06100.

Krause, G.H., Grafflage, S., Rumich-Bayer, S., & Somersalo, S. (1988). Effects of freezing on plant mesophyll cells. *Symposia of the Society Experimental Biology* **42:** 311-327.

Kreps. J.A., & Simon, A.E. (1997). Environmental and genetic effects on circadian clock-regulated gene expression in Arabidopsis. *Plant Cell* **9:** 297-304.

Kumar, S., Stecher, G., Li, M., Knyaz, C., & Tamura, K. (2018). MEGA X: Molecular Evolutionary Genetics Analysis across computing platforms. *Molecular Biology and Evolution* **35:** 1547-1549.

Kunst, L., Browse, J., & Somerville, C. (1988). Altered regulation of lipid biosynthesis in a mutant of Arabidopsis deficient in chloroplast glycerol-3-phosphate acyltransferase activity. *Proc. Natl. Acad. Sci.* USA **85:** 4143–4147.

Kurepin, L.V., Dahal, K.P., Savitch, L.V., Singh, J., Bode, R., Ivanov, A.G., Hurry, V., & Huner, N.P.A. (2013). Role of CBFs as integrators of chloroplast redox, phytochrome and plant hormone signaling during cold acclimation. *International Journal of Molecular Sciences* **14:** 12729-12763.

Kusvuran, S., Dasgan, H.Y., & Abak, K. (2013). Citrulline is an important biochemical indicator in tolerance to saline and drought stresses in melon. *The Scientific World Journal* **2013:** 253414.

Lata, C., & Prasad, M. (2011). Role of DREBs in regulation of abiotic stress responses in plants. *Journal of Experimental Botany* **62:** 4731-4748.

Lebreton, A., Saveanu, C., Decourty, L., Rain, J-C., Jacquier, A., & Fromont-Racine, M. (2006). A functional network involved in the recycling of nucleocytoplasmic pre-60S factors. *Journal of Cell Biology* **173:** 349-360.

Lee, J-Y., Colinas, J., Wang, J.Y., Mace, D., Ohler, U., & Benfey, P.N. (2006). Transcriptional and posttranscriptional regulation of transcription factor expression in Arabidopsis roots. *PNAS* **103:** 6055-6060.

Leff, B., Ramankutty, N., & Foley, J.A. (2004). Geographic distribution of major crops across the world. *Global Biogeochemical Cycles* **18**(1)**:** 1-27.

Lehmann, S., Funck, D., Szabados, L., & Rentsch D. (2010). Proline metabolism and transport in plant development. *Amino Acids* **39**(4)**:** 949-962.

Lemoine, R., La Camera, S., Atanassova, R., Dedaldechamp, F., Allario, T., Pourtau, N., Bonnemain, J.L., Laloi, M., Coutos-Thevenot, P., Maurousset, L., et al. (2013). Source-to-sink transport of sugar and regulation by environmental factors. *Frontiers in Plant Science* **4:** Article 272.

Lester, R.L., & Dickson, R.C. (1993). Sphingolipids with inositolphosphate containing head groups. *Advances in Lipid Research* **26:** 253–276.

Levitt, J. (1980). Responses of plants to environmental stresses. Volume I. *Chilling, freezing and high temperature stresses.*, Vol 2. New York: Academic Press.

Li, H-X., Cao, L-L., Yan, X., Li, C., Shi, H-Y., Wang, J-W., & Ye, Y-H. (2013). Cerebroside C increases tolerance to chilling injury and alters lipid composition in wheat roots. *PLOS ONE* **8:** e73380.

Li, L., Nelson, C. J., Trösch, J., Castleden, I., Huang, S., & Millar, A. H. (2017). Protein degradation rate in *Arabidopsis thaliana* leaf growth and development. *Plant Cell* **29:** 207-228.

Li, Q., Zheng, Q., Shen, W., Cram, D., Fowler, D.B., Wei, Y., & Zou, J. (2015a). Understanding the biochemical basis of temperature-induced lipid pathway adjustments in plants. *Plant Cell* **27:** 86–103.

Li, W., Li, M., Zhang, W., Welti, R., & Wang, X. (2004). The plasma membrane-bound phospholipase Dδ enhances freezing tolerance in *Arabidopsis thaliana*. *Nature Biotech.* **22:** 427–33.

Li, X., Cai, J., Liu, F., Dai, T., Cao, W., & Jiang, D. (2014). Spring freeze effect on wheat yield is modulated by winter temperature fluctuations: evidence from meta-analysis and simulating experiment. *Journal of Agronomy and Crop Science* **201**(4)**:** 288-300.

Li, X., Cai, J, Liu, F., Zhou, Q., Dai, T., Cao, W., & Jiang, D. (2015b). Wheat plants exposed to winter warming are more susceptible to low temperature stress in the spring. *Plant Growth Regulation* **77**(1)**:** 11-19.

Liang, H., Yao, N., Song, J.T., Luo, S., Lu, H., & Greenberg, J.T. (2003). Ceramide phosphorylation modulates programmed cell death in plants. *Genes and Development* **17:** 2636–2641.

Liang, X., Zhang, L., Natarajan, S.K., & Becker, D.F. (2013). Proline mechanisms of stress survival. *Antioxidants & Redox Signaling* **19**(9)**:** 998-1011.

Liebisch, G., Vizcaíno, J.A., Kofeler, H., Trotzmüller, M., Griffiths, W.J., Schmitz, G., Spener, F., & Wakelam, M.J. (2013). Shorthand notation for lipid structures derived from mass spectrometry. *Journal of Lipid Research* **54:** Article 1523e1530.

Liljas, A, & Sanyal, S (2018). The enigmatic ribosomal stalk. *Quarterly Reviews of Biophysics* **51:** e12, 1–10.

Limin, A.E., & Fowler, D.B. (2006). Low-temperature tolerance and genetic potential in wheat (*Triticum aestivum* L): response to photoperiod, vernalization, and plant development. *Planta* **224**(2)**:** 360-366.

Lissarre, M., Ohta, M., Sato, A., & Miura, K. (2010). Cold-responsive gene regulation during cold acclimation in plants. *Plant Signaling & Behavior* **5**(8)**:** 948-952.

Liu, Q., Kasuga, M., Sakuma, Y., Abe, H., Miura, S., Yamaguchi-Shinozaki, K., & Shinozaki, K. (1998). Two transcription factors, DREB1 and DREB2, with an EREBP/AP2 DNA binding domain separate two cellular signal transduction pathways in drought- and low-temperature-responsive gene expression, respectively, in Arabidopsis. *Plant Cell* **10:** 1391–1406.

Liu, Z., Xin, M., Qin, J., Peng, H., Ni, Z., Yao, Y. & Sun, Q. (2015). Temporal transcriptome profiling reveals expression partitioning of homeologous genes contributing to heat and drought acclimation in wheat (*Triticum aestivum* L.). *BMC Plant Biology* **15:** Article 152.

Livingston, D.P.I., Tuong, T. D., Isleib, T. G., Murphy, J. P. (2016). Differences between wheat genotypes in damage from freezing temperatures during reproductive growth. *European Journal of Agronomy* **74:** 164-172.

Llanes, A., Bertazza, G., Palacio, G., & Luna, V. (2013). Different sodium salts cause different solute accumulation in the halophyte *Prosopis strombulifera*. *Plant Biol. (Stuttg.)* **15:** (Suppl. 1), 118–125.

Lo, K.Y., Li, Z.H., Bussiere, C., Bresson, S., Marcotte, E.M., & Johnson, A.W. (2010). Defining the pathway of cytoplasmic maturation of the 60S ribosomal subunit. *Molecular Cell* **39:** 196-208.

Lobell, D.B., & Gourdji, S.M. (2012). The influence of climate change on global crop productivity. *Plant Physiology* **160:** 1686-1697.

Loescher, W.H., Tyson, R.H., Everard, J.D., Redgwell, R.J., & Bieleski, R.L. (1992). Mannitol synthesis in higher plants: evidence for the role and characterization of a NADPH-dependent mannose 6-phosphate reductase. *Plant Physiology* **98:** 1396-1402.

Lokhande, V.H., & Suprasanna, P. (2012). Prospects of halophytes in understanding and managing abiotic stress yolerance. In *Environmental Adaptations and Stress Tolerance of Plants in the Era of Climate Change*, Ahmad, P., Prasad, M.N.V., Eds., Springer New York: New York, NY, USA, pp. 29–56, doi:10.1007/978-1-4614-0815-4_2.

Los, D.A., & Murata, N. (2004). Membrane fluidity and its roles in the perception of environmental signals. *Biochim. Biophys. Acta* **1666:** 142–157.

Loukoianov, A., Yan, L., Blechl, A., Sanchez, A., & Dubcovsky, J. (2005). Regulation of VRN-1 vernalization genes in normal and transgenic polyploidy wheat. *Plant Physiology* **138:** 2364-2373.

Lu, J., Xu, Y., Wang, J., Singer, S.D., & Chen, G. (2020). The role of triacylglycerol in plant stress response. *Plants* **9:** Article 472.

Lu, Y., & Sharkey, T.D. (2006). The importance of maltose in transitory starch breakdown. *Plant Cell Environ.* **29:** 353–366.

Luo, M-C., et al. (2017). Genome sequence of the progenitor of the wheat D genome *Aegilops tauschii. Nature* **551:** 498–502.

Luttgeharm, K.D., Kimberlin, A.N., & Cahoon, E.B. (2016). Plant sphingolipid metabolism and function. In: Nakamura Y., Li-Beisson Y. (eds) *Lipids in Plant and Algae Development. Subcellular Biochemistry*, vol **86**. Springer, Cham.

Lynch, D.V., & Steponkus, P.L. (1987). Plasma membrane lipid alterations associated with cold acclimation of winter rye seedlings (*Secale cereale* L. cv. Puma). *Plant Physiology* **83:** 761–767.

Lynch, D.V. (1993). Sphingolipids. In: Moore Jr TS, ed. *Lipid metabolism in plants*. Boca Raton, FL, USA: CRC Press, 285–308.

Lynch, D.V. & Dunn, T.M. (2004). An introduction to plant sphingolipids and a review of recent advances in understanding their metabolism and function. *New Phytologist* **161:** 677-702.

Ma, C., Wu, S., Li, N., Chen, Y., Yan, K., Li, Z., Zheng, L., Lei, J., Woolford, J.L. Jr., & Gao, N. (2017). Structural snapshot of cytoplasmic pre-60S ribosomal particles bound by Nmd3, Lsg1, Tif6 and Reh1. *Nat. Struct. Mol. Biol.* **24:** 214–220.

Ma, N.Y., Rahmat, Z., & Lam, S.S. (2013). A review of the "omics" approach to biomarkers of oxidative stress in Oryza sativa. *Int. J. Mol. Sci.* **14:** 7515-754.

Machakova, I., Hanisova, A., & Krekule, J. (1989). Levels of ethylene, ACC, MACC, ABA and proline as indicators of cold hardening and frost resistance in winter wheat. *Physiologia Plantarum* **76:** 603-607.

Mahajan, S., & Tuteja, N. (2005). Cold, salinity and drought stresses: An overview. *Arch. Biochem. Biophys.* **444:** 139–158.

Marcelis, L.F. (1996). Sink strength as a determinant of dry matter partitioning in the whole plant. *J. Exp. Bot.* **47:** 1281–1291.

Marcellos, H., & Single, W.V. (1975). Temperatures in wheat during radiation frost. *Australian Journal of Experimental Agriculture* **15**(77)**:** 818-822.

March, T., Knights, S., Biddulph, B., Ogbonnaya, F., Maccallum, R., & Belford, R. (2015). The GRDC National Frost Initiative. Availabe online: https://grdc.com.au/Research-and-Development/GRDC-Update-Papers/2015/02/The-GRDC-National-Frost-Initiative.

Margutti, M.P., Reyna, M., Meringer, M.V., Racagni, G.E., & Villasuso, A.L. (2017). Lipid signalling mediated by PLD/PA modulates proline and H_2O_2 levels in barley seedlings exposed to short- and long-term chilling stress. *Plant Physiology and Biochemistry* **113:** 149-160.

Margutti, M.P., Gavegliob, V.L., Reyna, M., Pasquare, S.J., Racagnia, G.E. & Villasuso, A.L. (2018). Differential phosphatidic acid metabolism in barley leaves and roots induced by chilling temperature. *Plant Physiology and Biochemistry* **132:** 174-182.

Margutti, M.P., Reyna, M., Vilchez, A.C., & Villasuso, A.L. (2019). Lipid profiling shows tissue-specific differences in barley for glycerolipid composition in response to chilling. *Environmental and Experimental Botany* **158:** 150-160.

Markham, J.E., Lynch, D.V., Napier, J.A., Dunn, T.M., & Cahoon, E.B. (2013). Plant sphingolipids: function follows form. *Current opinion in Plant Biology* **16:** 350-357.

Martin, M.L., & Busconi, L. (2001). A rice membrane-bound calcium-dependent protein kinase is activated in response to low temperature. *Plant Physiology* **125:** 1442-1449.

Martin, T.E., & Hartwell, L.H. (1970). Resistance of active yeast ribosomes to dissociation by KCl. *Journal of Biological Chemistry* **245:** 1504-1506.

Martiniere, A., Shvedunova, M., Thomson, A.J.W., Evans, N.H., Penfield, S., Runions, J., McWatters, H.G. (2011). Homeostasis of plasma membrane viscosity in fluctuating temperatures. *New Phytologist* **192:** 328-337.

Maruyama, K., Sakuma, Y., Kasuga, M., Ito, Y., Seki, M., Goda, H., Shimada, Y., Yoshida, S., Shinozaki, K., & Yamaguchi-Shinozaki, K. (2004). Identification of cold-inducible downstream genes of the Arabidopsis DREB1A/CBF3 transcriptional factor using two microarray systems. *The Plant Journal* **38:** 982-993.

Maruyama, K., Urano, K., Yoshiwara, K., Morishita, Y., Sakurai, N., Suzuki, H., Kojima, M., Sakakibara, H., Shibata, D., Saito, K., Shinozaki, K., & Yamaguchi-Shinozaki, K. (2014). Integrated analysis of the effects of cold and dehydration on rice metabolites, phytohormones, and gene transcripts. *Plant Physiology* **164:** 1759-1771.

Matsuo, Y., Granneman, S., Thoms, M., Manikas, R.G., Tollervey, D., & Hurt, E. (2014). Coupled GTPase and remodelling ATPase activities form a checkpoint for ribosome export. *Nature* **505:** 112-116.

Matsuo, Y., Granneman, S., Thoms, M., Manikas, R.G., Tollervey, D., & Hurt, E. (2014). Coupled GTPase and remodelling ATPase activities form a checkpoint for ribosome export. *Nature* **505:** 112-116.

Mayer, R.R., Cherry, J.H., & Rhodes, D. (1990). Effects of heat shock on amino acid metabolism of cowpea cells. *Plant Physiology* **94:** 796-810.

Mazzucotelli, E., Mastrangelo, A.M., Crosatti, C., Guerra, D., Stanca, A.M., & Cattivelli, L. (2008). Abiotic stress response in plants: when post-transcriptional and post-translational regulations control transcription. *Plant Science* **174:** 420-431.

Mazzucotelli, E., Tartari, A., Cattivelli, L., & Forlani, G. (2006). Metabolism of gamma-aminobutyric acid during cold acclimation and freezing and its relationship to frost tolerance in barley and wheat. *Journal of Experimental Botany* **57**(14)**:** 3755-3766.

McCarty, R. E., &]agendorf, A.T. (1965). Chloroplast damage due to enzymatic hydrolysis of endogenous lipids. *Plant Physiology* **40:** 725-735.

Meijer, H.J., & Munnik, T. (2003). Phospholipid-based signaling in plants. *Annual Review of Plant Biology* **54:** 265-306.

Meinke, D.W. (2019). Genome ‐ wide identification of EMBRYO ‐ DEFECTIVE (EMB) genes required for growth and development in Arabidopsis. *New Phytologist* doi: 10.1111/nph.16071.

Merrill, Jr. A.H., & Sweeley, C.C. (1996). Sphingolipids: metabolism and cell signalling. In: Vance DE, Vance JE, eds. *New comprehensive biochemistry: biochemistry of lipids, lipoproteins and membranes*. Amsterdam, the Netherlands: Elsevier, 309–340.

Meyerowitz, E.M., Bowman, J.L., Brockman, L.L., Drews, G.N., Jack, T., Sieburth, L.E., & Weigel, D. (1991). A genetic and molecular model for flower development in Arabidopsis thaliana. *Development* **1:** 157-167.

Michaelson, L.V., Longman, A.J., Sayanova, O., Stobart, A.K., Napier, J.A. (2002). Isolation and characterization of a cDNA encoding a Δ8 sphingolipid desaturase from *Aquilegia vulgaris. Biochemical Society Transactions* **30:** 1073–1075.

Minami, A., Takahashi, D., Kawamura, Y., & Uemura, M. (2017). Isolation of plasma membrane and plasma membrane microdomains. In *Methods in Molecular Biology, Isolation of plant organelles and structures: methods and protocols*, Taylor N.L. and Miller A.H. (ed.), 199-211. New York: Humana Press.

Miquel, M. et al. (1993). Arabidopsis requires polyunsaturated lipids for low-temperature survival. *Proc. Natl. Acad. Sci. U. S. A.* **90:** 6208–6212.

Mitroshin, I. V., Garber, M. B., & Gabdulkhakov, A. G. (2016). Investigation of Structure of the Ribosomal L12/P Stalk. Biochemistry (Moscow), **81:** 1589-1601.

Miura, K., & Furumoto, T. (2013). Cold signaling and cold response in plants. *International Journal of Molecular Sciences* **14**(3)**:** 5312-5337.

Miura, K., & Tada, Y. (2014). Regulation of water, salinity, and cold stress responses by salicylic acid. *Frontiers in Plant Science* **5:** Article 4.

Mizoi, J., Shinozaki, K., & Yamaguchi-Shinozaki, K. (2012). AP2/ERF family transcription factors in plant abiotic stress responses. *Biochimica et Biophysica Acta* **1819:** 86-96.

Moellering, E.R., Muthan, B. & Benning, C. (2010). Freezing tolerance in plants requires lipid remodeling at the outer chloroplast membrane. *Science* **330:** 226-228.

Moellering, E.R., & Benning, C. (2011). Galactoglycerolipid metabolism under stress: a time for remodeling. *Trends in Plant Science* **16:** 2.

Monroy, A.F., Dryanova, A., Malette, B., Oren, D.H., Ridha, Farajalla, M., Liu, W., Danyluk, J., Ubayasena, L.W.C., Kane, K., Scoles, G.J., Sarhan, F., & Gulick, P.J. (2007). Regulatory gene candidates and gene expression analysis of cold acclimation in winter and spring wheat. *Plant Molecular Biology* **64:** 409-423.

Moon, B.Y., Higashi, S., Gombos, Z., & Murata, N. (1995). Unsaturation of the membrane lipids of chloroplasts stabilizes the photosynthetic machinery against low-temperature photoinhibition in transgenic tobacco plants. *Proc. Natl. Acad. Sci. USA* **92:** 6219–6223.

Morgan, J. (1992). Osmotic components and properties associated with genotypic differences in osmoregulation in wheat. *Functional Plant Biology* **19**(1)**:** 67-76.

Morita, D., Miyoshi, K., Matsui, Y., Toh-e, A., Shinkawa, H., Miyakawa, T., & Mizuta, K. (2002). Rpf2p, an evolutionarily conserved protein, interacts with ribosomal protein L11 and is essential for the processing of 27 SB Pre-rRNA to 25 S rRNA and the 60 S ribosomal subunit assembly in Saccharomyces cerevisiae. *J. Biol. Chem.* **277:** 28780-28786.

Morran, S., Eini, O., Pyvovarenko, T., Parent, B., Singh, R., Ismaguk, A., Eliby, S., Shirley, N., Langridge, P., & Lopato, S. (2011). Improvement of stress tolerance of wheat and barley by modulation of expression of DREB/CBF factors. *Plant Biotechnology Journal* **9:** 230-249.

Morsy, M.R., Jouve, L., Hausman, J.F., Hoffman, L., & Stewart, J.M. (2007). Alteration of oxidative and carbohydrate metabolism under abiotic stress in two rice (Oryza sativa L.) genotypes contrasting in chilling tolerance. *Journal of Plant Physiology* **164:** 157-167.

Munnik, T. & Vermeer, J.E.M. (2010). Osmotic stress-induced phosphoinositide and inositol phosphate signalling in plants. *Plant, Cell and Environment* **33**(4)**:** 655-669.

Murakami, Y., Tsuyama, M., Kobayashi, Y., Kodama, H., Iba, K. (2000). Trienoic fatty acids and plant tolerance of high temperature. *Science* **287:** 476-479.

Murata, N. & Yamaya, J. (1984). Temperature-dependent phase behavior of phosphatidylglycerols from chilling-sensitive and chilling-resistant plants. *Plant Physiol.* **74**(4)**:** 1016–10124.

Murata, N., Wada, H., & Gombos, Z. (1992). Modes of fatty-acid desaturation in cyanobacteria. *Plant Cell Physiol.* **33:** 933–941.

Nahar, K., Hasanuzzaman, M., & Fujita, M. (2016). Roles of osmolytes in plant adaptation to drought and salinity. In *Osmolytes and Plants Acclimation to Changing Environment: Emerging Omics Technologies*, Iqbal, N., Nazar, R.A., Khan, N., Eds., Springer India: New Delhi, India, pp. 37–68, doi:10.1007/978-81-322-2616-1_4.

Nakamura, Y. (2017). Plant phospholipid diversity: Emerging functions in metabolism and protein–lipid interactions. *Trends in Plant Science* **22:** 1027-1040.

Narayanan, S., Tamura, P.J., Roth, M.R., Prasad, P.V., & Welti, R. (2016a). Wheat leaf lipids during heat stress: I. High day and night temperatures result in major lipid alterations. *Plant, Cell and Environment* **39**(4)**:** 787-803.

Narayanan, S., Prasad, P.V.A., & Welti, R. (2016b). Wheat leaf lipids heat stress: II. Lipids experiencing coordinated metabolism are detected by analysis of lipid co-occurrence. *Plant, Cell and Environment* **39:** 608-617.

Natera, S.H.A., Hill, C. B., Rupasinghe, T. W. T., & Roesner, U. (2016) Salt-stress induced alterations in the root lipidome of two barley genotypes with contrasting responses to salinity. *Functional Plant Biology* **43**(2)**:** 207-219.

Navari-Izzo, F., Ricci, F., Vazzana, C., & Quartacci, M.F. (1995). Unusual composition of thylakoid membranes of the resurrection plant *Boea hygroscopica*: Changes in lipids upon dehydration and rehydration. *Physiol. Plant.* **94:** 135–142.

Nejadsadeghi, L., Maali-Amiri, R., Zeinali, H., Ramezanpour, S., & Sadeghzade, B. (2015). Membrane fatty acid compositions and cold-induced responses in tetraploid and hexaploid wheats. *Molecular Biology Reports* **42:** 363-372.

Nielsen, K.F., & Humphries, E.C. (1966). Effect of temperature on plant growth. *Soils Fert.* **29:** 1–7.

Nishiyama, I. (1984). Climatic influence on pollen formation and fertilization. In S. Tsunoda & N. Takahashi (eds), *Biology of rice* (pp. 153-171). Amsterdam: Elsevier.

Noblet, A., Leymarie, J., & Bailly, C. (2017). Chilling temperature remodels phospholipidome of *Zea mays* seeds during imbibition. *Scientific Reports* **7:** Article 8886.

Ohlrogge, J. & Browse, J. (1995). Lipid biosynthesis. *Plant Cell* **7:** 957–970.

Oliver, S.N., Van Dongen, J.T., Alfred, S.C., Mamun, E.A., Zhao, X., Saini, H.S., Fernandes, S.F., Blanchard, C.L., Sutton, B.G., Geigenberger. P., Dennis, E.S., & Dolferus, R. (2005). Cold-induced repression of the rice anther-specific cell wall invertase gene *OSINV4* is correlated with sucrose accumulation and pollen sterility. *Plant, Cell and Environment* **28**(12)**:** 1534–1551.

Ortiz, R., Sayre, K.D., Govaerts, B., Gupta, R., Subbarao, G.V., Ban, T., Hodson, D., Dixon, J.M., Ortiz-Monasterio, J.I., & Reynolds, M. (2008). Climate change: can wheat beat the heat? *Agriculture, Ecosystems and Environment* **126:** 46-58.

Ouellet, F., & Charron, J.B. (2013). Cold acclimation and freezing tolerance in plants. *Encyclopedia of Life Sciences,* doi: 10.1002/9780470015902.a0020093.

Pagter, M., & Arora, R. (2013). Winter survival and deacclimation of perennials under warming climate: physiological perspectives. *Physiologia Plantarum* **147**(1)**:** 75-87.

Pagter, M., Alpers, J., Erban, A., Kopka, J., Zuther, E., & Hincha, D.K. (2017). Rapid transcriptional and metabolic regulation of the deacclimation process in cold acclimated *Arabidopsis thaliana*. *BMC Genomics* **18:** Article 731.

Palta, J.P., & Weiss, L.S. (1993). Ice formation and freezing injury: an overview on the survival mechanisms and molecular aspects of injury and cold acclimation in

herbaceous plants. *In* P.H. Li & L. Christersson (eds), *Advances in plant cold hardiness* (pp. 143-176). Boca Raton (Florida): CRC Press.

Park, S., Lee, C., Doherty, C.J., Gilmour, S.J., Kim, Y.S., & Thomashow, M.F. (2015). Regulation of the Arabidopsis CBF regulon by a complex low-temperature regulatory network. *Plant Journal* **82:** 193-207.

Parnell, K.M., & Bass, B.L. (2009). Functional redundancy of yeast proteins Reh1 and Rei1 in cytoplasmic 60S subunit maturation. *Mol Cell Biol* **29:** 4014–4023.

Paulsen, G.M., & Heyne, E.G. (1983). Grain production of winter wheat after spring freeze injury. *Agron. J.* **75**: 705–707.

Perez-Riverol, Y. Et al., (2019). The PRIDE database and related tools and resources in 2019: improving support for quantification data. *Nucleic Acids Research* **47:** D442-D450.

Petr, J. (Ed.), (1991). Weather and Yield. Elsevier, pp. 288, Amsterdam.

Pocock, T.H., Hurry, V., Savitch, L.V., & Huner, N.P. (2001). Susceptibility to low-temperature photoinhibition and the acquisition of freezing tolerance in winter and spring wheat: The role of growth temperature and irradiance. *Physiologia Plantarum* **113:** 499-506.

Pogson, B.J., Ganguly, D., & Albrecht-Borth, V. (2015). Insights into chloroplast biogenesis and development. *Biochim. Biophys. Acta—Bioenerg.* **1847:** 1017–1024.

Porter, J.R., & Gawith, M. (1999). Temperatures and the growth and development of wheat: a review. *European Journal of Agronomy* **10:** 23-36.

Pyke, K.A. (1999). Plastid division and development. *Plant Cell* **11:** 549–556.

Qin, D., Wu, H., Peng, H., Yao, Y., Ni, Z., Li, Z., Zhou, C., & Sun, Q. (2008). Heat stress-responsiveness transcriptome analysis in heat susceptible and tolerant wheat (*Tritucm aestivum* L.) by using Wheat Genome Array. *BMC Genomics* **9:** Article 432.

Qin, F., Sakuma, Y., Li, J., Liu, Q., Li, Y., Shinozaki, K., Yamaguchi-Shinozaki, K. (2004). Cloning and functional analysis of a novel DREB1/CBF transcription factor involved in cold-responsive gene expression in *Zea mays* L. *Plant Cell Physiol.* **45:** 1042–1052.

Quartacci, M.F., Pinzino, C., Sgherri, C.L.M., & Navari-Izzo, F. (1995). Lipid composition and protein dynamics in thylakoids of two wheat cultivars differently sensitive to drought. *Plant Physiol.* **108:** 191–197.

Radomiljac, J.D., Whelan, J., & van der Merwe, M. (2013). Coordinating metabolite changes with our perception of plant abiotic stress responses: Emerging views revealed by integrative-omic analyses. *Metabolites* **3:** 761–786.

Rapacz, M. (2002). Regulation of frost resistance during cold de-acclimation and re-acclimation in oilseed rape. A possible role of PSII redox state. *Physiologia Plantarum* **115**(2)**:** 236-243.

Rawlinson, C., Kamphuis, L.G., Gummer, J.P.A., Singh, K.P., & Trengove, R.D. (2015). A rapid method for profiling of volatile and semi-volatile phytohormones using methyl chloroformate derivatisation and GC-MS. *Metabolomics* **11**(6)**:** 1922-1933.

Ren, M., Phoon, C.K., & Schlame, M. (2014). Metabolism and function of mitochondrial cardiolipin. *Prog. Lipid Res.* **55:** 1–16.

Rerkasem, B. (1996). A general survey of the incidence of wheat sterility. In H.M. Rawson & K.D. Subedi (eds), *Sterility in wheat in subtropical Asia: extent, causes and solutions*, Vol 72 (pp. 8-12). Pokhara (Nepal): ACIAR Proceedings, LumJe Agricultural Research Centre.

Reynolds, M.P., Pellegrineschi, A., & Skovmand, B. (2005). Sink-limitation to yield and biomass: A summary of some investigations in spring wheat. *Ann. Appl. Biol.* **146:** 39–49.

Richards, R.A., Rebetzke, G.J., Watt, M., Condon, A.G., Spielmeyer, W., & Dolferus, R. (2010). Breeding for improved water productivity in temperate cereals: phenotyping, quantitative trait loci, markers and the selection environment. *Functional Plant Biology* **37**(2)**:** 85-97.

Rimando, A.M., & Perkins-Veazie, P.M. (2005). Determination of citrulline in watermelon rind. *Journal of Chromatography A* **1078**(1-2)**:** 196-200.

Ritchie, M.E., Phipson, B., Wu, D., Hu, Y., Law, C.W., Shi, W., & Smyth, G.K. (2015). Limma powers differential expression analyses for RNA-sequencing and microarray studies. *Nucleic Acids Research* **43:** e47.

Rizhsky, L., Liang, H., Shuman, J., Shulaev, V., Davletova, S., & Mittler, R. (2004). When defense pathways collide. The response of Arabidopsis to a combination of drought and heat stress. *Plant Physiol.* **134:** 1683–1696.

Rocha, M., Licausi, F., Araujo, W.L., Nunes-Nesi, A., Sodek, L., Fernie, A.R., & van Dongen, J.T. (2010). Glycolysis and the tricarboxylic acid cycle are linked by alanine aminotransferase during hypoxia induced by waterlogging of *Lotus japonicus*. *Plant Physiol.* **152:** 1501–1513.

Roche, I.A., Andrews, C.J., Pomeroy, MK., Weinberger, P., & Kates, M. (1972). Lipid changes in winter wheat seedlings (*Triticum aestivum*) at temperatures inducing cold hardiness. *Canadian Journal of Botany* **50:** 2401-2409.

Roessner, U., Luedemann, A., Brust, D., Fiehn, O., Linke, T., Willmitzer, L., & Fernie, A.R. (2001). Metabolic profiling allows comprehensive phenotyping of genetically or environmentally modified plant systems. *Plant Cell* **13:** 11-29.

Rosso, M.G., Li, Y., Strizhov, N., Reiss, B., Dekker, K., & Weisshaar, B. (2003). An *Arabidopsis thaliana* T-DNA mutagenized population (GABI-Kat) for flanking sequence tag-based reverse genetics. *Plant Molecular Biology* **53:** 247-259.

Routaboul, J.M., Fischer, S.F., & Browse, J. (2000). Trienoic fatty acids are required to maintain chloroplast function at low temperatures. *Plant Physiol.* **124:** 1697–1705

Ruelland, E., Cantrel, C., Gawer, M., Kader, J.C., & Zachowski, A. (2002). Activation of phospholipases C and D is an early response to a cold exposure in Arabidopsis suspension cells. *Plant Physiol.* **130:** 999–1007.

Ruelland, E., Vaultier, M-N., Zachowski, A., & Hurry, V. (2009). Chapter 2: Cold signalling and cold acclimation in plants. In K. Jean-Claude & D. Michel (eds), *Advances in Botanical Research*, Vol 49 (pp. 35-150). Academic Press.

Ruelland, E., & Zachowski, A. (2010). How plants sense temperature. *Environ. Exp. Bot.* **69:** 225–232.

Rugen, N., Straube, H., Franken, L. E., Braun, H. P., & Eubel, H. (2019). Complexome profiling reveals association of PPR proteins with ribosomes in the mitochondria of plants. *Mol. Cell. Proteomics* **18:** 1345–1362.

Saez-Vasquez, J., & Delseny, M. (2019). Ribosome biogenesis in plants: From functional 45S ribosomal DNA organization to ribosome assembly factors. *Plant Cell* **31:** 1945-1967.

Sakai, A., & Larcher, W. (1987). Frost Survival of Plants: Responses and Adaptation to Freezing Stress, Ecological Studies,Vol.62, pp. 124–131. Springer Verlag, New York, USA.

Salih, K.J., Duncan, O., Li, L., Troesch, J., & Millar, A.H. (2019). Refining the composition of the *Arabidopsis thaliana* 80S cytosolic ribosome. *bioRxiv* 764316

Santra, D.K., Santra, M., Allan, R.E., Campbell, K.G., & Kidwell, K.K. (2009). Genetic and molecular characterization of vernalization genes Vrn-A1, Vrn-B1, and Vrn-D1 in pring wheat Germplasm from the Pacific Northwest Region of the U.S.A. *Plant Breeding* **128:** 576-584.

Sarabia, L.D., Hill, C.B., Boughton, B., & Roessner, U. (2018). Advancs of metabolite profiling of plants in challenging environments. In Roberts J (ed), *Annual Plant Reviews* (pp. 1-45), Volume 1. John Wiley and Sons: New York.

Sarabia, L.D., Boughton, B., Rupasinghe, T.W.T., van de Menee, A.M.L., Callahan, D.M., Hill, C.B., & Roessner, U. (2019). High-mass-resolution MALDI mass spectrometry imaging reveals detailed spatial distribution of metabolites and lipids in roots of barley seedlings in response to salinity stress. *Metabolomics* **14:** 63.

Satake, T., Nishiyama, I., Ito, N., & Hayase, H. (1969). Male sterility caused by cooling treatment at the meiotic stage in rice plants. I. Methods of growing rice plants and inducing sterility in the phytotron. *Japanese Journal of Crop Science* **38:** 603-609.

Schiefelbein, J.W., & Benfey, P.N. (1991). The development of plant roots: new approaches to underground problems. *Plant Cell* **3:** 1147–1154.

Schmidt, S., Dethloff, F., Beine-Golovchuk, O., Kopka, J. (2013). The REIL1 and REIL2 proteins of Arabidopsis thaliana are required for leaf growth in the cold. *Plant Physiology* **163:** 1623–1639.

Schmidt, S., Dethloff, F., Beine-Golovchuk, O., Kopka, J. (2014). REIL proteins of *Arabidopsis thaliana* interact in yeast-2-hybrid assays with homologs of the yeast Rlp24, Rpl24A, Rlp24B, Arx1, and Jjj1 proteins. *Plant Signal Behaviour* **9:** e28224.

Scholl, R.I., Ma, S.T., Ware, D.H. (2000). Seed and molecular resources for Arabidopsis. *Plant Physiology* **124:** 1477-1480.

Seki, M., Narusaka, M., Abe, H., Kasuga, M., Yamaguchi-Shinozaki, K., Carninci, P., Hayashizaki, Y., Shinozaki, K. (2001). Monitoring the expression pattern of 1300 Arabidopsis genes under drought and cold stresses by using a full-length cDNA microarray. *Plant Cell* **13:** 61–72.

Shavrukov, Y., Kurishbayev, A., Jatayev, S., Shvidchenko, V., Zotova, L., Koekemoer, F., de Groot, S., Soole, K., & Langridge, P. (2017). Early flowering as a drought escape mechanism in plants: how can it aid wheat production? *Frontiers in Plant Science* **8:** Article 1950.

Shi, H., & Chan, Z. (2014). Improvement of plant abiotic stress tolerance through modulation of the polyamine pathway. *Journal of Integrative Plant Biology* **56**(2)**:** 114-121.

Shi, Z., Fujii, K., Kovary, K. M., Genuth, N. R., Röst, H. L., Teruel, M. N., & Barna, M. (2017). Heterogeneous ribosomes preferentially translate distinct subpools of mRNAs genome-wide. *Molecular Cell* **67:** 71-83.

Shinkawa, R., Morishita, A., Amikura, K., Machida, R., Murakawa, H., Kuchitsu, K., et al. (2013). Abscisic acid induced freezing tolerance in chilling-sensitive suspension cultures and seedlings of rice. *BMC Res Notes.* **6:** 351.

Shulaev, V., Cortes, D., Miller, G., & Mittler, R. (2008). Metabolomics for plant stress responses. *Physiologia Plantarum* **132:** 199-208.

Simon-Plas, F., Perraki, A., Bayer, E., Gerbau-Pissot, P., & Mongrand, S. (2011). An update on plant membrane rafts. *Current Opinion in Plant Biology* **14:** 642-649.

Simsek, D., Tiu, G. C., Flynn, R. A., Byeon, G. W., Leppek, K., Xu, A. F., Chang, H.Y., & Barna, M. (2017). The mammalian ribo-interactome reveals ribosome functional diversity and heterogeneity. *Cell* **169:** 1051-1065.

Single, W.V (1966). Studies on frost injury to wheat. III. Screening of varieties for resistance to ear and stem frosting. *Aust. J. Agric. Res.* **17:** 601–610.

Slama, I., Abdelly, C., Bouchereau, A., Flowers, T., & Savouré, A. (2015). Diversity, distribution and roles of osmoprotective compounds accumulated in halophytes under abiotic stress. *Annals of Botany* **115**(3)**:** 433-447.

Smallwood, M., & Bowles, D.J. (2002). Plants in a cold climate. *Philosophical Transactions of the Royal Society B: Biological Sciences* **357**(1423)**:** 831-847.

Smith, A.R., & Zhao, D. (2016). Sterility caused by floral organ degeneration and abiotic stresses in Arabidopsis and cereal grains. *Frontiers in Plant Science* **7:** Article1503.

Smith, M.R., Rao, I.M., & Merchant, A. (2018). Source-sink relationships in crop plants and their influence on yield development and nutritional quality. Frontiers in Plant Science **9:** Article 1889.

Somerville, C., & Koornneef, M. (2002). A fortunate choice: the history of Arabidopsis as a model plant. *Nature Reviews Genetics* **3:** 883–889.

Somssich, M., Abbas Khan, G., & Persson, S. (2016). Cell wall heterogeneity in root development of Arabidopsis. *Frontiers in Plant Science* **7:** Article 1242.

Sormani, R., Masclaux-Daubresse, C., Daniel-Vedele, F., & Chardon, F. (2011). Transcriptional regulation of ribosome components are determined by stress according to cellular compartments in *Arabidopsis thaliana*. *PLoS ONE* **6:** e28070.

Sperling, P., Franke, S., Luthje, S., & Heinz, E. (2005). Are glucocerebrosides the predominant sphingolipids in plant plasma membranes? *Plant Physiol. Biochem.* **43:** 1031-1038.

Steponkus, P.L. (1984). Role of the plasma membrane in freezing injury and cold acclimation. *Annual Review of Plant Physiology* **35:** 543-584.

Steponkus, P.L., Lynch, D.V., & Uemura, M. (1990). The influence of cold acclimation on the lipid composition and cryobehavior of the plasma membrane of isolated rye

protoplasts. *Philosophical Transactions of the Royal Society of London B* **326:** 571–583.

Steponkus, P.L., Uemura, M., & Webb, M.S. (1993). A contrast of the cryostability of the plasma membrane of winter rye and spring oat-two species that widely differ in their freezing tolerance and plasma membrane lipid composition. In P.L. Steponkus (ed.), *Advances in Low-Temperature Biology*, Vol. 2 (pp. 211–312). London: JAI Press.

Steponkus, P.L., Uemura, M., Balsamo, R.A., Arvinte, T., Lynch, D.V. (1988). Transformation of the cryobehavior of rye protoplasts by modification of the plasma membrane lipid composition. *Proceedings of the National Academy of Sciences, USA* **85:** 9026–9030.

Steponkus, P.L., Uemura, M., Joseph, R.A., Gilmour, S.J., Thomashow, M.F. (1998). Mode of action of the *COR15a* gene on the freezing tolerance of *Arabidopsis thaliana*. *Proc. Natl. Acad. Sci. USA* **95:** 14570–14575.

Stitt, M., & Hurry, V. (2002). A plant for all seasons: alterations in photosynthetic carbon metabolism during cold acclimation in Arabidopsis. *Current Opinion in Plant Biology* **5:** 199-206

Stockinger, E.J., Gilmour, S.J., & Thomashow, M.F. (1997). *Arabidopsis thaliana* CBF1 encodes an AP2 domain-containing transcriptional activator that binds to the C-repeat/DRE, a cis-acting DNA regulatory element that stimulates transcription in response to low temperature and water deficit. *Proc Natl Acad Sci USA* **94:** 1035–104.

Strand, A., Hurry, V., Gustafsson, P., & Gardestrom, P. (1997). Development of *Arabidopsis thaliana* leaves at low temperatures releases the suppression of photosynthesis and photosynthetic gene expression despite the accumulation of soluble carbohydrates. *Plant Journal* **12**(3)**:** 605-614.

Subedi, K., Gregory, P., Summerfield, R., & Gooding, M. (1998a). Cold temperatures and boron deficiency caused grain set failure in spring wheat (*Triticum aestivum* L.). *Field crops research* **57**(3)**:** 277-288.

Subedi, K.D., Floyd, C.N., & Budhathoki, C.B. (1998b). Cool temperature-induced sterility in spring wheat (*Triticum aestivum* L.) at high altitudes in Nepal: variation among cultivars in response to sowing date. *Field Crops Research* **55**(1-2)**:** 141-151.

Subedi, K.D., Gregory, P.J., Summerfield, R.J., & Gooding, M.J. (2000). Pattern of grain set in boron-deficient and cold-stressed wheat (*Triticum aestivum* L). *The Journal of Agricultural Science* **134**(1)**:** 25-31.

Sumner, L.W., Amberg, A., Barrett, D., Beale, M.H., Beger, R., Daykin, C.A., (2007). Proposed minimum reporting standards for chemical analysis Chemical Analysis Working Group (CAWG) Metabolomics Standards Initiative (MSI). *Metabolomics* **3**(3)**:** 211-221.

Sumner, L.W., Lei, Z., Nikolau, B.J., & Saito, K. (2015). Modern plant metabolomics: advanced natural product gene discoveries, improved technologies, and future prospects. *Natural Product reports* **32:** 212-229.

Swart, C., Martínez-Jaime, S., Gorka, M., Zander, K., & Graf, A. (2018). Hit-Gel: Streamlining in-gel protein digestion for high-throughput proteomics experiments. *Scientific Reports* **8:** Article 8582.

Taji, T., Ohsumi. C., Iuchi, S., Seki, M., Kasuga, M., Kobayashi, M., Yamaguchi-Shinozaki, K., & Shinozaki, K. (2002). Important roles of drought- and cold-inducible genes for galactinol synthase in stress tolerance in *Arabidopsis thaliana*. *Plant Journal* **29:** 417-426.

Tan, W., Yang, Y., Huang, L., Xu, L., Chen, Q., Yu, L., & Xiao, S. (2018). Diacylglycerol acyltranferase and diacylglycerol kinase modulate triacylglycerol and phosphatidic acid production in the plant response to freezing stress. *Plant Physiology* **177:** 1303-1318.

Teige, M., Scheikl, E., Eulgem, T. et al., (2004). The MKK2 pathway mediates cold and salt stress signaling in Arabidopsis. *Molecular Cell* **15:** 141-152.

Testerink, C., & Munnik, T. (2005). Phosphatidic acid: a multifunctional stress signalling lipid in plants. *Trends in Plant Science* **10:** 368-375.

Thakur, P., Kumar, S., Malika, J.A., Berger, J.D., & Nayyar, H. (2010). Cold stress effects on reproductive development in grain crops: An overview. *Environ. Exp. Bot.* **67:** 429–443.

Thomas, A.H., Catala, A., & Vignoni, M. (2016). Soybean phosphotidylcholine liposomes as model membranes to study lipid peroxidation photoinduced by pterin. *Biochimica et Biophysica Acta* **1858:** 139-145.

Thomashow, M.F. (1999). Plant cold acclimation: Freezing tolerance genes and regulatory mechanisms. *Annu. Rev. Plant Physiol. Plant Mol. Biol.* **50:** 571–599.

Thomashow, M.F. (2001). So what's new in the field of plant cold acclimation? Lots! *Plant Physiology* **125:** 89-93.

Thomashow, M.F. (2010). Molecular basis of plant cold acclimation: insights gained from studying the CBF cold response pathway. *Plant Physiology* **154:** 571-577.

Thomson, E., Ferreira-Cerca, S., & Hurt, E. (2013). Eukaryotic ribosome biogenesis at a glance. *Journal of Cell Science* **126:** 4815-4821.

Tian, T., Liu, Y., Yan, H., You, Q., Yi, X., Du, Z., Xu, W., & Su, Z. (2017). AgriGO v2.0: a GO analysis toolkit for the agricultural community, 2017 update. *Nucleic Acids Research* **45:** W122-W129.

Travert, S., Valerio, L., Fouraste, I., Boudet, A.M., & Teulieres, C. (1997). Enrichment in specific soluble sugars of two Eucalyptus cell-suspension cultures by various treatments enhances their frost tolerance via a noncolligative mechanism. *Plant Physiology* **114:** 1433-1442.

Uemura, M., & Steponkus, P.L. (1994). A contrast of the plasma membrane lipid composition of oat and rye leaves in relation to freezing tolerance. *Plant Physiology* **104:** 479–496.

Uemura, M., Joseph, R. A., & Steponkus, P. L. (1995a). Effect of cold acclimation on the lipid composition of the inner and outer membrane of the chloroplast envelope isolated from rye leaves. *Plant Physiol.* **109:** 15-30.

Uemura, M., Joseph, R.A., & Steponkus, P.L. (1995b). Cold acclimation of *Arabidopsis thaliana*. Effect on plasma membrane lipid composition and freeze-induced lesions. *Plant Physiology* **109:** 15–30.

Uemura, M., Warren, G., & Steponkus, P.L. (2003). Freezing sensitivity in the *sfr4* mutant of Arabidopsis is due to low sugar content and is manifested by loss of osmotic responsiveness. *Plant Physiology* **131:** 1800-1807.

Uesono, Y., & Toh-e, A. (2002). Transient inhibition of translation initiation by osmotic stress. *Journal of Biological Chemistry* **277:** 13845-13855.

Upchurch, R.G. (2008). Fatty acid unsaturation, mobilization, and regulation in the response of plants to stress. *Biotechnology Letters* **30**(6)**:** 967-977.

Usadel, B., Blasing, O.E., Gibon, Y., Poree, F., Hohne, M., Gunter, M., Trethewey, R., Kamlage, B., Poorter, H., & Stitt, M. (2008). Multilevel genomic analysis of the response of transcripts, enzyme activities and metabolites in Arabidopsis rosettes to a progressive decrease of temperature in the non-freezing range. *Plant, Cell and Environment* **31:** 518-547.

Vágújfalvi, A., Kerepesi, I., Galiba, G., Tischner, T., & Sutka, J. (1999). Frost hardiness depending on carbohydrate changes during cold acclimation in wheat. *Plant Science* **144**(2)**:** 85-92.

Vágújfalvi, A., Galiba, G., Cattivelli, L., & Dubcovsky, J. (2003). The cold-regulated transcriptional activator Cbf3 is linked to the frost-tolerance locus Fr-A2 on wheat chromosome 5A. *Mol. Genet. Genomics* **269:** 60–67.

Valluru, R., Lammens, W., Claupein, W., & Van den Ende, W. (2008). Freezing tolerance by vesicle-mediated fructan transport. *Trends in Plant Science* **13**(8)**:** 409-414.

Van Buskirk, H.A., & Thomashow, M.F. (2006). *Arabidopsis* transcription factors regulating cold acclimation. *Physiologia Plantarum* **126:** 72-80.

Van den Elzen, A.M.G., Schuller A., Green, R., & Seraphin, B. (2014). Dom34-Hbs1 mediated dissociation of inactive 80S ribosomes promotes restart of translation after stress. *The EMBO Journal* **33:** 265-276.

Van Lijsebettens, M., Vanderhaeghen, R., De Block, M., Bauw, G., Villarroel, R., Van Montagu, M. (1994). An S18 ribosomal protein gene copy at the *Arabidopsis* PFL locus affects plant development by its specific expression in meristems. *EMBO Journal* **13:** 3378–3388.

Van Meer, G., Voelker, D.R., & Feigenson, G.W. (2008). Membrane lipids: where they are and how they behave. *Nature Reviews Molecular Cell Biology* **9:** 112-124.

Vance, D.E., & Vance, J.E. (2008). CHAPTER 8—Phospholipid biosynthesis in eukaryotes. In *Biochemistry of Lipids, Lipoproteins and Membranes*, 5th ed., Vance, D.E., Vance, J.E., Eds., Elsevier: San Diego, CA, USA, pp. 213–244.

Vanková, R., Kosová, K., Dobrev, P., Vítámvás, P., Trávníčková, A., Cvikrová, M., Pešek, B., Gaudinová, A., Prerostová, S., Musilová, J., Galiba, G., & Prášil, I.T. (2014). Dynamics of cold acclimation and complex phytohormone responses in *Triticum monococcum* lines G3116 and DV92 differing in vernalization and frost tolerance level. *Environmental and Experimental Botany* **101:** 12-25.

Vigh, L., Horvath, L.I., Horvath, I., Dudits, D., & Farkas, T. (1979). Protoplast plasmalemma fluidity of hardened wheats correlates with frost resistance. *FEBS Letters* **107**(2)**:** 291-294.

Vigh, L., Horvàth, I., van Hasselt, P.R., & Kuiper, P.J.C. (1985). Effect of frost hardening on lipid and fatty acid composition of chloroplast thylakoid membranes in two wheat varieties of contrasting hardiness. *Plant Physiology* **79:** 756-759.

Vitamvas, P, & Prasil, I.T. (2008). WCS120 protein family and frost tolerance during cold acclimation, deacclimation and reacclimation of winter wheat. *Plant Physiology and Biochemistry* **46**(11)**:** 970-976.

Vothknecht, U.C., & Westhoff, P. (2001). Biogenesis and origin of thylakoid membranes. *Biochim. Biophys. Acta—Mol. Cell Res.* **1541:** 91–101.

Vu, H.S., Roth, M.R., Tamura, P., Samarakoon, T., Shiva, S., Honey, S., Lowe, K., Schmelz, E.A., Williams, T.D., & Welti, R. (2014). Head-group acylation of monogalactosyldiacylglycerol is a common stress response, and the acyl-galactose acyl composition varies with the plant species and applied stress. Physiologia Plantarum 150: 517-528.

Wahlquist, A. (2012). Researchers probe warming climate frost puzzle. In: *Grains Research and Development Corporation*, Kingston, ACT, Australia.

Waltz, F., Nguyen, T. T., Arrivé, M., Bochler, A., Chicher, J., Hammann, P., Kuhn, L., Quadrado M., Mireau H., Hashem, Y., & Giegé, P. (2019). Small is big in Arabidopsis mitochondrial ribosome. *Nature Plants* **5:** 106-117.

Wang, X., & Chapman, K.D. (2013). Lipid signaling in plants. Frontiers in Plant Science **4:** *Article 216*.

Wang, X., Devaiah, S. P., Zhang W. & Welti, R. (2006). Signaling functions of phosphatidic acid. *Prog. Lipid Research* **45:** 250-278.

Wang, X., Li, W., Li, M., Welti, R. (2006). Profiling lipid changes in plant response to low temperatures. *Physiologia Plantarum* **126**(1)**:** 90-96.

Wanner, L.A., & Junttila, O. (1999). Cold-induced freezing tolerance in Arabidopsis. *Plant Physiology* **120:** 391-400.

Warnecke, D., & Heinz, E. (2003). Recently discovered functions of glucosylceramides in plants and fungi. *Cellular and Molecular Life Sciences* **60:** 919–941.

Webb, M.S., & Green, B.R. (1991). Biochemical and biophysical properties of thylakoid acyl lipids. *Biochim. Biophys. Acta Bioenerg* **1060:** 133–158.

Weckwerth, W. (2011). Green systems biology—From single genomes, proteomes and metabolomes to ecosystems research and biotechnology. *J. Proteom.* **75:** 284–305.

Weis, B.L., Kovacevic, J., Missbach, S., & Schleiff, E. (2015). Plant-specific features of ribosome biogenesis. *Trends in Plant Science* **20:** 11.

Welti, R., Li, W., Li, M., Sang, Y., Biesiada, H., Zhou, H., Rajashekar, C.B., Williams, T.D., & Wang, X. (2002). Profiling membrane lipids in plant stress responses. *Journal of Biological Chemistry* **277**(35)**:** 31994-32002.

Welti, R., Shah, J., Li, W., Li, M., Chen, J., Burke, J.J., Fauconnier, M.L., Chapman, K., Chye, M.L., & Wang, X. (2007). Plant lipidomics: discerning biological function by

profiling plant complex lipids using mass spectrometry. *Frontiers in Bioscience* **12:** 2494-2506.

Williams, M., & Harwood, J.L. (1997). Effect of drought on volatile production by the lipoxygenase pathway in olive fruit. *Biochem. Soc. Trans.* **25:** 499S.

Winfield, M.O., Lu, C., Wilson, I.D., Cognill, J.A., & Edwards, K.J. (2010). Plant responses to cold: transcriptome analysis of wheat. *Plant Biotechnology Journal* **8:** 749-771.

Wolfe, J., & Bryant, G. (1999). Freezing, drying, and/or vitrification of membrane-solute-water systems. *Cryobiology* **39:** 103–129.

Wong, H.L., & Shimamoto, K. (2009). Sending ROS on a bullet train. *Science Signaling* **2:** pp.pe60.

Xia, J., & Wishart, D.S. (2016). Using MetaboAnalyst 3.0 for comprehensive metabolomics data analysis. *Curr. Protoc. Bioinform.* **55:** https://doi.org/10.1002/cpbi.11.

Xiong, L.M., Schumaker, K.S., & Zhu, J.K. (2002). Cell signaling during cold, drought, and salt stress. *Plant Cell* **14:** S165–S183.

Xiong, Y., McCormack, M., Li, L., Hall, Q., Xiang, C., & Sheen, J. (2013). Glucose-TOR signalling reprograms the transcriptome and activates meristems. *Nature* **496:** 181-186.

Xu, Q., Truong, T.T., Barrero, J.M., Jacobsen, J.V., Hocart, C.H., & Gubler, F. (2016). A role for jasmonates in the release of dormancy by cold stratification in wheat. *Journal of Experiemental Botany* **67:** 3497-3508.

Xue, S., & Barna, M. (2012). Specialized ribosomes: A new frontier in gene regulation and organismal biology. *Nature Reviews Molecular Cell Biology* **13:** 355-369.

Yadav, S.K. (2010). Cold stress tolerance mechanisms in plants. A review. *Agron. Sustain. Dev.* **30:** 515-527.

Yan, L., Li, G., Yu, M., Fang, T., Cao, S., & Carver, B.F. (2015). Genetic mechanisms of vernalization requirement duration in winter wheat cultivars. In: Ogihara Y, Takumi S, Handa H. (eds) *Advances in Wheat Genetics: From Genome to Field.* Springer, Tokyo. Page 117-126.

Yang, R.L. et al. (2013). The reference genome of the halophytic plant *Eutrema salsugineum. Frontiers in Plant Science* **4:** Article 46.

You, J., & Chan, Z. (2015). ROS regulation during abiotic stress responses in crop plants. *Frontiers in Plant Science. **6*****:** Article 1092.

Yu, D., Rupasinghe, T.W.T., Boughton, B.A., Natera, S.H.A., Hill, C.B., Tarazona, P., Feussner, I., & Roessner, U. (2018). A high-resolution HPLC-QqTOF platform using

parallel reaction monitoring for in-depth lipid discovery and rapid profiling. *Analytica Chimica Acta* **1026:** 87-100.

Yu, D., Boughton, B.A., Hill, C.B., Feussner, I., Roessner, U., Rupasinghe, T.W.T. (2020). Insights into oxidized lipid modification in barley roots as an adaptation mechanism to salinity stress. *Frontiers in Plant Science* **11:** Article 1.

Yu, H. et. al. (2020). STCH4/REIL2 confers cold stress tolerance in Arabidopsis by promoting rRNA processing and CBF protein translation. *Cell Reports* **30:** 229-242.

Yu, X., Peng, Y.H., Zhang, M.H., Shao, Y.J., Su, W.A., & Tang, Z.C. (2006). Water relations and an expression analysis of plasma membrane intrinsic proteins in sensitive and tolerant rice during chilling and recovery. *Cell Research* **16:** 599-608.

Zadoks, J.C., Chang, T.T., & Konzak, C.F. (1974). A decimal code for the growth stages of cereals. *Weed Research* **14:** 415-421.

Zhang, H., Dong, J., Zhao, X., Zhang, Y., Ren, J., Xing, L., Jiang, C., Wang, X, Wang, J., Zhao, S., & Yu, H. (2019). Research progress in membrane lipid metabolism and molecular mechanism in peanut cold tolerance. *Frontiers in Plant Science* **10:** Article 838.

Zhang, W., Yu, L., Zhang, Y., & Wang, X. (2005). Phospholipase D in the signaling networks of plant response to abscisic acid and reactive oxygen species. *Biochimica et Biophysica Acta* **1736**(1)**:** 1-9.

Zhang, W., Zhang, J., Xu, C., Li, N., Liu, H., Ma, J., Zhu, Y., & Xie, H. (2012). LFQuant: label-free fast quantitative analysis tool for high-resolution LC-MS/MS proteomics data. *Proteomics* **12:** 3475–3484.

Zhang, X.D., Wang, R.P., Zhang, F.J., Tao, F.Q., & Li, W.Q. (2013). Lipid profiling and tolerance to low-temperature stress in *Thellungiella salsuginea* in comparison with *Arabidopsis thaliana*. *Biol. Plant.* **57:** 149–153.

Zhang, Y., Zhu, H., Zhang, Q., Li, M., Yan, M., Wang, R., Wang, L., Welti, R., Zhang, W., & Wang, X. (2009). Phospholipase D_1 and phosphatidic acid regulate NADPH oxidase activity and production of reactive oxygen species in ABA-mediated stomatal closure in Arabidopsis. *Plant Cell* **21:** 2357–2377.

Zhen, Y., Dhakal, P., & Ungerer, M.C. (2011). Fitness benefits and costs of cold acclimation in *Arabidopsis thaliana. The American Naturalist* **178:** 44-52.

Zheng, B., Chapman, S.C., Christopher, J.T., Frederiks, T.M., & Chenu, K. (2015). Frost trends and their estimated impact on yield in the Australian wheatbelt. *Journal of Experimental Botany* **66**(12)**:** 3611-3623.

Zheng, G., Li, L., & Li, W. (2016). Glycerolipidome responses to freezing- and chilling-induced injuries: examples in Arabidopsis and rice. *BMC Plant Biology* **16:** Article 70.

Zheng, G., Tian, Bo., Zhang, F., Tao, F., Li, W. (2011). Plant adaptation to frequent alterations between high and low temperatures: remodeling of membrane lipids and maintenance of unsaturation levels. *Plant, Cell and Environment* **34:** 1431-1442.

Zinselmeier, C., Lauer, M.J., & Boyer, J.S. (1995). Reversing drought-induced losses in grain yield—Sucrose maintains embryo growth in maize. *Crop Science* **35:** 1390–1400.

Zinselmeier, C., Westgate, M., Schussler, J., & Jones, R. (1995). Low water potential disrupts carbohydrate metabolism in maize (*Zea mays* L.) ovaries. *Plant Physiology* **107:** 385–391.

Zylber, E.A., & Penman, S. (1970). The effect of high ionic strength on monomers, polyribosomes, and puromycin-treated polyribosomes. *Biochim Biophys Acta* **204:** 221-229.

Appendices

Appendix A: Supplemental Data and Tables for Chapter 2, Part I

Supplemental Data I-S2-1: Methodology for Phytohormone Analysis

1. Preparation of calibration and internal standards for the ten phytohormones and organic acids [Three organic acids that serve as precursors for phytohormones: benzoic acid (BA), *trans*-Cinnamic acid (CA), 12-oxo phytodienoic acid (OPDA); Seven phytohormones: Salicylic acid (SA), Jasmonic acid (JA), Jasmonoyl-isoleucine (JA-ile), Indole-3-acetic acid (IAA), Indole-3-carboxylic acid (ICA), Indole-3-butyric acid (IBA), 2-cis-4-trans-Abscisic acid (ABA)]

A) Preparation of phytohormone calibration standard mixture, 5 ug/ml

M1 = 50 ug/ml original concentration for each phytohormone and organic acid,

V1 = x ul, M2 = 5, V2 = 2000 uL

M1V1 = M2V2

V1 = 200 uL

- Take each 200 uL of the 10 phytohormones and organic acid to make the 2000 uL mixture, kept at -80°C

B) Preparation of phytohormone calibration standard mixture, 0.5 ug/ml

M1 = 5 ug/ml, V1 = x, M2 = 0.5 ug/ml, V2 = 1000 uL

M1V1 = M2V2

V1 = 100 uL

- Take 100 uL of **A** and 900 uL MEOH (methanol) to make the 1000 uL mixture, kept at -80°C

C) Preparation of phytohormone calibration standard 0.05 ug/ml

M1 = 0.5 ug/ml, V1 = x, M2 = 0.05 ug/ml, V2 = 1000 uL

M1V1 = M2V2

V1 = 100 uL

- Take 100 uL of **B** and 900 uL MEOH to make the 1000 uL mixture, kept at -80°C

D) Preparation of phytohormone calibration standard 0.005 ug/ml

M1 = 0.05 ug/ml, V1 = x, M2 = 0.005 ug/ml, V2 = 1000 uL

M1V1 = M2V2

V1 = 100 uL

- Take 100 uL of **B** and 900 uL MEOH to make the 1000 uL mixture, kept at -80°C

E) Preparation of ISTD (internal standard) mixture (d_2IAA, d_5BA, d_6ABA, d_6SA, d_7CA, H_2JA)

M1 = 50 ug/ml, V1 = 100 uL, M2 = x, V2 = 600 uL

M1V1 = M2V2

M2 = 8.3 ug/ml

- Take each 100 uL of the 6 ISTD to make the 600 uL mixtures, kept at -80°C
- (the final ISTD conc. in each calibration standard is 145.3 ng/ml, by adding 7 ul of 8.3 ug/ml stock mixtures in a total volume of 400 ul, refer to the table below)

F) Valine ISTD, kept in -80°C until use

M1 = 50 ug/ml, V1 = 100 uL, M2 = x, V2 = 600 uL

M1V1 = M2V2

M2 = 8.3 ug/ml

- Take each 100 uL of the M1 and top up with 500 ul MEOH to make the 600 uL mixtures, kept at -80°C
- (the final Valine ISTD conc. in each calibration standard is 145.3 ng/ml, by adding 7 ul of 8.3 ug/ml stock mixtures in a total volume of 400 ul, refer to the table below)

2. Preparation of phytohormone and organic acids calibration standards (containing ISTD) by referring to the table below.

Calibration standard (ug/ml)	**A)** 5 ug/ml stock mixture (uL)	**B)** 0.5 ug/ml stock mixture (uL)	**C)** 0.05 ug/ml stock mixture (uL)	**D)** 0.005 ug/ml stock mixture (uL)	**E)** ISTD stock mixture 8.3 ug/ml (uL)	**F)** Valine ISTD stock 8.3 ug/ml (uL)	1 % NaOH (uL) + suspend	MEOH(uL)	Pyridine (uL) + Vortex vigorously for 25-30s
0.00025				20	7	7	200	133	34
0.0005				40	7	7	200	113	34
0.001				80	7	7	200	73	34
0.0025			20		7	7	200	133	34
0.005			40		7	7	200	113	34
0.01			80		7	7	200	73	34
0.025		20			7	7	200	133	34
0.05		40			7	7	200	113	34
0.1		80			7	7	200	73	34
0.25	20				7	7	200	133	34
0.5	40				7	7	200	113	34
1	80				7	7	200	73	34
2	153				7	7	200	0	34

3. Extraction of the phytohormones and organic acids from the flag leaf tissues of Wyalkatchem and Young

The extraction of phytohormones from the leaf samples was carried out according to Cao et al., (2017) with some modifications. Briefly, the samples were ground with pestle and mortar in liquid nitrogen and frozen immediately. Then, a 100 mg was weighed for each of the sample and put into a 2 ml centrifuge tube. 1 ml of extraction solvent (containing 956 µL of 70% methanol and 44 µL of 8.3 ug/ml ISTD mixture) was added to the sample, vortexed and extracted with a thermoshaker at 4 °C, 1400 rpm for 30 minutes. The samples were centrifuged at 16,100 X g for 10 mins. The supernatants were taken and transferred to new centrifuge tubes. The residues were extracted again with 500 µL of extraction solvent (without ISTD) with the same extraction steps. The first and second supernatants were combined and kept at – 80 °C until further use.

4. Derivatization of samples

For the methyl-chloroformate derivatization of the samples, the protocols were referred to Rawlinson et al., (2015) with some modifications. Briefly, 600 µL of the supernatant for each sample was taken, dried down and re-dissolved with 160 µL methanol. Then, 8.3 ug/ml of $^{13}C5$, N-labelled L-Valine (another internal standard) was added. 34 µL of pyridine was added to the mixture and vortexed vigorously for 25-30s. After that, 200 µL of 1% NaOH solution was added to the mixture and suspended. This 400 µL mixture was derivatized with 20 µL of methyl chloroformate (MCF) and vortexed vigorously for 25-30s. Another 20 µL of methyl chloroformate (MCF) was added and repeated the vortex. Next, 400 µL of chloroform was added to the mixture and vortexed for 10s, followed by an addition of 400 µL of 50 mM sodium bicarbonate. The mixture was vortexed for 10-15s and centrifuged for 30s at 16,100 xg. The upper aqueous layer was discarded, and the bottom organic layer was kept at -80 °C until further analysis.

5. Quantification and analysis of samples using GC-Triple Quadruple-MS

For the quantification of phytohormones, samples (1 µL) were injected into a GC–QqQ–MS system comprising of a Gerstel 2.5.2 Autosampler, a 7890A Agilent gas chromatograph and a 7010 Agilent triple-quadrupole MS (Agilent, Santa Clara, USA) with an electron impact (EI) ion source. The GC was operated in constant pressure mode (20 psi) with helium as the carrier gas. The MS was adjusted according to the manufacturer's recommendations using tris-

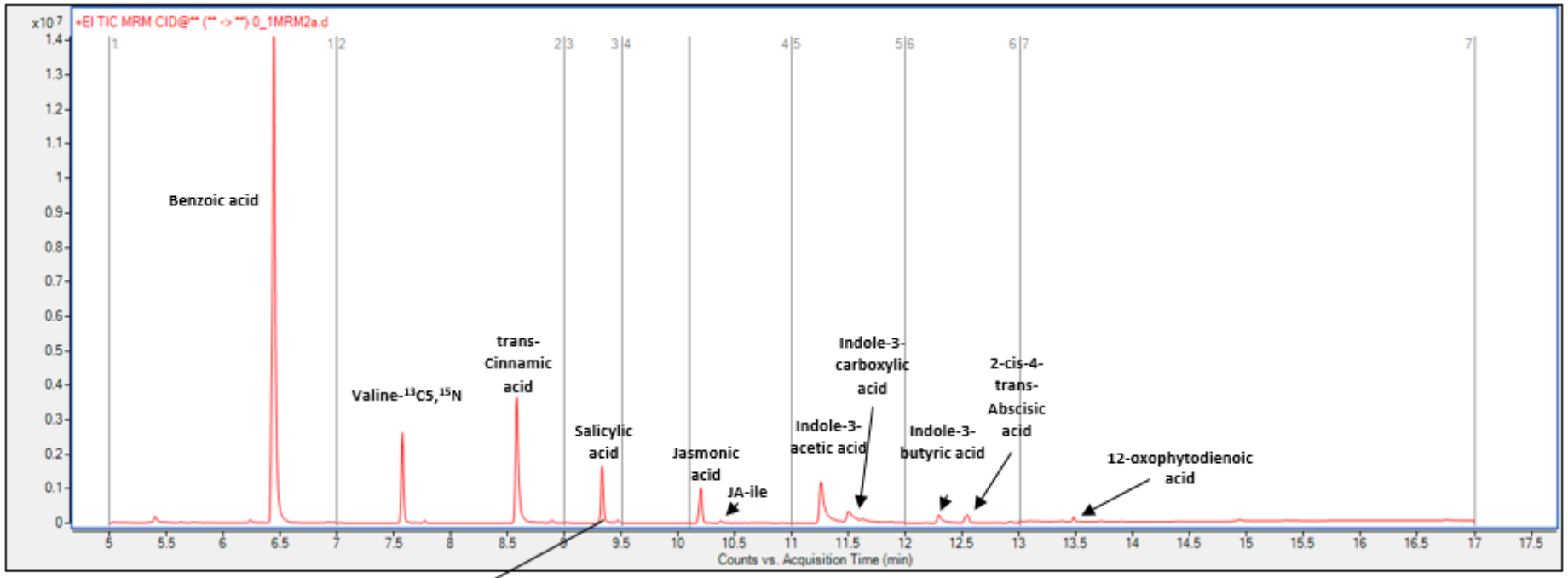
(perfluorobutyl)- amine (CF43). A J&W Scientific VF-5MS column (30m long with 10m guard column, 0.25mm inner diameter, 0.25um film thickness) was used. The injection temperature was set at 250 °C, the MS transfer line at 250 °C, the ion source was adjusted to 250 °C and the quadrupole at 150 °C. Helium was used as the carrier gas at a flow rate of $1mLmin^{-1}$. Nitrogen (UHP 5.0) was used as the collision cell gas at a flow rate of $1.5mLmin^{-1}$. Helium (UHP 5.0) was used as the quenching gas at a flow rate of $2.25mLmin^{-1}$. The following temperature program (Rawlinson et al., 2015) with modification was used; injection at 40 ◦C, hold for 1 min, followed by a 20 $°Cmin^{-1}$ oven temperature and ramped to 255 ◦C, followed by a 15 $°Cmin^{-1}$ oven temperature and ramped to 282 ◦C, then back to 20 $°Cmin^{-1}$ oven temperature and ramped to 320 ◦C and a final hold for 2 min. The total run time was 17.583 min. For method optimization, calibration and internal standards were subsequently analyzed on the GC–QqQ–MS to obtain the retention times and to identify a corresponding unique precursor ion. For each precursor ion, two product ion scans were carried out using four collision energies (0, 5, 10 and 20 V) to identify product ions in which two product ions were identified. Subsequently, for the two generated products the collision energies for each major reaction monitoring (MRM) transition was optimized using a series of collision energies (CEs) between 0 and 30 V. Collision energy optimization plots for each compound are presented in **Point 6** below. Once collision energies were optimized for each MRM transition, a product ion was selected as the corresponding target ion (T) and the subsequent MRM transition was deemed as the qualifier ion (Q). Absolute concentrations (ug/ml) of targeted phytohormones/organic acids were quantified using a MRM target ion based on the linear response of the calibration. Together, all the ten phytohormones and organic acids were detected from the flag leaf samples (refer to the chromatogram in **Point 7** below). However, only six of them [trans-Cinnamic acid (CA), Salicylic acid (SA), Jasmonic acid (JA), Jasmonoyl-isoleucine (JA-ile), Indole-3-acetic acid (IAA) and 2-cis-4-trans-Abscisic acid (ABA)] were managed to be quantified in this study. Benzoic acid (BA) although was detected in high amount, but this was largely due to the contribution from the LC-MS grade methanol solvent. Meanwhile, and 12-oxo phytodienoic acid (OPDA), Indole-3-carboxylic acid (ICA) and Indole-3-butyric acid (IBA) were absent or present in low amount in some of the samples, thus couldn’t be quantified.

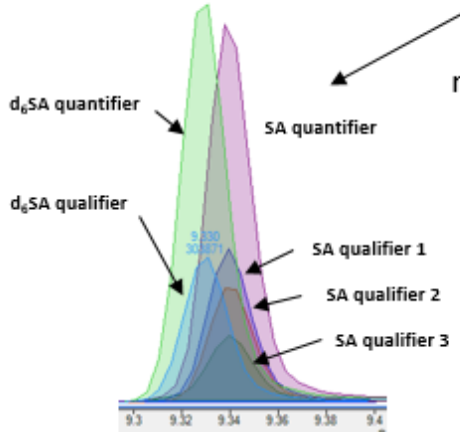
6. Multiple Reaction Monitoring (MRM) developed for the phytohormone and organic acid analyses

	Compound name	Internal standard (/)	Precursor Ion (m/z)	Product ion	Collision Energy	Retention Time (min)
Quantifier	Benzoic acid (BA)		105	77.1	16	6.450
Qualifier 1			105	51	28	
Qualifier 2			136.1	105	8	
Qualifier1	D_5BA	/	110.1	54.1	28	6.432
Quantifier		/	110.1	82.1	16	
Quantifier	Valine-$^{13}C_5$,^{15}N	/	134.9	103.1	12	7.58
Qualifier1		/	134.9	75.1	14	
Qualifier2		/	117.9	86	5	
Qualifier3		/	103.1	59.1	6	
Quantifier	trans-Cinnamic acid (CA)		131.1	103.1	12	8.604
Qualifier1			162.1	103.1	28	
Qualifier2			162.1	131	28	
Quantifier	D_7CA	/	138.1	82.1	28	8.582
Qualifier2			169.1	110.1	28	
Qualifier1			138.1	110.1	16	
Quantifier	Salicylic acid (SA)		135.1	77.1	16	9.337
Qualifier1			135.1	92	20	
Qualifier2			121	93	8	
Qualifier3			121	65.1	20	
Qualifier1	D_6SA	/	139.1	96.1	20	9.327
Quantifier			139.1	81.1	16	
Qualifier2	Jasmonic acid (JA)		224.2	151	4	10.192
Qualifier1			151.1	133.1	4	

Quantifier			151.1	93.1	4	
Quantifier	Jasmonic acid-Isoleucine (Jaile)		151.1	93	4	10.376
Qualifier1			224.1	150.8	4	
Qualifier1	H_2JA	/	153.1	83	20	10.203
Quantifier			153.1	97.1	8	
Quantifier	Indole-3-acetic acid (IAA)		130.1	103.1	20	11.256
Qualifier			189.1	130	20	
Quantifier	D_2IAA	/	191.1	132	20	11.247
Quantifier	Indole-3-carboxylic acid (ICA)		144	89.1	28	11.494
Qualifier2			175	89	28	
Qualifier1			144	116	20	
Quantifier	Indole-3-butyric acid (IBA)		130.1	103.1	20	12.291
Qualifier1			217.1	130	20	
Qualifier2			217.7	142.9	20	
Quantifier	2-cis-4-trans Abscisic acid (ABA)		190.1	162	8	12.55
Qualifier1			190.1	91	28	
Qualifier2			162.1	134	4	
Quantifier	D_6ABA	/	194.1	165.8	8	12.526
Qualifier3	12-oxophytodienoic acid (OPDA)		238.2	148.9	20	13.479
Qualifier2			163.1	121.1	10	
Quantifier			121.1	77	20	
Qualifier4			238.2	206	4	
Qualifier1			121.1	93	8	

7. Chromatogram for the phytohormones and organic acids





Extracted multiple reaction monitoring (MRM) for salicylic acid (SA)

Table I-S2-1. The Multiple Reaction Monitorings (MRMs) established for the authentic sugars, organic acids, amino acids/amines and phytohormones used for identification and quantification in this study. T = Quantifier, Q = Qualifier

Compound name	Precursor ion (m/z)	Product ion (m/z)	Transition	Retention Time (min)	MSI Level	PubChem ID
Sugars and organic acids						
$^{13}C_6$-Sorbitol (Internal standard)	323	132	T	21.497	1	137553928
2-Ketogluconic acid	349	201	T	20.62	1	10198044
2-Ketogluconic acid	349	186	Q		1	
2-Oxoglutarate	198	154	T	16.51	1	51
2-Oxoglutarate	198	167	Q		1	
Aconitate	375	211	T	18.93	1	309
Aconitate	375	285	Q		1	
Caffeic acid	219	191	T	24.437	1	1549111
Citrate	183	138.7	T	19.92	1	311
Ferulic acid	308	219	T	23.904	1	445858
Ferulic acid	308	293	Q		1	
Fumarate	245	217	T	12.21	1	444972
Fumarate	245	170.9	Q		1	
Isocitrate	257	200.7	T	19.93	1	1198
Itaconate	215	132.8	T	12.04	1	811
Itaconate	259	130.8	Q		1	
Malate	233	189	T	14.61	1	525
Maleate	245	216.7	T	11.326	1	5288227
Maleate	245	132.7	Q		1	
Malonate	233	142.8	T	9.446	1	9084
Malonate	233	216.8	Q		1	
Nicotinic acid	180	105.9	T	11.256	1	938
Nicotinic acid	180	135.9	Q		1	
Pipecolate	156	83.9	T	12.46	1	849
Pipecolate	156	127.9	Q		1	
Quinate	255	239	T	20.468	1	6508
Quinate	345	255.1	Q		1	
Salicylate	267	209	T	15.057	1	338
Salicylate	209	91	Q		1	
Shikimate	255	239	T	19.79	1	8742
Shikimate	204	189	Q		1	
Succinate	172	112.9	T	11.514	1	
Succinate	172	155.9	Q		1	1110
Syringic acid	327	312	T	21.19	1	10742
Arabinose	307	217	T	17.446	1	66308
beta-Gentibiose	361	243	T	31.916	1	441422
Fructose	307	217	T	20.617	1	439709
Galactose	319	157	T	20.903	1	6036
Glucose	319	129	T	20.98	1	5793
Maltose	361	169	T	31.06	1	10991489

Mannose	319	129	T	20.848	1	18950
Melezitose	361	169	T	37.6	1	92817
Melibiose	361	169	T	32.33	1	11458
Raffinose	361	169	T	36.946	1	10542
Rhamnose	364	160	T	18.31	1	25310
Ribose	307	217	T	17.683	1	5779
Sucrose	361	169	T	30.02	1	5988
Trehalose	361	169	T	31.13	1	7427
Turanose	361	169	T	31.18	1	5460935
Xylose	307	217	T	17.19	1	135191
Fructose-6-phosphate	204	189	T	26.35	1	69507
Glucose-6-phosphate	364	160	T	26.505	1	5958
Arabitol	319	129	T	18.332	1	827
Erythritol	307	217	T	14.864	1	222285
Galactitol	319	129	T	21.6	1	11850
Glucuronate	364	160	T	21.537	1	94715
Inositol	305	217	T	23.666	1	892
Mannitol	319	157	T	21.429	1	6251

Amino acids and amines	Precursor ion (m/z)	Product ion (m/z)	Transition	Retention Time (min)	MSI Level	PubChem ID
Valine-$^{13}C_5$,^{15}N (Internal standard)	294	171	T	11	1	12164856
gamma-Aminobutyric acid	274	171	T	9.767	1	119
4-Hydroxyproline	302	171	T	12.741	1	825
Alanine	260	171	T	8.446	1	5950
Asparagine	303	171	T	6.147	1	6267
Arginine	345	171	T	6.394	1	6322
Aspartate	304	171	T	7.469	1	5960
beta-Alanine	260	171	T	8.446	1	239
Citrulline	346	171	T	7.582	1	9750
Cysteine	292	171	T	13.995	1	5862
Glutamate	318	171	T	7.769	1	33032
Glutamine	317	171	T	6.781	1	5961
Glycine	246	171	T	7.025	1	750
Histidine	326	171	T	5.425	1	6274
Homoserine	290	171	T	7.94	1	12647
Isoleucine	302	171	T	12.741	1	6306
Leucine	302	171	T	12.908	1	6106
Lysine	244	171	T	10.037	1	5962
Methionine	320	171	T	11.069	1	6137
Octopamine	324	171	T	10.648	1	4581
Ornithine	237	171	T	9.485	1	6262
Phenyalanine	336	171	T	13.122	1	6140
Proline	286	171	T	8.961	1	145742
Putrescine	215	171	T	10.056	1	1045

Serine	276	171	T	6.753	1	5951
Threonine	290	171	T	7.94	1	6288
Tryptophan	375	171	T	13.486	1	6305
Tyramine	308	171	T	11.62	1	5610
Tyrosine	352	171	T	10.981	1	6057
Valine	288	171	T	11.156	1	6287

Phytohormones and the precursor organic acids	Precursor ion (m/z)	Product ion (m/z)	Transition	Retention Time (min)	MSI Level	PubChem ID
Benzoic acid (BA)	105	77.1	T	6.45	1	243
Benzoic acid (BA)	105	51	Q		1	
Benzoic acid (BA)	136.1	105	Q		1	
trans-Cinnamic acid (CA)	131.1	103.1	T	8.604	1	444539
trans-Cinnamic acid (CA)	162.1	103.1	Q		1	
trans-Cinnamic acid (CA)	162.1	131	Q		1	
Salicylic acid (SA)	135.1	77.1	T	9.337	1	338
Salicylic acid (SA)	135.1	92	Q		1	
Salicylic acid (SA)	121	93	Q		1	
Salicylic acid (SA)	121	65.1	Q		1	
Jasmonic acid (JA)	151.1	93.1	T	10.192	1	5281166
Jasmonic acid (JA)	224.2	151	Q		1	
Jasmonic acid (JA)	151.1	133.1	Q		1	
Jasmonic acid-Isoleucine (Jaile)	151.1	93	T	10.376	1	126961093
Jasmonic acid-Isoleucine (Jaile)	224.1	150.8	Q		1	
Indole-3-acetic acid (IAA)	130.1	103.1	T	11.256	1	802
Indole-3-acetic acid (IAA)	189.1	130	Q		1	
Indole-3-carboxylic acid (ICA)	144	89.1	T	11.494	1	69867
Indole-3-carboxylic acid (ICA)	175	89	Q		1	
Indole-3-carboxylic acid (ICA)	144	116	Q		1	
Indole-3-butyric acid (IBA)	130.1	103.1	T	12.291	1	8617
Indole-3-butyric acid (IBA)	217.1	130	Q		1	
Indole-3-butyric acid (IBA)	217.7	142.9	Q		1	
2-cis-4-trans Abscisic acid (ABA)	190.1	162	T	12.55	1	5280896
2-cis-4-trans Abscisic acid (ABA)	190.1	91	Q		1	
2-cis-4-trans Abscisic acid (ABA)	162.1	134	Q		1	
12-oxophytodienoic acid (OPDA)	121.1	77	T	13.479	1	5280411
12-oxophytodienoic acid (OPDA)	238.2	148.9	Q		1	
12-oxophytodienoic acid (OPDA)	163.1	121.1	Q		1	
12-oxophytodienoic acid (OPDA)	238.2	206	Q		1	
12-oxophytodienoic acid (OPDA)	121.1	93	Q		1	
D_5BA (Internal standard)	110.1	82.1	T	6.432	1	24852996
D_5BA (Internal standard)	110.1	54.1	Q		1	
D_7CA (Internal standard)	138.1	82.1	T	8.582	1	16213746
D_7CA (Internal standard)	169.1	110.1	Q		1	
D_7CA (Internal standard)	138.1	110.1	Q		1	

D_6SA (Internal standard)	139.1	81.1	T	9.327	1	71309006
D_6SA (Internal standard)	139.1	96.1	Q		1	
H_2JA (Internal standard)	153.1	97.1	T	10.203	1	2519057
H_2JA (Internal standard)	153.1	83	Q		1	
D_2IAA (Internal standard)	191.1	132	T	11.247	1	24872781
D_6ABA (Internal standard)	190.1	162	T	12.526	1	46779839
D_6ABA (Internal standard)	190.1	91	Q		1	
D_6ABA (Internal standard)	162.1	134	Q		1	
Valine-$^{13}C_5$,^{15}N (Internal standard)	134.9	103.1	T	7.58	1	12164856
Valine-$^{13}C_5$,^{15}N (Internal standard)	134.9	75.1	Q		1	
Valine-$^{13}C_5$,^{15}N (Internal standard)	117.9	86	Q		1	
Valine-$^{13}C_5$,^{15}N (Internal standard)	103.1	59.1	Q		1	

Table I-S2-2. The Multiple Reaction Monitorings (MRMs) established for the five external authentic lipids, and 70 phospholipids used for identification in this study.

Compound Group	Compound Name	Precursor Ion	Product Ion	Retention Time (min)	Lipid Name searched by using LIPIDMAPS and LIPIDMATCH	MSI Level
LPC (Lysophosphatidylcholine)	LPC_482.2	482.2	184.1	5	LPC(15:0)	2
	LPC_496.8	496.8	184.1	4.403	LPC(16:0)	2
	LPC_510.6	510.6	184.1	5.3	LPC(17:0)	2
	LPC_518.6	518.6	184.1	2.268	LPC(18:3)	2
	LPC_520.3	520.3	184.1	3.593	LPC(18:2)	2
	LPC_522.4	522.4	184.1	4.447	LPC(18:1)	2
	LPC_600.0	600	184.1	4.334	LPC(24:4)	2
	LPC_674.5	674.5	184.1	4.649	LPC(29:2)	2
	LPC_680.5	680.5	184.1	5.974	LPC(30:6)	2
	LPC(17:0), external standard, PubChem ID 24779413	510.6	184.1	5.3	LPC(17:0)	1
PC (Phosphatidylcholine)	PC_728.4	728.4	184.1	7.547	PC(32:3)	2
	PC_730.5	730.5	184.1	7.524	PC(32:2)	2
	PC_732.4	732.4	184.1	5.231	PC(32:1)	2
	PC_734.6	734.6	184.1	5	PC(32:0)	2
	PC_740.6	740.6	184.1	7.927	PC(33:4)	2
	PC_742.5	742.5	184.1	6.848	PC(33:3)	2
	PC_744.6	744.6	184.1	7.005	PC(33:2)	2
	PC_746.5	746.5	184.1	6.645	PC(33:1)	2
	PC_754.8	754.8	184.1	5.453	PC(34:4)	2
	PC_756.6	756.6	184.1	5.385	PC(34:3)	2
	PC_758.8	758.8	184.1	6.262	PC(34:2)	2
	PC_760.6	760.6	184.1	4.958	PC(34:1)	2
	PC_762.8	762.8	184.1	7.093	PC(34:0)	2
	PC_766.7	766.7	184.1	6.44	PC(35:5)	2
	PC_768.4	768.4	184.1	7.092	PC(35:4)	2
	PC_770.7	770.7	184.1	6.822	PC(35:3)	2
	PC_772.8	772.8	184.1	6.596	PC(35:2)	2
	PC_774.0	774.7	184.1	6.798	PC(35:1)	2
	PC_776.5	776.5	184.1	5.18	PC(35:0)	2
	PC_778.6	778.6	184.1	8	PC(36:6)	2
	PC_780.7	780.7	184.1	9.674	PC(36:5)	2
	PC_782.7	782.7	184.1	7.494	PC(36:4)	2
	PC_784.8	784.8	184.1	9.381	PC(36:3)	2
	PC_786.6	786.6	184.1	7.74	PC(36:2)	2
	PC_788.0	788	184.1	6.796	PC(36:1)	2

	PC_790.7	790.7	184.1	7.267	PC(36:0)	2
	PC_794.5	794.5	184.1	8.054	PC(37:5)	2
	PC_796.8	796.8	184.1	8.188	PC(37:4)	2
	PC_806.5	806.5	184.1	8.075	PC(38:6)	2
	PC_808.8	808.8	184.1	7.49	PC(38:5)	2
	PC_810.8	810.8	184.1	7.445	PC(38:4)	2
	PC_812.8	812.8	184.1	6.478	PC(38:3)	2
	PC_814.6	814.6	184.1	8.95	PC(38:2)	2
	PC_820.6	820.6	184.1	5	PC(39:6)	2
	PC_824.5	824.5	184.1	8.612	PC(39:4)	2
	PC_826.7	826.7	184.1	7.78	PC(39:3)	2
	PC_828.5	828.5	184.1	7.128	PC(39:2)	2
	PC_848.3	848.3	184.1	7.329	PC(41:6)	2
	PC_850.7	850.7	184.1	6.924	PC(41:5)	2
	PC(34:1), external standard, PubChem ID 5497103	760.6	184.1	4.958	PC(16:0/18:1)	1
PE (Phosphatidylethanolamine)	PE_686.3	686.34	545.2	7.591	PE(32:3)	2
	PE_688.3	688.3	547.2	7.781	PE(32:2)	2
	PE_690.4	690.4	549.3	7.972	PE(32:1)	2
	PE_700.3	700.3	559.2	7.781	PE(33:3)	2
	PE_702.2	702.2	561.1	7.937	PE(33:2)	2
	PE_704.2	704.2	563.1	6.551	PE(33:1)	2
	PE_712.1	712.1	571	7.711	PE(34:4)	2
	PE_714.3	714.3	573.2	7.902	PE(34:3)	2
	PE_716.3	716.3	575.2	8.092	PE(34:2)	2
	PE_718.3	718.3	577.2	8.239	PE(34:1)	2
	PE_720.3	720.3	579.2	8.239	PE(34:0)	2
	PE_722.4	722.4	581.3	7.451	PE(35:6)	2
	PE_726.3	726.3	585.2	7.832	PE(35:4)	2
	PE_728.3	728.3	587.2	8.005	PE(35:3)	2
	PE_736.3	736.3	595.2	7.598	PE(36:6)	2
	PE_738.2	738.2	597.1	7.788	PE(36:5)	2
	PE_740.3	740.3	599.2	7.952	PE(36:4)	2
	PE_742.3	742.3	601.2	7.943	PE(36:3)	2
	PE_744.4	744.4	603.3	8.332	PE(36:2)	2
	PE_758.4	758.4	617.3	6.229	PE(38:9)	2
	PE_764.4	764.4	623.3	7.873	PE(38:6)	2
	PE_766.2	766.2	625.1	8.002	PE(38:5)	2
	PE_768.3	768.3	627.2	8.192	PE(38:4)	2
	PE_770.4	770.4	629.3	8.426	PE(38:3)	2
	PE_772.4	772.4	631.3	8.556	PE(38:2)	2
	PE_784.5	784.5	643.4	6.331	PE(40:10)	2
	PE_786.3	786.3	645.2	6.555	PE(40:9)	2

	PE_794.3	794.3	653.2	8.286	PE(40:5)	2
	PE_796.3	796.3	655.2	8.424	PE(40:4)	2
	PE_806.3	806.3	665.2	7.706	PE(41:6)	2
	PE_808.3	808.3	667.2	7.818	PE(41:5)	2
	PE_810.4	810.4	669.3	8.225	PE(41:4)	2
	PE(34:0), external standard, PubChem ID 46891875	720.3	579.3	669.3	PE(17:0/17:0)	1
PG (Phosphatidylglycerol)	PG_738.3	738.3	549.3	7.398	PG(32:1)	2
	PG_740.4	740.4	551.4	7.45	PG(32:0)	2
	PG_760.3	760.3	571.3	7.077	PG(34:4)	2
	PG_762.3	762.3	573.3	7.172	PG(34:3)	2
	PG_764.3	764.3	575.3	7.336	PG(34:2)	2
	PG_766.3	766.3	577.3	7.517	PG(34:1)	2
	PG_784.4	784.4	595.4	6.841	PG(36:6)	2
	PG_786.3	786.3	597.3	7.014	PG(36:5)	2
	PG_788.2	788.2	599.2	7.412	PG(36:4)	2
	PG_790.1	790.1	601.1	7.429	PG(36:3)	2
	PG(34:1), external standard, PubChem ID 5283509	764.3	575.2	7.336	PG(16:0/18:1)	1
PI (Phosphatidylinositol)	PI_792.1	792.1	515.1	8.078	PI(30:4)	2
	PI_848.2	848.2	571.2	7.073	PI(34:4)	2
	PI_850.2	850.2	573.2	6.917	PI(34:3)	2
	PI_852.2	852.2	575.2	7.134	PI(34:2)	2
	PI_872.1	872.1	595.1	6.623	PI(36:6)	2
	PI_874.2	874.2	597.2	6.804	PI(36:5)	2
	PI_876.2	876.2	599.2	6.986	PI(36:4)	2
	PI_878.2	878.2	601.2	7.254	PI(36:3)	2
	PI_880.3	880.3	603.3	6.839	PI(36:2)	2
	PI_892.4	892.4	615.4	9.072	PI(37:3)	2
	PI_906.5	906.5	629.5	8.916	PI(38:3)	2
	PI(36:2), external standard, PubChem ID not found	880.3	603.3	6.839	PI(18:1/18:1)	1
PA (Phosphatidic acid)	PA(34:0), external standard, PubChem ID 16219855	677.5	153	7	PA(17:0/17:0)	1
PS (Phosphatidylserine)	PS_680.2	680.2	495.2	8.964	PS(28:0)	2

	PS_842.1	842.1	657.1	7.824	PS(40:3)	2
	PS_844.2	844.2	659.2	7.959	PS(40:2)	2
	PS_858.1	858.1	673.1	8.115	PS(41:2)	2
	PS_870.1	870.1	685.1	8.137	PS(42:3_	2
	PS(34:0), external standard, PubChem ID 46891783	764.5	676	7	PS(17:0/17:0)	1
Galactosyl lipids	DGDG_932.2	932.2	591.2	7.944	DGDG(34:3)	2
	DGDG_954.3	954.3	613.3	7.677	DGDG(36:6)	2
	DGDG_960.3	960.3	619.3	8.22	DGDG(36:3)	2
	DGDG_982.4	982.4	641.4	7.907	DGDG(38:6)	2
	MGDG_792.2	792.2	613.2	8.081	MGDG(36:6)	2
	MGDG_794.2	794.2	615.2	8.247	MGDG(36:5)	2
	MGDG_796.2	796.2	617.2	8.396	MGDG(36:4)	2
	SQDG_834.1	834.1	591.1	6.997	SQDG(34:3)	2
	SQDG_856.2	856.2	613.2	6.684	SQDG(36:6)	2

The files sizes and the datasets in excel sheets for Supplemental Tables **I-S2-3** to **I-S2-13** are too large to insert in this thesis. Therefore, only the captions are given here. These supplemental tables can be accessed via the link of the published journal (Cheong et al., 2019), i.e. https://link.springer.com/article/10.1007/s11306-019-1606-2, under *Electronic supplementary material: Supplementary material 3 (XLSX 837 kb)*.

Table I-S2-3. Concentrations for the measured metabolites (sugars, organic acids, aminoacids/amines and phytohormones) in the Wyalkatchem's and Young's flag leaves across all the time points.

Table I-S2-4. Lipid responses for the measured phospholipids in the Wyalkatchem's and Young's flag leaves across all the time points.

Table I-S2-5. Fold changes ± sem for the pair-wise comparisons of metabolites in Young and Wyalkatchem.

Table I-S2-6. Fold changes ± sem for the pair-wise comparisons of phospholipids in Young and Wyalkatchem.

Table I-S2-7. Multiple comparisons of metabolites in Wyalkatchem, Young, Wyalkatchem vs. Young across all the time points by using One-Way ANOVA, with FDR-adjusted $p < 0.05$ as significance.

Table I-S2-8. Multiple comparisons of phospholipids in Wyalkatchem, Young, Wyalkatchem vs. Young across all the time points by using One-Way ANOVA, with FDR-adjusted $p < 0.05$ as significance.

Table I-S2-9. Tukey test for metabolites that significantly changed in Wyalkatchem, Young, Wyalkatchem *vs.* Young.

Table I-S2-10. Tukey test for phospholipids that significantly changed in Wyalkatchem, Young, Wyalkatchem *vs.* Young.

Table I-S2-11. The unsaturation to saturation ratio in Wyalkatchem and Young.

Table I-S2-12. Group of 11 lipids that consistently higher in Wyalkatchem compared to Young.

Table I-S2-13. Group of 18 lipids that consistently higher in Young compared to Wyalkatchem.

Appendix A: Supplemental Data and Tables for Chapter 2, Part II

Table II-S2-1. Multiple Reaction Monitoring (MRMs) established for authentic sugars, organic acids, amino acids and amines used for identification and quantification of these compounds in this study. T = Quantifier, Q = Qualifier

Compound name	Precursor ion (m/z)	Product ion (m/z)	Transition	Retention Time (min)	MSI Level	PubChem ID
Sugars and organic acids						
$^{13}C_6$-Sorbitol (Internal standard)	323	132	T	21.497	1	137553928
2-Ketogluconic acid	349	201	T	20.62	1	10198044
2-Ketogluconic acid	349	186	Q		1	
2-Oxoglutarate	198	154	T	16.51	1	51
2-Oxoglutarate	198	167	Q		1	
Aconitate	375	211	T	18.93	1	309
Aconitate	375	285	Q		1	
Caffeic acid	219	191	T	24.437	1	1549111
Citrate	183	138.7	T	19.92	1	311
Ferulic acid	308	219	T	23.904	1	445858
Ferulic acid	308	293	Q		1	
Fumarate	245	217	T	12.21	1	444972
Fumarate	245	170.9	Q		1	
Isocitrate	257	200.7	T	19.93	1	1198
Itaconate	215	132.8	T	12.04	1	811
Itaconate	259	130.8	Q		1	
Malate	233	189	T	14.61	1	525
Maleate	245	216.7	T	11.326	1	5288227
Maleate	245	132.7	Q		1	
Malonate	233	142.8	T	9.446	1	9084
Malonate	233	216.8	Q		1	
Nicotinic acid	180	105.9	T	11.256	1	938
Nicotinic acid	180	135.9	Q		1	
Pipecolate	156	83.9	T	12.46	1	849
Pipecolate	156	127.9	Q		1	
Quinate	255	239	T	20.468	1	6508
Quinate	345	255.1	Q		1	
Salicylate	267	209	T	15.057	1	338
Salicylate	209	91	Q		1	
Shikimate	255	239	T	19.79	1	8742
Shikimate	204	189	Q		1	
Succinate	172	112.9	T	11.514	1	
Succinate	172	155.9	Q		1	1110
Syringic acid	327	312	T	21.19	1	10742
Arabinose	307	217	T	17.446	1	66308
beta-Gentibiose	361	243	T	31.916	1	441422

Fructose	307	217	T	20.617	1	439709
Galactose	319	157	T	20.903	1	6036
Glucose	319	129	T	20.98	1	5793
Maltose	361	169	T	31.06	1	10991489
Mannose	319	129	T	20.848	1	18950
Melezitose	361	169	T	37.6	1	92817
Melibiose	361	169	T	32.33	1	11458
Raffinose	361	169	T	36.946	1	10542
Rhamnose	364	160	T	18.31	1	25310
Ribose	307	217	T	17.683	1	5779
Sucrose	361	169	T	30.02	1	5988
Trehalose	361	169	T	31.13	1	7427
Turanose	361	169	T	31.18	1	5460935
Xylose	307	217	T	17.19	1	135191
Fructose-6-phosphate	204	189	T	26.35	1	69507
Glucose-6-phosphate	364	160	T	26.505	1	5958
Arabitol	319	129	T	18.332	1	827
Erythritol	307	217	T	14.864	1	222285
Galactitol	319	129	T	21.6	1	11850
Glucuronate	364	160	T	21.537	1	94715
Inositol	305	217	T	23.666	1	892
Mannitol	319	157	T	21.429	1	6251

Amino acids and amines	Precursor ion (m/z)	Product ion (m/z)	Transition	Retention Time (min)	MSI Level	PubChem ID
Valine-$^{13}C_5$,^{15}N (Internal standard)	294	171	T	11	1	12164856
gamma-Aminobutyric acid	274	171	T	9.767	1	119
4-Hydroxyproline	302	171	T	12.741	1	825
Alanine	260	171	T	8.446	1	5950
Asparagine	303	171	T	6.147	1	6267
Arginine	345	171	T	6.394	1	6322
Aspartate	304	171	T	7.469	1	5960
beta-Alanine	260	171	T	8.446	1	239
Citrulline	346	171	T	7.582	1	9750
Cysteine	292	171	T	13.995	1	5862
Glutamate	318	171	T	7.769	1	33032
Glutamine	317	171	T	6.781	1	5961
Glycine	246	171	T	7.025	1	750
Histidine	326	171	T	5.425	1	6274
Homoserine	290	171	T	7.94	1	12647
Isoleucine	302	171	T	12.741	1	6306
Leucine	302	171	T	12.908	1	6106
Lysine	244	171	T	10.037	1	5962
Methionine	320	171	T	11.069	1	6137
Octopamine	324	171	T	10.648	1	4581

Ornithine	237	171	T	9.485	1	6262
Phenyalanine	336	171	T	13.122	1	6140
Proline	286	171	T	8.961	1	145742
Putrescine	215	171	T	10.056	1	1045
Serine	276	171	T	6.753	1	5951
Threonine	290	171	T	7.94	1	6288
Tryptophan	375	171	T	13.486	1	6305
Tyramine	308	171	T	11.62	1	5610
Tyrosine	352	171	T	10.981	1	6057
Valine	288	171	T	11.156	1	6287

Table II-S2-2. Multiple Reaction Monitoring (MRMs) established for the seven external authentic lipids, and 95 phospholipids used for identification of these compounds in this study.

Compound Group	Compound Name	Precursor Ion	Product Ion	Retention Time (min)	Lipid Name searched by using LIPIDMAPS and LIPIDMATCH	MSI Level
LPC (Lysophosphatidylcholine)	LPC_482.2	482.2	184.1	5	LPC(15:0)	2
	LPC_496.8	496.8	184.1	4.403	LPC(16:0)	2
	LPC_510.6	510.6	184.1	5.3	LPC(17:0)	2
	LPC_518.6	518.6	184.1	2.268	LPC(18:3)	2
	LPC_520.3	520.3	184.1	3.593	LPC(18:2)	2
	LPC_522.4	522.4	184.1	4.447	LPC(18:1)	2
	LPC_600.0	600	184.1	4.334	LPC(24:4)	2
	LPC_674.5	674.5	184.1	4.649	LPC(29:2)	2
	LPC_680.5	680.5	184.1	5.974	LPC(30:6)	2
	LPC(17:0), external standard, PubChem ID 24779463	510.6	184.1	5.3	LPC(17:0)	1
PC (Phosphatidylcholine)	PC_728.4	728.4	184.1	7.547	PC(32:3)	2
	PC_730.5	730.5	184.1	7.524	PC(32:2)	2
	PC_732.4	732.4	184.1	5.231	PC(32:1)	2
	PC_734.6	734.6	184.1	5	PC(32:0)	2
	PC_740.6	740.6	184.1	7.927	PC(33:4)	2
	PC_742.5	742.5	184.1	6.848	PC(33:3)	2
	PC_744.6	744.6	184.1	7.005	PC(33:2)	2
	PC_746.5	746.5	184.1	6.645	PC(33:1)	2
	PC_754.8	754.8	184.1	5.453	PC(34:4)	2
	PC_756.6	756.6	184.1	5.385	PC(34:3)	2
	PC_758.8	758.8	184.1	6.262	PC(34:2)	2
	PC_760.6	760.6	184.1	4.958	PC(34:1)	2
	PC_762.8	762.8	184.1	7.093	PC(34:0)	2
	PC_766.7	766.7	184.1	6.44	PC(35:5)	2
	PC_768.4	768.4	184.1	7.092	PC(35:4)	2
	PC_770.7	770.7	184.1	6.822	PC(35:3)	2
	PC_772.8	772.8	184.1	6.596	PC(35:2)	2
	PC_774.0	774.7	184.1	6.798	PC(35:1)	2
	PC_776.5	776.5	184.1	5.18	PC(35:0)	2
	PC_778.6	778.6	184.1	8	PC(36:6)	2
	PC_780.7	780.7	184.1	9.674	PC(36:5)	2
	PC_782.7	782.7	184.1	7.494	PC(36:4)	2
	PC_784.8	784.8	184.1	9.381	PC(36:3)	2
	PC_786.6	786.6	184.1	7.74	PC(36:2)	2
	PC_788.0	788	184.1	6.796	PC(36:1)	2

	PC_790.7	790.7	184.1	7.267	PC(36:0)	2
	PC_794.5	794.5	184.1	8.054	PC(37:5)	2
	PC_796.8	796.8	184.1	8.188	PC(37:4)	2
	PC_806.5	806.5	184.1	8.075	PC(38:6)	2
	PC_808.8	808.8	184.1	7.49	PC(38:5)	2
	PC_810.8	810.8	184.1	7.445	PC(38:4)	2
	PC_812.8	812.8	184.1	6.478	PC(38:3)	2
	PC_814.6	814.6	184.1	8.95	PC(38:2)	2
	PC_820.6	820.6	184.1	5	PC(39:6)	2
	PC_824.5	824.5	184.1	8.612	PC(39:4)	2
	PC_826.7	826.7	184.1	7.78	PC(39:3)	2
	PC_828.5	828.5	184.1	7.128	PC(39:2)	2
	PC_848.3	848.3	184.1	7.329	PC(41:6)	2
	PC_850.7	850.7	184.1	6.924	PC(41:5)	2
	PC(34:1), external standard, PubChem ID 5497103	760.6	184.1	4.958	PC(16:0/18:1)	1
PE (Phosphatidylethanolamine)	PE_686.3	686.34	545.2	7.591	PE(32:3)	2
	PE_688.3	688.3	547.2	7.781	PE(32:2)	2
	PE_690.4	690.4	549.3	7.972	PE(32:1)	2
	PE_700.3	700.3	559.2	7.781	PE(33:3)	2
	PE_702.2	702.2	561.1	7.937	PE(33:2)	2
	PE_704.2	704.2	563.1	6.551	PE(33:1)	2
	PE_712.1	712.1	571	7.711	PE(34:4)	2
	PE_714.3	714.3	573.2	7.902	PE(34:3)	2
	PE_716.3	716.3	575.2	8.092	PE(34:2)	2
	PE_718.3	718.3	577.2	8.239	PE(34:1)	2
	PE_720.3	720.3	579.2	8.239	PE(34:0)	2
	PE_722.4	722.4	581.3	7.451	PE(35:6)	2
	PE_726.3	726.3	585.2	7.832	PE(35:4)	2
	PE_728.3	728.3	587.2	8.005	PE(35:3)	2
	PE_736.3	736.3	595.2	7.598	PE(36:6)	2
	PE_738.2	738.2	597.1	7.788	PE(36:5)	2
	PE_740.3	740.3	599.2	7.952	PE(36:4)	2
	PE_742.3	742.3	601.2	7.943	PE(36:3)	2
	PE_744.4	744.4	603.3	8.332	PE(36:2)	2
	PE_758.4	758.4	617.3	6.229	PE(38:9)	2
	PE_764.4	764.4	623.3	7.873	PE(38:6)	2
	PE_766.2	766.2	625.1	8.002	PE(38:5)	2
	PE_768.3	768.3	627.2	8.192	PE(38:4)	2
	PE_770.4	770.4	629.3	8.426	PE(38:3)	2
	PE_772.4	772.4	631.3	8.556	PE(38:2)	2
	PE_784.5	784.5	643.4	6.331	PE(40:10)	2

	PE_786.3	786.3	645.2	6.555	PE(40:9)	2
	PE_794.3	794.3	653.2	8.286	PE(40:5)	2
	PE_796.3	796.3	655.2	8.424	PE(40:4)	2
	PE_806.3	806.3	665.2	7.706	PE(41:6)	2
	PE_808.3	808.3	667.2	7.818	PE(41:5)	2
	PE_810.4	810.4	669.3	8.225	PE(41:4)	2
	PE(34:0), external standard, PubChem ID 46891875	720.3	579.3	669.3	PE(17:0/17:0)	1
PG (Phosphatidylglycerol)	PG_738.3	738.3	549.3	7.398	PG(32:1)	2
	PG_740.4	740.4	551.4	7.45	PG(32:0)	2
	PG_760.3	760.3	571.3	7.077	PG(34:4)	2
	PG_762.3	762.3	573.3	7.172	PG(34:3)	2
	PG_764.3	764.3	575.3	7.336	PG(34:2)	2
	PG_766.3	766.3	577.3	7.517	PG(34:1)	2
	PG_784.4	784.4	595.4	6.841	PG(36:6)	2
	PG_786.3	786.3	597.3	7.014	PG(36:5)	2
	PG_788.2	788.2	599.2	7.412	PG(36:4)	2
	PG_790.1	790.1	601.1	7.429	PG(36:3)	2
	PG(34:1), external standard, PubChem ID 5283509	764.3	575.2	7.336	PG(16:0/18:1)	1
PI (Phosphatidylinositol)	PI_792.1	792.1	515.1	8.078	PI(30:4)	2
	PI_848.2	848.2	571.2	7.073	PI(34:4)	2
	PI_850.2	850.2	573.2	6.917	PI(34:3)	2
	PI_852.2	852.2	575.2	7.134	PI(34:2)	2
	PI_872.1	872.1	595.1	6.623	PI(36:6)	2
	PI_874.2	874.2	597.2	6.804	PI(36:5)	2
	PI_876.2	876.2	599.2	6.986	PI(36:4)	2
	PI_878.2	878.2	601.2	7.254	PI(36:3)	2
	PI_880.3	880.3	603.3	6.839	PI(36:2)	2
	PI_892.4	892.4	615.4	9.072	PI(37:3)	2
	PI_906.5	906.5	629.5	8.916	PI(38:3)	2
	PI(36:2), external standard, PubChem ID not found	880.3	603.3	6.839	PI(18:1/18:1)	1
PA (Phosphatidic acid)	PA(34:0), external standard, PubChem ID 16219855	677.5	153	7	PA(17:0/17:0)	1

PS (Phosphatidylserine)	PS_680.2	680.2	495.2	8.964	PS(28:0)	2
	PS_842.1	842.1	657.1	7.824	PS(40:3)	2
	PS_844.2	844.2	659.2	7.959	PS(40:2)	2
	PS_858.1	858.1	673.1	8.115	PS(41:2)	2
	PS_870.1	870.1	685.1	8.137	PS(42:3_	2
	PS(34:0), external standard, PubChem ID 46891783	764.5	676	7	PS(17:0/17:0)	1
Galactolipids	DGDG_932.2	932.2	591.2	7.944	DGDG(34:3)	2
	DGDG_954.3	954.3	613.3	7.677	DGDG(36:6)	2
	DGDG_960.3	960.3	619.3	8.22	DGDG(36:3)	2
	DGDG_982.4	982.4	641.4	7.907	DGDG(38:6)	2
	MGDG_792.2	792.2	613.2	8.081	MGDG(36:6)	2
	MGDG_794.2	794.2	615.2	8.247	MGDG(36:5)	2
	MGDG_796.2	796.2	617.2	8.396	MGDG(36:4)	2
	SQDG_834.1	834.1	591.1	6.997	SQDG(34:3)	2
	SQDG_856.2	856.2	613.2	6.684	SQDG(36:6)	2
	SQDG_848.2	848.2	605.2		SQDG(36:1)	2
	SQDG_888.6	888.6	645.5		SQDG(38:4)	2

The files sizes and the datasets in excel sheets for Supplemental Tables **II-S2-3** to **II-S2-10** are too large to insert in this thesis. Therefore, only the captions are given here. These supplemental tables can be accessed via the link of the published journal (Cheong et al., 2020), i.e. http://www.mdpi.com/2073-4409/9/5/1309/s1.

Table II-S2-3. Concentrations of primary metabolites (sugars, organic acids, amino acids and amines) measured in Wyalkatchem and Young spikes across all time points.

Table II-S2-4. Normalized lipid responses for the measured lipids in the Wyalkatchem and Young spikes across all the time points.

Table II-S2-5. Fold changes ± sem for the pair-wise comparisons of metabolites in Young and Wyalkatchem spikes.

Table II-S2-6. Fold changes ± sem for the pair-wise comparisons of lipids in Young and Wyalkatchem spikes.

Table II-S2-7. Multiple comparisons of primary metabolites in Wyalkatchem, Young, Wyalkatchem vs. Young across all time points using One-Way ANOVA (with FDR-adjusted

p<0.05), followed by Tukey test to determine which specific two groups are significantly different.

Table II-S2-8. Multiple comparisons of phospholipids in Wyalkatchem, Young, Wyalkatchem vs. Young across all time points using One-Way ANOVA (with FDR-adjusted p<0.05), followed by Tukey test to determine which specific two groups are significantly different.

Table II-S2-9. Changes in the unsaturated to saturated lipid ratio in Wyalkatchem and Young during the time-course experiment.

Table II-S2-10. One-Way ANOVA analysis and Tukey test for comparison of primary metabolite levels between flag leaves and spikes in Wyalkatchem and Young.

Appendix B: Supplemental Data and Tables for Chapter 3

Supplemental Table S3-1. Fold-changes of total 273 lipid species in the three developmental root zones of cold-sensitive Wyalkatchem and cold-tolerant Young at the unstressed stage (control 21°C), after subjected to chilling (4°C) and freezing (-3°C) stress.

	Comparisons in Wyalkatchem						Comparisons in Young						Comparisons between Young vs. Wyalkatchem								
	MZ		EZ		DZ		MZ		EZ		DZ		MZ	EZ	DZ	MZ	EZ	DZ	MZ	EZ	DZ
Significant x-fold changes (mean) of the 273 lipid species. Significance of differences were determined by FDR-adjusted *p*-value < 0.05 as cut-off and highlighted with yellow colour.	Chilling 4°C vs Control 21°C	Freezing -3°C vs Control 21°C	Chilling 4°C vs Control 21°C	Freezing -3°C vs Control 21°C	Chilling 4°C vs Control 21°C	Freezing -3°C vs Control 21°C	Chilling 4°C vs Control 21°C	Freezing -3°C vs Control 21°C	Chilling 4°C vs Control 21°C	Freezing -3°C vs Control 21°C	Chilling 4°C vs Control 21°C	Freezing -3°C vs Control 21°C	Control (21°C)	Control (21°C)	Control (21°C)	Chilling (4°C)	Chilling (4°C)	Chilling (4°C)	Freezing (-3°C)	Freezing (-3°C)	Freezing (-3°C)
LysoPC(16:0)	1.0	1.2	1.2	1.7	-1.2	1.1	-1.0	1.2	1.0	1.4	-1.1	1.0	3.2	4.9	3.0	3.0	4.3	3.3	3.1	4.1	2.9
LysoPC(16:1)	-1.4	-1.2	-1.1	1.1	-1.2	1.1	-1.1	1.1	1.1	1.4	-1.0	1.3	2.5	3.3	1.9	3.2	4.2	2.3	3.5	4.3	2.4
LysoPC(18:1)	1.1	1.4	-1.1	1.4	-2.1	-1.6	1.1	1.3	1.0	1.4	-1.4	-1.6	2.7	3.8	2.7	2.7	4.2	4.0	2.4	3.7	2.6
LysoPC(18:2)	1.2	1.4	1.2	1.7	-1.3	1.0	1.1	1.3	1.2	1.7	1.0	1.2	3.2	4.2	2.5	3.0	4.1	3.3	3.1	4.1	2.9
LysoPC(18:3))	1.3	1.5	1.6	2.3	1.0	1.4	-1.0	1.2	1.1	1.9	1.2	1.3	2.9	3.6	2.3	2.2	2.5	2.6	2.3	3.0	2.2
LysoPC(20:1	1.6	1.8	1.2	1.8	-1.5	-1.0	1.2	1.6	1.5	2.3	-1.1	-1.1	3.9	4.5	5.2	3.0	5.7	7.2	3.4	5.6	4.7
LysoPC(20:2)	1.2	1.4	1.4	1.9	-1.1	1.1	-1.1	1.1	1.1	1.9	1.1	1.1	3.6	4.8	3.7	2.6	3.8	4.6	2.8	4.8	3.8
LysoPC(22:1)	1.3	1.3	1.5	2.1	-1.4	-1.3	1.0	1.3	1.4	1.8	-1.1	-1.4	3.7	5.9	4.9	3.0	5.5	6.5	4.0	5.1	4.4
LysoPC(24:1)	1.2	1.4	1.5	1.8	1.0	1.0	1.2	1.3	1.4	1.8	1.1	-1.1	3.4	5.7	5.9	3.4	5.2	6.7	3.1	5.6	5.1
LysoPE(14:0)	-1.3	-1.3	-1.1	-1.2	-1.2	-1.1	-1.0	-1.1	-1.2	1.0	-1.2	1.1	2.5	3.3	2.6	3.0	3.1	2.6	2.7	4.2	3.0
LysoPE(16:1)	-3.3	-3.4	-2.1	-2.8	-2.6	-2.9	1.5	1.9	1.3	1.9	1.3	2.7	1.6	2.4	1.3	7.5	6.4	4.0	10.4	12.4	10.1
LysoPE(18:1)	-1.3	-1.0	-1.3	1.1	-2.1	-1.5	1.1	1.5	1.1	1.6	-1.3	-1.0	2.1	3.1	2.9	3.0	4.5	4.4	3.2	4.4	4.1

LysoPE(18:2)	1.2	1.4	1.2	1.7	-1.2	1.1	1.1	1.3	1.2	1.6	-1.1	1.2	3.4	5.1	3.3	3.1	5.0	3.7	3.3	4.9	3.6
LysoPE(18:3)	1.5	1.8	1.6	2.3	1.0	1.3	-1.0	1.3	1.1	1.7	-1.1	1.1	2.9	3.8	2.7	1.9	2.5	2.5	2.1	2.9	2.4
LysoPE(20:1)	1.2	1.3	1.2	1.7	-1.4	1.0	1.0	1.3	1.2	1.7	-1.2	-1.1	2.8	4.1	4.1	2.3	3.9	4.5	2.8	4.3	3.7
LysoPE(20:2)	-1.1	-1.1	1.1	1.4	-1.4	-1.1	-1.1	1.0	-1.1	1.2	-1.3	-1.1	2.7	4.9	3.7	2.5	4.3	3.9	2.9	4.3	3.9
LysoPE(22:1)	1.1	1.2	1.3	1.5	-1.4	-1.2	1.0	1.2	1.3	1.6	-1.1	-1.2	3.0	3.8	3.8	2.7	3.7	4.8	2.9	3.8	3.7
LysoPE(22:2)	-1.1	-1.2	-1.1	-1.2	-1.4	-1.2	-1.2	-1.1	-1.1	1.0	-1.3	-1.4	2.3	3.4	3.8	2.2	3.5	4.2	2.6	4.1	3.2
LysoPG(16:0)	1.2	1.2	1.3	1.8	-1.1	1.1	1.0	1.2	1.2	1.6	-1.1	-1.0	2.3	2.8	2.2	2.0	2.5	2.2	2.3	2.5	1.9
LysoPG(18:1)	-1.3	-1.1	-1.3	1.1	-1.9	-1.4	1.1	1.5	1.1	1.5	-1.4	-1.2	1.5	1.9	1.8	2.1	2.8	2.5	2.5	2.5	2.1
LysoPG(18:2)	1.2	1.3	1.1	1.5	-1.1	1.1	1.1	1.3	1.3	1.5	-1.1	1.1	2.3	2.8	2.1	2.0	3.0	2.3	2.3	2.8	2.0
LysoPG(18:3)	1.5	1.6	1.6	2.1	1.2	1.4	1.0	1.3	1.2	1.9	-1.0	1.0	1.8	2.1	2.1	1.2	1.6	1.8	1.5	1.9	1.6
LysoPI(18:2)	1.4	1.6	1.3	1.8	-1.1	1.0	-1.0	1.2	1.1	1.4	-1.1	1.1	2.6	2.7	1.8	1.9	2.3	1.8	2.0	2.2	1.9
LysoPI(18:3)	1.6	1.9	1.6	2.2	1.0	1.2	-1.1	1.1	-1.0	1.5	-1.1	-1.0	2.4	2.4	2.1	1.4	1.5	1.8	1.5	1.7	1.7
LysoPS(18:2)	1.4	2.0	1.2	1.8	-1.1	1.0	1.1	1.4	-1.0	1.3	-1.1	1.2	2.5	2.4	1.6	2.0	1.9	1.6	1.7	1.8	1.8
PC(32:0)_PC(16:0_16:0)	1.3	1.8	1.2	1.3	1.2	1.2	-1.2	-1.0	-1.1	1.1	-1.2	1.1	1.1	-1.3	-1.6	-1.4	-1.8	-2.2	-1.7	-1.6	-1.8
PC(32:1)_PC(16:0_16:1)	-1.2	1.1	1.0	1.3	-1.0	-1.0	-1.1	1.0	-1.2	1.0	-1.4	1.0	-1.4	-1.4	-1.6	-1.3	-1.8	-2.3	-1.5	-1.7	-1.5
PC(32:2)_PC(14:0_18:2)	-1.1	1.2	-1.1	1.1	-1.2	-1.0	-1.2	-1.1	-1.2	-1.2	-1.3	1.1	1.1	-1.2	-1.8	1.0	-1.3	-1.9	-1.2	-1.5	-1.5
PC(32:3)_PC(14:0_18:3)	-1.0	1.3	1.3	1.6	1.2	1.3	-1.3	1.0	-1.2	1.1	-1.1	1.1	-1.2	-1.3	-1.8	-1.5	-2.1	-2.2	-1.4	-2.0	-2.0
PC(34:1)_PC(16:0_18:1)	1.2	1.9	1.1	1.3	-1.4	-1.2	-1.0	1.1	-1.2	1.0	-1.5	-1.3	-1.1	-1.6	-1.8	-1.4	-2.0	-1.9	-1.9	-2.1	-2.0
PC(34:2)_PC(16:0_18:2)	1.2	1.7	1.4	1.5	1.1	1.2	-1.0	1.1	-1.1	1.2	-1.1	1.1	-1.0	-1.3	-1.6	-1.3	-1.9	-2.0	-1.6	-1.7	-1.8
PC(34:3)_PC(16:0_18:3)	1.4	1.8	1.6	1.8	1.3	1.4	-1.2	1.1	-1.1	1.2	-1.1	1.1	-1.1	-1.5	-1.6	-1.8	-2.7	-2.1	-1.9	-2.3	-2.0
PC(34:3)_PC(16:1_18:2)	1.0	1.3	1.2	1.3	-1.0	1.1	-1.1	-1.1	-1.1	1.1	-1.0	1.2	-1.1	-1.4	-1.9	-1.1	-1.8	-1.9	-1.5	-1.7	-1.7
PC(34:4)_PC(16:1_18:3)	1.1	1.5	1.7	1.9	1.1	1.1	-1.1	-1.1	-1.1	1.4	1.2	1.7	-1.2	-1.6	-2.9	-1.3	-3.2	-2.5	-2.0	-2.4	-1.9
PC(36:1)_PC(18:0_18:1)	1.1	1.8	-1.2	1.1	-2.5	-1.9	1.2	1.3	-1.1	1.3	-1.8	-1.6	-1.2	-1.9	-1.5	-1.1	-1.7	-1.1	-1.6	-1.5	-1.2
PC(36:2)_PC(18:0_18:2)	1.3	1.8	1.3	1.5	-1.2	-1.0	1.1	1.3	1.0	1.6	-1.1	1.1	-1.0	-1.4	-1.3	-1.2	-1.8	-1.2	-1.4	-1.4	-1.2
PC(36:2)_PC(18:1_18:1)	1.1	1.7	-1.2	1.0	-2.1	-1.7	1.1	1.2	-1.2	1.1	-1.6	-1.5	-1.4	-2.1	-1.9	-1.4	-2.3	-1.5	-1.9	-2.1	-1.7
PC(36:3)_PC(18:0_18:3)	1.4	2.1	1.8	2.1	1.1	1.3	-1.0	1.1	-1.1	1.6	-1.0	1.0	-1.2	-1.6	-1.3	-1.8	-3.0	-1.4	-2.3	-2.0	-1.6
PC(36:3)_PC(18:1_18:2)	1.3	2.0	1.1	1.3	-1.4	-1.2	1.1	1.2	-1.1	1.2	-1.4	-1.2	-1.2	-1.8	-1.9	-1.4	-2.3	-1.8	-2.0	-2.1	-1.8
PC(36:4)_PC(18:1_18:3)	1.4	2.2	1.4	1.7	-1.1	-1.1	-1.1	1.2	-1.2	1.2	-1.3	-1.3	-1.3	-2.0	-1.9	-2.0	-3.3	-2.1	-2.5	-2.7	-2.2
PC(36:4)_PC(18:2_18:2)	1.2	1.7	1.3	1.5	1.0	1.2	-1.0	1.2	-1.0	1.3	-1.0	1.2	-1.0	-1.4	-1.9	-1.3	-2.0	-2.0	-1.5	-1.6	-1.8
PC(36:5)_PC(18:2_18:3)	1.4	1.9	1.7	1.9	1.3	1.4	-1.2	1.1	-1.0	1.5	1.2	1.3	-1.1	-1.7	-2.0	-1.8	-3.0	-2.1	-1.9	-2.2	-2.0
PC(36:6)_PC(18:3_18:3)	1.7	2.3	2.5	2.7	1.8	1.8	-1.2	1.0	-1.1	1.9	1.7	1.7	-1.2	-2.2	-2.6	-2.4	-5.8	-2.7	-2.6	-3.1	-2.7

PC(38:2)_PC(18:1_20:1)	1.3	2.0	1.0	1.2	-1.9	-1.5	1.2	1.2	1.0	1.2	-1.5	-1.6	-1.5	-2.3	-1.9	-1.6	-2.3	-1.5	-2.3	-2.3	-2.0
PC(38:2)_PC(18:2_20:0)	1.1	1.6	1.3	1.4	-1.2	-1.1	-1.0	-1.0	-1.1	1.3	-1.2	-1.2	1.0	-1.3	-1.2	-1.2	-1.9	-1.2	-1.6	-1.4	-1.3
PC(38:3)_PC(18:2_20:1)	1.3	2.0	1.3	1.6	-1.1	1.2	1.2	1.4	1.0	1.4	-1.0	1.2	-1.3	-1.7	-1.9	-1.4	-2.2	-1.8	-2.0	-1.9	-1.8
PC(38:4)_PC(18:2_20:2)	1.4	1.9	1.6	1.7	1.3	1.3	-1.1	1.1	-1.1	1.3	1.0	1.2	-1.1	-1.4	-1.5	-1.6	-2.5	-2.0	-1.8	-1.8	-1.7
PC(38:4)_PC(18:3_20:1)	1.5	2.5	1.8	2.3	1.4	1.6	1.0	1.3	-1.0	1.6	1.2	1.3	-1.4	-1.8	-1.7	-2.0	-3.3	-2.0	-2.9	-2.5	-2.2
PC(38:5)_PC(18:2_20:3)	1.2	1.7	1.6	1.6	1.4	1.5	-1.2	-1.1	-1.4	1.0	-1.0	1.2	-1.1	-1.4	-1.7	-1.7	-3.1	-2.3	-2.3	-2.3	-2.0
PC(38:5)_PC(18:3_20:2)	1.5	2.4	2.2	2.2	2.0	1.8	-1.2	-1.1	-1.1	1.7	1.2	1.3	-1.1	-1.9	-1.4	-2.0	-4.6	-2.3	-2.9	-2.5	-1.9
PC(38:6)_PC(18:3_20:3)	1.4	1.9	1.5	1.7	1.3	1.3	-1.2	1.0	-1.0	1.2	-1.1	1.1	1.0	-1.6	-1.5	-1.6	-2.5	-2.0	-1.9	-2.2	-1.8
PC(40:4)_PC(18:3_22:1)	1.7	2.5	2.2	2.3	1.4	1.5	1.0	1.1	1.4	1.5	1.2	1.3	-1.2	-1.9	-1.5	-1.9	-2.8	-1.8	-2.8	-2.8	-1.8
PC(42:2)_PC(18:2_24:0)	1.4	1.6	1.4	1.5	-1.2	-1.1	-1.1	-1.1	1.1	1.2	-1.1	-1.1	1.4	-1.3	-1.3	-1.1	-1.6	-1.2	-1.3	-1.6	-1.2
PC(42:3)_PC(18:2_24:1)	1.6	2.0	1.9	1.9	1.3	1.2	1.2	1.1	1.4	1.4	1.2	1.2	1.0	-1.4	-1.3	-1.2	-1.8	-1.4	-1.7	-1.8	-1.3
PC(42:3)_PC(18:3_24:0)	1.6	2.2	1.5	1.8	-1.0	1.0	-1.3	-1.0	1.1	1.3	-1.2	-1.2	1.2	-1.5	-1.2	-1.6	-2.1	-1.4	-1.9	-2.0	-1.4
PC(42:4)_PC(18:3_24:1)	1.8	2.4	2.3	2.2	1.6	1.5	1.1	1.2	1.3	1.4	1.3	1.1	-1.2	-1.6	-1.3	-1.9	-2.9	-1.6	-2.4	-2.5	-1.7
PC(44:4)_PC(18:3_26:1)	1.6	2.0	2.0	2.1	1.4	1.2	-1.0	1.0	1.0	1.3	1.1	1.1	-1.4	-1.8	-1.6	-2.3	-3.7	-2.1	-2.7	-2.9	-1.8
PE(30:1)_PE(14:0_16:1)	-3.1	-4.9	-2.0	-3.7	-1.6	-2.0	1.4	2.1	1.2	2.2	2.1	4.6	-4.2	-5.0	-6.4	1.1	-2.2	-1.9	2.5	1.7	1.4
PE(32:0)_PE(16:0_16:0)	-1.7	-1.6	-2.1	-3.0	-2.8	-3.3	1.6	1.8	1.2	1.4	1.4	3.3	-1.2	-1.9	-4.4	2.3	1.2	-1.1	2.5	2.1	2.5
PE(32:1)_PE(16:0_16:1)	-2.8	-3.3	-1.4	-3.5	-1.9	-2.9	1.5	1.8	1.2	1.6	1.4	3.3	-2.1	-2.4	-3.7	2.1	-1.4	-1.4	2.9	2.4	2.6
PE(32:2)_PE(14:0_18:2)	-1.1	1.1	1.1	1.1	1.1	1.1	-1.1	1.6	-1.0	-5.4	-1.4	-5.6	6.6	3.9	3.3	6.1	3.6	2.3	9.2	-1.5	-1.8
PE(32:2)_PE(16:1_16:1)	-2.2	-2.2	-1.5	-1.9	-1.2	-1.7	1.5	2.7	1.2	2.7	2.0	4.6	-2.9	-3.9	-7.9	1.2	-2.2	-3.2	2.0	1.3	1.0
PE(32:3)_PE(14:0_18:3)	1.1	22.4	1.4	1.7	-1.0	1.2	-1.2	1.5	-1.1	-6.0	-1.6	-5.7	5.1	5.3	3.5	4.0	3.4	2.1	-2.9	-1.9	-1.9
PE(34:1)_PE(16:0_18:1)	-1.4	1.1	-1.2	1.0	-1.9	-1.6	-1.0	1.1	-1.2	1.0	-1.4	1.0	-1.4	-1.8	-2.2	-1.0	-1.8	-1.6	-1.4	-1.7	-1.3
PE(34:2)_PE(16:0_18:2)	1.2	1.5	1.3	1.4	1.1	1.2	-1.1	1.1	-1.0	1.1	-1.1	1.1	1.0	-1.3	-1.6	-1.2	-1.8	-2.0	-1.3	-1.7	-1.8
PE(34:2)_PE(16:1_18:1)	-5.8	-5.1	-2.6	-4.6	-3.1	-3.8	1.4	1.7	1.1	1.4	1.3	2.6	-2.5	-2.5	-4.0	3.2	1.1	1.0	3.4	2.5	2.5
PE(34:3)_PE(16:0_18:3)	1.4	2.0	1.6	1.9	1.2	1.3	-1.1	1.1	-1.1	1.3	-1.0	1.1	1.0	-1.5	-1.7	-1.6	-2.5	-2.1	-1.7	-2.2	-1.9
PE(34:3)_PE(16:1_18:2)	-1.2	1.0	1.2	1.3	1.1	1.0	-1.0	1.2	-1.1	1.1	1.1	1.2	-1.1	-1.3	-2.0	1.1	-1.6	-2.1	1.0	-1.5	-1.7
PE(36:2)_PE(18:0_18:2)	1.3	1.7	1.2	1.5	-1.2	-1.2	1.1	1.3	1.0	1.4	-1.1	1.2	1.2	-1.1	-1.1	-1.0	-1.3	-1.0	-1.2	-1.2	1.2
PE(36:2)_PE(18:1_18:1)	-2.6	-1.8	-1.6	-1.4	-2.5	-2.2	1.2	1.4	-1.0	1.2	-1.3	1.2	-2.6	-2.3	-2.8	1.3	-1.5	-1.5	-1.0	-1.3	-1.0
PE(36:3)_PE(18:0_18:3)	1.7	2.7	1.7	2.2	1.1	1.3	-1.0	1.3	-1.0	1.6	1.0	1.0	1.0	-1.4	-1.2	-1.8	-2.5	-1.3	-2.1	-2.0	-1.5
PE(36:3)_PE(18:1_18:2)	1.3	2.2	1.2	1.6	-1.2	1.0	1.1	1.4	-1.0	1.3	-1.3	-1.1	-1.1	-1.5	-1.6	-1.4	-1.8	-1.6	-1.8	-1.8	-1.8
PE(36:4)_PE(18:1_18:3)	1.7	2.6	1.6	2.0	-1.0	1.2	-1.1	1.2	-1.1	1.4	-1.2	-1.2	-1.2	-1.8	-1.6	-2.2	-3.1	-1.9	-2.5	-2.6	-2.1
PE(36:4)_PE(18:2_18:2)	1.4	1.8	1.4	1.5	1.1	1.2	1.0	1.2	1.1	1.3	-1.0	1.2	1.0	-1.3	-1.7	-1.3	-1.7	-2.0	-1.4	-1.6	-1.7

PE(36:5)_PE(18:2_18:3)	1.8	2.3	1.8	2.0	1.2	1.4	1.0	1.3	1.1	1.7	1.2	1.4	1.1	-1.6	-1.9	-1.6	-2.7	-2.0	-1.7	-1.9	-1.9
PE(36:6)_PE(18:3_18:3)	2.0	3.0	2.4	2.7	1.5	1.6	-1.1	1.3	1.1	2.0	1.3	1.5	-1.1	-1.9	-2.1	-2.3	-4.4	-2.3	-2.6	-2.7	-2.3
PE(38:2)_PE(18:2_20:0)	1.3	1.9	1.3	1.5	-1.1	-1.1	-1.1	-1.0	-1.0	1.2	-1.1	1.2	1.3	-1.2	-1.4	-1.0	-1.5	-1.4	-1.4	-1.5	1.0
PE(38:3)_PE(18:2_20:1)	1.3	2.0	1.4	1.6	1.1	1.2	1.2	1.3	1.1	1.3	-1.1	1.3	-1.0	-1.5	-1.6	-1.2	-1.8	-1.8	-1.6	-1.7	-1.4
PE(38:3)_PE(18:3_20:0)	1.5	2.3	1.6	1.9	-1.0	1.0	-1.2	1.0	-1.1	1.2	-1.2	1.1	1.1	-1.4	-1.3	-1.6	-2.4	-1.5	-2.0	-2.1	-1.2
PE(38:4)_PE(18:2_20:2)	1.1	1.4	1.4	1.3	1.2	1.2	-1.1	-1.0	-1.2	-1.0	-1.2	1.2	1.0	-1.2	-1.7	-1.2	-1.9	-2.4	-1.4	-1.6	-1.7
PE(38:4)_PE(18:3_20:1)	1.7	2.7	1.9	2.3	1.3	1.4	1.1	1.4	1.1	1.6	-1.0	1.2	-1.2	-1.7	-1.5	-1.9	-3.0	-2.0	-2.4	-2.5	-1.9
PE(38:5)_PE(18:2_20:3)	1.3	-1.1	2.4	3.8	1.1	1.3	-1.1	-1.4	-1.6	-1.1	-1.0	-1.4	-1.2	1.9	-1.7	-1.6	-2.0	-2.0	-1.6	-2.2	-3.1
PE(38:5)_PE(18:3_20:2)	1.5	1.9	1.8	1.8	1.3	1.2	-1.3	-1.0	-1.2	1.3	-1.1	1.0	1.1	-1.4	-1.5	-1.9	-2.9	-2.1	-1.8	-2.0	-1.7
PE(38:6)_PE(18:3_20:3)	1.5	1.9	2.0	1.9	1.3	1.3	-1.3	1.0	-1.2	1.4	-1.0	1.1	-1.1	-1.7	-1.8	-2.2	-4.2	-2.4	-2.1	-2.3	-2.0
PE(40:2)_PE(18:2_22:0)	1.2	1.6	1.2	1.4	-1.2	-1.1	-1.1	-1.0	1.2	1.2	-1.2	1.1	1.4	-1.1	-1.1	1.1	-1.1	-1.1	-1.2	-1.3	1.1
PE(40:3)_PE(18:2_22:1)	1.5	2.1	1.5	1.6	1.1	1.1	1.3	1.3	1.3	1.3	1.0	1.2	-1.1	-1.4	-1.5	-1.3	-1.7	-1.6	-1.7	-1.8	-1.3
PE(40:3)_PE(18:3_22:0)	1.5	2.3	1.7	2.0	1.0	1.0	-1.1	1.0	-1.0	1.2	-1.1	1.2	1.2	-1.2	-1.3	-1.4	-2.1	-1.5	-1.9	-2.1	-1.1
PE(40:4)_PE(18:2_22:2)	1.0	1.3	1.3	1.4	1.1	1.0	-1.0	-1.0	-1.0	-1.1	-1.1	1.1	-1.0	-1.1	-1.6	-1.1	-1.5	-1.9	-1.4	-1.7	-1.5
PE(40:4)_PE(18:3_22:1)	1.6	2.5	1.8	2.2	1.2	1.1	1.0	1.2	1.0	1.3	-1.1	1.1	-1.1	-1.4	-1.5	-1.7	-2.6	-2.0	-2.3	-2.3	-1.5
PE(40:5)_PE(18:3_22:2)	1.4	1.7	1.6	1.6	1.3	1.2	-1.2	-1.0	-1.2	1.0	-1.1	1.0	-1.1	-1.2	-1.4	-1.7	-2.4	-2.0	-1.8	-1.9	-1.7
PE(42:3)_PE(18:2_24:1)	1.7	2.1	1.7	1.8	1.2	1.1	1.2	1.2	1.4	1.4	1.1	1.3	1.1	-1.5	-1.5	-1.3	-1.9	-1.5	-1.6	-1.9	-1.3
PE(42:3)_PE(18:3_24:0)	1.7	2.3	1.7	2.0	-1.1	-1.0	-1.2	-1.0	1.0	1.2	-1.1	-1.0	1.2	-1.4	-1.4	-1.6	-2.4	-1.5	-2.0	-2.3	-1.4
PE(42:4)_PE(18:3_24:1)	2.1	3.1	2.3	2.4	1.5	1.4	1.2	1.3	1.3	1.6	1.3	1.3	-1.0	-1.6	-1.5	-1.8	-2.8	-1.8	-2.5	-2.5	-1.6
PG(30:1)_PG(14:0_16:1)	-2.3	-3.1	-1.5	-2.1	-1.5	-2.0	1.1	1.9	-1.1	1.9	1.5	3.3	-2.4	-2.8	-4.3	1.0	-2.0	-2.0	2.5	1.4	1.5
PG(32:0)_PG(16:0_16:0)	1.2	1.6	1.6	1.9	-1.0	1.1	-1.3	-1.1	-1.3	1.3	-1.1	1.1	1.3	-1.4	-1.8	-1.2	-2.9	-1.9	-1.3	-2.0	-1.8
PG(32:1)_PG(16:0_16:1)	-2.5	-3.5	-1.3	-3.0	-1.7	-2.4	1.6	2.0	1.3	1.7	1.4	2.9	-2.7	-3.5	-5.7	1.5	-2.2	-2.4	2.5	1.5	1.3
PG(32:2)_PG(14:0_18:2)	1.2	1.4	1.4	1.5	1.0	1.2	-1.1	1.0	-1.0	1.1	-1.0	1.2	-1.0	-1.4	-2.2	-1.4	-2.0	-2.3	-1.4	-2.0	-2.0
PG(32:2)_PG(16:1_16:1)	-1.9	-2.4	-1.6	-2.3	-1.1	-1.6	1.8	3.3	1.4	2.5	2.2	4.8	-2.3	-3.0	-5.7	1.5	-1.4	-2.3	3.4	1.9	1.3
PG(32:3)_PG(14:0_18:3)	1.3	1.3	1.6	1.8	1.3	1.3	-1.3	-1.1	-1.3	1.3	-1.0	1.2	-1.1	-1.9	-2.0	-1.8	-3.8	-2.6	-1.6	-2.6	-2.2
PG(34:1)_PG(16:0_18:1)	-1.3	1.1	-1.1	1.2	-1.7	-1.3	-1.1	1.2	-1.1	1.3	-1.2	-1.0	-1.5	-2.5	-2.8	-1.4	-2.6	-2.0	-1.4	-2.2	-2.2
PG(34:2)_PG(16:0_18:2)	1.3	1.6	1.5	1.6	1.1	1.2	1.0	1.2	1.1	1.3	1.1	1.3	-1.0	-1.6	-2.2	-1.3	-2.3	-2.2	-1.3	-1.9	-2.1
PG(34:2)_PG(16:1_18:1)	-3.7	-3.5	-1.7	-3.2	-1.6	-2.0	1.7	2.2	1.4	1.8	1.9	3.4	-2.3	-3.0	-4.3	2.7	-1.3	-1.4	3.3	1.9	1.6
PG(34:3)_PG(16:0_18:3)	1.5	1.9	1.7	1.9	1.2	1.3	-1.0	1.2	-1.0	1.4	1.0	1.2	-1.1	-1.8	-2.0	-1.8	-3.0	-2.4	-1.8	-2.4	-2.2
PG(34:3)_PG(16:1_18:2)	-1.1	1.2	1.2	1.2	1.2	1.3	1.0	1.1	-1.1	-1.0	1.1	1.4	-1.2	-1.3	-2.0	-1.1	-1.7	-2.2	-1.3	-1.6	-1.9
PG(36:1)_PG(16:0_20:1)	1.5	2.0	1.4	1.7	-1.2	-1.0	1.0	1.3	1.0	1.3	-1.2	-1.2	-1.1	-1.7	-1.5	-1.7	-2.4	-1.5	-1.7	-2.2	-1.8

PG(36:1)_PG(18:0_18:1)	-2.9	-2.2	-1.9	-1.5	-2.8	-2.4	-1.7	1.0	-1.5	1.1	-1.8	-1.3	-2.1	-2.2	-2.5	-1.2	-1.7	-1.6	1.1	-1.4	-1.3
PG(36:2)_PG(18:0_18:2)	1.3	1.4	1.1	1.3	-1.4	-1.3	1.0	1.3	1.1	1.6	-1.1	1.2	1.1	-1.4	-1.4	-1.1	-1.4	-1.1	1.0	-1.1	1.1
PG(36:2)_PG(18:1_18:1)	-2.0	-1.6	-1.6	-1.4	-2.8	-2.4	1.1	1.7	-1.1	1.1	-1.6	-1.3	-2.8	-2.9	-2.9	-1.2	-2.1	-1.7	-1.0	-1.9	-1.6
PG(36:3)_PG(18:1_18:2)	1.3	1.9	1.2	1.4	-1.3	-1.1	1.1	1.4	1.1	1.3	-1.1	1.0	-1.2	-2.0	-2.2	-1.4	-2.2	-1.7	-1.6	-2.0	-1.9
PG(36:4)_PG(18:1_18:3)	1.6	2.2	1.5	1.7	-1.1	-1.0	1.1	1.3	1.1	1.4	-1.0	1.0	-1.4	-2.1	-2.3	-2.0	-2.9	-2.1	-2.2	-2.6	-2.2
PG(36:4)_PG(18:2_18:2)	1.3	1.7	1.5	1.6	1.1	1.2	1.1	1.4	1.3	1.5	1.2	1.6	-1.1	-1.5	-2.2	-1.3	-1.7	-2.0	-1.3	-1.6	-1.7
PG(36:5)_PG(18:2_18:3)	1.6	1.9	1.9	2.0	1.2	1.3	-1.0	1.3	1.1	1.6	1.3	1.6	-1.2	-1.7	-2.3	-1.9	-2.8	-2.1	-1.8	-2.1	-2.0
PG(36:6)_PG(18:3_18:3)	1.8	2.0	2.2	2.5	1.6	1.6	-1.2	1.2	1.1	1.8	1.3	1.4	-1.5	-2.3	-2.3	-3.0	-4.7	-2.9	-2.4	-3.3	-2.6
PI(32:0)_PI(16:0_16:0)	-1.1	1.5	1.0	1.3	-1.4	-1.3	-1.2	1.2	-1.0	1.1	-1.5	1.0	-1.2	-2.1	-2.0	-1.4	-2.3	-2.2	-1.5	-2.5	-1.5
PI(32:2)_PI(14:0_18:2)	-1.2	1.5	1.2	1.3	1.1	-1.0	-1.1	-1.2	-1.2	-1.1	-1.1	1.2	1.1	-1.3	-2.0	1.1	-1.7	-2.4	-1.6	-1.7	-1.6
PI(32:3)_PI(14:0_18:3)	1.2	1.8	1.4	2.1	1.0	1.0	-1.3	-1.2	-1.3	-1.0	-1.2	1.1	-1.1	-1.5	-1.8	-1.7	-2.6	-2.1	-2.3	-3.2	-1.7
PI(34:1)_PI(16:0_18:1)	1.2	2.1	-1.3	1.2	-2.3	-1.8	-1.2	1.1	-1.2	1.2	-1.5	-1.3	-1.0	-2.3	-2.4	-1.4	-2.3	-1.6	-2.0	-2.3	-1.8
PI(34:2)_PI(16:0_18:2)	1.3	1.9	1.4	1.7	-1.0	-1.1	-1.1	1.1	-1.1	1.3	1.0	1.3	1.1	-1.6	-2.3	-1.4	-2.3	-2.2	-1.5	-2.0	-1.7
PI(34:3)_PI(16:0_18:3)	1.4	2.1	1.6	1.9	1.5	1.4	-1.2	1.0	-1.2	1.2	-1.0	1.2	1.0	-1.6	-1.6	-1.7	-3.0	-2.4	-2.0	-2.5	-1.8
PI(34:3)_PI(16:1_18:2)	1.4	1.8	1.5	1.6	1.4	1.6	-1.2	1.1	-1.1	1.2	-1.0	1.3	23.4	1.9	19.3	14.0	10.5	13.5	13.4	13.4	14.7
PI(36:3)_PI(18:1_18:2)	1.3	1.7	1.4	1.5	1.0	1.1	1.0	1.1	1.1	1.2	1.0	1.2	-1.0	-1.6	-1.9	-1.3	-2.2	-1.9	-1.6	-2.0	-1.8
PI(36:4)_PI(18:1_18:3)	1.4	2.0	1.6	1.7	1.2	1.3	-1.1	1.1	-1.0	1.3	-1.0	1.2	-1.1	-1.8	-1.8	-1.7	-2.8	-2.3	-2.0	-2.4	-2.0
PI(36:4)_PI(18:2_18:2)	1.4	1.8	1.3	1.5	1.1	1.2	1.1	1.3	1.3	1.4	1.2	1.5	1.0	-1.6	-2.2	-1.2	-1.6	-1.9	-1.3	-1.7	-1.7
PI(36:5)_PI(18:2_18:3)	1.3	1.8	1.4	1.7	1.1	1.2	-1.2	1.1	-1.0	1.0	-1.3	-1.0	-1.1	-1.2	-1.1	-1.7	-1.8	-1.7	-1.8	-2.0	-1.3
PI(36:6)_PI(18:3_18:3)	1.8	2.2	2.0	2.5	1.5	1.5	-1.2	1.2	-1.0	1.5	1.2	1.4	-1.3	-1.9	-1.9	-2.9	-3.9	-2.4	-2.5	-3.1	-2.0
PS(34:3)_PS(16:0_18:3)	1.2	2.0	1.4	1.9	1.2	1.3	-1.1	1.1	1.0	1.3	-1.1	1.3	1.0	-1.4	-1.9	-1.3	-1.9	-2.5	-1.8	-2.1	-1.9
PS(34:3)_PS(16:1_18:2)	-1.7	-1.4	-1.4	-1.5	-1.3	-1.3	1.2	2.0	1.2	1.6	-1.0	1.6	-1.7	-2.0	-2.1	1.2	-1.2	-1.7	1.6	1.2	1.0
PS(36:1)_PS(18:0_18:1)	1.1	1.9	-1.0	1.1	-1.8	-1.6	1.0	1.1	-1.2	1.1	-1.5	-1.4	-1.2	-1.9	-1.7	-1.2	-2.1	-1.4	-1.9	-1.8	-1.5
PS(36:4)_PS(18:2_18:2)	1.0	1.7	-1.0	1.4	-1.2	1.0	1.0	1.4	1.1	1.1	-1.4	1.1	1.1	-1.1	-1.5	1.1	1.0	-1.7	-1.1	-1.3	-1.4
PS(36:5)_PS(18:2_18:3)	1.3	2.3	1.2	1.7	1.0	1.3	1.0	1.6	1.2	1.4	-1.1	1.3	-1.1	-1.5	-1.8	-1.4	-1.5	-2.1	-1.6	-1.7	-1.7
DGDG(32:2)_DGDG(14:0_18:2)	-1.3	-1.2	1.2	2.3	1.0	1.1	1.2	-1.1	-1.2	-1.5	2.0	2.1	-1.7	-1.0	-3.5	-1.0	-1.5	-1.8	-1.6	-3.5	-1.9
DGDG(34:1)_DGDG(16:0_18:1)	1.1	1.5	1.3	1.5	1.1	1.2	-1.2	-1.1	-1.1	-1.0	-1.2	1.0	1.0	-1.3	-1.7	-1.3	-1.9	-2.1	-1.6	-2.0	-2.0
DGDG(34:2)_DGDG(16:0_18:2)	1.0	1.4	1.2	1.3	1.0	1.1	-1.2	-1.1	-1.1	1.0	-1.1	1.1	1.1	-1.3	-1.7	-1.1	-1.7	-1.9	-1.4	-1.7	-1.7
DGDG(34:3)_DGDG(16:0_18:3)	1.2	1.6	1.5	1.7	1.2	1.3	-1.3	-1.1	-1.1	1.1	-1.1	1.1	1.0	-1.5	-1.7	-1.5	-2.4	-2.2	-1.7	-2.2	-1.9
DGDG(34:3)_DGDG(16:1_18:2)	1.4	1.9	1.6	1.7	1.3	1.4	-1.2	-1.0	-1.0	1.4	1.0	1.3	1.0	-1.7	-1.8	-1.7	-2.8	-2.3	-1.9	-2.2	-1.9
DGDG(36:2)_DGDG(18:0_18:2)	1.2	1.9	1.2	1.3	-1.3	-1.1	1.0	1.2	-1.0	1.3	-1.3	-1.1	-1.2	-1.8	-1.8	-1.4	-2.1	-1.8	-1.9	-1.9	-1.8

DGDG(36:2)_DGDG(18:1_18:1)	1.1	1.8	1.1	1.3	-1.4	-1.1	-1.1	1.0	-1.2	1.1	-1.4	-1.3	-1.1	-1.7	-1.6	-1.4	-2.2	-1.7	-2.0	-2.1	-1.9
DGDG(36:3)_DGDG(18:1_18:2)	1.2	1.7	1.3	1.5	1.1	1.2	-1.0	1.1	-1.0	1.2	-1.2	1.2	-1.0	-1.4	-1.7	-1.3	-1.9	-2.1	-1.6	-1.8	-1.7
DGDG(36:4)_DGDG(18:1_18:3)	-1.1	1.3	-1.1	1.1	-1.6	-1.3	-1.2	1.1	-1.2	1.1	-1.3	-1.1	-1.2	-1.9	-2.1	-1.3	-2.1	-1.8	-1.4	-2.0	-1.8
DGDG(36:4)_DGDG(18:2_18:2)	-1.3	-1.0	-1.0	1.0	-1.3	-1.1	-1.1	-1.2	-1.1	-1.5	-1.1	1.1	1.4	1.4	-1.0	1.6	1.3	1.2	1.2	-1.1	1.2
DGDG(36:5)_DGDG(18:2_18:3)	1.2	1.6	1.3	1.4	1.0	1.0	-1.0	1.0	1.1	1.2	1.0	1.3	1.3	-1.1	-1.3	1.1	-1.4	-1.4	-1.2	-1.3	-1.1
DGDG(36:6)_DGDG(18:3_18:3)	1.3	1.9	1.8	1.9	1.2	1.2	-1.1	-1.1	-1.1	1.2	-1.0	1.2	1.2	-1.3	-1.9	-1.3	-2.5	-2.3	-1.8	-2.1	-1.9
DGMG(16:0)	1.4	1.4	2.0	1.5	-1.0	1.5	-1.2	-1.2	-1.5	-1.6	-1.2	-1.2	4.3	4.4	2.6	2.6	1.5	2.2	2.5	1.9	1.5
DGMG(18:1)	1.1	1.5	-1.1	1.3	-2.0	-1.6	1.2	1.3	1.0	1.4	-1.4	-1.3	3.2	3.3	2.5	3.5	3.8	3.5	2.6	3.6	3.0
DGMG(18:2)	1.4	1.6	1.1	1.5	-3.6	-2.6	-1.2	-1.1	-1.1	1.2	-1.2	1.1	9.0	10.9	2.7	5.8	8.7	7.8	5.1	8.7	7.3
DGMG(18:3)	-1.2	1.2	-1.3	-1.1	-1.2	-1.2	-1.1	-1.0	-1.2	1.2	-1.2	1.1	6.0	5.5	4.8	6.6	6.3	4.5	4.8	7.3	6.4
MGDG(32:2)_MGDG(16:1_16:1)	-2.6	-2.8	-1.4	-3.1	-1.7	-2.7	1.5	1.6	1.2	1.6	1.4	3.1	-1.9	-2.3	-3.5	2.0	-1.4	-1.5	2.3	2.1	2.4
MGDG(34:2)_MGDG(16:1_18:1)	1.1	1.8	1.1	1.3	-1.3	-1.1	-1.1	1.1	-1.1	-1.0	-1.5	-1.2	-1.2	-1.7	-1.6	-1.4	-2.0	-1.9	-2.0	-2.2	-1.9
MGDG(36:3)_MGDG(18:0_18:3)	1.2	1.6	1.2	1.4	-1.1	-1.0	1.0	1.2	1.1	1.2	-1.1	-1.1	-1.0	-1.3	-1.2	-1.2	-1.4	-1.2	-1.4	-1.4	-1.3
MGMG(16:0)	1.4	1.9	1.4	1.5	1.1	1.4	-1.1	1.1	-1.1	1.0	-1.2	1.2	1.1	-1.1	-1.2	-1.4	-1.6	-1.6	-1.5	-1.6	-1.4
MGMG(18:2)	1.2	1.5	1.2	1.6	-1.2	1.1	1.1	1.3	1.1	1.4	-1.1	1.2	3.2	4.5	2.8	2.7	4.0	3.1	2.9	3.8	3.0
MGMG(18:3)	1.5	1.3	1.2	1.5	-1.4	-1.2	-1.1	1.1	1.0	1.2	-1.4	1.1	3.3	4.2	3.7	2.0	3.6	3.7	2.7	3.3	4.9
SQDG(32:3)_SQDG(14:0_18:3)	1.3	1.7	1.5	1.6	1.1	1.3	-1.1	1.1	-1.1	1.2	-1.2	1.1	-1.1	-1.5	-1.6	-1.6	-2.6	-2.2	-1.7	-2.0	-1.9
SQDG(34:2)_SQDG(16:0_18:2)	1.1	1.6	1.4	1.5	1.2	1.3	-1.0	1.1	-1.1	1.1	-1.1	1.1	-1.1	-1.4	-1.6	-1.3	-2.0	-2.1	-1.7	-1.8	-1.8
SQDG(34:3)_SQDG(16:0_18:3)	1.4	1.9	1.6	1.8	1.4	1.5	-1.2	1.1	-1.1	1.2	-1.1	1.0	-1.1	-1.6	-1.4	-1.9	-2.9	-2.1	-2.0	-2.3	-2.0
SQDG(36:2)_SQDG(18:0_18:2)	1.1	2.0	1.3	1.8	-1.4	-1.1	1.1	1.1	1.1	1.5	1.0	1.3	1.0	-1.4	-1.6	1.1	-1.7	-1.1	-1.7	-1.8	-1.1
SQDG(36:2)_SQDG(18:1_18:1)	-1.0	1.5	-1.1	-1.0	-2.3	-1.8	1.1	1.3	-1.2	1.0	-1.6	-1.4	-1.6	-2.1	-2.1	-1.5	-2.2	-1.5	-1.9	-2.0	-1.6
SQDG(36:3)_SQDG(18:0_18:3)	1.5	2.2	1.9	2.2	1.0	1.3	-1.0	1.1	-1.0	1.6	-1.0	-1.0	-1.1	-1.6	-1.3	-1.7	-3.0	-1.4	-2.2	-2.1	-1.7
SQDG(36:3)_SQDG(18:1_18:2)	1.2	2.0	1.1	1.3	-1.3	-1.1	1.1	1.2	-1.1	1.2	-1.4	-1.3	-1.3	-1.8	-1.8	-1.4	-2.1	-1.8	-2.1	-2.0	-2.2
SQDG(36:4)_SQDG(18:1_18:3)	1.4	2.1	1.5	1.6	-1.1	1.0	-1.0	1.2	-1.1	1.2	-1.3	-1.3	-1.4	-2.3	-1.7	-2.0	-4.0	-2.1	-2.5	-3.1	-2.3
SQDG(36:4)_SQDG(18:2_18:2)	1.2	1.7	1.3	1.4	1.1	1.2	-1.0	1.2	-1.1	1.3	-1.0	1.2	-1.1	-1.6	-1.9	-1.4	-2.2	-2.1	-1.6	-1.7	-1.8
SQDG(36:5)_SQDG(18:2_18:3)	1.4	1.8	1.7	1.8	1.3	1.4	-1.2	1.0	-1.1	1.4	1.1	1.3	-1.1	-1.8	-1.8	-1.8	-3.3	-2.1	-2.0	-2.3	-2.1
SQDG(36:6)_SQDG(18:3_18:3)	1.7	2.8	2.5	2.8	1.6	1.7	-1.3	1.1	-1.0	2.2	1.4	1.6	-1.2	-2.3	-2.6	-2.7	-5.9	-3.0	-3.3	-3.0	-2.8
SQMG(16:0)	1.0	1.3	1.2	1.6	-1.2	1.1	-1.1	1.1	1.0	1.4	-1.1	1.0	3.2	4.3	2.9	3.0	3.8	3.0	2.8	3.8	2.8
SQMG(18:0)	-1.1	2.6	1.6	1.7	-2.5	-1.4	-1.1	1.6	2.0	3.7	-1.6	-1.6	1.8	5.6	12.4	1.8	6.9	19.7	1.1	12.1	11.5
SQMG(18:2)	1.1	1.4	1.2	1.6	-1.2	1.1	1.1	1.3	1.1	1.6	1.0	1.2	3.0	3.8	2.3	2.8	3.7	2.9	2.8	3.8	2.6
SQMG(18:3)	1.2	1.4	1.5	2.1	-1.1	1.2	-1.1	1.1	-1.0	1.6	1.0	1.3	3.2	4.0	2.1	2.4	2.6	2.3	2.5	3.1	2.3

DAG(14:0_18:2)	1.2	1.7	1.1	1.2	1.2	1.3	-1.2	1.1	-1.5	-1.3	-1.5	1.0	1.0	1.1	-1.1	-1.3	-1.5	-2.0	-1.5	-1.4	-1.4
DAG(14:0_18:3)	1.2	2.0	2.2	2.0	1.8	1.8	-1.6	-1.1	-1.4	1.0	-1.4	1.1	-1.0	1.0	1.2	-2.0	-3.1	-2.1	-2.2	-2.0	-1.4
DAG(16:0_16:0)	1.0	1.7	1.0	1.0	-1.4	-1.3	-1.4	-1.1	-1.8	-1.3	-2.4	-1.4	1.3	1.6	1.9	-1.1	-1.2	1.1	-1.4	1.2	1.7
DAG(16:0_18:0)	1.2	1.5	1.2	-1.2	-1.2	-1.2	-1.5	-1.0	-1.6	-1.2	-2.0	1.1	1.3	1.4	1.4	-1.4	-1.3	-1.3	-1.1	1.4	1.7
DAG(16:0_18:1)	1.8	2.6	1.1	1.1	-1.7	-1.6	-1.0	1.5	-1.3	1.0	-1.9	-1.7	-1.1	-1.6	-1.4	-1.9	-2.2	-1.5	-1.8	-1.7	-1.5
DAG(16:0_18:2)	1.6	2.2	1.5	1.4	1.0	1.1	-1.1	1.3	-1.1	1.1	-1.3	1.0	1.2	-1.0	-1.2	-1.5	-1.6	-1.7	-1.4	-1.3	-1.3
DAG(16:0_18:3)	1.7	2.8	1.9	1.8	1.4	1.4	-1.3	1.2	-1.3	1.2	-1.4	1.0	-1.0	-1.2	-1.1	-2.3	-2.9	-2.1	-2.4	-1.8	-1.5
DAG(16:1_18:1)	-1.6	-1.3	-1.0	1.1	-2.3	-2.4	-1.1	1.3	-1.3	1.0	-1.5	1.1	-1.3	1.3	-1.8	1.1	1.0	-1.2	1.2	1.3	1.5
DAG(16:1_18:2)	1.1	1.3	1.4	1.4	1.1	1.2	-1.2	1.1	-1.6	-1.2	-1.2	1.1	-1.3	1.0	-1.3	-1.7	-2.2	-1.8	-1.5	-1.6	-1.5
DAG(18:0_18:0)	1.1	1.5	1.2	-1.1	1.1	-1.2	-1.9	-1.0	-1.7	-1.3	-1.8	-1.1	1.2	1.1	1.1	-1.7	-1.9	-1.8	-1.3	-1.1	1.2
DAG(18:0_18:1)	1.4	2.1	-1.2	1.0	-2.7	-2.3	-1.2	1.3	-1.5	-1.0	-2.0	-1.8	-1.0	-1.5	-1.3	-1.7	-1.9	-1.0	-1.7	-1.6	-1.1
DAG(18:0_18:2)	2.2	2.8	1.6	1.7	-1.4	-1.2	1.3	1.8	1.1	1.8	-1.1	1.1	1.1	-1.2	-1.1	-1.5	-1.6	1.2	-1.4	-1.1	1.2
DAG(18:0_18:3)	2.3	3.6	1.9	2.3	1.0	1.1	1.0	1.7	-1.1	1.8	-1.1	-1.0	-1.1	-1.2	1.0	-2.4	-2.4	-1.2	-2.2	-1.6	-1.1
DAG(18:1_18:1)	1.8	2.7	-1.0	1.0	-2.2	-2.1	1.0	1.7	-1.2	1.3	-1.6	-1.6	-1.2	-2.1	-1.6	-2.1	-2.4	-1.2	-1.9	-1.7	-1.2
DAG(18:1_18:2)	1.9	2.8	1.2	1.3	-1.5	-1.4	1.2	1.8	-1.0	1.3	-1.5	-1.3	-1.1	-1.6	-1.5	-1.8	-2.0	-1.4	-1.7	-1.6	-1.4
DAG(18:1_18:3)	2.0	3.4	1.7	1.8	-1.1	-1.1	-1.0	1.6	-1.2	1.4	-1.4	-1.3	-1.1	-1.6	-1.3	-2.4	-3.1	-1.7	-2.3	-2.0	-1.5
DAG(18:1_20:1)	2.3	3.1	1.3	1.2	-1.8	-1.9	1.2	1.8	1.0	1.3	-1.4	-1.8	-1.3	-2.2	-1.7	-2.5	-2.8	-1.3	-2.2	-2.2	-1.7
DAG(18:2_18:2)	1.6	2.3	1.5	1.5	1.1	1.2	-1.1	1.4	-1.0	1.2	-1.2	1.2	1.0	-1.2	-1.4	-1.7	-2.0	-1.8	-1.7	-1.5	-1.3
DAG(18:2_18:3)	1.7	2.6	2.2	2.0	1.6	1.7	-1.3	1.2	-1.1	1.3	-1.1	1.3	1.0	-1.2	-1.2	-2.1	-2.9	-2.0	-2.1	-1.8	-1.5
DAG(18:2_20:1)	2.5	3.3	1.7	1.8	-1.1	1.1	1.4	2.1	1.3	1.7	-1.0	1.0	-1.2	-1.6	-1.4	-2.1	-2.0	-1.3	-1.8	-1.6	-1.5
DAG(18:2_20:2)	2.2	2.4	2.1	1.7	1.3	1.3	-1.2	1.3	-1.1	1.4	1.1	1.2	1.1	-1.3	-1.3	-2.4	-2.9	-1.6	-1.6	-1.6	-1.4
DAG(18:2_22:0)	2.0	2.4	1.7	1.8	-1.0	-1.2	1.3	1.5	1.1	1.4	-1.1	1.0	1.4	1.1	-1.4	-1.1	-1.4	-1.5	-1.1	-1.2	-1.1
DAG(18:2_22:2)	1.1	1.0	-1.1	-1.5	-1.1	-1.9	-1.6	-1.3	-1.3	-1.5	-1.7	-1.4	1.3	-1.2	-1.0	-1.3	-1.3	-1.6	-1.0	-1.2	1.3
DAG(18:2_24:0)	5.2	6.4	4.4	4.9	2.9	3.1	2.0	2.6	2.1	3.3	2.6	3.5	1.6	-1.1	-1.5	-1.6	-2.2	-1.7	-1.5	-1.6	-1.4
DAG(18:2_24:1)	5.8	7.2	5.5	5.6	3.4	4.1	2.1	3.2	2.3	3.8	2.6	3.1	1.3	-1.2	-1.3	-2.1	-2.9	-1.7	-1.8	-1.9	-1.7
DAG(18:3_18:3)	1.6	2.7	2.6	2.5	1.9	1.9	-1.7	-1.0	-1.4	1.2	-1.3	1.2	1.1	-1.0	1.2	-2.6	-3.8	-2.2	-2.5	-2.0	-1.4
DAG(18:3_20:1)	2.9	4.2	2.4	2.5	1.3	1.5	1.1	2.0	1.2	2.0	1.1	1.1	-1.3	-1.9	-1.4	-3.4	-3.7	-1.6	-2.7	-2.3	-2.0
DAG(18:3_22:0)	1.6	1.8	1.4	1.4	-1.4	-1.7	-1.4	-1.3	-1.2	-1.1	-1.3	-1.3	1.8	1.1	-1.3	-1.3	-1.5	-1.2	-1.3	-1.3	1.0
DAG(18:3_22:1)	2.2	3.5	1.6	1.8	-1.0	-1.1	-1.4	1.3	-1.2	1.1	-1.5	-1.3	1.3	-1.1	1.1	-2.4	-2.1	-1.4	-2.1	-1.7	-1.1
DAG(18:3_24:0)	4.3	6.4	4.5	5.4	2.3	2.9	1.4	2.0	1.9	3.4	2.2	2.7	1.4	-1.4	-1.6	-2.2	-3.2	-1.7	-2.3	-2.2	-1.8
DAG(18:3_24:1)	4.8	7.2	4.9	5.7	2.7	3.3	1.4	2.6	1.7	2.9	1.7	2.0	1.1	-1.3	-1.1	-3.1	-3.9	-1.8	-2.5	-2.6	-1.9

ASG.16:0-Glc-campesterol	-1.8	-1.3	-1.4	-1.3	-1.2	-1.4	-2.5	-1.7	-2.3	-1.9	-1.9	-1.3	2.0	1.3	-1.3	1.5	-1.3	-2.0	1.5	-1.1	-1.2
ASG.16:0-Glc-sitosterol	-1.7	-1.2	-1.4	-1.4	-1.3	-1.4	-2.4	-2.0	-2.2	-2.0	-1.8	-1.3	2.7	1.5	-1.2	1.9	1.0	-1.6	1.7	1.1	-1.0
ASG.18:1-Glc-campesterol	-1.1	1.5	-1.1	1.1	-1.2	-1.2	-1.8	-1.1	-1.6	-1.2	-1.3	-1.2	1.3	-1.4	-1.8	-1.2	-2.0	-2.1	-1.3	-1.7	-1.8
ASG.18:1-Glc-sitosterol	1.2	2.0	-1.1	1.1	-1.3	-1.3	-1.9	-1.3	-1.7	-1.2	-1.5	-1.1	2.4	-1.0	-1.5	1.0	-1.6	-1.8	-1.1	-1.4	-1.3
ASG.18:2-Glc-campesterol	-1.6	-1.1	-1.6	-1.5	-1.2	-1.5	-2.0	-1.6	-1.8	-1.8	-1.7	-1.1	1.8	1.3	-1.7	1.4	1.1	-2.4	1.2	1.1	-1.3
ASG.18:2-Glc-sitosterol	-1.7	-1.4	-1.7	-1.6	-1.3	-1.5	-2.3	-1.9	-1.7	-1.8	-1.6	-1.2	2.5	1.5	-1.2	1.9	1.5	-1.5	1.8	1.3	1.0
ASG.18:3-Glc-campesterol	-1.7	-1.1	-1.5	-1.2	-1.2	-1.4	-2.3	-1.7	-2.2	-2.0	-2.0	-1.3	1.5	1.1	-1.5	1.2	-1.3	-2.3	1.0	-1.4	-1.4
ASG.18:3-Glc-sitosterol	-1.6	-1.2	-1.4	-1.2	-1.3	-1.4	-2.3	-2.0	-2.0	-1.8	-1.9	-1.3	2.2	1.5	-1.2	1.6	1.1	-1.7	1.4	-1.0	-1.1
ASG.20:1-Glc-sitosterol	-1.0	1.7	-1.1	1.0	-1.5	-1.4	-2.2	-1.7	-1.8	-1.4	-1.5	-1.2	2.6	1.1	-1.4	1.2	-1.5	-1.4	-1.1	-1.3	-1.2
ASG.22:1-Glc-sitosterol	-1.7	-1.3	-1.1	-1.2	-1.2	-1.6	-2.5	-1.9	-2.4	-1.5	-1.9	-1.3	2.3	1.2	-1.2	1.6	-1.8	-1.9	1.6	-1.1	1.0
Cer(t18:0_22:0)	-1.7	1.3	-2.6	-1.1	-3.0	-1.2	-2.4	-1.3	-3.1	-1.6	-3.4	-1.6	1.7	1.2	1.1	1.2	1.0	-1.1	-1.0	-1.2	-1.3
Cer(t18:0_22:1)	-1.0	3.2	-1.3	2.2	-1.6	1.7	-2.0	1.9	-1.8	2.0	-2.0	1.3	-1.1	-1.3	-1.2	-2.3	0.5	-1.5	-1.9	-1.5	-1.5
Cer(t18:0_22:1-OH)	-1.6	1.6	-2.3	1.1	-1.9	-1.0	-2.1	1.0	-2.2	-1.5	-3.3	-1.7	1.5	1.4	1.5	1.1	1.4	-1.2	-1.0	-1.1	-1.1
Cer(t18:0_23:0-OH)	-2.7	-1.5	-2.2	-1.1	-1.8	-1.7	-2.7	-1.4	-2.5	-1.8	-1.8	-1.5	1.4	1.3	-1.1	1.5	1.1	-1.1	1.6	-1.2	1.1
Cer(t18:0_24:0)	-1.9	-1.4	-3.0	-2.6	-3.7	-3.1	-2.2	-1.8	-2.7	-3.1	-4.0	-3.4	1.4	-1.0	-1.2	1.2	1.0	-1.3	1.1	-1.3	-1.3
Cer(t18:0_24:1)	1.1	1.5	-1.2	-1.1	-1.7	-1.7	-1.8	-1.1	-1.7	-1.5	-2.0	-2.0	1.0	-1.4	-1.4	-1.8	-2.1	-1.7	-1.6	-1.9	-1.7
Cer(t18:0_24:1-OH)	-1.8	-1.3	-2.2	-2.2	-2.7	-2.7	-2.0	-1.4	-2.2	-2.8	-2.7	-3.1	1.6	1.4	1.3	1.4	1.4	1.3	1.5	1.1	1.1
Cer(t18:0_25:0-OH)	-1.2	-1.0	-1.2	-1.6	-1.7	-2.0	-1.7	-1.5	-1.8	-2.1	-1.6	-1.8	1.3	-1.2	-1.6	-1.1	-1.9	-1.5	-1.1	-1.6	-1.5
Cer(t18:0_25:1-OH)	-2.3	-2.5	-1.9	-2.0	-2.5	-3.1	-3.0	-2.1	-2.5	-2.6	-1.9	-1.9	1.7	2.1	-1.1	1.3	1.6	1.2	2.0	1.6	1.5
Cer(t18:0_26:0)	-1.7	-1.2	-2.2	-2.2	-3.1	-3.3	-2.0	-1.5	-2.5	-2.7	-3.3	-2.8	1.4	-1.1	-1.4	1.2	-1.3	-1.5	1.1	-1.3	-1.2
Cer(t18:0_26:1)	-1.1	-1.0	-1.3	-1.6	-1.8	-2.4	-1.6	-1.4	-1.9	-2.2	-2.1	-2.5	1.0	-1.6	-1.7	-1.5	-2.4	-1.9	-1.3	-2.1	-1.7
Cer(t18:0_26:1-OH)	-2.0	-1.6	-2.1	-2.2	-2.6	-2.8	-2.7	-2.1	-2.3	-2.9	-2.4	-2.1	1.9	1.7	1.1	1.4	1.6	1.1	1.5	1.3	1.4
Cer(t18:1_22:0)	1.9	5.0	1.3	2.6	-1.3	1.7	-1.3	1.8	-1.3	1.8	-1.4	1.5	1.1	-1.4	-1.3	-2.3	-2.2	-1.5	-2.6	-2.0	-1.5
Cer(t18:1_22:0-OH)	1.0	2.2	-1.1	1.4	-1.2	-1.1	-1.7	1.2	-1.8	1.1	-1.5	-1.2	1.5	1.2	1.2	-1.2	-1.4	-1.1	-1.2	-1.1	1.1
Cer(t18:1_23:0-OH)	1.0	1.9	1.3	2.0	-1.1	-1.0	-1.2	1.9	-1.7	-1.0	1.0	1.4	1.0	1.1	-1.7	-1.2	-2.0	-1.5	1.1	-1.8	-1.1
Cer(t18:1_24:0)	1.2	2.0	-1.1	1.3	-1.7	-1.3	-1.8	1.0	-2.1	-1.0	-2.1	-1.2	-1.1	-1.7	-1.9	-2.4	-3.2	-2.3	-2.1	-2.2	-1.7
Cer(t18:1_24:0-OH)	1.0	1.4	-1.1	1.1	-1.3	-1.3	-1.9	1.0	-1.9	-1.0	-1.8	-1.2	1.6	1.1	1.0	-1.2	-1.7	-1.3	1.1	-1.0	1.1
Cer(t18:1_24:1-OH)	1.7	2.6	1.7	1.5	1.1	1.0	-1.3	1.4	-1.2	1.4	-1.3	-1.0	1.1	-1.3	-1.1	-2.0	-2.6	-1.7	-1.7	-1.4	-1.2
Cer(t18:1_25:0-OH)	-1.2	-1.2	-1.1	1.1	-1.2	-1.4	-2.5	-1.6	-1.4	1.0	-1.7	1.0	1.2	-1.2	-1.5	-1.7	-1.7	-2.1	-1.1	-1.3	-1.0
Cer(t18:1_26:0)	1.8	3.1	1.9	2.1	1.0	1.0	-1.4	1.4	-1.1	2.1	-1.2	1.3	-1.1	-1.9	-2.0	-2.9	-4.2	-2.5	-2.5	-1.9	-1.6
Cer(t18:1_26:0-OH)	-1.0	1.2	1.3	1.2	-1.2	-1.4	-1.7	-1.2	-1.4	1.2	-1.5	-1.0	1.4	-1.0	-1.2	-1.2	-1.7	-1.6	-1.0	1.0	1.1

HexCer(d18:1_16:0-OH)	-1.2	1.4	-1.2	-1.3	-1.5	-1.5	-1.7	-1.2	-1.6	-1.9	-2.2	-1.8	1.5	1.4	1.3	1.0	1.1	-1.1	-1.2	-1.1	1.1
HexCer(d18:1_20:0-OH)	-1.1	1.3	-1.2	-1.2	-1.3	-1.4	-1.4	-1.1	-1.4	-1.5	-1.3	-1.4	1.5	1.3	-1.0	1.3	1.1	-1.1	1.2	1.0	-1.1
HexCer(d18:1_24:0-OH)	-1.0	1.3	-1.1	-1.2	-1.4	-1.9	-1.5	-1.0	-1.4	-1.4	-1.5	-2.0	1.8	1.3	1.1	1.2	-1.0	1.0	1.4	1.0	1.1
HexCer(d18:2_14:0)	1.7	2.4	1.5	1.6	-1.1	1.1	-1.5	1.2	-1.1	1.2	-1.2	-1.2	1.3	-1.3	-1.4	-1.8	-2.1	-1.5	-1.5	-1.7	-1.8
HexCer(d18:2_14:0-OH)	1.2	1.6	1.1	1.1	-1.3	-1.1	-1.5	1.1	-1.7	-1.1	-1.5	-1.3	1.1	-1.2	-1.2	-1.8	-2.3	-1.4	-1.4	-1.5	-1.4
HexCer(d18:2_16:0)	2.0	3.6	2.3	2.8	1.2	1.5	-1.3	1.5	1.4	1.6	-1.3	1.4	1.4	1.3	1.1	-1.9	-1.3	-1.4	-1.7	-1.4	1.0
HexCer(d18:2_16:0-OH)	1.0	1.7	-1.1	-1.1	-1.4	-1.3	-1.6	-1.0	-1.6	-1.5	-2.3	-1.6	1.3	1.2	1.3	-1.2	-1.3	-1.3	-1.3	-1.1	1.1
HexCer(d18:2_16:1-OH)	-1.2	1.3	-1.2	-1.2	-1.4	-1.5	-1.6	1.0	-1.9	-1.2	-1.6	-1.6	1.1	1.0	1.1	-1.3	-1.6	-1.0	-1.2	1.0	-1.0
HexCer(d18:2_18:0-OH)	-1.1	1.6	1.0	-1.0	-1.1	-1.1	-1.7	-1.0	-1.6	-1.3	-2.0	-1.2	1.3	1.2	1.2	-1.1	-1.3	-1.4	-1.3	-1.0	1.2
HexCer(d18:2_18:1-OH)	-1.3	1.3	-1.1	-1.1	-1.5	-1.6	-1.8	-1.1	-1.6	-1.6	-2.1	-1.5	1.4	1.6	1.3	1.0	1.1	-1.1	-1.0	1.1	1.4
HexCer(d18:2_20:0-OH)	1.1	1.6	1.1	1.0	-1.1	-1.1	-1.5	1.1	-1.5	-1.0	-1.5	-1.2	1.3	-1.0	-1.1	-1.3	-1.7	-1.4	-1.2	-1.1	-1.2
HexCer(d18:2_20:1-OH)	-1.0	1.8	1.1	1.1	-1.1	-1.1	-1.7	-1.0	-1.6	-1.3	-2.0	-1.3	1.1	-1.0	1.1	-1.5	-1.8	-1.7	-1.7	-1.4	-1.1
HexCer(d18:2_22:0-OH)	1.3	1.8	1.1	1.1	-1.2	-1.3	-1.4	1.2	-1.4	-1.0	-1.5	-1.3	1.4	1.0	1.0	-1.2	-1.5	-1.2	-1.0	-1.1	1.0
HexCer(d18:2_22:1-OH)	1.3	1.9	1.3	1.3	1.1	1.0	-1.4	1.1	-1.4	1.0	-1.4	-1.3	1.3	-1.1	1.0	-1.5	-2.0	-1.4	-1.4	-1.3	-1.3
HexCer(d18:2_23:0-OH)	1.1	1.5	1.4	1.3	-1.1	-1.2	-1.4	1.2	-1.2	1.1	-1.4	-1.1	-1.0	-1.2	-1.3	-1.6	-2.1	-1.8	-1.2	-1.4	-1.2
HexCer(d18:2_23:1-OH)	1.2	1.9	1.2	1.2	1.1	1.0	-1.6	-1.0	-1.6	-1.4	-1.3	-1.1	1.6	1.4	-1.1	-1.3	-1.3	-1.6	-1.3	-1.2	-1.2
HexCer(d18:2_24:0)	1.6	2.1	1.3	1.5	-1.0	-1.0	-1.3	1.5	-1.1	1.5	1.0	-1.1	1.2	-1.4	-1.6	-1.7	-2.0	-1.5	-1.2	-1.4	-1.7
HexCer(d18:2_24:0-OH)	1.3	1.8	1.1	1.1	-1.2	-1.2	-1.4	1.2	-1.4	-1.0	-1.5	-1.3	1.4	-1.0	1.0	-1.3	-1.7	-1.2	-1.1	-1.1	-1.1
HexCer(d18:2_24:1-OH)	1.4	2.0	1.3	1.2	-1.1	-1.1	-1.4	1.1	-1.4	-1.0	-1.5	-1.4	1.2	-1.2	-1.1	-1.7	-2.2	-1.5	-1.5	-1.5	-1.4
HexCer(d18:2_25:0-OH)	1.1	1.3	1.1	1.0	-1.1	-1.3	-1.4	1.3	-1.5	1.1	-1.5	-1.2	-1.2	-1.6	-1.5	-1.9	-2.8	-2.0	-1.3	-1.4	-1.3
HexCer(d18:2_25:1-OH)	1.2	1.5	1.2	1.2	-1.1	-1.2	-1.6	1.1	-1.9	-1.1	-1.7	-1.3	-1.0	-1.2	-1.1	-2.0	-2.8	-1.7	-1.3	-1.6	-1.2
HexCer(d18:2_26:0)	2.1	2.7	1.6	1.8	1.1	1.1	-1.1	1.6	1.0	1.6	1.1	1.2	1.2	-1.4	-1.7	-1.9	-2.2	-1.7	-1.4	-1.6	-1.6
HexCer(d18:2_26:0-OH)	1.1	1.6	1.1	1.1	-1.1	-1.2	-1.4	1.2	-1.5	-1.0	-1.5	-1.2	1.1	-1.2	-1.3	-1.4	-1.9	-1.7	-1.2	-1.3	-1.3
HexCer(d18:2_26:1-OH)	1.3	1.8	1.2	1.2	-1.1	-1.1	-1.6	1.1	-1.7	-1.1	-1.6	-1.4	1.1	-1.3	-1.1	-1.8	-2.6	-1.6	-1.5	-1.6	-1.4
HexCer(t18:0_22:0-OH)	1.2	1.6	-1.1	-1.1	1.1	-1.0	-1.4	1.2	-1.4	-1.3	-1.5	-1.3	1.5	1.2	1.1	-1.1	-1.1	-1.5	1.1	-1.0	-1.2
HexCer(t18:0_22:1-OH)	-1.3	-1.1	-2.0	-1.8	-1.3	-1.1	-1.7	-1.2	-1.8	-2.4	-1.5	-3.1	1.8	1.6	2.0	1.3	1.8	1.7	1.6	1.2	-1.5
HexCer(t18:0_24:1-OH)	-1.3	-1.0	-1.9	-1.9	-1.5	-1.6	-1.6	-1.2	-1.6	-2.3	-1.7	-2.3	1.7	1.3	1.1	1.3	1.5	-1.0	1.4	1.1	-1.3
HexCer(t18:1_16:0-OH)	1.1	1.6	-1.1	-1.1	-1.3	-1.2	-1.5	1.0	-1.5	-1.5	-1.6	-1.6	1.6	1.3	1.0	-1.0	-1.1	-1.1	1.1	-1.0	-1.3
HexCer(t18:1_18:0-OH)	1.0	1.5	-1.3	-1.2	-1.2	-1.1	-1.7	-1.2	-1.4	-1.5	-2.0	-1.4	1.6	1.2	1.2	-1.1	1.1	-1.5	-1.0	1.0	-1.1
HexCer(t18:1_20:0-OH)	1.1	1.6	1.1	1.0	-1.0	1.0	-1.7	-1.2	-1.4	-1.4	-1.7	-1.3	1.8	1.6	1.4	1.0	1.1	-1.2	-1.0	1.1	1.0
HexCer(t18:1_22:0-OH)	1.2	1.7	1.0	-1.0	-1.1	-1.1	-1.5	1.0	-1.5	-1.4	-1.6	-1.4	1.8	1.5	1.2	-1.0	1.0	-1.2	1.0	1.1	-1.1

HexCer(t18:1_22:1-OH)	1.2	1.8	1.1	1.1	-1.1	-1.1	-1.5	1.0	-1.4	-1.3	-1.6	-1.6	1.5	1.3	1.2	-1.2	-1.2	-1.2	-1.2	-1.1	-1.2
HexCer(t18:1_23:0-OH)	1.2	1.4	-1.1	-1.1	-1.2	-1.3	-1.1	1.3	-1.5	-1.2	-1.5	1.0	-1.0	-1.2	-1.6	-1.3	-1.7	-1.9	-1.2	-1.3	-1.2
HexCer(t18:1_23:1-OH)	1.1	1.5	1.1	1.1	1.1	-1.1	-1.4	1.0	-1.4	-1.1	-1.4	-1.1	1.1	1.0	-1.2	-1.4	-1.5	-1.7	-1.4	-1.1	-1.3
HexCer(t18:1_24:0)	1.3	1.5	-1.0	1.0	-1.4	-1.3	-1.6	1.1	-1.5	-1.3	-1.5	-1.7	1.1	-1.1	-1.3	-1.8	-1.5	-1.5	-1.2	-1.4	-1.7
HexCer(t18:1_24:0-OH)	1.2	1.7	-1.0	-1.0	-1.2	-1.2	-1.5	1.1	-1.5	-1.2	-1.6	-1.4	1.5	1.1	1.0	-1.2	-1.3	-1.4	-1.0	-1.1	-1.2
HexCer(t18:1_24:1-OH)	1.3	1.9	1.2	1.1	-1.1	-1.1	-1.4	1.1	-1.4	-1.2	-1.6	-1.3	1.2	1.0	-1.0	-1.5	-1.7	-1.5	-1.4	-1.3	-1.3
HexCer(t18:1_25:0-OH)	1.1	1.3	1.0	-1.1	-1.1	-1.3	-1.4	1.2	-1.4	-1.1	-1.6	-1.2	-1.2	-1.3	-1.5	-1.8	-2.0	-2.1	-1.3	-1.4	-1.4
HexCer(t18:1_25:1-OH)	1.2	1.4	1.1	-1.0	-1.1	-1.2	-1.4	1.1	-1.8	-1.2	-1.7	-1.2	-1.0	-1.2	-1.3	-1.7	-2.4	-2.0	-1.4	-1.4	-1.3
HexCer(t18:1_26:0-OH)	1.2	1.5	-1.0	1.0	-1.1	-1.2	-1.5	1.1	-1.5	-1.1	-1.7	-1.3	1.4	1.0	-1.2	-1.3	-1.5	-1.7	-1.0	-1.1	-1.2
HexCer(t18:1_26:1-OH)	1.3	1.7	1.2	1.1	-1.1	-1.1	-1.5	1.0	-1.5	-1.1	-1.8	-1.4	1.2	-1.1	-1.0	-1.7	-2.0	-1.7	-1.4	-1.4	-1.4
SG. campesteryl glucoside	-1.3	1.0	-1.3	-1.4	-1.5	-1.4	-2.0	-1.5	-1.8	-1.5	-1.6	-1.5	1.4	1.4	1.2	-1.0	-1.0	1.1	-1.1	1.2	1.1
SG. cholesteryl glucoside	1.3	1.9	-1.0	-1.0	-1.0	-1.1	-1.5	-1.1	-1.2	-1.6	-1.9	-1.2	1.2	1.0	1.5	-1.6	-1.1	-1.2	-1.8	-1.5	1.4
SG. sitosteryl glucoside	-1.7	-1.1	-1.8	-1.8	-1.6	-1.6	-2.3	-1.7	-2.1	-2.0	-2.0	-1.7	2.0	1.8	1.7	1.5	1.5	1.3	1.2	1.6	1.6

Appendix C: Supplemental Data and Tables for Chapter 4

The files sizes and the datasets in excel sheets for Supplemental Tables **S4-1** to **S4-7** are too large to insert in this thesis. Therefore, only the captions are given here and links are given here for access to examiners. These supplemental tables can be accessed from the additional supplemental file for Chapter 4.

Supplemental Table S4-1. Abundance analysis of ribosome complexes (40S SSU, 60S LSU, 80S monosomes and polysomes) from roots of single-paralog *reil* mutants (*reil1-1, reil2-1, reil2-2*) and double mutants (*reil1-1 reil2-1* and *reil1-1 reil2-2*) compared to wild type Col-0 at non-acclimated (20°C, 0 day) and cold-acclimating states (10°C, 1 day, 3 days, 7 days, and 21 days).

Supplemental Table S4-2. Gene expression profiles and statistical data analyses of roots from the non-acclimated and 10°C cold acclimating *reil1-1 reil2-1* and *reil1-1 reil2-2* mutants compared to Col-0 wild type. Genes are listed by name, description, probe identifier and probe sequence (columns A-E). The table contains differential profiles of *reil1-1 reil2-1* and *reil1-1 reil2-2* compared to Col-0 at different time points, namely at 0 day (non-acclimated state), 1 day or 7 days after cold shift (columns G-L), 2-way analyses of variance (ANOVA) (columns N-P), and pairwise heteroscedastic Student´s *t*-test results of differential gene expression in the mutants (column R-Y) with significance calls at $p < 0.01$ (column U and Y) and 1-way ANOVA of the cold shift response in Col-0 (column AA) with *t*-test results of cold acclimating Col-0 compared to non-acclimated Col-0 (column AB-AE). Differential profiles of mutants and Col-0 were compared to non-acclimated Col-0 (columns AG-AO) with respective standard errors (columns AQ-AY) and *P* values of t-tests (Column BA-BI). Note that gene expression values were averaged across redundant probes, if multiple probes per gene model were available. Only the first probe identifiers and respective probe sequences of each gene are listed. Three biological replicates (n=3) in which each replicate was a pool of roots from at least three plants grown in the same cultivation container were analyzed. Note the eight genes that were constitutively and highly expressed in both *reil* double mutants compared to wild type Col-0 regardless of the length of cold acclimation. These genes were selected by applying filters of $p < 0.05$ to each of the columns R-T and V-X. Two of these genes were also found to be consistently differentially expressed in the leaf transcriptome that was analyzed previously (Beine-Golovchuk et al., 2018). Paste values from any row below into row 3 is for visualization of differential gene expression.

Supplemental Table S4-3. Functional enrichment analysis of differential gene expression in non-acclimated (0 day) and cold-acclimating roots of *Arabidopsis thaliana* Col-0 and the *reil1-1 reil2-1* and *reil1-1 reil2-2* mutants at 1 day or 7 days after shift to 10°C cold. Differential gene expression was determined relative to non-acclimated Col-0 that was cultivated at 20°C, i.e. optimized cultivation temperature. Mean $\log_2$-fold changes (Log_2-FC), z-scores, and *P*-values of gene set enrichments of 2145 GO terms were calculated by parametric analysis of gene set enrichment (Tian et al., 2017). GO identifiers, ontology domain, description and number of constituent genes are listed (columns A-D). Mean $\log_2$-FC changes are color coded by a scale ranging from +1.5 (red) to -1.5 (blue).

Supplemental Table S4-4. Proteomic characterization of ribosome preparations obtained from root material by sucrose density gradient fractionation experiments DS1 and DS2 (Selection of analyzed samples from Pride repository data set PXD016292). Ribosome complexes are characterized by sums of label-free quantification (LFQ)-intensities of all detected RPs of 40S, 60S, and organelle 30S or 50S subunits within each fraction. Non-translating immature 60S subunits are assessed by Arabidopsis homologs eIF6A and NMD3 of yeast cytosolic 60S maturation factors. Experiments DS1 and DS2 compare the ribo-proteome of 6 fractions after sucrose density gradient fractionation. Samples of Arabidopsis thaliana Col-0 wild type are compared to the double mutants, *reil1-1 reil2-1* (DS2) and *reil1 1 reil2-2* (DS1) at day 0 (non-acclimated) and day 7 after shift to 10°C. Sums of LFQ-intensities of cytosolic and organelle ribosome subunits are reported (* not analyzed because of low peptide count).

Supplemental Table S4-5. Fold changes (FC) of total RP abundances in the proteomic analyses of roots from the *reil1 reil2* double mutants compared to Col-0 wild type at 20°C and 7 days after shift to 10°C cold. Numbers of detected proteins and sums of LFQ-abundances across all sedimentation fractions are reported.

Supplemental Table S4-6. List and specificity analysis of detected cytosolic RPs and ribosome associated proteins.

Supplemental Table S4-7. Differential accumulation of cytosolic RPs and RP associated proteins (RAPs) in non-translating ribosome fractions of the *reil1-1 reil2-1* (DS2) and *reil1-1 reil2-2* (DS1) mutants relative to *Arabidopsis thaliana* Col-0 wild type. This list contains changes that are shared between the reil1 reil2 mutants 7 days after shift to 10°C and respective observations at 20°C prior to the shift. Supplemental Table S4-7A contains shared $\log_2$-fold changes in the non-translating 60S and 60/80S fractions after normalization of protein LFQ-abundances by LFQ-abundance sums of all detected 60S RPs. Supplemental Table S4-7B contains shared $\log_2$-fold changes in the non-translating 30/S40S fraction after normalization of protein LFQ-abundances by LFQ-abundance sums of all detected 40S RPs. Presence in mutants relative to absence in Col-0 are classified as increase, absence in mutants relative to presence in Col-0 as decrease.

Appendix D: Supplemental Data and Tables for Chapter 5

Supplemental Data S5-1. The coding sequences of *Arabidopsis thaliana REIL1* and *REIL2*.

Arabidopsis thaliana REIL1 (AT4G31420.1), accession number NM_202923.2

aaaaaggctaaaagaatgggccaaatgggctactcttgtatcgggtcaggaacgggtcagttccaacccgatcggatctaaaatgggcgg
ggcgccttccttttcattttgatggcaatcaatcatcatcaatcgacgctttttagagacaaacacgatcgccgatccatttacgagccgtcgtt
gctctacacatatcaacaacaaatcttatcctcccaactatcttttctctgattttcttttcttctccagtttccatttctagaatcgatcgatattgaag
gagagaagatgcctggtttaacatgtaacgcgtgtaacatggagttcaaggacgaagaagaacgtaaccttcattacaaatccgattggcac
cgctacaatctcaagcgcaaggtggctggagttcctggagttacagaagccttgtttgaggctagacaatctgctcttgctcaggagaagaat
aaatcaaatgaagcacctatgctttatacttgtgcaatctgtgctaaaggttacaggagttccaaggctcatgagcagcatcttcagtcgcgtcc
atgttttgcgggtttcacaagggacatcaatcaacggagaggaggatatagcgattatcaggcaacttcctcgccgtgttcaacacaggggtt
ccattgatgatgatagtgaagatgaatgggtggaggttgattctgacgaggaattggctgctgaagaagcctctgattctttgtctaagttgaat
gtgaatgagtctggatctgctgaagatatggatgatgatggtgatgcagataagtatgagctggatccaacctgctgtttgatgtgtgacaaaa
aacataagaccttagagagctgtatgcttcacatgcataagcatcatggtttctttattcccgatattgagtatctcaaggatcctgaagggcttct
cacttaccttggtcttaaggtcaagagagacttcatgtgtctgtactgcaatgagctgtgccgtccattcagcagcttagaagctgtaagaaaat
atggaagcaaagagtcattgcaaactgcattatggtgatggtgatgatgaagaagatgctgagctagaagagttttatgactacagcagcag
cagctatgttgatgaagctggaaagcaaattgttgtatctggtgaaacagacaatactgtagaactcgttggtggttctgagctcttgatcacgg
agaagtccgagaacacaacaacgtctaaaactctcgggtcccgtgaattcatgcgttactacagacagaagccacgcccaacttctcaaac
agcaaccagataattgcctctttatcttcaaggtacaagagcctgggtctgaagacagtaccgtcgaaagaggagactttgaggatgaaagt
gcgcaaggagatgagcaagagaggcgagacaatgcgtaccaagatcggagtgaagagtaatgtcataagaaacttgcccaataacgtcc
catattagtttctgtgtatgtgccacttgttctcaagtgttggattgtatgatgatttcatgtacttttgagtctttgaccaagttgtgttgctacttgga
ataagagtaagctttaaaaagagtatgttcactgaaatagaaatgttaaaaattaatacacgaacgttgacttctga

Arabidopsis thaliana REIL 2 (AT2G24500), accession number AY114695.1

agatttggagatttgtcgttaaacaaatttcgccgacctacgtatgagccgtcgcctccaatataaaccaaagccatccctaatcctcgaattctt
cctctctgagttttattctgagatagagaaagatgtcaggtttagcttgtaattcgtgtaacaaagacttcgaagacgacgctgagcagaagttt
cactacaaatccgaatggcaccgttacaatctcaagcgcaagatagctggtgttcctggagtaacagaggcactatttgaagctagacaagc
tgctatagctcaagagaaggttaaagctgttgaagcaccgatgctttatagttgtggaatctgtaacaaaggttacaggagttccaaggctcat
gagcagcatcttaagtcgaagagtcatgttttgaaggcttcgacgagtactggagaggaggataaagcgatcatcaagcagcttccgcctgt
cgtgttgagaagaataacactgctcaattgaagggttcgattgaggaggaagagagtgaagatgaatggattgaggttgattcggatgagat
ttggatgcggaaatgaatgaggatggtgaagaagaagatatggatgaagatggtattgaatttgagttggatccggcttgttgtttgatgtgtat
aagaagcataagactatagagaaatgtatggttcatatgcataagtttcatgggttcttcattcctgatattgagtacttgaaggatcctaaaggg
tttctgacctacctcggtctaaaggtcaagagagacttcgtgtgtctgtactgcaatgaattgtgccatccatttagtagtttggaagctgttcgta
agcatatggacgccaaaggtcattgcaaagtgcattatggtgatggtggtgatgaagaagatgcagaacttgaagagttctatgactacagc
agcagctatgtcaatggagacgaaaatcagatggttgtgtccggtgagtcagtgaacactgtagagctttttggtgggtctgagcttgtgatca
ccaagagaaccgataacaaagtaacgtctaggactcttgggtctcgagaattcatgcgctactacaaacagaagccagcaccgtcttctcag
aagcatattgtcaactctctaacctccaggtacaagatgatgggtctagcaacagtgcagtcaaaggaggccatagtgaggatgaaggtgat
gagagagatgaacaaaagaggagcgaaaagcagtgtcaggctcggaatgaagagcaacgtcatcaggaatctgcccaacaatgtcacct
attagtcttgctcctcgattttcaggtctctcctctttgtttgattttgtgaccagagttttggtgagtaaatctatctaagtttttcactagtactcaagt
atcttaggcccatttgggtctctgttttgtctgatttagtcttttgaaaatgttacgttttggctgagtttgtatctcttgcccagtgctttgtacactcta
cattaatctatatttcatttggtagaagatcaagagctaatcaatctttatctgctaaatcataaatctagtacacttttcacttatctatacatttgtttt

agataacgaatgctctcgacttcactttctctagctatcttgataaattgtataaaggtaaatgcacaggtcgatttacgagttcctcacaaaccg
cgagtaaatctcgacacgaatatcttgcatcatccactatatctctttattatttatcactctattgctctctcttacaggcactactgtttcaaaaga
gagaggaacaagtttaaagcctaactctttccaaagtccaacagcccaacttcacaggagcccatcgaaatcataagtcttctaaaccggaa
agcttttgagtcgaataaactgaactgagagtaaaccggag

Supplemental Data S5-2. REIL amino acid sequences used for phylogenetic tree construction, * represents the stop codon.

Arabidopsis thaliana REIL1
MPGLTCNACNMEFKDEEERNLHYKSDWHRYNLKRKVAGVPGVTEALFEARQSALAQE
KNKSNEAPMLYTCAICAKGYRSSKAHEQHLQSRSHVLRVSQGTSINGEEDIAIIRQLPRV
QHRGSIDDDSEDEWVEVDSDEELAAEEASDSLSKLNVNESGSAEDMDDDGDADKYELD
PTCCLMCDKKHKTLESCMLHMHKHHGFFIPDIEYLKDPEGLLTYLGLKVKRDFMCLYC
NELCRPFSSLEAVRKHMEAKSHCKLHYGDGDDEEDAELEEFYDYSSSYVDEAGKQIVS
GETDNTVELVGGSELLITEKSENTTTSKTLGSREFMRYYRQKPRPTSQDSNQIIASLSSRY
KSLGLKTVPSKEETLRMKVRKEMSKRGETMRTKIGVKSNVIRNLPNNVPY*

Arabidopsis thaliana REIL2
MSGLACNSCNKDFEDDAEQKFHYKSEWHRYNLKRKIAGVPGVTEALFEARQAAIAQEK
VKAVEAPMLYSCGICNKGYRSSKAHEQHLKSKSHVLKASTSTGEEDKAIIKQLPPRRVK
NNTAQLKGSIEEEESEDEWIEVDSDEDLDAEMNEDGEEEDMDEDGIEFELDPACCLMCD
KKHKTIEKCMVHMHKFHGFFIPDIEYLKDPKGFLTYLGLKVKRDFVCLYCNELCHPFSL
EAVRKHMDAKGHCKVHYGDGGDEEDAELEEFYDYSSSYVNGDENQMVVSGESVNTE
LFGGSELVITKRTDNKVTSRTLGSREFMRYYKQKPAPSSQKHIVNSLTSRYKMMGLATV
QSKEAIVRMKVMREMNKRGAKSSVRLGMKSNVIRNLPNNVTY*

Wheat_Aegilops_REIL
MPTVTCNACNAAFEEEEEQRLHYRSEWHRYNLKRKVAGVPGVTEALFIARQTVLAEGS
NSTIAPPMSYSCALCGKGYRSAKAHAQHLTTRSHLLRASQEPNASTAAVVKPLPERVPR
RAPSAMEEDEDEDEDEEEEWVEVDPSELESTSNMQVDEDSKSDDEMADLEMLDPSDCF
MCDLKHDNIEDCMIHMHKKHGFFIPDSEYLKDPNGLLIYVGLKVKRDFMCLYCNDRCQ
PFQSLEAVRKHMDAKGHCKLRYGDGGEDEDADLEDFYDYSSSYVDVEGKQLVTAGM
DNSIELGGGGSELVITSKSEKGRRVTTLGSREFIRYYRQKPRPSVAADRALALSLASSYKS
MGLVTVQSKEQMVRLKVLRAMNKSGVETMRTKIGMKSNVIRNLPKNVPY*

Wheat_Chinese Spring_REIL_7A
MPTVTCNACNAAFEEEEEQRLHYRSEWHRYNLKRKVAGVPGVTEALFIARQTVLAEGS
NSTVAPPMSYSCALCGKGYRSAKAHAQHLTTRSHLLRASQEPNASTAAVVKPLPERVP
RRAPSAMEEDEDEDEEEEEEWVEVDPSELESTSNMQVDEDSKSDDEMADLEMLDPSDC
FMCDLKHDNIEDCMIHMHKKHGFFIPDSEYLKDPNGLLIYVGLKVKRDFMCLYCNDRC
QPFQSLEAVRKHMDAKGHCKLRYGDGGEDEDADLEDFYDYSSSYVDVEGKQLVAAG
DMDNSIELGGGGSELVITSKSEKGRRVTTLGSREFIRYYRQKPRPSVAADRALALSLASS
YKSMGLVTVQSKEQMVRLKVLRAMNKSGVETMRTKIGMKSNVIRNLPKNVPY*

Wheat_Chinese Spring_REIL_7B
MPTVTCNACNAAFEEEEEQRLHYRSEWHRYNLKRKVAGVPGVTEALFIARQTVLAEGS
NSTVAPPMSYSCALCGKGYRSAKAHAQHLTTRSHLLRASQEPNASTAAVVKPLPERVP
RRAPSAMEEDEDEDEDEDEEEEWVEVDPSELESTSNMQVDEDSKSDDEMADLEMLDPS
VCFMCDLKHDNIEDCMIHMHKKHGFFIPDSEYLKDPNGLLIYVGLKVKRDFMCLYCND
RCQPFQSLEAVRKHMDAKGHCKLRYGDGGEDEDADLEDFYDYSSSYVDVEGKQLVAA
GDMDNSIELGGGGSELVITSKSEKGRRVTTLGSREFIRYYRQKPRPSVAADRALALSLAS
SYKSMGLVTVQSKEQMVRLKVLRAMNKSGVETMRTKIGMKSNVIRNLPKNVPY*

Wheat_Chinese Spring_REIL_7D
MPTVTCNACNAAFEEEEEQRLHYRSEWHRYNLKRKVAGVPGVTEALFIARQTVLAEGS
NSTIAPPMSYSCALCGKGYRSAKAHAQHLTTRSHLLRASQEPNASTAAVVKPLPERVPR
RAPSAMEEDEDEDEDEEEEWVEVDPSELESTSNMQVDEDSKSDDEMADLEMLDPSDCF
MCDLKHDNIEDCMIHMHKKHGFFIPDSEYLKDPNGLLIYVGLKVKRDFMCLYCNDRCQ
PFQSLEAVRKHMDAKGHCKLRYGDGGEDEDADLEDFYDYSSSYVDVEGKQLVTAGM
DNSIELGGGGSELVITSKSEKGRRVTTLGSREFIRYYRQKPRPSVAADRALALSLASSYKS
MGLVTVQSKEQMVRLKVLRAMNKSGVETMRTKIGMKSNVIRNLPKNVPY*

Wheat_TAM107_REIL_7A
MPTVTCNACNAAFEEEEEQRLHYRSEWHRYNLKRKVVAGVPGVTEALFIARQTVLAEG
SNSTVAPPMSYSCALCGKGYRSAKAHAQHLTTRSHLLRASQEPNASTAAVVKPLPERVP
RRAPSAMEEDEDEDEEEEEEWVEVDPSELESTSNMQVDEDSKSDDEMADLEMLDPSDC
FMCDLKHDNIEDCMIHMHKKHGFFIPDSEYLKDPNGLLIYVGLKVKRDFMCLYCNDRC
QPFQSLEAVRKHMDAKGHCKLRYGDGGEDEDADLEDFYDYSSSYVDVEGKQLVAAD
MDNSIELGGGGSELVITSKSEKGRRVTTLGSREFIRYYRQKPRPSVAADRALALSLASSK
SMGLVTVQSKEQMVRLKVLRAMNKSGVETMRTKIGMKSNVIRNLPKNVPY*

Wheat_TAM107_REIL_7B
MPTVTCNACNAAFEEEEEQRLHYRSEWHRYNLKRKVVAGVPGVTEALFIARQTVLAEG
SNSTVAPPMSYSCALCGKGYRSAKAHAQHLTTRSHLLRASQEPNASTAAVVKPLPERVP
RRAPSAMEEDEDEDEDEDEEEEWVEVDPSELESTSNMQVDEDSKSDDEMADLEMLDPS
VCFMCDLKHDNIEDCMIHMHKKHGFFIPDSEYLKDPNGLLIYVGLKVKRDFMCLYCND
RCQPFQSLEAVRKHMDAKGHCKLRYGDGGEDEDADLEDFYDYSSSYVDVEGKQLVAA
GDMDNSIELGGGGSELVITSKSEKGRRVTTLGSREFIRYYRQKPRPSVAADRALALSLAS
SYKSMGLVTVQSKEQMVRLKVLRAMNKSGVETMRTKIGMKSNVIRNLPKNVPY*

Wheat_TAM107_REIL_7D
MPTVTCNACNAAFEEEEEQRLHYRSEWHRYNLKRKVVAGVPGVTEALFIARQTVLAEG
SNSTIAPPMSYSCALCGKGYRSAKAHAQHLTTRSHLLRASQEPNASTAAVVKPLPERVR
RAPSAMEEDEDEDEDEEEEWVEVDPSELESTSNMQVDEDSKSDDEMADLEMLDPSDCF
MCDLKHDNIEDCMIHMHKKHGFFIPDSEYLKDPNGLLIYVGLKVKRDFMCLYCNDRCQ
PFQSLEAVRKHMDAKGHCKLRYGDGGEDEDADLEDFYDYSSSYVDVEGKQLVTAGM
DNSIELGGGGSELVITSKSEKGRRVTTLGSREFIRYYRQKPRPSVAADRALALSLASSYKS
MGLVTVQSKEQMVRLKVLRAMNKSGVETMRTKIGMKSNVIRNLPKNVPY*

Wheat_Manitou_REIL_7A
MPTVTCNACNAAFEEEEEQRLHYRSEWHRYNLKRKVAGVPGVTEALFIARQTVLAEGS
NSTIAPPMSYSCALCGKGYRSAKAHAQHLTTRSHLLRASEEPNAATAAVVKPLPERVPR
RAPSAMEEDEDEDEDEEEEGVEVDPSELESTSNMQVDEDSNQNDEMADLEMLDPSVCF
MCDLKHDNIEDCMIHMHKKHGFFIPDSEYLKDPNGLLIYVGLKVKRDFMCLYCNDRCQ
PFQSLEAVRKHMDAKGHCKLRYGDGGEDEDADLEDFYDYSSSYVDVEGKQLVAAGD
MDNSIELGGGGSELVITSKSEKGRRVTTLGSREFIRYYRQKPRPSVAADRALALSLASSY
KSMGLVTVQSKEQMVRLKVLRAMNKSGVETMRTKIGMKSNVIRNLPKNVPY*

Wheat_Manitou_REIL_7B
MPTVTCNACNAAFEEEEEQRLHYRSEWHRYNLKRKVAGVPGVTEALFIARQTVLAEGS
NSTVAPPMSYSCALCGKGYRSAKAHAQHLTTRSHLLRASQEPNASTAAVVKPLPERVP
RRAPSAMEEDEDEDEDEDEEEEWVEVDPSELESTSNMQVDEDSKSDDEMADLEMLDPS
VCFMCDLKHDNIEDCMIHMHKKHGFFIPDSEYLKDPNGLLIYVGLKVKRDFMCLYCND
RCQPFQSLEAVRKHMDAKGHCKLRYGDGGEDEDADLEDFYDYSSSYVDVEGKQLVAA
GDMDNSIELGGGGSELVITSKSEKGRRVTTLGSREFIRYYRQKPRPSVAADRALALSLAS
SYKSMGLVTVQSKEQMVRLKVLRAMNKSGVETMRTKIGMKSNVIRNLPKNVPY*

Wheat_Manitou_REIL_7D
MPTVTCNACNAAFEEEEEQRLHYRSEWHRYNLKRKVAGVPGVTEALFIARQTVLAEGS
NSTVAPPMSYSCALCGKGYRSAKAHAQHLTTRSHLLRASQEPNASTAAVVKPLPERVP
RRAPSAMEEDEDEDEDEEEEGVEVDPSELESTSNMQVDEDSKSDDEMADLEMLDPSVC
FMCDLKHDNIEDCMIHMHKKHGFFIPDSEYLKDPNGLLIYVGLKVKRDFMCLYCNDRC
QPFQSLEAVRKHMDAKGHCKLRYGDGGEDEDADLEDFYDYSSSYVDVEGKQLVTAGD
MDNSIELGGGGSELVITSKSEKGRRVTTLGSREFIRYYRQKPRPSVAADRALALSLASSY
KSMGLVTVQSKEQMVRLKVLRAMNKSGVETMRTKIGMKSNVIRNLPKNVPY*

Wheat_Wyalkatchem_REIL_7A
MPTVTCNACNAAFEEEEEQRLHYRSEWHRYNLKRKVAGVPGVTEALFIARQTVLAEGS
NSTVAPPMSYSCALCGKGYRSAKAHAQHLTTRSHLLRASQEPNASTAAVVKPLPERVR
RAPSAMEEDEDEDEEEEEEWVEVDPSELESTSNMQVDEDSKSDDEMADLEMLDPSDCF
MCDLKHDNIEDCMIHMHKKHGFFIPDSEYLKDPNGLLIYVGLKVKRDFMCLYCNDRCQ
PFQSLEAVRKHMDAKGHCKLRYGDGGEDEDADLEDFYDYSSSYVDVEGKQPVAACD
MDNSIELGGGGSQLVITSKSEKGRRLTTLGSRKFIRYYRQKPRPSVAADRALALSLASSY
KSMGLVTVQSKEQMVRLKVLRAMNKSGVETMRTKIGMKSNVIRNLPKNVPY*

Wheat_Wyalkatchem_REIL_7B
MPTVTCNACNAAFEEEEEQRLHYRSEWHRYNLKRKVAGVPGVTEALFIARQTVLAEGS
NSTFAPPMSYSCALCGKGYRSAKAHAQHLTTRSHLLRASQEPNASTAAVVKPLPERVPC
RAPSAMEEDEDEDEDEDEEEEWVEVDPSELESTSNMQVDEDSKSDDEMADLEMLDPSV
CFMCDLKHDNIEDCMIHMHKKHGFFIPDSEYLKDPNGLLIYVGLKVKRDFMCLYCNDR
CQPFQSLEAVRKHMDAKGHCKLRYGDGGEDEDADLEDFYDYSSSYVDVEGKQLVAAG
DMDNSIELGGGGSELVITSKSEKGRRVTTLGSREFIRYYRQKPRPSVAADRALALSLASY
KSMGLVTVQSKEQMVRLKVLRAMNKSGVETMRTKIGMKSNVIRNLPKNVPY*

Wheat_Wyalkatchem_REIL_7D
MPTVTCNACNAAFEEEEEQRLHYRSEWHRYNLKRKVAGVPGVTEALFIARQTVLAEGS
NSTIAPPMSYSCALCGKGYRSAKAHAQHLTTRSHLLRASQEPNASTAAVVKPLPERVPR
RAPSAMEEDEDEDEDEEEEWVEVDPSELESTSNMQVDEDSKSDDEMADLEMLDPSDCF
MCDLKHDNIEDCMIHMHKKHGFFIPDSEYLKDPNGLLIYVGLKVKRDFMCLYCNDRCQ
PFQSLEAVRKHMDAKGHCKLRYGDGGEDEDADLEDFYDYSSSYVDVEGKQLVTAGD
MDNSIELGGGGSELVITSKSEKGRRVTTLGSRKFIRYYRQKPRPSVAADRALALSLASSSY
KSMGLVTVQSKEQMVRLKVLRAMNKSGVETMRTKIGMKSNVIRNLPKNVPY*

Wheat_Young_REIL_7A
MPTVTCNACNAAFEEEEEQRLHYRSEWHRYNLKRKVAGVPGVTEALFIARQTVLAEGS
NSTVAPPMSYSCALCGKGYRSAKAHAQHLTTRSHLLRASQEPNASTAAVVKPLPERVR
RAPSAMEEDEDEDEEEEEEWVEVDPSELESTSNMQVDEDSKSDDEMADLEMLDPSDCF
MCDLKHDNIEDCMIHMHKKHGFFIPDSEYLKDPNGLLIYVGLKVKRDFMCLYCNDRCQ
PFQSLEAVRKHMDAKGHCKLRYGDGGEDEDADLEDFYDYSSSYVDVEGKQPVAACD
MDNSIELGGGGSQLVITSKSEKGRRLTTLGSRKFIRYYRQKPRPSVAADRALALSLASSSY
KSMGLVTVQSKEQMVRLKVLRAMNKSGVETMRTKIGMKSNVIRNLPKNVPY*

Wheat_Young_REIL_7B
MPTVTCNACNAAFEEEEEQRLHYRSEWHRYNLKRKVAGVPGVTEALFIARQTVLAEGS
NSTFAPPMSYSCALCGKGYRSAKAHAQHLTTRSHLLRASQEPNASTAAVVKPLPERVPC
RAPSAMEEDEDEDEDEDEEEEWVEVDPSELESTSNMQVDEDSKSDDEMADLEMLDPSV
CFMCDLKHDNIEDCMIHMHKKHGFFIPDSEYLKDPNGLLIYVGLKVKRDFMCLYCNDR
CQPFQSLEAVRKHMDAKGHCKLRYGDGGEDEDADLEDFYDYSSSYVDVEGKQLVAAD
MDNSIELGGGGSELVITSKSEKGRRVTTLGSREFIRYYRQKPRPSVAADRALALSLASSSK
SMGLVTVQSKEQMVRLKVLRAMNKSGVETMRTKIGMKSNVIRNLPKNVPY*

Wheat_Young_REIL_7D
MPTVTCNACNAAFEEEEEQRLHYRSEWHRYNLKRKVAGVPGVTEALFIARQTVLAEGS
NSTIAPPMSYSCALCGKGYRSAKAHAQHLTTRSHLLRASQEPNASTAAVVKPLPERVPR
RAPSAMEEDEDEDEDEEEEWVEVDPSELESTSNMQVDEDSKSDDEMADLEMLDPSDCF
MCDLKHDNIEDCMIHMHKKHGFFIPDSEYLKDPNGLLIYVGLKVKRDFMCLYCNDRCQ
PFQSLEAVRKHMDAKGHCKLRYGDGGEDEDADLEDFYDYSSSYVDVEGKQLVTAGM
DNSIELGGGGSELVITSKSEKGRRVTTLGSREFIRYYRQKPRPSVAADCALALSLASRYK
SMGLVTVQSKEQMVRLKVLRAMNKSGVETMRTEIGMKSNVIRDLPKNVPY*

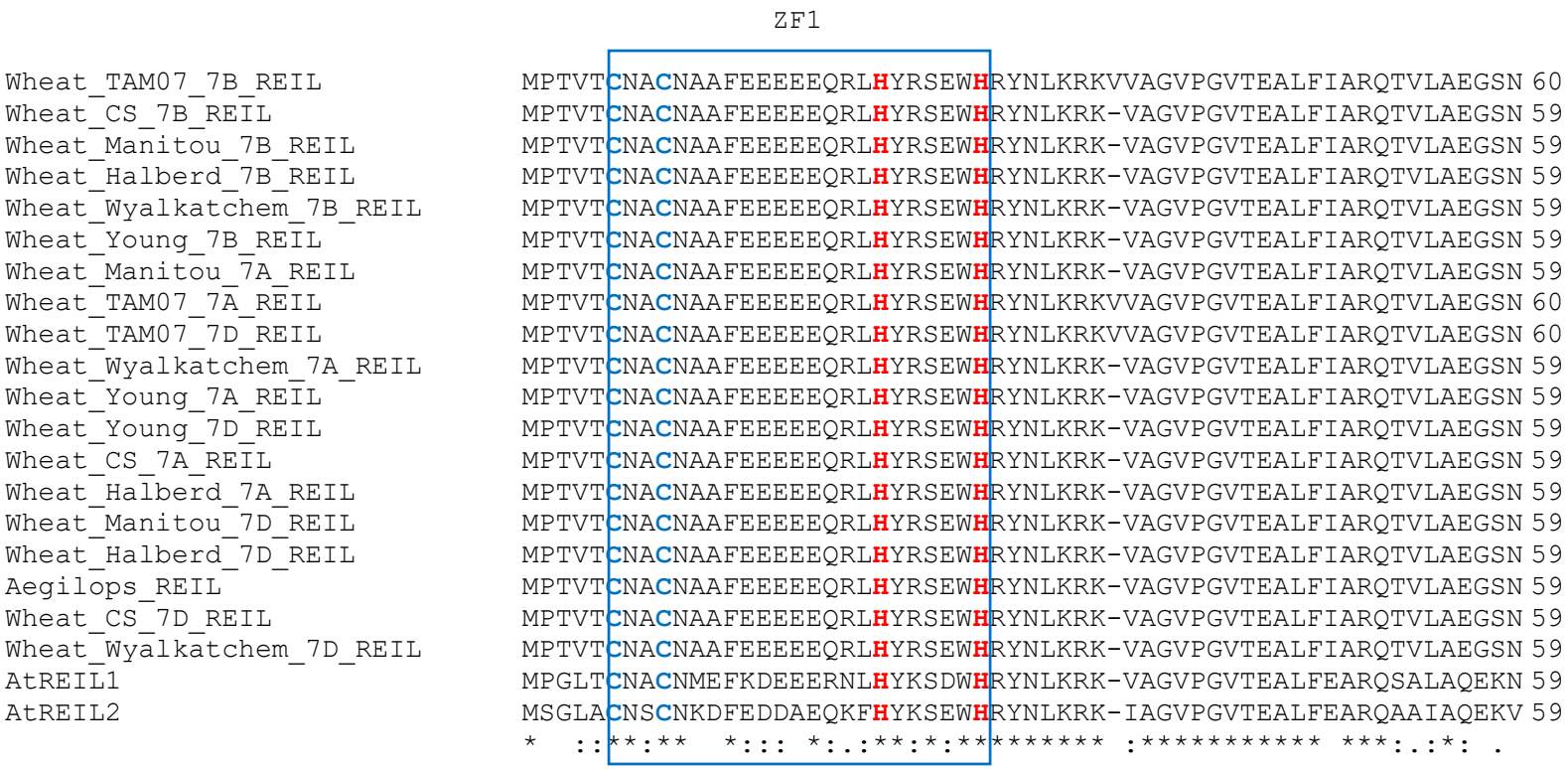
Wheat_Halberd_REIL_7A
MPTVTCNACNAAFEEEEEQRLHYRSEWHRYNLKRKVAGVPGVTEALFIARQTVLAEGS
NSTVAPPMSYSCALCGKGYRSAKAHAQHLTTRSHLLRASQEPNASTAAVVKPLPERVR
RAPSAMEEDEDEDEEEEEEWVEVDPSELESTSNMQVDEDSKSDDEMADLEMLDPSVCF
MCDLKHDNIEDCMIHMHKKHGFFIPDSEYLKDPNGLLIYVGLKVKRDFMCLYCNDRCQ
PFQSLEAVRKHMDGKGHCKLRYGDGGEDEDADLEDFYDYSSSYVDVEGKQLVAAGD
MDNSIELGGGGSELVITSKSEKGRRVTTLGSREFIRYYRQKPRPSVAADRALALSLASSSY
KSMGLVTVQSKEQMVRLKVLRAMNKSGVETMRTKIGMKSNVIRNLPKNVPY*

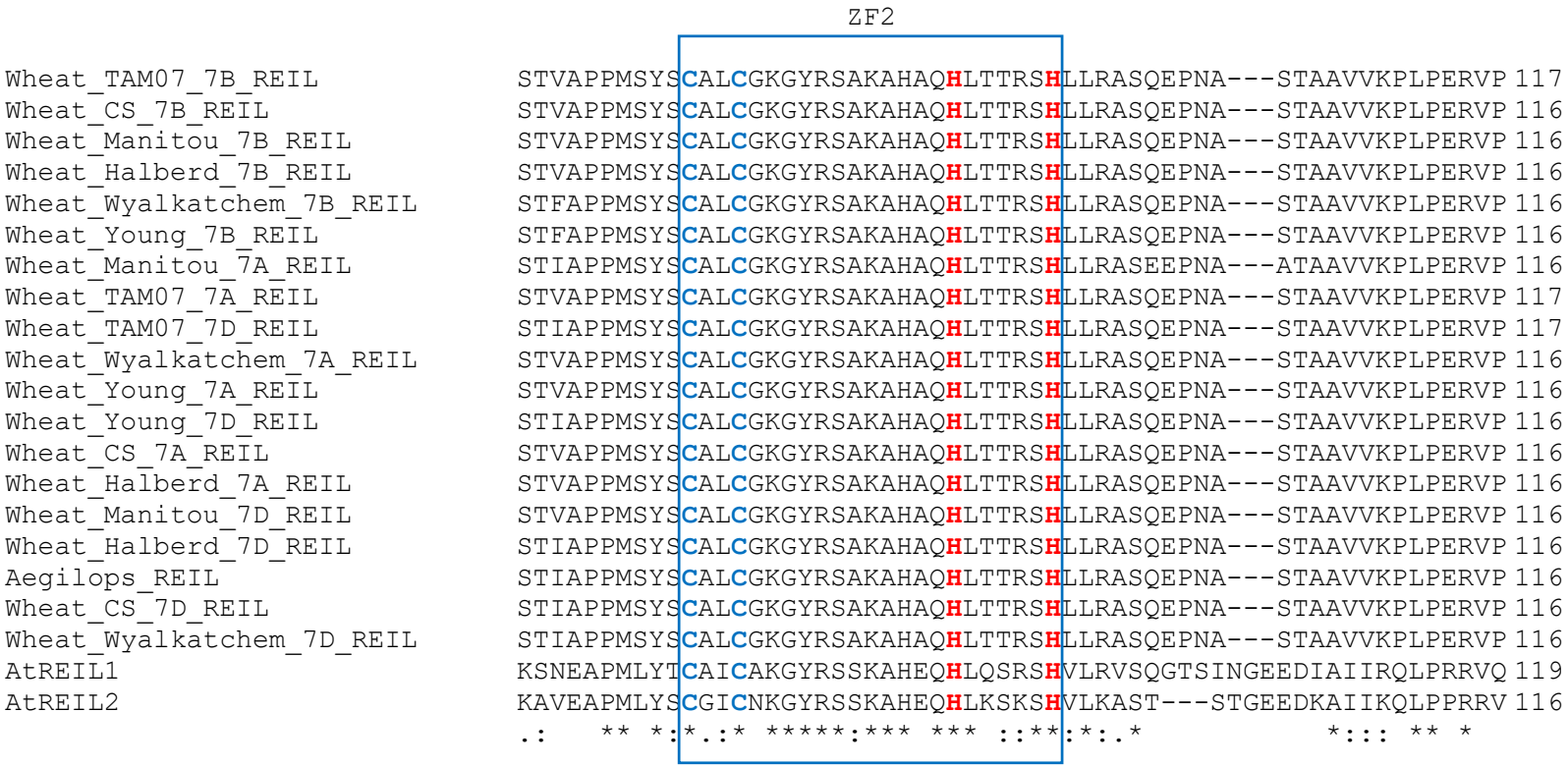
Wheat_Halberd_REIL_7B
MPTVTCNACNAAFEEEEEQRLHYRSEWHRYNLKRKVAGVPGVTEALFIARQTVLAEGS
NSTVAPPMSYSCALCGKGYRSAKAHAQHLTTRSHLLRASQEPNASTAAVVKPLPERVP
RRAPSAMEEDEDEDEDEDEEEEWVEVDPSELESTSNMQVDEDSKSDDEMADLEMLDPS
VCFMCDLKHDNIEDCMIHMHKKHGFFIPDSEYLKDPNGLLIYVGLKVKRDFMCLYCND
RCQPFQSLEAVRKHMDAKGHCKLRYGDGGEDEDADLEDFYDYSSSYVDVEGKQLVAA
GDMDNSIELGGGGSELVITSKSEKGRRVTTLGSREFIRYYRQKPRPSVAADRALALSLAS
SYKSMGLVTVQSKEQMVRLKVLRAMNKSGVETMRTKIGMKSNVIRNLPKNVPY*

Wheat_Halberd_REIL_7D
MPTVTCNACNAAFEEEEEQRLHYRSEWHRYNLKRKVAGVPGVTEALFIARQTVLAEGS
NSTIAPPMSYSCALCGKGYRSAKAHAQHLTTRSHLLRASQEPNASTAAVVKPLPERVPR
RAPSAMEEDEDEDEDEEEEWVEVDPSELESTSNMQVDEDSKSDDEMADLEMLDPSVCF
MCDLKHDNIEDCMIHMHKKHGFFIPDSEYLKDPNGLLIYVGLKVKRDFMCLYCNDRCQ
PFQSLEAVRKHMDAKGHCKLRYGDGGEDEDADLEDFYDYSSSYVDVEGKQLVTAGD
MDNSIELGGGGSELVITSKSEKGRRVTTLGSREFIRYYRQKPRPSVAADRALALSLASSY
KSMGLVTVQSKEQMVRLKVLRAMNKSGVETMRTKIGMKSNVIRNLPKNVPY*

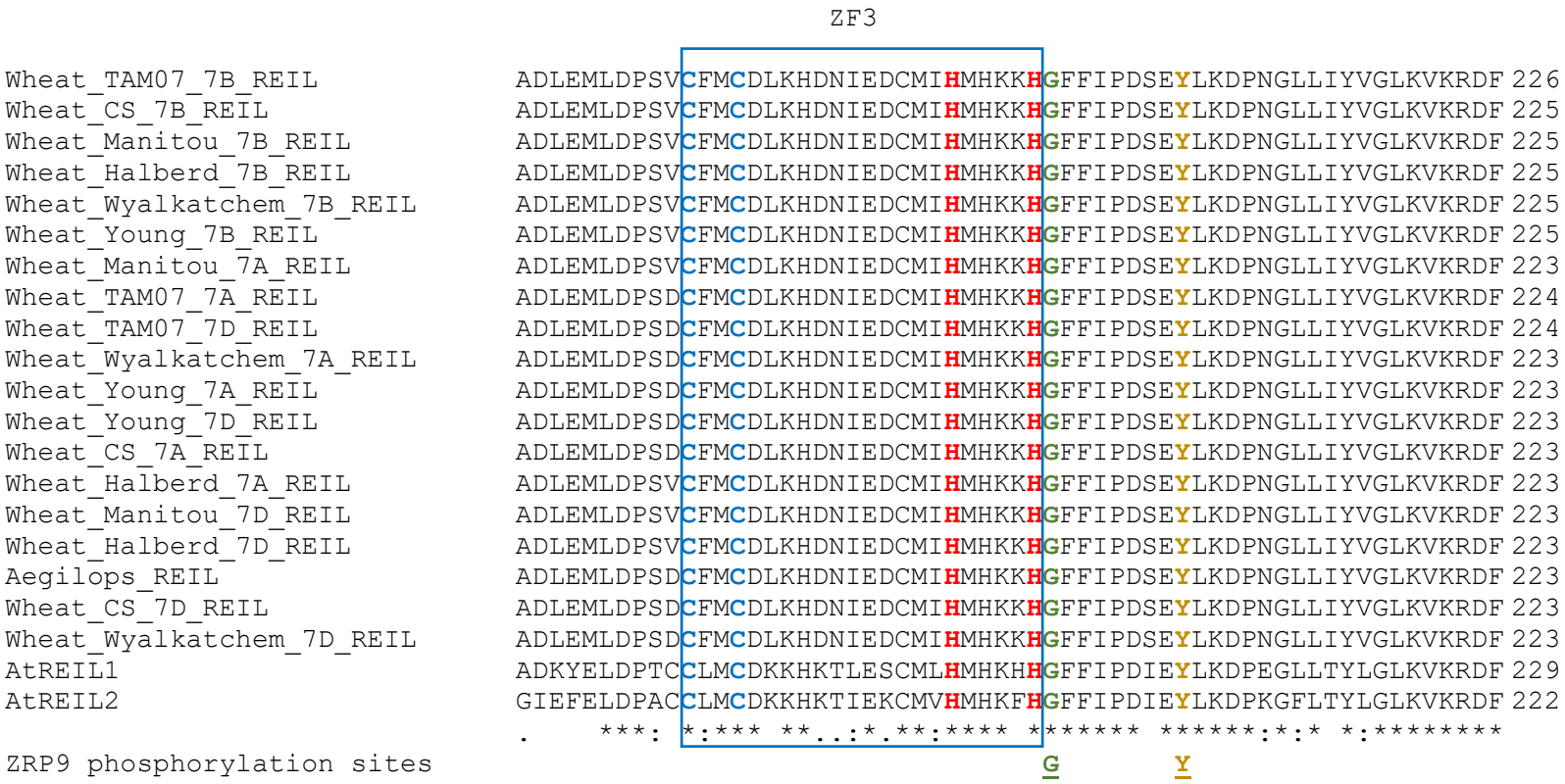
Supplemental Data S5-3. Multiple sequence alignments and phylogenetic analysis of REIL proteins in *Arabidopsis thaliana* and different wheat varieties

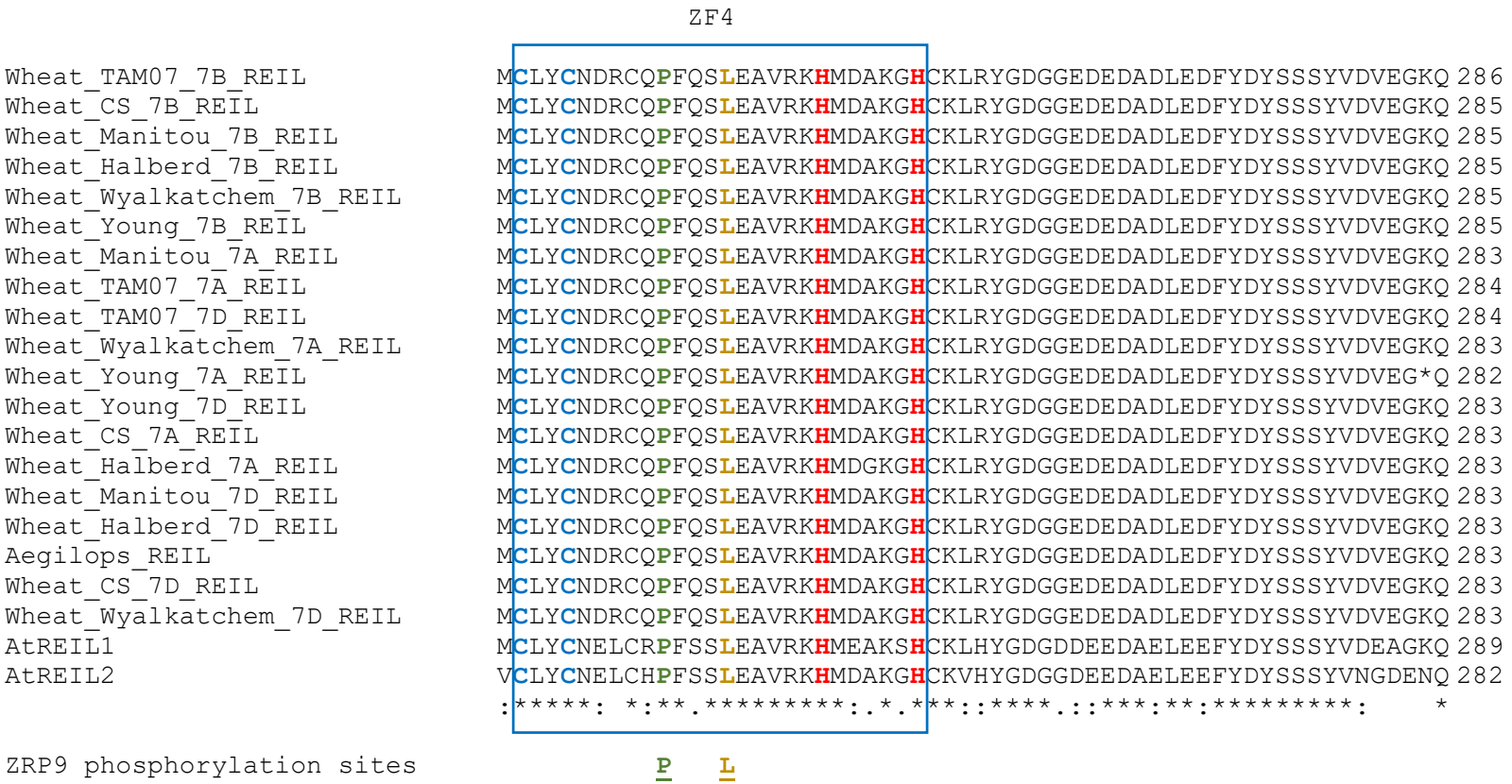
Abbreviation:
At = *Arabidopsis thaliana*
Manitou = Non-hardy spring wheat cultivar, cold-susceptible
CS = Chinese Spring = Spring wheat
TAM107 = Winter wheat, heat and drought tolerant
Aegilops = *Aegilops tauschii*, progenitor of the wheat D genome
Halberd = Australia spring wheat, cold tolerant
Wyalkatchem = Australia spring wheat, cold sensitive
Young = Australia spring wheat, cold tolerant
ZF = zinc finger
ZRP = Zinc Finger-like Protein9
CD = conserved domain

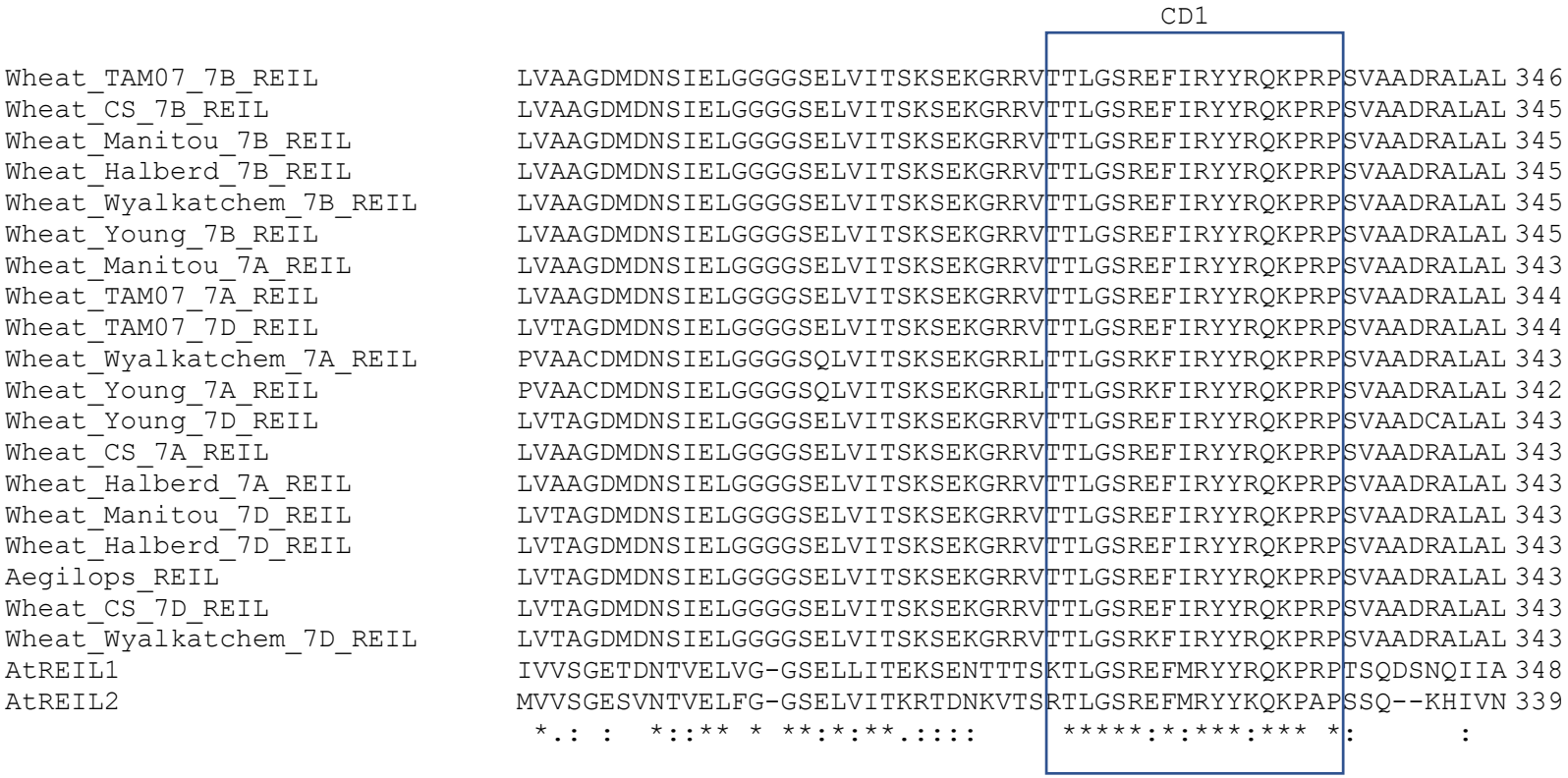

ZF1
Wheat_TAM07_7B_REIL MPTVTCNACNAAFEEEEEQRLHYRSEWHRYNLKRKVVAGVPGVTEALFIARQTVLAEGSN 60
Wheat_CS_7B_REIL MPTVTCNACNAAFEEEEEQRLHYRSEWHRYNLKRK-VAGVPGVTEALFIARQTVLAEGSN 59
Wheat_Manitou_7B_REIL MPTVTCNACNAAFEEEEEQRLHYRSEWHRYNLKRK-VAGVPGVTEALFIARQTVLAEGSN 59
Wheat_Halberd_7B_REIL MPTVTCNACNAAFEEEEEQRLHYRSEWHRYNLKRK-VAGVPGVTEALFIARQTVLAEGSN 59
Wheat_Wyalkatchem_7B_REIL MPTVTCNACNAAFEEEEEQRLHYRSEWHRYNLKRK-VAGVPGVTEALFIARQTVLAEGSN 59
Wheat_Young_7B_REIL MPTVTCNACNAAFEEEEEQRLHYRSEWHRYNLKRK-VAGVPGVTEALFIARQTVLAEGSN 59
Wheat_Manitou_7A_REIL MPTVTCNACNAAFEEEEEQRLHYRSEWHRYNLKRK-VAGVPGVTEALFIARQTVLAEGSN 59
Wheat_TAM07_7A_REIL MPTVTCNACNAAFEEEEEQRLHYRSEWHRYNLKRKVVAGVPGVTEALFIARQTVLAEGSN 60
Wheat_TAM07_7D_REIL MPTVTCNACNAAFEEEEEQRLHYRSEWHRYNLKRKVVAGVPGVTEALFIARQTVLAEGSN 60
Wheat_Wyalkatchem_7A_REIL MPTVTCNACNAAFEEEEEQRLHYRSEWHRYNLKRK-VAGVPGVTEALFIARQTVLAEGSN 59
Wheat_Young_7A_REIL MPTVTCNACNAAFEEEEEQRLHYRSEWHRYNLKRK-VAGVPGVTEALFIARQTVLAEGSN 59
Wheat_Young_7D_REIL MPTVTCNACNAAFEEEEEQRLHYRSEWHRYNLKRK-VAGVPGVTEALFIARQTVLAEGSN 59
Wheat_CS_7A_REIL MPTVTCNACNAAFEEEEEQRLHYRSEWHRYNLKRK-VAGVPGVTEALFIARQTVLAEGSN 59
Wheat_Halberd_7A_REIL MPTVTCNACNAAFEEEEEQRLHYRSEWHRYNLKRK-VAGVPGVTEALFIARQTVLAEGSN 59
Wheat_Manitou_7D_REIL MPTVTCNACNAAFEEEEEQRLHYRSEWHRYNLKRK-VAGVPGVTEALFIARQTVLAEGSN 59
Wheat_Halberd_7D_REIL MPTVTCNACNAAFEEEEEQRLHYRSEWHRYNLKRK-VAGVPGVTEALFIARQTVLAEGSN 59
Aegilops_REIL MPTVTCNACNAAFEEEEEQRLHYRSEWHRYNLKRK-VAGVPGVTEALFIARQTVLAEGSN 59
Wheat_CS_7D_REIL MPTVTCNACNAAFEEEEEQRLHYRSEWHRYNLKRK-VAGVPGVTEALFIARQTVLAEGSN 59
Wheat_Wyalkatchem_7D_REIL MPTVTCNACNAAFEEEEEQRLHYRSEWHRYNLKRK-VAGVPGVTEALFIARQTVLAEGSN 59
AtREIL1 MPGLTCNACNMEFKDEEERNLHYKSDWHRYNLKRK-VAGVPGVTEALFEARQSALAQEKN 59
AtREIL2 MSGLACNSCNKDFEDDAEQKFHYKSEWHRYNLKRK-IAGVPGVTEALFEARQAAIAQEKV 59
* ::**:** *::: *:.:**:*:********* :*********** ***:.:*: .

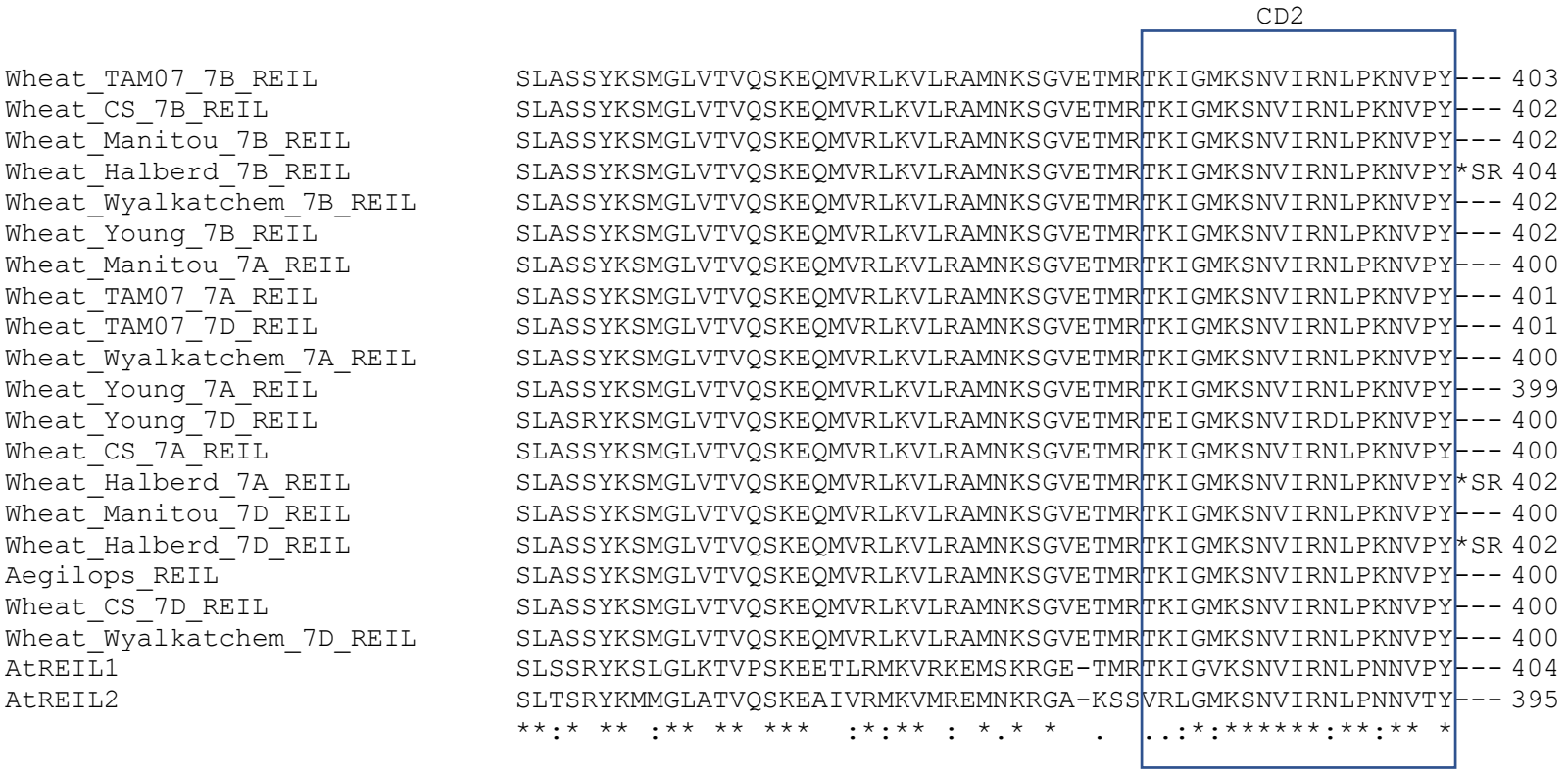

ZF2
Wheat_TAM07_7B_REIL STVAPPMSYSCALCGKGYRSAKAHAQHLTTRSHLLRASQEPNA---STAAVVKPLPERVP 117
Wheat_CS_7B_REIL STVAPPMSYSCALCGKGYRSAKAHAQHLTTRSHLLRASQEPNA---STAAVVKPLPERVP 116
Wheat_Manitou_7B_REIL STVAPPMSYSCALCGKGYRSAKAHAQHLTTRSHLLRASQEPNA---STAAVVKPLPERVP 116
Wheat_Halberd_7B_REIL STVAPPMSYSCALCGKGYRSAKAHAQHLTTRSHLLRASQEPNA---STAAVVKPLPERVP 116
Wheat_Wyalkatchem_7B_REIL STFAPPMSYSCALCGKGYRSAKAHAQHLTTRSHLLRASQEPNA---STAAVVKPLPERVP 116
Wheat_Young_7B_REIL STFAPPMSYSCALCGKGYRSAKAHAQHLTTRSHLLRASQEPNA---STAAVVKPLPERVP 116
Wheat_Manitou_7A_REIL STIAPPMSYSCALCGKGYRSAKAHAQHLTTRSHLLRASEEPNA---ATAAVVKPLPERVP 116
Wheat_TAM07_7A_REIL STVAPPMSYSCALCGKGYRSAKAHAQHLTTRSHLLRASQEPNA---STAAVVKPLPERVP 117
Wheat_TAM07_7D_REIL STIAPPMSYSCALCGKGYRSAKAHAQHLTTRSHLLRASQEPNA---STAAVVKPLPERVP 117
Wheat_Wyalkatchem_7A_REIL STVAPPMSYSCALCGKGYRSAKAHAQHLTTRSHLLRASQEPNA---STAAVVKPLPERVP 116
Wheat_Young_7A_REIL STVAPPMSYSCALCGKGYRSAKAHAQHLTTRSHLLRASQEPNA---STAAVVKPLPERVP 116
Wheat_Young_7D_REIL STIAPPMSYSCALCGKGYRSAKAHAQHLTTRSHLLRASQEPNA---STAAVVKPLPERVP 116
Wheat_CS_7A_REIL STVAPPMSYSCALCGKGYRSAKAHAQHLTTRSHLLRASQEPNA---STAAVVKPLPERVP 116
Wheat_Halberd_7A_REIL STVAPPMSYSCALCGKGYRSAKAHAQHLTTRSHLLRASQEPNA---STAAVVKPLPERVP 116
Wheat_Manitou_7D_REIL STVAPPMSYSCALCGKGYRSAKAHAQHLTTRSHLLRASQEPNA---STAAVVKPLPERVP 116
Wheat_Halberd_7D_REIL STIAPPMSYSCALCGKGYRSAKAHAQHLTTRSHLLRASQEPNA---STAAVVKPLPERVP 116
Aegilops_REIL STIAPPMSYSCALCGKGYRSAKAHAQHLTTRSHLLRASQEPNA---STAAVVKPLPERVP 116
Wheat_CS_7D_REIL STIAPPMSYSCALCGKGYRSAKAHAQHLTTRSHLLRASQEPNA---STAAVVKPLPERVP 116
Wheat_Wyalkatchem_7D_REIL STIAPPMSYSCALCGKGYRSAKAHAQHLTTRSHLLRASQEPNA---STAAVVKPLPERVP 116
AtREIL1 KSNEAPMLYTCAICAKGYRSSKAHEQHLQSRSHVLRVSQGTSINGEEDIAIIRQLPRRVQ 119
AtREIL2 KAVEAPMLYSCGICNKGYRSSKAHEQHLKSKSHVLKAST---STGEEDKAIIKQLPPRRV 116
.: ** *:*.:* *****:*** *** ::**:*:.* *::: ** *

```
Wheat_TAM07_7B_REIL          RRAPSAMEEDEDEDEDEEEEWVEVDPSELEST-------SNMQVDEDS----KSDDEM 166
Wheat_CS_7B_REIL             RRAPSAMEEDEDEDEDEEEEWVEVDPSELEST-------SNMQVDEDS----KSDDEM 165
Wheat_Manitou_7B_REIL        RRAPSAMEEDEDEDEDEEEEWVEVDPSELEST-------SNMQVDEDS----KSDDEM 165
Wheat_Halberd_7B_REIL        RRAPSAMEEDEDEDEDEEEEWVEVDPSELEST-------SNMQVDEDS----KSDDEM 165
Wheat_Wyalkatchem_7B_REIL    CRAPSAMEEDEDEDEDEEEEWVEVDPSELEST-------SNMQVDEDS----KSDDEM 165
Wheat_Young_7B_REIL          CRAPSAMEEDEDEDEDEEEEWVEVDPSELEST-------SNMQVDEDS----KSDDEM 165
Wheat_Manitou_7A_REIL        RRAPSAMEEDEDE--DEDEEEEGVEVDPSELEST-------SNMQVDEDS----NQNDEM 163
Wheat_TAM07_7A_REIL          RRAPSAMEEDEDE--DEEEEEEWVEVDPSELEST-------SNMQVDEDS----KSDDEM 164
Wheat_TAM07_7D_REIL          RRAPSAMEEDEDE--DEDEEEEWVEVDPSELEST-------SNMQVDEDS----KSDDEM 164
Wheat_Wyalkatchem_7A_REIL    RRAPSAMEEDEDE--DEEEEEEWVEVDPSELEST-------SNMQVDEDS----KSDDEM 163
Wheat_Young_7A_REIL          RRAPSAMEEDEDE--DEEEEEEWVEVDPSELEST-------SNMQVDEDS----KSDDEM 163
Wheat_Young_7D_REIL          RRAPSAMEEDEDE--DEDEEEEWVEVDPSELEST-------SNMQVDEDS----KSDDEM 163
Wheat_CS_7A_REIL             RRAPSAMEEDEDE--DEEEEEEWVEVDPSELEST-------SNMQVDEDS----KSDDEM 163
Wheat_Halberd_7A_REIL        RRAPSAMEEDEDE--DEEEEEEWVEVDPSELEST-------SNMQVDEDS----KSDDEM 163
Wheat_Manitou_7D_REIL        RRAPSAMEEDEDE--DEDEEEEGVEVDPSELEST-------SNMQVDEDS----KSDDEM 163
Wheat_Halberd_7D_REIL        RRAPSAMEEDEDE--DEDEEEEWVEVDPSELEST-------SNMQVDEDS----KSDDEM 163
Aegilops_REIL                RRAPSAMEEDEDE--DEDEEEEWVEVDPSELEST-------SNMQVDEDS----KSDDEM 163
Wheat_CS_7D_REIL             RRAPSAMEEDEDE--DEDEEEEWVEVDPSELEST-------SNMQVDEDS----KSDDEM 163
Wheat_Wyalkatchem_7D_REIL    RRAPSAMEEDEDE--DEDEEEEWVEVDPSELEST-------SNMQVDEDS----KSDDEM 163
AtREIL1                      H---------RGSI-DDDSEDEWVEVDSDEELAAEEASDSLSKLNVNESGSAEDMDDDGD 169
AtREIL2                      EKNNTAQL--KGSIEEEESEDEWIEVDSDEDLDAEM----------NEDGEEEDMDED-- 162
                                       ...  :::.*:* :*** .*   :            :*..     .:*
```


ZF3
Wheat_TAM07_7B_REIL ADLEMLDPSVCFMCDLKHDNIEDCMIHMHKKHGFFIPDSEYLKDPNGLLIYVGLKVKRDF 226
Wheat_CS_7B_REIL ADLEMLDPSVCFMCDLKHDNIEDCMIHMHKKHGFFIPDSEYLKDPNGLLIYVGLKVKRDF 225
Wheat_Manitou_7B_REIL ADLEMLDPSVCFMCDLKHDNIEDCMIHMHKKHGFFIPDSEYLKDPNGLLIYVGLKVKRDF 225
Wheat_Halberd_7B_REIL ADLEMLDPSVCFMCDLKHDNIEDCMIHMHKKHGFFIPDSEYLKDPNGLLIYVGLKVKRDF 225
Wheat_Wyalkatchem_7B_REIL ADLEMLDPSVCFMCDLKHDNIEDCMIHMHKKHGFFIPDSEYLKDPNGLLIYVGLKVKRDF 225
Wheat_Young_7B_REIL ADLEMLDPSVCFMCDLKHDNIEDCMIHMHKKHGFFIPDSEYLKDPNGLLIYVGLKVKRDF 225
Wheat_Manitou_7A_REIL ADLEMLDPSVCFMCDLKHDNIEDCMIHMHKKHGFFIPDSEYLKDPNGLLIYVGLKVKRDF 223
Wheat_TAM07_7A_REIL ADLEMLDPSDCFMCDLKHDNIEDCMIHMHKKHGFFIPDSEYLKDPNGLLIYVGLKVKRDF 224
Wheat_TAM07_7D_REIL ADLEMLDPSDCFMCDLKHDNIEDCMIHMHKKHGFFIPDSEYLKDPNGLLIYVGLKVKRDF 224
Wheat_Wyalkatchem_7A_REIL ADLEMLDPSDCFMCDLKHDNIEDCMIHMHKKHGFFIPDSEYLKDPNGLLIYVGLKVKRDF 223
Wheat_Young_7A_REIL ADLEMLDPSDCFMCDLKHDNIEDCMIHMHKKHGFFIPDSEYLKDPNGLLIYVGLKVKRDF 223
Wheat_Young_7D_REIL ADLEMLDPSDCFMCDLKHDNIEDCMIHMHKKHGFFIPDSEYLKDPNGLLIYVGLKVKRDF 223
Wheat_CS_7A_REIL ADLEMLDPSDCFMCDLKHDNIEDCMIHMHKKHGFFIPDSEYLKDPNGLLIYVGLKVKRDF 223
Wheat_Halberd_7A_REIL ADLEMLDPSVCFMCDLKHDNIEDCMIHMHKKHGFFIPDSEYLKDPNGLLIYVGLKVKRDF 223
Wheat_Manitou_7D_REIL ADLEMLDPSVCFMCDLKHDNIEDCMIHMHKKHGFFIPDSEYLKDPNGLLIYVGLKVKRDF 223
Wheat_Halberd_7D_REIL ADLEMLDPSVCFMCDLKHDNIEDCMIHMHKKHGFFIPDSEYLKDPNGLLIYVGLKVKRDF 223
Aegilops_REIL ADLEMLDPSDCFMCDLKHDNIEDCMIHMHKKHGFFIPDSEYLKDPNGLLIYVGLKVKRDF 223
Wheat_CS_7D_REIL ADLEMLDPSDCFMCDLKHDNIEDCMIHMHKKHGFFIPDSEYLKDPNGLLIYVGLKVKRDF 223
Wheat_Wyalkatchem_7D_REIL ADLEMLDPSDCFMCDLKHDNIEDCMIHMHKKHGFFIPDSEYLKDPNGLLIYVGLKVKRDF 223
AtREIL1 ADKYELDPTCCLMCDKKHKTLESCMLHMHKHHGFFIPDIEYLKDPEGLLTYLGLKVKRDF 229
AtREIL2 GIEFELDPACCLMCDKKHKTIEKCMVHMHKFHGFFIPDIEYLKDPKGFLTYLGLKVKRDF 222
. ***: *:*** **..:*.**:**** ******* ******:*:* *:********
ZRP9 phosphorylation sites G Y


ZF4
Wheat_TAM07_7B_REIL MCLYCNDRCQPFQSLEAVRKHMDAKGHCKLRYGDGGEDEDADLEDFYDYSSSYVDVEGKQ 286
Wheat_CS_7B_REIL MCLYCNDRCQPFQSLEAVRKHMDAKGHCKLRYGDGGEDEDADLEDFYDYSSSYVDVEGKQ 285
Wheat_Manitou_7B_REIL MCLYCNDRCQPFQSLEAVRKHMDAKGHCKLRYGDGGEDEDADLEDFYDYSSSYVDVEGKQ 285
Wheat_Halberd_7B_REIL MCLYCNDRCQPFQSLEAVRKHMDAKGHCKLRYGDGGEDEDADLEDFYDYSSSYVDVEGKQ 285
Wheat_Wyalkatchem_7B_REIL MCLYCNDRCQPFQSLEAVRKHMDAKGHCKLRYGDGGEDEDADLEDFYDYSSSYVDVEGKQ 285
Wheat_Young_7B_REIL MCLYCNDRCQPFQSLEAVRKHMDAKGHCKLRYGDGGEDEDADLEDFYDYSSSYVDVEGKQ 285
Wheat_Manitou_7A_REIL MCLYCNDRCQPFQSLEAVRKHMDAKGHCKLRYGDGGEDEDADLEDFYDYSSSYVDVEGKQ 283
Wheat_TAM07_7A_REIL MCLYCNDRCQPFQSLEAVRKHMDAKGHCKLRYGDGGEDEDADLEDFYDYSSSYVDVEGKQ 284
Wheat_TAM07_7D_REIL MCLYCNDRCQPFQSLEAVRKHMDAKGHCKLRYGDGGEDEDADLEDFYDYSSSYVDVEGKQ 284
Wheat_Wyalkatchem_7A_REIL MCLYCNDRCQPFQSLEAVRKHMDAKGHCKLRYGDGGEDEDADLEDFYDYSSSYVDVEGKQ 283
Wheat_Young_7A_REIL MCLYCNDRCQPFQSLEAVRKHMDAKGHCKLRYGDGGEDEDADLEDFYDYSSSYVDVEG*Q 282
Wheat_Young_7D_REIL MCLYCNDRCQPFQSLEAVRKHMDAKGHCKLRYGDGGEDEDADLEDFYDYSSSYVDVEGKQ 283
Wheat_CS_7A_REIL MCLYCNDRCQPFQSLEAVRKHMDAKGHCKLRYGDGGEDEDADLEDFYDYSSSYVDVEGKQ 283
Wheat_Halberd_7A_REIL MCLYCNDRCQPFQSLEAVRKHMDGKGHCKLRYGDGGEDEDADLEDFYDYSSSYVDVEGKQ 283
Wheat_Manitou_7D_REIL MCLYCNDRCQPFQSLEAVRKHMDAKGHCKLRYGDGGEDEDADLEDFYDYSSSYVDVEGKQ 283
Wheat_Halberd_7D_REIL MCLYCNDRCQPFQSLEAVRKHMDAKGHCKLRYGDGGEDEDADLEDFYDYSSSYVDVEGKQ 283
Aegilops_REIL MCLYCNDRCQPFQSLEAVRKHMDAKGHCKLRYGDGGEDEDADLEDFYDYSSSYVDVEGKQ 283
Wheat_CS_7D_REIL MCLYCNDRCQPFQSLEAVRKHMDAKGHCKLRYGDGGEDEDADLEDFYDYSSSYVDVEGKQ 283
Wheat_Wyalkatchem_7D_REIL MCLYCNDRCQPFQSLEAVRKHMDAKGHCKLRYGDGGEDEDADLEDFYDYSSSYVDVEGKQ 283
AtREIL1 MCLYCNELCRPFSSLEAVRKHMEAKSHCKLHYGDGDDEEDAELEEFYDYSSSYVDEAGKQ 289
AtREIL2 VCLYCNELCHPFSSLEAVRKHMDAKGHCKVHYGDGGDEEDAELEEFYDYSSSYVNGDENQ 282
:*****: *:**.*********:.*.***::****.::***:**:*********: *
ZRP9 phosphorylation sites P L


CD1
Wheat_TAM07_7B_REIL LVAAGDMDNSIELGGGGSELVITSKSEKGRRVTTLGSREFIRYYRQKPRPSVAADRALAL 346
Wheat_CS_7B_REIL LVAAGDMDNSIELGGGGSELVITSKSEKGRRVTTLGSREFIRYYRQKPRPSVAADRALAL 345
Wheat_Manitou_7B_REIL LVAAGDMDNSIELGGGGSELVITSKSEKGRRVTTLGSREFIRYYRQKPRPSVAADRALAL 345
Wheat_Halberd_7B_REIL LVAAGDMDNSIELGGGGSELVITSKSEKGRRVTTLGSREFIRYYRQKPRPSVAADRALAL 345
Wheat_Wyalkatchem_7B_REIL LVAAGDMDNSIELGGGGSELVITSKSEKGRRVTTLGSREFIRYYRQKPRPSVAADRALAL 345
Wheat_Young_7B_REIL LVAAGDMDNSIELGGGGSELVITSKSEKGRRVTTLGSREFIRYYRQKPRPSVAADRALAL 345
Wheat_Manitou_7A_REIL LVAAGDMDNSIELGGGGSELVITSKSEKGRRVTTLGSREFIRYYRQKPRPSVAADRALAL 343
Wheat_TAM07_7A_REIL LVAAGDMDNSIELGGGGSELVITSKSEKGRRVTTLGSREFIRYYRQKPRPSVAADRALAL 344
Wheat_TAM07_7D_REIL LVTAGDMDNSIELGGGGSELVITSKSEKGRRVTTLGSREFIRYYRQKPRPSVAADRALAL 344
Wheat_Wyalkatchem_7A_REIL PVAACDMDNSIELGGGGSQLVITSKSEKGRRLTTLGSRKFIRYYRQKPRPSVAADRALAL 343
Wheat_Young_7A_REIL PVAACDMDNSIELGGGGSQLVITSKSEKGRRLTTLGSRKFIRYYRQKPRPSVAADRALAL 342
Wheat_Young_7D_REIL LVTAGDMDNSIELGGGGSELVITSKSEKGRRVTTLGSREFIRYYRQKPRPSVAADCALAL 343
Wheat_CS_7A_REIL LVAAGDMDNSIELGGGGSELVITSKSEKGRRVTTLGSREFIRYYRQKPRPSVAADRALAL 343
Wheat_Halberd_7A_REIL LVAAGDMDNSIELGGGGSELVITSKSEKGRRVTTLGSREFIRYYRQKPRPSVAADRALAL 343
Wheat_Manitou_7D_REIL LVTAGDMDNSIELGGGGSELVITSKSEKGRRVTTLGSREFIRYYRQKPRPSVAADRALAL 343
Wheat_Halberd_7D_REIL LVTAGDMDNSIELGGGGSELVITSKSEKGRRVTTLGSREFIRYYRQKPRPSVAADRALAL 343
Aegilops_REIL LVTAGDMDNSIELGGGGSELVITSKSEKGRRVTTLGSREFIRYYRQKPRPSVAADRALAL 343
Wheat_CS_7D_REIL LVTAGDMDNSIELGGGGSELVITSKSEKGRRVTTLGSREFIRYYRQKPRPSVAADRALAL 343
Wheat_Wyalkatchem_7D_REIL LVTAGDMDNSIELGGGGSELVITSKSEKGRRVTTLGSRKFIRYYRQKPRPSVAADRALAL 343
AtREIL1 IVVSGETDNTVELVG-GSELLITEKSENTTTSKTLGSREFMRYYRQKPRPTSQDSNQIIA 348
AtREIL2 MVVSGESVNTVELFG-GSELVITKRTDNKVTSRTLGSREFMRYYKQKPAPSSQ--KHIVN 339


CD2
Wheat_TAM07_7B_REIL SLASSYKSMGLVTVQSKEQMVRLKVLRAMNKSGVETMRTKIGMKSNVIRNLPKNVPY--- 403
Wheat_CS_7B_REIL SLASSYKSMGLVTVQSKEQMVRLKVLRAMNKSGVETMRTKIGMKSNVIRNLPKNVPY--- 402
Wheat_Manitou_7B_REIL SLASSYKSMGLVTVQSKEQMVRLKVLRAMNKSGVETMRTKIGMKSNVIRNLPKNVPY--- 402
Wheat_Halberd_7B_REIL SLASSYKSMGLVTVQSKEQMVRLKVLRAMNKSGVETMRTKIGMKSNVIRNLPKNVPY*SR 404
Wheat_Wyalkatchem_7B_REIL SLASSYKSMGLVTVQSKEQMVRLKVLRAMNKSGVETMRTKIGMKSNVIRNLPKNVPY--- 402
Wheat_Young_7B_REIL SLASSYKSMGLVTVQSKEQMVRLKVLRAMNKSGVETMRTKIGMKSNVIRNLPKNVPY--- 402
Wheat_Manitou_7A_REIL SLASSYKSMGLVTVQSKEQMVRLKVLRAMNKSGVETMRTKIGMKSNVIRNLPKNVPY--- 400
Wheat_TAM07_7A_REIL SLASSYKSMGLVTVQSKEQMVRLKVLRAMNKSGVETMRTKIGMKSNVIRNLPKNVPY--- 401
Wheat_TAM07_7D_REIL SLASSYKSMGLVTVQSKEQMVRLKVLRAMNKSGVETMRTKIGMKSNVIRNLPKNVPY--- 401
Wheat_Wyalkatchem_7A_REIL SLASSYKSMGLVTVQSKEQMVRLKVLRAMNKSGVETMRTKIGMKSNVIRNLPKNVPY--- 400
Wheat_Young_7A_REIL SLASSYKSMGLVTVQSKEQMVRLKVLRAMNKSGVETMRTKIGMKSNVIRNLPKNVPY--- 399
Wheat_Young_7D_REIL SLASRYKSMGLVTVQSKEQMVRLKVLRAMNKSGVETMRTEIGMKSNVIRDLPKNVPY--- 400
Wheat_CS_7A_REIL SLASSYKSMGLVTVQSKEQMVRLKVLRAMNKSGVETMRTKIGMKSNVIRNLPKNVPY--- 400
Wheat_Halberd_7A_REIL SLASSYKSMGLVTVQSKEQMVRLKVLRAMNKSGVETMRTKIGMKSNVIRNLPKNVPY*SR 402
Wheat_Manitou_7D_REIL SLASSYKSMGLVTVQSKEQMVRLKVLRAMNKSGVETMRTKIGMKSNVIRNLPKNVPY--- 400
Wheat_Halberd_7D_REIL SLASSYKSMGLVTVQSKEQMVRLKVLRAMNKSGVETMRTKIGMKSNVIRNLPKNVPY*SR 402
Aegilops_REIL SLASSYKSMGLVTVQSKEQMVRLKVLRAMNKSGVETMRTKIGMKSNVIRNLPKNVPY--- 400
Wheat_CS_7D_REIL SLASSYKSMGLVTVQSKEQMVRLKVLRAMNKSGVETMRTKIGMKSNVIRNLPKNVPY--- 400
Wheat_Wyalkatchem_7D_REIL SLASSYKSMGLVTVQSKEQMVRLKVLRAMNKSGVETMRTKIGMKSNVIRNLPKNVPY--- 400
AtREIL1 SLSSRYKSLGLKTVPSKEETLRMKVRKEMSKRGE-TMRTKIGVKSNVIRNLPNNVPY--- 404
AtREIL2 SLTSRYKMMGLATVQSKEAIVRMKVMREMNKRGA-KSSVRLGMKSNVIRNLPNNVTY--- 395
:* ** : ** *** :*:** : *.* * . ..:*:******:**:** *

Supplemental Table S5-1. Primers used in this study.

Gene	Primers	Forward (Fw)/Reverse (Rv)	T_m (meting temperature, °C)
Ubiquitin	5' CCTTCACTTGGTTCTCCGTCT 3'	Fw	64.4
	5' AACGACCAGGACGACAGACACA 3'	Rv	69.2
*REIL*7A	5' CAGCTGTGCTCTTTGTGGAA 3'	Fw	64.2
	5' TTCCTCCTCCTCCTCATCCT 3'	Rv	64.1
*REIL*7B	5' GGCTACAGGAGTGCAAAAGC 3'	Fw	63.8
	5' CAACCCACTCTTCCTCCTCA 3'	Rv	64.3
*REIL*7D	5' CAGCTGTGCTCTTTGTGGAA 3'	Fw	64.2
	5' CCTCCTCATCCTCATCCTCA 3'	Rv	64.3

Supplemental Table S5-2. Relative expression of *REIL* compared to Ubiquitin in each of the wheat variety.

REIL gene	Wheat variety and condition	*REIL* expression relative to Ubiquitin (value averaged from three technical replicates)	Standard error mean (sem)
7A	Wyalkatchem_Control_1 (Biological replicate 1)	1.13E+00	0.098029612
7A	Wyalkatchem_Control_2 (Biological replicate 2)	3.98E-01	0.001248105
7A	Wyalkatchem_Cold-treated_1 (Biological replicate 1)	1.37E+00	0.049236225
7A	Wyalkatchem_Cold-treated_2 (Biological replicate 2)	7.54E-01	0.036481667
7A	Young_Control_1 (Biological replicate 1)	6.73E-01	0.010811916
7A	Young_Control_2 (Biological replicate 2)	1.13E+00	0.020408882
7A	Young_Cold-treated_1 (Biological replicate 1)	1.11E+00	0.003651271
7A	Young_Cold-treated_2 (Biological replicate 2)	6.21E-01	0.012017242
7B	Wyalkatchem_Control_1 (Biological replicate 1)	1.12E+00	0.069304983
7B	Wyalkatchem_Control_2 (Biological replicate 2)	4.58E-01	0.016691983
7B	Wyalkatchem_Cold-treated_1 (Biological replicate 1)	1.57E+00	0.1082681

7B	Wyalkatchem_Cold-treated_2 (Biological replicate 2)	5.75E-01	0.039048516
7B	Young_Control_1 (Biological replicate 1)	6.43E-01	0.038109898
7B	Young_Control_2 (Biological replicate 2)	1.09E+00	0.037980738
7B	Young_Cold-treated_1 (Biological replicate 1)	1.29E+00	0.049931456
7B	Young_Cold-treated_2 (Biological replicate 2)	7.23E-01	0.027574101
7D	Wyalkatchem_Control_1 (Biological replicate 1)	1.10E+00	0.076212256
7D	Wyalkatchem_Control_2 (Biological replicate 2)	4.12E-01	0.020767696
7D	Wyalkatchem_Cold-treated_1 (Biological replicate 1)	1.39E+00	0.088559918
7D	Wyalkatchem_Cold-treated_2 (Biological replicate 2)	6.10E-01	0.045414588
7D	Young_Control_1 (Biological replicate 1)	7.10E-01	0.028117885
7D	Young_Control_2 (Biological replicate 2)	1.23E+00	0.049266037
7D	Young_Cold-treated_1 (Biological replicate 1)	1.22E+00	0.020434002
7D	Young_Cold-treated_2 (Biological replicate 2)	6.99E-01	0.013274354

Metabolomics (2019) 15:144
https://doi.org/10.1007/s11306-019-1606-2

ORIGINAL ARTICLE

Phenotyping reproductive stage chilling and frost tolerance in wheat using targeted metabolome and lipidome profiling

Bo Eng Cheong[1] · William Wing Ho Ho[1,5] · Ben Biddulph[3] · Xiaomei Wallace[2] · Tina Rathjen[2] · Thusitha W. T. Rupasinghe[4] · Ute Roessner[1,4] · Rudy Dolferus[2]

Received: 12 February 2019 / Accepted: 10 October 2019
© The Author(s) 2019

Abstract

Introduction Frost events lead to A$360 million of yield losses annually to the Australian wheat industry, making improvement of chilling and frost tolerance an important trait for breeding.

Objectives This study aimed to use metabolomics and lipidomics to explore genetic variation in acclimation potential to chilling and to identify metabolite markers for chilling tolerance in wheat.

Methods We established a controlled environment screening assay that is able to reproduce field rankings of wheat germplasm for chilling and frost tolerance. This assay, together with targeted metabolomics and lipidomics approaches, were used to compare metabolite and lipid levels in flag leaves of two wheat varieties with contrasting chilling tolerance.

Results The sensitive variety Wyalkatchem showed a strong reduction in amino acids after the first cold night, followed by accumulation of osmolytes such as fructose, glucose, putrescine and shikimate over a 4-day period. Accumulation of osmolytes is indicative of acclimation to water stress in Wyalkatchem. This response was not observed for tolerant variety Young. The two varieties also displayed significant differences in lipid accumulation. Variation in two lipid clusters, resulted in a higher unsaturated to saturated lipid ratio in Young after 4 days cold treatment and the lipids PC(34:0), PC(34:1), PC(35:1), PC(38:3), and PI(36:4) were the main contributors to the unsaturated to saturated ratio change. This indicates that Young may have superior ability to maintain membrane fluidity following cold exposure, thereby avoiding membrane damage and water stress observed for Wyalkatchem.

Conclusion Our study suggests that metabolomics and lipidomics markers could be used as an alternative phenotyping method to discriminate wheat varieties with differences in cold acclimation.

Keywords Cold tolerance · Flowering · Lipid · Metabolite · Phenotyping · Wheat

Electronic supplementary material The online version of this article (https://doi.org/10.1007/s11306-019-1606-2) contains supplementary material, which is available to authorized users.

✉ Rudy Dolferus
rudy.dolferus@csiro.au

Bo Eng Cheong
cheongb@student.unimelb.edu.au

William Wing Ho Ho
whho@unimelb.edu.au

Ben Biddulph
ben.biddulph@dpird.wa.gov.au

Xiaomei Wallace
xiaomei.wallace@csiro.au

Tina Rathjen
tina.rathjen@csiro.au

Thusitha W. T. Rupasinghe
tru@unimelb.edu.au

Ute Roessner
u.roessner@unimelb.edu.au

[1] School of BioSciences, The University of Melbourne, Melbourne, VIC 3010, Australia

[2] CSIRO Agriculture & Food, GPO Box 1700, Canberra, ACT 2601, Australia

[3] Department of Primary Industries and Regional Development, 3 Baron Hay Court, South Perth, WA 6151, Australia

[4] Metabolomics Australia, School of BioSciences, The University of Melbourne, Melbourne, VIC 3010, Australia

[5] Melbourne Integrative Genomics, Schools of Mathematics and Statistics and of BioSciences, The University of Melbourne, Melbourne, VIC 3010, Australia

Published online: 20 October 2019

1 Introduction

For important food crops, such as cereals, chilling and frost are major constraints to yield and productivity (Gray et al. 1997; Leff et al. 2004; Lobell and Gourdji 2012). Climate change affects atmospheric conditions, increasing the probability of weather extremes. This is likely to result in more frequent crop losses in the future (Lobell and Gourdji 2012). Warmer winters and more frequent spring frosts have increasingly affected wheat yields in China between 1961 and 2000 (Li et al. 2014, 2015). In Southern Australia, spring frosts have become significantly more frequent since 1960 and the overall length of the frost season has increased by 1 month, resulting in more frequent occurrences of frost damage to wheat crops (Crimp et al. 2015; Zheng et al. 2015). In Australia, spring wheat varieties are sown in autumn, flower in early spring and are harvested in late spring (Zheng et al. 2015). Radiant frosts in spring are caused by heat loss from the soil surface to the night sky on cold and dry days with clear skies. This leads to a rapid cooling of the crop canopy and associated frost damage if crops are at susceptible stages (Marcellos and Single 1975). The associated increase in risk of frost damage requires wheat cultivars with improved frost tolerance. Reoccurring frost events cost the Australian wheat industry an estimated A$360 million of direct and indirect yield losses annually (March et al. 2015; Zheng et al. 2015).

Above zero degree temperatures (chilling; typically 10 to 0 °C) cause an acclimation or adaptation response in plant tissues. Below zero degree temperatures (frosts) cause an additional challenge to plant tissues due to the formation of ice crystals. Quantitative and/or qualitative differences in the acclimation response during the chilling period may provide various degrees of frost tolerance. Wheat tolerates frosts during vegetative growth, but becomes more frost-sensitive during flowering in early spring. Chilling conditions during flowering can cause pollen sterility and grain loss in wheat (Demotes-Mainard et al. 1996; Rerkasem 1996; Subedi et al. 1998a, b, 2000; Chakrabarti et al. 2011). Exposure of plants to chilling conditions ("hardening") enhances freezing tolerance in a process called cold acclimation (Palta and Weiss 1993; Guy 1999; Tomashow 1999; Wanner and Junttila 1999). In wheat, cold acclimation during reproductive stages remains poorly characterised. Although most genes involved in cold acclimation are expressed after 24 h of exposure (Monroy et al. 2007; Kurepin et al. 2013), the full establishment of the response may require prolonged or repeated exposures to cold (Levitt 1980; Guy 1990; Ruelland et al. 2009). Cold acclimation can be lost during warmer fluctuating winter conditions, but it remains unclear whether re-acclimation can occur following de-acclimation (Rapacz 2002; Kalberer et al. 2006; Vitamvas and Prasil 2008), particularly after crops transition into reproductive stages. Loss of cold acclimation during spring makes wheat crops particularly vulnerable to unexpected frosts (Frederiks et al. 2011, 2012). Cold temperatures, in combination with increasing day-length, accelerate the transition from vegetative to reproductive growth as the vernalization and photoperiod requirements are met (Fowler et al. 2001; Limin and Fowler 2006). Proper management of sowing time and phenology of wheat (flowering time, response to day-length) minimise frost damage, but the unpredictability of frost events requires genetic improvement in frost tolerance to manage yield stability (Limin and Fowler 2006; Zheng et al. 2015), particulary in Southern Australia where the length of the frost season is increasing (Crimp et al. 2015) and crop development can not be delayed further.

Induction of cold acclimation and freezing tolerance involves physiological and biochemical changes in plants (Wanner and Junttila 1999). Cold-tolerant plants have a higher proportion of unsaturated fatty acids in the plasma membrane and are better at maintaining membrane fluidity at lower temperatures (Vigh et al. 1979; Steponkus et al. 1993; Bohn et al. 2007). Plants tend to increase the degree of fatty acid unsaturation and the content of phospholipids when they are exposed to low, non-freezing temperatures (Welti et al. 2007). In Arabidopsis, phophatidylcholines (PC), phosphatidylethanolamines (PE), phosphatidylglycerols (PG) and monogalactosyldiacylglycerols (MGDG) containing two polyunsaturated acyl species, including 36:5 (18:2/18:3) and 36:6 (di-18:3), increased during cold acclimation (Welti et al. 2002). Chilling conditions also lead to the accumulation of osmolytes, compatible solutes or cryoprotectants such as sugars (fructose, glucose, trehalose, raffinose) and amino acids or amines such as proline and gamma-aminobutyric acid (GABA). This response is not specific to chilling and is also induced by other stressors that cause osmotic stress (e.g., drought, salinity, heat; Beck et al. 2007). Apart from playing a role in compensating for water loss during osmotic adjustment, osmolytes are also important for protecting membrane integrity and scavenging of reactive oxygen species (Guy 1999; Wanner and Junttila 1999; Smallwood and Bowles 2002; Valluru et al. 2008; Javadian et al. 2010; Verslues et al. 2006; Janmohammadi 2012). Cold acclimation in spring and winter *Triticum monococcum* lines affects the steady-state levels of phytohormones, including abscisic acid (ABA), salicylic acid, ethylene, jasmonic acid, gibberellins, cytokinins and auxin (Horvath et al. 2007; Machakova et al. 1989; Vanková et al. 2014). Increased ABA levels are correlated with cold-induced water deficit in plants. ABA is implicated in plasma membrane lipid alterations during cold stress (Bohn

et al. 2007). ABA induces the expression of phospholipase D (AtPLD) in Arabidopsis, causing hydrolysis of structural phospholipids (Zhang et al. 2005; Meijer and Munnik 2003).

Studying quantitative and qualitative differences in metabolite and lipid accumulation during cold acclimation is an important tool to understand chilling and frost tolerance in wheat. Targeted metabolomics and lipidomics using gas/liquid chromatography, coupled to a triple-quadruple MS (GC/LC-QqQ-MS) approach offers higher sensitivity, selectivity, reproducibility and robust quantification over a broad dynamic range (Douglas 2009; Sumner et al. 2015; Jorge et al. 2016). Dias et al. (2015) were able to quantify 76 primary metabolites (sugars, organic acids and amino acids/amines) in two chickpea cultivars with contrasting responses to salinity using GC- and LC-QqQ-MS. Natera et al. (2016) reported the quantification of 63 phospholipids in the roots of two barley genotypes with contrasting responses to salinity using LC-QqQ-MS. We therefore applied these approaches to study the cold acclimation response in wheat.

Reliable phenotyping for chilling and frost tolerance in the field is challenging due to unpredictability, variability in severity, duration, and timing of these events. In this study we established a reliable controlled environment (CE) phenotyping method to discriminate genetic variation in cold and frost tolerance in wheat. This CE phenotyping method, together with targeted metabolomics and lipidomics approaches, were then used to identify quantitative and qualitative differences in metabolite and lipid accumulation in two wheat varieties with differential chilling-tolerance. As starting tissue we used flag leaves from wheat plants harvested at the young microspore (YM) stage of pollen development, the reproductive stage with highest sensitivity to various abiotic stresses -including cold (Dolferus et al. 2013). The results indicate that two Australian spring wheat varieties with contrasting chilling tolerance (cold-tolerant Young and cold-sensitive Wyalkatchem) differed significantly in the accumulation of metabolites (amino acids, osmolytes) and levels of unsaturated versus saturated membrane lipids, indicating that metabolite profiling could be used to select wheat varieties with differences in cold acclimation.

2 Materials and methods

2.1 Controlled environment wheat growing, cold treatment and sample collection

Wheat varieties Wyalkatchem (cold-sensitive) and Young (cold-tolerant) used in this study were obtained via the National Frost Initiative, Australia (http://www.nvtonline.com.au/frost/). Seeds were sown in trays (36 × 25 × 13 cm, L × W × H; 15 plants/tray) filled with soil (100% composted soil, containing 1 g l^{-1} fertilizer: 14.4% N/6.6% P/5% K). Plants were grown in the glasshouse under natural lighting conditions and controlled temperature regime (24/16 °C, L/D); watering occurred once daily. The young microspore (YM) stage of pollen development was determined using auricle distance measurements (Ji et al. 2010; Dolferus et al. 2013). The Zadoks scale was used to determine growth stages other than YM (Zadoks et al. 1974). Cold treatments were carried out at the YM stage in a Conviron PGC 20 growth chamber. The treatment cycle consisted of 12 h incubation at 21 °C in the light, followed by a linear cooling gradient descending from 21 to − 3 °C over a period of 4 h, then followed by a continuous cold period at − 3 °C over 8 h in the dark (12/12 light/dark cycle, using 400 µmol m^{-2} s^{-1} light intensity; see Fig. S1a). The whole experiment was run over four consecutive days and samples were harvested in the morning immediately after a cold treatment at day one (TP_1—short cold stress), day four (TP_3—prolonged cold stress), and corresponding day-time samples were harvested 6 h into the normal temperature (21 °C) light cycle after day one and day four respectively (TP_2 and TP_4; see Fig. S1f). One tray of plants was used as untreated control to harvest T_0 samples. In the trays for stress treatments, tillers that reached the YM stage were tagged before cold-treatment. Three flag leaves were harvested from three different tagged plants at each of the time points (TP_0 to TP_4) and pooled as one replicate for metabolite measurements. For each time point, we harvested four biological replicates per variety (n = 4) for all the metabolite and lipid analyses, except for phytohormone analyses where three replicates were used (n = 3). For sterility measurements, plants were returned to the glasshouse after cold treatment, and spike grain number of tagged tillers was determined at maturity.

2.2 Analysis of sugars, organic acids, amino acids, amines and phytohormones

All chemicals and solvents for metabolite measurements were purchased from Sigma-Aldrich (Australia) and were of analytical or mass spectrometry grades. For sugars, organic acids and amines, tissue extraction was performed according to Dias et al. (2015), with some modifications. Aliquots of frozen leaf material (50 mg per replicate × four replicates) were weighed into Cryomill tubes (Precellys 24, Bertin Technologies). Subsequently, 500 µl of methanol containing 4% of internal standard (from a stock solution containing 0.5 mg ml^{-1} of $^{12}C_6$-sorbitol and 0.5 mg ml^{-1} $^{13}C_5$-^{15}N-L-valine) was added to the samples, followed by vortexing for 30 s and homogenization at − 10 °C using a Cryomill (3 × 45 s at 6100 rpm). The samples were then extracted for 15 min at 30 °C in a thermomixer at 850 rpm, and subsequently centrifuged for 5 min at 4 °C at 13,000 rpm. The supernatants were transferred into new tubes, and 500 µl of

water containing 0.2% formic acid was added into the Cryomill tubes containing the previously ground tissue pellet. The samples were vortex-mixed for 30 s, and centrifuged at 13,000 rpm for 5 min at 4 °C. The supernatants were then transferred and combined with the methanolic extracts from the previous centrifugation. A 200 µl of dichloromethane was added to the combined supernatants to separate chlorophylls. The combined supernatants were vortexed, centrifuged at 13,000 rpm for 2 min at 4 °C. The supernatants were taken and stored at − 80 °C for subsequent sugars, organic acids and amine analyses.

For the analysis of sugars and organic acids, 5 µl and 125 µl aliquots of the supernatants was transferred into new glass vial inserts, and dried *in vacuo* for sugars and organic acids analyses using GC-QqQ-MS. Prior to the GC-QqQ-MS analysis, the dried extracts were derivatized with methoxyamine hydrochloride in pyridine and bis-(trimethylsilyl)-trifluoroacetamide (BFTFA) as described by Dias et al. (2015). Briefly, All samples were re-dissolved in 20 µl of 30 mg ml^{-1} methoxyamine hydrochloride in pyridine and derivatized at 37 °C for 120 min with mixing at 500 rpm. The samples were incubated for 30 min with mixing at 500 rpm after addition of 20 µl *N*,*O*-bis-(trimethylsilyl)-trifluoroacetamide (BSTFA). Each derivatized sample was allowed to rest for 60 min prior to injection. Later, the derivatized samples (injection volume of 1 µl for each sample) were injected into a GC-QqQ-MS system comprising of a Gerstel 2.5.2 Autosampler, a 7890A Agilent gas chromatograph and a 7000 Agilent triple-quadruple MS (Agilent Santa Clara, USA) with an electron impact (EI) ion source. The instrument settings were the same as described by Dias et al. (2015). For calibration and quantification of sugars and organic acids in the flag leaf samples, we used serial concentrations of calibration authentic standards (Table S1), including 24 sugars (sugars, sugar phosphates, sugar acids and sugar alcohols) and 19 organic acids, derivatized and subjected to GC-QqQ-MS analysis–as described by Dias et al. (2015).

For the amino acid and amine analyses with LC-QqQ-MS, 10 µl of supernatants were transferred into new glass vial inserts. The amino acids and amines in the supernatants were then derivatized with 6-aminoquinolyl-*N*-hydrosysuccinimidyl carbamate (AQC) reagent as described in Boughton et al. (2011) and Dias et al. (2015). Briefly, 10 µl samples were added to 70 µl of borate buffer (200 mM, pH 8.8 at 25 °C) containing 10 mM TCEP, 1 mM ascorbic acid and 50 µM 2-aminobutyrate. The resulting solution was vortexed before adding 20 µl of 6-aminoquinolyl-*N*-hydrosysuccinimidyl carbamate (AQC) reagent [200 mM dissolved in 100% acetonitrile (ACN)] and then immediately vortexed. The samples were heated with shaking at 55 °C for 10 min, then centrifuged at 13,000 rpm at room temperature and transferred to HPLC vials containing inserts (Agilent, springless glass inserts, 250 µl) prior to injection. The derivatized samples (injection volume of 1 µl for each sample) were immediately injected into a LC-QqQ-MS system comprising of an Agilent 1200 LC-system coupled to an Agilent 6410 Electrospray Ionization-Triple Quadruple-MS. The setting of the LC–MS instrument were as described by Dias et al. (2015). For calibration and quantification of amino acids and amines in the flag leaf samples, a series of concentrations of calibration authentic standards (Table S1), comprising of 29 amino acids and amines mixed with sulfur-containing compound solution were prepared, derivatized and subjected to LC-QqQ-MS analysis same as described by Dias et al. (2015).

Seven phytohormones and phytohormone-related compounds [salicylic acid (SA), jasmonic acid (JA), jasmonoyl-isoleucine (JA-ile), indole-3-acetic acid (IAA), indole-3-carboxylic acid (ICA), indole-3-butyric acid (IBA) and 2-cis-4-trans-abscisic acid (ABA)], as well as three organic acids which are precursors for phytohormones [(benzoic acid (BA), trans-cinnamic acid (CA) and 12-oxo-phytodienoic acid (OPDA) were analysed in this study. Extraction for phytohormone analysis was carried out using a slightly modified procedure of Cao et al. (2017). Briefly, the flag leaf samples were ground with pestle and mortar in liquid nitrogen and frozen immediately. A 100 mg of sample was weighed for each of the samples and transferred to a dried 2 ml centrifuge tube that was pre-washed with MS grade methanol. 1 ml of extraction solvent, containing 956 µl of 70% methanol and 44 µl of 8.3 µg ml^{-1} internal standard mixtures (d_2IAA, d_5BA, d_6ABA, d_6SA, d_7CA, H_2JA), was added to the sample, then vortexed and agitated at 4 °C, and spun at 1400 rpm for 30 min. The samples were then centrifuged at 16,100×*g* for 10 min. The supernatants were transferred to fresh centrifuge tubes. The residues were re-extracted and centrifuged with 500 µl of extraction solvents (without internal standards). Finally, the first and second supernatant was combined and kept at − 80 °C until further derivatization steps using methyl-chloroformate (MCF). The subsequent derivatization steps were carried out according to Rawlinson et al. (2015), with some modifications. While Rawlinson et al. used GC coupled with single MS, our analysis used triple quadruple GC–MS (GC-QqQ-MS) with newly developed multiple reaction monitorings (MRMs) which were developed for each of the measured phytohormone and organic acids. Briefly, 600 µl of the supernatant for each sample was taken, dried down and re-dissolved with 160 µl methanol. Then, 8.3 µg ml^{-1} of $^{13}C_5$-^{15}N-L-Valine (another internal standard) was added. 34 µl of pyridine was then added to the mixture, followed by vortexing vigorously for 25–30 s. 200 µl of 1% NaOH solution was then added to the mixture. This ~ 400 µl mixture was then derivatized with 20 µl of methyl chloroformate (MCF) and vortexed vigorously for 25–30 s. Another 20 µl of methyl chloroformate (MCF)

was added, followed by vortexing. 400 µl of chloroform was then added to the mixture, vortexed again for 10 s, followed by an addition of 400 µl of 50 mM sodium bicarbonate. The mixture was vortexed for 10–15 s and centrifuged for 30 s at 16,100×*g*. The upper aqueous layer was discarded and the bottom organic layer was taken (1 µl for each sample) and injected into a GC-QqQ-MS system comprising a Gerstel 2.5.2 Autosampler, a 7890A Agilent gas chromatograph and a 7010 Agilent triple-quadrupole MS (Agilent, Santa Clara, USA) with an electron impact (EI) ion source. More details for the preparation of calibration and internal standards, extraction, derivatization steps and GC-QqQ-MS instrument settings can be found in Supplementary Data S1 (Methodology for phytohormone analysis).

2.3 Analysis of lipid content

The extraction of lipids was carried according to Folch et al. (1957), with modifications. Briefly, 30 mg freshly frozen flag leaf samples were homogenized in 500 µl of a 2:1 methanol:chloroform mixture using a Cryomill (Precellys 24, Bertin technologies) for 3 × 45 s at 6100 rpm (− 10 °C). The extracts were shaken at 750 rpm for 15 min at 30 °C, and centrifuged at 13,000 rpm for 15 min. The supernatants were transferred to new tubes, while 500 µl of 2:1 methanol:chloroform mixture was added again to each of the remaining residue, vortexed and centrifuged at 13,000 rpm for 15 min. The supernatants were combined with the previous supernatants. The combined supernatants were dried down *in vacuo* and re-constituted in 100 µl of 1:1 butanol:methanol for the subsequent LC-QqQ-MS analysis using an Agilent 1200 LC-system coupled to an Agilent 6410 Electrospray Ionization-Triple Quadruple-MS system. An injection of 5 µl of each total lipid extract was chromatographically separated on an Ascentis Express RP-Amide 50 × 2.1 mm, 2.7 µm HPLC column (Sigma-Aldrich, Castle Hill, NSW) using an 8 min gradient from 0% A to 100% B, which was then held for 2 min and followed by a 4 min column re-equilibration with a flow rate of 0.18 ml min^{-1}. The mobile phases were: A, 10 mM ammonium formate in water: methanol: tetrahydrofuran (50: 20: 30, v/v/v); B, 10 mM ammonium formate in water: methanol: tetrahydrofuran (5: 20: 75, v/v/v). Lipid species were identified and quantified based on multiple reaction monitorings (MRMs) established using external lipid standards and references from the LIPIDMATCH database (https://github.com/GarrettLab-UF/LipidMatch/releases/tag/v2.0.2) as listed in Table S2, with a 5–20 ms dwell time for the simultaneous measurements of up to 100 compounds. We used optimised parameters for capillary (4000 V), fragmentor (60–160 V) and collision voltages (20–40 V). In all cases, the collision gas was nitrogen with a flow rate of 7 l min^{-1}. The external lipid standards used (Table S2) were lysophosphatidylcholine LPC(17:0), phospatidylcholine PC(34:1), phosphatidylethanolamine PE(34:0), phosphatidylglycerol PG(34:1), phosphatidylinositol PI(36:2), phosphatidic acid (PA) and phosphatidylserine PS(34:0). Detected lipid species are annotated as follows: lipid class designation (total number of carbon atoms in the fatty acid chains: total number of double bonds in the fatty acid chains).

2.4 Data processing and statistical analysis of metabolite data

Raw metabolite and lipid data were processed and analyzed using Quantitative Analysis MassHunter Workstation software for QQQ (Agilent Technologies, Santa Clara, CA, USA). The level of identification was carried out based on the Metabolomics Standards Initiative (MSI) requirements (Sumner et al. 2007). For all measured metabolites (sugars, organic acids, amines and phytohormones), absolute quantities were determined while the concentration unit was expressed as picomole/mg of fresh weight (Table S3), using MSI Level 1 as the identification was based on Multiple Reaction Monitorings (MRMs) established using authentic standards (Table S1). Meanwhile, for lipids, responses were normalized to mg fresh weight (Table S4). Although single authentic lipid species were used for each of the phospholipid class, the identification of individual lipid species was based on the MRM experiment and retention time (MSI Level 2, Table S2). The processed metabolite and lipid data were first subjected to multiple comparison statistical analyses using Analysis of Variance (ANOVA), with a false discovery rate (FDR)-adjusted p value of 0.05 and using the Benjamini–Hochberg method (1995) to determine the metabolites and lipids that changed significantly across all time points or over the 4-day cold stress period, followed by the Tukey's honestly significant difference (HSD) post hoc test in order to determine which pair-wise combinations showed significant differences for both primary metabolites and lipids using Graphpad Prism 7.0 (GraphPad Software, La Jolla California USA). Next, we determined which metabolites/lipids responded specifically to short cold stress (TP_1), prolonged cold stress (TP_3), diurnal fluctuations when the plants were exposed to normal day-time temperature of 21 °C for 6 h (TP_2 and TP_4). We therefore performed pair-wise comparisons of the selected two groups TP_1 versus TP_0 (for short cold stress), TP_3 versus TP_1 (for prolonged cold stress), TP_2 versus TP_1 and TP_4 versus TP_3 (for recovery and the effect of diurnal fluctuations on metabolite levels) within each variety, and comparisons in every time point between the two varieties (varietal differences). The comparisons for metabolites were presented as Log_2-transformed of fold change values (Figs. 1, 3; Table S5). A similar approach was also performed for the lipid data (Figs. 2, 4; Table S6). Statistical significance of differences observed between samples

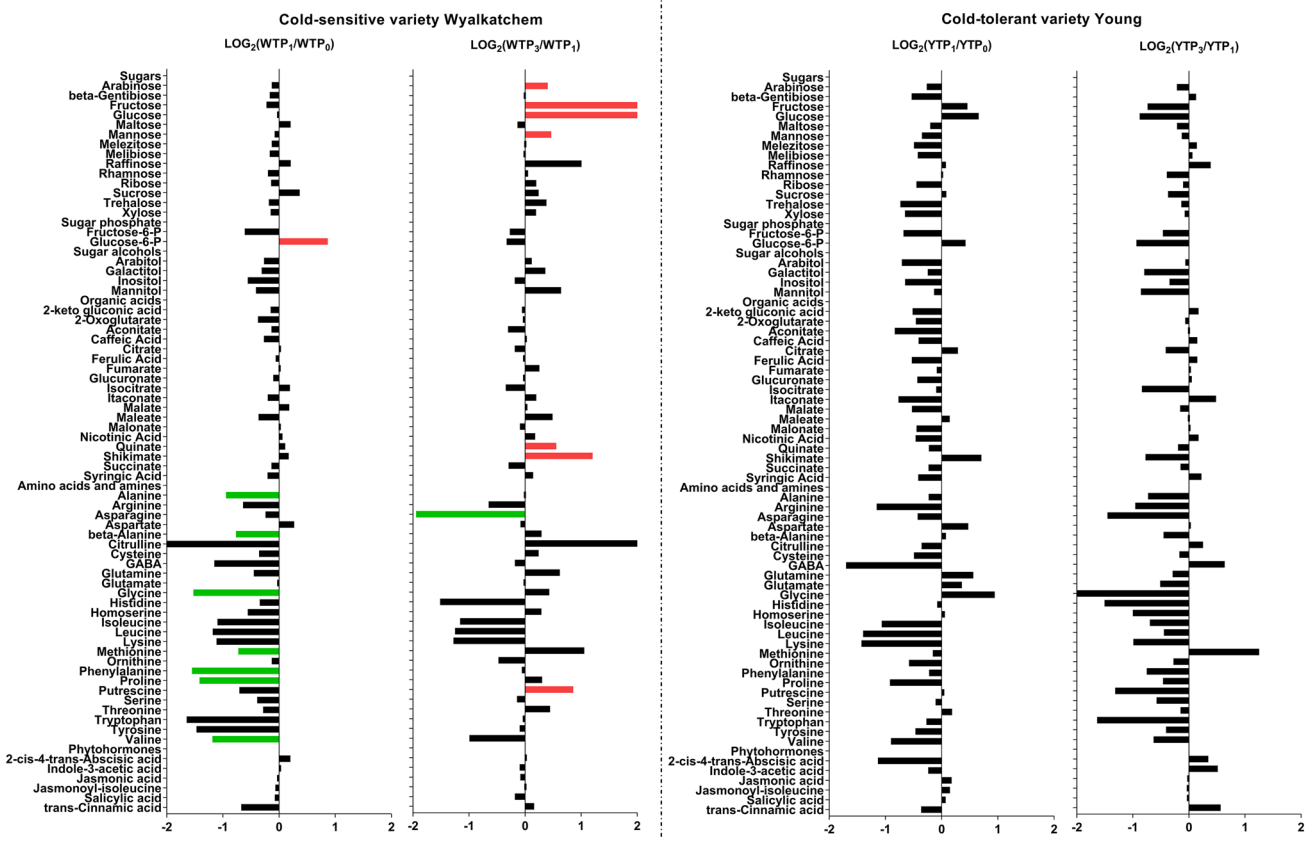


Fig. 1 Log_2-fold changes of primary metabolites in the flag leaves of the cold-sensitive Wyalkatchem (W) and cold-tolerant Young (Y) after one night (TP_1 vs. TP_0) and prolonged (TP_3 vs. TP_1) of cold treatment. Fold changes were calculated by dividing the concentration of the variety at a time point (e.g., TP_1) to the concentration of that variety at the previous time point (e.g., TP_0), then Log_2-transformed. Significance of difference was determined by Benjamini and Hochberg method (Benjamini and Hochberg 1995) with false discovery rate (FDR)-adjusted *p*-value of 0.05 as the cut-off. *Green* significant decrease, *Red* significant increase. There were four biological replicates (n = 4) for all the measured metabolites, except phytohormones (n = 3)

was evaluated with the Student's *t*-test in Excel, with a false discovery rate (FDR)-adjusted *p*-value of 0.05 as the cut-off (Benjamini and Hochberg 1995). The statistical analysis for the comparison of the unsaturation to saturation ratio between Wyalkatchem and Young at different time points was also performed with Student's *t*-test using GraphPad Prism 7.0 software (GraphPad Software, La Jolla, CA, USA). All bar plots were created using the same software.

3 Results

3.1 Establishment of a controlled environment assay for chilling tolerance

To establish a controlled environment phenotyping method for chilling and frost tolerance in wheat, we used two wheat varieties that consistently performed better (Young) and worse (Wyalkatchem) in terms of grain yield in the Australian National Frost Initiative (NFI) field trials. We used a linear cooling gradient descending from 21 to − 3 °C over a period of 4 h, followed by a continuous cold period at − 3 °C over 8 h (Fig. S1a). A four-day chilling treatment at the YM stage showed that the average spike grain number relative to unstressed control plants was consistently higher for Young compared to Wyalkatchem, with Wyalkatchem grain number reduced to an average of 76.3% of control (Fig. S1b). Reduced spike grain number in Wyalkatchem was often associated with the development of larger grains (Fig. S1c). A 4-day cold treatment during different stages of reproductive development showed that sensitivity to chilling in Wyalkatchem was highest at Zadok stages 41 to 47 and from 57 to 65, which corresponded to the YM stage and anthesis respectively. Spike grain numbers in Young were not significantly affected at both stages (Fig. S1d). A time course experiment shows that spike grain numbers in Wyalkatchem were reduced considerably after three days of treatment, while in Young spike grain numbers were reduced

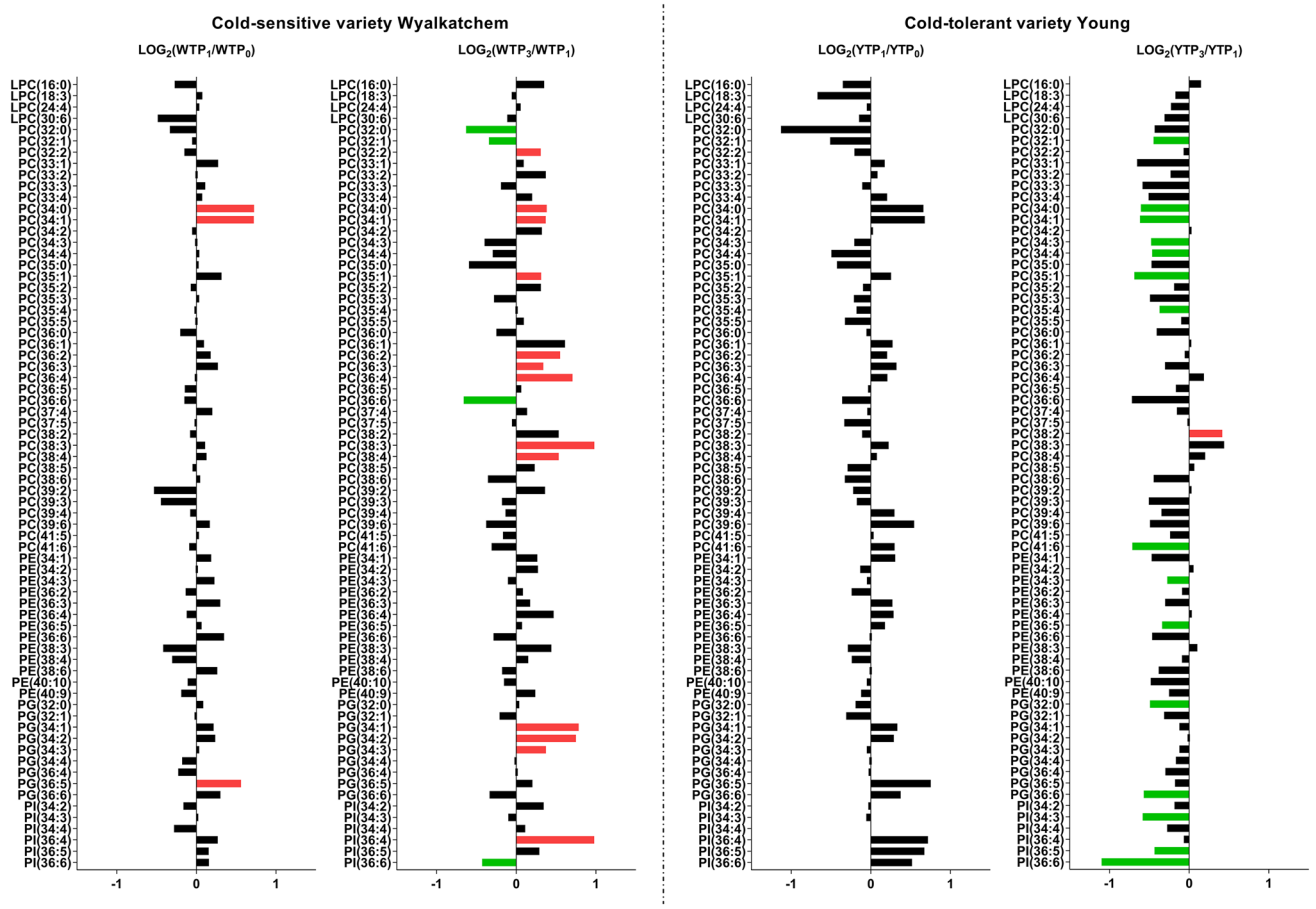


Fig. 2 Log_2-fold changes of phospholipids in the flag leaves of the cold-sensitive Wyalkatchem (W) and cold-tolerant Young (Y) after one night (TP_1 vs. TP_0) and prolonged (TP_3 vs. TP_1) of cold treatment. Fold changes were calculated by dividing the normalized response of the variety at a time point (e.g., TP_1) to the normalized response of that variety at the previous time point (e.g., TP_0), then Log_2-transformed. Statistical method and cut-offs are as stated in Fig. 1. *Green* significant decrease, *Red* significant increase. There were four biological replicates (n = 4) for all the measured lipids

significantly from 5 days treatment onwards (Fig. S1e). We therefore standardised on a 4-day YM stage treatment to discriminate the two varieties.

3.2 Four-day chilling treatment induces significant changes in metabolites and lipids in Young and Wyalkatchem

To develop a workable field phenotyping method, we focused on cold-induced metabolite changes in the flag leaf, a tissue that is easier to collect in a non-destructive way compared to YM stage spikes. In the field, wheat plants often experience consecutive nights of chilling and frost events throughout flowering, as frost events are linked to large scale climatic patterns and regularly occur over successive nights, while day time temperatures can be normal (~ 20 °C). Previous chilling events can influence metabolite levels at any harvest time. A time course experiment was therefore designed to identify metabolite changes that were stable over consecutive cold events and were not subject to day-time recovery or to circadian fluctuations. In addition, metabolite markers for chilling tolerance have to accumulate to significantly different levels in the cold-tolerant and sensitive wheat lines.

Using ANOVA multiple comparison analysis and a false discovery rate (FDR)-adjusted *p*-value of 0.05, significant changes of metabolites and lipids were observed in each variety and between the two varieties across all the time points (Table 1, S7, S8). Cold treatment of cold-sensitive Wyalkatchem revealed significantly more changes in both primary metabolites (25) and lipids (19) compared to cold-tolerant Young which showed only one metabolite and ten lipid changes across all the time points (Table 1). When comparing quantitative and qualitative differences in cold acclimation between the two varieties, a total of 43 metabolites and 47 lipids were found to differ across all time points (Table 1). All metabolites and lipids listed in Table 1 were further analysed with Tukey's honestly significant difference

Table 1 Metabolites and lipids that changed significantly over the 4-day of cold stress in the flag leaves of cold-sensitive Wyalkatchem (W) and cold-tolerant Young (Y), analyzed by One-way ANOVA with FDR-adjusted $p < 0.05$ as significance, followed by Tukey Test

Flag leaves_within variety				Flag leaves_between the two varieties	
Wyalkatchem		Young		Wyalkatchem versus Young	
Metabolites	Lipids	Metabolites	Lipids	Metabolites	Lipids
				2-cis-4-trans-Abscisic acid	LPC(30:6)
2-Oxoglutarate	PC(32:0)		PC(32:0)	2-Oxoglutarate	PC(32:0)
			PC(32:1)	Aconitate	PC(32:1)
Alanine				Alanine	PC(32:2)
				Arabinose	PC(33:1)
	PC(33:2)			Arabitol	PC(33:2)
Arginine				Arginine	PC(33:3)
Asparagine				Asparagine	PC(33:4)
beta-Alanine	PC(34:0)		PC(34:0)	beta-Alanine	PC(34:0)
Citrate	PC(34:1)		PC(34:1)	Citrate	PC(34:1)
Citrulline				Citrulline	PC(34:2)
Fructose	PC(34:3)		PC(34:3)	Fructose	PC(34:3)
				Fructose-6-P	PC(34:4)
GABA	PC(35:0)			GABA	PC(35:0)
	PC(35:1)			Galactitol	PC(35:1)
Glucose				Glucose	PC(35:2)
Glucose-6-P			PC(35:3)	Glucose-6-P	PC(35:3)
Glycine				Glycine	PC(35:4)
Histidine				Histidine	PC(35:5)
				Homoserine	PC(36:1)
	PC(36:2)			Inositol	
	PC(36:3)			Isocitrate	PC(36:3)
Isoleucine	PC(36:4)			Isoleucine	PC(36:4)
Leucine	PC(36:6)			Leucine	PC(36:6)
Lysine				Lysine	PC(37:4)
	PC(38:3)			Maltose	PC(38:3)
Mannose	PC(38:4)			Mannose	PC(38:4)
				Methionine	PC(38:6)
Phenylalanine				Phenylalanine	PC(39:3)
Proline				Proline	PC(41:6)
Putrescine				Putrescine	PE(34:3)
				Quinate	PE(36:4)
				Raffinose	PE(36:6)
				Ribose	PE(38:3)
				Salicylic acid	PE(38:6)
				Serine	PE(40:10)
Shikimate		Shikimate	PG(32:0)	Shikimate	PG(32:0)
Sucrose				Sucrose	PG(32:1)
	PG(34:1)			trans-Cinnamic acid	PG(34:1)
	PG(34:2)			Trehalose	PG(34:2)
Tryptophan	PG(34:3)				PG(34:3)
Tyrosine				Tyrosine	PG(36:4)
Valine	PG(36:5)		PG(36:5)	Valine	PG(36:5)
				Xylose	PG(36:6)
					PI(34:3)
	PI(36:4)				PI(36:4)
			PI(36:5)		PI(36:5)
	PI(36:6)		PI(36:6)		PI(36:6)

(HSD) post hoc test in order to determine which pair-wise combinations showed significant differences for both primary metabolites and lipids (Tables S9, S10). Many pair-wise combinations were shown to differ significantly for both metabolites (387; highlighted in Table S9) and lipids (470; highlighted in Table S10) for the two wheat varieties and across all time points. But only some of these comparisons are relevant for identification of potential metabolite markers for chilling and frost tolerance phenotyping. Comparisons between TP_1 versus TP_0 (short cold treatment) and TP_3 versus TP_1 (stability over prolonged cold treatment during cold acclimation), as well as comparisons between the day and night-time samples (TP_2 vs. TP_1 and TP_4 vs. TP_3; effect of diurnal fluctuations on metabolite levels), and comparison between these time points for the two wheat varieties are essential to identify those metabolites that could be used as stable markers for cold-tolerance phenotyping. To achieve this particular aim we performed additional Student's *t*-test to carry out pair-wise comparisons to identify candidate metabolite markers that are able to differentiate the response in cold acclimation and cold tolerance between the two wheat varieties.

3.3 A 4-day chilling time course reveals significant differences in cold acclimation in Wyalkatchem and Young flag leaves

Sample comparisons: TP_1 versus TP_0, TP_2 versus TP_1, TP_3 versus TP_1 and TP_4 versus TP_3 for both varieties After the first night of cold exposure, the sensitive variety Wyalkatchem showed the most dramatic changes in primary metabolite levels (WTP_1 vs. WTP_0). As shown in Fig. 1, seven amino acids and amines were significantly decreased, including alanine (− 1.9-fold), beta-alanine (− 1.7-fold), glycine (− 2.9-fold), methionine (− 1.7-fold), phenylalanine (− 2.9-fold), proline (− 2.7-fold) and valine (− 2.3-fold). One sugar increased significantly at TP_1: glucose-6-phosphate (+ 1.8-fold). There was no significant change in phytohormones. Three lipids increased significantly after overnight cold exposure of Wyalkatchem (Fig. 2): PC(34:0) (+ 1.6-fold), PC(34:1) (+ 1.6-fold) and PG(36:5) (+ 1.4-fold). In contrast to Wyalkatchem, the cold tolerant variety Young did not show any significant changes in primary metabolites or lipids at TP_1 compared to TP_0 (Figs. 1, 2).

To test for recovery and the effect of diurnal fluctuations on metabolite levels we harvested the TP_2 samples 6 h after the TP_1 samples, when plants were allowed to experience day-light and normal temperatures (21 °C) for 6 h. Comparison of TP_2 and TP_1 metabolite levels revealed that some of the significant changes we observed at TP_1 in Wyalkatchem flag leaves were partially reversed, but some were maintained and new changes also appeared (Table S5, Fig. S2). Some amino acids and amine levels changed from being decreased at TP_1 to being significantly increased at TP_2 and regaining T_0 levels: citrulline (+ 14.9-fold), glycine (+ 2.3-fold), homoserine (+ 2.2-fold), methionine (+ 1.6-fold) and putrescine (+ 3.0-fold). Tryptophan decreased further at TP_2 compared to TP_1: (− 1.9-fold). There were no differences in phytohormone levels, nor were there any significant changes in lipid levels between TP_2 and TP_1 Wyalkatchem flag leaves (Table S6, Fig. S3). Comparing TP_2 to TP_1 in Young showed a significant increase for citrulline (+ 2.8-fold) (Table S5, Fig. S2). There were no significant lipid changes (Table S6, Fig. S3).

After prolonged four-night cold treatment (TP_3), more significant accumulation of sugars and organic acids were observed in Wyalkatchem flag leaves compared to the first overnight exposure to cold (WTP_1; Fig. 1). Fructose (+ 4.1-fold) and glucose (+ 6.0-fold) increased significantly in Wyalkatchem flag leaves. Also, arabinose (+ 1.3-fold) and mannose (+ 1.4-fold) were higher compared to TP_1. Two organic acids, quinate (+ 1.5-fold) and shikimate (+ 2.3-fold), and one amine, putrescine (+ 1.8-fold), were significantly higher. One amino acid, asparagine (− 3.9-fold) was markedly lower at WTP_3 compared to WTP_1. Prolonged cold treatment of Wyalkatchem also resulted in more lipid changes at WTP_3 compared to WTP_1. Four lipids were significantly reduced, one being a saturated species [PC(32:0)] and the remaining three being unsaturated species [PC(32:1), PC(36:6), PI(36:6)]. Another 13 lipids increased significantly; one of them was a saturated lipid, while 12 others were unsaturated species (Fig. 2, Table S6). In Young, none of the primary metabolites were significantly changed at YTP_3 compared to YTP_1 (Fig. 1). The most notable changes after prolonged cold stress (YTP_3) in Young flag leaves compared to the shorter cold stress (YTP_1) were in the lipid levels. Fifteen lipids were significantly reduced compared to TP_1, while one polyunsaturated lipid species, PC(38:2), was significantly higher (1.4-fold). Of the 15 lipids with reduced levels, two were saturated species while a majority (13) were unsaturated species (Fig. 2, Table S6). Comparing TP_4 day-time samples to TP_3 in Wyalkatchem and Young revealed that there were no significant differences in primary metabolites (Table S5, Fig. S2), while only one polyunsaturated lipid species, PC(41:6) was increased (+ 1.5-fold) in Young flag leaves (Table S6, Fig. S3).

3.4 Young and Wyalkatchem show significant varietal differences in cold acclimation across time points

Sample comparisons: WTP versus YTP at each time point In the unstressed plants (TP_0), there were no significant differences in the levels of primary metabolites or lipids between

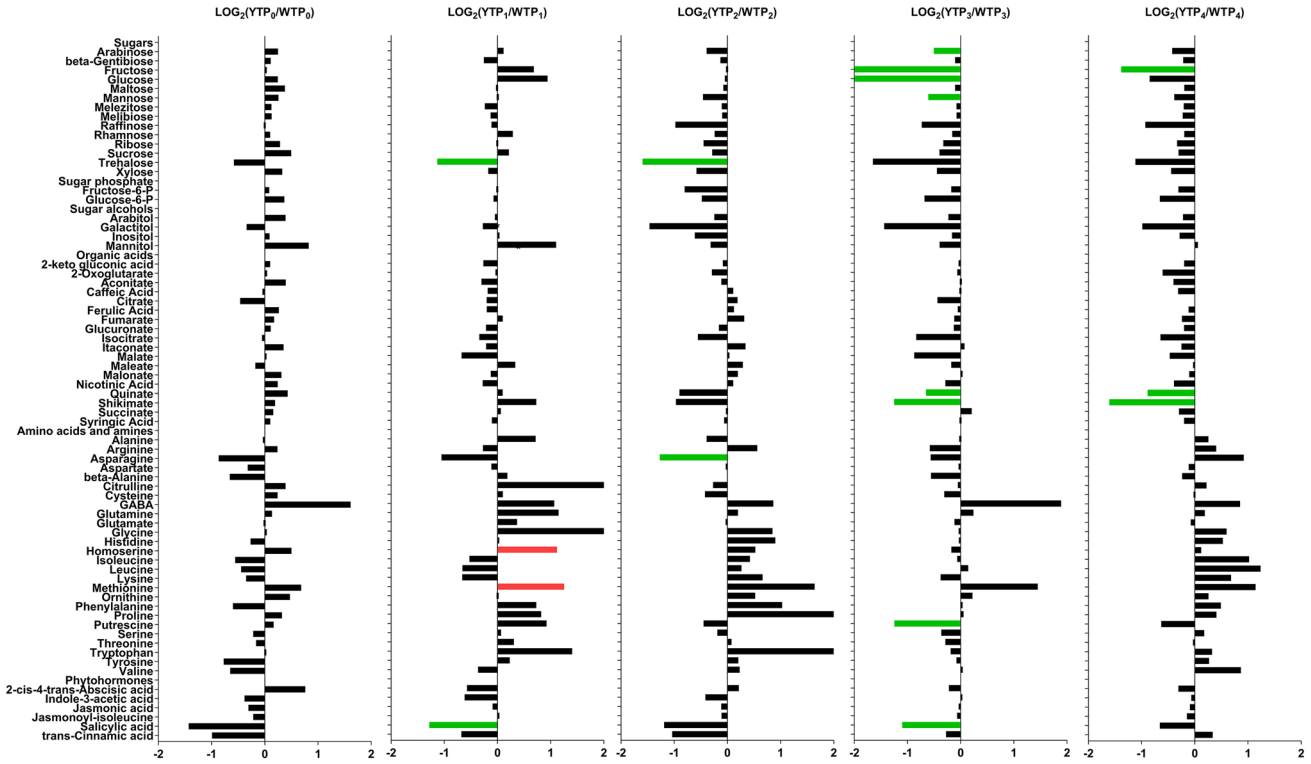


Fig. 3 Log_2-fold changes of primary metabolites in the flag leaves of cold-tolerant Young (Y) compared to the cold-sensitive Wyalkatchem (W) at each time point. Fold changes were calculated by dividing the concentration of Y to the concentration of W at that particular time point, then Log_2-transformed. Statistical method and cut-offs are as stated in Fig. 1. *Green* significantly lower in Young/higher in Wyalkatchem; *Red* significantly higher in Young/lower in Wyalkatchem. There were four biological replicates (n = 4) for all the measured primary metabolites, except phytohormones (n = 3)

Wyalkatchem and Young flag leaves (Figs. 3, 4). However, several metabolites with potential roles in stress responses were slightly higher in Young compared to Wyalkatchem: sucrose (+ 1.4-fold), mannitol (+ 1.8-fold), GABA (+ 3.1-fold), ABA (+ 1.7-fold). At TP_0, there were no significant differences between Wyalkatchem and Young in terms of lipid content. However, some lipid levels appeared to be different in Wyalkatchem and Young flag leaves. Some lipids were lower in Young compared to Wyalkatchem when a cut-off of 0.1 was used: PC(33:4) (− 1.5-fold), PG(36:6) (− 1.6-fold) and PI(36:6) (− 1.6-fold). Others were higher in Young compared to Wyalkatchem ($p < 0.1$): PC(35:1) (+ 1.5-fold), PG(34:1) (+ 1.4-fold) and PG(34:2) (+ 1.4-fold) (Fig. 4). Although these lipids (indicated by asterisks) did not satisfy the significance threshold ($p < 0.05$) at TP_0, they did become significantly different ($p < 0.05$) after the first night of cold treatment (TP_1; Fig. 4). This may indicate that the lipid composition in Wyalkatchem and Young may be different before cold treatment. This is also reflected by the fact that at TP_0, the unsaturated to saturated lipid ratio of Young (218.6 ± 10.6) was significantly lower than in Wyalkatchem flag leave samples (265.2 ± 16.0; Fig. 5a, Table S11).

After overnight exposure to cold (TP_1), two amino acids and amines were significantly higher in Young compared to Wyalkatchem (Fig. 3): homoserine (+ 2.2-fold) and methionine (+ 2.4-fold). Trehalose (+ 2.2-fold) was the only sugar that was significantly higher in Wyalkatchem flag leaves. The phytohormone salicylic acid decreased in Young compared to Wyalkatchem (− 2.4-fold). Lipids showed the most dramatic difference between the two varieties at TP_1. Fourteen lipid species were significantly higher in Young TP_1 samples and all were polyunsaturated lipids. Thirteen lipid species were significantly higher in Wyalkatchem compared to Young, and all were also unsaturated lipids (Fig. 4, Table S6). The lipid unsaturation to saturation ratio was not significantly different between Wyalkatchem and Young flag leaves at this time point (Fig. 5a). When comparing the TP_2 samples between the two wheat varieties (YTP_2 vs. WTP_2), two metabolites in Young were significantly lower compared to Wyalkatchem (Fig. 3): trehalose (− 3.0-fold), and asparagine (− 2.4-fold). None of the lipid species were significantly different in Young compared to Wyalkatchem at this time point (Fig. 4, Table S6).There was no significant difference in the lipid unsaturation to saturation ratio between the two varieties at TP_2 (Fig. 5a, Table S11).

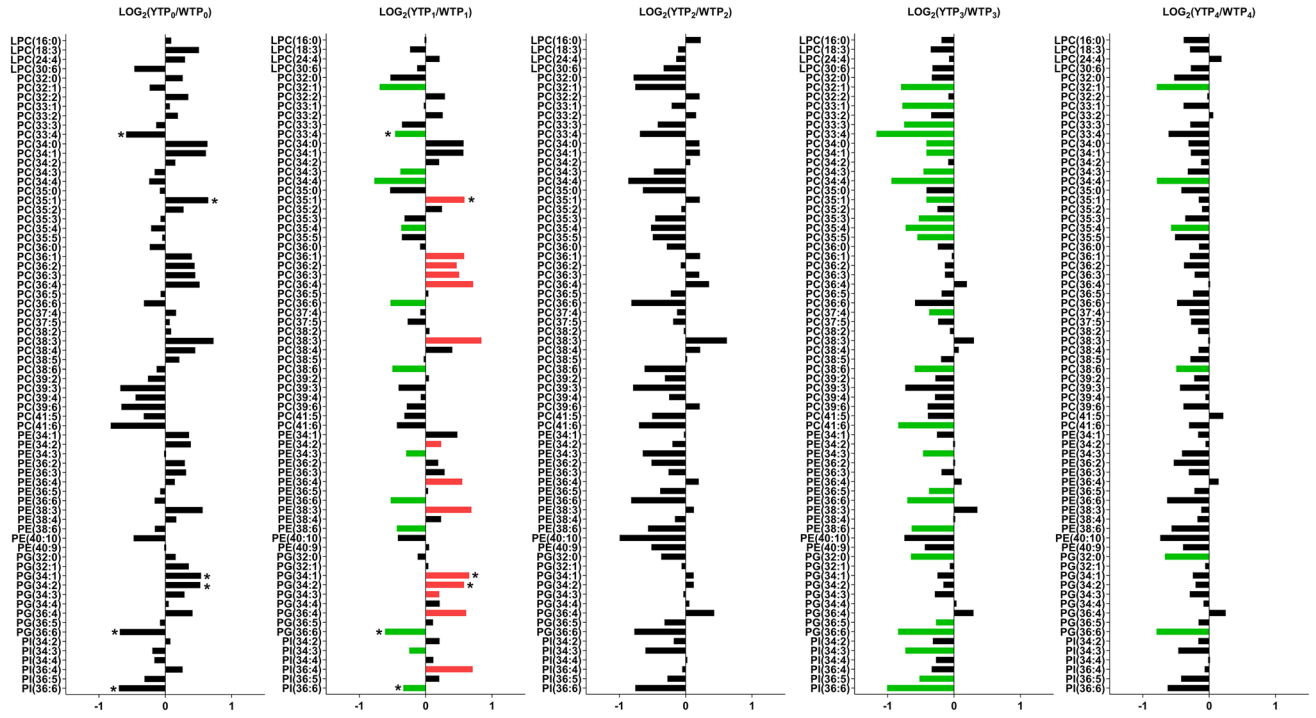


Fig. 4 Log_2-fold changes of phospholipids in the flag leaves of the cold-tolerant Young (Y) compared to the sensitive Wyalkatchem (W) at each time point. Fold changes were calculated by dividing the concentration of Y to the concentration of W at that particular time point, then Log_2-transformed. Statistical method and cut-offs are as stated in Fig. 1. *Green* significantly lower in Young/higher in Wyalkatchem; *Red* significantly higher in Young/lower in Wyalkatchem. There were four biological replicates (n = 4) for all the measured lipids. Three lipids: PC(33:4), PG(36:6) and PI(36:6) were lower in Young compared to Wyalkatchem, while another three lipids: PC(35:1), PG(34:1) and PG(34:2) were higher in Young compared to Wyalkatchem when a cut-off of 0.1 was used. Although these six lipids (indicated with asterisks at TP_0 and TP_1) did not satisfy the significance threshold ($p < 0.05$) at TP_0, they did become significantly different after the first night of cold treatment (TP_1)

After prolonged cold stress exposure (TP_3; Fig. 3), some metabolites were significantly lower in Young compared to Wyalkatchem, including arabinose (− 1.4-fold), fructose (− 4.2-fold), glucose (− 5.7-fold), mannose (− 1.5-fold), quinate (− 1.6-fold), shikimate (− 2.4-fold), putrescine (− 2.4-fold) and salicylic acid (− 2.1-fold). Comparison of the lipids at TP_3 again showed the biggest difference between the two varieties. Twenty-five lipid species were significantly lower at TP_3 in Young compared to Wyalkatchem (Fig. 4, Table S6). The total lipid unsaturation to saturation ratio was significantly higher in Young compared to Wyalkatchem at this stage (Fig. 5a, Table S11). Comparison of TP_4 samples between Young and Wyalkatchem (YTP_4 vs. WTP_4) showed that only three metabolites were significantly lower in Young compared to Wyalkatchem (Fig. 3): fructose (− 2.6-fold), quinate (− 1.8-fold) and shikimate (− 3.0-fold). In addition, six lipids were significantly lower in Young when compared to Wyalkatchem (Fig. 4, Table S6). They were PC(32:1), PC(34:4), PC(35:4), PC(38:6), PG(32:0) and PG(36:6). All of these six lipids were the same as those found to be lower in Young at previous time points (TP_1 to TP_3). The unsaturation to saturation ratio of Young was again significantly higher than Wyalkatchem at this stage (Fig. 5a, Table S11).

3.5 Quantitative changes in two groups of lipids may account for differences in membrane fluidity and cold tolerance between Young and Wyalkatchem

The time course experiment revealed that the unsaturated to saturated lipid ratio changed progressively from being higher in Wyalkatchem compared to Young at TP_0, to higher in Young at TP_3 and TP_4 (Fig. 5a). This shift in unsaturated to saturated lipid ratio is correlated with differences in the expression profile of two main groups of lipids from TP_0 onwards (Fig. 5b, c). The first group of 11 lipids was higher in Wyalkatchem after the first cold exposure (TP_1) and remained higher than in Young throughout the 4-day time course (Fig. 5b, Table S12). In contrast, another group of 18 lipids (Fig. 5c, Table S13) were on average higher in Young compared to Wyalkatchem from the first exposure to cold

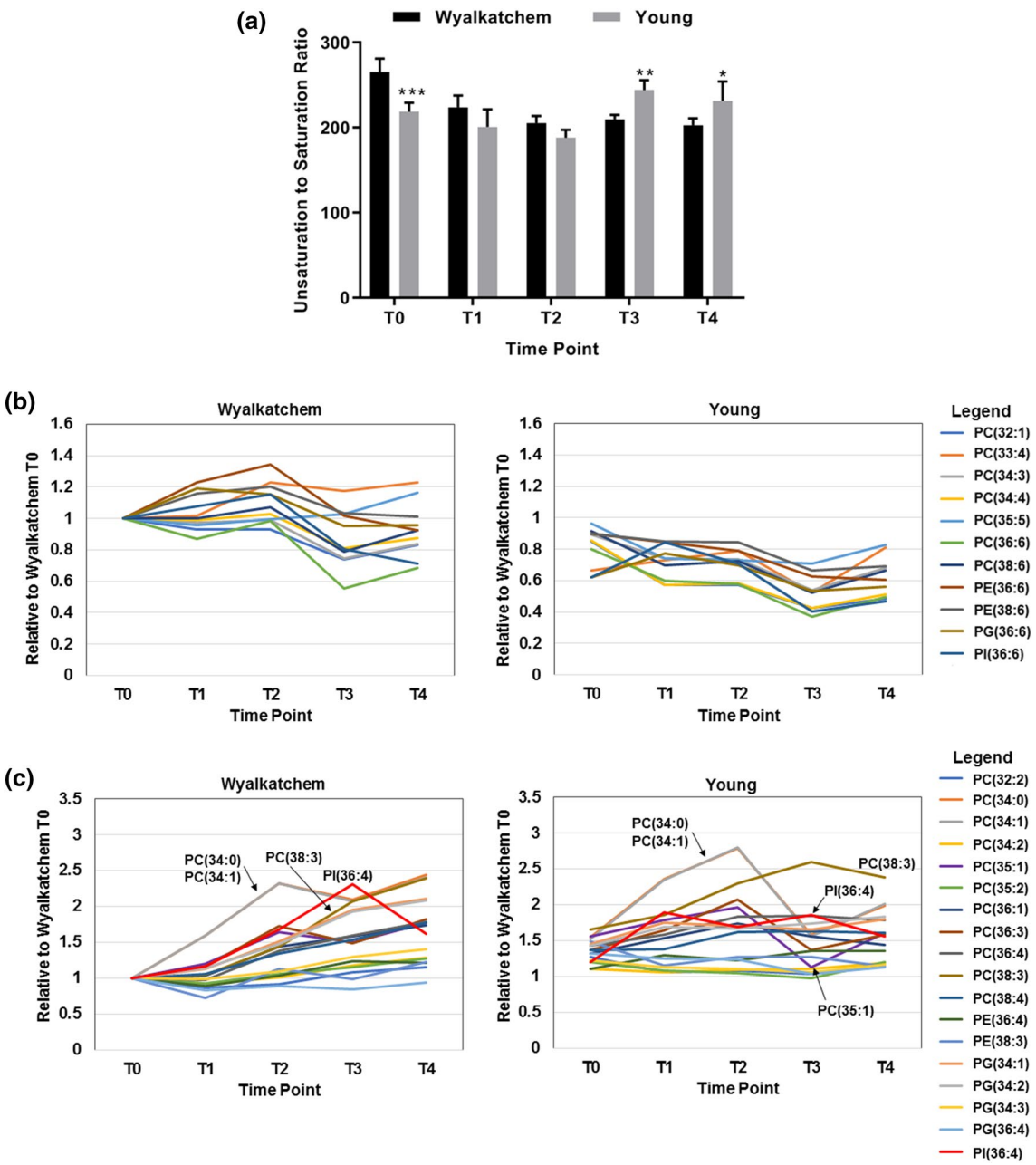


Fig. 5 **a** Unsaturation to saturation ratio in Wyalkatchem and Young across the time points. Student's t-test was used to compare the ratio values between Wyalkatchem and Young at each time point. Error bars indicate the standard deviation (SD) of four biological replicates (n = 4) and asterisks indicate significance levels: *p < 0.05, **p < 0.01 and ***p < 0.001. **b** Expression levels of a group of 11 lipids with higher expression from TP_1 onwards in the cold-sensitive Wyalkatchem compared to Young [(PC(32:1), PC(33:4), PC(34:3), PC(34:4), PC(35:5), PC(36:6), PC(38:6), PE (36:6), PE(38:6), PG(36:6), PI(36:6)]. These lipids had higher levels in Wyalkatchem after the first cold treatment and most of them remained higher than in Young throughout the treatment. **c** Expression levels of a group of 18 lipids with higher expression from TP_1 onwards in the cold-tolerant Young compared to Wyalkatchem [(PC(32:2), PC(34:0), PC(34:1), PC(34:2), PC (35:1), PC(35:2), PC(36:1), PC(36:3), PC(36:4), PC(38:3), PC(38:4), PE(36:4), PE(38:3), PG(34:1), PG(34:2), PG(34:3), PG(36:4), PI(36:4)]. Arrows indicate three lipids, PC(34:0), PC(34:1) and PC(35:1), that changed drastically from TP_2 onwards in Young. **b** and **c** illustrate how these lipids behaved after long term exposure to cold and how they respond to diurnal rhythms

onwards (TP_1), but 5 members of this group behaved quite differently in the two wheat varieties (Fig. 5c). The saturated species PC(34:0), monounsaturated species PC(34:1) and PC (35:1) were significantly increased in both Wyalkatchem and Young after one overnight cold stress event (TP_1), but were then reduced drastically in Young compared to Wyalkatchem after the fourth night of cold stress (TP_3). A fourth lipid, PI(36:4), was increased in Young from time points

TP_1 to TP_3, but was induced more strongly in Wyalkatchem after prolonged cold exposure (TP_3). The unsaturated lipid species PC(38:3) was always significantly higher in Young compared to Wyalkatchem from TP_0 onwards and is gradually increased during prolonged cold exposure and was not subjected to diurnal fluctuations (TP_2 and TP_4). PC(38:3) was only increased in Wyalkatchem from TP_3 onwards. The combined changes in these two lipid groups and the differential expression behaviour of some members in these lipid groups may contribute towards the observed increase in the ratio of unsaturated to saturated lipids in Young compared to Wyalkatchem (Fig. 5a, Table S11).

4 Discussion

4.1 Wheat chilling and frost tolerance: field versus controlled environment phenotyping

In the field, phenotyping for wheat frost tolerance is complicated by the unpredictability and spatial/temporal variation in the severity of frost events (Frederiks et al. 2012). Field phenotyping has focused on the presence/absence of tissue damage and yield effects caused by frosts. Frost events at the critical stage of flowering are often catastrophic, leading to the assumption that there is little genetic variation for frost tolerance in wheat (Frederiks et al. 2012; Zheng et al. 2015; Barlow et al. 2015). Non-freezing, chilling conditions occur far more frequently in the field, but the associated sterility and loss in spike grain number has received less attention (Subedi et al. 1998a, b; Chakrabarti et al. 2011; Smith and Zhao 2016). In rice, cold-induced pollen sterility causing loss in grain yield is commonly used as a phenotyping trait (Hayase et al. 1969; Satake et al. 1969; Nishiyama 1984; Oliver et al. 2005). Similar to drought and heat stress, phenotyping for chilling and frost tolerance in the field is compromised by avoidance or escape mechanisms such as phenology of flowering (Fleury et al. 2010; Richards et al. 2010; Shavrukov et al. 2017). Controlled environment phenotyping can overcome some of the pitfalls associated with field work. Occurrence and severity of cold events can be monitored and repeated consistently, as well as their timing during reproductive growth controlled, making it possible to study the physiological and molecular basis of cold tolerance without the interference of avoidance or escape mechanisms or the complexity of changes in frost severity and duration between events. We established a controlled environment screening method based on maintenance of grain number under chilling conditions using two wheat cultivars that were reproducibly shown to be more tolerant (Young) and sensitive (Wyalkatchem) to field chilling and frost conditions. This screening method allowed us to reproduce the field rankings for the two cultivars, as well as the cold tolerance rankings for several other tolerant and sensitive wheat cultivars from the National Frost Initiative (Dolferus et al., unpublished results). Chilling conditions led to a reduction in spike grain number in wheat and we show that the YM and anthesis stages are the two most sensitive stages to chilling stress.

4.2 Metabolomics as alternative phenotyping tool for chilling and frost tolerance in wheat

Tolerance to frost requires the establishment of an acclimation response in plant tissues. Cold acclimation starts below a certain non-freezing threshold temperature before below-zero temperatures cause ice formation and desiccation and freezing damage to plant tissues (Livingston et al. 2016). It remains unclear how much time it takes for effective cold acclimation to reach maximal potential, nor do we know whether there is genetic variation in quantitative or qualitative aspects of cold acclimation (Pagter and Arora 2013; Vanková et al. 2014; Chen et al. 2014; Fiebelkorn and Rahman 2016). Understanding what acclimation to non-freezing or chilling conditions involves is essential to understand how frost tolerance (cold, chilling/dessication and freezing) can be improved.

Acclimation to abiotic stresses such as cold leads to accumulation of metabolites in plant tissues to protect cellular functions (Morgan 1992; Ruelland et al. 2009; Ouellet and Charron 2013; Miura and Furumoto 2013). Some of these compounds act as osmoprotectants to protect against abiotic stresses that affect the water balance of plants (Vágújfalvi et al. 1999; Uemura et al. 2003; Chen et al. 2014). Osmolytes are small, electrically neutral, water-soluble organic compounds that efficiently maintain osmotic balance and stabilize membranes and macromolecules under water stress conditions. They include betaines, amino acids, polyols and non-reducing sugars (Burg and Ferraris 2008; Slama et al. 2015; Nahar et al. 2016; Argiolas et al. 2016). Osmolytes also protect membranes and act as scavengers for toxic reactive oxygen species. They are induced by a variety of other abiotic stresses that affect the water balance (drought, heat, salinity), making them therefore less specific markers for cold tolerance per se (Beck et al. 2007). There is no clear evidence available as to how quantitative or qualitative differences in accumulation of these compounds directly contribute to cold tolerance. We compared changes in the concentrations of metabolites and lipids during cold acclimation for two wheat varieties that differ in cold tolerance. Many metabolites are subject to day-night circadian fluctuations and cold or frost events usually occur during the night. It has been demonstrated that there is a substantial overlap between cold and circadian-regulated genes, suggesting that cold acclimation is tightly linked to circadian rhythms (Espinoza et al. 2010; Sanchez et al. 2011). However, it is

expected that some compounds that accumulate after an initial chilling or frost event during the night remain present in plant tissues as a protection against subsequent chilling events. To investigate this, we designed an experiment where we compared metabolite levels in leaves harvested in the morning immediately after a chilling event and 6 h later, when plants were allowed to recover in the light at normal temperatures. We also compared these samples for a single and four consecutive chilling cycles. Because our focus is on using metabolites as diagnostic markers for cold acclimation, we first used the easy-to-collect flag leaves.

4.3 Effect of prolonged/consecutive chilling treatments on wheat flag leaf metabolites and lipids

Cumulative changes with respect to TP_0, TP_1 and TP_3 for both Wyalkatchem and Young flag leaves show significant changes occurring after the first cold night (TP_1), with additional changes appearing after prolonged cold treatment (TP_3). However, fewer changes were observed in the daytime samples (TP_2 and TP_4), suggesting that partial recovery takes place during normal day temperatures for some metabolites. Day-night fluctuation in levels of some metabolite is likely due to circadian rhythms and fluctuation of photosynthetic activity and associated metabolism and needs to be taken into account for field sampling and cold tolerance phenotyping. After the first night of cold treatment, a significant reduction in the levels of most amino acids and amines was evident in Wyalkatchem, but not in Young. Most amino acids and amines were higher in Young compared to Wyalkatchem from the first overnight cold treatment (TP_1). Interestingly, the amino acids proline and citrulline, which are known to accumulate in plant tissues under a variety of stresses that affect water relations (drought, salinity, cold, heat; Mayer et al. 1990; Ashraf and Foolad 2007; Lehmann et al. 2010; Hayat et al. 2012; Liang et al. 2013), behaved quite differently in Wyalkatchem compared to Young. Proline was found to decrease significantly after one night cold treatment in Wyalkatchem but increased in Young flag leaves. Citrulline behaved in a similar fashion, but was only found to change significantly at a more relaxed cut-off of ($p < 0.1$) in both wheat lines. Citrulline has hydroxyl radical scavenging and antioxidant properties and can protect DNA and enzymes from oxidative injuries (Kawasaki et al. 2000; Akashi et al. 2001; Rimando and Perkins-Veazie 2005; Kusvuran et al. 2013).

In Young, a significant increase in citrulline was observed in the TP_2 samples. GABA, an amine with cryo-protective properties (Bouche and Fromm 2004; Mazzucotelli et al. 2006) was also marginally increased-albeit below significance levels. After the prolonged cold treatment (TP_3), amino acid levels in Wyalkatchem did not fully recover and citrulline increased further. Accumulation of citrulline occurred predominantly in Wyalkatchem and only temporarily in Young (TP_1). Wyalkatchem also showed a threefold increase for the polyamine putrescine, an amino acid breakdown product with growth-regulatory properties known to play a role in abiotic stresses (Gill and Tuteja 2010; Shi and Chan 2014). Shikimate, a substrate for the synthesis of lignin and various aromatic compounds such as quinate (Herrmann and Weaver 1999; Guo et al. 2014) was increased in Wyalkatchem but decreased in Young. The enzymes of this pathway have been shown to be involved in defence responses (Kasai et al. 2005). Furthermore, compatible osmolytes such as sugars (arabinose, glucose, glucose-6-P,fructose and raffinose) and the sugar alcohol mannitol also accumulated in Wyalkatchem upon cold treatment, but not in Young flag leaves. Sugars and sugar alcohols play a role as osmo-and cryo-protectants (Loescher et al. 1992; Travert et al. 1997; Burg and Ferraris 2008; Slama et al. 2015). The accumulation of these osmolytes indicates that Wyalkatchem is responding to water or desiccation stress as a consequence of cold treatment. Repression of amino acid synthesis in Wyalkatchem may also contribute to this situation. None of these symptoms was observed in tolerant variety Young. Osmolytes can therefore serve as markers for chilling sensitivity; they may be indicative of water stress as a result of membrane damage caused by chilling and frost. But osmolytes point to a secondary effect of cold treatment and their accumulation is therefore not specific for low temperature stress. Osmolyte accumulation can be activated by other abiotic stresses as well (drought, heat, salinity; Beck et al. 2007). We did not observe many significant differences in phytohormone levels between Wyalkatchem and Young. Interestingly, the only phytohormone that showed significant differences between the two wheat varieties was salicylic acid. Trans-cinnamic acid (significant at TP_2), one of the precursors of salicylic acid biosynthesis (Hayat et al. 2007), follows the same abundance profile as salicylic acid. Salicylic acid levels were consistently higher in Wyalkatchem compared to Young at both short and prolonged cold stress exposures. Salicylic acid is known for its role in plant pathogen responses, but also plays a role in abiotic stress in regulating stomatal closure under water stress. When applied to plants, salicylic acid was shown to reduce freezing tolerance and at high levels causes oxidative stress and increased stress sensitivity (Lissarre et al. 2010; Miura and Tada 2014; Eremina et al. 2016).

Cold treatment of Wyalkatchem and Young flag leaves resulted in quantitative and qualitative changes in the lipid composition and the lipid changes outnumber those observed for the primary metabolites. The most prevalent changes in cold-stressed Wyalkatchem and Young flag leaves were

observed for the phospatidylcholine (PC) class of lipids. PCs are the most abundant plasma membrane lipids in plants and animals. Differences between Wyalkatchem and Young PC levels in response to cold may therefore contribute to changes in plasma membrane fluidity and permeability (Upchurch 2008; van Meer et al. 2008). The saturated lipid species PC(34:0), monounsaturated species PC(34:1) and PC(35:1) increased in both wheat varieties after the first exposure to cold (TP_1) and then decreased after prolonged cold treatment (TP_3) (Fig. 5c). However, the decrease of these PCs at TP_3 was faster in Young compared to Wyalkatchem and this may have contributed to a higher level of unsaturated lipids in Young compared to Wyalkatchem (Fig. 5c). Even at TP_0, Young and Wyalketchem flag leaves show a different lipid saturation:unsaturation ratio and some lipid levels are marginally different, but become significantly different after the first night of cold treatment. This seems to indicate that Young is better adapted to cold from the beginning. The change in the unsaturated to saturated lipid ratio is the result of a change in relatively few lipid species and this may be the result of a modification in the expression of a small number of genes. The fact that Young and Wyalkatchem show a different lipid content before and after cold treatment may indicate that both lines are adapted differently to cold temperatures and this may be due to genetic variation in the regulation or function of lipid biosynthesis gene/genes. Using lipids as phenotyping markers may enable us to identify those genes using a mapping population. The superior ability of the tolerant variety Young to adjust and remodel its membrane composition may be the key factor to overcome prolonged cold exposure. We do not know to what extend the differences in lipid content between Young and Wyalkatchem flag leaves can protect against frost (temperature threshold) or whether the observed differences are sufficient to survive more severe frost conditions. But using lipidomics to screen wheat germplasm collections for varieties with higher lipid unsaturation levels than Young may hold the key to improving frost tolerance in wheat. Plants produce a large variety of lipid species in their chloroplasts and the fact that the spectrum of synthesised lipids depends significantly on the reigning environmental conditions (e.g., temperature) indicates that modification of membrane lipid composition is an important environmental adaption mechanism (Aid 2019).

Phosphatidylglycerol lipids (PGs) are the main phospholipid class of thylakoid membranes in higher plants (Ren et al. 2014). PGs are the second largest lipid group that is affected by cold in wheat flag leaves. The saturated lipid PG(32:0) is lower in Young and higher in Wyalkatchem flag leaves after the prolonged cold stress (TP_3), indicating that this lipid species may also contribute to the higher degree of lipid unsaturation in membranes of the tolerant variety Young. Phosphotidylinositol (PI) lipids are the third most abundant extraplastidic lipid. PIs are involved in membrane signalling under abiotic stress conditions such as osmotic stress (Munnik and Vermeer 2010; Zheng et al. 2016). PIs increase by 50% after freezing in Arabidopsis and contribute to frost tolerance (Zheng et al. 2016). Significantly higher levels in Young compared to Wyalkatchem of polyunsaturated PI species such PI(36:4) at TP_1 may also contribute to better membrane protection for the tolerant variety during cold stress.

Plants respond with complex changes in lipid composition during cold acclimation to maintain membrane integrity (Uemura and Steponkus 1994; Uemura et al. 1995; Degenkolbe et al. 2012). The amount of double bonds in unsaturated lipids improves membrane fluidity at lower temperatures. To maintain optimum membrane fluidity, unsaturation levels of lipids decreases at higher temperatures and increases at lower temperatures (Narayanan et al. 2016a, b; Zheng et al. 2016). The significant increase in the ratio of unsaturated to saturated lipids after prolonged cold treatment suggests that Young is better able to adapt its membrane composition to low temperatures. Failure of Wyalkatchem to modify lipid composition in favour of unsaturated to saturated lipids may lead to membrane damage, causing electrolyte leakage and water loss, leading to the osmotic stress response observed in this variety. The lipid changes we observed in Young and Wyalkatchem flag leaves are part of an acclimation response to cold; they are amplified during prolonged cold treatment, they are not subjected to diurnal fluctuations and they are specific for low temperature adaptation. Lipids are therefore suitable markers for chilling and frost tolerance phenotyping.

5 Conclusion

In conclusion, combined metabolome and lipidome analyses in flag leaves have shed light on important differences in cold acclimation between the cold-sensitive Wyalkatchem and cold-tolerant Young varieties. The main differences between the two wheat cultivars were the differential modification of membrane lipids in both varieties and the establishment of an osmotic stress-like response in the sensitive varieties Wyalkatchem. There is a gradual change in the ratio of unsaturated versus saturated lipids that favors higher levels of unsaturated lipids being incorporated in the tolerant variety Young. As a consequence, Young may acquire a superior ability to adapt membrane fluidity to cold conditions and avoid membrane damage. Diagnostic metabolites, including sugars and lipids, can therefore serve as tools to improve the reliability of phenotyping for chilling and frost tolerance in wheat. Furthermore, metabolomics and lipidomics can be combined with transcriptome analysis and genomics approaches to identify the genetic mechanism driving the

observed differences in metabolite accumulation and this could lead to future DNA marker-based approaches for frost tolerance breeding in wheat.

Acknowledgements Cold treatments were carried out using growth chambers from the High- Resolution Plant Phenomics Centre in Canberra (HRPPC; https://www.plantphenomics.org.au/tag/high-resolution-plant-phenomics-centre/). The authors thank Mrs Cheka Kehelpannala from the School of Biosciences, Mrs Nirupama Jayasinghe, Mrs Himasha Mendis, Ms. Veronica Lui and Dr Siria Natera from Metabolomics Australia for the metabolite, lipid and phytohormone analyses. Metabolomics Australia (School of BioSciences, The University of Melbourne, Australia) is a National Collaborative Research Infrastructure Strategy initiative under Bioplatforms Australia Pty Ltd (http://www.bioplatforms.com/).

Author contributions BEC performed part of the metabolite, lipid and phytohormone experiments and analysed the data. WWHH and TWTR contributed to the data analysis. UR designed the metabolite analysis and contributed to data analysis, statistical analysis and manuscript writing. RD conceived the project, designed the experiments and contributed to the writing of the manuscript. RD, XW, and TR established the controlled environmental conditions for chilling treatments and harvested the plant tissue samples for metabolite analysis. BB provided advice on the wheat germplasm to best use in this study and provided field climatic information, as well as advice to establish the controlled environmental conditions most likely to provide discriminating damage based on field experience in phenotyping the same material. BEC, WWHH, TWTR and RD wrote the manuscript.

Funding This research was supported by Grants of the Australian Grains Research and Development Corporation (GRDC projects CSP00143 and CSP00202).

Data availability statement All the data sets that support the findings of this study are available as Supplemental data files (Microsoft Excel 2013 files).

Compliance with ethical standards

Conflict of interest The authors declare that they have no conflict of interest.

Research involved human and animal participants This article does not contain any studies with human and/or animal participants performed by any of the authors.

Open Access This article is distributed under the terms of the Creative Commons Attribution 4.0 International License (http://creativecommons.org/licenses/by/4.0/), which permits unrestricted use, distribution, and reproduction in any medium, provided you give appropriate credit to the original author(s) and the source, provide a link to the Creative Commons license, and indicate if changes were made.

References

Aid, F. (2019). Plant lipid metabolism. In R. V. Baez (Ed.), *Lipid metabolism*. Vienna: IntechOpen.

Akashi, K., Miyake, C., & Yokota, A. (2001). Citrulline, a novel compatible solute in drought-tolerant wild watermelon leaves, is an efficient hydroxyl radical scavenger. *FEBS Letters, 508*(3), 438–442.

Argiolas, A., Puleo, G. L., Sinibaldi, E., & Mazzolai, B. (2016). Osmolyte cooperation affects turgor dynamics in plants. *Scientific Reports, 6,* 30139.

Ashraf, M., & Foolad, M. R. (2007). Roles of glycine betaine and proline in improving plant abiotic stress resistance. *Environmental and Experimental Botany, 59*(2), 206–216.

Barlow, K. M., Christy, B. P., O'Leary, G. J., Riffkin, P. A., & Nuttall, J. G. (2015). Simulating the impact of extreme heat and frost events on wheat crop production: A review. *Field Crops Research, 171,* 109–119.

Beck, E. H., Fettig, S., Knake, C., Hartig, K., & Bhattarai, T. (2007). Specific and unspecific responses of plants to cold and drought stress. *Journal of Biosciences, 32*(3), 501–510.

Benjamini, Y., & Hochberg, Y. (1995). Controlling the false discovery rate: A practical and powerful approach to multiple testing. *Journal of the Royal Statistical Society (Series B), 57*(1), 289–300.

Bohn, M., Luthje, S., Sperling, P., Heinz, E., & Dorffling, K. (2007). Plasma membrane lipid alterations induced by cold acclimation and abscisic acid treatment of winter wheat seedlings differing in frost resistance. *Journal of Plant Physiology, 164*(2), 146–156.

Bouche, N., & Fromm, H. (2004). GABA in plants: Just a metabolite? *Trends in Plant Science, 9*(3), 110–115.

Boughton, B. B., Callahan, D. L., Silva, C., Bowne, J., Nahid, A., Rupasinghe, T., et al. (2011). Comprehensive profiling and quantitation of amine group containing metabolites. *Analytical Chemistry, 83,* 7523–7530.

Burg, M. B., & Ferraris, J. D. (2008). Intracellular organic osmolytes: Function and regulation. *Journal of Biological Chemistry, 283*(12), 7309–7313.

Cao, D., Lutz, A., Hill, C. B., Callahan, D. L., & Roessner, U. (2017). A quantitative profiling method of phytohormones and other metabolites applied to barley roots subjected to salinity stress. *Frontiers in Plant Science, 7,* 2070.

Chakrabarti, B., Singh, S. D., Nagarajan, S., & Aggarwal, P. K. (2011). Impact of temperature on phenology and pollen sterility of wheat varieties. *Australian Journal of Crop Science, 5*(8), 1039–1043.

Chen, Y., Jiang, J., Chang, Q., Gu, C., Song, A., Chen, S., et al. (2014). Cold acclimation induces freezing tolerance via antioxidative enzymes, proline metabolism and gene expression changes in two *Chrysanthemum* species. *Molecular Biology Reports, 41*(2), 815–822.

Crimp, S., Bakar, K. S., Kokic, P., Jin, H., Nicholls, N., & Howden, M. (2015). Bayesian space-time model to analyse frost risk for agriculture in Southeast Australia. *International Journal of Climatology, 35*(8), 2092–2108.

Degenkolbe, T., Giavalisco, P., Zuther, E., Seiwert, B., Hincha, D. K., & Willmitzer, L. (2012). Differential remodeling of the lipidome during cold acclimation in natural accessions of *Arabidopsis thaliana*. *Plant Journal, 72*(6), 972–982.

Demotes-Mainard, S., Doussinault, G., Meynard, J. M., & Gate, P. (1996). Is it possible to diagnose at harvest a problem of pollen sterility in wheat? *European Journal of Agronomy, 5*(3–4), 169–180.

Dias, D. A., Hill, C. B., Jayasinghe, N. S., Atieno, J., Sutton, T., & Roessner, U. (2015). Quantitative profiling of polar primary metabolites of two chickpea cultivars with constrasting responses to salinity. *Journal of Chromatography B, 1000,* 1–13.

Dolferus, R., Powell, N., Ji, X., Ravash, R., Edlington, J., Oliver, S., et al. (2013). The physiology of reproductive-stage abiotic stress tolerance in cereals. In G. Rout & A. Das (Eds.), *Molecular stress physiology of plants* (pp. 193–216). India: Springer.

Douglas, D. J. (2009). Linear quadruples in mass spectrometry. *Mass Spectrometry Reviews, 28,* 937–960.

Eremina, M., Rozhon, W., & Poppenberger, B. (2016). Hormonal control of cold stress responses in plants. *Cellular and Molecular Life Sciences, 73*(4), 797–810.

Espinoza, C., Degenkolbe, T., Caldana, C., Zuther, E., Leisse, A., Willmitzer, L., et al. (2010). Interaction with diurnal and circadian regulation results in dynamic metabolic and transcriptional changes during cold acclimation in *Arabidopsis*. *PLoS ONE, 5*(11), e14101.

Fiebelkorn, D., & Rahman, M. (2016). Development of a protocol for frost-tolerance evaluation in rapeseed/canola (*Brassica napus* L). *Crop Journal, 4*(2), 147–152.

Fleury, D., Jefferies, S., Kuchel, H., & Langridge, P. (2010). Genetic and genomic tools to improve drought tolerance in wheat. *Journal of Experimental Botany, 61*(12), 3211–3222.

Folch, J., Lees, M., & Stanley, G. H. S. (1957). A simple method for the isolation and purification of total lipids from animal tissues. *Journal of Biological Chemistry, 226,* 497–509.

Fowler, D. B., Breton, G., Limin, A. E., Mahfoozi, S., & Sarhan, F. (2001). Photoperiod and temperature interactions regulate low-temperature-induced gene expression in barley. *Plant Physiology, 127*(4), 1676–1681.

Frederiks, T. M., Christopher, J. T., Fletcher, S. E. H., & Borrell, A. K. (2011). Post head-emergence frost resistance of barley genotypes in the northern grain region of Australia. *Crop and Pasture Science, 62*(9), 736–745.

Frederiks, T. M., Christopher, J. T., Harvey, G. L., Sutherland, M. W., & Borrell, A. K. (2012). Current and emerging screening methods to identify post-head-emergence frost adaptation in wheat and barley. *Journal of Experimental Botany, 63*(15), 5405–5416.

Gill, S. S., & Tuteja, N. (2010). Polyamines and abiotic stress tolerance in plants. *Plant Signaling & Behavior, 5,* 26–33.

Gray, G. R., Chauvin, L.-P., Sarhan, F., & Huner, N. P. (1997). Cold acclimation and freezing tolerance (a complex interaction of light and temperature). *Plant Physiology, 114,* 467–474.

Guo, J., Carrington, Y., Alber, A., & Ehlting, J. (2014). Molecular characterization of quinate and shikimate metabolism in *Populus trichocarpa*. *Journal of Biological Chemistry, 289,* 23846–23858.

Guy, C. L. (1990). Cold acclimation and freezing stress tolerance: Role of protein metabolism. *Annual Review of Plant Physiology and Plant Molecular Biology, 41,* 187–223.

Guy, C. (1999). Molecular responses of plants to cold shock and cold acclimation. *Journal of Molecular Microbiology Biotechnology, 1*(2), 231–242.

Hayase, H., Satake, T., Nashiyama, I., & Ito, N. (1969). Male sterility caused by cooling treatment at the meiotic stage in rice plants. II. The most sensitive stage to cooling and fertilizing ability of pistils. *Proceedings of the Crop Science. Society of Japan, 38,* 706–711.

Hayat, S., Ali, B., & Ahmad, A. (2007). Salicylic acid: Biosynthesis, metabolism and physiological role in plants. In S. Hayat & A. Ahmad (Eds.), *Salicylic acid: A plant hormone* (pp. 1–14). Dordrecht: Springer.

Hayat, S., Hayat, Q., Alyemeni, M. N., Wani, A. S., Pichtel, J., & Ahmad, A. (2012). Role of proline under changing environments: A review. *Plant Signaling & Behavior, 7*(11), 1456–1466.

Herrmann, K. M., & Weaver, L. M. (1999). The shikimate pathway. *Annual Review of Plant Physiology and Plant Molecular Biology, 50,* 473–503.

Horvath, E., Szalai, G., & Janda, T. (2007). Induction of abiotic stress tolerance by salicylic acid signaling. *Journal of Plant Growth Regulation, 26*(3), 290–300.

Janmohammadi, M. (2012). Metabolomic analysis of low temperature responses in plants. *Current Opinion in Agriculture, 1,* 1–6.

Javadian, N., Karimzadeh, G., Mahfoozi, S., & Ghanati, F. (2010). Cold-induced changes of enzymes, proline, carbohydrates, and chlorophyll in wheat. *Russian Journal of Plant Physiology, 57*(4), 540–547.

Ji, X., Shiran, B., Wan, J., Lewis, D. C., Jenkins, C. L. D., Condon, A. G., et al. (2010). Importance of pre-anthesis anther sink strength for maintenance of grain number during reproductive stage water stress in wheat. *Plant, Cell and Environment, 33*(6), 926–942.

Jorge, T. F., Rodrigues, J. A., Caldana, C., Schmist, R., van Dongen, J. T., Thomas-Oates, J., et al. (2016). Mass spectrometry-based plant metabolomics: Metabolite responses to abiotic stress. *Mass Spectrometry Reviews, 35,* 620–649.

Kalberer, S. R., Wisniewski, M., & Arora, R. (2006). Deacclimation and reacclimation of cold-hardy plants: Current understanding and emerging concepts. *Plant Science, 171*(1), 3–16.

Kasai, K., Kanno, T., Akita, M., Ikejiri-Kanno, Y., Wakasa, K., & Tozawa, Y. (2005). Identification of three shikimate kinase genes in rice: characterization of their differential expression during panicle development and of the enzymatic activities of the encoded proteins. *Planta, 222*(3), 438–447.

Kawasaki, S., Miyake, C., Kohchi, T., Fujii, S., Uchida, M., & Yokota, A. (2000). Responses of wild watermelon to drought stress: Accumulation of an ArgE homologue and citrulline in leaves during water deficits. *Plant and Cell Physiology, 41*(7), 864–873.

Kurepin, L. V., Dahal, K. P., Savitch, L. V., Singh, J., Bode, R., Ivanov, A. G., et al. (2013). Role of CBFs as integrators of chloroplast redox, phytochrome and plant hormone signaling during cold acclimation. *International Journal of Molecular Sciences, 14*(6), 12729–12763.

Kusvuran, S., Dasgan, H. Y., & Abak, K. (2013). Citrulline is an important biochemical indicator in tolerance to saline and drought stresses in melon. *The Scientific World Journal, 2013,* 253414.

Leff, B., Ramankutty, N., & Foley, J. A. (2004). Geographic distribution of major crops across the world. *Global Biogeochemical Cycles, 18*(1), 1–27.

Lehmann, S., Funck, D., Szabados, L., & Rentsch, D. (2010). Proline metabolism and transport in plant development. *Amino Acids, 39*(4), 949–962.

Levitt, J. (1980). *Responses of plants to environmental stresses. Volume I. Chilling, freezing and high temperature stresses*. New York: Academic Press.

Li, X., Cai, J., Liu, F., Dai, T., Cao, W., & Jiang, D. (2014). Spring freeze effect on wheat yield is modulated by winter temperature fluctuations: Evidence from meta-analysis and simulating experiment. *Journal of Agronomy and Crop Science, 201*(4), 288–300.

Li, X., Cai, J., Liu, F., Zhou, Q., Dai, T., Cao, W., et al. (2015). Wheat plants exposed to winter warming are more susceptible to low temperature stress in the spring. *Plant Growth Regulation, 77*(1), 11–19.

Liang, X., Zhang, L., Natarajan, S. K., & Becker, D. F. (2013). Proline mechanisms of stress survival. *Antioxidants & Redox Signaling, 19*(9), 998–1011.

Limin, A. E., & Fowler, D. B. (2006). Low-temperature tolerance and genetic potential in wheat (*Triticum aestivum* L): Response to photoperiod, vernalization, and plant development. *Planta, 224*(2), 360–366.

Lissarre, M., Ohta, M., Sato, A., & Miura, K. (2010). Cold-responsive gene regulation during cold acclimation in plants. *Plant Signaling & Behavior, 5*(8), 948–952.

Livingston, D. P. I., Tuong, T. D., Isleib, T. G., & Murphy, J. P. (2016). Differences between wheat genotypes in damage from freezing temperatures during reproductive growth. *European Journal of Agronomy, 74,* 164–172.

Lobell, D. B., & Gourdji, S. M. (2012). The influence of climate change on global crop productivity. *Plant Physiology, 160,* 1686–1697.

Loescher, W. H., Tyson, R. H., Everard, J. D., Redgwell, R. J., & Bieleski, R. L. (1992). Mannitol synthesis in higher plants: Evidence for the role and characterization of a NADPH-dependent

mannose 6-phosphate reductase. *Plant Physiology, 98,* 1396–1402.
Machakova, I., Hanisova, A., & Krekule, J. (1989). Levels of ethylene, ACC, MACC, ABA and proline as indicators of cold hardening and frost resistance in winter wheat. *Physiologia Plantarum, 76,* 603–607.
Marcellos, H., & Single, W. V. (1975). Temperatures in wheat during radiation frost. *Australian Journal of Experimental Agriculture, 15*(77), 818–822.
March, T., Knights, S., Biddulph, B., Ogbonnaya, F., Maccallum, R., & Belford, R. (2015). *The GRDC National Frost Initiative, Vol 2015.*
Mayer, R. R., Cherry, J. H., & Rhodes, D. (1990). Effects of heat shock on amino acid metabolism of cowpea cells. *Plant Physiology, 94,* 796–810.
Mazzucotelli, E., Tartari, A., Cattivelli, L., & Forlani, G. (2006). Metabolism of gamma-aminobutyric acid during cold acclimation and freezing and its relationship to frost tolerance in barley and wheat. *Journal of Experimental Botany, 57*(14), 3755–3766.
Meijer, H. J., & Munnik, T. (2003). Phospholipid-based signaling in plants. *Annual Review of Plant Biology, 54,* 265–306.
Miura, K., & Furumoto, T. (2013). Cold signaling and cold response in plants. *International Journal of Molecular Sciences, 14*(3), 5312–5337.
Miura, K., & Tada, Y. (2014). Regulation of water, salinity, and cold stress responses by salicylic acid. *Frontiers in Plant Science, 5,* 4.
Monroy, A. F., Dryanova, A., Malette, B., Oren, D. H., Ridha Farajalla, M., Liu, W., et al. (2007). Regulatory gene candidates and gene expression analysis of cold acclimation in winter and spring wheat. *Plant Molecular Biology, 64*(4), 409–423.
Morgan, J. (1992). Osmotic components and properties associated with genotypic differences in osmoregulation in wheat. *Functional Plant Biology, 19*(1), 67–76.
Munnik, T., & Vermeer, J. E. M. (2010). Osmotic stress-induced phosphoinositide and inositol phosphate signalling in plants. *Plant, Cell and Environment, 33*(4), 655–669.
Nahar, K., Hasanuzzaman, M., & Fujita, M. (2016). Roles of osmolytes in plant adaptation to drought and salinity. In N. Iqbal, R. Nazar, & N. A. Khan (Eds.), *Osmolytes and plants acclimation to changing environment: Emerging omics technologies* (pp. 37–68). India: Springer.
Narayanan, S., Prasad, P. V., & Welti, R. (2016a). Wheat leaf lipids during heat stress: II. Lipids experiencing coordinated metabolism are detected by analysis of lipid co-occurrence. *Plant, Cell and Environment, 39*(3), 608–617.
Narayanan, S., Tamura, P. J., Roth, M. R., Prasad, P. V., & Welti, R. (2016b). Wheat leaf lipids during heat stress: I. High day and night temperatures result in major lipid alterations. *Plant, Cell and Environment, 39*(4), 787–788.
Natera, S. H. A., Hill, C. B., Rupasinghe, T. W. T., & Roesner, U. (2016). Salt-stress induced alterations in the root lipidome of two barley genotypes with contrasting responses to salinity. *Functional Plant Biology, 43*(2), 207–219.
Nishiyama, I. (1984). Climatic influence on pollen formation and fertilization. In S. Tsunoda & N. Takahashi (Eds.), *Biology of rice* (pp. 153–171). Amsterdam: Elsevier.
Oliver, S. N., Van Dongen, J. T., Alfred, S. C., Mamun, E. A., Zhao, X., Saini, H. S., et al. (2005). Cold-induced repression of the rice anther-specific cell wall invertase gene *OSINV4* is correlated with sucrose accumulation and pollen sterility. *Plant, Cell and Environment, 28*(12), 1534–1551.
Ouellet, F., & Charron, J. B. (2013). Cold acclimation and freezing tolerance in plants. *Encyclopedia of Life Sciences*. https://doi.org/10.1002/9780470015902.a0020093.
Pagter, M., & Arora, R. (2013). Winter survival and deacclimation of perennials under warming climate: Physiological perspectives. *Physiologia Plantarum, 147*(1), 75–87.
Palta, J. P., & Weiss, L. S. (1993). Ice formation and freezing injury: An overview on the survival mechanisms and molecular aspects of injury and cold acclimation in herbaceous plants. In P. H. Li & L. Christersson (Eds.), *Advances in plant cold hardiness* (pp. 143–176). Boca Raton (Florida): CRC Press.
Rapacz, M. (2002). Regulation of frost resistance during cold deacclimation and re-acclimation in oilseed rape. A possible role of PSII redox state. *Physiologia Plantarum, 115*(2), 236–243.
Rawlinson, C., Kamphuis, L. G., Gummer, J. P. A., Singh, K. P., & Trengove, R. D. (2015). A rapid method for profiling of volatile and semi-volatile phytohormones using methyl chloroformate derivatisation and GC-MS. *Metabolomics, 11*(6), 1922–1933.
Ren, M., Phoon, C. K. L., & Schlame, M. (2014). Metabolism and function of mitochondrial cardiolipin. *Progress in Lipid Research, 55,* 1–6.
Rerkasem, B. (1996). A general survey of the incidence of wheat sterility. In H. M. Rawson & K. D. Subedi (Eds.), A*CIAR Proceedings of the Sterility in wheat in subtropical Asia: extent, causes and solutions*, Vol 72 (pp. 8–12). Pokhara (Nepal): LumJe Agricultural Research Centre.
Richards, R. A., Rebetzke, G. J., Watt, M., Condon, A. G., Spielmeyer, W., & Dolferus, R. (2010). Breeding for improved water productivity in temperate cereals: Phenotyping, quantitative trait loci, markers and the selection environment. *Functional Plant Biology, 37*(2), 85–97.
Rimando, A. M., & Perkins-Veazie, P. M. (2005). Determination of citrulline in watermelon rind. *Journal of Chromatography A, 1078*(1–2), 196–200.
Ruelland, E., Vaultier, M.-N., Zachowski, A., & Hurry, V. (2009). Chapter 2: Cold signalling and cold acclimation in plants. In K. Jean-Claude & D. Michel (Eds.), *Advances in botanical research* (Vol. 49, pp. 35–150). New York: Academic Press.
Sanchez, A., Shin, J., & Davis, S. J. (2011). Abiotic stress and the plant circadian clock. *Plant Signaling and Behaviour, 6*(2), 223–231.
Satake, T., Nishiyama, I., Ito, N., & Hayase, H. (1969). Male sterility caused by cooling treatment at the meiotic stage in rice plants. I. Methods of growing rice plants and inducing sterility in the phytotron. *Japanese Journal of Crop Science, 38,* 603–609.
Shavrukov, Y., Kurishbayev, A., Jatayev, S., Shvidchenko, V., Zotova, L., Koekemoer, F., et al. (2017). Early flowering as a drought escape mechanism in plants: How can it aid wheat production? *Frontiers in Plant Science, 8,* 950.
Shi, H., & Chan, Z. (2014). Improvement of plant abiotic stress tolerance through modulation of the polyamine pathway. *Journal of Integrative Plant Biology, 56*(2), 114–121.
Slama, I., Abdelly, C., Bouchereau, A., Flowers, T., & Savouré, A. (2015). Diversity, distribution and roles of osmoprotective compounds accumulated in halophytes under abiotic stress. *Annals of Botany, 115*(3), 433–447.
Smallwood, M., & Bowles, D. J. (2002). Plants in a cold climate. *Philosophical Transactions of the Royal Society B: Biological Sciences, 357*(1423), 831–847.
Smith, A. R., & Zhao, D. (2016). Sterility caused by floral organ degeneration and abiotic stresses in *Arabidopsis* and cereal grains. *Frontiers in Plant Science, 7,* 1503.
Steponkus, P. L., Uemura, M., & Webb, M. S. (1993). A contrast of the cryostability of the plasma membrane of winter rye and spring oat-two species that widely differ in their freezing tolerance and plasma membrane lipid composition. In P. L. Steponkus (Ed.), *Advances in low-temperature biology* (Vol. 2, pp. 211–312). London: JAI Press.
Subedi, K. D., Floyd, C. N., & Budhathoki, C. B. (1998a). Cool temperature-induced sterility in spring wheat (*Triticum aestivum* L.)

at high altitudes in Nepal: Variation among cultivars in response to sowing date. *Field Crops Research, 55*(1–2), 141–151.

Subedi, K., Gregory, P., Summerfield, R., & Gooding, M. (1998b). Cold temperatures and boron deficiency caused grain set failure in spring wheat (*Triticum aestivum* L.). *Field crops research, 57*(3), 277–288.

Subedi, K. D., Gregory, P. J., Summerfield, R. J., & Gooding, M. J. (2000). Pattern of grain set in boron-deficient and cold-stressed wheat (*Triticum aestivum* L). *The Journal of Agricultural Science, 134*(1), 25–31.

Sumner, L. W., Amberg, A., Barrett, D., Beale, M. H., Beger, R., & Daykin, C. A. (2007). Proposed minimum reporting standards for chemical analysis Chemical Analysis Working Group (CAWG) Metabolomics Standards Initiative (MSI). *Metabolomics, 3*(3), 211–221.

Sumner, L. W., Lei, Z., Nikolau, B. J., & Saito, K. (2015). Modern plant metabolomics: Advanced natural product gene discoveries, improved technologies, and future prospects. *Natural Product Reports, 32,* 212–229.

Tomashow, M. F. (1999). Plant cold acclimation: Freezing tolerance genes and regulatory mechanisms. *Annual Review of Plant Physiology and Plant Molecular Biology, 50,* 571–599.

Travert, S., Valerio, L., Fouraste, I., Boudet, A. M., & Teulieres, C. (1997). Enrichment in specific soluble sugars of two Eucalyptus cell-suspension cultures by various treatments enhances their frost tolerance via a noncolligative mechanism. *Plant Physiology, 114,* 1433–1442.

Uemura, M., Joseph, R. A., & Steponkus, P. L. (1995). Cold acclimation of *Arabidopsis thaliana* - effect on plasma membrane lipid composition and freeze-induced lesions. *Plant Physiology, 109,* 15–30.

Uemura, M., & Steponkus, P. L. (1994). A contrast of the plasma membrane lipid composition of oat and rye leaves in relation to freezing tolerance. *Plant Physiology, 104,* 479–496.

Uemura, M., Warren, G., & Steponkus, P. L. (2003). Freezing sensitivity in the *sfr4* mutant of *Arabidopsis* is due to low sugar content and is manifested by loss of osmotic responsiveness. *Plant Physiology, 131,* 1800–1807.

Upchurch, R. G. (2008). Fatty acid unsaturation, mobilization, and regulation in the response of plants to stress. *Biotechnology Letters, 30*(6), 967–977.

Vágújfalvi, A., Kerepesi, I., Galiba, G., Tischner, T., & Sutka, J. (1999). Frost hardiness depending on carbohydrate changes during cold acclimation in wheat. *Plant Science, 144*(2), 85–92.

Valluru, R., Lammens, W., Claupein, W., & Van den Ende, W. (2008). Freezing tolerance by vesicle-mediated fructan transport. *Trends in Plant Science, 13*(8), 409–414.

Van Meer, G., Voelker, D. R., & Feigenson, G. W. (2008). Membrane lipids: Where they are and how they behave. *Nature Reviews Molecular Cell Biology, 9,* 112–124.

Vanková, R., Kosová, K., Dobrev, P., Vítámvás, P., Trávníčková, A., Cvikrová, M., et al. (2014). Dynamics of cold acclimation and complex phytohormone responses in *Triticum monococcum* lines G3116 and DV92 differing in vernalization and frost tolerance level. *Environmental and Experimental Botany, 101,* 12–25.

Verslues, P. E., Agarwal, M., Katiyar-Agarwal, S., Zhu, J., & Zhu, J-K. (2006). Methods and concepts in quantifying resistance to drought, salt and freezing, abiotic stresses that affect plant water status. *Plant Journal, 45,* 523–539.

Vigh, L., Horvath, L. I., Horvath, I., Dudits, D., & Farkas, T. (1979). Protoplast plasmalemma fluidity of hardened wheats correlates with frost resistance. *FEBS Letters, 107*(2), 291–294.

Vitamvas, P., & Prasil, I. T. (2008). WCS120 protein family and frost tolerance during cold acclimation, deacclimation and reacclimation of winter wheat. *Plant Physiology and Biochemistry, 46*(11), 970–976.

Wanner, L. A., & Junttila, O. (1999). Cold-induced freezing tolerance in *Arabidopsis*. *Plant Physiology, 120,* 391–400.

Welti, R., Li, W., Li, M., Sang, Y., Biesiada, H., Zhou, H., et al. (2002). Profiling membrane lipids in plant stress responses. *Journal of Biological Chemistry, 277*(35), 31994–32002.

Welti, R., Shah, J., Li, W., Li, M., Chen, J., Burke, J. J., et al. (2007). Plant lipidomics: Discerning biological function by profiling plant complex lipids using mass spectrometry. *Frontiers in Bioscience, 12,* 2494–2506.

Zadoks, J. C., Chang, T. T., & Konzak, C. F. (1974). A decimal code for the growth stages of cereals. *Weed Research, 14,* 415–421.

Zhang, W., Yu, L., Zhang, Y., & Wang, X. (2005). Phospholipase D in the signaling networks of plant response to abscisic acid and reactive oxygen species. *Biochimica et Biophysica Acta, 1736*(1), 1–9.

Zheng, B., Chapman, S. C., Christopher, J. T., Frederiks, T. M., & Chenu, K. (2015). Frost trends and their estimated impact on yield in the Australian wheatbelt. *Journal of Experimental Botany, 66*(12), 3611–3623.

Zheng, G., Li, L., & Li, W. (2016). Glycerolipidome responses to freezing- and chilling-induced injuries: Examples in Arabidopsis and rice. *BMC Plant Biology, 16,* 70.

Publisher's Note Springer Nature remains neutral with regard to jurisdictional claims in published maps and institutional affiliations.

cells

MDPI

Article

Phenotyping the Chilling and Freezing Responses of Young Microspore Stage Wheat Spikes Using Targeted Metabolome and Lipidome Profiling

Bo Eng Cheong [1], Olive Onyemaobi [2], William Wing Ho Ho [1], Thomas Ben Biddulph [3], Thusitha W. T. Rupasinghe [1], Ute Roessner [1] and Rudy Dolferus [2,*]

1 School of BioSciences, The University of Melbourne, Melbourne, VIC 3010, Australia; cheongb@student.unimelb.edu.au (B.E.C.); whho@unimelb.edu.au (W.W.H.H.); tru@unimelb.edu.au (T.W.T.R.); u.roessner@unimelb.edu.au (U.R.)
2 CSIRO Agriculture & Food, GPO Box 1700, Canberra, ACT 2601, Australia; olive.onyemaobi@csiro.au
3 Department of Primary Industries and Regional Development, 3 Baron Hay Court, South Perth, WA 6151, Australia; ben.biddulph@dpird.wa.gov.au
* Correspondence: rudy.dolferus@csiro.au; Tel.: +61-2-6246 5010

Received: 15 April 2020; Accepted: 20 May 2020; Published: 25 May 2020



Abstract: Chilling and frost conditions impose major yield restraints to wheat crops in Australia and other temperate climate regions. Unpredictability and variability of field frost events are major impediments for cold tolerance breeding. Metabolome and lipidome profiling were used to compare the cold response in spikes of cold-tolerant Young and sensitive variety Wyalkatchem at the young microspore (YM) stage of pollen development. We aimed to identify metabolite markers that can reliably distinguish cold-tolerant and sensitive wheat varieties for future cold-tolerance phenotyping applications. We scored changes in spike metabolites and lipids for both varieties during cold acclimation after initial and prolonged exposure to combined chilling and freezing cycles (1 and 4 days, respectively) using controlled environment conditions. The two contrasting wheat varieties showed qualitative and quantitative differences in primary metabolites involved in osmoprotection, but differences in lipid accumulation most distinctively separated the cold response of the two wheat lines. These results resemble what we previously observed in flag leaves of the same two wheat varieties. The fact that this response occurs in tissue types with very different functions indicates that chilling and freezing tolerance in these wheat lines is associated with re-modelling of membrane lipid composition to maintain membrane fluidity.

Keywords: wheat; spike; cold tolerance; phenotyping; reproductive development; metabolomics; lipidomics

1. Introduction

Frost events can cause major yield losses to cereal crops in many temperate climate regions in the world. Wheat crops in Australia are grown during winter and they flower in early spring to avoid the hot summers and to take advantage of available soil moisture. The sensitive stage of flowering is therefore frequently exposed to frost. The annual yield loss due to frost events to the Australian grains industry is estimated to be A$360 million [1–5]. The problem is exacerbated by climate change. In China and Australia, spring frosts have become increasingly frequent since the 1960s and the length of the frost season has been extended by one month, leading to more frequent yield losses due to frost damage [5–8].

In field conditions, severity, occurrence, and timing of frosts during plant development are highly variable, making screening and selection for wheat germplasm with higher frost tolerance very difficult.

Using controlled environment experiments is complicated by the fact that radiative frost conditions are difficult to simulate [9–12]. Phenology and flowering time play an important role in avoiding exposure of the sensitive reproductive structures, anthers in particular, to frosts [5,7,13,14]. The increased frequency of frost occurrences in field environments indicates the need for wheat germplasm with improved tolerance to frost conditions.

Acclimation to non-freezing chilling or cold conditions (above zero degrees, low temperatures) plays an important role in establishing tolerance to freezing (below zero degree) temperatures. Frosts occur when ice crystallization takes place in plant tissues due to a combination of freezing temperatures, humidity, and temperatures falling below the dew point [4,9]. Plants respond during the chilling period by mounting an acclimation response to protect macromolecules and cellular functions against reactive oxygen species (ROS) and to protect tissues against ensuing freezing and frost conditions [15–18]. Low temperatures were shown to lead to accumulation of osmolytes (various sugars, polyols, betaines, amines, and amino acids) that may act as cryo-protectants to protect the cells against freezing and associated water loss [19–23]. Importantly, protection of membrane fluidity through changes in unsaturated lipid levels in the membrane was also found to play an important role in protecting plant tissues against frost damage [24–26]. However, it remains unclear how quantitative and qualitative differences in the accumulation of these compounds during the acclimation response correlates with differences in frost tolerance levels and information about physiological differences in cold-acclimation responses between cold-tolerant and sensitive germplasm is also missing.

Changes in metabolite composition provide a powerful tool to explore cold acclimation and potentially tolerance to chilling and frost conditions. Metabolomics is therefore a technology that can contribute to more accurate and reliable phenotyping of physiological changes in plant tissues [27–29]. Metabolite and lipidome analyses in wheat flag leaves revealed significant differences in the cold response to chilling of frost-tolerant and sensitive wheat lines: membrane fluidity was maintained mainly by increasing unsaturated lipid levels in cold-tolerant wheat. This response was absent in cold-sensitive wheat, where a water stress-type response was observed instead [30].

The aim of this study was to use metabolomics and lipidomics profiling to investigate changes in cold acclimation in the reproductive tissues (spikes) of two wheat varieties with contrasting cold tolerance. Herein we used the same wheat varieties with our previously published paper, which are the cold-tolerant Young and cold-sensitive Wyalkatchem [30]. Metabolites that can reliably differentiate the response of a cold-tolerant and sensitive wheat line are useful as "diagnostic markers" in wheat cold-tolerance phenotyping. To achieve this, we will have to test the reliability of candidate metabolite markers identified in this study first on a wider range of wheat chilling/freezing tolerant and sensitive germplasm before using these markers in routine phenotyping tasks. We scored metabolite and lipidome changes during cold acclimation after initial exposure (1 day) and prolonged exposure to cold (4 days) in order to identify diagnostic metabolite markers that could reliably distinguish the cold-tolerant wheat variety from the cold-sensitive one. We then compared the cold acclimation response between spikes and flag leaves for the two wheat varieties to identify differences in cold acclimation and to determine which tissue is most suitable for cold tolerance phenotyping. Wheat spikes are physiologically different from flag leaves in that the former are actively developing sink tissues, while the latter are static photosynthetic source tissues. Comparison of the primary metabolite and lipid changes in response to cold for both wheat varieties will enable us to distinguish which metabolites are critically important for cold acclimation.

Abiotic stresses such as cold affect sink–source relationships and distribution of sugars in the plant [31]. Source and sink tissues may therefore react differently to cold and reveal accumulation of different metabolites during cold acclimation. At the young microspore (YM) stage and during grain-filling, the reproductive structures in cereals represent the strongest sink strength of the plant. This is essential to attract sugars for reproductive development and grain filling. Sink strength is highest during pollen formation after meiosis and during grain development after fertilization [32–37]. Abiotic stresses such as cold and drought reduce sink strength in anthers of stress-sensitive lines,

while stress tolerance was correlated with a higher potential to maintain sink strength [38,39]. In this study we demonstrate that cold acclimation in spikes and flag leaves shows some similarities in terms of accumulation of compounds involved in osmoprotection and defense against reactive oxygen species (ROS). However, more importantly, both tissues share a similar mechanism in modifying their membrane lipid composition in response to cold. These findings highlight the importance of preserving membrane fluidity and functionality in different plant tissues during cold acclimation in wheat. Metabolomics and lipidomics can be exploited as a phenotyping strategy to discriminate cold-tolerant from cold-sensitive wheat germplasm.

2. Materials and Methods

2.1. Controlled Environment Wheat Growth, Cold Treatment, and Tissue Sampling

Wheat varieties Wyalkatchem (cold-sensitive) and Young (cold-tolerant), plant growth, and cold treatment conditions were as previously described [30]. The two wheat varieties we used were chosen based on their performance in field chilling and frost trials and can be differentiated in controlled environment assays based on spike sterility levels after a four-day chilling/freezing treatment [30]. Plants were grown in the glasshouse under natural lighting conditions and controlled temperature regime (24/16 °C light/dark). When plants reached the YM stage of pollen development, the YM-stage tillers were tagged and plants were transferred to a Conviron PGC 20 growth chamber (Conviron, Winnipeg, Canada) with the following settings (Figure 1A): 12 h at 21 °C (light period), 4 h linear cooling gradient in the dark to −3 °C, followed by 8 h in the dark at constant −3 °C (12/12 light/dark cycle, using 400 $\mu mol.m^{-2}.s^{-1}$ light intensity) as a cold cycle. The cold-treatment uses a simplified profile of a typical mid-August early morning chilling/frost event in the Southern Australian wheat growing areas. The linear temperature decline in the profile allows induction of an acclimation response before a period of freezing temperatures. Despite the use of below-zero temperatures, this treatment does not cause ice crystal formation. Ice crystallization depends on humidity and dew point which is hard to control in controlled environments. Super-cooling above the canopy [9] or treatments with ice-nucleating agents can cause ice crystallization but were avoided because of secondary effects and because ice formation is not essential for this study that focuses on varietal differences in acclimation to chilling conditions. YM-stage spike samples were harvested at the start of the treatment (TP_0, TP = time point), at the end of the first overnight cold cycle (TP_1), and 6 h into the light cycle after the first cold treatment (TP_2). Samples TP_3 and TP_4 are equivalent to TP_1 and TP_2, but samples were harvested after the fourth consecutive cold treatment to study the effect of long-term cold treatment on the acclimation response [30] (Figure 1A). Each sample used for metabolite measurements consisted of three spikes, harvested from different plants, and for each time point we collected three biological repeat samples for both the cold-tolerant and sensitive wheat varieties.

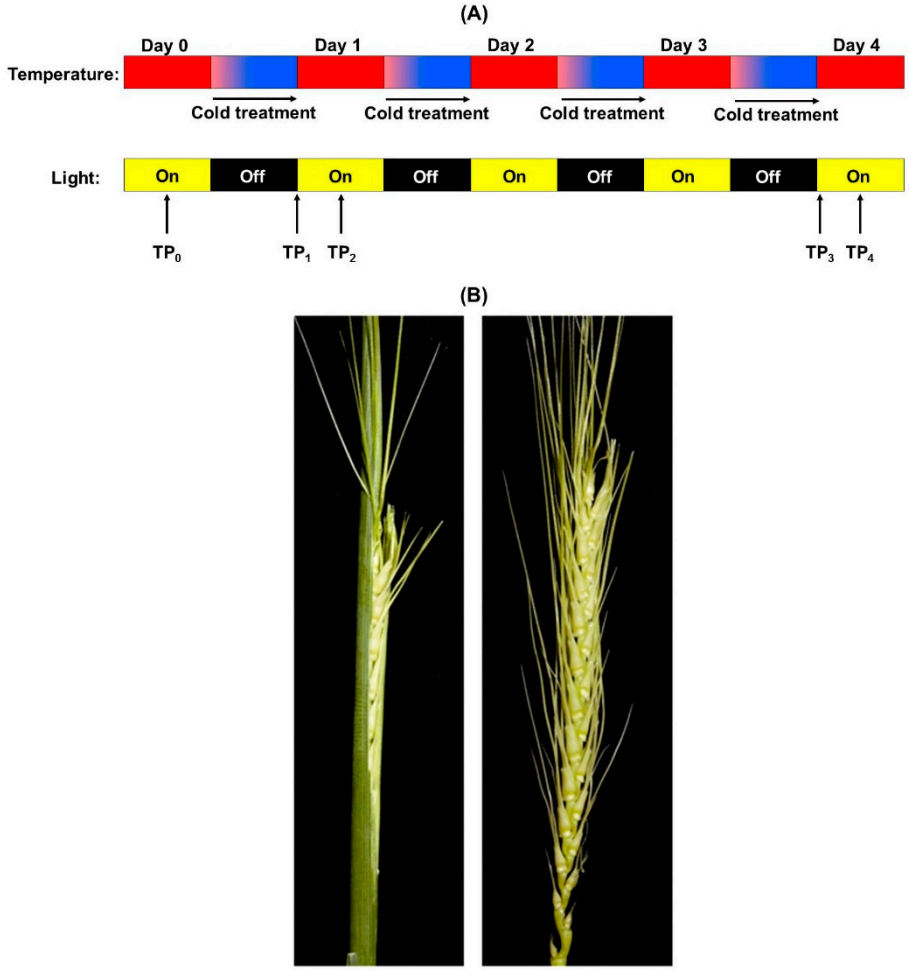


Figure 1. (**A**) Schematic diagram showing the controlled environment design of the cold treatments and lighting conditions (see Section 2.1). Yellow bars show day-light conditions, black bars dark conditions. Arrows labelled TPx indicate where samples were harvested from wheat plants. (**B**) Pictures showing the morphological stage of the young microspore (YM) stage wheat spikes used in this study. At the YM stage, wheat spikes have been shielded from light exposure by the surrounding leaf sheaths (left picture). The picture on the right shows the dissected spike used for metabolite measurements.

2.2. Analysis of Sugars, Organic Acids, Amino Acids, and Amines

All chemicals and solvents for metabolite measurements were purchased from Sigma-Aldrich (Castle Hill, NSW, Australia) and were of analytical or mass spectrometry grades. For sugars, organic acids, and amines, tissue extraction was performed as previously described [30,40], with some modifications. Aliquots of 20 mg of frozen spike material were weighed in Cryomill tubes (Precellys 24, Bertin Technologies, Rockville, MD, USA). To each sample, 500 µL of methanol containing 4% of internal standards (from a stock solution containing 0.5 mg/mL of $^{12}C_6$-sorbitol and 0.5 mg/mL ^{13}C5-^{15}N-L-valine) was added, followed by vortexing for 30 s and homogenization at −10 °C using a Cryomill (3 × 45 s at 6100 rpm). The samples were then extracted for 15 min at 30 °C in a thermomixer at 850 rpm, and subsequently centrifuged for 15 min at 4 °C at 13,000 rpm. The supernatants were combined into new tubes and 500 µL of 0.2% formic acid (in water) was added into the Cryomill tubes containing the previously ground tissue pellet. The samples were vortexed for 30 s, and spun at 13,000 rpm for 15 min at 4 °C. The supernatants were then combined with the methanolic extracts from the previous centrifugation and stored at −80 °C for subsequent analyses.

For the analyses of sugars and organic acids, an 80 µL aliquot of the supernatants was transferred into new glass vial inserts and dried in vacuo without heating. Prior to the GC-QqQ-MS

analysis, the dried extracts were derivatized with methoxyamine hydrochloride in pyridine and bis-(trimethylsilyl)-trifluoroacetamide (BFTFA) as previously described [40]. Briefly, samples were re-dissolved in 20 µL of 30 mg/mL methoxyamine hydrochloride in pyridine and derivatized at 37 °C for 120 min with mixing at 500 rpm. After addition of 20 µL N,O-bis-(trimethylsilyl)-trifluoroacetamide (BSTFA), the samples were incubated for 30 min with mixing at 500 rpm at 37 °C. Derivatized samples were allowed to equilibrate for 60 min and 1 µL aliquots of each sample were injected into a GC-QqQ-MS system, consisting of a Gerstel 2.5.2 Autosampler, a 7890A Agilent gas chromatograph, and a 7000 Agilent triple-quadruple MS (Agilent Technologies, Santa Clara, CA, USA) with an electron impact (EI) ion source. The instrument settings were the same as described previously [30,40]. For calibration and quantification of sugars and organic acids in the flag leaf samples, we used serial concentrations of calibration standards (Table S1). Standards included 24 sugars (sugars, sugar phosphates, sugar acids, and sugar alcohols) and 19 organic acids, derivatized and subjected to GC-QqQ-MS analysis as described previously [30,40].

For the amino acid and amine analyses with LC-QqQ-MS, 10 µL of supernatants were transferred into new glass vial inserts. The amino acids and amines in the supernatants were then derivatized with 6-aminoquinolyl-N-hydrosysuccinimidyl carbamate (AQC) reagent [30,40,41]. Briefly, 10 µL samples were added to 70 µL of borate buffer (200 mM, pH 8.8 at 25 °C) containing 10 mM TCEP, 1 mM ascorbic acid, and 50 µM 2-aminobutyrate. The resulting solution was vortexed before adding 20 µL of 6-aminoquinolyl-N-hydrosysuccinimidyl carbamate (AQC) reagent (200 mM dissolved in 100% acetonitrile, ACN) and then vortexed immediately. The samples were heated with shaking at 55 °C for 10 min and centrifuged at 13,000 rpm at room temperature and then transferred to HPLC vials containing inserts (Agilent, spring-less glass inserts, 250 µL) prior to injection. Aliquots (1 µL) of the derivatized samples were immediately injected into a LC-QqQ-MS system comprising of an Agilent 1200 LC-system coupled to an Agilent 6410 Electrospray Ionization-Triple Quadruple-MS. The settings of the LC-MS instrument were previously described [30,40]. For calibration and quantification of amino acids and amines in the flag leaf samples, a series of concentrations of calibration authentic standards comprising of 29 amino acids and amines (Table S1), mixed with a sulfur-containing compound solution, were prepared, derivatized, and subjected to LC-QqQ-MS analysis same as previously described [30,40].

2.3. Analysis of Lipids

The extraction of lipids was carried out as described previously [30,42], with modifications. Briefly, 20 mg freshly frozen spike samples were homogenized in 500 µL of a 2:1 methanol:chloroform mixture using a Cryomill (Precellys 24, Bertin Technologies, Rockville, MD, USA) for 3 × 45 s at 6100 rpm (−10 °C). The extracts were shaken at 750 rpm for 15 min at 30 °C and centrifuged at 13,000 rpm for 15 min. The supernatants were transferred to new tubes, while 500 µL of a 2:1 methanol:chloroform mixture was added again to the remaining residue. The tubes were vortexed and centrifuged again at 13,000 rpm for 15 min. The supernatants were combined and dried down in vacuo and then re-constituted in 100 µL of 1:1 butanol:methanol for the subsequent LC-QqQ-MS analysis using an Agilent 1200 LC-system coupled to an Agilent 6410 Electrospray Ionization-Triple Quadruple-MS system. An injection of 5 µL of each total lipid extract was chromatographically separated on an Ascentis Express RP-Amide 50 × 2.1 mm, 2.7 µm HPLC column (Sigma-Aldrich, Castle Hill, NSW, Australia) using an 8 min gradient from 0% A to 100% B, which was then held for 2 min and followed by a 4 min column re-equilibration with a flow rate of 0.18 mL/min. The mobile phases were A: 10 mM ammonium formate in water:methanol:tetrahydrofuran (50:20:30, v:v:v); B: 10 mM ammonium formate in water:methanol:tetrahydrofuran (5:20:75, v:v:v). Lipid species were identified and quantified based on multiple reaction monitoring (MRMs) established using external lipid standards and references from the LIPIDMATCH database (https://github.com/GarrettLab-UF/LipidMatch/releases/tag/v2.0.2) as listed in Table S2, with a 5–20 ms dwell time for the simultaneous measurements of up to 100 compounds. We used optimized parameters for capillary (4000 V), fragmentor (60–160 V), and collision voltages

(20–40 V). In all cases, the collision gas was nitrogen with a flow rate of 7 L/min. The external lipid standards used were lysophosphatidylcholine LPC (17:0), lysophophatidylglycerol LPG (16:0), phospatidylcholine PC (20:0) and PC (34:1), phosphatidylethanolamine PE (34:0), phosphatidylglycerol PG (34:1) and PG (36:0), phosphatidylinositol PI (34:2) and PI (36:2), and phosphatidylserine PS (34:0) (Table S2). Detected lipid species were annotated by lipid class designation, followed by the "total number of carbon atoms in the fatty acid chains" and the "total number of double bonds in the fatty acid chains", separated by a colon sign.

2.4. Processing of Raw Data

Raw metabolite and lipid data were processed and analyzed using Quantitative Analysis MassHunter Workstation software for QQQ (Agilent Technologies, Santa Clara, CA, USA). The level of identification was carried out based on the Metabolomics Standards Initiative (MSI) requirements [43]. For all measured metabolites (sugars, organic acids, amino acids, and amines), absolute concentrations were determined for all the metabolites except for fructose-6-phosphate and glucose-6-phophate as the linear standard curves for these two metabolites could not be generated for quantification due to very high abundance of these two metabolites in the spike samples. The concentration unit for all the metabolites was expressed as picomole/mg of fresh weight except responses normalized to mg of fresh weight for fructose-6-phosphate and glucose-6-phophate (Table S3). All the metabolites measured at MSI Level 1, as the identification was based on multiple reaction monitoring (MRMs) established using authentic standards (Table S1). For lipids, responses were normalized to mg of fresh weight, FW (Table S4). Although single authentic lipid species were used for each of the phospholipid class, the identification of individual lipid species was based on both the MRM experiment and retention time and was therefore measured at MSI Level 2 (Table S2).

2.5. Statistical Analysis of Metabolite and Lipid Data

The statistical analysis for metabolite and lipid data was performed by using MetaboAnalyst v3.0 [44]. For normalization of metabolite data which are expressed as absolute quantity (picomole/mg of fresh weight), the data was $\log_2$-transformed and mean-centered. For normalization of lipid data which in response/mg of fresh weight, the data was first normalized by median, $\log_2$-transformed, mean-centered, and divided by the standard deviation of each variable. Next, for the statistical significance determination of metabolites and lipids in each variety or between varieties, the normalized data was subjected to one-way analysis of variance (ANOVA), with a false discovery rate (FDR)-adjusted p-value of 0.05 as significance level [45]. This was followed by the Tukey's honestly significant difference (HSD) post-hoc test to perform significant pairwise comparisons using MetaboAnalyst 3.0 or Graphpad Prism 7.0 (GraphPad Software, La Jolla California, CA, USA). In order to determine which metabolites or lipids responded specifically to short cold stress (TP_1), prolonged cold stress (TP_3), diurnal fluctuations when the spikes were exposed to normal day-time temperature of 21 °C for 6 h (TP_2 and TP_4), we performed pairwise comparisons of the selected two groups: TP_1 vs. TP_0 (for short cold stress), TP_3 vs. TP_1 (for prolonged cold stress), TP_2 vs. TP_1, and TP_4 vs. TP_3 (for recovery and the effect of diurnal fluctuations on metabolite levels) in each variety, and also comparisons at every time point between the two varieties (varietal differences) via Student's t-test using MetaboAnalyst and GraphPad Prism software. The Student's t-test for comparing the unsaturation to saturation lipid ratio (using the response/mg values) between Wyalkatchem and Young at different time points was performed in Microsoft-Excel. All plots shown in the results section were generated either using GraphPad Prism 7.0 software, MetaboAnalyst 3.0 software, and the Venn diagram webtool (http://bioinformatics.psb.ugent.be/webtools/Venn/).

3. Results

3.1. Metabolite and Lipid Profiling Using YM Stage Wheat Spikes

The spike tissues analyzed in this study were collected from the same plant material treated by the same controlled environment cold treatment as the previously analyzed flag leaf samples [30]. YM stage spikes are actively developing sink tissues inside the leaf sheaths of the wheat plant where they lack direct exposure to light (Figure 1B). This material needs to be destructively harvested (i.e., plants will not produce seeds) for metabolite analysis. The cold-tolerant wheat variety Young used in this study consistently performs better than the cold-sensitive variety Wyalkatchem in terms of spike grain yield in both field trials of the Australian National Frost Program (ANFP) and our controlled environment assays [30]. The aim of the time-course experiment was to capture changes in cold acclimation after a single night of exposure to cold ($TP_{1,2}$) and after a prolonged 4-day treatment ($TP_{3,4}$). To be able to measure the effect of daytime recovery and circadian rhythms, we also compared metabolite levels in samples harvested in the morning immediately after overnight cold treatment ($TP_{1,3}$) to the samples harvested after 6 h of day-time recovery at normal temperatures following the respective cold treatments ($TP_{2,4}$). We quantified 58 primary metabolites, including 21 sugars/sugar phosphates/polyols, 13 organic acids, and 24 amino acids (including amines). A total of 95 lipid species were detected and measured in the spikes of both varieties, including 86 phospholipids such as PCs (phosphotidylcholine), PEs (phosphotidylethanolamine), PGs (phosphotidylglycerolipid), PIs (phosphoinositide), and lysophospholipids. In addition, we also quantified nine galactosyl lipids (galactosyldiaclyglycerols) in the spikes: digalactosyldiacylglycerols (DGDG), monogalactosyldiacylglycerols (MGDG), and sulfoquinovosyl diacylglycerols (SQDG).

3.2. Cold Treatment Affects Spike Metabolites in Wyalkatchem More than Young Spikes

A short overnight cold treatment (≈12 h) revealed that four primary metabolites and one lipid were significantly affected in Wyalkatchem spikes: maltose (+17.8-fold), fructose-6-phosphate (+4.2-fold), glucose-6-phosphate (+4.7-fold), beta-alanine (+2.0-fold), and the lipid PG(36:5) (+1.2-fold) were all significantly increased (TP_1 vs. TP_0; Figure 2A). In contrast, the comparison of TP_1 vs. TP_0 in Young showed no significant changes in primary metabolites and only one lipid, i.e., PC (37:5), was significantly reduced (−16.5-fold; Figure 2B). The TP_2 spike samples were harvested after 6 h of day-light and normal temperatures (21 °C) following the first night cold exposure (TP_1). Comparison of TP_2 to TP_1 in Wyalkatchem spikes showed that only two metabolites were significantly changed: rather than induced at TP_1, maltose was this time strongly repressed back to TP_0 levels (−20-fold) and levels stay the same at TP_2 and TP_4, while 2-oxoglutarate was induced (+3.1-fold). There were no significant changes in the lipids at TP_2 vs. TP_1, indicating that the observed change in PG (36:5) at TP_1 was maintained during day-time recovery (Supplementary Figures S1 and S2). In Young spikes, maltose was also repressed compared to TP_1 (−10.7-fold) and we also found a significant increase in methionine levels at TP_2 (+2.1-fold). There were no significant changes in the lipids, again indicating that the PC (37:5) lipid change at TP_1 was maintained at TP_2 (Supplementary Figures S1 and S2).

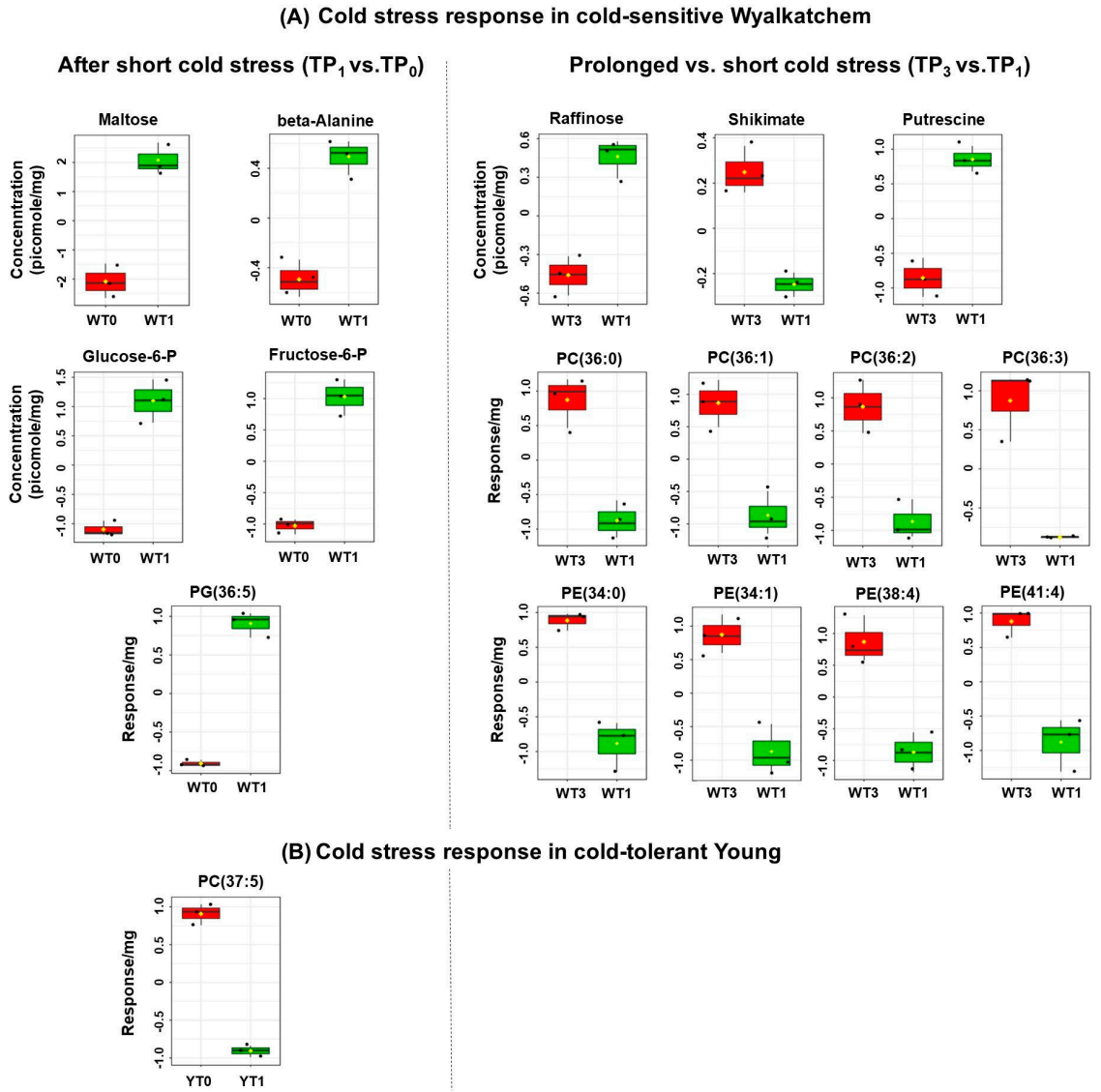


Figure 2. Pairwise comparisons of normalized and $\log_2$-transformed primary metabolites and lipids in the spikes of cold-sensitive Wyalkatchem (**A**) and cold-tolerant Young (**B**) after one night (TP_1 vs. TP_0) and prolonged (TP_3 vs. TP_1) of cold treatment. Metabolites and lipids shown are significantly different and the significance levels were determined using the Benjamini and Hochberg method [45] with a false discovery rate (FDR)-adjusted *p*-value of 0.05 as cut-off. There were three biological replicates (n = 3) for all the measured metabolites and lipids. W = Wyalkatchem; Y = Young

After a prolonged four-night cold treatment (TP_3 vs. TP_1 comparison), three primary metabolites changed significantly in Wyalkatchem spikes: raffinose (+1.9-fold), shikimate (−1.4-fold), and putrescine (+3.2-fold). Additionally, a series of saturated and unsaturated PC (36:x) lipids were significantly reduced at TP_3 compared to TP_1: PC (36:0) (−1.6-fold), PC (36:1) (−1.5-fold), PC (36:2) (−1.5-fold), PC (36:3) (−1.2-fold). Four PE lipid species were also significantly reduced: PE (34:0) (−1.4-fold), PE (34:1) (−1.4-fold), PE (38:4) (−1.2-fold), and PE (41:4) (−1.4-fold) (Figure 2A). In Young spikes, the prolonged cold treatment (TP_3) did not cause any significant changes in primary metabolites and lipids compared to TP_1 (Figure 2B). Comparing the prolonged cold treatment samples with their equivalent day-time samples (TP_4 vs. TP_3) showed the same significant reduction in maltose levels (−8.8-fold) as observed in Wyalkatchem spikes between TP_2 and TP_1, as well as an increase in quinate levels (+1.7-fold). There were no significant changes in lipid levels (Supplementary Figures S1 and S2). In Young spikes, the TP_4 vs. TP_3 pairwise comparison did not reveal any significant changes in primary

metabolites or lipids (Supplementary Figures S1 and S2). These data indicate that the cold treatment has a more drastic effect on spikes of the cold-sensitive line Wyalkatchem compared to the tolerant line Young.

3.3. Varietal Differences in Metabolite and Lipid Levels before and after Cold Treatment

Before the plants were subjected to cold stress (TP_0), there were already significant differences in the levels of primary metabolites and lipids in the spikes of cold-tolerant Young and cold-sensitive Wyalkatchem. Nine primary metabolites were significantly higher in Young compared to Wyalkatchem at TP_0: glucose (+1.4-fold), sucrose (+3.1-fold), trehalose (+2.5-fold), fructose-6-phosphate (+2.2-fold), glucose-6-phosphate (+1.8-fold), beta-alanine (+1.7-fold), glutamate (+1.4-fold), glycine (+1.3-fold), and proline (+1.9-fold). Two metabolites were significantly lower in Young compared to Wyalkatchem spikes: histidine (−2.8-fold) and phenethylamine (−2.9-fold) (Figure 3). Three unsaturated lipid species were significantly higher at TP_0 in Young spikes compared to Wyalkatchem: PC (37:5) (+12.9-fold), PC (39:4) (+2.2-fold), and PG (32:1) (+2.3-fold). In contrast, six unsaturated lipids were significantly lower at TP_0 in Young spikes compared to Wyalkatchem: LPC (18:2) (−9.2-fold), PC (33:1) (−1.2-fold), PC (35:5) (−1.3-fold), PE (33:1) (−1.7-fold), PE (35:3) (−1.7-fold), and PE (35:4) (−1.5-fold) (Figure 4). Before the start of the cold treatment, there was no significant difference in the overall unsaturated to saturated lipid ratio between the two varieties (Figure 5A).

After one night of cold exposure (TP_1), three metabolites were found to be significantly different between the two varieties. The osmolyte mannitol accumulated to significantly higher levels (+1.5-fold), while ribose (−1.5-fold) and shikimate (−2.1-fold) were significantly lower in Young compared to Wyalkatchem spikes (Figure 3). Two lysophosphatidylcholine lipids were significantly lower in Young spikes compared to Wyalkatchem: LPC (17:0) (−1.8-fold) and LPC (18:1) (−3.8-fold). Two lipids that contain two polyunsaturated acyl chains in their structures, PC (36:6) (+1.3-fold) and PE (36:6) (+1-3-fold), had significantly higher levels in Young spikes compared to Wyalkatchem at TP_1 (Figure 4). However, again, at TP_1 there was no significant difference in the overall ratio of unsaturated to saturated lipids between the two varieties (Figure 5A).

When comparing the TP_2 day-time samples between the two varieties, seven metabolites were significantly higher in Young compared to Wyalkatchem spikes. All of them were either amino acids or amines: alanine (+1.7-fold), beta-alanine (+1.7-fold), GABA (+1.7-fold), glutamate (+1.3-fold), methionine (+1.8-fold), proline (+2.8-fold), and threonine (+1.2-fold). Three sugars (fucose, −1.5-fold; ribose, −1.6-fold; xylose, −1.6-fold), one organic acid (shikimate, −2.3-fold), and one amine (phenethylamine, −2.3-fold) were significantly reduced at TP_2 in Young spikes compared to Wyalkatchem (Figure 3). There were no significant differences in the lipids between the two varieties at TP_2, but for the first time, Young spikes showed a significantly higher ratio in unsaturated to saturated lipids compared to the ratio in Wyalkatchem spikes (Figure 5A).

After prolonged cold exposure (TP_3), three metabolites were decreased significantly in Young spikes compared to Wyalkatchem: quinate (−1.8-fold), methionine (−2.2-fold), and putrescine (−3.8-fold) (Figure 3). The largest difference between both wheat varieties at TP_3 was in the lipid levels. Three lysophosphatidylcholines with a carbon backbone of 18 were significantly lower in Young spikes compared to Wyalkatchem: LPC (18:1) (−5.0-fold), LPC (18:2) (−7.3-fold), and LPC (18:3) (−3.6-fold). Coincidently, 25 lipids with a higher carbon backbone length of 36 and a higher poly-unsaturation level were increased significantly in Young spikes compared to Wyalkatchem (Figure 4). Interestingly, 10 of these 25 lipid species were found to contain two polyunsaturated acyl chains in their structures: PC (36:5) (+1.3-fold), PC (36:6) (+1.6-fold), PC (38:5) (+1.3-fold), PC (38:6) (+1.3-fold), PE (36:6) (+1.6-fold), PE (38:6) (+1.2-fold), PG (36:6) (+1.1-fold), PG (36:7) (+2.4-fold), PI (36:6) (+1.9-fold), and DGDG (36:6) (+1.2-fold). This change in the lipid spectrum at TP_3 resulted in Young spikes showing a significantly higher unsaturated to saturated lipid ratio compared to Wyalkatchem (Figure 5A).

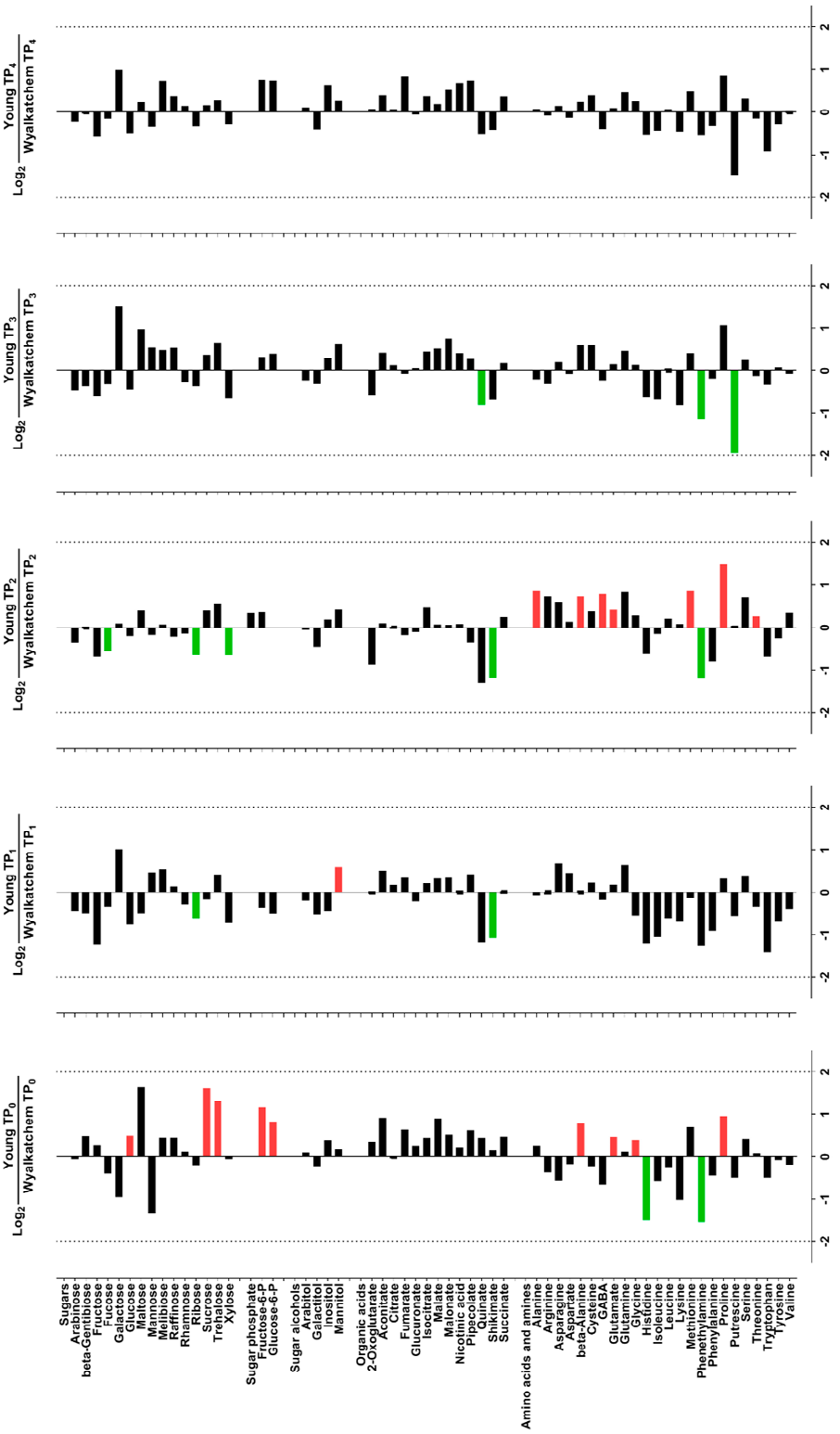


Figure 3. Log_2-fold changes of primary metabolites in spikes of cold-tolerant Young (Y) compared to cold-sensitive Wyalkatchem (W) at each time point. Fold changes were calculated by dividing the concentration of Young by the concentration of Wyalkatchem at each time point, followed by log_2-transformation. FDR-adjusted *p*-value of 0.05 was set as the cut-off. Green = significantly lower in Young, or higher in Wyalkatchem; red = significantly higher in Young, or lower in Wyalkatchem. $n = 3$.

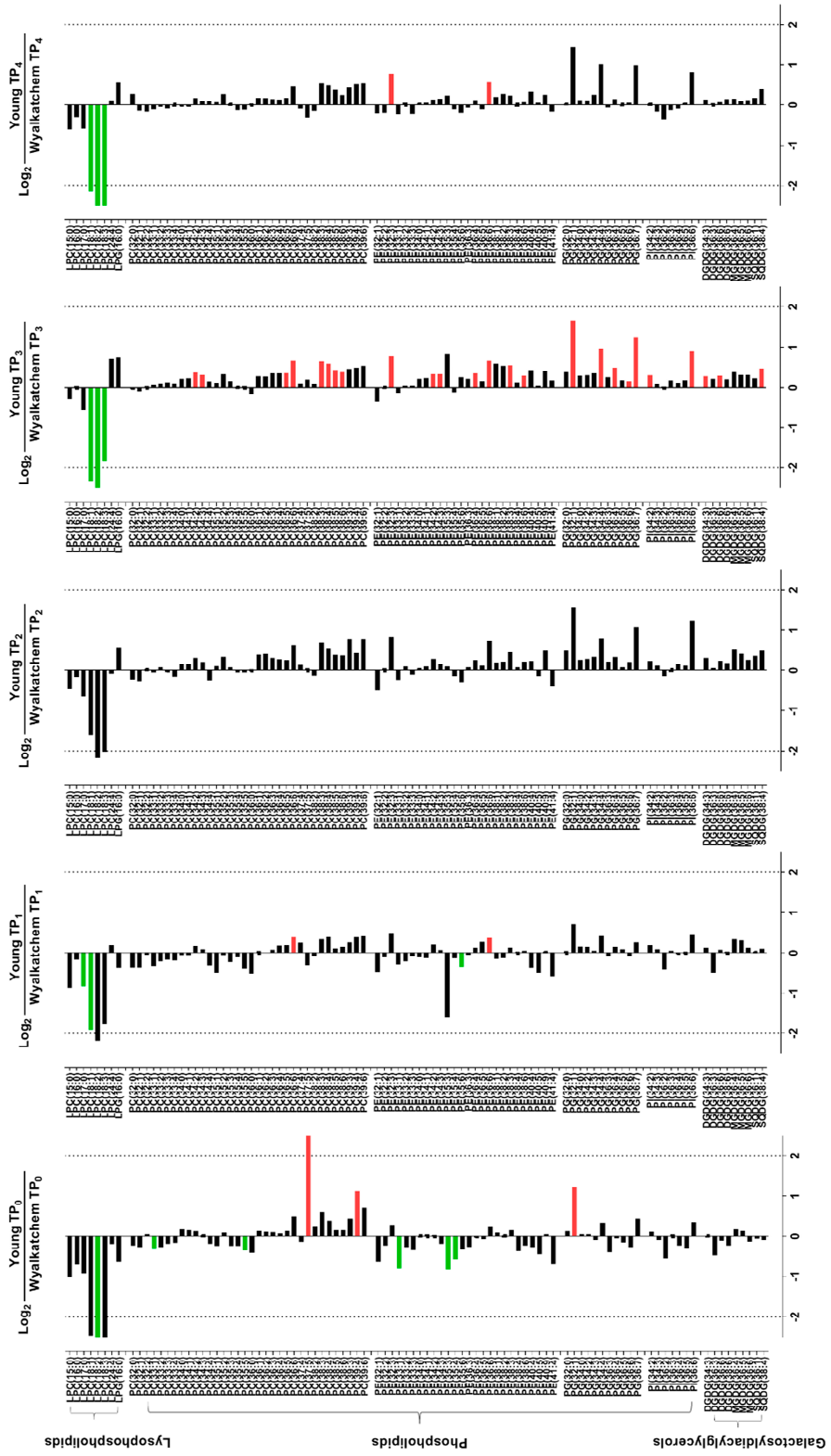


Figure 4. Log_2-fold changes of lipids in the spikes of cold-tolerant Young (Y) compared to cold-sensitive Wyalkatchem (W) at each time point. Fold changes were calculated by dividing the concentration of Young by the concentration of Wyalkatchem at each time point, followed by log_2-transformation. FDR-adjusted *p*-value of 0.05 was set as the cut-off. Green = significantly lower in Young, or higher in Wyalkatchem; red = significantly higher in Young, or lower in Wyalkatchem. $n = 3$.

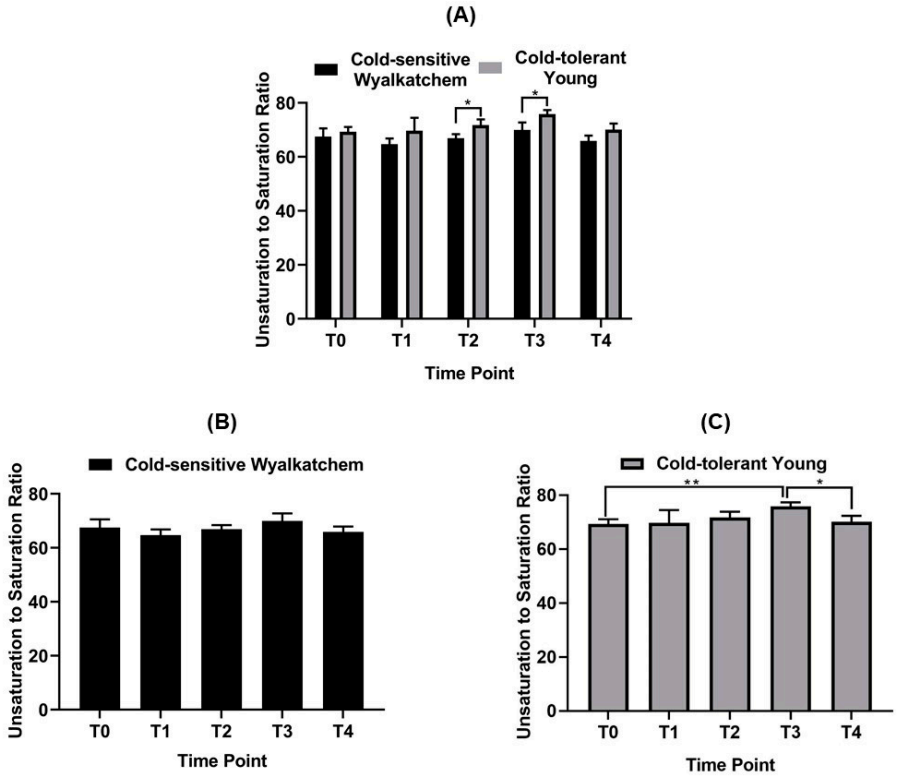


Figure 5. (**A**) Comparison of unsaturated to saturated lipid ratio between Wyalkatchem and Young across the time points. (**B**) Comparison of unsaturated to saturated lipid ratio in Wyalkatchem across the time points. (**C**) Comparison of unsaturated to saturated lipid ratio in Young across the time points. Student's *t*-test was used to compare the ratio for a time point with its following time point. Error bars indicate the standard error mean (SEM) of three biological replicates ($n = 3$). Significantly different ratios were labelled with an asterisk (* = $p < 0.05$, ** = $p < 0.01$).

Comparison between Young and Wyalkatchem at the last day-time sampling point (TP_4) showed that there were no significant differences in primary metabolites between the two wheat varieties (Figure 3). In terms of lipids, three lysophosphatidylcholines were again significantly lower in Young compared to Wyalkatchem spikes: LPC (18:1) (−4.5-fold), LPC (18:2) (−7.6-fold), and LPC (18:3) (−5.9-fold). However, two unsaturated phosphatidylethanolamine lipids species, PE (32:3) (+1.7-fold) and PE (36:6) (+1.5-fold), were significantly higher in Young spikes compared to Wyalkatchem (Figure 4). At TP_4, there was no significant difference in the unsaturated to saturated lipid ratio between the two varieties (Figure 5A).

3.4. Differences in Primary Metabolite Levels between Spikes and Flag Leaves of Wyalkatchem and Young

The spikes and flag leaves of the two wheat varieties showed significant differences in sugars and organic acids that are part of glycolysis and tricarboxylic acid (TCA) cycle. Twelve amino acids, putrescine, gamma-aminobutyric acid (GABA), and two organic acids (quinate and shikimate) that are involved in amino acid metabolism, showed significant differences between the spikes and flag leaves of the two wheat varieties (Figures 6 and 7; for one-way ANOVA, see Supplementary Table S10). Of these 16 metabolites, eight were found to be significantly higher in the spikes compared to the flag leaves over the 4-day cold treatment: tyrosine, phenylalanine, quinate, shikimate, proline, glutamine, beta-alanine, and asparagine. Five amino acids (glutamate, aspartate, threonine, serine, and cysteine) and GABA were significantly lower in the spikes compared to the flag leaves. Putrescine was slightly lower in the spikes compared to the flag leaves, especially in the cold-tolerant variety Young. Interestingly, the response of alanine increased significantly from TP_1 to TP_3 in spikes, while it decreased for the same time points in flag leaves of both varieties. The results in Figures 6 and 7 reveal that the overall

response of metabolites to cold is quantitatively stronger in the reproductive tissues (spikes) compared to the flag leaves for both the sensitive and tolerant wheat line.

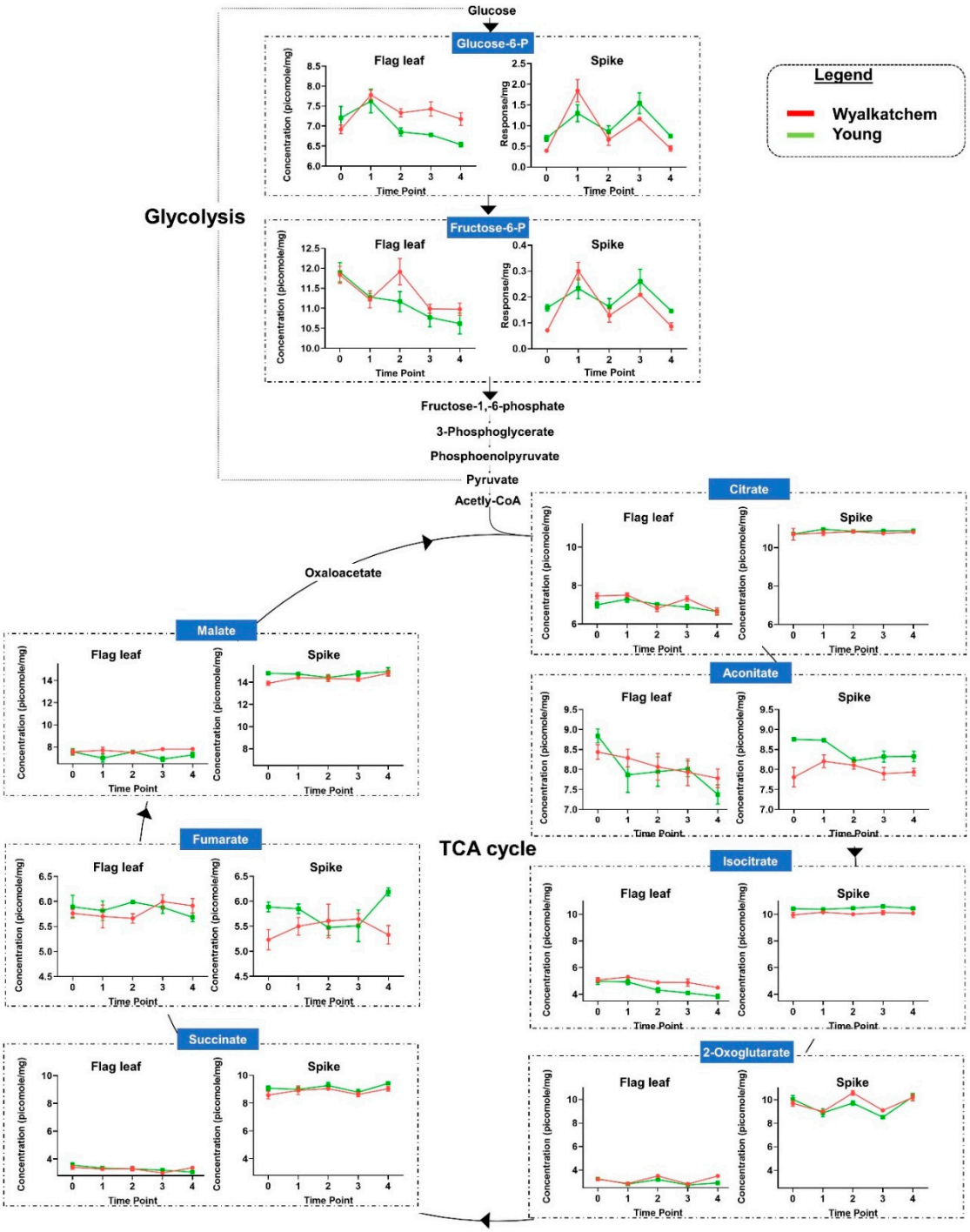


Figure 6. Comparison of primary metabolites involved in glycolysis and the tricarboxylic acid **cycle** (TCA) cycle, the two main energy-providing pathways of the cell. The graphs show differences in relevant primary metabolite concentrations (picomole/mg of fresh weight, Log_2-transformed) between flag leaf and spike metabolite data. For glucose-6-phosphate and fructose-6-phosphate, the spike data compare the response normalized per mg of fresh weight. The graphs reveal differences in accumulation levels of these metabolites in cold-tolerant Young and cold-sensitive Wyalkatchem spikes. $n = 4 \pm$ SEM for flag leaf, $n = 3 \pm$ SEM for spike.

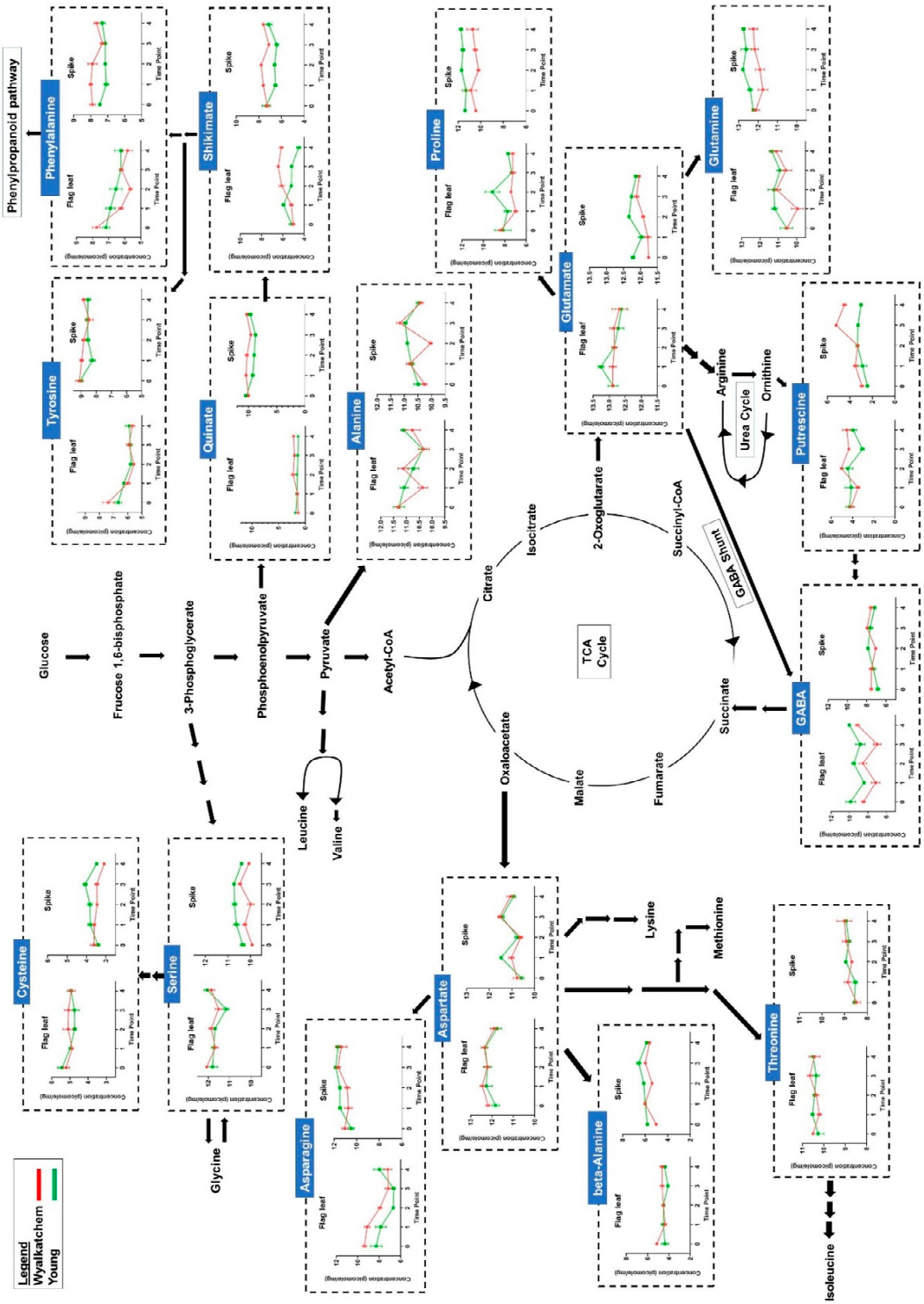
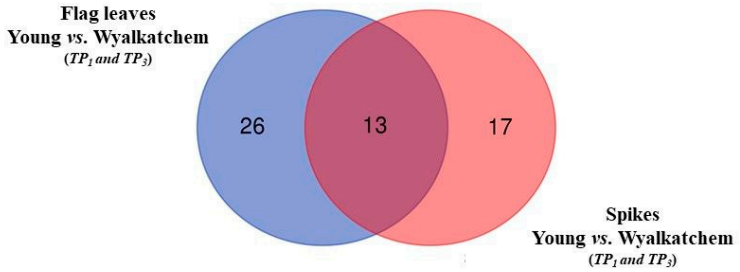


Figure 7. Comparison of amino acid and amine levels (picomole/mg of fresh weight and Log_2-transformed), as well as their relationship to the main energy providing pathways (glycolysis and TCA cycle). The graphs show differences in metabolite levels between flag leaf and spike metabolite data, as well as differences in accumulation levels of those metabolites in cold-tolerant Young and cold-sensitive Wyalkatchem spikes. $n = 4 \pm$ SEM for flag leaf, $n = 3 \pm$ SEM for spike.

3.5. Differences in Metabolite and Lipid Levels between Spikes and Flag Leaves of Wyalkatchem and Young

The most dramatic changes in primary metabolites and lipids occur at TP_1 and TP_3. We therefore compared the response at these time points between flag leaves and spikes for Young and

Wyalkatchem. In terms of primary metabolites, cold treatment only affected 10 and six primary metabolites in flag leaves and spikes, respectively, and only three of these metabolites were common to both tissues: putrescine, quinate, and shikimate (Supplementary Figure S3). Interestingly, all three of these overlapping metabolites were lower in both Young flag leaves and spikes compared to Wyalkatchem. We observed a larger number of changes in lipid composition for both wheat varieties at TP_1 and TP_3 (Figure 8). The results show that there were both similarities and differences in lipid accumulation between flag leaves and spikes (Figure 8). Thirteen lipids were found to overlap between the lipid species of flag leaves and spikes and all of them were polyunsaturated lipids. Of the common lipids, five were accumulating to higher levels in both spike and flag leaf tissues of cold-tolerant Young compared to cold-sensitive Wyalkatchem: PC (38:3), PE (34:2), PE (36:4), PE (38:3), and PG (36:4). Eight unsaturated lipids were found to be lower in Young flag leaves when compared to Wyalkatchem, but their levels were higher in Young spikes compared to Wyalkatchem spikes: PC (34:4), PC (36:6), PC (38:6), PE (34:3), PE (36:6), PE (38:6), PG (36:6), and PI (36:6). Interestingly, levels of all these 13 polyunsaturated lipid species showed quantitatively higher levels in Young compared to Wyalkatchem spikes (Figure 8). These results indicate that there are quantitative and qualitative differences in cold acclimation between sensitive variety Wyalkatchem and tolerant Young.



Differences in expression behavior of 13 overlapping lipids between flag leaves and spikes of Young and Wyalkatchem (TP_1 and TP_3 samples)

Overlapped (13)	Higher in Young Flag leaves	Lower in Young Flag Leaves	Higher in Young Spikes	Lower in Young Spikes
PC(38:3)	√		√	
PE(34:2)	√		√	
PE(36:4)	√		√	
PE(38:3)	√		√	
PG(36:4)	√		√	
PC(34:3)		√	√	
PC(36:6)		√	√	
PC(38:6)		√	√	
PE(34:3)		√	√	
PE(36:6)		√	√	
PE(38:6)		√	√	
PG(36:6)		√	√	
PI(36:6)		√	√	

Figure 8. Differences in differentially expressed lipid species between flag leaves and spikes of cold-tolerant Young and cold-sensitive Wyalkatchem. The Venn diagrams show the degree of overlap between differentially expressed cold-induced lipid species in flag leaves and spikes for Young and Wyalkatchem. Thirteen lipid species were commonly expressed in flag leaves and spikes at TP_1 and TP_3. The table below the diagram shows how these 13 lipid species are expressed differently in flag leaves and spikes of Wyalkatchem and Young.

4. Discussion

4.1. Are Wheat Spikes or Flag Leaves Better for Cold Tolerance Phenotyping?

We have previously compared the effect of cold stress on metabolite levels during cold acclimation in flag leaves of cold-tolerant Young and cold-sensitive Wyalkatchem [30]. For the ultimate aim of phenotyping, flag leaves are easy to collect, especially in the field. The motivation to also study metabolite changes in wheat spikes during cold acclimation came from the fact that spikes are the organs of the wheat plant where grain yield is determined. Spike material at the stage of highest sensitivity to cold, the YM stage of pollen development [30], is harder to collect. However, this tissue may provide metabolite information that is more directly correlated with the cold tolerance/sensitivity mechanism. If we can prove that the metabolite changes in flag leaves and spikes show significant similarities, then we can be confident that flag leaf material suits our phenotyping needs.

An important difference between flag leaf and YM stage spike tissues is that the former is a static photosynthetic source tissue, whilst the latter is a young and actively growing tissue in need of sugar supply to drive reproductive development (sink tissue). YM stage spikes are shielded from daylight by the surrounding leaf sheaths and have a light-green appearance; there may be a low amount of chlorophyll and photosynthetically active chloroplasts in cells of the outside tissue layers of the florets (glumes, lemma, and awns), but the anthers that produce pollen inside the florets are yellow and at the YM stage are non-photosynthetic sink tissues [38,39]. Sink strength is defined as the competitive ability of an organ to attract and store assimilates [46]. At the reproductive stage, developing wheat spikes need a strong sink strength to attract sugars for reproductive development and grain filling [32–34,36,47]. In rice and wheat, cold and drought stress reduce sink strength in lines that are more sensitive to those stresses and stress tolerance correlates with a higher capability to maintain sink strength [38,48]. The higher sugar levels in Young compared to Wyalkatchem spikes before cold exposure therefore indicate that Young spikes have a higher sink strength than Wyalkatchem spikes.

The spikes of the cold-tolerant variety Young did not show any significant primary metabolite changes upon short or prolonged exposure to cold, while cold-sensitive Wyalkatchem did show some metabolites that were significantly affected by cold. In the flag leaves there were more changes in primary metabolites in response to the same cold treatment [30]. It is possible that the cold treatment at the spike level is somewhat less stringent compared to the flag leaf. While the flag leaf is directly exposed to cold air, at the YM stage the spike is still protected inside the leaf sheath of the flag leaf and the penultimate leaf. However, spikes of both wheat varieties show a clear lipid response to cold, which is similar to that of the flag leaf [30]. This indicates that the YM stage spikes have experienced cold stress. Alternatively, they responded to a cold stress signal coming from the vegetative plant parts.

Most metabolites that were detected are present at higher levels in actively growing spikes than in flag leaves and are therefore easier to detect in spike tissues. Despite quantitative and qualitative differences in the cold acclimation response between spike and flag leaves, the message we obtained in terms of metabolite profiles and differences in cold acclimation between the tolerant and sensitive wheat line is quite similar. This observation also strengthens the conclusion that the response we observed is a true defensive acclimation response to the chilling/freezing treatment we imposed.

4.2. Spikes of Cold-Tolerant Young Are Potentially Better Prepared for Low Temperature Stress

Levels of important sugars (glucose, sucrose, trehalose, fructose-6-phosphate, and glucose-6-phosphate) were significantly higher under unstressed conditions (TP_0) in spikes of cold-tolerant Young compared to cold-sensitive Wyalkatchem. Higher levels of these sugars may indicate that Young spikes have a higher sink strength and are more metabolically active than Wyalkatchem spikes under normal growth conditions. High sugar levels also play a role in osmotic adjustment and membrane protection during water and cold stress [49]. In addition, proline and β-alanine levels were also significantly higher in Young spikes before cold stress treatment. Proline is an osmolyte with protective functions in plant tissues under a variety of stresses (drought, salinity, cold, and heat) [50–54]. β-Alanine in spikes

of the sensitive variety Wyalkatchem is only increased after the first night of cold exposure. β-Alanine is a non-proteinogenic amino acid that is increased during abiotic stress conditions [50,55,56]; it is a coenzyme A precursor that is involved in the tricarboxylic acid cycle, as well as phospholipid and fatty acid metabolism [57]. β-Alanine serves also as a substrate for β-alanine betaine synthesis, a quaternary ammonium compound with osmo-protective functions under stress conditions [58–61]. The polyol sugar mannitol accumulates to higher levels in Young spikes after the first cold night (TP_1). Mannitol acts as a radical scavenger to protect against ROS under abiotic stress conditions [62–64]. The flag leaf study showed similar observations [30].

Some other sugars with protective functions are mainly accumulating in spikes of the sensitive line Wyalkatchem. Maltose levels increase after the first night of cold stress exposure, but in Young the increase in maltose remained insignificant. Maltose is a transitory starch breakdown product and this breakdown is induced during the day under photorespiratory conditions. Maltose metabolism is regulated by the circadian clock, day-length, and temperature [65]. Maltose plays a role in stabilizing membranes and proteins [66,67]. In Arabidopsis, maltose functions as a compatible solute and a stabilizing factor in the chloroplast stroma during temperature stress [55]. In vitro assays indicate that maltose protects proteins, membranes, and the photosynthetic electron transport chain during freezing stress. Increased maltose levels under cold stress could be caused by increased expression of β-amylase [55,65].

Spikes of the cold-sensitive variety Wyalkatchem also showed increased levels of putrescine and raffinose after prolonged cold stress (TP_3). Putrescine is a polyamine and amino acid breakdown product with growth-regulatory properties that plays a role in abiotic stresses [68,69]. Raffinose is a soluble galactosyl-sucrose carbohydrate that plays a role in stabilizing photosystem II during freeze-thaw cycles in Arabidopsis [70]. Raffinose acts as an antioxidant that can protect cells from oxidative stress damage by scavenging ROS [62–64,71,72].

In contrast to Young, where a protection mechanism involving higher sink strength and accumulation of osmolytes (sugars, amino acids) appears to be constitutively present, Wyalkatchem activates primary metabolite changes after the first night and during prolonged cold exposure. Spikes of cold-tolerant Young may therefore be better prepared against cold stress from the start. This knowledge can be exploited in phenotyping approaches for cold tolerance. The primary metabolite response in cold-sensitive Wyalkatchem is a cold stress response. Being a sensitive variety, Wyalkatchem responds with osmolyte synthesis, possibly to control water loss caused by membrane damage, and with activation of a signature oxidative stress and ROS protection mechanism. The same type of response was also observed in Wyalkatchem flag leaves. Osmolytes can therefore be used as indicator for the secondary water stress response caused by cold-induced membrane damage [30,73].

4.3. Lipid Re-Modelling Is Critical for Cold Acclimation in Wheat Spikes

Modifying membrane lipid composition forms an important part of cold acclimation. Similar to what we found for flag leaves, in wheat spikes chilling stress had a more drastic effect on lipids compared to primary metabolites. Under unstressed conditions, Young spikes showed higher levels of three unsaturated phospholipids, with PC (37:5) being the most prevalent one. Unstressed Wyalkatchem spikes had higher levels of five different unsaturated phospholipids. Interestingly, in Young spikes the high level of PC (37:5) was reduced drastically after overnight cold stress. PC (37:5) was much lower in unstressed Wyalkatchem spikes, nor was the level of this lipid strongly repressed by overnight cold treatment. Instead, Wyalkatchem increased PG (36:5) levels upon cold exposure. PG (32:1) is higher in Young compared to Wyalkatchem at the unstressed and prolonged cold stress stage (TP_3). PG lipids are the main phospholipid class in thylakoid membranes of higher plants [74]. Plant cells contain proplastids that can multiply and develop into specialised plastids such as chloroplasts. Plants increase the degree of fatty acid unsaturation and the content of phospholipids when they are exposed to low, non-freezing temperatures [75,76]. PG lipids contain trans-Δ3-hexadecenoic acid (C16:1t), a monounsaturated 16-carbon fatty acid with a trans-double bond at position C-3); they are major

fatty acids involved in decreasing the phase transition temperature of thylakoid PG and maintaining membrane fluidity at lower temperatures [74,77–80]. The highly unsaturated PG (36:5) lipid in Wyalkatchem spikes consists of 18:2 and 18:3 acyl chains and may protect the plastidial/thylakoid membranes. Interestingly, this species was also found to increase significantly in the flag leaves of the same variety after overnight cold stress (TP_1) [30].

After prolonged cold stress, a series of PC (36:x, with x ranging from 0 to 3) lipids, as well as several saturated and polyunsaturated PE lipids, were decreased in cold-sensitive Wyalkatchem and not in cold-tolerant Young spikes. This may be a consequence of their utilization as substrates to produce PAs by phospholipases to trigger a further response against cold stress. Alternatively, the decrease in those PC and PE lipids in Wyalkatchem could be the consequence of membrane damage and/or lipid degradation.

In Young spikes, the first cold night increased the levels of the polyunsaturated lipids PC (36:6) and PE (36:6). The result is a net increase in the degree of fatty acid unsaturation and phospholipid content in Young spikes. In Arabidopsis, PC lipids are amongst a group of lipids that increased during cold acclimation [81]. The higher lipid unsaturation to saturation ratio in Young compared to Wyalkatchem improves the ability to maintain membrane fluidity at low temperatures.

Under unstressed conditions, and particularly after prolonged exposure to cold, most short-chain lysophospholipids (LPC) were higher in Wyalkatchem spikes compared to Young. PCs and PEs are the most abundant plasma membrane lipids in plants and animals [30]. Plants can lower the ratio of PC to PE during cold stress via a hydrolysis reaction catalyzed by phospholipase D (PLDα). Hydrolysis of PC lipids at the sn-1 or sn-2 positions of the glycerol backbone results in formation of LPC and phosphatidic acid (PA), a signaling molecule involved in cold and ABA signaling [82–90]. LPC levels are generally higher in Wyalkatchem spikes at all time points, but most obviously after prolonged cold treatment ($TP_{3,4}$). This was not observed in flag leaves, where none of the LPC lipids were significantly different between Wyalkatchem and Young. In Young spikes, cold-induced PC (37:5) catabolism does not seem to impact LPC levels. PC (39:4) is also higher in unstressed Young spikes; this lipid does not seem to be reduced as dramatically as PC (37:5), but is also induced in Wyalkatchem to a level similar to Young after overnight cold exposure. Both PC (37:5) and PC (39:4) can serve as substrates for PLDα to produce the cold response signaling molecule PA [87,88], so Young could initially benefit from higher levels of these lipids to produce PA and trigger a cold response quicker and more efficiently than Wyalkatchem. Higher levels of LPC (18:1), LPC (18:2) and LPC (18:3) in Wyalkatchem spikes after prolonged cold stress (TP_3 and TP_4) may indicate that prolonged cold stress has caused degradation of PC lipids, causing damage to the plasma membrane. This may then lead to water loss and electrolyte leakage.

Maintenance of plastid functionality during chilling conditions also requires changes in membrane lipid composition. The wheat spike consists of several tissue types (glumes, lemma, awns, anthers, and ovule), most of which will become photosynthetically active when the spike extrudes from the leaf sheath of the flag leaf later on in development. As mentioned earlier, plant cells contain proplastids that can multiply and develop into specialized plastids such as chloroplasts. Light exposure leads to synthesis of photosynthetically active thylakoid membranes and differentiation into chloroplasts [91–93]. The thylakoid membrane of chloroplasts is composed mainly of galactosylglycerolipids, consisting of 50% MGDG, 26% DGDG, and 24% SQDG lipids, as well as other galactosylglycerolipid species and PG lipids [94]. Low temperature acclimation can lead to an increased proportion of highly unsaturated fatty acids in galactolipids, such as linolenic acid (C18:3) [95]. Levels of DGDG (34:3), DGDG (36:6), and SQDG (38:4) in Young spikes after prolonged cold treatment (TP_3) may help this cold-tolerant variety to maintain better chloroplast functionality. Higher levels of DGDG improves ionic permeability of the chloroplasts and preserves activity of membrane proteins [96,97]. Experiments using desaturase enzyme mutants in Arabidopsis have illustrated the importance of glycerolipid composition and the degree of fatty acid desaturation in controlling membrane performance during cold stress [77].

5. Conclusions

Profiling of primary metabolite and lipid changes in response to cold treatment of wheat spikes provided a better understanding about differences in cold acclimation of cold-tolerant Young and cold-sensitive Wyalkatchem. The changes in metabolomes and lipidomes of spikes were similar to those of flag leaves in many ways [30], but there were clearly some interesting quantitative and qualitative differences in accumulation of osmolytes, ROS protective compounds, and lipids. This means that both flag leaf and spike metabolite and lipidome analysis are complementary in terms of physiological information, and they can be used interchangeably for cold tolerance phenotyping in wheat. Flag leaf tissue is easier to collect, while spike tissue offers an advantage in terms of detectability because of the presence of higher levels of some of the metabolites. Both the flag leaf and spike datasets pointed out that re-modelling of membrane lipids is critical for adaptation to low temperature stress. Controlling the unsaturated lipid levels to maintain membrane fluidity at low temperatures appears to be a distinguishing factor between cold-tolerant line Young and cold-sensitive Wyalkatchem. However, the change in the ratio of saturated to unsaturated lipids is small and there are also important changes in the saturated lipid spectrum. We do not know the biochemical structure of the lipid species that are affected by cold, nor do we know their exact role in controlling membrane functionality or which cellular membranes they are associated with. We identified some individual lipid species that stand out in the response of the cold-tolerant and sensitive wheat line, but for phenotyping purposes we will at this stage observe changes in the entire lipid spectrum. Experiments are in progress to demonstrate whether lipid profiling proves to be reliable in a wider variety of cold-tolerant and sensitive wheat lines and whether the changes in lipid spectrum matches the ones observed in Young and Wyalkatchem. When lipid profiling proves to be reliable, we can deploy the technology in QTL mapping or genome-wide association studies (GWAS) to identify to identify genetic markers that can be used to predict the cold tolerance phenotype. In addition, the data presented here have provided new avenues to investigate genes involved in metabolic and lipid biochemical processes using transcriptome analysis. Combination of metabolome and transcriptome analysis can further improve our understanding of how cold tolerance is controlled in wheat.

Supplementary Materials: The following supplementary data files are available online at http://www.mdpi.com/2073-4409/9/5/1309/s1, Figure S1: $\log_2$-fold changes of primary metabolite concentrations in the spikes of cold-sensitive Wyalkatchem (W) and cold-tolerant Young (Y) after one night (TP_1 vs. TP_0) and prolonged (TP_3 vs. TP_1) exposure to cold, and the day-time recoveries after each of these cold treatments (TP_2 vs. TP_1 and TP_4 vs. TP_1), Figure S2: $\log_2$-fold changes of lipid concentrations in the spikes of the cold-sensitive Wyalkatchem (W) and cold-tolerant Young (Y) after one night (TP_1 vs. TP_0) and prolonged (TP_3 vs. TP_1) exposure to cold, and the day-time recoveries after each of these cold treatments (TP_2 vs. TP_1 and TP_4 vs. TP_3), Figure S3: Differences in differentially expressed primary metabolites between flag leaves and spikes of cold-tolerant Young and cold-sensitive Wyalkatchem. The Venn diagrams show the degree of overlap between differentially expressed cold-induced metabolites in flag leaves and spikes for Young and Wyalkatchem. Three metabolites were commonly expressed in flag leaves and spikes at TP_1 and TP_3. The table below shows how these three metabolites are expressed differently in Wyalkatchem and Young flag leaves and spikes, Table S1: Multiple reaction monitoring (MRMs) established for authentic sugars, organic acids, amino acids, and amines used for identification and quantification of these compounds in this study, Table S2: Multiple reaction monitoring (MRMs) established for the seven external authentic lipids, and 95 phospholipids used for identification of these compounds in this study, Table S3: Concentrations of primary metabolites (sugars, organic acids, amino acids, and amines) measured in Wyalkatchem and Young spikes across all time points, Table S4: Normalized lipid responses for the measured lipids in the Wyalkatchem and Young spikes across all the time points, Table S5: Fold changes ± SEM for the pairwise comparisons of metabolites in Young and Wyalkatchem spikes, Table S6: Fold changes ± SEM for the pairwise comparisons of lipids in Young and Wyalkatchem spikes, Table S7: Multiple comparisons of primary metabolites in Wyalkatchem, Young, Wyalkatchem vs. Young across all time points using one-way ANOVA (with FDR-adjusted $p < 0.05$), followed by Tukey test to determine which specific two groups are significantly different, Table S8: Multiple comparisons of phospholipids in Wyalkatchem, Young, Wyalkatchem vs. Young across all time points using one-way ANOVA (with FDR-adjusted $p < 0.05$), followed by Tukey test to determine which specific two groups are significantly different, Table S9: Changes in the unsaturated to saturated lipid ratio in Wyalkatchem and Young during the time-course experiment, Table S10: One-way ANOVA analysis and Tukey test for comparison of primary metabolite levels between flag leaves and spikes in Wyalkatchem and Young.

Author Contributions: Conceptualization, R.D.; Formal analysis, B.E.C., O.O., W.W.H.H., T.W.T.R. and U.R.; Funding acquisition, R.D.; Investigation, B.E.C., O.O., W.W.H.H. and R.D.; Methodology, W.W.H.H., T.B.B., T.W.T.R. and R.D.; Project administration, U.R. and R.D.; Resources, T.B.B.; Supervision, U.R. and R.D.; Writing—original draft, B.E.C. and R.D.; Writing—review and editing, B.E.C., O.O., W.W.H.H., T.B.B., U.R. and R.D. All authors have read and agreed to the published version of the manuscript.

Funding: This research was supported by grants of the Australian Grains Research and Development Corporation (GRDC projects CSP00143 and CSP00202).

Acknowledgments: Cold treatments were carried out using growth chambers from the High-Resolution Plant Phenomics Centre in Canberra (HRPPC; https://www.plantphenomics.org.au/tag/high-resolution-plant-phenomics-centre/). The authors would like to thank Xiaomei Wallace, Sue Kleven and Tina Rathjen from CSIRO Agriculture and Food for excellent technical assistance. The authors also thank Nirupama Jayasinghe, Himasha Mendis, Veronica Lui, and Siria Natera from Metabolomics Australia for the metabolite and lipid analyses. Metabolomics Australia (School of BioSciences, The University of Melbourne, Australia) is a National Collaborative Research Infrastructure Strategy initiative under Bioplatforms Australia Pty Ltd. (http://www.bioplatforms.com/).

Conflicts of Interest: The authors declare no conflict of interest.

References

1. Paulsen, G.M.; Heyne, E.G. Grain production of winter wheat after spring freeze injury. *Agron. J.* **1983**, *75*, 705–707. [CrossRef]
2. Boer, R.; Campbell, L.C.; Fletcher, D.J. Characteristics of frost in a major wheat-growing region of Australia. *Aust. J. Agric. Res.* **1993**, *44*, 1731–1743. [CrossRef]
3. Gu, L.; Hanson, P.J.; Post, W.M.; Kaiser, D.P.; Yang, B.; Nemani, R.; Pallardy, S.G.; Meyers, T. The 2007 Eastern US spring freeze: Increased cold damage in a warming world? *BioScience* **2008**, *58*, 253–262. [CrossRef]
4. Frederiks, T.M.; Christopher, J.T.; Sutherland, M.W.; Borrell, A.K. Post-head-emergence frost in wheat and barley: Defining the problem, assessing the damage, and identifying resistance. *J. Exp. Bot.* **2015**, *66*, 3487–3498. [CrossRef]
5. Zheng, B.; Chapman, S.C.; Christopher, J.T.; Frederiks, T.M.; Chenu, K. Frost trends and their estimated impact on yield in the Australian wheatbelt. *J. Exp. Bot.* **2015**, *66*, 3611–3623. [CrossRef]
6. Li, X.; Cai, J.; Liu, F.; Dai, T.; Cao, W.; Jiang, D. Spring freeze effect on wheat yield is modulated by winter temperature fluctuations: Evidence from meta-analysis and simulating experiment. *J. Agron. Crop Sci.* **2014**, *201*, 288–300. [CrossRef]
7. Crimp, S.; Bakar, K.S.; Kokic, P.; Jin, H.; Nicholls, N.; Howden, M. Bayesian space–time model to analyse frost risk for agriculture in Southeast Australia. *Int. J. Climatol.* **2015**, *35*, 2092–2108. [CrossRef]
8. Li, X.; Cai, J.; Liu, F.; Zhou, Q.; Dai, T.; Cao, W.; Jiang, D. Wheat plants exposed to winter warming are more susceptible to low temperature stress in the spring. *Plant Growth Regul.* **2015**, *77*, 11–19. [CrossRef]
9. Marcellos, H.; Single, W.V. Temperatures in wheat during radiation frost. *Aust. J. Exp. Agric.* **1975**, *15*, 818–822. [CrossRef]
10. March, T.; Knights, S.; Biddulph, B.; Ogbonnaya, F.; Maccallum, R.; Belford, R. The GRDC National Frost Initiative. Available online: https://grdc.com.au/Research-and-Development/GRDC-Update-Papers/2015/02/The-GRDC-National-Frost-Initiative (accessed on 4 April 2020).
11. Frederiks, T.M.; Christopher, J.T.; Harvey, G.L.; Sutherland, M.W.; Borrell, A.K. Current and emerging screening methods to identify post-head-emergence frost adaptation in wheat and barley. *J. Exp. Bot.* **2012**, *63*, 5405–5416. [CrossRef]
12. Single, W.V. Studies on frost injury to wheat. III. Screening of varieties for resistance to ear and stem frosting. *Aust. J. Agric. Res.* **1966**, *17*, 601–610. [CrossRef]
13. Fowler, D.B.; Breton, G.; Limin, A.E.; Mahfoozi, S.; Sarhan, F. Photoperiod and temperature interactions regulate low-temperature-induced gene expression in barley. *Plant Physiol.* **2001**, *127*, 1676–1681. [CrossRef]
14. Limin, A.E.; Fowler, D.B. Low-temperature tolerance and genetic potential in wheat (*Triticum aestivum* L.): Response to photoperiod, vernalization, and plant development. *Planta* **2006**, *224*, 360–366. [CrossRef]
15. Mahajan, S.; Tuteja, N. Cold, salinity and drought stresses: An overview. *Arch. Biochem. Biophys.* **2005**, *444*, 139–158. [CrossRef]
16. Wong, H.L.; Shimamoto, K. Sending ROS on a bullet train. *Sci. Signal.* **2009**, *2*, pe60. [CrossRef]
17. Das, K.; Roychoudhury, A. Reactive oxygen species (ROS) and response of antioxidants as ROS-scavengers during environmental stress in plants. *Front. Environ. Sci.* **2014**, *2*. [CrossRef]

18. You, J.; Chan, Z. ROS regulation during abiotic stress responses in crop plants. *Front. Plant Sci.* **2015**, *6*. [CrossRef]
19. Vágújfalvi, A.; Kerepesi, I.; Galiba, G.; Tischner, T.; Sutka, J. Frost hardiness depending on carbohydrate changes during cold acclimation in wheat. *Plant Sci.* **1999**, *144*, 85–92. [CrossRef]
20. Uemura, M.; Warren, G.; Steponkus, P.L. Freezing sensitivity in the *sfr4* mutant of Arabidopsis is due to low sugar content and is manifested by loss of osmotic responsiveness. *Plant Physiol.* **2003**, *131*, 1800–1807. [CrossRef]
21. Bouche, N.; Fait, A.; Zik, M.; Fromm, H. The root-specific glutamate decarboxylase (GAD1) is essential for sustaining GABA levels in Arabidopsis. *Plant Mol. Biol.* **2004**, *55*, 315–325. [CrossRef]
22. Burg, M.B.; Ferraris, J.D. Intracellular Organic Osmolytes: Function and regulation. *J. Biol. Chem.* **2008**, *283*, 7309–7313. [CrossRef]
23. Nahar, K.; Hasanuzzaman, M.; Fujita, M. Roles of osmolytes in plant adaptation to drought and salinity. In *Osmolytes and Plants Acclimation to Changing Environment: Emerging Omics Technologies*; Iqbal, N., Nazar, R.A., Khan, N., Eds.; Springer: New Delhi, India, 2016; pp. 37–68. [CrossRef]
24. Los, D.A.; Murata, N. Membrane fluidity and its roles in the perception of environmental signals. *Biochim. Biophys. Acta* **2004**, *1666*, 142–157. [CrossRef] [PubMed]
25. Upchurch, R.G. Fatty acid unsaturation, mobilization, and regulation in the response of plants to stress. *Biotechnol. Lett.* **2008**, *30*, 967–977. [CrossRef]
26. Ruelland, E.; Zachowski, A. How plants sense temperature. *Environ. Exp. Bot.* **2010**, *69*, 225–232. [CrossRef]
27. Keurentjes, J.J. Genetical metabolomics: Closing in on phenotypes. *Curr. Opin. Plant Biol.* **2009**, *12*, 223–230. [CrossRef]
28. Weckwerth, W. Green systems biology—From single genomes, proteomes and metabolomes to ecosystems research and biotechnology. *J. Proteom.* **2011**, *75*, 284–305. [CrossRef]
29. Radomiljac, J.D.; Whelan, J.; van der Merwe, M. Coordinating metabolite changes with our perception of plant abiotic stress responses: Emerging views revealed by integrative-omic analyses. *Metabolites* **2013**, *3*, 761–786. [CrossRef]
30. Cheong, B.E.; Ho, W.W.H.; Biddulph, B.; Wallace, X.; Rathjen, T.; Rupasinghe, T.W.T.; Roessner, U.; Dolferus, R. Phenotyping reproductive stage chilling and frost tolerance in wheat using targeted metabolome and lipidome profiling. *Metab. Off. J. Metab. Soc.* **2019**, *15*, 144. [CrossRef]
31. Smith, M.R.; Rao, I.M.; Merchant, A. Source-sink relationships in crop plants and their influence on yield development and nutritional quality. *Front. Plant Sci.* **2018**, *9*, 1889. [CrossRef]
32. Zinselmeier, C.; Lauer, M.J.; Boyer, J.S. Reversing drought-induced losses in grain yield—Sucrose maintains embryo growth in maize. *Crop Sci.* **1995**, *35*, 1390–1400. [CrossRef]
33. Zinselmeier, C.; Westgate, M.; Schussler, J.; Jones, R. Low water potential disrupts carbohydrate metabolism in maize (*Zea mays* L.) ovaries. *Plant Physiol.* **1995**, *107*, 385–391. [CrossRef] [PubMed]
34. Clément, C.; Burrus, M.; Audran, J.-C. Floral organ growth and carbohydrate content during pollen development in *Lilium*. *Am. J. Bot.* **1996**, *83*, 459–469. [CrossRef]
35. Clément, C.; Laporte, P.; Audran, J.C. The loculus content and tapetum during pollen development in *Lilium*. *Sex. Plant Reprod.* **1998**, *11*, 94–106. [CrossRef]
36. Reynolds, M.P.; Pellegrineschi, A.; Skovmand, B. Sink-limitation to yield and biomass: A summary of some investigations in spring wheat. *Ann. Appl. Biol.* **2005**, *146*, 39–49. [CrossRef]
37. Castro, A.J.; Clément, C. Sucrose and starch catabolism in the anther of *Lilium* during its development: A comparative study among the anther wall, locular fluid and microspore/pollen fractions. *Planta* **2007**, *225*, 1573–1582. [CrossRef]
38. Oliver, S.N.; Van Dongen, J.T.; Alfred, S.C.; Mamun, E.A.; Zhao, X.; Saini, H.S.; Fernandes, S.F.; Blanchard, C.L.; Sutton, B.G.; Geigenberger, P.; et al. Cold-induced repression of the rice anther-specific cell wall invertase gene *OSINV4* is correlated with sucrose accumulation and pollen sterility. *Plant Cell Environ.* **2005**, *28*, 1534–1551. [CrossRef]
39. Ji, X.; Shiran, B.; Wan, J.; Lewis, D.C.; Jenkins, C.L.D.; Condon, A.G.; Richards, R.A.; Dolferus, R. Importance of pre-anthesis anther sink strength for maintenance of grain number during reproductive stage water stress in wheat. *Plant Cell Environ.* **2010**, *33*, 926–942. [CrossRef]

40. Dias, D.A.; Hill, C.B.; Jayasinghe, N.S.; Atieno, J.; Sutton, T.; Roessner, U. Quantitative profiling of polar primary metabolites of two chickpea cultivars with contrasting responses to salinity. *J. Chromatogr. B* **2015**, *1000*, 1–13. [CrossRef]
41. Boughton, B.A.; Callahan, D.L.; Silva, C.; Bowne, J.; Nahid, A.; Rupasinghe, T.; Tull, D.L.; McConville, M.J.; Bacic, A.; Roessner, U. Comprehensive profiling and quantitation of amine group containing metabolites. *Anal. Chem.* **2011**, *83*, 7523–7530. [CrossRef]
42. Folch, J.; Lees, M.; Sloane Stanley, G.H. A simple method for the isolation and purification of total lipids from animal tissues. *J. Biol. Chem.* **1957**, *226*, 497–509.
43. Sumner, L.W.; Amberg, A.; Barrett, D.; Beale, M.H.; Beger, R.; Daykin, C.A.; Fan, T.W.M.; Fiehn, O.; Goodacre, R.; Griffin, J.L.; et al. Proposed minimum reporting standards for chemical analysis Chemical Analysis Working Group (CAWG) Metabolomics Standards Initiative (MSI). *Metab. Off. J. Metab. Soc.* **2007**, *3*, 211–221. [CrossRef]
44. Xia, J.; Wishart, D.S. Using MetaboAnalyst 3.0 for comprehensive metabolomics data analysis. *Curr. Protoc. Bioinform.* **2016**, *55*, 14.10.11–14.10.91. [CrossRef] [PubMed]
45. Benjamini, Y.; Hochberg, Y. Controlling the False Discovery Rate: A practical and powerful approach to multiple testing. *J. R. Stat. Soc. Ser. B (Methodol.)* **1995**, *57*, 289–300. [CrossRef]
46. Marcelis, L.F. Sink strength as a determinant of dry matter partitioning in the whole plant. *J. Exp. Bot.* **1996**, *47*, 1281–1291. [CrossRef] [PubMed]
47. Lemoine, R.; La Camera, S.; Atanassova, R.; Dedaldechamp, F.; Allario, T.; Pourtau, N.; Bonnemain, J.L.; Laloi, M.; Coutos-Thevenot, P.; Maurousset, L.; et al. Source-to-sink transport of sugar and regulation by environmental factors. *Front. Plant Sci.* **2013**, *4*, 272. [CrossRef]
48. Thakur, P.; Kumar, S.; Malika, J.A.; Berger, J.D.; Nayyar, H. Cold stress effects on reproductive development in grain crops: An overview. *Environ. Exp. Bot.* **2010**, *67*, 429–443. [CrossRef]
49. Lokhande, V.H.; Suprasanna, P. Prospects of halophytes in understanding and managing abiotic stress yolerance. In *Environmental Adaptations and Stress Tolerance of Plants in the Era of Climate Change*; Ahmad, P., Prasad, M.N.V., Eds.; Springer: New York, NY, USA, 2012; pp. 29–56. [CrossRef]
50. Mayer, R.R.; Cherry, J.H.; Rhodes, D. Effects of heat shock on amino acid metabolism of cowpea cells. *Plant Physiol.* **1990**, *94*, 796–810. [CrossRef]
51. Ashraf, M.; Foolad, M.R. Roles of glycine betaine and proline in improving plant abiotic stress resistance. *Environ. Exp. Bot.* **2007**, *59*, 206–216. [CrossRef]
52. Lehmann, S.; Funck, D.; Szabados, L.; Rentsch, D. Proline metabolism and transport in plant development. *Amino Acids* **2010**, *39*, 949–962. [CrossRef]
53. Hayat, S.; Hayat, Q.; Alyemeni, M.N.; Wani, A.S.; Pichtel, J.; Ahmad, A. Role of proline under changing environments: A review. *Plant Signal. Behav.* **2012**, *7*, 1456–1466. [CrossRef]
54. Liang, X.; Zhang, L.; Natarajan, S.K.; Becker, D.F. Proline mechanisms of stress survival. *Antioxid. Redox Signal.* **2013**, *19*, 998–1011. [CrossRef] [PubMed]
55. Kaplan, F.; Guy, C.L. beta-Amylase induction and the protective role of maltose during temperature shock. *Plant Physiol.* **2004**, *135*, 1674–1684. [CrossRef]
56. Rizhsky, L.; Liang, H.; Shuman, J.; Shulaev, V.; Davletova, S.; Mittler, R. When defense pathways collide. The response of Arabidopsis to a combination of drought and heat stress. *Plant Physiol.* **2004**, *134*, 1683–1696. [CrossRef]
57. Broeckling, C.D.; Huhman, D.V.; Farag, M.A.; Smith, J.T.; May, G.D.; Mendes, P.; Dixon, R.A.; Sumner, L.W. Metabolic profiling of *Medicago truncatula* cell cultures reveals the effects of biotic and abiotic elicitors on metabolism. *J. Exp. Bot.* **2005**, *56*, 323–336. [CrossRef] [PubMed]
58. Hanson, A.D.; Rathinasabapathi, B.; Chamberlin, B.; Gage, D.A. Comparative physiological evidence that β-alanine betaine and choline-O-sulfate act as compatible osmolytes in halophytic *Limonium* species. *Plant Physiol.* **1991**, *97*, 1199–1205. [CrossRef] [PubMed]
59. Rocha, M.; Licausi, F.; Araujo, W.L.; Nunes-Nesi, A.; Sodek, L.; Fernie, A.R.; van Dongen, J.T. Glycolysis and the tricarboxylic acid cycle are linked by alanine aminotransferase during hypoxia induced by waterlogging of *Lotus japonicus*. *Plant Physiol.* **2010**, *152*, 1501–1513. [CrossRef] [PubMed]
60. Rocha, M.; Sodek, L.; Licausi, F.; Hameed, M.W.; Dornelas, M.C.; van Dongen, J.T. Analysis of alanine aminotransferase in various organs of soybean (*Glycine max*) and in dependence of different nitrogen fertilisers during hypoxic stress. *Amino Acids* **2010**, *39*, 1043–1053. [CrossRef]

61. Hanson, A.D.; Rathinasabapathi, B.; Rivoal, J.; Burnet, M.; Dillon, M.O.; Gage, D.A. Osmoprotective compounds in the Plumbaginaceae: A natural experiment in metabolic engineering of stress tolerance. *Proc. Natl. Acad. Sci. USA* **1994**, *91*, 306–310. [CrossRef]
62. Morsy, M.R.; Jouve, L.; Hausman, J.F.; Hoffmann, L.; Stewart, J.M. Alteration of oxidative and carbohydrate metabolism under abiotic stress in two rice (*Oryza sativa* L.) genotypes contrasting in chilling tolerance. *J. Plant Physiol.* **2007**, *164*, 157–167. [CrossRef]
63. Folgado, R.; Panis, B.; Sergeant, K.; Renaut, J.; Swennen, R.; Hausman, J.F. Unravelling the effect of sucrose and cold pretreatment on cryopreservation of potato through sugar analysis and proteomics. *Cryobiology* **2015**, *71*, 432–441. [CrossRef]
64. Llanes, A.; Bertazza, G.; Palacio, G.; Luna, V. Different sodium salts cause different solute accumulation in the halophyte *Prosopis strombulifera*. *Plant Biol.* **2013**, *15* (Suppl. 1), 118–125. [CrossRef] [PubMed]
65. Lu, Y.; Sharkey, T.D. The importance of maltose in transitory starch breakdown. *Plant Cell Environ.* **2006**, *29*, 353–366. [CrossRef] [PubMed]
66. Wolfe, J.; Bryant, G. Freezing, drying, and/or vitrification of membrane-solute-water systems. *Cryobiology* **1999**, *39*, 103–129. [CrossRef] [PubMed]
67. Ambroise, V.; Legay, S.; Guerriero, G.; Hausman, J.-F.; Cuypers, A.; Sergeant, K. The roots of plant frost hardiness and tolerance. *Plant Cell Physiol.* **2019**, *61*, 3–20. [CrossRef] [PubMed]
68. Gill, S.S.; Tuteja, N. Polyamines and abiotic stress tolerance in plants. *Plant Signal. Behav.* **2010**, *5*, 26–33. [CrossRef] [PubMed]
69. Shi, H.; Chan, Z. Improvement of plant abiotic stress tolerance through modulation of the polyamine pathway. *J. Integr. Plant Biol.* **2014**, *56*, 114–121. [CrossRef]
70. Knaupp, M.; Mishra, K.B.; Nedbal, L.; Heyer, A.G. Evidence for a role of raffinose in stabilizing photosystem II during freeze-thaw cycles. *Planta* **2011**, *234*, 477–486. [CrossRef]
71. Keunen, E.; Peshev, D.; Vangronsveld, J.; Van Den Ende, W.; Cuypers, A. Plant sugars are crucial players in the oxidative challenge during abiotic stress: Extending the traditional concept. *Plant Cell Environ.* **2013**, *36*, 1242–1255. [CrossRef]
72. Couée, I.; Sulmon, C.; Gouesbet, G.; El Amrani, A. Involvement of soluble sugars in reactive oxygen species balance and responses to oxidative stress in plants. *J. Exp. Bot.* **2006**, *57*, 449–459. [CrossRef]
73. Beck, E.H.; Fettig, S.; Knake, C.; Hartig, K.; Bhattarai, T. Specific and unspecific responses of plants to cold and drought stress. *J. Biosci.* **2007**, *32*, 501–510. [CrossRef]
74. Ren, M.; Phoon, C.K.; Schlame, M. Metabolism and function of mitochondrial cardiolipin. *Prog. Lipid Res.* **2014**, *55*, 1–16. [CrossRef] [PubMed]
75. Murata, N.; Wada, H.; Gombos, Z. Modes of fatty-acid desaturation in cyanobacteria. *Plant Cell Physiol.* **1992**, *33*, 933–941. [CrossRef]
76. Welti, R.; Shah, J.; Li, W.; Li, M.; Chen, J.; Burke, J.J.; Fauconnier, M.L.; Chapman, K.; Chye, M.L.; Wang, X. Plant lipidomics: Discerning biological function by profiling plant complex lipids using mass spectrometry. *Front. Biosci.* **2007**, *12*, 2494–2506. [CrossRef] [PubMed]
77. Li, Q.; Zheng, Q.; Shen, W.; Cram, D.; Fowler, D.B.; Wei, Y.; Zou, J. Understanding the biochemical basis of temperature-induced lipid pathway adjustments in plants. *Plant Cell* **2015**, *27*, 86–103. [CrossRef] [PubMed]
78. Williams, M.; Harwood, J.L. Effect of drought on volatile production by the lipoxygenase pathway in olive fruit. *Biochem. Soc. Trans.* **1997**, *25*, 499S. [CrossRef] [PubMed]
79. Campos, P.; Quartin, V.; Ramalho, J.; Nunes, M. Electrolyte leakage and lipid degradation account for cold sensitivity in leaves of *Coffea* sp. plants. *J. Plant Physiol.* **2003**, *160*, 283–292. [CrossRef]
80. Moon, B.Y.; Higashi, S.; Gombos, Z.; Murata, N. Unsaturation of the membrane lipids of chloroplasts stabilizes the photosynthetic machinery against low-temperature photoinhibition in transgenic tobacco plants. *Proc. Natl. Acad. Sci. USA* **1995**, *92*, 6219–6223. [CrossRef]
81. Welti, R.; Li, W.; Li, M.; Sang, Y.; Biesiada, H.; Zhou, H.E.; Rajashekar, C.B.; Williams, T.D.; Wang, X. Profiling membrane lipids in plant stress responses. Role of phospholipase D alpha in freezing-induced lipid changes in Arabidopsis. *J. Biol. Chem.* **2002**, *277*, 31994–32002. [CrossRef]
82. Zhang, X.D.; Wang, R.P.; Zhang, F.J.; Tao, F.Q.; Li, W.Q. Lipid profiling and tolerance to low-temperature stress in *Thellungiella salsuginea* in comparison with *Arabidopsis thaliana*. *Biol. Plant.* **2013**, *57*, 149–153. [CrossRef]

83. Vance, D.E.; Vance, J.E. CHAPTER 8—Phospholipid biosynthesis in eukaryotes. In *Biochemistry of Lipids, Lipoproteins and Membranes*, 5th ed.; Vance, D.E., Vance, J.E., Eds.; Elsevier: San Diego, CA, USA, 2008; pp. 213–244. [CrossRef]
84. Guschina, I.A.; Harwood, J.L. Mechanisms of temperature adaptation in poikilotherms. *FEBS Lett.* **2006**, *580*, 5477–5483. [CrossRef]
85. Ruelland, E.; Cantrel, C.; Gawer, M.; Kader, J.C.; Zachowski, A. Activation of phospholipases C and D is an early response to a cold exposure in Arabidopsis suspension cells. *Plant Physiol.* **2002**, *130*, 999–1007. [CrossRef] [PubMed]
86. Murata, N.; Yamaya, J. Temperature-dependent phase behavior of phosphatidylglycerols from chilling-sensitive and chilling-resistant plants. *Plant Physiol.* **1984**, *74*, 1016–1024. [CrossRef] [PubMed]
87. Bargmann, B.O.; Munnik, T. The role of phospholipase D in plant stress responses. *Curr. Opin. Plant Biol.* **2006**, *9*, 515–522. [CrossRef] [PubMed]
88. Testerink, C.; Munnik, T. Phosphatidic acid: A multifunctional stress signaling lipid in plants. *Trends Plant Sci.* **2005**, *10*, 368–375. [CrossRef]
89. Guo, L.; Mishra, G.; Taylor, K.; Wang, X. Phosphatidic acid binds and stimulates Arabidopsis sphingosine kinases. *J. Biol. Chem.* **2011**, *286*, 13336–13345. [CrossRef]
90. Barbaglia, A.M.; Hoffmann-Benning, S. Long-distance lipid signaling and its role in plant development and stress response. *Subcell Biochem.* **2016**, *86*, 339–361. [CrossRef]
91. Pyke, K.A. Plastid division and development. *Plant Cell* **1999**, *11*, 549–556. [CrossRef]
92. Pogson, B.J.; Ganguly, D.; Albrecht-Borth, V. Insights into chloroplast biogenesis and development. *Biochim. Biophys. Acta—Bioenerg.* **2015**, *1847*, 1017–1024. [CrossRef]
93. Vothknecht, U.C.; Westhoff, P. Biogenesis and origin of thylakoid membranes. *Biochim. Biophys. Acta—Mol. Cell Res.* **2001**, *1541*, 91–101. [CrossRef]
94. Dörmann, P. Galactolipids in plant membranes. *eLS* **2013**. [CrossRef]
95. Routaboul, J.M.; Fischer, S.F.; Browse, J. Trienoic fatty acids are required to maintain chloroplast function at low temperatures. *Plant Physiol.* **2000**, *124*, 1697–1705. [CrossRef] [PubMed]
96. Quartacci, M.F.; Pinzino, C.; Sgherri, C.L.M.; Navari-Izzo, F. Lipid composition and protein dynamics in thylakoids of two wheat cultivars differently sensitive to drought. *Plant Physiol.* **1995**, *108*, 191–197. [CrossRef] [PubMed]
97. Navari-Izzo, F.; Ricci, F.; Vazzana, C.; Quartacci, M.F. Unusual composition of thylakoid membranes of the resurrection plant *Boea hygroscopica*: Changes in lipids upon dehydration and rehydration. *Physiol. Plant.* **1995**, *94*, 135–142. [CrossRef]



© 2020 by the authors. Licensee MDPI, Basel, Switzerland. This article is an open access article distributed under the terms and conditions of the Creative Commons Attribution (CC BY) license (http://creativecommons.org/licenses/by/4.0/).